Vol. 66 September, 1962 No. 9

THE JOURNAL OF PHYSICAL CHEMISTRY

(Registered in U. S. Patent Office)

CONTENTS

Contents continued on page 1A

THE JOURNAL OF PHYSICAL CHEMISTRY

(Registered in U. S. Patent Office)

Published monthly by the American Chemical Society at 20th and Northampton Sts., Easton, Pa. Second-class postage paid at Easton, Pa.

The *Journal of Physical Chemistry* is devoted to the publication of selected symposia in the broad field of physical chemistry and to other contributed papers.

Manuscripts originating in the British Isles, Europe, and Africa should be sent to F. C. Tompkins, The Faraday Society, 6 Gray's Inn Square, London W. C. 1, England.

Manuscripts originating elsewhere should be sent to W. Albert Noyes, Jr., Department of Chemistry, University of Rochester, Rochester 20, N. Y.

Correspondence regarding accepted copy, proofs, and reprints should be directed to Assistant Editor, Allen D. Bliss, ACS Office, Mack Printing Company, 20th and Northampton Sts., Easton, Pa.

Advertising Office: Reinhold Publishing Corporation, 430 Park Avenue, New York 22, N. Y.

Articles must be submitted in duplicate, typed, and double spaced. They should have at the beginning a brief Abstract, in no case exceeding 300 words. Original drawings should accompany the manuscript. Lettering at the sides of graphs (black on white or blue) may be pencilled in and will be typeset. Figures and tables should be held to a minimum consistent with adequate presentation of information. Photographs will not be printed on glossy paper except by special arrangement. All footnotes and references to the literature should be numbered consecutively and placed in the manuscript at the proper places. Initials of authors referred to in citations should be given. Nomenclature should conform to that used in *Chemical Abstracts*, mathematical characters be marked for italic, Greek letters carefully made or annotated, and subscripts and superscripts clearly shown. Articles should be written as briefly as possible consistent with clarity and should avoid historical background unnecessary for specialists.

Notes describe fragmentary or incomplete studies but do not otherwise differ fundamentally from articles and are subjected to the same editorial appraisal as are articles. In their preparation particular attention should be paid to brevity and conciseness. Material included in Notes must be definitive and may not be republished subsequently.

Communications to the Editor are designed to afford prompt preliminary publication of observations or discoveries whose value to science is so great that immediate publication is imperative. The appearance of related work from other laboratories is in itself not considered sufficient justification for the publication of a Communication, which must in addition meet special requirements of timeliness and significance. Their total length may in no case exceed 1000 words or their equivalent. They differ from Articles and Notes in that their subject matter may be republished.

Symposium papers should be sent in all cases to Secretaries of Divisions sponsoring the symposium, who will be responsible for their transmittal to the Editor. The Secretary of the Division by agreement with the Editor will specify a time after which symposium papers cannot be accepted. The Editor reserves the right to refuse to publish symposium articles, for valid scientific reasons. Each symposium paper may not exceed four printed pages (about sixteen double spaced typewritten pages) in length except by prior arrangement with the Editor.

Remittances and orders for subscriptions and for single copies, notices of changes of address and new professional connections, and claims for missing numbers should be sent to the Subscription Service Department, American Chemical Society, 1155 Sixteenth St., N. W., Washington 6, D. C. Changes of address for the *Journal of Physical Chemistry* must be received on or before the 30th of the preceding month. Please include an old address label with the notification.

Claims for missing numbers will not be allowed (1) if received more than sixty days from date of issue (because of delivery hazards, no claims can be honored from subscribers in Central Europe, Asia, or Pacific Islands other than Hawaii), (2) if loss was due to failure of notice of change of address to be received before the date specified in the preceding paragraph, or (3) if the reason for the claim is "missing from files."

Subscription rates (1962): members of American Chemical Society, $12.00 for 1 year; to non-members, $24.00 for 1 year. Postage to countries in the Pan-American Union $0.80; Canada, $0.40; all other countries, $1.20. Single copies, current volume, $2.50; foreign postage, $0.15; Canadian postage $0.10; Pan-American Union, $0.10. Back volumes (Vol. 56–65) $30.00 per volume; foreign postage, per volume $1.20, Canadian, $0.40; Pan-American Union, $0.80. Single copies: back issues, $3.00; for current year, $2.50; postage, single copies: foreign, $0.15; Canadian, $0.10; Pan-American Union, $0.10.

The American Chemical Society and the Editors of the *Journal of Physical Chemistry* assume no responsibility for the statements and opinions advanced by contributors to THIS JOURNAL.

The American Chemical Society also publishes *Journal of the American Chemical Society, Chemical Abstracts, Industrial and Engineering Chemistry*, International Edition of *Industrial and Engineering Chemistry, Chemical and Engineering News, Analytical Chemistry, Journal of Agricultural and Food Chemistry, Journal of Organic Chemistry, Journal of Chemical and Engineering Data, Chemical Reviews, Chemical Titles, Journal of Chemical Documentation, Journal of Medicinal and Pharmaceutical Chemistry, Inorganic Chemistry, Biochemistry*, and *CA — Biochemical Sections*. Rates on request.

Contents continued

NOTES

COMMUNICATION TO THE EDITOR

AUTHOR INDEX

Special Notice to Authors

Beginning with the January issue, 1963, a page charge for publication will go into effect. The ACS position is described in detail *via* a series of questions and answers in "The Case for Page Charges," *Chem. Eng. News*, March 19, 1962, p. 92. The editors of the Journal of Physical Chemistry wish to emphasize the following points.

1. The page charge is a publication service charge designed to aid in covering the costs of publishing an article in a journal. The page charge covers only costs of setting the article in type and preparing it for the presses. As administered by the ACS, it will also include 100 reprints supplied to the author.

2. Manuscripts received after August 15, 1962, or accepted for publication after September 15, may be published in January, 1963, and subsequent issues, and therefore be subject to the page charge.

3. Payment is expected from sponsored funds supporting the research reported. Page charge payment is not a condition for publication.

4. The editor's decision to publish is made before assessment of page charges and the editor's office will not be advised on charges or payment.

5. With the institution of page charges, subscription rates to ACS journals should be stabilized at current levels for an indefinite period of time.

Complete your search for original sources in chemistry . . . with CA's 1961 LIST OF PERIODICALS

The new edition of this famous LIST is now available. It offers up-to-date information on virtually all chemical journals published today. It makes CHEMICAL ABSTRACTS fully useful by answering the important question of where to find the original paper from which an abstract is taken. Non-CA subscribers will find it equally helpful.

What the LIST Contains

The 1961 LIST gives 8,150 entries which locate abstracted *serials* and 1,532 entries which locate *nonserial* volumes (largely proceedings of meetings, plus memorial volumes, lectures, and edited compilations of signed papers). With discontinued journals, references from former titles and from other forms of title to the one used in CA, there is a grand total of 12,543 entries.

YOU WILL FIND:

(1) names and addresses of publishers or those who sell these publications

(2) a key to 334 cooperating libraries in the U. S. and foreign countries where these periodicals may be found or copies of papers purchased.

Under each journal, code numbers are printed, which key the user to the cooperating libraries shown in the front of the book. You can readily decide whether to write for a journal or use a nearby library where it can be studied or borrowed.

Useful to Every Researcher

No library will want to be without the 1961 LIST OF PERIODICALS, and no researcher will want to work without it handy. Annual supplements will keep this listing current. Not only CA subscribers but any chemist in research can benefit from the timely information in this volume. It is among the most basic of searching tools.

397 pages. **Paper bound.** **Price: $5.00**

Order from:

Special Issues Sales/American Chemical Society/1155 Sixteenth St., N. W./Washington 6, D. C.

THE JOURNAL OF
PHYSICAL CHEMISTRY

(Registered in U. S. Patent Office)

VOLUME 66 SEPTEMBER 19, 1962. NUMBER 9

FREE RADICALS FROM THE DECOMPOSITION OF TOLUENE AND BUTENE-1[1]

BY STANLEY DEUTSCH[2] AND K. A. KRIEGER

Department of Chemistry, University of Pennsylvania, Philadelphia, Penna.

Received September 22, 1961

A tracer method, using a frozen radioactive iodine mirror, has been utilized for the detection of free radicals from the decomposition of toluene and butene-1. At 500°, the major decomposition fragment from toluene is the benzyl free radical. A catalytic effect is observed over chromia, where a decrease in the concentration of benzyl radicals, with a corresponding increase in the phenyl free radical concentration, is observed. Butene-1 has been found to decompose at 690° to yield methyl radicals and considerably lower concentrations of ethyl radicals over alumina and platinum surfaces. In the temperature range 300–500°, a significant change in the rate of isomerization of butene-1 to butene-2 has been shown to take place over alumina. However, at these temperatures, the surface free radical concentration is essentially invariant, indicating that the isomerization process does not proceed by a free radical mechanism.

Introduction

Fleming,[3] and Fleming and Krieger[4] have investigated the heterogeneous decomposition of butane using solid iodine-131 as a scavenger for the free radicals formed. The purpose of this study is to extend the work of Fleming, using a modified apparatus and procedure, to an investigation of the heterogeneous decomposition of an aromatic hydrocarbon, toluene, and an olefin, butene-1.

Experimental

Procedure.—The reactant, either toluene or butene-1, is allowed to flow through a previously evacuated system at a pressure such that the mean free path of vapor is greater than the distance from a heated catalyst surface to a molecular radio-iodine mirror (see Fig. 1). Hence, free radicals which are formed on the reaction surface, and which leave the surface, will react with the iodine to form stable, radioactive, organic iodides. These products are collected in a cold trap at the termination of the experiment. The excess iodine is removed by appropriate chemical means, and carrier iodides, corresponding to the suspected compounds formed, are added. These carriers are separated by methods which will be considered shortly, and the radioactivity of each fraction is measured to determine which free radicals were initially present.

In the toluene experiments, excess radio-iodine was removed by vigorous shaking with 0.1 *N* sodium thiosulfate until the aqueous layer showed no significant radioactivity. An improved extraction method was employed in the butene-1 experiments. Independent check experiments showed that if iodine dissolved in organic solvents or in iodides is vacuum-distilled through sodium thiosulfate crystals (6/16 mesh) supported on a porous glass filter, a quantitative separation of the iodine from the various organic iodides takes place. This method is rapid, eliminates the possibility of hydrolytic breakdown of iodides, and, particularly important for the butene-1 experiments, allows small quantities of carrier substance to be manipulated.

After extraction of the iodine by either method, carrier iodides are added. In the toluene runs, 10 ml. each of methyl iodide, iodobenzene, and in later experiments, *p*-iodotoluene, were added along with 5 ml. of benzyl iodide.

Distillation proved unsuccessful for the quantitative separation of the lower-boiling iodides, and the only acceptable data from these preliminary runs were for the fraction of the total activity which appeared in the benzyl iodide (Table I). Furthermore, since in this procedure benzyl iodide was the residue from a distillation, it was necessary to show that the measured radioactivity was due to benzyl iodide, and not some other high-boiling impurity. This was done by two separate methods: the radioactive benzyl iodide was slowly cooled to its melting point (24°), and after partial crystallization, the liquid and solid portions were separated and measured for radioactivity. This procedure was repeated on the separated phases for as many times as was experimentally feasible. It is most unlikely that any impurity present would distribute itself equally, at each crystallization step, between the liquid and solid phases. Hence, a radioactive substance (other than benzyl iodide) would concentrate itself in the solid or liquid fractions as the separations are continued. From the measurements of the specific activity of each phase at each crystallization, no such concentration of activity was observed. A further check on the

(1) Abstracted from a dissertation submitted by S. Deutsch to the Graduate School of Arts and Sciences of the University of Pennsylvania in partial fulfillment of the requirements for the degree of Doctor of Philosophy.

(2) Radiation Chemistry Research Group, Department of Chemical Engineering, Columbia University, New York 27, N. Y.

(3) S. Fleming, Dissertation, University of Pennsylvania, 1954.

(4) S. Fleming and K. A. Krieger, *J. Am. Chem. Soc.*, **79**, 4003 (1957).

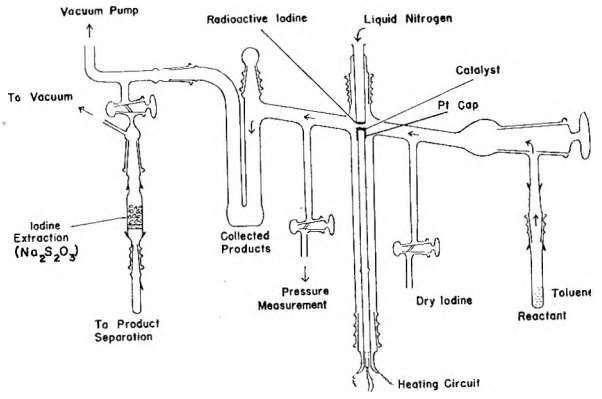

Fig. 1.—Apparatus for detection of free radicals.

An entirely different method, however, was employed for the separation of the butene-1 carrier substances. The mixture of products from butene-1, after removal of iodine and addition of carriers, was analyzed by gas chromatography using a dinonyl phthalate column. The effluent was trapped in a liquid nitrogen cooled coil,[5] continuously monitored by a scintillation counter. The resulting cumulative activity record, compared with a usual gas chromatographic trace, gave the distribution of radioactive products, as shown in Fig. 2.

Since the catalyzed isomerization of butene-1 to butene-2 has been reported,[6] it was thought that the results of the butene-1 decomposition studies, using the same catalysts, might cast some light on the mechanism of the isomerization reaction. Hence, the catalytic conversion of butene-1 to butene-2 as a function of temperature, over the same alumina catalyst used for the decomposition reactions, was studied from 300–500°. The reactant gas was passed over the heated catalyst, condensed, and analyzed by passage through a chromatographic column containing a diethylene

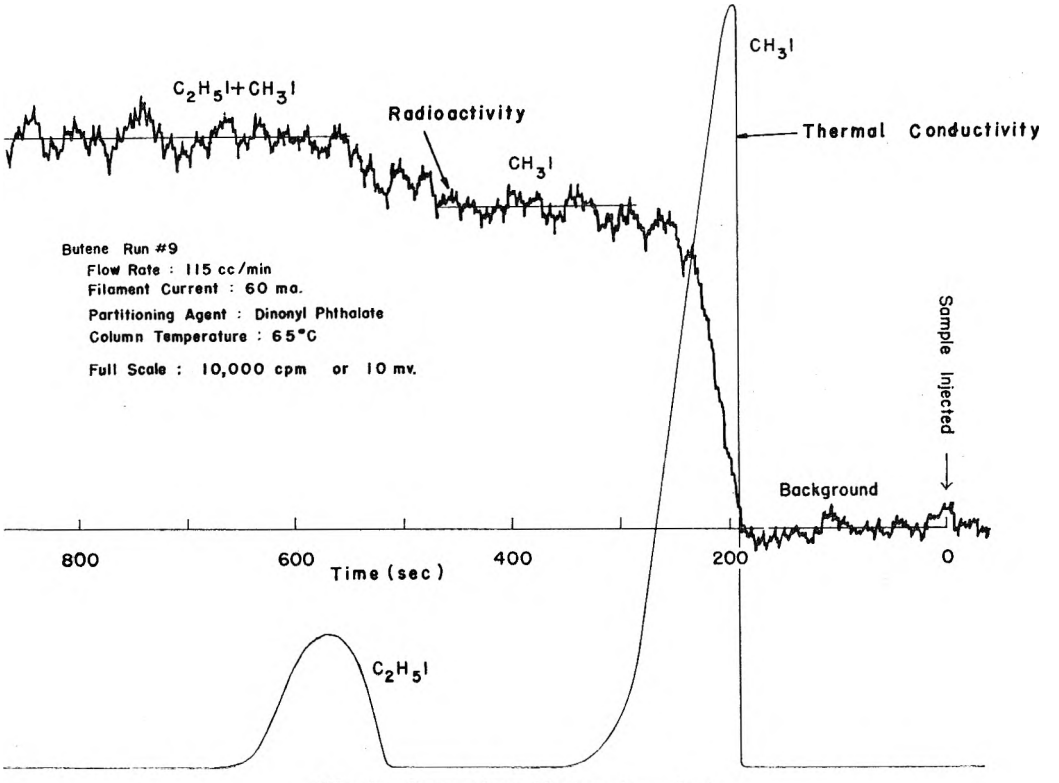

Fig. 2.—Separation of butene-1 products.

benzyl iodide purity was made by precipitating AgI (in alcoholic solution) with $AgNO_3$, dissolving the precipitate in KCN, and measuring the radioactivity in the aqueous layer. This procedure revealed that other radioactive substances were present to the extent, on the average, of less than 5%. The values in Table I have been corrected for these non-precipitable iodides.

To avoid decomposition of the thermally labile benzyl iodide during distillation, this compound was removed by precipitation with AgF (silver nitrate caused decomposition of the other iodides present) after the other precipitable carrier substance, methyl iodide, was distilled off. The precipitate was filtered, washed, and its radioactivity taken as a measure of the benzyl iodide activity. The remaining components, which included iodobenzene, *p*-iodotoluene, and heptane (used to facilitate solution transfer) then were distilled. Two-ml. distillate fractions were removed and measured for radioactivity. These results are shown in Table II and graphically in Fig. 3 and 4.

The experimental arrangement for the formation and capture of free radicals from the decomposition of butene-1 was similar to that used in the toluene experiments, with modifications for metering in the reactant gas at low pressures (one micron) and for gas volume measurements.

glycol monomethyl ether (carbitol) partitioning agent. The result, showing decreasing conversion with increasing temperature between 300 and 500°, is shown in Fig. 5.

Apparatus.—The main reaction train already has been described. The pressure in the system was measured by an internally calibrated Phillips-type cold cathode ionization gage which agreed satisfactorally with McLeod gage readings.

The catalyst surface was heated by means of a high resistance Chromel heating element positioned external to the vacuum system and separated from it by a cylindrical tube (see Fig. 1). The temperature fluctuation during a run at 500° was ±5°.

The reaction temperature was measured by a platinum–platinum, 10% rhodium thermocouple. The hot junction was the center of the thin platinum cap which was molded around the top of the cylindrical quartz tube to provide a support for the catalyst. The temperature of the thin catalyst surface (when a catalyst was used) was taken to be the same as that of the platinum. The thermocouple setup

(5) P. H. Emmett, private communication.

(6) C. Matignon, H. Moureu, and M. Dode, *Bull. soc. chim. France*, **2**, 1169 (1935).

was calibrated against a National Bureau of Standards thermocouple.

The separation of carrier substances in the toluene decomposition studies was accomplished by distillation, either at normal or reduced pressures. Column-head temperatures were measured by an iron–constantan thermocouple and continuously recorded.

The distillate samples from the toluene experiments, as well as the total activity before chromatographic analysis of the products from the butene experiments, were counted in a well-type multigeiger tube apparatus. The tubes were wired in parallel and were powered by the high voltage supply of a Model 163 Instrument Development Laboratory scalar whose efficiency for counting I-131 gammas was determined, using known amounts of radio-iodine, to be 0.2%. From this it was possible to obtain absolute disintegration rates.

As already mentioned, the carrier substances in the butene-1 studies were separated by chromatographic means. The column, 2.5 m. in length, was of the gas–liquid partition type, with the active highboiling liquid, in this instance dinonyl phthalate, adsorbed on an inert carrier. The scintillation counter was a Nuclear Chicago Corp. DS5-5 well-type counter with a thallium-activated sodium iodide crystal. The efficiency of the scintillation counter was measured by injecting known amounts of radioactive methyl iodide into the column and condensing the effluent vapor with liquid nitrogen in coils immediately adjacent to the scintillator crystal. The absolute activity of the methyl iodide was previously measured in the multiple geiger tube setup. When compared with the activity obtained from the scintillation counter, an efficiency of 5.6% was found.

The thermal conductivity cell was obtained from the Gow-Mac Co. and, for greater sensitivity, was insulated from ambient temperature variation by a heated, thermostated transite container.

Preparation of Materials.—The methyl iodide, iodobenzene, and *p*-iodotoluene which were added as carriers were distilled once and stored in the dark over cleaned copper wire. Ethyl iodide and heptane were distilled, passed through silica gel to remove any unsaturates, shaken with red phosphorus to remove any iodine, filtered to remove the red phosphorus, and redistilled.

The toluene reactant was a high-purity sulfur-free product of the Eastman Kodak Co. The only chemical treatment employed was the addition of sodium ribbon to remove any water vapor which may have been absorbed by the toluene during its transfer to the reaction system.

Butene-1 was obtained from the K & K Laboratories, New York, and was listed as 99+% pure. Mass spectrographic analysis indicated only 96.5% butene-1, with hydrogen and propene as the major impurities. The hydrogen, and any air that may have been present, was removed by condensing the butene at −195° and pumping for 10 min. It is not believed that the propene present, less than 1.0%, could have interfered with the butene-1 reactions being studied.

The benzyl iodide was prepared in this Laboratory by the exchange of sodium iodide with benzyl chloride in acetone solution.[7] After refluxing for 30 min., all the solvent was removed, the crude benzyl iodide was recrystallized from ethyl alcohol at least twice, and tested for purity by its pale yellow color and melting point. If not prepared for immediate use, it was sealed in an evacuated tube and stored at −10°. Synthetic radioactive benzyl iodide was prepared in a similar manner, with radioactive KI being dissolved in the acetone solvent at the start of the reaction.

Reliability.—The limit of reliability can be seen by comparing the results shown in Table II for the two runs over platinum. One possible explanation for the lack of close reproducibility may have been the purity of the reactant toluene. Though obtained sulfur-free, dried in the reaction chamber with sodium, analyzed chromatographically and for correct boiling point, it was not "pre-pyrolyzed" in the sense of Szwarc.[8]

Results and Discussion

Toluene.—In every experiment on toluene decomposition, the major product was benzyl iodide, indicating predominance of C–H bond cleavage at

(7) E. Spath, *Monatsh.*, **34**, 1995 (1914).

(8) M. Szwarc, *J. Chem. Phys.*, **16**, 128 (1948).

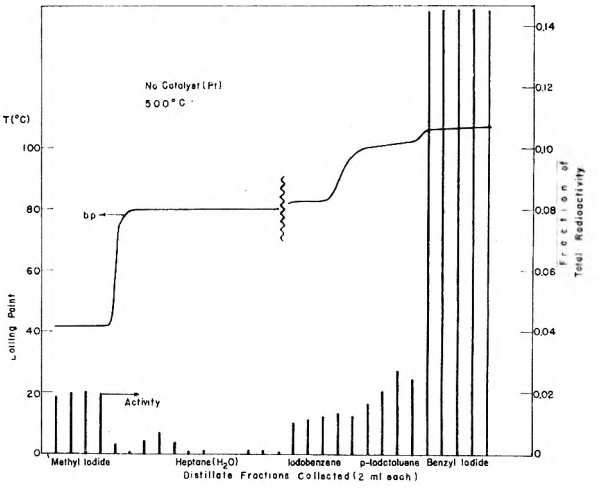

Figure 3.

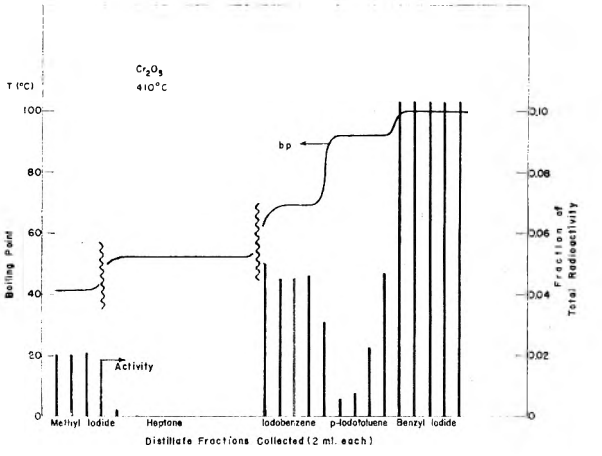

Figure 4.

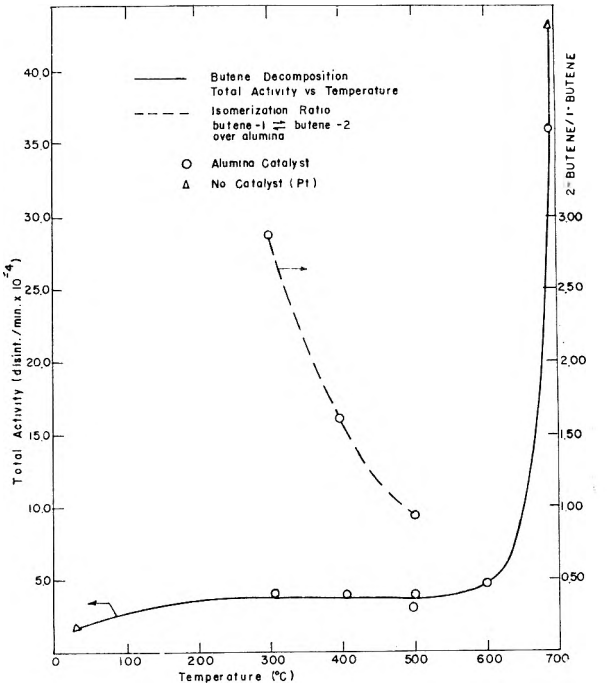

Figure 5.

the methyl side chain. As can be seen from Table I, a definite catalytic effect exists over Cr_2O_3, with smaller effects observable over Al_2O_3 and sugar charcoal. To fully appreciate the extent of the catalytic action of chromia, it must be emphasized that these results were obtained at a temperature approximately 100° lower than with any other catalyst or with bare platinum surfaces. At this temperature, the total activity obtained over all surfaces except chromia was too low to analyze.

TABLE I

PRODUCTS FROM DECOMPOSITION OF TOLUENE

Catalyst	Temp. (°C.)	Fraction of total activity as benzyl iodide
Al_2O_3	490	0.79
Al_2O_3	532	.79
None (Pt)	520	.89
Sugar charcoal	540	.74
Cr_2O_3	395	.51

The fraction of the total activity appearing as benzyl iodide was decreased to 0.51 (Table I), in close agreement with the value obtained by the precipitation method, the results of which are shown in Table II and Fig. 3 and 4. In Fig. 4, in which the fraction of the total radioactivity is plotted, for each two-ml. distillate cut, as a function of its boiling point, the drop in benzyl iodide activity[9] can be accounted for largely by the increase in iodobenzene activity. It appears that the Cr_2O_3 accelerates the cleavage of the side-chain C–C bond in toluene. This is in agreement with the work of Coonradt and Lerman,[10] in which chromia and chromia-containing catalysts were employed successfully as demethylation catalysts.

TABLE II

PRODUCTS FROM THE DECOMPOSITION OF TOLUENE

		Fraction of total activity			
Catalyst	Temp. (°C.)	Methyl iodide	Iodobenzene	*p*-Iodotoluene	Benzyl iodide
None (Pt)	505	0.19	0.02	0.11	0.68
None (Pt)	500	.10	.06	.12	.72
Cr_2O_3	410	.11	.23	.09	.52

p-Iodotoluene was added as a carrier in an attempt to observe the presence of a tolyl free radical, possibly the result of the removal of a hydrogen atom from the benzene ring. The results are inconclusive, and the unequal, steadily rising distribution of activity among the *p*-iodotoluene fractions (Fig. 3 and 4) suggests the presence of some non-precipitable iodide with a boiling point higher than any of the iodotoluenes, possibly a binuclear iodide resulting from the reaction of a primary free radical with adsorbed toluene.

It had been hoped that the results of this investigation might have some bearing on the controversial Szwarc mechanism for toluene decomposition.[8] By trapping and tagging the initial reaction fragments, the primary decomposition process might have been elucidated. However, the experiments were carried out at a vapor pressure of toluene which corresponds to a P/P_0 ratio of 0.15, indicating the presence of at least a monolayer of toluene at the surface of the frozen radio-iodine mirror. Hence many of the radicals from the primary decomposition may have reacted with adsorbed toluene before reacting with iodine, with the final observed products representing the sum of these primary and secondary interactions. If this experiment could have been carried out at a vapor pressure of toluene low enough to eliminate significant amounts of condensed toluene, a clearer picture of the primary decomposition step would be available.

Butene-1.—Two reactions of butene-1, isomerization to butene-2 and decomposition, have been studied. These will be discussed separately.

The mechanism of the isomerization reaction over catalysts considered to be "acidic," as alumina, has been studied. It is generally conceded that a carbonium ion mechanism prevails.[11,12] A proton from the catalyst adds to the olefin, followed by rearrangement of the resulting carbonium ion, with final loss of the proton to the catalyst, yielding an olefin of new structure. The best experimental evidence to support this is the work of Turkevich and Smith.[13] They found that the rate of exchange of tritium between butene-1 and a phosphoric acid catalyst, when corrected for isotope effects, was equal to the rate of the observed double bond migration. The experiments obtained in this Laboratory are in agreement with this type of mechanism. From the fact that the concentration of radicals formed during this reaction is invariant with temperature in the temperature range 300–500° while the rate of isomerization changes markedly as a function of temperature[14] (Fig. 5), only a mechanism which does not require free radicals is acceptable.

It might be argued that a free radical mechanism might nevertheless exist, but that no radicals leave the catalyst surface. This, under the experimental conditions employed here, must be considered unlikely. With bonds being continually broken and reformed, at least a small fraction would be expected to "boil off." Under the conditions of these experiments, only 1 in 10^8 radicals would need to be evaporated from the surface for detection.

From the radioactivity observed in each carrier substance in Table III, the ratio of methyl to ethyl radicals formed over alumina and platinum surfaces, at 690°, can be seen to be 16:1 and approximately 4.5:1. These high values, particularly over alumina, are in agreement with the mechanism for homogeneous butene-1 decomposition as proposed by Szwarc.[8] According to his suggested reaction scheme, the primary decomposition step leads to the formation of a methyl and an allyl free radical.

(9) The benzyl iodide fractions, as already mentioned, were not actually distilled. They are placed on the activity distribution graphs for comparative purposes only.

(10) H. L. Coonradt and W. K. Lerman, U. S. Patent 2,773,917 (1956).

(11) B. S. Greenfelder, H. H. Voge, and G. M. Good, *Ind. Eng. Chem.*, **41**, 2573 (1949).

(12) P. H. Emmett, Ed., "Catalysis," Vol. VI, Reinhold Publ. Corp., New York, N. Y., 1958, pp. 98–101.

(13) J. Turkevich and R. K. Smith, *J. Chem. Phys.*, **16**, 466 (1948).

(14) The observed results do not merely reflect a shift in equilibrium. The ratios of butene-2/butene-1 plotted in Fig. 5 are all far from the equilibrium values.[15]

(15) P. H. Emmett, ref. 12, pp. 167–169.

TABLE III
PRODUCTS FROM THE HIGH TEMPERATURE DECOMPOSITION OF BUTENE-1

Catalyst	Temp. (°C.)	Carrier substance	Radioactivity (counts/min.)
Al_2O_3	690	CH_3I	3230
		C_2H_5I	200
Platinum	690	CH_3I	3090
		C_2H_5I	700

For the heterogeneous case, however, if two-point adsorption by the double-bonded carbons of butene-1 is assumed, only ethyl radicals would be expected. But at these elevated temperatures, it is likely that the catalytic action, particularly of alumina, results in the equilibrium or near-equilibrium concentrations of butene-1 with its isomers, butene-2 and isobutene. Both isobutene and butene-2, again assuming two-point adsorption, would yield two methyl radicals for each molecule decomposed. In fact, if two-point adsorption and equilibrium are both attained prior to the decomposition step, the ratio of methyl to ethyl radicals would be quite high, about 9:1. Thus it appears from the data that these assumptions are more correct for alumina than for platinum, a substance which is not known to be a particularly good catalyst for olefin isomerization.

Although allyl iodide was looked for in a few of the runs, none was detected. This may have been due to the strong adherence of the unsaturated allyl radical to the catalyst surface.

Acknowledgment.—Acknowledgment is made to the donors of The Petroleum Research Fund, administered by the American Chemical Society, for support of this research.

THERMOGRAVIMETRIC STUDY OF THE KINETICS OF THE REDUCTION OF CUPRIC OXIDE BY HYDROGEN[1]

BY W. D. BOND

Oak Ridge National Laboratory, Oak Ridge, Tennessee, Operated by Union Carbide Nuclear Company for the U. S. Atomic Energy Commission

Received September 23, 1961

The reaction $CuO(s) + H_2(g) \rightarrow Cu(s) + H_2O(g)$ occurs in three stages: an induction stage, an acceleration or autocatalytic stage terminating at about 35% reduction of the oxide, and a decreasing-rate stage. The rate of reduction in each stage is dependent on the nature and the degree of subdivision of the initial oxide and on the temperature. The same mole fraction is reduced in a given time regardless of the initial mass of oxide. The acceleration and decay stages are very closely approximated by a semi-empirical equation of the Prout–Tompkins type, which is based on the initial reaction occurring on certain active nuclei followed by a rapid growth of these nuclei by a branching-chain mechanism. As a result, the reduction rate is not necessarily proportional to the initial surface area. The reduction rate reaches a maximum and subsequently decreases, as considerable interference occurs among the branching nuclei. Arrhenius plots give an activation energy of 13.5 ± 1.2 kcal. for the reduction. Addition of the reaction product copper has no measurable effect on the reaction. Water vapor in concentrations of 25 mg./l. of hydrogen completely inhibits reaction initiation at 112°. The inhibiting effect decreases rapidly as the temperature is increased and disappears entirely at 190°. Once reduction starts, water vapor has practically no effect.

Many studies of the nature of the reduction of copper oxide by hydrogen have been reported in the literature. All investigators agree that the reduction consists of three stages—induction, autocatalytic or acceleratory, and decay—and that the reactions occur on certain active nuclei. There are, however, several areas of disagreement in the results of these studies. Several workers[2-5] have reported that water vapor markedly affects the beginning of the reduction, although little effect is observed once the reaction has begun. However, Pavlyuchenko and Rubinchik[6] report that water vapor has no measurable effect on the onset of the reaction. Some workers[2,3] have reported that the autocatalysis of the reaction is primarily a result of the solid product, copper, whereas others[6,7] report that copper has no measurable effect and that the autocatalysis is the result chiefly of the crystal structure of the initial oxide. Mathematical expressions for the reduction rate at various per cent of reduction differ widely.[3-5] The reduction has been shown to involve adsorbed hydrogen, with the rate only slightly affected by hydrogen pressure in the 200–700 mm. range.[5-6]

(1) Presented at the 138th National Meeting of the American Chemical Society, New York, N. Y., September 11–16, 1960.

(2) (a) R. N. Pease and H. S. Taylor, *J. Am. Chem. Soc.*, **43**, 2179 (1921); (b) A. T. Larson and F. E. Smith, *ibid.*, **47**, 346 (1925).

(3) Y. Okayama, *J. Soc. Chem. Ind. Japan*, **31**, 300 (1928); *Chem. Abstr.*, **23**, 2873 (1929).

(4) G. I. Chufarov, *et al.*, *Zhur. Fiz. Khim.*, **26**, 31 (1952).

(5) S. Hasegawa, *Proc. Imp. Acad. Tokyo*, **19**, 393 (1943).

(6) M. M. Pavlyuchenko and Ya. S. Rubinchik, *J. Appl. Chem. USSR*, **24**, 751 (1951).

(7) J. S. Lewis, *J. Chem. Soc.*, 820 (1932).

Experimental

Chemicals.—Three types of CuO were used: a wire form of reagent grade CuO obtained from Mallinckrodt Chemical Co., CuO prepared by calcination of $Cu(NO_3)_2 \cdot 3H_2O$, and CuO prepared by calcination of $Cu(OH)_2$ which was obtained by precipitation from a copper nitrate solution with ammonium hydroxide. All chemicals used in the preparations were reagent grade.

Cupric oxide was prepared from the nitrate by weighing 150 g. of $Cu(NO_3)_2 \cdot 3H_2O$ in a 250-ml. evaporating dish, carefully heating on a hot plate until most of the water of hydration had been removed, and then heating in a muffle furnace at 400° for 22 hr. The product was lightly crushed and sieved. About 75% of the material was found to be $<44\ \mu$.

The preparation of CuO from $Cu(OH)_2$ consisted in neutralizing 1 l. of 1 *M* $Cu(NO_3)_2$ with 2 *M* NH_4OH to form the hydroxide, decanting the supernatant liquid, washing the precipitate by decantation with three 500-ml. portions of deionized water, transferring the precipitate to a suction

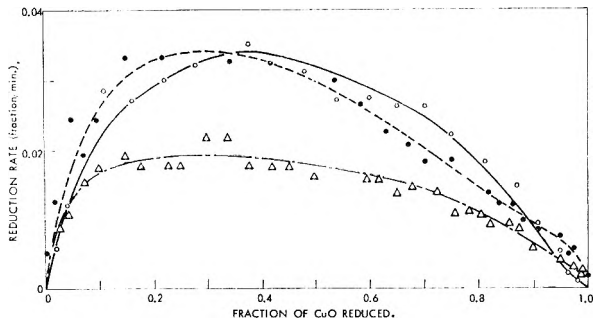

Fig. 1.—Dependence of reduction rate on fraction of CuO (<44 μ particle size) reduced by H_2, 2.0 l./min: ●, temperature = 190°, CuO from calcining of $Cu(OH)_2$, initial surface area 0.43 m.²/g.; ○, temperature = 148°, CuO from calcining of $Cu(NO_3)_2 \cdot 3H_2O$, initial surface 0.49 m.²/g.; △, 148°, commercial grade CuO, initial surface = 0.22 m.²/g.

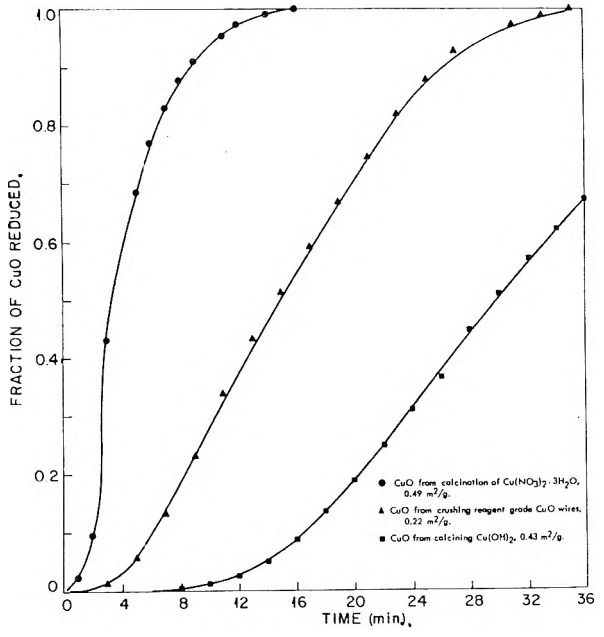

Fig. 2.—Effect of nature of oxide on rate of reduction of CuO by hydrogen. Particle size <44 μ; hydrogen flow rate 2.0 l./min.; temperature 190°.

filter, and air drying for 24 hr. The dried precipitate was calcined in a muffle furnace at 400° for 20 hr., and the product was crushed and sieved.

The wire-form CuO was crushed to <44 μ. Each preparation was dried for 20 hr. at 600° under a stream of dry oxygen flowing at a rate of 1.6 l./hr. before use. The hydrogen, obtained as electrolytic hydrogen from the Southern Oxygen Co., was passed through a platinum–asbestos catalytic recombiner and then through a charcoal trap cooled by liquid nitrogen to remove any traces of oxygen and water. The catalytic recombiner was a commercial model (Baker and Co., Newark, N. J.) with a capacity of 5 ft.³/hr. at 50 p.s.i.

Hydrogen reduction of all three types of oxides gave the theoretical weight loss for reduction to pure Cu. X-Ray diffraction analysis of the initial oxides showed lines for CuO only. Surface areas were determined by nitrogen adsorption.

Apparatus and Procedure.—The apparatus used has been described previously.[8] Basically, it consisted of a reduction chamber and a semiautomatic recording thermogravimetric balance. The reduction chamber was a cylindrical nickel vessel, 2 in. i.d., equipped with a helium seal through which the sample was suspended from the balance. The reduction vessel was heated by a platinum-wound resistance furnace and the temperature was controlled to ±2° by a platinum–rhodium thermocouple connected to a Pyr-o-vane controller and recorder. The recorder was calibrated with a glass thermometer for different temperature settings. The sample was contained in a platinum pail 1 in. in diam. and 1/8 in. deep. The hydrogen was preheated by spiraling the entrance 1/4-in. o.d. nickel tubing into 12 turns around the reaction vessel. The gas flow was measured by calibrated rotameters.

One-gram samples of CuO were weighed in the tared platinum pail on an analytical balance to the nearest 0.2 mg. The pail was then hung on a nichrome wire and lowered into the reduction chamber, and the recording balance was set for automatic control. Dry helium was admitted at a flow rate of 2 l./min. The volume of the reduction chamber and the associated gas lines was about 500 ml. so that the helium was displaced in less than 1 min. if complete mixing is assumed. The inert atmosphere was necessary when the reduction chamber was above room temperature to prevent formation of reducible nickel oxides. The furnace was then turned on and, when the desired temperature had been obtained, an additional 1–2 hr. was allowed for any weight loss due to adsorbed water. No decrease in weight was observed for any of the samples as the temperature was raised from ambient to the reduction temperature.

Hydrogen then was admitted to the reduction chamber, the helium was immediately shut off, and the final regulation was made to a flow rate of 2.0 l./min. This whole operation required about 0.5 min. After reaction had stopped, helium was admitted to the reduction chamber, the hydrogen was shut off, and the sample was allowed to cool to room temperature under an atmosphere of flowing helium. The sample then was removed from the chamber and weighed in air on an analytical balance as a check on the recording balance.

Reduction–Time Curves.—Curves of fraction reduced *vs.* time were typically sigmoid. The same curve was obtained with 1 or 2 g. of oxide when the data were normalized to fraction reduced, which shows that the reduction curve is independent of the mass of the oxide. Self-heating effects would result if too large a sample was used. The reduction curves were reproducible to ±3% when the H_2 flow rate was between 2 and 4 l./min. The reduction rate reached a maximum at 20–40% reduction regardless of the nature of the oxide (Fig. 1).

Effect of Method of Preparing the CuO and its Surface Area.—The oxide produced from calcination of $Cu(NO_3)_2 \cdot 2H_2O$ at 400° was reduced more rapidly than that obtained from calcination of $Cu(OH)_2$ at 400° or from oxidized copper wires crushed to <44 μ (Fig. 2). For example, at 190° the oxide from calcining of $Cu(NO_3)_2 \cdot 3H_2O$ was reduced completely in 16 min., whereas the oxides from calcining of $Cu(OH)_2$ and from oxidizing of copper wires required 98 and 35 min., respectively, for complete reduction. The initial reduction rates for the different oxides were markedly different (Fig. 2).

The reactivity of the oxide is clearly an effect of the nature of the oxide, and probably depends on the crystallite structure within the individual particles, since a wide difference in reactivity is observed between different oxides of the same mesh size classification and approximately the same initial nitrogen-adsorption surface area. This difference also shows that reaction occurs on certain active nuclei; otherwise, the initial rates would be approximately the same. The total surface area is not necessarily related to the number of active nuclei for the adsorption or reaction of specific gases. The nitrogen-adsorption surface area of the copper product is much higher than that of the initial copper oxide (Table I). The precision of the sur-

(8) L. M. Ferris, *Ind. Eng. Chem.*, **51**, 200 (1959).

face area measurements is ±15%, so that within experimental error the product surface areas do not differ greatly.

TABLE I

SURFACE AREA OF INITIAL OXIDES AND REDUCTION PRODUCTS

Redn. temp., °C.	CuO preparation	Size of CuO, μ	Surface area,[a] m.²/g. CuO	Cu prod.
190	Calcination of $Cu(NO_3)_2 \cdot 3H_2O$ at 400°	<44	0.49	1.1
	Calcination of $Cu(OH)_2$ at 400°	<44	.43	1.3
148	Crushing of reagent grade CuO wires and calcining at 600°	<44	.22	0.98
	Calcination of $Cu(NO_3)_2 \cdot 3H_2O$ at 400°	<44	.49	1.3
	Crushing of reagent grade CuO wires (contained some Cu_2O)	149–297	.019	0.82

[a] Determined by nitrogen adsorption.

Effect of Temperature.—Increasing the temperature of the reduction markedly increased the rate of reduction of all oxides regardless of the method of preparation. The time required for complete reaction decreased by factors of 6 to 10, depending on the oxide, as the temperature was raised from 148 to 216°.

Effect of Mesh Size.—The effect of mesh size was investigated only very briefly. A single massive piece of CuO weighing 1.6 g., obtained by calcining $Cu(NO_3)_2 \cdot 3H_2O$, was reduced at 216° and the results were compared with those from the same material crushed at <44 μ. The reduction time was only about twice as great for the single massive piece. There was little difference in the rate until 90% reduction was reached, beyond which point the reaction slowed rapidly for the massive CuO. This probably is a result of the CuO becoming completely covered with metallic copper, after which diffusion of hydrogen to the reaction site or water vapor from the reaction site controlled the rate. Similar results were observed with <44 μ and with 149 to 297 μ oxides from crushed CuO wires.

Effect of Water Vapor.—Saturation of the hydrogen with water vapor at 27° completely prevented initial reaction from taking place at 112°, but this effect for the oxide prepared from calcination of $Cu(NO_3)_2 \cdot 2H_2O$ disappeared at 190°. Once reaction had begun, however, the water vapor had no appreciable effect on the reduction rate. These results indicate that water vapor is adsorbed at active sites in preference to hydrogen at lower temperatures. At 112° the adsorbed water vapor completely masked the active sites from hydrogen. The decrease in the inhibiting effect of water vapor with increasing temperature indicates that hydrogen is more strongly adsorbed than water vapor at higher temperature.

The results are consistent with those of previous workers. Pavlyuchenko and Rubinchik[6] state that water vapor had practically no effect on the reduction, but their conclusions were based on experiments performed at 183°, which was too high a temperature for the inhibiting effect of water to be observed. Since adsorption phenomena are involved, the temperature for observation of the inhibition of the reduction by water vapor will depend upon the nature of the oxide and the partial pressure of water vapor.

Effect of Metallic Copper.—The addition of copper powder, obtained from a previous experiment under the same conditions, to the oxide prior to reduction had no measurable effect, within experimental error, on the reduction rate at 112 or 190°. Copper metal *per se* therefore is not responsible for the autocatalysis of the reaction.

These results are in agreement with the data of some previous workers[6,7] but are contrary to the observations of Pease and Taylor,[2a] who reported a marked increase in the initial reduction rate as a result of added copper granules. This difference is not understood. Acceleration of the reduction could not be produced by stirring metal into the oxide or by placing metal as a layer on the oxide.

Kinetic Equation.—Several theories and mathematical expressions have been developed for explaining the autocatalytic nature of the thermal decomposition of solids.[9] These theories and equations also are applicable to reactions between a gas and a solid when the rate is controlled by chemical reaction and not by adsorption or diffusion of the reactant gas to the solid surface. Since in this study the reaction rate was independent of the flow rate and was only slightly affected by hydrogen pressure in the range 200–700 mm. in a previous study,[5,6] the rate of reduction of CuO by hydrogen is considered to be governed by either chemical reaction or diffusion of water away from the reaction site. Also, since Pavlyuchenko and Rubinchik[6] have shown that the reaction involves adsorbed hydrogen, the reduction may be visualized as taking place in essentially the same way as a thermal decomposition reaction

$$CuO + H_2 \longrightarrow CuO:H_2$$

$$CuO:H_2 \longrightarrow Cu + H_2O$$

where the colon denotes the adsorption boundary layer. If the adsorption step is much faster than the decomposition step, the over-all behavior of the reaction is like that of a thermal decomposition reaction.

Prout and Tompkins[10] have derived an equation of applicability for autocatalytic decomposition reactions which proceed by the growth of chains. When the maximum rate is observed at 50% decomposition, their equation is

$$dx/dt = kx(1 - x) \qquad (1)$$

where

dx/dt = rate of reaction
x = fraction decomposed

(9) W. E. Garner, "The Chemistry of the Solid State," Butterworth, London, 1955.

(10) E. G. Prout and F. C. Tompkins, *Trans. Faraday Soc.*, **40**, 488 (1954).

$1 - x$ = fraction remaining
k = specific rate constant

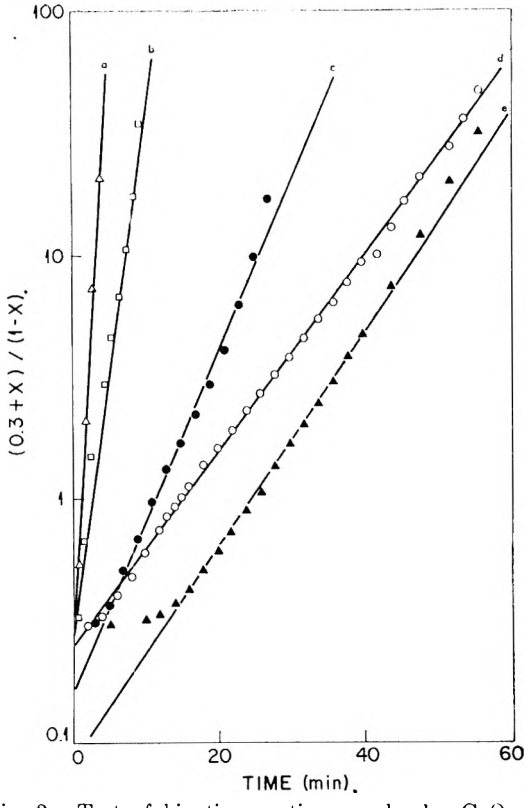

Fig. 3.—Test of kinetic equation. a, b, d: CuO prepared by calcining $Cu(NO_3)_2 \cdot 3H_2O$, <44 μ size; respective reduction temperatures, 216, 190, and 148°; c: commercial grade CuO, <44 μ size; reduction temperature 190°; e: CuO prepared by calcining $Cu(OH)_2$; <44 μ size; reduction temperature 190°.

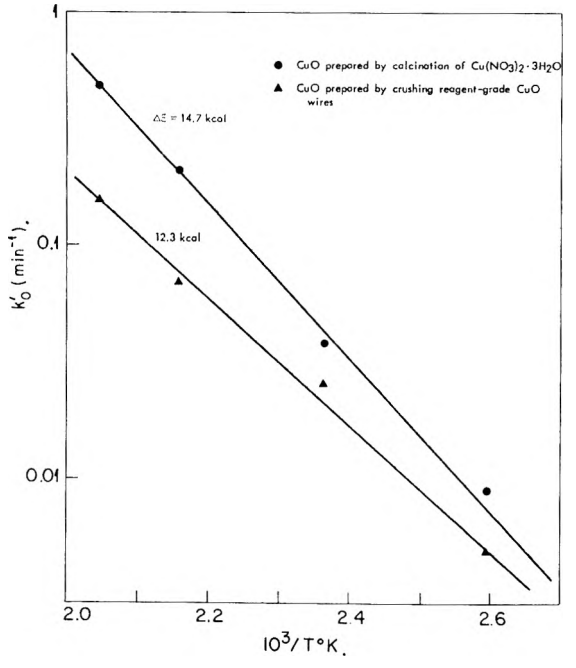

Fig. 4.—Temperature dependence of rate constants for reduction of CuO by H_2.

Integration and rearrangement of the equation leads to

$$\log (x/(1 - x)) = k_1 t + C \qquad (2)$$

where $C = -kt_{max}$, and t_{max} = time at which the rate is a maximum.

In general, two constants are required, one for the period of increasing rate and one for the period of decreasing rate. This is a result of the asymmetry of the x–t curves. However, there is little difference in the numerical values of the constants. Prout and Tompkins attributed the asymmetry to a cessation of mechanical disintegration of the original crystals at the maximum rate of decomposition and were able to observe this circumstance microscopically.

When the maximum rate occurs at a value different from $x = 0.5$, it is necessary to integrate Prout and Tompkins' original equation with different boundary conditions. When this is done eq. 3 results.

$$\frac{dx}{dt} = \frac{k_1}{2x_i}(1 - 2x_i + x)(1 - x) \qquad (3)$$

where x, $1-x$, k are defined as in eq. 1 and x_i = fraction reacted at dx/dt = max. Equation 3 is valid for a maximum rate occurring at values of $0 < x < 0.5$. It is obvious that the equations have no physical reality above $x = 0.5$ since dx/dt becomes negative for the onset of the reaction.

Integration of eq. 3 gives

$$\log \frac{1 - 2x_i + x}{1 - x} = \frac{1 - x_i}{x_i}(k_1 t + C) \qquad (4)$$

Substituting $x_i = 0.35$, which is a good average of nine reductions, and rearranging gives

$$\log \frac{0.3 + x}{1 - x} = k_0' t + c_0' \qquad (5)$$

where

$$k_0' = 1.86 k_1$$

$$c_0' = 1.86 C$$

An average value of x_i was used rather than individual values because of the flatness of the dx/dt *vs.* x curves near the maxima.

Prout and Tompkins explain adherence to eq. 2 by the formation of certain active nuclei which grow by a branched-chain mechanism as a result of the reaction process. The reaction rate reaches a maximum when the rate of growth of branches is equal to their rate of termination by interference with each other, and the rate will subsequently decrease as interference among the growing chains steadily increases.

Plots of the data according to eq. 5 show that this equation closely approximates the reduction process (Fig. 3). The equation is obeyed from 3 to 90% reduction. Only one constant is used to describe the whole reduction rather than one for acceleration and one for decay. A slightly better fit of the data would be obtained if two constants were used, but in this case little would be added to the

interpretation of the over-all reduction process. One constant sufficiently approximates the data with only a slight amount of sinusoidal curvature about the straight line drawn through the experimental points. The fit of the data to eq. 5 is remarkably good, considering the fact that an average value of x_i was used over a fraction range from 0.2 to 0.4. This relative insensitivity to the x_i value is due to the fact the maximum rate does not peak sharply (Fig. 1).

Deviations from eq. 3 would be expected at the very beginning and at the end of the reaction since any small error in measurement of the fractions reduced will introduce large errors in the value of $(0.3 + x)/(1 - x)$. However, they will not be so great as the variations shown toward the end of the reduction. The equation is not obeyed beyond 90% reduction. It is likely that the remaining CuO is enclosed completely in the copper particles with little chance of growth of existing nuclei and that the reaction rate is controlled by diffusion.

Activation Energy.—Arrhenius plots gave an apparent activation energy of 14.7 kcal. for the oxide from calcination of copper nitrate and 12.3 kcal. for the oxide from oxidized copper wires after crushing (Fig. 4). The activation energy for the reduction of CuO from calcining of $Cu(OH)_2$ was not determined since only one temperature was used. Within the accuracy of the plots (±20%), the activation energy is considered to be the same for the two oxides used.

Acknowledgments.—The author is indebted to the following individuals for assistance in carrying out this research project: J. F. Talley for technical assistance; W. R. Laing for surface area determinations; R. L. Sherman for X-ray diffraction analyses; and L. M. Ferris and C. E. Schilling for stimulating discussions.

POLYFUNCTIONAL ADDITION POLYMERIZATION (THEORY AND EXPERIMENT)

BY NORMAN T. NOTLEY[1]

Photo Products Department, E. I. du Pont de Nemours & Company, Parlin, N. J.

Received November 10, 1961

The photopolymerization of a polyfunctional monomer (triethylene glycol diacrylate) was studied quantitatively with particular emphasis on the extent to which the reaction can go to completion. Dilution with high molecular weight material (cellulose acetate) sharply reduced the limiting degree of conversion which could be restored by partial replacement with inert solvent (triethylene glycol dipropionate). The limiting degree of conversion increased with the concentration of photoinitiator, $\Phi = c'$ [Initiator]$^{0.21} = k'(R_i)^{0.21}$ and with the intensity of photo exposure (I_0). $\Phi = c'(I_0)^{0.24} = k''(R_i)^{0.24}$. From a theoretical model in which propagation occurs only in virgin pockets and the passage of the growing chain by growth diffusion excludes further reaction in its environs, a theoretical relationship was derived $\Phi = c(R_i)^{0.25}$. The experimental dependence of polymerization rate upon the concentration of initiator and upon the intensity of photo exposure at high conversions was found to be consistent with the theoretical postulates.

Introduction

Investigations of free-radical polymerization kinetics usually are made at low conversion or in dilute solution. This allows use of dilatometry or refractive index measurement for following the reaction and simplifies interpretation of the results. These methods of measurement require, however, that the polymerizing system have sufficient fluidity to conform to the shape of its containing vessel. Where the polymerizing system is in whole or in part of polyfunctional monomer, then the products pull away from the container during the reaction and the standard kinetic methods are not applicable.

The heat output is a convenient measure of reaction, especially where conditions approximate to adiabatic. Significant results are possible providing the reaction is photoinitiated and the temperature does not rise sufficiently for thermal initiation to make an appreciable contribution. A hundredfold excess of photo over thermal polymerization rate was achieved with photosensitized triethyleneglycol diacrylate. With α-methoxy-α-phenyl-acetophenone (benzoin methyl ether) as photoinitiator reaction temperatures up to 80° were possible without the complication of significant thermal initiation.

The temperature rise during polymerization of pure triethylene glycol diacrylate could be as high as 150° if there were no heat losses from the system. In these conditions there would be charring and loss of light transmission and the temperature would unduly favor thermal initiation. These difficulties occur if a thick sample is used. With a thin sample, heat loss to the container prevents excessive temperature rise, but calculation of heat output of the reaction is impractical.

It was found highly desirable to give the monomer dimensional stability by making it the plasticizer of a non-interfering polymer, cellulose acetate. This technique eliminated the need for a containing vessel for the monomer, thus simplifying the heat-loss corrections. Part of the heat output of polymerization was now shared with the bulking polymer and some lost by radiation to the outside. The first loss was calculated readily and the latter obtained readily by experiment. There was some diminution of actinic intensity through these samples. However, it was not very serious with a thickness of one millimeter, and the effect was minimized by keeping the sample thickness within close tolerance.

(1) Metal Box Co., Kendal Avenue, London, W.3, England.

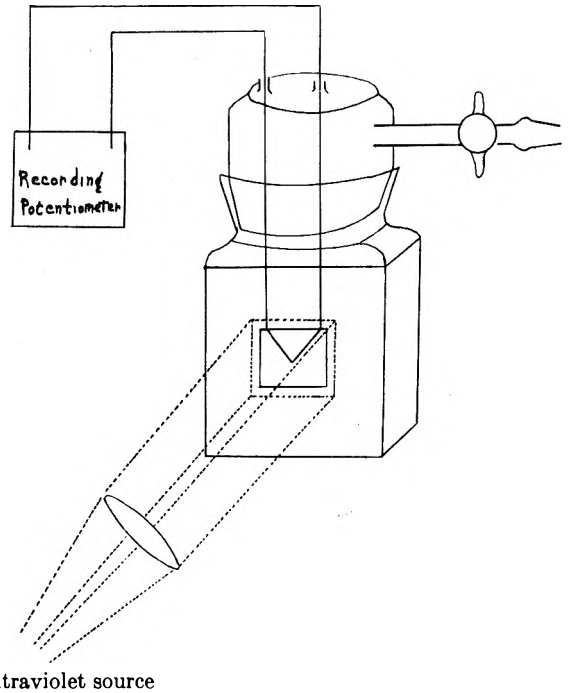

Fig. 1.—Photopolymerization apparatus.

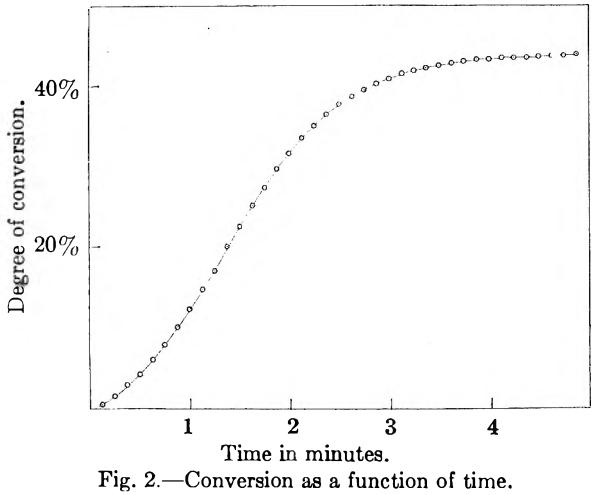

Fig. 2.—Conversion as a function of time.

Experimental

Temperature of the monomer was recorded continuously during controlled ultraviolet exposure. A cooling curve obtained under the same experimental conditions allowed a heat-loss correction and calculation of the temperatures which would have been observed under adiabatic conditions (T_{corr}). Then the degree of conversion after t sec. was given by the integral

$$\text{D.C.} = \int_0^t \frac{1}{HM} \cdot \frac{d(T_{corr})}{dt} \cdot S_T \cdot dt \qquad (1)$$

where S_T = heat capacity of polymerization system at $T°$
H = molar heat of polymerization
M = moles of monomer per gram of polymerization system

Materials

Triethyleneglycol diacrylate was prepared by an esterification reaction in benzene at reflux. The polyfunctional monomer was purified by a series of aqueous washes and filtration through a 40-cm. column of alumina before removal of the solvent by evaporation. Cellulose acetate (Textile Fibres Department, E. I. du Pont de Nemours & Co.) was a film grade polymer from "cotton linters" cellulose and required no purification. Its 55% combined acetic acid indicated 1.8 acetate groups per ring. Benzoin methyl ether[2] was prepared by passing hydrogen chloride into a solution of benzoin in methanol at 50° and recrystallizing the product from ethanol.

Cellulose acetate (60 g.), triethyleneglycol diacrylate (40 g.), and benzoin methyl ether (0.4 g.) were dissolved in acetone (200 cc.)/ethyl alcohol (20 cc.). After the solution was degassed and spread between dams which confined an area of 1300 cm.², slow evaporation gave a clear bubble-free sheet 0.6 mm. thick.

An iron–constantan thermocouple was made by butt-joining 0.2 mm. wires and enclosing the junction centrally between two pieces of the monomer each 2 cm. by 2.5 cm. The sandwich was pressed between polished platens at 150° to make a sample for a photopolymerization experiment.

Heat Capacity.—The heat capacity (S_T) of the polymerization system was measured in a differential calorimeter. The sample was sealed in a small brass calorimeter which was centrally located inside a second brass cylinder which was evenly heated, with the temperature maintained exactly 5° above that of the inner calorimeter. A temperature–time curve was obtained under these highly reproducible conditions of heating and compared with similar heating curves for the empty calorimeter and for the same calorimeter filled with powdered sapphire. The heat capacity then could be calculated as a continuous function of temperature.

The composition, cellulose acetate (40%)/triethyleneglycol diacrylate (60%) has a heat capacity of 0.46 cal. per gram and cellulose acetate (60%)/triethyleneglycol diacrylate (40%) of 0.40 cal. per gram. For both compositions the measurement is independent of temperature in the measured range of 30 to 100°. Heat capacity for a polymer/plasticizer system is expected to be additive,[3] so heat capacities for these polymerization systems can be summarized as: S = 0.30(cellulose acetate) + 0.56(triethylene glycol diacrylate) cal./g. Since this value is independent of temperature, and is expected to be essentially independent of the extent of polymerization of the monomer,[4] it does not change during the course of photo exposure.

So $$\text{D.C.} = (S/H\,M)\,\Delta T_{corr} \qquad (2)$$

Heat of Polymerization. The heat of polymerization of methyl acrylate has been determined[4] as $-\Delta H$ = 20.2 ± 1.0 kcal. per mole. We rely on evidence that the molar heat of polymerization of an ester of an ethylenically unsaturated acid is essentially independent of the saturated esterifying group.[5] So this value of ΔH is applied to the present polymerization of acrylate groups remembering that the full molar heat of polymerization for triethylene glycol diacrylate becomes 2 × 20.2 kcal. per mole.

Photopolymerization Procedure.—The ultraviolet light source, a 100 watt mercury vapor arc lamp, was supplied by a stabilized power circuit. Mounted on an optical bench with a quartz lens system, it gave a sharply collimated beam. An iris diaphragm at a focal point of the optical system controlled the intensity, independently of wave length distribution. Intensity was measured, in arbitrary units, with a "photometer probe" in the plane of the polymerizable system. The sample was supported in a sealed cell (Fig. 1) by the iron/constantan leads of its thermocouple, connected to a high vacuum system, and sealed off at a pressure lower than 10^{-4} mm. The sample was irradiated through an optically flat side of the cell and its temperature was followed continuously with a recording potentiometer.

(2) E. Fischer, *Ber.*, **26**, 2412 (1893).

(3) S. M. Skuratov and M. S. Shkitov, *Compt. rend. acad. sci. URSS*, **53**, 627 (1946).

(4) A. G. Evans and E. Tyrrall, *J. Polymer Sci.*, **2**, 387 (1947).

(5) L. K. J. Tong and W. O. Kenyon, *J. Am. Chem. Soc.*, **68**, 1355 (1946).

The apparatus was calibrated by recording a cooling curve on a sample which had been polymerized already. The thermocouple wires were used to heat the sample initially to a temperature just above that which was encountered in photopolymerization. The cooling curve which was obtained under standard operating conditions of high vacuum and photo exposure was the basis for calculating values of T_{corr}, temperatures which would have been recorded in a polymerization experiment had the reaction conditions been strictly adiabatic.

Results

Degree of Conversion.—A typical polymerization curve is illustrated in Fig. 2. The degree of conversion does not approach unity even with very long polymerization times. This behavior had been observed qualitatively by Melville,[6] but now the limiting value is shown to vary widely with monomer concentration and with rate of initiation. It also has been observed that post-cures of even rather high exposure intensity give only slight increase in the conversion. This is particularly interesting when compared with the theoretical treatment developed below, in which the immobilization of unsaturated groups is primarily dependent on the coil size of growth paths in the polymerized network, consequently depending on the polymerization history as well as the subsequent temperature or intensity of irradiation.

The dependence of the limiting degree of conversion upon the ratio of monomer to filler was examined throughout the range experimentally accessible and is illustrated in Fig. 3. The range 50 to 70% filler in which very rapid change of limiting degree of conversion occurs is also the region in which a very sharp change in the macroscopic flow property occurs. At the mid-point of this range, a composition 60% filler under a stress of 100 p.s.i. at 50° flows 1.5% per hour; 70% filler on the one hand gives a rather rigid structure while 50% filler on the other is only just sufficient to prevent a visible rate of flow under no loading.

It was somewhat surprising that degrees of conversion over 80% should be recorded since 50% of all unsaturation is available only as potential crosslinks. These high values suggested that the estimate of heat of polymerization might err on the low side. This possibility was probed by looking for ways of further increasing the degree of conversion. The present observations could not be extended to lower concentrations of filler since such compositions lacked dimensional stability.

However it was observed that the limiting degree of conversion could be raised by diluting the monomer with triethylene glycol dipropionate, the filler concentration being unchanged (67% cellulose acetate). This lead was pursued in order to see whether the anomaly of conversions higher than unity would occur. In Table I it appears that dilution of the monomer gives a rapid increase in limiting conversion but only until a plateau of 65% limiting conversion is reached. At lower filler concentrations this boosting effect may be entirely absent, *e.g.*, with 60% filler the limit apparently is unchanged at 73% even through very heavy replacement by non-polymerizable plasticizer.

Effect of Initiation Rate.—The relation between the limiting degree of conversion (Φ) and the initiation rate was examined through a range of exposure intensities and as a function of photoinitiator concentration.

The light intensity was controlled with the iris diaphragm/photometer, and fivefold range of intensity was possible without reducing the rate of photo reaction to the point where the thermal

(6) H. W. Melville, *Proc. Roy. Soc.* (London), **A237**, 149 (1956).

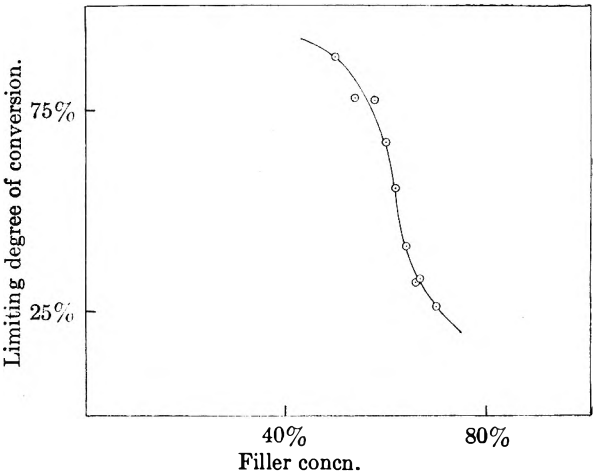

Figure 3.

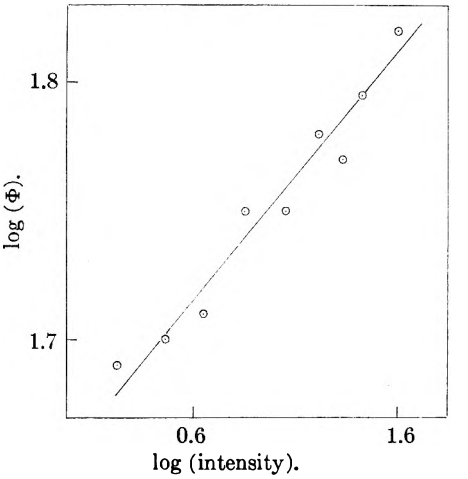

Fig. 4.—Degree of conversion as a function of intensity.

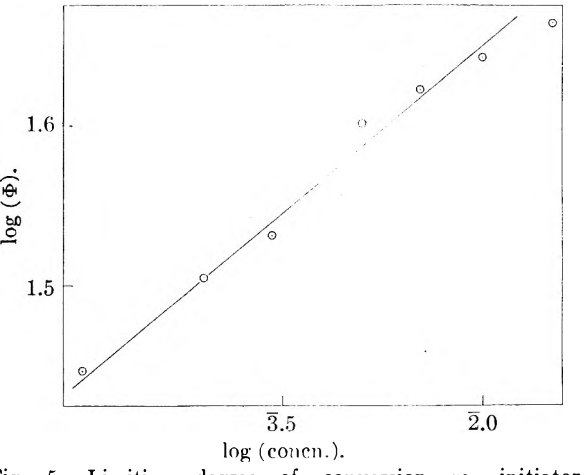

Fig. 5.—Limiting degree of conversion *vs.* initiator concentration.

TABLE I

Monomer in plasticizer mixture, %	100	83	75	67	50	40	35	30	25	20	10	Plateau value (root mean square)
Degree of conversion, % 67% filler	34	45	..	54	65	63	66	70	61	66	61	65 ± 1
Degree of conversion, % 60% filler	68	..	65	..	80	73	70	72	84	68	..	73 ± 2

(dark) reaction made a significant contribution. The limiting degree of conversion decreased from 66 to 50%. The data are represented logarithmically in Fig. 4, which suggests a relation between limiting degree of conversion (Φ) and exposure intensity (I_0): $\Phi = k(I_0)^{0.24} = k(R_i)^{0.24}$, where R_i is the rate of initiation.

In the alternative experimental approach the photoinitiator (benzoin methyl ether) concentration was varied through a fifteenfold range from 1.5 to 0.1 grams per hundred grams of monomer. It was established that the contribution of direct photoinitiation under the conditions of exposure described was less than 3% even at the lowest photoinitiator concentration. The concentration of inert polymer with which dimensional stability of sample was secured was exactly the same in each polymerization (although not the same as in the exposure intensity studies, above). The limiting degree of conversion decreased from 46% to 28%. The representation of Fig. 5 suggests $\Phi = k[\text{Initiator}]^{0.21} = k(R_i)^{0.21}$.

Theory.—The kinetics of free radical polymerization have been most rigorously derived for the bifunctional addition reaction in dilute solution, or in bulk at low conversions. Anomalous results are found in some solutions at higher concentrations and in most bulk monomers at higher conversions.[7] Autoacceleration or the "gel effect" has been observed at conversions of less than 1% when the polymer is not soluble in the polymerizing system, *e.g.*, methyl methacrylate polymerizing from a solution in heptane or cyclohexane.[8] It is interpreted as a decreasing termination rate constant, since decreasing diffusional mobility affects polymeric diffusion, particularly polymer–polymer contacts, before it restricts the movement of monomer.

If this gelation occurs early in the reaction, as it does in a polyfunctional polymerization, then the reaction slows up and stops before complete conversion of the monomer. A special case of incomplete polymerization has been considered by Tobolsky.[9] The catalyzed polymerization of isoprene has a limiting degree of conversion which can be quantitatively explained as exhaustion of catalyst. However, if a photoinitiated polymerization were controlled by catalyst exhaustion, higher intensities of exposure would lower the limiting degree of conversion. The present polymerization clearly does not follow this course.

To explain the incomplete polymerization of polyfunctional monomers, one might postulate a continuously declining propagation rate constant. This does not lead to an explanation of the wide variations of conversion with catalyst concentration and it takes insufficient account of the obvious immobility of 50% of the monomer units which are immobilized by the polymerization of their monomer partners and yet to some extent still polymerize.

It is proposed here that all translational motion, whether of monomer or of polymer, is restricted from quite early in the reaction. Polymerization still can proceed, monomer units being gathered when the active end of a live chain progresses on a random walk by "growth diffusion." The growing chain depletes its immediate environs to such an extent that no other chain can grow through its path. The polymerizing system is visualized as a fine mixture of "forbidden pockets" and "virgin pockets." In the "forbidden pockets" there are reacted functional groups and unreacted groups together, but no further reaction is possible. Further polymerization occurs only in the virgin pockets. So conditions at the site of polymerization are unchanging, except for a moderate temperature rise, and for most of the reaction, excluding only the early stages, the rate constants of propagation and of termination are unchanging. From this postulate of prohibited translational motion, relations between the limiting degree of conversion and the process conditions can be developed.

The concentration of functional units is represented as unity and the extent of reaction, that is the ratio of reacted to total units, is X. The extent of reaction reaches its limiting value (Φ) when the growth paths are just touching, when all functional groups are embraced by the forbidden pockets. So in forbidden pockets the ratio of total functional groups to reacted functional groups is $1/\Phi$. When the extent of reaction is X, there are X reacted groups in forbidden pockets and a total of X/Φ functional groups therein. So the chance of a free radical being in a virgin pocket, of being in a growth situation, is $(1 - X/\Phi)$. This is the effective monomer concentration, and the rate of propagation is

$$R_p = k_p[\text{M}\cdot]\frac{\Phi - X}{\Phi} \qquad (3)$$

where $[\text{M}\cdot]$ is the total concentration of free radicals and k_p the propagation rate constant.

The path of the growing polymer chain should approximate to a random walk in three dimensions. This reaction path has no separate existence in the final polymer, being subsequently attached at many points to the three dimensional network. The (root mean square) displacement length or end-to-end distance of a random walk has been calculated[10] as

$$\sqrt{\overline{r^2}} = cn^{1/2}$$

where n is the number of repeating units, here the number of reacted functional groups, and c is a measure of their individual length. The total

(7) G. V. Schulz and G. Harborth, *Makromol. Chem.*, **1**, 106 (1947).
(8) R. G. W. Norrish and R. R. Smith, *Nature*, **150**, 336 (1942).
(9) A. V. Tobolsky, *J. Am. Chem. Soc.*, **80**, 5927 (1958).
(10) Lord Rayleigh, *Phil. Mag.*, **37**, 321 (1919); W. Kuhn, *Kolloid Z.*, **76**, 258 (1936).

number of functional groups, reacted and trapped together, is equal to the volume of this gelled region or proportional to the cube of any linear dimension. The limiting degree of conversion may be written as the ratio of reacted to total functional groups; so

$$\Phi = \text{const.}\ (n/c^3n^{3/2}) = c(n)^{-1/2}$$

The length of the polymer chain is determined by the ratio of propagation to initiation rate so

$$\Phi = c\sqrt{(R_i/R_p)} \qquad (4)$$

While the average chain length cannot be obtained rigorously, an estimate may be obtained by introducing the median value of R_i/R_p, the value at half-reaction.

Then $X = \Phi/2$ and from (3), $R_p = {}^1/_2k_p[M\cdot]$. The ultimate loss of free radicals is by growth collisions which, like diffusional collision, involve two free radicals, so

$$R_t = k_t[M\cdot]^2$$

and

$$R_p = {}^1/_2k_p(R_t/k_t)^{1/2}, \text{ at half-reaction}$$

At some point in the reaction the rate of termination approaches closely the rate of initiation. If this stationary condition prevails through most of the polymerization, then the limiting degree of conversion

$$\Phi = c(R_i)^{0.25}$$

where $c = \sqrt{2}c'k_t^{1/4}/k_p^{1/2}$. This relation agrees very closely with the experiments which have been discussed, both for varying concentration and for varying intensity of photo exposure.

Now it is possible to examine the rate of polymerization in greater detail. A conventional plot of polymerization rate (R_p) against monomer concentration ($1 - X$) would suggest that either the propagation rate constant or the free radical concentration declines substantially during the reaction. However eq. 3 above brings attention to the relation between R_p and $(\Phi - X)/\Phi$ which one might call the "available monomer."

A disturbing feature of the polymerization in Fig. 2 is the region of retardation which persists until nearly 20% of the ethylenic groups have reacted. The monomer contained 0.1% of a phenolic inhibitor which had been necessary in the preparation of the triethylene glycol diacrylate from acrylic acid, and which was helpful in preparing the acrylate/cellulose acetate compositions reproducibly. The thermal inhibitor may be acting as a retarder in the photopolymerization. On the other hand part of this apparent retardation might be otherwise explained as a pre-stationary state in which the rate of radical initiation exceeds the termination rate.

In view of this complication, the data relating to higher levels of conversion are more significant. In Fig. 6 rates of polymerization derived from Fig. 2 are plotted against available monomer. The wide range of linearity in the relationship shows a stationary value for $k_p[M\cdot]$. Remembering that conditions are not isothermal all through the reaction, the constancy of k_p is not immediately evident. In fact non-linearity at rather high available monomer concentrations (Fig. 6) may be explained as a lower temperature and a lower value of k_p. However, toward the end of reaction the slower heat output is closely balanced by the heat losses, giving a more constant temperature and propagation rate constant (k_p).

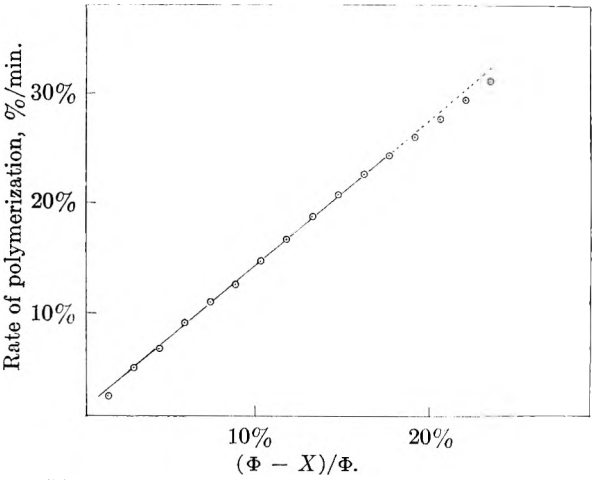

Fig. 6.—Rate *vs.* effective monomer concentration.

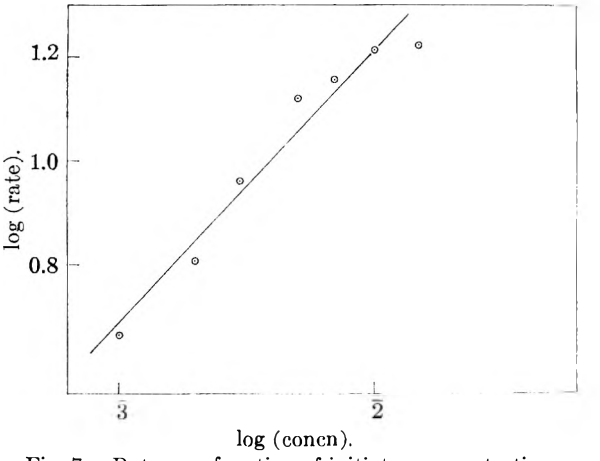

Fig. 7.—Rate as a function of initiator concentration.

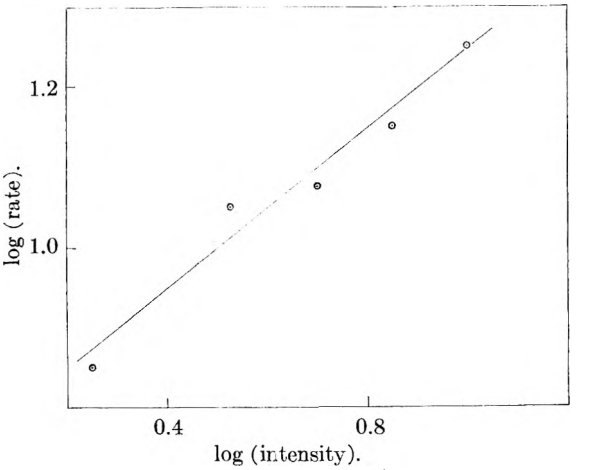

Fig. 8.—Rate as a function of intensity.

We may use the measurements of polymerization rate to check the stationary state postulate. Taking a generalized form of the termination rate

$$R_t = k_t[M\cdot]^a$$

and the stationary state relation

$$R_t = R_i = k_i[\text{Initiator}]I_0$$

where I_0 is the intensity of actinic radiation. We have $k_t[M\cdot]^a = k_i[\text{Initiator}]I_0$ and a plot of log $\{dR_p/d(\phi - X)/\Phi)\}$ against logarithm of the photoinitiator concentration has a gradient $1/a$.

With benzoin methyl ether as photoinitiator, the data are shown in Fig. 7 where the gradient is 0.52 and

$$R_t = k_t[M\cdot]^{1.92}$$

This experimental relation also has been explored by changing the intensity of photo exposure. The logarithmic plot of Fig. 8 suggests $1/a = 0.49$, or

$$R_t = k_t[M\cdot]^{2.03}$$

This demonstrates a general consistency among the quantitative aspects of the postulated mechanism. The broad assumption of a heterogeneous polymerization system in which most of the propagation reaction occurs in virgin pockets has yielded a relation between the limiting degree of conversion and the initiator concentration or the intensity of photo exposure. This is in close agreement with the experimental work with a polyfunctional monomer.

Acknowledgment.—The author wishes to acknowledge helpful conversations with many colleagues in the Photo Products Department of E. I. du Pont de Nemours Co., and especially with Mr. W. R. Saner and Dr. D. R. White.

THE KINETICS OF EXCHANGE OF COPPER(II) BETWEEN ETHYLENEDIAMINETETRAACETIC ACID AND ERIOCHROME BLUE BLACK R

BY DONALD W. ROGERS, DAVID A. AIKENS, AND CHARLES N. REILLEY

Department of Chemistry, University of North Carolina, Chapel Hill, North Carolina

Received November 13, 1961

The exchange of Cu(II) between EDTA and Eriochrome Blue Black R, 1-(2-hydroxy-1-naphthylazo)-2-naphthol-4-sulfonic acid, a typical *o,o'*-dihydroxyazo compound, occurs by acid-catalyzed dissociation of the chelates below pH 5 and by second-order displacement reactions above pH 5. Bonding of the attacking ligand to the Cu chelate followed by competition between the two ligands is postulated for the second-order reactions. EDTA, in order to displace Erio R from Cu effectively, must possess at least one proton, which weakens the phenolic Erio R–Cu bond in an S_E2 step. The rate of attack of Erio R on Cu-EDTA depends on the fraction of the Erio R having one unprotonated phenolic group, suggesting an S_N2 reaction in which the activated complex involves one chelate ring with the attacking ligand. The formation of Cu–OH–EDTA enhances the rate of this reaction since the Cu–Erio R product is stabilized more by mixed hydroxide complex formation than is Cu–EDTA. Effective second-order rate constants for the combination of Cu(II) with Erio R and with EDTA at pH 3.3 calculated from the dissociation rates of the Cu chelates are of the order of $10^6\ M^{-1}$ sec.$^{-1}$ for both ligands.

Introduction

The importance of ethylenediaminetetraacetic acid (EDTA) as a chelating agent has led naturally to study of the kinetic behavior of its metal chelates. The bulk of this work, which has been concerned with the exchange of aquated metal ions with metal chelates, has been reviewed by Margerum.[1] The interesting related problem of the exchange of a metal ion between two multidentate ligands has, as yet, received little attention for ligands of the aminopolycarboxylate type, the work of Bosnich, Dwyer, and Sargeson on the exchange of metal ions between the *d* and *l* isomers of 1,2-propylenediaminetetraacetic acid being the only example.[2]

The exchange of a metal between EDTA and a second multidentate ligand of contrasting structure is of interest since it allows speculation on the relation between the observed rates and the structures of the entering and leaving ligands. Eriochrome Blue Black R, 1-(2-hydroxy-1-naphthylazo)-2-naphthol-4-sulfonic acid (Erio R), was chosen as the second ligand as representative of the *o,o'*-dihydroxyazo type of ligand, the Cu chelates of which are of appropriate stability and of well defined structure.

(1) D. W. Margerum, *J. Phys. Chem.*, **63**, 336 (1959).

(2) B. Bosnich, F. P. Dwyer, and A. M. Sargeson, *Nature*, **186**, 966 (1960).

Experimental

Reagents.—Solutions of EDTA were standardized against copper metal. Erio R (Color Index No. 202, supplied by American Cyanamid Company, New York, N. Y.) was freed of metallic impurities by three precipitations from aqueous solution by the addition of hydrochloric acid. The precipitated dye was dried at 60° under vacuum. The purified dye contained less than 2% metal impurity transferable to EDTA, as judged from the increase in absorbance at 635 mμ of a dye solution at pH 9.3 on addition of a 100-fold excess of EDTA. Solutions of Erio R were prepared daily and standardized against copper by photometric titration. Stock solutions of copper–Erio R, about $2 \times 10^{-4}\ M$, were prepared in 0.001 *M* acetate buffer, pH 5, and used within 8 hr. to avoid deterioration. Stock EDTA solutions were prepared and converted to Cu–EDTA by addition of the appropriate amount of Cu(II). In both Cu–EDTA and Cu–Erio R, a 1% excess of the ligand was present to prevent interference by free Cu(II). Demineralized water was used in all solutions.

All kinetic and equilibrium measurements were made at $I = 0.1$, maintained with sodium nitrate. Chloroacetate, acetate, phosphate, carbonate, and borate buffers were used at 0.01 *M* concentration, giving pH control during the course of a reaction to within 0.02 pH unit, the limit of detection. A properly calibrated Leeds and Northrup Model 7664 pH meter equipped with a Leeds and Northrup STD. 1199-30 glass electrode was used for all pH determinations. Because of the sensitivity of Erio R and Cu–Erio R solutions to slow aggregation at low pH in the presence of electrolytes, and to oxidation of the dye at high pH, the buffer and sodium nitrate were incorporated in the EDTA and Cu–EDTA solutions.

Procedure. Rate Data.—All spectrophotometric measure-

ments were made with a Cary Model 14 recording spectrophotometer with the cell compartment thermostated at 25.0 ± 0.2°. Rate constants were obtained from the limiting rate of change of absorbance at 545 mμ extrapolated to zero time. The reaction was initiated by mixing the reactants directly in a stoppered spectrophotometer cell, permitting the absorbance to be monitored within 10 sec. of the start of the reaction. In a typical experiment 2.00 ml. of 2.0×10^{-5} M Cu–EDTA (or EDTA) was placed in the cell and 1.00 ml. of 3.00×10^{-5} M Erio R (or Cu–Erio R) was blown from a calibrated pipet into the cell, which was capped and inverted several times. The concentration of Cu–EDTA (or EDTA) solution was varied from about 1.0×10^{-5} M when the reaction rate constant was of the order of 10^2 M^{-1} sec.$^{-1}$ to about 1.0×10^{-3} M when the rate constant was of the order of 1 M^{-1} sec.$^{-1}$. The Cu–Erio R (or Erio R) concentration was of the order of 1×10^{-5} M.

The rate of reaction is related to the rate of change of absorbance by the expression

$$\frac{d(Z)}{dt} = \frac{1}{(a_Z - a_{CuZ})b} \frac{dA}{dt}$$

where dA/dt is the rate of change of absorbance extrapolated to zero time, a_Z and a_{CuZ} are the absorptivities of Erio R and Cu–Erio R, respectively, $d(Z)/dt$ is the rate of appearance (or disappearance) of Erio R at zero time, and b is the cell length. The contribution of Cu–EDTA to the absorbance change can be neglected as its absorptivity is less than that of the Erio R species by a factor of at least a hundred.

The reproducibility of the rate data from day to day was of the order of 30% in spite of precautions to standardize the experimental techniques. This variation may be caused by irreproducibility in the mixing technique and by variations in the Erio R and Cu–Erio R solutions, such as undetected aggregation. In addition, the inherent difficulty in determining the slope of the absorbance *vs.* time plot is undoubtedly a factor. The problem of reproducibility was accentuated below pH 5 where the reaction rate was independent of the concentration of the attacking ligand. Above pH 5, the second order of the reaction allowed ready adjustment of the reaction rate to a convenient value.

Equilibrium Data.—The acid dissociation constants of Erio R were determined spectrophotometrically as described by Hildebrand and Reilley[3] and the formation constant of the hydroxide derivative of Cu–EDTA spectrophotometrically as described by Bennett and Schmidt.[4] The effective equilibrium constant for the exchange reaction was determined from the absorbance of mixtures containing Erio R and Cu–Erio R in approximately equal concentrations and at least a fivefold excess of both EDTA and Cu–EDTA. The absolute stability constant of Cu–Erio R was estimated from spectral measurement of the dissociation of the chelate in acid solution containing a tenfold excess of Cu(II) as described by Rogers.[5]

Results

Equilibrium data for the exchange reaction are presented in terms of effective constants based on total concentrations of ligand and chelate species without regard to such factors as chelate derivative formation or the degree of protonation of ligands. Such constants are useful as the numerical magnitudes reflect directly the composite effects of all the competing equilibria involved. Effective exchange constants are readily derived from the absolute stability constants of the chelates by consideration of all the competitive equilibria.

Equilibrium Data.—The successive pK_a's of Erio R are 1, 7.3, and 13.6. The first value, that for the sulfonic acid proton, is somewhat uncertain because of the small spectral difference between the acid and base forms. The latter values, for the phenolic protons, are much more reliable and are in good agreement with those of previous workers.[3,6]

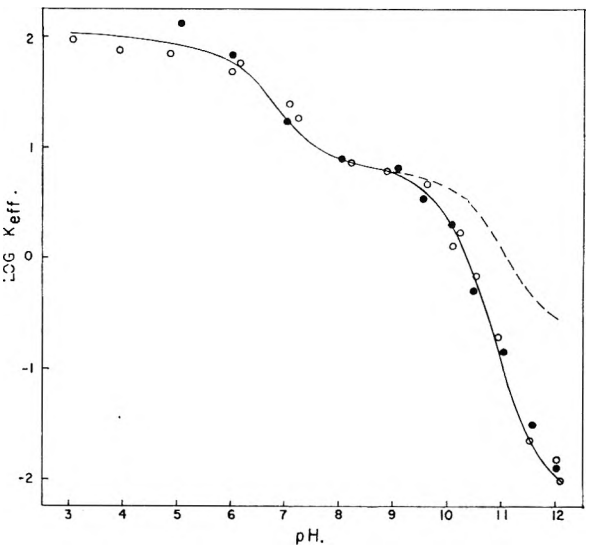

Fig. 1.—Effective equilibrium constant for the exchange reaction CuZ + Y → CuY + Z as a function of pH: solid line, calculated from formation constants of the chelates, acid–base constants of the ligands, and formation constants of mixed ligand chelates with hydroxide; dashed line, as above, except formation of Cu–OH–Erio R neglected; filled circles, ratio k_f/k_r; open circles, measured values of k_{eff}.

The effective equilibrium constant, K_{eff}, for the exchange reaction (1) where Y is EDTA and Z is Erio

$$CuZ + Y \longrightarrow CuY + Z \qquad (1)$$

R, is given from pH 3 to pH 12 in Fig. 1. Experimental values of K_{eff} determined by direct measurement (open circles) agree within 0.2 pK unit with values calculated from $k_{f_{eff}}/k_{r_{eff}}$, the ratio of the forward and reverse effective rate constants (filled circles) above pH 5. The relation of the rate data to the equilibrium constant below pH 5, where the reaction rates are independent of the concentration of the attacking ligand, is more complex and will be discussed separately.

Agreement between the two experimental sets of K_{eff} and values calculated from the effective stability constants of the two chelates (solid line) is between 0.1 and 0.2 pK unit, if the formation of hydroxide derivatives of Cu–EDTA and Cu–Erio R is considered. The directly measured value of the equilibrium constant for the formation of the former from Cu–EDTA and hydroxide is 2.1 log units, in good agreement with the value found by Bennett and Schmidt.[4] The formation constant of Cu–OH–Erio R cannot be determined directly by spectral methods because of the similar spectra of the chelate and its hydroxide derivative, but a value can be inferred readily from the pH dependence of measured values of K_{eff}. Neglect of this species results in large discrepancies between measured and calculated values of K_{eff} above pH 9 (dashed line), while a value of 4.0 log units for its formation constant gives excellent agreement to pH 12. Calculated values of K_{eff} are based on data quoted and the

(3) G. P. Hildebrand and C. N. Reilley, *Anal. Chem.*, **29**, 259 (1957).

(4) M. C. Bennett and N. O. Schmidt, *Trans. Faraday Soc.*, **51**, 1412 (1955).

(5) D. W. Rogers, Ph.D. Thesis, University of North Carolina, 1960.

(6) G. Schwarzenbach and W. Biedermann, *Helv. Chim. Acta*, **31**, 678 (1948).

acid–base constants of EDTA given by Schwarzenbach and Ackermann,[7] and the stability constant of Cu–EDTA as determined by Schwarzenbach, Gut, and Anderegg.[8]

Kinetic Data.—The rate of reaction of EDTA with Cu–Erio R in M^{-1} sec.$^{-1}$ is given by the expression

$$1.6 \times 10^{1}(\mathrm{CuZ})(\mathrm{H}) + 7 \times 10^{1}(\mathrm{CuZ})(\mathrm{H_2Y}) + 1.5 \times 10^{2}(\mathrm{CuZ})(\mathrm{HY}) + 1.5 \times 10^{2}(\mathrm{CuZOH})(\mathrm{HY})$$

from pH 3 to 13 and the rate of the reaction of Erio R with Cu–EDTA in the same pH range by

$$8.4 \times 10^{-4}(\mathrm{CuHY}) + 2 \times 10^{-1}(\mathrm{CuY})(\mathrm{H_2Z}) + 2.1 \times 10^{1}(\mathrm{CuY})(\mathrm{HZ}) + 3.1 \times 10^{2}(\mathrm{CuYOH})(\mathrm{HZ})$$

In each case the reaction rate is independent of the concentration of the attacking ligand below pH 5 and first order in the attacking ligand above pH 5. The reaction pairs chosen for the formulation of the rate law are not necessarily unique and other combinations of the same over-all stoichiometry will fit the data as well. However, except for the last term of the rate law for the reaction of EDTA with Cu–Erio R, a reasonable and mechanistically consistent choice can be made simply by formulating the rate law in terms of the predominant species of each reactant. This criterion cannot be applied to the term in question as the pH of the CuZ/CuZOH transformation (pH 10.0) is nearly equal to the pH of the HY/Y transformation (pH 10.3) and appreciable concentrations of all four species exist near pH 10. Although this suggests that both the path (CuZ)(Y) and the path (CuZOH)(HY) may be important in the reaction above pH 10, indirect evidence presented in the Discussion section strongly favors the latter pair, which has been chosen for the formulation of the rate law.

The second-order rate constants for both exchange reactions are valid over a 100-fold range of reactant concentration product and from reactant concentration ratios of 0.2 to 5.0. The rate constant for the reaction of EDTA with Cu–Erio R fluctuated between 1.1×10^{2} and 1.4×10^{2} M^{-1} sec.$^{-1}$ at pH 7.0 as the concentrations of EDTA and of Cu–Erio R were increased simultaneously by up to tenfold from their lower limits of 1.0×10^{-5} and 2.1×10^{-6} M, respectively. The rate constant for the reaction of Erio R with Cu–EDTA at pH 8.5 varied randomly between 20 and 24 M^{-1} sec.$^{-1}$ with the same variation in the EDTA and Erio R species. The pH value for each reaction was chosen to minimize variation of reaction rate with pH between experiments.

The reaction of EDTA with Cu–Erio R at pH 3.26 gives consistent first-order rate constants over an EDTA concentration range of 2.0×10^{-6} to 3.3×10^{-5} M. At EDTA concentrations above 3.3×10^{-5} M, the effect of the concurrent second-order reaction becomes apparent. Data for the first-order path of the reaction of Erio R with Cu–EDTA at pH 3.15 are limited to Erio R concentrations greater than 1.0×10^{-5} M and less than 1.0×10^{-4} M, the first because of the unfavorable equilibrium constant of the reaction, and the second because of the high absorptivity of Erio R. Over this range of Erio R concentrations no deviation from first-order kinetics is observable.

The reactions of EDTA with Cu–Erio R and of Erio R with Cu–EDTA both follow pseudo-first order kinetics above pH 5 over 95% of the reaction when carried out with a large excess of attacking ligand. If more than one Cu chelate species is present, equilibrium among them is rapid. Good agreement was found between the pseudo-first order rate constants and those calculated from the limiting rate of change of absorbance.

Discussion

Chelate Stability Constants.—The absolute stability constant of Cu–Erio R is estimated as 21.2 log units, somewhat higher than would be expected from published stability constants of metal ions with EDTA and with Erio R. The absolute stability constants of Ca–EDTA and Ca–Erio R are 10.7 and 5.2 log units, respectively, while that of Cu–EDTA is 18.8 log units,[3,6] so that the order of stability of the copper chelates is opposite to that of the calcium chelates.

This increase in the relative stability of Cu–Erio R is due to the large ligand field of the aromatic ligand, and may be caused in part by the effect of π-bonding between the d electrons of Cu(II) and the conjugated aromatic ring system of the dye. Qualitatively, the stability of the complex is enhanced by delocalization of the electrons in the t_g orbitals of the central ion over the vacant π-orbitals of the ligand as discussed by Orgel.[9] As EDTA has no delocalized π-orbitals, its chelates cannot benefit from π-bonding.

Second-Order Displacement Reactions.—The observation of second-order kinetics above pH 5 in the reaction of EDTA with Cu–Erio R and in the reaction of Erio R with Cu–EDTA does not in itself shed much light on the actual reaction mechanism. Because of the large number of bonds involved, a one-step reaction is very unlikely. Rather it is quite probable that a stepwise reaction occurs, the first step of which is the bonding of the attacking ligand to a loosely chelated or unchelated site (or sites) of the Cu chelate to form a mixed ligand chelate in a second-order step. This is followed by stepwise replacement of the ligand coördination sites of the original chelate by those of the attacking ligand. The activated complex is associated with the formation of a certain critical number of bonds between Cu(II) and the attacking ligand.

Whether these steps proceed primarily by dissociation of the individual metal–chelate bonds (S$_N$1) or by displacement of the original chelate coordination links by the attacking ligand (S$_N$2) or by some other path must be deduced from detailed examination of the rate data. This second phase of the reaction is undoubtedly complex, but consideration of the rate data together with the acid–base constants of the ligands and the chelate formation

(7) G. Schwarzenbach and H. Ackermann, *Helv. Chim. Acta*, **30**, 1798 (1947).

(8) G. Schwarzenbach, R. Gut, and H. Anderegg, *ibid.*, **37**, 937 (1954).

(9) L. E. Orgel, "An Introduction to Transition Metal Chemistry," Methuen, London, 1960, pp. 106–108.

constants of the ligands allows some interesting mechanistic speculation. For convenience, the formation of a mixed complex will be discussed first, followed by consideration of the replacement phase of the reaction.

The mixed ligand complex EDTA–Cu–Erio R formed in the exchange reactions, as inferred from the second-order kinetics, exists in low concentration relative to the reactants. First, attempts to detect this intermediate spectrophotometrically were unsuccessful. The absorbance of the reaction mixture, extrapolated to zero time, was equal within experimental error to that expected from the sum of the reactants. Second, the reaction of EDTA with Cu–Erio R remained second order even in the presence of a fivefold excess of EDTA. Formation of a significant concentration of mixed ligand intermediate would result in a lowering of the apparent order of reaction in the presence of excess attacking ligand.

The inference of a mixed ligand complex involving multidentate ligands is supported by a considerable amount of indirect evidence. The existence of derivatives of Cu–EDTA is well known. Mixed bidentate ligand complexes of Cu(II) have been demonstrated by Watters.[10] Mixed ligand Cu(II) chelates involving *o,o'*-dihydroxyazobenzene were studied by Jonassen and Oliver,[11] who concluded that 8-hydroxyquinoline can occupy two coördination sites in such chelates. In the case of substitution-inert Ni(II) species, mixed ligand intermediates have been detected in kinetic experiments. In the reaction of Ni–EDTA with cyanide, Margerum, Bydalek, and Bishop[12] identified Ni–EDTA–CN and Ni–EDTA–$(CN)_2$ as intermediates in the forward reaction and found evidence for Ni–EDTA–$(CN)_3$ as an intermediate in the reverse reaction. Although cyanide is a monodentate ligand, the analogy of the mixed complexes to those proposed in the present study is clear. Another mixed complex of Ni(II) with tetraethylenepentamine and Erio T, an analog of Erio R, has been reported by Reilley and Schmid.[13]

Some insight into the mechanism of the exchange reactions at individual coördination sites is given by consideration of the magnitudes of the terms in the rate laws for the exchange reactions. In addition, estimates of the proton affinities of the coördination sites of the *coördinated* ligands and of the relative stabilities of individual metal–ligand bonds in the two chelates are necessary. The equilibrium constant for the protonation of Cu–EDTA (formation of a binuclear H–EDTA–Cu species), presumably at one of the carboxylate groups, is 3.0 log units.[7] Data for the amine sites is not available, nor is there any data for the protonation of Cu–Erio R. As a rough approximation, the proton affinities of the coördination sites of the chelated ligands have been equated with the proton affinities of the free ligands. The errors introduced tend to cancel to a large extent since the *difference* in proton affinities of the two ligands is important, and both are coördinated to some extent to Cu in the activated complex.

The average strength of the bonds between Cu and Erio R is obviously much higher than the average strength of the bonds in Cu–EDTA. Erio R, with its *o,o'*-dihydroxyazo structure, can occupy three coördination sites around Cu(II),[14] yet the stability constant of Cu–Erio R is 21.2 log units, while the stability of Cu–EDTA with five or six metal–ligand bonds is only 18.8 log units. Although rather crude, this evaluation of the relative strength of the bonds in the two chelates is sufficiently clear cut for the present purposes.

The rate of attack of monoprotonated Erio R on Cu–EDTA (21) is of the order of 100-fold faster than the rate of attack of the diprotonated form of Erio R (0.2). Although the diprotonated form has one free coördination site available for bonding to Cu–EDTA, its ability to participate in further bonding is limited. The high proton affinity of the Erio R ($pK_1 = 7.3$) and the low proton affinities of the EDTA sites, ($pK_1 = 2.0$ (COO^-), $pK_2 = 2.8$ (COO^-), $pK_3 = 6.2$ (N)) preclude the operation of a concerted Se2 reaction in which the proton on the attacking Erio R assists in breaking the Cu–EDTA bonds. Further, the high proton affinity of the Erio R impedes the formation of a strong bond between the Cu and the phenolic group of Erio R. Removal of the first phenolic proton allows the Erio R phenolic site to act as an effective displacing agent for the EDTA carboxylate group in an Sn2 step by virtue of the higher stability of the bonds between Cu and Erio R. A carboxylate seems more likely to be displaced than an amine because the peripheral nature of the former requires the breaking of only one metal–ligand bond.

Removal of the second proton from Erio R has much less, if any, effect on the rate. At pH 13, where 20% of the Erio R is unprotonated, no increase in rate of attack on Cu–EDTA over the monoprotonated species is observed. Apparently the formation of the first chelate ring between Cu and Erio R is rate-determining.

The rate of attack of EDTA on Cu–Erio R is nearly constant from pH 5 to 10, the range in which EDTA exists as a diprotonated or monoprotonated species, with a sharp decrease above pH 10. A choice between the alternative terms 150 (CuZOH)(HY) and 300(CuZ)(Y) applicable above pH 10 can be made by comparison of the reactivities of both forms of each species, as reflected in rate law coefficients. The coefficient for the term (CuZ)(HY) is 150, while in contrast that for the term (CuZOH)(Y) is of the order of 0.3, even if the total rate of the reaction is attributed to this path at pH 13, where these are the major species. The critical factor in determining the rate is therefore the presence of a proton on the attacking EDTA, and on this basis, the rate law term (CuZOH)(HY) has been chosen. The role of the proton is very likely to at least weaken the Cu–Erio R phenolic bond in an Se2 step, followed by a displacement of the weakened bond by the EDTA. It is extremely unlikely that an EDTA coördination group could

(10) J. I. Watters, *J. Am. Chem. Soc.*, **81**, 1560 (1959).
(11) H. Jonassen and J. Oliver, *ibid.*, **80**, 2347 (1958).
(12) D. W. Margerum, J. T. Bydalek, and John J. Bishop, *ibid.*, **83**, 1791 (1961).
(13) C. N. Reilley and R. W. Schmid, *Anal. Chem.*, **31**, 887 (1959).
(14) H. D. K. Drew and J. K. Landquist, *J. Chem. Soc.*, 292 (1938).

effectively displace Erio R from its Cu bond, based on the prior estimates of bond stabilities.

A twofold increase in rate does occur as the pH is increased above 6, coincident with the transformation of H_2Y into HY. The coefficient for the term $(H_2Y)(CuZ)$ is 7×10^1, while that for the term $(HY)(CuZ)$ is 1.5×10^2. In H_2Y both amine groups are protonated, while in HY the proton probably is localized between the two nitrogens as suggested by Olson and Margerum.[15] The amine nitrogens in HY are probably in a *cis* orientation and both could readily attack the Cu–Erio R chelate. In H_2Y, however, it is likely that the nitrogens are better described as in a *trans* orientation, due to the electrostatic repulsion of the two protons. Thus if one of the nitrogens is oriented to attack Cu–Erio R, an internal rotation about one of the C–C or C–N bonds in the ethylenediamine nucleus is necessary before the second nitrogen is in a position to attack the Cu chelate structure. An alternative explanation is that the protonation of both nitrogens in H_2Y reduces the ability of these groups to bond to Cu, simply because the nitrogens already are coördinately saturated. Because EDTA has at least 4 free coördination sites above pH 5, it is not possible to speculate as to the number of points of attachment of EDTA to Cu–Erio in the activated complex except to note that 3 sites on Cu–Erio are unchelated and could be involved.

Superimposed on the basic reaction mechanism is the effect of formation of hydroxy derivatives of the chelates. The formation of Cu–OH–EDTA is associated with an increase in the rate of attack of Erio R on Cu–EDTA above pH 11. The rate increase reflects the relatively greater stabilization of Cu–Erio R (compared to Cu–EDTA) by hydroxide derivative formation, the formation constants of the two derivatives being 4.0 and 2.1 log units. The reaction of Cu–OH–EDTA with Erio R brings together in one step all the reactants needed for the formation of Cu–OH–Erio R, with a resultant stabilization of the activated complex.

Dissociation Reactions.—Below pH 5, the rates of both exchange reactions become independent of the concentration of the attacking ligand, suggesting dissociation of the chelates as the rate controlling process. Further, the rates increase with acidity analogous to the observations of Cook and Long[16] and Jones and Long[17] on the dissociation of the Ni and Fe chelates of EDTA. The rate of the reaction of Cu–Erio R with EDTA is given by 16(CuZ)(H) and that of Cu–EDTA with Erio R by 8.4×10^{-4} (Cu–H–EDTA), the formation constant of Cu–H–EDTA being taken as 3.0 log units.[7] No evidence for the formation of a protonated chelate derivative such as Cu–H–Erio R was found in pH titrations of Cu–Erio R.

Further evidence for a dissociation mechanism is the inhibiting effect of free Erio R on the *initial* rate of reaction of EDTA and Cu–Erio R. A mechanism consisting of a slow dissociation of Cu–Erio R, followed by competition between Erio R and EDTA for the free Cu(II), yields the following expression on assuming a steady state concentration of Cu(II). The rate of dissociation of Cu–EDTA is negligible and is not considered.

$$R = k_{dCuZ}(CuZ)\frac{k_y(Y) - k_z(Z)}{k_y(Y) + k_z(Z)}$$

where

R is the observed initial rate of reaction
k_{dCuZ} is the effective first-order dissociation rate constant of Cu–Erio R (rate/(CuZ))
k_y and k_z are effective rate constants for the combination of Cu(II) with EDTA and with Erio R

A test of the rate law at pH 3.30 gives general agreement between observed and predicted rates. The initial rate decreases from 8×10^{-8} to 1.6×10^{-8} M^{-1} sec.$^{-1}$ as the concentration of free Erio R is increased from zero to 6×10^{-5} M. The concentrations of EDTA and Cu–Erio R are both 1×10^{-5} M.

In addition to aiding in the elucidation of the reaction mechanism, these data allow an estimation of both the ratio k_y/k_z and of the magnitude of k_z. Although the scatter in the data precludes an exact determination, k_y is roughly a factor of five greater than k_z. Even though the effective stability constant of Cu–EDTA is about a hundredfold greater than that of Cu–Erio R, the effective rates of formation differ only by a factor of five. The effective value of k_z estimated from the product of k_{dCuZ} (8×10^{-3}) and the effective stability constant of CuZ at pH 3.30 (8×10^6) is 6×10^4.

Acknowledgment.—D. W. R. wishes to acknowledge the financial assistance of the American Viscose Corporation. Part of this research was supported by the United States Air Force through Air Force Office of Scientific Research, Air Research and Development Command, contract No. AF 49(638)-333. Presented at the Combined Meeting, Southeastern and Southwestern Sections of the American Chemical Society, New Orleans, La., Dec. 7–9, 1961.

(15) D. C. Olson and D. W. Margerum, *J. Am. Chem. Soc.*, **82**, 5602 (1960).
(16) C. M. Cook, Jr., and F. A. Long, *ibid.*, **80**, 33 (1958).
(17) S. S. Jones and F. A. Long, *J. Phys. Chem.*, **56**, 25 (1952).

ELECTROMOTIVE FORCE, POLAROGRAPHIC, AND CHRONOPOTENTIOMETRIC STUDIES IN MOLTEN BISMUTH–BISMUTH TRIBROMIDE SOLUTIONS[1]

BY L. E. TOPOL AND R. A. OSTERYOUNG

Atomics International, A Division of North American Aviation, Inc., Canoga Park, California

Received November 21, 1961

E.m.f. and polarographic measurements on cells of the type C, Bi(N_1), $BiBr_3(1 - N_1)||BiBr_3(1 - N_2)$, Bi($N_2$), C where N denotes mole fraction and N_2 varied from 10^{-4} to about 0.08, were made at 226, 235, 250, 275, 300, and 325°. In addition, a chronopotentiometric study was performed on a cell containing N_2's of 0.0027 to 0.0210 at 285–290° and $N_2 = 0.0027$, 0.0072, and 0.0128 at 240°. The e.m.f. and polarography results were similar to those found in the Bi–$BiCl_3$ system. The e.m.f. data were consistent with the reaction $4BiBr = Bi_4Br_4$ and the equilibrium constant, K_N, can be expressed as $\log K_N = (2.83 \pm 0.83)(10^3/T\ °K. - 1.852) + 3.98 \pm 0.25$ for $N_{Bi} < 0.08$. It also was found that if liquid junction potentials are not negligible, Bi_5Br_5 instead of Bi_4Br_4 species actually may be present. Polarograms yielded anodic waves indicating the oxidation of a soluble entity, and it was concluded that the electrode reaction probably is reversible. Anodic limiting current *vs.* Bi concentration plots were linear to about 0.2 mole % Bi, and an activation energy of 5.1 ± 0.9 kcal. was determined for the current-limiting process. The chronopotentiograms appear to indicate that oxidation of the bismuth species occurs without any apparent complications. The transition time constant, $i\tau^{1/2}/C$, was found to vary somewhat with concentration at each temperature and also increased with decreasing current. However, plots of the average $i\tau^{1/2}$ *vs.* C for all the runs resulted in straight lines at each temperature, and diffusion coefficients of about 0.62×10^{-5} and 0.30×10^{-5} cm.²/sec. at 285 and 240°, respectively, and an activation energy of diffusion of 7.3 kcal. were calculated.

Introduction

In previous electrochemical studies, polarographic[2] and e.m.f.[3] measurements were made in Bi–$BiCl_3$ melts. The polarography results indicated that the dissolved Bi metal formed an oxidizable entity, and the e.m.f. data were found to be consistent with the species BiCl and $(BiCl)_4$. A similar investigation on the Bi–$BiBr_3$ system should not only yield information on the species present, but also should enable a comparison to be made between the two systems. In addition, it was decided to test the feasibility of chronopotentiometry on a metal–metal salt system.

Experimental

Materials.—The $BiBr_3$ was synthesized either by direct combination of the elements in a sealed Vycor tube or by treating Bi_2O_3 with an excess of HBr and evaporating to dryness. In both cases final purification of the product was achieved by subliming the salt *in vacuo*. The $BiBr_3$ thus prepared had a melting point of 219°.

The purification of bismuth has been described in previous studies.[2,3]

Apparatus and Procedure.—The cells and procedures for the e.m.f. and polarographic measurements were identical to those used for the Bi–$BiCl_3$ work.[2,3] For the chronopotentiometry, the cells and method of coulometric addition of bismuth also were similar to those for the polarographic investigation. However, instead of two microelectrodes, a single 1/8-in. diameter tungsten rod, sealed in Kovar glass with the metal surface cut flush with the glass, was used as the indicator electrode (exposed area = 7.9 mm.²). Constant currents of known magnitude were applied between the indicator electrode and a working electrode by means of a d.c. power supply connected in series to decade resistance boxes. The chronopotentiograms, measured against a Bi–$BiBr_3$ reference electrode, were recorded on a Moseley Autograph Model 2-S X-Y recorder.

Results

A. E.m.f.—The e.m.f.'s of cells of the type

$$C, Bi(N_1), BiBr_3(1 - N_1)||BiBr_3(1 - N_2), Bi(N_2), C \quad (1)$$

where N denotes mole fraction, were measured at 226, 235, 250, 275, 300, and 325°. As with $BiCl_3$,[2,3] $BiBr_3$ upon melting was found to contain an initial amount of lower-valent Bi species. These concentrations of Bi were computed from the polarographic limiting current *vs.* added Bi plots for each cell (see below) and were of the order of 10^{-5} to 10^{-4} mole fraction. The e.m.f. results, corrected for the initial Bi concentration, are shown in Fig. 1a and 1b. The plots resemble those for the chloride melts[3] in that they depict an initial linear portion and then a change in slope. However, the change in slope is more gradual and is seen to occur at higher metal concentrations than in the chloride system. The agreement between N_{Bi} and the mole fraction of the reference half-cell at zero e.m.f., within 3 to 8% (Fig. 1a, 1b), was not as good as in the Bi–$BiCl_3$ study. The discrepancies probably are due to diffusion of bismuth from the reference half-cell since the asbestos fibers used in these cells were thicker than those used previously. The initial slopes of the curves, corrected for the original Bi, yielded a Nernst n of 1.96 ± 0.09.

B. Polarography.—The polarographic measurements were made with tungsten microelectrodes for all the cells described above. In general, polarograms were run with potentials initially positive to those at which the anodic limiting reaction occurs and then increased in the negative direction. The useful voltage span in pure $BiBr_3$ was about 0.6 v. at 300°; the cathodic limiting reaction represents the reduction of Bi(III) while the anodic reaction is the evolution of Br_2. The current–voltage curves were similar in appearance to those found in the Bi–$BiCl_3$ investigation[2]; the anodic waves indicate that the oxidation of a lower-valent Bi species occurs at the microelectrode. As reproducible anodic waves were found with "pure" molten $BiBr_3$, it was assumed some metal was present in the original melt. Plots of the anodic limiting current *vs.* the concentration of Bi added coulometrically yielded straight lines to about 0.2 mole % Bi as before,[2] and extrapolation

(1) This work was carried out under the auspices of the Research Division of the U. S. Atomic Energy Commission.

(2) L. E. Topol and R. A. Osteryoung, *J. Electrochem. Soc.*, **108**, 573 (1961).

(3) L. E. Topol, S. J. Yosim, and R. A. Osteryoung, *J. Phys. Chem.*, **65**, 1511 (1961).

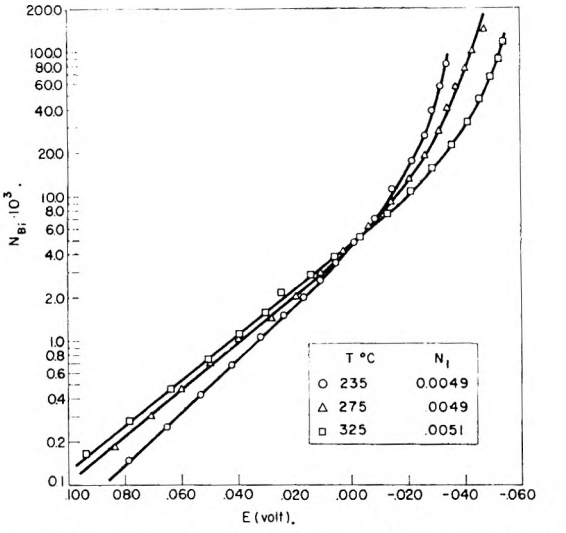

Fig. 1a.—Log N *vs.* E results for cells of the type: Bi(N_1), $BiBr_3$‖$BiBr_3$, Bi(N_{Bi}).

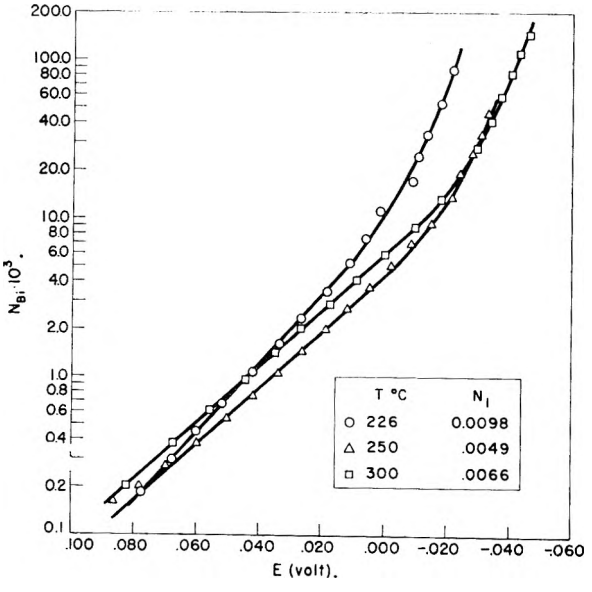

Figure 1b.

of these lines to zero current yielded the initial quantity of Bi present in the fused salt.

C. Chronopotentiometry.—Chronopotentiograms with the indicator electrode anodic were run in a cell at 285–290° and at 240°. At the higher temperature, runs were carried out at 12 concentrations over a range of 500 to 4000 microequivalents Bi/27.80 g. $BiBr_3$ (0.27 to 2.10 mole % Bi); at the lower temperature, measurements were made at 500, 1350, and 2400 microequivalents Bi (0.27, 0.72, and 1.28 mole % Bi). At each concentration a number of runs were made over a current range that varied by a factor of 1.5 to 3, and the transition times, *i.e.*, the time required for the bulk concentration of electroactive species to be reduced to zero at the electrode, were read from the chronopotentiograms at +0.15 v.; although the transition times varied over a range of 0.5 to 11 sec., most values were of the order of a few seconds. No readings were made below concentrations of 500 microequivalents, as the breaks were too sharp to permit accurate determinations of the transition times. The chronopotentiograms appear to indicate that oxidation of the lower-valent bismuth species occurs without any apparent complications. Two typical chronopotentiograms, one with the indicator electrode first made cathodic then anodic, and the other with the electrode anodic throughout, are shown in Fig. 2. The effect of increasing the concentration of oxidizable species at the electrode surface (by cathodization) is, as expected, to increase the time of the subsequent anodic halt.

Discussion

A. E.m.f.—The reaction at an electrode in cell (1) may be written

$$Bi_x^{+y} = xBi^{+3} + (3x - y)e^- \qquad (2)$$

where x and y are integers and y may also equal zero. For a reversible half-cell, assuming the mole fraction N of $BiBr_3$ and the activity coefficients are essentially unity or constant, one can derive the expression

$$E = \frac{RT}{(3x - y)F} \ln N_{Bi} + \text{constant} \qquad (3)$$

for the concentration range where one Bi_x^{+y} species predominates.[3]

Thus, the apparent Nernst n's of 2 found for the initial linear portion in Fig. 1a and 1b indicate the species $Bi_x^{+(3x-2)}$ is present, and as in the chloride case[3] $Bi^+(x = 1)$ appears to be the most reasonable entity. If liquid junction potentials are negligible or constant, the change in slope in the e.m.f. *vs.* log N plots of Fig. 1a and 1b at higher Bi concentrations may be ascribed to a departure of the system from Henry's law behavior, and as in the Bi–$BiCl_3$ system[3] this departure may be interpreted in terms of the existence of another low-valent Bi species such as $(BiBr)_z$. (The reader is referred to ref. 3 for the detailed method of calculation.) The data for this work, as for the previous,[3] are most consistent with the monomer–tetramer equilibrium, and the equilibrium constants for the reaction

$$4BiBr = Bi_4Br_4 \qquad (4)$$

as a function of temperature (Fig. 3) can be expressed by

$$\log K_N = (2.83 \pm 0.83)\left(\frac{10^3}{T\ °K.} - 1.852\right) + 3.98 \pm 0.25 \qquad (5)$$

where $1.852 = 10^3$ times the reciprocal of the mean temperature of the measurements. Thus the chloride and bromide systems are very similar, and the monomer subhalide is more important in the bromide (*e.g.*, at 300° $K_N = (8.1 \pm 1.7) \times 10^5$ and $(4.8 \pm 1.9) \times 10^3$ for the chloride and bromide, respectively) as might be expected from an acid–base viewpoint; *i.e.*, Bi^+ is less acid than Bi_4^{+4} and thus should become increasingly stabilized as the anion becomes less basic.

From relation 5, values of ΔH^0 and ΔF^0 of -12.9 ± 3.8 and -9.6 ± 0.7 kcal., respectively, are obtained for the hypothetical pure liquid standard state at 300°. These quantities yield a ΔS^0 of -5.8 ± 6.7 e.u. as compared to the $\Delta S^0 = -8.7 \pm 4.5$ e.u. found for the analogous chloride reaction. One would expect a much closer agreement between the entropies for the two reactions, but the largest part of this discrepancy is undoubtedly due to the greater scatter in the data in this investigation (Fig. 3).

The species above, *i.e.*, BiBr and $(BiBr)_4$, may be compared with those postulated in other studies. A cryoscopic approach[4] can be interpreted in terms of the entity BiBr in dilute Bi melts, *i.e.*, under 2 mole %, but in more concentrated Bi solutions (10 to 20%) the freezing point data appear to approach the species Bi_3Br_3. The results of a vapor pressure investigation,[5] although not sensitive enough to distinguish species in dilute solutions, can be shown in a manner similar to that used by Corbett[6] to be similar to the cryoscopic observations and become consistent with Bi_4Br_4 at Bi concentrations of 20 mole % and above. Although the various approaches do not lead to consistent results, a similar inconsistency was found in the chloride case.[3] Here, an X-ray[7] and a spectrophotometric[8] study both yielded evidence favoring Bi_3^{+3} for non-dilute Bi solutions rather than Bi_4^{+4} found in our previous investigation. Since the results of this investigation as well as those of a spectrophotometric study[9] indicated that the bromide and chloride systems are very similar, a strong argument could be advanced for the existence of Bi_3Br_3. In the interpretation of the e.m.f. results, it was assumed that liquid junction potentials either were negligible or constant for the concentration ranges covered, *i.e.*, that most of the current is carried by the anions; as in the Bi–$BiCl_3$ system, no electronic conduction is evident. If this assumption is in error, and if Bi^+, Bi^{+3}, and Br^- are all involved in the transport of current, then the following relation[10] holds

$$E = \frac{-RT}{nF} \ln \frac{[Bi^{+3}(2)][Bi^{+}(1)][BiBr_3(1)]^{(2/3)t_{+3}}[BiBr(1)]^{2t_+}}{[Bi^{+3}(1)][Bi^{+}(2)][BiBr_3(2)]^{(2/3)t'_{+3}}[BiBr(2)]^{2t'_+}} \quad (6)$$

$$= E_{n.t.} - \frac{2RT}{nF} \ln \frac{[BiBr_3(1)]^{(1/3)t_{+3}}[BiBr(1)]^{t_+}}{[BiBr_3(2)]^{(1/3)t'_{+3}}[BiBr(2)]^{t'_+}} \quad (7)$$

where t_{+3} and t'_{+3} are the transference numbers of Bi^{+3} in the two half-cells, t_+ and t'_+ those for Bi^+, $E_{n.t.}$ the e.m.f. of the cell without transference,

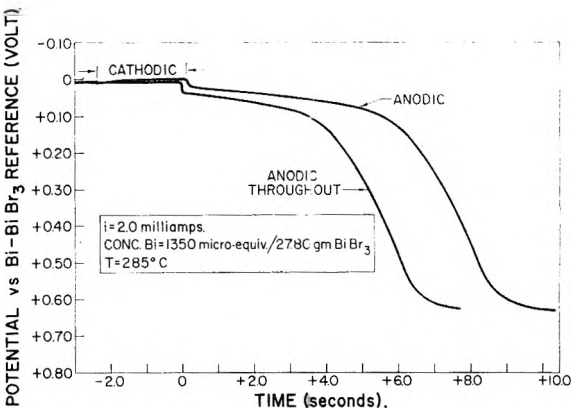

Fig. 2.—Chronopotentiogram-potential of Bi–$BiBr_3$ melt *vs.* time

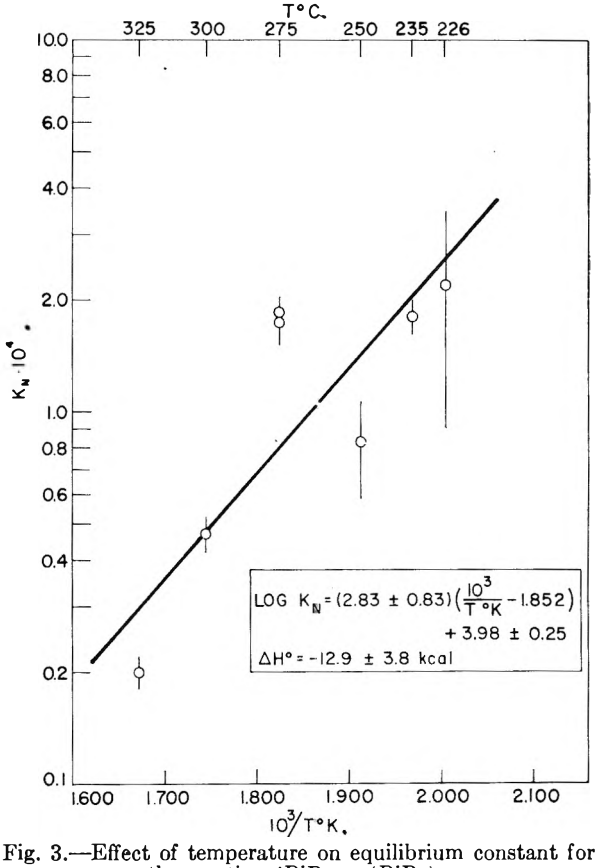

Fig. 3.—Effect of temperature on equilibrium constant for the reaction $4BiBr = (BiBr)_4$.

and the concentration of Bi(2) is greater than Bi(1). Thus, the difference between $E_{n.t.}$ and the measured E depends on the ratios of both the Bi–Br_3 and BiBr activities raised to the appropriate powers. Now, $[BiBr(2)] > [BiBr(1)]$, $[BiBr_3(2)] < [BiBr_3(1)]$, $t'_+ > t_+$, and $t'_{+3} < t_{+3}$, so that the two ratios in the logarithm of eq. 7 act in opposite directions and no definite conclusion can be

(4) S. J. Yosim, L. D. Ransom, R. A. Sallach, and L. E. Topol, *J. Phys. Chem.*, **66**, 28 (1962).

(5) D. Cubicciotti and F. J. Keneshea, Jr., *ibid.*, **62**, 999 (1958).

(6) J. D. Corbett, *ibid.*, **62**, 1149 (1958).

(7) H. A. Levy, M. A. Bredig, M. D. Danford, and P. Agron, *ibid.*, **64**, 1959 (1960).

(8) C. R. Boston and G. P. Smith, ORNL-2988, July, 1960, pp. 9–16.

(9) C. R. Boston and G. P. Smith, Abstracts of the XVIIIth International Congress of Pure and Applied Chemistry, Montreal, Canada, August, 1961, B3-13, p. 184.

(10) For the cell:

$Bi(2), BiBr_3(2) \| BiBr_3(1), Bi(1)$

the simple electrode reaction is

$Bi^+(2) + Bi^{+3}(1) = Bi^{+3}(2) + Bi^+(1)$

whereas the transference expression is given by

$^2/_3 t'_{+3} Bi^{+3}(2) + 2t'_+ Bi^+(2) + 2(1 - t_{+3} - t_+)\, Br^-(1) = {}^2/_3 t_{+3} Bi^{+3}(1) + 2t_+ Bi^+(1) - 2(1 - t'_{+3} - t'_+) Br^-(2)$

Combining terms of these two equations, one gets the total cell reaction for which eq. 6 holds.

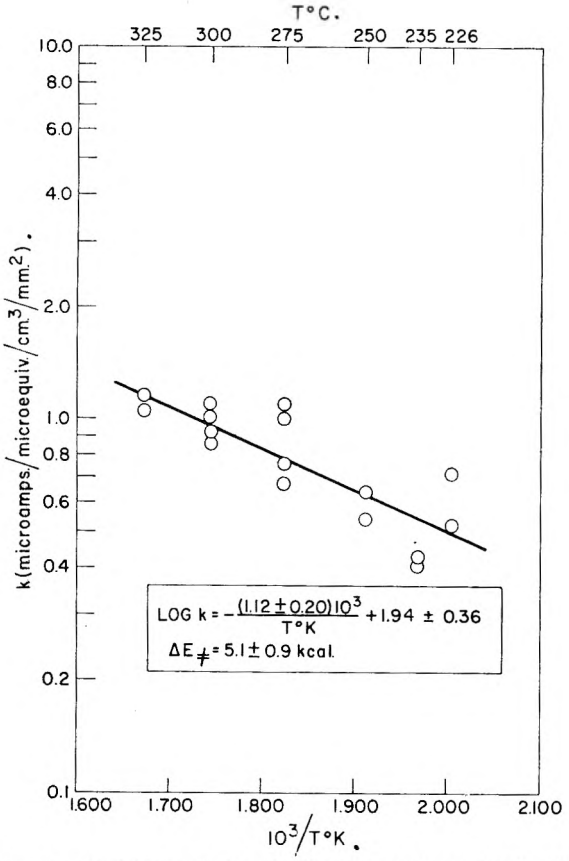

Fig. 4.—Variation of the limiting current constant with temperature.

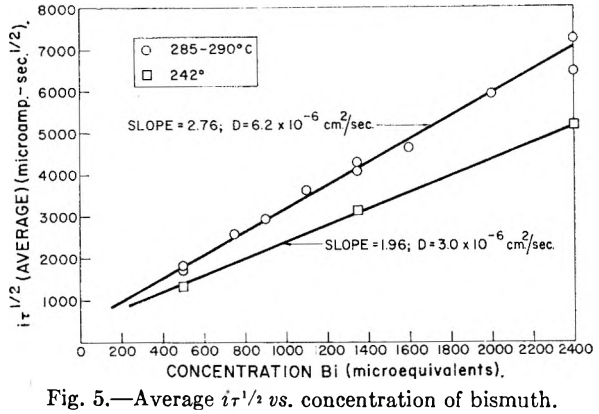

Fig. 5.—Average $i\tau^{1/2}$ *vs.* concentration of bismuth.

drawn. However, since the change in the $BiBr_3$ ratio as well as the difference in Bi^{+3} transference numbers should be much less than that for BiBr for the concentrations in question, it would appear, as a first approximation, that the logarithm of the $BiBr_3$ ratio can be neglected. If this assumption is made, then the logarithm expression in (7) is positive. This may be seen more readily by writing

$$\frac{2RT}{nF} \ln \frac{[BiBr(1)]^{t'_+}}{[BiBr(2)]^{t''_+}} = \frac{2RT}{nF}(t_+) \ln [BiBr(1)] \left\{1 - \frac{t'_+ \ln [BiBr(2)]}{t_+ \ln [BiBr(1)]}\right\} \quad (8)$$

Now, generally the value in the braces will be negative as the ratio of transference numbers (which is greater than one) will be much greater than the ratio of log [BiBr] (which is less than one). Since ln [BiBr(1)] is always negative (activity is less than unity), the value of expression 8 is positive, and $E_{n.t.}$ is greater than the measured E. If this is true, *i.e.*, if Bi^+ carries an important fraction of the current, then the results from the e.m.f. data would be shifted in the direction of higher polymer formation, *e.g.*, $(BiBr)_5$ rather than trimers.

An attempt to measure roughly the Bi^+ transference number in $BiBr_3$ was made employing a six-compartment cell. Four compartments were joined in a row by means of ultra-fine glass frits, and two reference half-cells consisting of known quantities of Bi and $BiBr_3$ were joined to the second and third compartments. The first and fourth compartments were utilized as the cathode and anode, respectively. Compartment 2, the half-cell adjoining the cathode, contained a small amount of Bi, *e.g.*, 0.1 mole %, while compartment 3, that between 2 and the anode, contained a larger amount of metal, *e.g.*, in one case 1% and in the other 10%. After a known amount of current was passed between 1 and 4, the increase in Bi^+ concentrations in half-cell 2 was determined from the e.m.f. change, *i.e.*

$$\Delta E = \frac{RT}{2F} \ln \frac{[Bi]_{final}}{[Bi]_{initial}} \quad (9)$$

as Henry's law has been shown to hold for dilute Bi concentrations, and the $[BiBr_3]$ ratio before and after electrolysis is essentially constant. Thus, t_+, the mean transference number of Bi^+ between the concentrations in compartments 2 and 3, could be calculated with the relation

$$t_+ = \frac{\text{g. equiv. } Bi^+ \text{ gained in 2}}{\text{g. equiv. current passed}} \quad (10)$$

Values of t_+ of about 0.007 and 0.07–0.08 thus were found at 280° when compartment 3 contained 1.0 and 10.0 mole % Bi, respectively. Although these t_+ values are for large concentration differences, it is interesting to note that the Bi^+ appears to carry an amount of current directly proportional to its concentration. This transference behavior, if true, would confirm the assumption above that the log expression in eq. 7 is positive, and if large enough, pentamers rather than tetramers may indeed be present.

B. Polarography.—The polarographic behavior found in this system suggests that (a) the electrode reactions involved probably are reversible as the current–voltage curve crossed the zero current axis at maximum slope, and (b) the dissolved metal yields a species that is subject to oxidation. From the relation

$$i_l = kAC \quad (11)$$

where i_l is the measured limiting current, A the electrode area, and C the formal concentration of bismuth calculated from the weight and density[11]

(11) F. J. Keneshea, Jr., and D. Cubicciotti, *J. Phys. Chem.*, **63**, 1112 (1959).

of $BiBr_3$ in the compartment, values of the limiting current constant k were determined. These values in units of microamperes/microequivalent/cm.^{3}/mm.^{2} are very slightly lower than those reported for Bi–$BiCl_3$.[2] As discussed previously[2] a plot of log k *vs.* $1/T$ should yield the activation energy of the limiting process. Such a plot is shown in Fig. 4, and a least squares treatment results in an activation energy for the current-limiting process of 5.1 ± 0.9 kcal., about the same as that found in the chloride (5.8 ± 1.1 kcal.).[2]

C. Chronopotentiometry.—To check the applicability of the basic equation of chronopotentiometry[12]

$$\frac{i\tau^{1/2}}{C} = \frac{\pi^{1/2}nFD^{1/2}}{2} \qquad (12)$$

where i is the current density, τ the transition time, and C and D the bulk concentration and the diffusion coefficient of the electroactive species, respectively, various relations were examined. Plots of log τ *vs.* log i at constant C yielded lines of slope which varied from −1.90 to −2.30, but most of the slopes were close to the theoretical value of −2.0. However, at constant concentration, the transition time constant $i\tau^{1/2}/C$ was not independent of C but varied from 3.5 to 2.9 at 285° and from 2.7 to 2.2 at 240° as the concentration of metal increased. Further, the transition time constant was not independent of i but increased somewhat with decreasing i. This behavior has been found in practically every chronopotentiometric study to date[13] and suggests that semi-infinite linear diffusion is not the only means of mass transfer of the electroactive species to the electrode surface. However, the solid electrode used was sealed in glass and mounted horizontally to achieve near-optimum conditions.[13] Similar electrode geometries have been used in other fused salt studies.[14,15] Although the diffusion coefficients may not be very meaningful, plots of the average $i\tau^{1/2}$ for each concentration *vs.* C for all the runs did result in straight lines at each temperature, as demonstrated in Fig. 5. From the slopes of these two lines and eq. 12, diffusion constants for Bi^+ of about 0.62×10^{-5} and 0.30×10^{-5} cm.^{2}/sec. at 285 and 240°, respectively, and an activation energy for diffusion of about 7.3 kcal. were calculated. This value for the activation energy of diffusion is in fair agreement with that found polarographically. (It is assumed that the current-limiting process in the polarography is diffusion controlled.) Although theoretically, chronopotentiometry should give a more direct determination of diffusion parameters than does voltammetry at solid electrodes, experimentally, ideal conditions are more difficult to achieve.

(12) P. Delahay, "New Instrumental Methods in Electrochemistry," Interscience Publishers, Inc., New York, N. Y., 1954, Chap. 8.

(13) A. J. Bard, *Anal. Chem.*, **33**, 11 (1961).

(14) H. A. Laitinen and W. S. Ferguson, *ibid.*, **29**, 4 (1957).

(15) H. A. Laitinen and H. C. Gaur, *Anal. Chim. Acta*, **18**, 1 (1958)

PEROXIDE DECOMPOSITION AND CAGE EFFECT

BY W. BRAUN,[1] L. RAJBENBACH, AND F. R. EIRICH

Institute of Polymer Research, Polytechnic Institute of Brooklyn, Brooklyn, N. Y.

Received January 6, 1962

After assuming that the lifetime of the acetoxy radical is of the same order as the "lifetime" of a "geminate diffusive combination" reaction (cage) and assuming that ethane results from the geminate combination of methyl radicals, it is possible to relate the amount of ethane formed to microscopic diffusion parameters and the lifetime of the acetoxy radical, while assuming "free" diffusion of the radical pairs. The calculations lead to results consistent with these assumptions. The rate constant for the decarboxylation of the acetoxy radical was calculated to be $k = 1.6 \times 10^9$ sec.$^{-1}$, at 60°, and the activation energy, 6.6 kcal./mole. In order to evaluate the possibility of the reaction scheme involving the geminate combination of a methyl radical with an acetoxy radical to explain the "cage" methyl acetate experimentally observed, a calculation was carried out assuming this mechanism. The ratio of cage methyl acetate to cage ethane was thus calculated and it agreed remarkably well with the experimentally observed ratio.

If two free radicals (fragments) formed by the decomposition of the *same* molecule become initially separated by an average distance of at least several molecular diameters, the surrounding liquid can then be considered as a continuum and interactions between the two fragments can be neglected. In other words, the fragments can be treated as if they were undergoing *random* displacements. The probability that they meet again, *i.e.*, that "geminate diffusive combination" occurs, can be evaluated as a function of their initial separation. Two methyl radicals, for example, formed by a two-step thermal decomposition of a diacetyl peroxide molecule, apparently satisfy this condition. It will be shown that it is possible to calculate the extent of radical combination (ethane formation) as a function of the viscosity of the hydrocarbon solvent medium and of the lifetime of the intermediate acetoxy radical, while treating the fragments as undergoing free diffusion and justifiably neglecting proximity effects normally encountered in cage (re)combination problems.[2] The latter is a particularly significant point since cage (re)combination problems invariably involve (a) neglecting the effect of the primary cage, although the radical pair immediately subsequent to formation is still caged in by the surrounding solvent molecules, and (b) assuming that the radicals undergo free diffusion after escaping the primary cage and are separated by

(1) Taken in part from a thesis to be submitted in partial fulfillment of the requirements for the Ph.D., by this author.

(2) R. M. Noyes, *Z. Elektrochem.*, **64**, 153 (1960).

less than several molecular diameters. Completely free diffusion, as has been pointed out by Noyes,[2] can only be assumed after the radical pair has separated by at least several molecular diameters. It is this phase of the (re)combination process which will be referred to as "geminate diffusive (re)combination."

The thermal[3] decomposition of a diacetyl peroxide molecule in solution results initially in the formation of two acetoxy radicals ($CH_3CO_2\cdot$) and subsequently in the geminate "cage" production of ethane and methyl acetate.[4] We will assume that the "lifetime" of the acetoxy radical is of the same order of magnitude as the "lifetime"[5] of the "geminate diffusive combination" reaction and at least an order of magnitude longer than the "lifetime" of the "geminate primary combination" reaction. We will further assume that ethane formation can occur only after both acetoxy radicals decarboxylate to give two CO_2 molecules and a pair of methyl radicals. The latter will then be separated by an average distance of at least several molecular diameters due to the relative diffusion of the acetoxy radical pair.

Consistent with these assumptions, the "geminate diffusive combination" of the two methyl radicals can be treated as follows: The probability that one of the two acetoxy radicals formed at $t = 0$ will have decarboxylated during time t is $(1 - \exp(-kt))$, where k is the unimolecular rate constant for the decarboxylation of an acetoxy radical. The probability that one acetoxy radical will have decarboxylated during time t, and the other between time t and $t + dt$, is $2(1 - \exp(-kt))k \exp(-kt)\, dt$. If $R(t)$ is the average separation of a methyl radical *pair* formed at time t then, assuming a gaussian distribution of separations, the probability of ultimate (geminate) combination of the methyl radical pair (between time t and $t = \infty$) is approximately[6] $1.13\rho/R(t)$, where ρ is the collision diameter of a methyl radical.

It is also possible for methyl acetate to form during time t; therefore, ethane formation will further depend on the probability of this occurrence. Including this, the probability, dX, of a methyl radical pair forming between t and $t + dt$ and ultimately resulting in ethane formation (between t and $t = \infty$) is given by eq. 1. $Y(t)$ is the probability of methyl acetate formation during time t, and the quantity $(1 - Y(t))$ is the probability that the acetoxy radical pair escapes methyl acetate formation prior to methyl radical *pair* formation.

$$dX = (1 - Y(t))(1.13\rho/R(t))\, 2(1 - \exp(-kt))\, k \exp(-kt)\, dt \quad (1)$$

If we make the simplifying assumption that $Y(t)$ reaches a limiting value rapidly while $\int_0^t dX$ is still small, we can substitute $Y_{(t=\infty)} = Y_\infty$ for $Y(t)$, enabling integration of eq. 1. Since Y_∞ is the fraction of decomposing acetoxy radical pairs which form methyl acetate (experimentally measured) and is reasonably small, the error introduced by replacing $(1 - Y(t))$ by $(1 - Y_\infty)$ is expected to be small.

The treatment above considers *one* acetoxy radical decomposing between t and $t + dt$. This fragment diffuses t seconds as an acetoxy radical. The displacement distance is $\bar{d}_a = (V_a l_a t)^{1/2}$ where V_a and l_a are the average velocity and the length of one diffusive displacement, respectively, for an acetoxy radical. The other acetoxy radical decomposes between $t = 0$ and t, and as a good approximation we assume that the radical diffuses $t/2$ seconds as an acetoxy radical, and $t/2$ seconds as a methyl radical. The displacement distance of this particle between $t = 0$ and time t is $\bar{d}_{am} = (\frac{1}{2}V_a l_a t + \frac{1}{2}V_m l_m t)^{1/2}$, where the subscripts a and m refer to the acetoxy radical and methyl radical, respectively. If the average separation of the two methyl groups at $t = 0$ (approximately equal to the distance between the methyls in the peroxide molecule) is R_0, then $R(t) = (R_0^2 + At)^{1/2}$, where the parameter $A = (\frac{3}{2})V_a l_a + \frac{1}{2}V_m l_m$.

Substituting for $R(t)$ in eq. 1 and integrating from $t = 0$ to $t = \infty$, 2 is obtained

$$X_\infty = 2.26(1 - Y_\infty)\rho\{(k^{1/2}/A^{1/2})\, 0.519 - 0.733\bar{R}_0^2 k^{1.5}/A^{1.5} + \ldots\} \quad (2)$$

X_∞ is the fraction of decomposing diacetyl peroxide molecules which result in ethane formation *via* geminate diffusive combination of methyl radicals. The parameter A can be calculated using the equation $l = kT/\pi\eta v r$ relating l, the length of a diffusive displacement, to the velocity of the particle, v, the radius of the diffusing particle, r, and the solvent viscosity, η.

This calculation is the result of an attempt to predict quantitatively the effect of solvent viscosity on the cage products formed on decomposing diacetyl peroxide. The latter was decomposed isothermally in a homologous series of paraffins and the products were determined quantitatively. These experiments will be described in the Experimental section.

Table I summarizes the effect of viscosity on the "cage" products formed, and also the effect on the rate constant for the thermal decomposition of diacetyl peroxide at 60°.

Using the experimental values for X_∞ and $(1 - Y_\infty)$, and calculating the parameter A using the approximate values for the constants $\rho = 3 \times 10^{-8}$ cm., $r_m = 1.1 \times 10^{-8}$ cm. = radius of a methyl radical, and $r_a = 1.8 \times 10^{-8}$ cm. = radius of an acetoxy radical, the rate constant k can be calculated using the iterative method. Over the range of viscosity studied X_∞ is adequately described using only the first term in the expansion (eq. 2). The parameter A is inversely proportional

(3) A. Rembaum and M. Szwarc, *J. Am. Chem. Soc.*, **76**, 5975 (1954).

(4) L. Herk, M. Feld, and M. Szwarc, *ibid.*, **83**, 2998 (1961).

(5) Here the meaning of "lifetime" of a "cage" reaction refers to that time interval during which (re)combination can occur with a finite probability, or after which there is negligible chance of an encounter occurring. For an estimate of the magnitude of this time interval refer to R. M. Noyes, *ibid.*, **77**, 2042 (1955).

(6) If two radicals are initially separated by a distance r, the probability of ultimate cage recombination is approximately equal to ρ/r (R. M. Noyes, *J. Am. Chem. Soc.*, **78**, 5486 (1956)). The factor 1.13 is introduced after assuming a gaussian distribution of methyl radical pair separations.

TABLE I

DECOMPOSITION OF DAP AT 60° IN SEVERAL HYDROCARBON SOLVENTS

Solvent	η, cp.	Rate constant (sec.$^{-1}$) for decomp. of DAP	X_∞ = Ratio of "cage" C_2H_6 to DAP decomp.	Y_∞ = Ratio of "cage" MeCAc to DAP decomp.	$\frac{Y_\infty}{\left[\frac{X_\infty}{1 - Y_\infty}\right]}$
n-C_6H_{14}	0.25	$(0.34 \pm 0.01) \times 10^{-5}$	0.034 ± 0.003	0.13 ± 0.02	3.3
n-C_8H_{18}	.35	$(.29 \pm .01) \times 10^{-5}$	.055 ± .002	.18 ± .02	2.7
i-C_8H_{18}	.35	$(.29 \pm .01) \times 10^{-5}$	.055 ± .002	.18 ± .02	2.7
n-$C_{12}H_{26}$	.75	$(.23 \pm .01) \times 10^{-5}$	.071 ± .002	.21 ± .02	2.6
n-$C_{14}H_{30}$	1.13	$(.20 \pm .01) \times 10^{-5}$	.089 ± .001	.24 ± .02	2.0
n-$C_{18}H_{38}$	2.07	$(.19 \pm .01) \times 10^{-5}$	.100 ± .002	.27 ± .02	2.0

to η and a plot of $X_\infty/(1 - Y_\infty)$ *vs.* $\eta^{1/2}$ should result in a straight line plot. The experimental values of $X_\infty/(1 - Y_\infty)$ when plotted against $\eta^{1/2}$ (cp.)$^{1/2}$ results in a linear plot, the slope of which equals 0.100 (cp.)$^{-1/2}$. This value is equal to $1.17\ \rho k^{1/2}/[(kT/\pi)^{1/2}((3/2)r_a) + (1/2)r_m))^{1/2}]$ from eq. 2. Using the approximate values of the constants ρ, r_a, and r_m, k can be numerically evaluated as $k = 1.6 \times 10^9$ sec.$^{-1}$ = rate constant for the decarboxylation of an acetoxy radical. Previous authors[3] have estimated the rate constant at 65° of the order 10^9 to 10^{10} sec.$^{-1}$ and an activation energy of about 5 kcal.

Using the first term in the expansion for X_∞ (eq. 2) the dependence of the ratio $X_\infty/(1 - Y_\infty)$ on temperature can be predicted by eq. 3.

$$\ln (X_\infty/(1 - Y_\infty)) = \ln (\text{const.}) - 1/2(1/RT) \times (\Delta E_1^* - \Delta E_2^*) - 1/2 \ln T \quad (3)$$

ΔE_1^* is the activation energy for the decarboxylation of an acetoxy radical and ΔE_2^* is the activation energy for viscous flow ($\eta = \eta_0 \Delta E_2^*/RT$). Clearly, if $\Delta E_1^* = \Delta E_2^*$ there should be little effect of temperature on the ratio. If $\Delta E_1^* > \Delta E_2^*$ the ratio must increase with increasing temperature.

Diacetyl peroxide was thermally decomposed at various temperatures in n-octane and the data are summarized in Table II. A plot of log $X_\infty/(1 - Y_\infty) + 1/2 \log T$ *vs.* $1/T$ results in a straight line, the slope of which should equal $-(\Delta E_1^* - \Delta E_2^*)/(2.303)(2)(RT)$ from eq. 3. $(\Delta E_1^* - \Delta E_2^*)$ was calculated to be 4.5 kcal./mole. Since ΔE_2^*, the viscosity activation energy, is 2.1 kcal./mole, ΔE_1^*, the activation energy of the acetoxy radical decarboxylation, is 6.6 kcal./mole. The frequency factor calculated from $k = 1.6 \times 10^9$ at 60° and $\Delta E_1^* = 6.6$ kcal./mole is 3.5×10^{13} sec.$^{-1}$.

TABLE II

EFFECT OF TEMPERATURE ON THE "CAGE" PRODUCTS

Temp., °C.	$\frac{\text{"Cage" ethane}}{\text{DAP decomp.}} = X_\infty$	$\frac{\text{"Cage" MeOAc}}{\text{DAP decomp.}} = Y_\infty$
40	0.0476 ± 0.0013	0.14 ± 0.02
60	.055 ± .002	.18 ± .02
80	.065 ± .001	.16 ± .01
100	.0776 ± .0010	.16 ± .02

At this point several conclusions can be made concerning some of the initial assumptions in the derivation. It was assumed, for example, that the lifetime of the acetoxy radical was long compared to the lifetime of any "primary geminate recombination reaction" (generally assumed to be of the order of 10^{-11} sec.) so that ethane formation should result from a "geminate diffusive recombination reaction." The half-lifetime of the acetoxy radical being $\approx 4.3 \times 10^{-10}$ sec., as calculated from $k = 1.6 \times 10^9$ sec.$^{-1}$, is consistent with this assumption. The average separation of the two methyl radicals, assuming that the radical pair is formed at the half-lifetime of the acetoxy radical, can be calculated from $R(t_{1/2}) = (\bar{R}_0^2 + At_{1/2})^{1/2}$. This value is approximately 50 Å. in n-octane (viscosity 0.35 cp.), and is consistent with the fact that the higher order terms in eq. 2 containing $\bar{R}_0$ can be neglected.

Within experimental error (Table II) there does not appear to be any significant temperature effect on the ratio methyl acetate/peroxide decomposed. It has been suggested by Szwarc[3] that methyl acetate possibly forms by the reaction of two acetoxy radicals. If this were the case, the activation energy would have to be very small.

To explore the possibility that methyl acetate results from the combination of a methyl radical from a decarboxylated acetoxy radical and an undecomposed acetoxy radical, we attempt to treat the problem in the following manner.

We previously utilized the relationship

$$\frac{1.13\rho}{R(\tau)} = \frac{1.13\rho}{(\bar{R}_0^2 + A\tau)^{1/2}}$$

to evaluate the probability that the methyl radical pair, formed at time τ subsequent to the initial scission of the peroxide molecule, ultimately combines to yield ethane.

The quantity $(\bar{R}_0^2 + A\tau)^{1/2}$ is the average separation of the radical pair. We define the function $P(t)$ in eq. 4 and assume that $P(t)$ is a monotonically decreasing function and that $P(t)dt$ is the probability that the pair combines in the interval between t and $t + dt$ where $t \geq \tau$.

$$\int_\tau^\infty P(t)dt = \frac{1.13\rho}{(\bar{R}_0^2 + A\tau)^{1/2}} \quad (4)$$

On differentiating eq. 4

$$P(t) = \frac{A1.13\rho}{2(\bar{R}_0^2 + At)^{3/2}}$$

The combination of methyl radicals can now be evaluated using this function[7] from eq. 5

(7) R. M. Noyes has previously used a function containing the separation distance to the $-3/2$ power. See for example, *J. Am. Chem. Soc.*, **77**, 2042 (1955); and ref. 6.

$$X_\infty = (1 - Y_\infty)\cdot\int_0^\infty (1 - \exp(-kt))^2\, P(t)\mathrm{d}t \quad (5)$$

The quantity $(1 - \exp(-kt))^2$ ensures that the methyl radical pair exists at time t, and $P(t)\mathrm{d}t$ is the probability that the pair combines in the interval $\mathrm{d}t$. $(1 - Y_\infty)$ is introduced, as before, to eliminate the radical pairs combining to form MeOAc. The parameter A, as previously defined, is equal to $^3/_2 V_a l_a + {}^1/_2 V_m l_m$. On integrating eq. 5 we again obtain eq. 2.

We similarly define the function $P'(t)$ by eq. 6

$$\int_\tau^\infty P'(t)\mathrm{d}t = \frac{1.13\rho'}{(\bar{R}_0'^2 + A'\tau)^{1/2}} \quad (6)$$

so that ρ' is the effective collision diameter of a methyl radical and an acetoxy radical and $(\bar{R}_0'^2 + A'\tau)^{1/2}$ defines the average separation of a methyl and acetoxy radical at τ, the time the pair is formed. As soon as one of two acetoxy radicals decomposes the *pair* is defined and we can calculate the initial separation of the pair by treating the relative diffusion of two acetoxy radicals; thus A' is equal to $2V_a l_a$.

Methyl acetate formed *via* the "geminate diffusive combination" of a methyl radical and an acetoxy radical can be calculated from eq. 7

$$Y_\infty = \int_0^\infty 2(1 - \exp(-kt))\cdot\exp(-kt)\cdot P'(t)\mathrm{d}t \quad (7)$$

where the factor $2(1 - \exp(-kt))\cdot\exp(-kt)$ is the probability that the radical pair comprises a methyl radical and an acetoxy radical at time t and $P'(t)\mathrm{d}t$ is the probability that the pair combines in the time interval between t and $t + \mathrm{d}t$.

On solving the expression for Y_∞, we obtain

$$Y_\infty = 2.26\rho'\left[\frac{0.734k^{1/2}}{A'^{1/2}} - \frac{2k\bar{R}_0'}{A'} + \ldots\right] \quad (8)$$

The negative term contributes approximately 20% of the value of the first term for the decomposition in *n*-octane and increases as the viscosity of the solvent increases (A' decreases), and may explain the fact that the ratio $Y_\infty/[X_\infty/(1 - Y_\infty)]$ decreases as the viscosity of the solvent increases (see Table I). From eq. 2 and 8, retaining only the first terms in the expansions, the ratio $Y_\infty/[X_\infty/(1 - Y_\infty)]$ can be evaluated as

$$\frac{\rho'}{\rho}\frac{A^{1/2}}{A'^{1/2}}\frac{0.734}{0.519}$$

If we assume that $\rho'/\rho \approx 1.5$ and $r_a/r_m \approx 2$, then $Y_\infty/[X_\infty/(1 - Y_\infty)] \approx 2.4$. Considering the uncertainty in the choice of the parameters, the calculated ratio comes reasonably close to the experimental values.

Several factors were assumed in the above treatment; for example, the implicit assumption that a methyl radical and an acetoxy radical recombine essentially at very encounter, *e.g.*, with a very small activation energy. This may not actually be the case. We also failed to account for the possibility that two acetoxy radicals recombine to re-form a peroxide molecule. If the latter did occur it would have to be considered in eq. 7.

The authors in ref. 4 conclude that acetoxy radicals do not undergo recombination since O^{18}-labeled keto groups are not mixed with –C–O– during partial decomposition of diacetyl peroxide in *n*-pentane. This would suggest that the activation energy for the recombination of acetoxy radicals is at least several kcal.

Table I indicates a definite trend of decreasing rate constant for the decomposition of DAP as the viscosity of the solvent increases. These data would suggest that acetoxy radicals recombine; in view of the O^{18}-labeled experiments, however, it does not seem likely that this is the case and the effect may be due to slight changes in the solvent properties.

There may also be a solvent effect on the lifetime of the acetoxy radical; we have not considered this in our calculations. It may prove interesting to examine the dependence of ethane on temperature for other solvent systems, particularly for dissimilar solvents, where interaction properties vary sufficiently so that one might observe a noticeable effect on the acetoxy radical decarboxylation activation energy.

Conclusion

The calculation of methyl acetate formation *via* the geminate diffusive (re)combination of an acetoxy radical and methyl radical suggests that it is possible that all of the methyl acetate experimentally observed results from this mechanism, although this would assume a very small activation energy for the recombination of the radical pair.

The success of our calculations in predicting a reasonable value for the rate constant for the decarboxylation of an acetoxy radical, and the fact that the observed temperature dependence of ethane agrees well with our initial assumption that the lifetime of the acetoxy radical is longer than the lifetime of the primary cage, *i.e.*, the activation energy is significantly larger than the expected activation energy for the diffusion of an acetoxy radical, gives us good reason to believe that ethane formation results from the combination of a methyl radical pair and that the combination can be treated assuming free diffusion of the radical fragments.

Furthermore, the temperature dependence of "cage" ethane offers a convenient experimental determination of the activation energy for the dissociation of the acetoxy radical.

Experimental

The *n*-octane, *n*-dodecane, *n*-tetradecane, and *n*-octadecane solvents were obtained from Humphrey-Wilkinson, Inc., and were of high purity, olefin-free grade. It was considered particularly important that no olefins be present to avoid scavenging of methyl radicals and thus reduce the quantity of methane resulting from those methyl radicals which escape geminate combination, and abstracting H from the solvent. The solvents were refluxed for several hours over sodium ribbon and then carefully distilled. The middle fractions were taken for the experiments. Several experiments, however, were carried out in solvent that was not previously treated and the results did not differ noticeably from those obtained with solvent refluxed over sodium.

Isooctane (2,2,4-trimethylpentane), research grade, was obtained from Phillips, and *n*-hexane, chromatoquality, from Matheson Coleman & Bell. These solvents were treated as above.

Diacetyl peroxide was prepared by the procedure described by Brice and Morita (*J. Am. Chem. Soc.*, **75**, 3685 (1953)) with a modification according to Rembaum and

Szwarc.[3] Solutions, approximately 0.01 M, were prepared from 0.1 M stock solutions of diacetyl peroxide in the various hydrocarbon solvents. The exact peroxide concentrations were determined according to the titration procedure described by Wagner, Smith, and Peters (*Anal. Chem.*, 19, 976 (1947)). It was found that if the stock solutions were stored over Molecular Sieve, better reproducibility generally was obtained. Some earlier experiments resulted in a rapid decomposition of the peroxide and formation of acetic acid often even at room temperature, indicating that perhaps water may have been introduced and peroxide hydrolysis occurred. These experimental results were irreproducible and discarded. Care was taken to ensure that no acetic acid was formed during the course of each experiment, by infrared analysis (1722 cm.$^{-1}$) of the solutions after partial decomposition.

The rate constants for the decomposition of diacetyl peroxide in n-hexane, n-octane, and n-tetradecane were determined from the slopes of plots of log (optical density of diacetyl peroxide absorption at 1802 cm.$^{-1}$) *vs.* time. The peroxide was decomposed to at least 30% completion and in one case to near completion—the plots were linear in all cases as they should be, since first-order kinetics apply.

Methyl acetate formation can be followed as a function of time by measuring the methyl acetate absorption peak at 1760 cm.$^{-1}$.

The gas analyses were performed as follows. Solutions of diacetyl peroxide of known concentration (usually about 0.01 M) were outgassed several times, sealed, and thermally decomposed at 60° to about 5% completion and the gases were collected in a vacuum system. After the total pressure of gas (CO_2, ethane, and methane) was measured, the gas sample was compressed into a sampling capillary and injected into a Perkin–Elmer fractometer (154B) and the relative amounts of the three components were analyzed. A Perkin–Elmer "J" column (silica gel) was used to resolve the gases. The height ratios of the peaks on the chromatogram were related to the molar ratios of the components using as a calibration a known mixture of approximately the same composition. Reproducibility between runs in a given solvent was found to be excellent.

The amount of peroxide decomposed was calculated from CO_2 evolved plus methyl acetate formed and the rate constant calculated from this agreed within experimental error with the rate constants from the infrared data.

Methyl acetate/peroxide decomposed was calculated from stoichiometry considerations, namely from $2x/1+x$ where

x = moles MeOAc/moles CO_2 = 1.00 − (moles CH_4/moles CO_2) − 2(moles C_2H_6/moles CO_2), and

ethane/peroxide decomposed = 2(moles ethane/moles CO_2)/1 + x

The rate constant for methyl acetate formation was determined in n-tetradecane by following methyl acetate formation in the infrared (1760 cm.$^{-1}$) as a function of time. The ratio of methyl acetate/peroxide decomposed calculated from this data was in excellent agreement with the ratio computed from the stoichiometry as described above.

Herk, Feld, and Szwarc[4] have demonstrated that methyl acetate and ethane form in a "cage" reaction, *i.e.*, they result from fragments from the *same* molecule. Prior to our knowledge of their experiments, we were confronted with the same problem of experimentally verifying that this is indeed the case. We carried out a number of experiments using "ionol" (2,6-di-*t*-butyl-4-methylphenol) at about 0.01 M concentration as a scavenger. "Ionol" is a solid at room temperature, is easily purified, and also is easily removed from the reaction mixture. The -4, methyl hydrogens are very easily abstracted and consequently this compound serves as a convenient source of hydrogen. To demonstrate that methyl radicals from different peroxide molecules do not recombine, and also that the ester absorption peak at 1760 cm.$^{-1}$ was due to methyl acetate rather than due to hydrocarbon acetate (possibly formed from a reaction of a hydrocarbon radical with a peroxide molecule), we sought for any effect of ionol on the ratios of ethane/CO_2 and CH_4/CO_2. These ratios remained invariant. The infrared absorption spectrum of ionol before reaction was compared to the spectrum after reaction and was identical with the exception of the appearance of vibrations due to the formation of $-CH_2-$ modes. Ionol radicals dimerize and changes in the spectra should be proportional to the amount of dimerization. We did not calibrate the system but there is good reason to expect that most of the methane formed from the decomposition of diacetyl peroxide resulted from hydrogen abstraction from the ionol. The fact that the presence of ionol does not affect the ratios of ethane/CO_2 and methane/CO_2 corroborates the results obtained by the authors of reference 4 who used a similar argument.

Acknowledgment.—We are greatly indebted to the Air Force Office of Scientific Research for financial support during the course of this study.

ELECTROLYTE SOLUTIONS THAT UNMIX TO FORM TWO LIQUID PHASES. SOLUTIONS IN BENZENE AND IN DIETHYL ETHER

BY HAROLD L. FRIEDMAN

International Business Machines Corporation, Thomas Watson Research Center, Yorktown Heights, New York

Received January 15, 1962

Some simple solutions of electrolytes in solvents of low dielectric constant exhibit a miscibility gap corresponding to the coexistence of two liquid phases. An explanation is given in terms of electrical forces among ion pairs. An approximation to the effect of these forces is based on the interaction of a simple ion pair with an ideal dielectric having the dielectric constant of the solution. The dielectric constant as a function of composition is measured for NH_4FeCl_4 in $(C_2H_5)_2O$, which unmixes, and is found to be consistent with the theory, as are other less complete dielectric constant data for other unmixing solutions. However, the observed osmotic coefficients of these solutions approach unity much more slowly with increasing dilution than one deduces from the simple theory, a discrepancy which seems to be due to pairwise association of ion pairs in the real solutions.

One of the earliest reported examples of an electrolyte solution that unmixes is $HFeCl_4$ in diethyl ether.[1] According to Houben and Fischer a solution containing HCl and $FeCl_3$ in equimolar amounts separates into two liquid phases, the denser being dark green and the other nearly colorless. It is not at first obvious that $HFeCl_4$ is an electrolyte or even that it exists in this form rather than as separate HCl and $FeCl_3$ molecules in the ether solution. However, later experience shows that chloroanions such as $FeCl_4^-$ have negligible basic properties although they may associate with solvated protons to form ion pairs. Furthermore, the green

(1) J. Houben and W. Fischer, *J. prakt. Chem.*, **123**, 89 (1929).

color in $Fe^{III}-Cl^-$ systems is characteristic of $FeCl_4^-$ and is not formed by dissolving $FeCl_3$ in ether.[2]

Another example of an electrolyte solution that unmixes is $(i\text{-}C_5H_{11})_4N$ picrate in benzene. It has been reported[3] that a little benzene added to the solid solute is sufficient to make it liquefy to form a heavy oil, but enough benzene to reduce the solute concentration below 0.1 molal must be added to get this oil all in solution. A more completely investigated[4] system is NH_4GaCl_4 in diethyl ether, for which the two phases in equilibrium at 25° have been found to be 0.45 and 0.88 molal and to have the same (4.00) chlorine to nitrogen atom ratio. In the case of another unmixing solution, NH_4FeCl_4 in diethyl ether, the absorption spectrum[2] of the light phase is closely similar to that of a solution that is even more concentrated than the dense phase.

Another example is Ga_2Cl_4 in benzene, which has a miscibility gap[5] below the concentration (1.7 molal) at which crystalline solute, of formula[6] $Ga_2Cl_4 \cdot C_6H_6$, first appears as the solution is concentrated. In this case the solute has been shown[7] to be $Ga^+GaCl_4^-$.

In addition to these two-component systems there are several systems with a larger number of components in which unmixing occurs in a very similar way. Examples are $AgClO_4$ in wet C_6H_6[8] and isopropyl ether extracts of aqueous solutions of HCl and $FeCl_3$.[9] In the last case the extracted species is essentially $H_9O_4^+FeCl_4^-$ and in some composition ranges there are three liquid phases in equilibrium, one mainly aqueous and the others mainly ethereal. It is the separation of the two ethereal phases that is analogous to the other systems that we discuss.

In all of these cases the electrolyte in both phases is disposed mainly as ion pairs rather than as free ions. It is proposed here that a general explanation of this kind of phase separation can be given along the following lines.

An ion pair has a very large dipole moment, approximately 20 debyes for an ideal ion pair consisting of two rigid spherical ions of unit plus and minus electronic charge and with centers about 4 Å. apart. A separation of about this amount is obtained from conductivity data by the Bjerrum–Fuoss theory for ion pairs like those in the examples above. As the concentration of such a solution is increased, the dielectric constant may increase drastically because of the contributions from the large dipoles. Whether or not this large increase occurs depends on whether the solute dipoles tend to line up in a parallel or antiparallel fashion when they collide. This seems to be well understood as a matter of principle[10-12] although detailed calculations would be difficult. However *if* the dielectric constant increases strongly enough with concentration, then instability must occur, for the solute dipoles are stabilized (relative to their state in the pure solvent) by increasing dielectric constant, and this stabilization may become so great that the activity of the solute no longer increases with increasing concentration. Then the phase becomes unstable with respect to separating into two phases of different concentrations. This thermodynamic criterion for phase separation is the same as the one usually used in discussing the liquid–vapor equilibrium of a substance in terms of its equation of state and indeed the dipole–dielectric constant interaction discussed here provides an alternative to the usual qualitative explanation of the low volatility of polar substances as compared with nonpolar substances.

An alternative to the explanation of the unmixing proposed here is to assume a series of association equilibria among the ion pairs as Myers and Metzler[9] did. A solution of given molality m may then be characterized by a polymerization number $n(m)$ that is experimentally defined as the ratio of the stoichiometric concentration to the colligative concentration. In this case we deduce the stability condition to be $d \ln n/d \ln m < 1$, but without a theory of the successive association equilibria one cannot obtain a molecular theory of the unmixing by this method.

In order to test the present proposal, it has been cast in the form of an approximate theory which relates the dielectric constant, the concentration of unmixing, and certain properties of the ion pairs. The only relevant dielectric constant data in the literature[7,10,13] do not extend up to the unmixing point; some measurements were therefore made on NH_4FeCl_4–$(C_2H_5)_2O$ in order to have one complete set of data to compare with the theory.

Theory.—We assume that the electrical interaction of a molecule of species i with the other molecules in a mixture makes a contribution to the free energy of the amount

$$[\mu_i^2/8b_i^3][1 - 1/D(m)] \qquad (1)$$

where μ_i is the electric dipole moment, b_i is a distance parameter representing the distance of closest approach of the dielectric medium to the dipole, and $D(m)$ is the macroscopic dielectric constant of the mixture of molality m. This free energy term is the Born solvation energy[14] of a dipole in a structureless medium of dielectric constant D, provided it is assumed that the dipole is constituted of a pair of rigid spherical ions in contact, each ion having a radius b_i and charge $\pm\mu_i/2b_i$. In a mixture of an electrolyte with a polar solvent there is a term like (1) for solvent molecules as well as solute molecules. For the present purpose it is adequate to use the same b parameter for the solvent as for the solute.

We neglect all other kinds of interactions except the ideal free energy of mixing. Then the Gibbs free energy change to form a mixture of m moles of

(2) H. L. Friedman, *J. Am. Chem. Soc.*, **74**, 5 (1952).
(3) R. M. Fuoss and C. A. Kraus, *ibid.*, **55**, 3617 (1933).
(4) H. L. Friedman and H. Taube, *ibid.*, **72**, 3362 (1950).
(5) H. L. Friedman, unpublished observation, 1947.
(6) R. C. Carlston, E. Griswold, and J. Kleinberg, *J. Am. Chem. Soc.*, **80**, 1532 (1958).
(7) R. K. McMullan and John D. Corbett, *ibid.*, **80**, 4761 (1958).
(8) A. E. Hill, *ibid.*, **44**, 1163 (1922).
(9) R. J. Myers and D. E. Metzler, *ibid.*, **72**, 3772 (1950).
(10) G. S. Hooper and C. A. Kraus, *ibid.*, **56**, 2265 (1934).
(11) R. M. Fuoss, *ibid.*, **56**, 1027 (1934).
(12) J. G. Kirkwood, *J. Chem. Phys.*, **7**, 911 (1939).
(13) J. W. Williams and R. J. Allgeier, *J. Am. Chem. Soc.*, **49**, 2416 (1927).
(14) M. Born, *Z. Physik*, **1**, 45 (1920).

ion pairs with one kilogram of the solvent from the components in their standard states (hypothetical 1 M for the solute, pure liquid for the solvent) is given by

$$\Delta G = RT[-m + m \ln m - B_w f/M_w - mBf] \quad (2)$$

where we employ the definitions

$$B_i \equiv \mu_i^2/8b^3kTD(0) \quad (3)$$

$$f \equiv 1 - D(0)/D(m) \quad (4)$$

The first two terms in brackets in (2) are the ideal terms for an unsymmetrical mixture.[15] The next term is the contribution of (1) for the solvent species, with M_w equal to the molecular weight of the solvent in kg./mole. The last term is the contribution of (1) for the solute species, for which the subscript is omitted. The use of f as a measure of the dielectric constant in this problem is natural because of the form of (1). If μ_i is in debyes and b in Ångstrom units, then at 25° eq. 3 reads $B_i = 3.00\mu_i^2/b^3 D(0)$.

In a stable phase the chemical potential of any species must increase when its concentration is increased. From this we deduce that $\partial^2\Delta G/\partial m^2 > 0$ in a stable phase. We call a state for which $\partial^2 \Delta G/\partial m^2 = 0$ a *spinodal* state because on a temperature–composition diagram the locus of such states is called the spinodal curve.[16] On such a diagram the spinodal curve always lies within the coexistence curve except at the critical point, where they are tangent. At a given temperature in a two-component mixture with miscibility gap, one must have

$$m_c < m_s < m_s' < m_c'$$

where m_c and m_c' are the molalities of the phases in equilibrium and m_s and m_s' are the molalities of the spinodal states. All of these remarks have their exact analogies for the more familiar case of liquid–vapor equilibrium. The main point to be made is that m_c and m_c', which are of primary interest, are determined by conditions that are far more complicated to apply than the condition that determines the spinodal states. For the rest we shall neglect the difference between m_c and m_s and, because of the lack of data for the more concentrated phase, shall not attempt any calculations relating to m_s' and m_c'.

In the spinodal state we have

$$\frac{1}{RT}\frac{\partial^2\Delta G}{\partial m^2} = \frac{1}{m} - 2B\frac{\partial f}{\partial m} - [mB + B_w/M_w]\frac{\partial^2 f}{\partial m^2} = 0 \quad (5)$$

The application of these equations is greatly simplified if we make the approximation that in the concentration range of interest $f(m)$ has the form

$$f = Am^p \quad (6)$$

(15) H. L. Friedman, *J. Chem. Phys.*, **32**, 1351 (1960).

(16) I. Prigogine and R. Defay, "Chemical Thermodynamics," Longmans, Green and Co., New York, N. Y., 1954, p. 246.

where A and p depend on the temperature and on the components. Then in the spinodal state m_s we have

$$B = \frac{1 - \dfrac{B_w p[p-1]f_s}{m_s M_w}}{[p^2 + p]f_s} \quad (7)$$

where $f_s = f(m_s)$.

In order to compare theory with experiment, eq. 7 is combined with eq. 3 to calculate b from experimental values of all of the other parameters. For polar solvents, b appears in B_w as well as in B, but the equation is readily solved for b. We use a value of the solute dipole moment μ obtained from the dielectric constant data for the most dilute solutions. If b calculated in this way is found to be of the order of molecular dimensions, then the dipole–dielectric interaction is adequate to account for the unmixing.

For comparison of this elementary theory with another kind of experiment we note that the polymerization number n is, to an accuracy adequate for our purpose, the reciprocal of the molal osmotic coefficient. This may readily be calculated[15] from eq. 2. We obtain

$$n = \frac{1}{1 - pBf - [1-p]B_w f/mM_w} \quad (8)$$

This may be compared with n determined by measuring a colligative property.

It is of interest to inquire whether eq. 5 has exactly two roots, corresponding to the two spinodal states. It is easily seen that if (6) is assumed for all m, then there is only one root if $0.5 < p < 1$, which is the range of interest here. However, there is in general no reason to expect that a particular function $f(m)$ that pertains to the range $m \leqslant m_s$ will also pertain to the range $m > m_s'$. Therefore, to apply the theory to the denser phase we would have to measure $f(m)$ for $m > m_c'$.

Comparison with Experiment.—The data are given in Fig. 1 in a form suitable for applying eq. 7 and the calculations are summarized in Table I. System I, which does not unmix, is included here because it represents a marginal case. Thus, Hill[8] pointed out that the temperature dependence of the solubility of the solid solute is similar to that for a system in which two liquid phases coexist. Moreover he found that three liquid phases, two of them benzene-rich, form if a little water is added to I at temperatures below 22°.

For each system the solute dipole moment μ has been calculated by applying Kirkwood's theory[12] to the dielectric constant data at lowest concentration. These moments are somewhat higher than the values, 11.7, 19.4, and 8.9 D., obtained for systems I, II, and III by the original investigators. This is due, at least in part, to their use of the Clausius–Mossotti–Debye equation to calculate the moments. The Kirkwood theory should give more exact results even though we, like the original investigators, have neglected the contributions of induced moments.

The a parameter in Table I is the ratio of μ to the

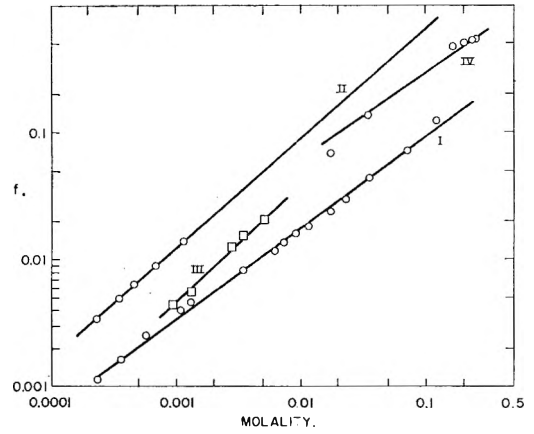

Fig. 1.—Concentration dependence of the dielectric constant function f.

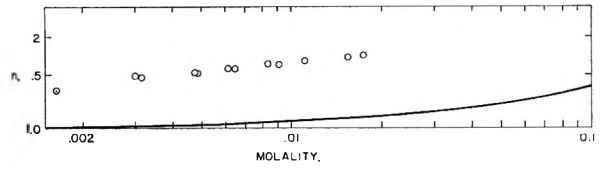

Fig. 2.—Polymerization number as a function of molality in $AgClO_4$–C_6H_6. Both scales are logarithmic. The circles are data at 5.5° obtained by F. M. Batson and C. A. Kraus, *J. Am. Chem. Soc.*, **56**, 2018 (1934). The curve is calculated for the parameters in Table I.

electronic charge. If our model were exact in all details we should have $a = 2b$. Since b is larger than $a/2$, we may conclude that the dipole–dielectric constant interaction is more than strong enough to account for the unmixing. Of course for I there is uncertainty because the phase separation is not actually observed and for II and III because of the long extrapolations.

TABLE I

SUMMARY OF CALCULATIONS

System	I	II	III	IV
Solute	$AgClO_4$	$[i\text{-}C_5H_{11}]_4NPi$	Ga_2Cl_4	NH_4FeCl_4
Solvent	C_6H_6	C_6H_6	C_6H_6	$(C_5H_5)_2O$
Temp., °C.	25	25	25	23.5
m_c, molal	>0.25	0.1	<1.7	0.21
m_c, molal	...		<1.7	1.22
μ_w, debye	0	0	0	1.0
μ, debye, ±0.5	12.7	22.0	12.1	16.5
a, Å.	2.65	4.63	2.53	3.5
p	0.76	0.91	0.98	.74
f_s	>0.2	0.8	0.5	0.6
B_w	0	0	0	.006
B	4.6	0.76	1.10	1.35
b, Å.	>3.8	9.2	5.6	5.3
Ref.	10, 13	10	7	...

For system IV the dielectric constants do not conform well to eq. 6 and it may be suspected that the latitude in choosing the slope p may permit a wide range of calculated b values. However the calculation also has been carried out by applying eq. 5 more directly to the data. It is found that over a limited range of concentration $D(m)$ is of the form $A_1 + A_2m$. This expression is substituted in 4) and then in (5) in order to express B in terms of A_1, A_2, B_w, and m_s. The value of b obtained in this way is 4.7 Å. It is worth pointing out also that for this system the contribution of the solvent dipoles to eq. 4, while not negligible, is not overwhelming, either.

The result $b \sim 5$ Å. for system IV seems reasonable when compared with the sizes of the ions. Thus NH_4^+ has a crystal radius of about 1.4 Å. and $FeCl_4^-$ about 4 Å. The sum, 5.4 Å., might be expected for an effective dipole–dipole contact distance in the configuration +-+- and thus would correspond to $2b$ if the model were exact and the effect of the solvent dipoles negligible. Considerations such as this are necessarily uncertain, however, when the numbers are based on a theory which treats only one dipole at a time as a physical object while all the others are "smeared out" to constitute the dielectric medium. This is the same problem one has in interpreting ionic diameters obtained with the use of the Debye–Hückel theory or in interpreting ionic diameters obtained by comparing the Born charging equation with ionic solvation energies. In each case the distance parameter absorbs all of the weakness of the theory and cannot be given a sharp physical interpretation.

A more serious inadequacy of the present theory is illustrated in Fig. 2. Phase instability on a graph of this sort corresponds to unit slope and the experimental curve, if extended, is expected to rise almost this steeply in the concentration range above a few tenths molal. The discrepancy is the long range at low molality in which the experimental curve is nearly flat and n is larger than unity. This behavior at low molality cannot be obtained from eq. 2 but corresponds closely to what is calculated in the usual way for a dimerization equilibrium with an association constant of 770. Similar difficulties are encountered for the other systems.

The following considerations show that the discrepancy is not an indication of an error in our qualitative interpretation of the phase separation but only serves to emphasize that the interactions among dipoles are only crudely accounted for in eq. 2. In the first place the dimerization certainly results from dipole–dipole interactions, although the only quantitative treatment available[17] is inadequate for electrolytes with symmetrical ions. Figure 2 shows that the dipole–dielectric constant approach is not a good way to represent the pairwise interaction either. This remains an unsolved problem. In the second place, we may calculate the moment of an associated pair of dipoles (a dimer) from the $f(m)$ data for I around $m = 0.4$ molal where n approaches 2. We find for the dimer $\mu_2 = 9.5$ D. and then, from the unmixing condition, $b_2 > 3$ Å. Thus even if the dimerization is reasonably complete, the dipole–dipole reactions among *dimers* are large enough to lead to phase separation. System I offers the most severe test of this kind for in the other systems the tendency to form dimers is weaker.

Other Observations on the Chloroferrate Solutions. Ionization.—In Fig. 3 we show the equivalent conductance as a function of concentration. The highest value corresponds to roughly 5%

(17) R. M. Fuoss and C. A. Kraus, *J. Am. Chem. Soc.*, **57**, 1 (1935).

ionization. Although it is unlikely that the ionization plays a controlling role in the unmixing, it does complicate the measurements because of the large electrode polarization effects found with the conducting solutions.

Dispersion.—This has not been extensively studied but Fig. 4 illustrates the typical behavior. The increase in apparent dielectric constant below 20 Mc. has been repeatedly observed, even with platinized electrodes, and is extreme for the more concentrated solutions, leading to values of the apparent dielectric constant in excess of 10^4 at 400 c.p.s. This effect is certainly not a property of the bulk phase but is the result of an electrode polarization process.[18] That is, the true dielectric constant is doubtless independent of frequency below 20 Mc. but polarization effects at the electrodes introduce series capacitance in the circuit which leads to erroneous values of the dielectric constant. The observation of such effects is not novel[18] but they are not ordinarily encountered at such high frequencies.

The dispersion above 50 Mc. seems to be real and is attributable to a dissipative process involving the ion pairs.[19] It would be of interest to characterize this process more completely.

The Dense Phase.—The best values obtained for the electrical properties of the dense phase of system IV are $D = 13$ and $\Lambda = 16$ for a sample of 0.78 M solution. Unfortunately all of the samples of the dense phase we investigated were found to behave in a highly non-linear manner (see Experimental), an effect which possibly may be attributed to electrode polarization effects that are orders of magnitude greater than in the more dilute solutions. The degree of ionization corresponding to $\Lambda = 16$ is at least 20%, while a dielectric constant of 13 implies that a large proportion of the solute is still in the ion-pair form.

Wet Solutions.—The preliminary experiments made in working out the procedure for the electrical measurements were performed with diisopropyl ether extracts of aqueous HCl–$FeCl_3$ mixtures.[9] A series of solutions of varying solute concentration was formed by mixing this ether with samples of the light ether phase formed in the extraction in a suitable composition range. In this case the solute has quite nearly the composition $H_9O_4^+$-$FeCl_4^-$. The electrical properties of the solutions were found to be very similar to those shown in Fig. 3 and 4.

Experimental

Apparatus.—The electrical measurements were made with a commercial[20] Schering bridge having a range of 0.5 to 250 Mc. In some of the preliminary work conductivity cells of conventional design were used, but the extreme electrode polarization observed made it necessary to work at frequencies greater than 20 Mc. In this range the corrections for the lead inductances (1 μh. on one cell, 0.1 μh. on the other) were prohibitively large. For the rest, a cell based on the design of Lovell and Cole[21] was used. The most important modifications were heavy gold plating on the metal surfaces which came in contact with the solutions and provision to avoid the entry of moisture into the cell when the Teflon plunger is withdrawn. In the course of the work it developed that there are two serious defects in the cell design. (1) The Teflon plunger carries solution out of the cell proper on its surface when it is withdrawn in the course of the measurements. This solution tends to evaporate but the solute is returned to the cell when the plunger is depressed again, thereby increasing the concentration of the solution. (2) The volume of solution within the Teflon plunger contributes to the cell capacity in a way that is not consistent with the Lovell–Cole equations. This is most readily seen by considering a highly conducting solution of low dielectric constant. Then all the solution within the plunger tends to be at the same electrical potential as the inner conductor and, as a result, the total displacement current through the Teflon plunger is independent of plunger setting. This effect is not easily allowed for by calculation, but it should be eliminated by placing a Teflon cap at least 5 mm. long on the upper end of the inner conductor of the cell.

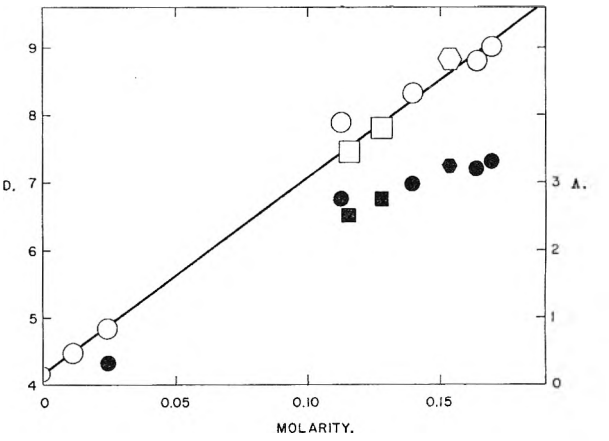

Fig. 3.—Electrical properties of system IV. The hollow figures represent dielectric constants, the solid figures equivalent conductivities. The different figures refer to different series of experiments as described in the Experimental section.

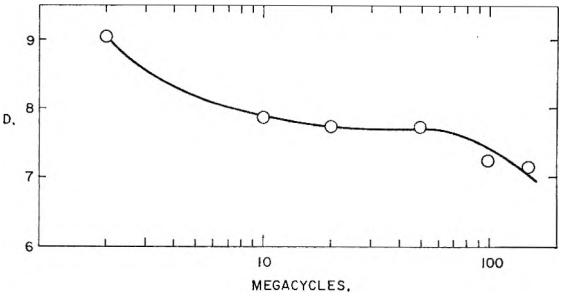

Fig. 4.—Dispersion of 0.116 M solution.

The cell was calibrated with air, CCl_4, and H_2O with the results for the cell parameters[21]: $C_g = 2.10$ pf./in.,[22] $\epsilon_T = 2.03$, $C_1/C_2 = 0.064$. By measurement of the conductivity of the cell filled with 0.001 M KCl(aq) an independent determination of C_g was obtained. $C_g = 2.10 \pm 0.01$ pf./in. for plunger displacements from 0.2 to 0.9 inch. Further checks were the dielectric constant of ether at 23° (found, 4.18; lit., 4.23) and 0.001 M KCl at 23.5° (found, 80.16; lit., 79.00). These are consistent with an accuracy of 1% in the measurement of D. The lead corrections, $L_1 = 0.018$ μh. and $C_1 = 0.0$ pf., were determined by loading the cell with 0.1 M KCl(aq), a strongly conducting medium for which the dielectric properties are known as a function of frequency.[23]

When possible, readings were taken at 0.20, 0.55, and 0.90-in. displacements of the plunger. (The plunger rested on the bottom of the cell at a reading of 0.10 in. on this scale.) The cell conductance and capacitance, after lead corrections,

(18) H. C. Chang and G. Jaffe, *J. Chem. Phys.*, **20**, 1071 (1952).

(19) M. Davies and G. Williams, *Trans. Faraday Soc.*, **56**, 1619 (1960).

(20) RX meter, type 250A, Boonton Radio Corporation, Boonton, N. J.

(21) S. E. Lovell and R. H. Cole, *Rev. Sci. Instr.*, **30**, 361 (1959).

(22) 1 pf. = 1 picofarad = 10^{-12} farad.

(23) J. B. Hasted, D. M. Ritson, and C. H. Collie, *J. Chem. Phys.*, **16**, 1 (1948).

were found to be linear in displacement within a few per cent, except when the heavy phase of system IV was in the cell. Even then the conductance was linear although the capacitance was strongly non-linear. We have not established whether this is due to the error in cell design, to extreme electrode polarization effects, or to the intrinsic behavior of the heavy phase. The last possibilities arise because in the bridge the voltage across the cell depends somewhat on the current through the cell.

Materials.—All operations with these materials were performed with rigorous exclusion of moisture. Reagent grade diethyl ether was used without further purification. Ammonium chloroferrate was prepared from $FeCl_3$ and NH_4Cl by first drying these materials separately by refluxing with freshly distilled $SOCl_2$, then mixing and filtering off the $SOCl_2$. Last traces of $SOCl_2$ were removed by pumping to 10^{-4} mm. overnight at room temperature and then for 1 hr. at 60°. The product was cooled in liquid nitrogen while ether was added and then the mixture was allowed to warm slowly to room temperature with occasional stirring. It was then stirred for several hours and finally filtered to yield a green 2.3 M solution of NH_4FeCl_4 and a solid residue consisting mostly of NH_4Cl, which had been in twofold excess. If the cooling step is omitted when the ether is added, local heating produces undesirable side reactions.

Analyses.—Samples of the ether solutions were taken volumetrically and analyzed for iron either gravimetrically (Fe_2O_3) or volumetrically (titration with $Hg_2(NO_3)_2$[24]). Some of the solutions were analyzed for chloride gravimetrically. In the 2.3 M stock solution the atom ratio Cl/Fe was found to be 4.00. In several cases the coexisting liquid phases at room temperature (23.4 ± 0.2°) were analyzed. The chloroferrate molarities found are (light phase/dense phase): 0.182/—, 0.147/0.804, 0.161/0.817. After considering the details of these experiments it was concluded that the phase equilibrium is slowly attained and that the second determination is the most reliable. This measurement was part of an attempt to determine the coexistence curve but the miscibility gap is only widened to 0.13/0.96 when the temperature is lowered to −80° and the method employed was not accurate enough to follow such small changes in detail.

Stability of Solutions.—The stock solution decomposed slightly during the course of a week, depositing a small amount of NH_4Cl. The properties of a solution derived from the week-old stock solution (Fig. 3, hexagon) were consistent with the main series of measurements (Fig. 3, circles) which were made during the first day after making the stock solution. Some results with a series of solutions prepared and handled in another less satisfactory way also are included in Fig. 3 (squares) to show that the properties of interest here are not largely determined by traces of impurities.

Densities.—In the range $c < 0.17$ M the densities (g./ml.) at 23.4° are given by $\rho = 0.710 + 0.2c$. Hence the molality is given by $m = c[1 + 0.02c]/0.710$. The density of a 0.817 M solution was found to be 0.85 g./ml.

(24) I. M. Kolthoff and P. J. Elving, "Treatise on Analytical Chemistry," Vol. 3, Interscience Publishers, New York, N. Y., 1961, Part II, p. 310.

Acknowledgment.—The author expresses his appreciation to T. Sun for the analyses.

TRANSPORT NUMBERS IN PURE FUSED SALTS

BY CESARE SINISTRI

Istituto di Chimica Fisica dell'Università, Pavia, Italy

Received January 17, 1962

The significance of cationic and anionic transport numbers of a pure fused salt is discussed, and particularly the importance of the reference system is pointed out. It is shown that in a pure fused salt the transport numbers are arbitrary quantities, which become defined automatically when the reference frame for velocities is fixed.

The significance of transport numbers in pure fused salts and the possibility of direct experimental measurement of them have been discussed for some years. However, very little attention has been given to the formalism of the reference frame, which is an important aspect of the problem. Therefore, it may be worthwhile to reconsider the whole matter from first principles.

Definitions.—Let us consider a salt $C_{\nu_+}A_{\nu_-}$ formed with ν_+ cationic constituents[1] of valency z_+ and molar volume concentration c_+, and with ν_- anionic constituents of valency z_- ($z_- < 0$) and concentration c_-. For the electroneutrality of the system, the following equation holds

$$z_+c_+ + z_-c_- = 0 \qquad (1)$$

The transport numbers are defined by means of the ratios of the partial electrical flows ($\vec{I}_+$ and $\vec{I}_-$) to the total electrical flow ($\vec{I}$)

$$t_+ \equiv \frac{\vec{I}_+}{\vec{I}} = \frac{z_+\vec{J}_+}{z_+\vec{J}_+ + z_-\vec{J}_-} \qquad (2a)$$

$$t_- \equiv \frac{\vec{I}_-}{\vec{I}} = \frac{z_-\vec{J}_-}{z_+\vec{J}_+ + z_-\vec{J}_-} = 1 - t_+ \qquad (2b)$$

where $\vec{I}_+ \equiv \mathfrak{F}z_+\vec{J}_+$, $\vec{I}_- \equiv \mathfrak{F}z_-\vec{J}_-$, $\vec{I} = \vec{I}_+ + \vec{I}_-$, $\mathfrak{F}$ is the Faraday constant, and $\vec{J}_+$, $\vec{J}_-$ are the respective cationic and anionic diffusion flows, as defined by

$$\vec{J}_+ \equiv c_+(\vec{v}_+ - \vec{\omega}), \quad \vec{J}_- \equiv c_-(\vec{v}_- - \vec{\omega}) \qquad (3)$$

In eq. 3, $\vec{v}_+$ and $\vec{v}_-$ are the average velocities of the cation and anion, whereas $\vec{\omega}$ is the reference velocity.

It is apparent from eq. 2 and 3 that the values of the transport numbers are functions of the value assumed for $\vec{\omega}$. When speaking of transport numbers, *it therefore is necessary to specify the adopted reference frame.*

Now, let us define the reference velocity. For a liquid medium, in which mechanical equilibrium can be considered established, the value for $\vec{\omega}$ is chosen by means of an averaging process[2]: this consists of attributing weights to the individual

(1) In what follows, the term "cationic" or "anionic constituent" is used in the meaning given by M. Spiro (*Trans. Faraday Soc.*, **55**, 1207 (1959)). In this way, one is freed from the complications which might arise from partial association or dissociation phenomena.

(2) See, *e.g.*, (a) S. R. de Groot, "Thermodynamics of Irreversible Processes," Amsterdam, 1951, p. 108; (b) R. Haase and H. Schönert, *Z. Elektrochem.*, **64**, 1155 (1960).

velocities of the components of the system. Thus we assume

$$\vec{} = p_+\vec{v}_+ + p_-\vec{v}_- \qquad (4)$$

with

$$p_+ + p_- = 1 \qquad (5)$$

In eq. 4 and 5, p_+ and p_- are "weight factors" for the cation and the anion, respectively. These factors can be arbitrarily defined within the limits imposed by (5).

From eq. 3, 4, and 5 there follows

$$\vec{J}_- = -\vec{J}_+ \frac{p_+c_-}{p_-c_+} \qquad (6)$$

As logically expected, this means that only one of the two flows defined in eq. 3 is independent.

Finally, by introduction of eq. 6 in both eq. 2a and 2b, the fundamental relations for t_+ and t_- are obtained

$$t_+ = p_-, \; t_- = p_+ \qquad (7)$$

Equations 7 clearly show that the transport numbers, t_+ and t_-, are automatically defined when the reference frame is defined.

Applications to the Most Common Reference Frames.—In what follows, an application of eq. 7 is made to the reference frames most widely employed. The symbols for transport numbers are provided with proper subscripts to identify the reference.

(a) **Hittorf's System.**—In this reference system a weight value of 1 is assigned to the velocity of one component and a weight 0 to all other components. In the present case, assigning the weight 1 to $\vec{v}_+$, we obtain

$$(t_+)_{h_+} = 0, \quad (t_-)_{h_+} = 1 \qquad (8)$$

or, when assigning the weight 1 to $\vec{v}_-$

$$(t_+)_{h_-} = 1, \quad (t_-)_{h_-} = 0 \qquad (9)$$

Equations 8 and 9 merely express the obvious fact that when the velocity of one of the two ions in the system is taken as the reference, the total electric current is carried solely by the other ion.

(b) **Velocity of the Center of Mass.**—In this reference system the weight ζ_i/ζ is assigned to the velocity of component i, ζ_i being the density of the ith component and ζ the total density. From eq. 7, by means of the relations $\zeta_+ = M_+c_+$ and $\zeta_- = M_-c_-$ (M_+ and M_- being the molecular weights of the cation and the anion), we obtain in our case

$$(t_+)_m = \frac{\nu_-M_-}{\nu_+M_+ + \nu_-M_-}, \; (t_-)_m = \frac{\nu_+M_+}{\nu_+M_+ + \nu_-M_-} \qquad (10)$$

In the case of a 1:1 electrolyte, eq. 10 become

$$(t_+)_m = \frac{M_-}{M_+ + M_-}, \; (t_-)_m = \frac{M_+}{M_+ + M_-} \qquad (11)$$

These equations are identical to those derived previously by Sundheim[3] for this reference frame by application of a criterion of moment conservation. However, there has been some objection[4] to this method.

(c) **Average Volume Velocity.**—In this reference system the weight c_iV_i is assigned to the velocity of component i, V_i being the partial molar volume and c_i the molar volume concentration of this component. By means of eq. 7 and taking V as the total volume of the salt, we write

$$(t_+)_V = \frac{\nu_-V_-}{V}, \; (t_-)_V = \frac{\nu_+V_+}{V} \qquad (12)$$

Conclusions.—Equations 7 clearly show that transport numbers in a pure fused salt can be defined only in an arbitrary manner. Expressions have been obtained in eq. 8 to 12 for reference systems most commonly employed in the liquid phase, and these values depend on the particular reference frame adopted. This is also in agreement with Pitzer's[5] statement that "a transference number in a single component fused salt can only be defined in an arbitrary manner."

Finally, some remarks on the transport numbers measured by means of porous glass diaphragm cells[6] may seem expedient. (a) First, it is clear that in this case the transport numbers are determined in the system *fused salt–porous diaphragm*, and not in the system *pure fused salt*. (b) The system then is formed with the porous diaphragm in addition to the single component of a pure salt; the analogy of the system glass–salt to the system water–salt, where water has been replaced by porous glass,[7] then is apparent. (c) Since considerable uncertainties are introduced by such unavoidable complicating factors as, *e.g.*, electroosmosis, glass–salt interactions, etc., that are certainly present—although not easily evaluable—an exact treatment does not appear to be easy.[8]

For all these reasons the meaning of transport numbers of the system *fused salt–porous diaphragm* appears to be rather uncertain.

On the other hand, as a consequence of eq. 7, any experimental method for the determination of transport numbers in the system *pure fused salt* has little significance.

(3) B. R. Sundheim, *J. Phys. Chem.*, **60**, 1381 (1956).

(4) See, *e.g.*, G. J. Janz, C. Solomons, and H. J. Gardner, *Chem Rev.*, **58**, 461 (1958).

(5) K. S. Pitzer, *J. Phys. Chem.*, **65**, 147 (1961).

(6) (a) F. R. Duke and R. W. Laity, *J. Am. Chem. Soc.*, **76**, 4046 (1954); *J. Phys. Chem.*, **59**, 549 (1955); and following papers; (b) H. Bloom and N. J. Doull, *ibid.*, **60**, 620 (1956).

(7) See also: F. R. Duke and B. Owens, *J. Electrochem. Soc.*, **105**, 548 (1958).

(8) Some reservations on the significance of these transport numbers also have been expressed by R. W. Laity, *J. Chem. Phys.*, **30**, 682 (1959).

STUDIES ON PHOTO-INDUCED ELECTRODE POTENTIALS[1]

BY JOHN J. SURASH AND DAVID M. HERCULES[2]

Departments of Chemistry, Lehigh University, Bethlehem, Pennsylvania, and Juniata College, Huntingdon, Pennsylvania

Received February 2, 1962

Photo-induced changes in the potential of a platinum electrode in contact with a solution of an organic compound in ethanol have been studied. Upon irradiation in the absence of air, the potentials rapidly became more negative (relative to an Ag/AgCl reference electrode), reached a limiting value, and decayed slowly when the exciting radiation was extinguished. The electroactive species is interpreted as being a free radical formed by a photochemical reaction of the solute with the solvent. Negative potentials are consistent with the Nernst equation. The effects of solute concentration, photoreduction product, viscosity, and wave length of exciting radiation have been studied. It has been demonstrated that the electroactive species is produced independent of the electrode. Absorbtion spectra and polymerization data are submitted as evidence that the intermediate is a free radical.

Introduction

The production of a potential difference between two electrodes immersed in a suitable electrolyte, when only one of them is illuminated, has been called the photovoltaic effect. Since Becquerel's original investigations,[3] this effect has been observed for different types of electrolytes and electrode systems. Work involving coated electrode–electrolyte systems[4-7] and semiconductor–electrolyte systems[8-10] indicated that direct irradiation of the electrode–solution interface was essential for the production of a photovoltaic effect. The effect described in the present communication can be produced without direct irradiation of the electrode–solution interface and therefore should be distinguished from the photovoltaic effects of earlier investigators.[4-10]

Levin, White, and co-workers investigated potentials produced by irradiation of platinum electrodes immersed in alcoholic solutions of organic compounds.[11-13] Their studies indicated that photopotentials were produced by the organic solute. Because Levin, *et al.*, failed to exclude oxygen from their solutions, thereby complicating interpretation of their data, the present investigation was begun to establish the nature of the physical processes giving rise to photo-induced electrode potentials.

Experimental

Materials.—Eastman Kodak White Label (or equivalent) chemicals were used throughout. They were further purified by one or a combination of the following methods: vacuum distillation, vacuum sublimation, and recrystallization from absolute ethanol.

U. S. I. (pure grade) absolute ethanol was employed as a solvent in most cases. No photopotential was observed for the solvent.

Apparatus.—The apparatus used in this investigation consisted of the following: Vycor, T-Shaped Cell.—This is shown in Fig. 1; it was made by joining together three 24/40 standard-taper Vycor joints to give a cell having a volume of about 30 ml. The entire cell was covered with black "Scotch" electrical tape except for an area of 1.5 cm.[2] where the exciting radiation entered the cell.

Platinum Indicator Electrode.—This electrode, 0.5 mm. in diameter, was sealed in a standard-taper Pyrex joint leaving approximately 2 mm. exposed. The electrode was supported in the cell against the irradiated side.

Silver–Silver Chloride Reference Electrode.—This electrode was made by anodizing a 1-mm. diameter silver wire in 2 *M* HCl for 5 min. at 5 ma. The reference electrode was placed in the long arm of the cell in a position where radiation could not strike it. Having the electrode in direct contact with the solution eliminated the necessity for a salt bridge. All potentials were measured relative to this electrode.

Hanovia, Air-Cooled, High-Pressure D.c. Xenon Arc (1000 Watts).—This served as a source of ultraviolet radiation and was focused on the sample cell by means of a quartz lens (focal length 14 cm.). The lamp to cell distance was 56 cm.

Filter System.—A Corning No. 7-54 filter and Corex glass No. 9863 (3.05 mm. thick) were used to isolate the 2400–4200 Å. region. A shutter system was used to control exposures.

Recording D.c. Electrometer.[14]—This instrument had an input impedance of 10^{12} ohms and a 1-sec. full-scale response time.

Procedures.—The following procedure was used to obtain potential time curves. A sample of 25.00 ml. was added to the Vycor cell at 25.0 ± 0.5°. The solution was flushed for 10 min. with oxygen-free nitrogen, prepared by passing tank nitrogen through separate containers of vanadous chloride,[15] water, ascarite, and calcium chloride. (An atmosphere of nitrogen was maintained above the sample at all times.) With the recorder running, radiation was made incident upon the indicator electrode by means of the camera shutter, and the potential–time curve was recorded.

To record potential–time curves as a function of wave length, the filter system was replaced by a Bausch and Lomb 500-mm. grating monochromator. The photopotentials recorded were corrected for variations in intensity of the xenon lamp as a function of wave length. Absorption spectra were obtained using a Warren Spectracord with matched, 1.00-cm. glass-stoppered fused-silica cells.

A special cleaning procedure was necessary for the platinum electrode in order to ensure reproducible results. The electrode was immersed in hot (110°) chromic acid cleaning solution for 3 min., rinsed with distilled water, cathodized for 10 min. in 1 *M* sulfuric acid at 5 ma., and rinsed with absolute ethanol. The electrode was always cleaned just prior to use.

(1) (a) Presented before the 138th National Meeting of the American Chemical Society, New York, N. Y., September 15, 1960; (b) this paper represents a part of the dissertation submitted by John J. Surash to the faculty of the Graduate School of Lehigh University in partial fulfillment of the requirements for the Degree of Doctor of Philosophy.

(2) Department of Chemistry, Juniata College, Huntingdon, Penna. Address all correspondence to this author.

(3) E. Becquerel, *Compt. rend.*, **9**, 144, 561 (1839).

(4) V. I. Veselovskii, *Zh. Fiz. Khim.*, **15**, 145 (1941).

(5) V. I. Veselovskii, *ibid.*, **20**, 269 (1946).

(6) V. I. Veselovskii, *ibid.*, **23**, 1095 (1949).

(7) V. I. Ginzburg and V. I. Veselovskii, *ibid.*, **24**, 366 (1950).

(8) W. H. Brattain and C. G. B. Garrett, *Bell System Tech. J.*, **34**, 129 (1955).

(9) H. Gobrecht, R. Kulinkies, and A. Tausend, *Z. Elektrochem.*, **63**, 541 (1959).

(10) R. Williams, *J. Chem. Phys.*, **32**, 1505 (1960).

(11) I. Levin and C. E. White, *ibid.*, **18**, 417 (1950).

(12) I. Levin and C. E. White, *ibid.*, **19**, 1079 (1951).

(13) I. Levin, J. R. Wiebush, M. B. Bush, and C. E. White, *ibid.*, **21**, 1654 (1953).

(14) R. R. H. Miron, Ph.D. Thesis, Lehigh University, 1959.

(15) L. Meites, "Polarographic Techniques," Interscience, New York, N. Y., 1955, p. 34.

Results and Discussion

Photopotentials.—Because Bolland and Cooper[16] studied the photochemical reaction of the anthraquinone system, 9,10-anthraquinone (hereafter called AQ) was selected as the model compound for most of our investigations. A typical photopotential–time curve for AQ is shown in Fig. 2. It is evident that the potential rapidly became more negative during illumination, reached a maximum negative potential, and slowly returned to a value near the initial potential after the exciting radiation was extinguished. Similar curves were observed for a variety of organic compounds in absolute ethanol, and their maximum negative potentials are recorded in Table I.

The following mechanism is proposed to account for the production of photopotentials in oxygen-free solutions of AQ in ethanol

$$AQ + h\bar{\nu} \longrightarrow AQ^* \quad (1)$$

$$AQ^* \longrightarrow AQ^{*\prime} \quad (2)$$

TABLE I

PHOTOPOTENTIALS OF ORGANIC COMPOUNDS IN ABSOLUTE ETHANOL[a]

Compound	Photopotential in mv.[b]
Acetophenone	−434
4-Aminoacetophenone	− 43
4-Bromoacetophenone	−210
4-Hydroxyacetophenone	− 62
4-Methoxyacetophenone	−350
4-Nitroacetophenone	− 42
9,10-Anthraquinone (0.0005 *M*)	−395
Anthraquinone 2,6-disulfonic acid disodium salt (0.005 *M*)	−250[c]
Benzaldehyde	−290
Benzhydrol	0
Benzoin	−409
Benzophenone	−400
4-Bromobenzophenone	−350
4,4′-Dimethylbenzophenone	−510
2-Hydroxy-5-chloro-benzophenone	0
Benzopinacol (0.005 *M*)	−330[d]
p-Benzoquinone	− 60
Benzoyl peroxide	−150
2,2′-Bipyridyl	−240
Diphenylamine	−465
Fluorescein	− 10
Tetrabromofluorescein (0.0001 *M*)	−200[e]
1,4-Naphthoquinone (0.001 *M*)	− 95
Phenazine (0.001 *M*)	−345
Tetraphenylhydrazine	+130[f]

[a] Potentials reported were measured against Ag/AgCl reference electrode. Excitation used was the 2400–4200 Å. component of the xenon lamp. Solutions were purged with nitrogen for 10 min. prior to measurement. Concentration is 0.01 *M* unless otherwise specified. [b] Reproducibility ±3%. [c] Solvent mixture used—60% water and 40% absolute ethanol by volume. [d] Used unfiltered radiation from xenon lamp. [e] Solution was 0.001 *M* in ascorbic acid. Also used unfiltered radiation from xenon lamp. [f] Solution used was the filtrate from a saturated solution of tetraphenylhydrazine in absolute ethanol. A 0.01 *M* solution of tetraphenylhydrazine in chloroform gave a photopotential of +155 mv.

(16) J. L. Bolland and H. R. Cooper, *Proc. Roy. Soc.* (London), **A225**, 405 (1954).

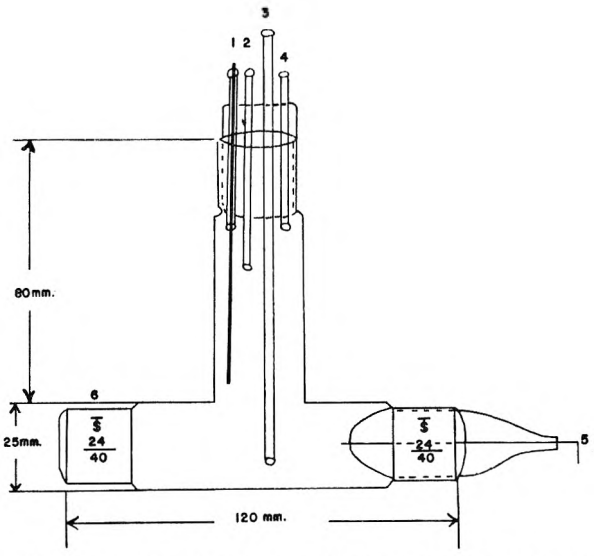

Fig. 1.—Vycor cell diagram: (1) Ag–AgCl electrode; (2) inlet for maintaining nitrogen atmosphere above solution; (3) inlet for bubbling nitrogen into solution; (4) opening to atmosphere; (5) platinum point electrode; (6) glass stopper, $\overline{\$}$ 24/40.

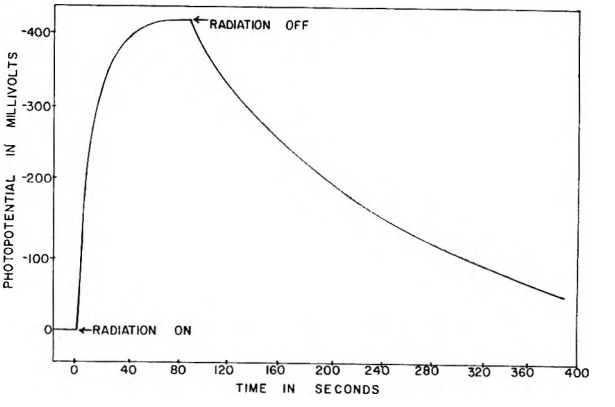

Fig. 2.—Photopotential–time curve for 9,10-anthraquinone (0.0005 *M*) in absolute ethanol in a nitrogen atmosphere.

$$AQ^{*\prime} + RCH_2OH \longrightarrow AQH\cdot^* + R\dot{C}HOH \quad (3a)$$

$$AQ^{*\prime} + RCH_2OH \longrightarrow AQH\cdot + R\dot{C}HOH \quad (3b)$$

$$AQH\cdot^* \longrightarrow AQH\cdot + h\bar{\nu}' \quad (4)$$

The primary process, eq. 1, must involve absorption of radiation in the 2400–4200 Å. region. Because the most intense absorption band for AQ in that region corresponds to a $\pi \rightarrow \pi^*$ transition it may be assumed that $\pi \rightarrow \pi^*$ absorption is the predominant primary process. The correlation between photopotentials and the absorption spectrum of AQ, shown in Fig. 3, enhances this point of view. However, the much weaker $n \rightarrow \pi^*$ transition cannot be ruled out, and probably contributes somewhat to the primary process. Equation 2 indicates conversion from the initial excited state of AQ to some other excited state prior to reaction with the solvent. Generally, it has been assumed

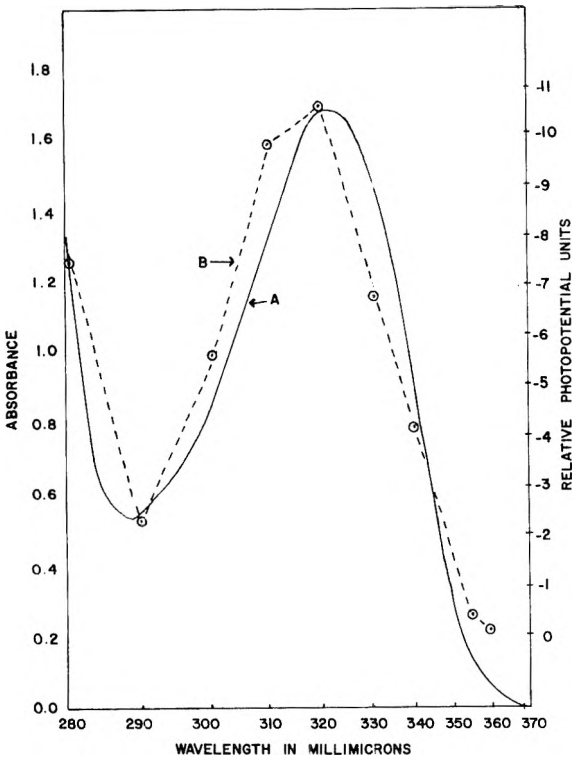

Fig. 3.—Correlation of photopotential and light absorption as a function of wave length of radiation for 9,10-anthraquinone (0.003 *M*) in absolute ethanol: curve A, light absorption—1.00 cm. cell; curve B, photopotential.

that photochemical reactions proceed *via* the triplet state (which in this case would be AQ*′) although the validity of this assumption has been questioned recently.[17] The excited AQ molecule then abstracts a hydrogen atom from the solvent (alcohol) to form a semiquinone radical and the corresponding alcohol radical as shown in eq. 3a and 3b. Evidence for such a reaction is supported by the study of Bolland and Cooper[16] on the photosensitized oxidation of ethanol, using anthraquinone-2,6-sulfonic acid, disodium salt, as the sensitizer.

At present it is not known whether eq. 3a or 3b is the predominant mode of radical production in the AQ system, although 3b seems more likely. If excited radical production does occur, one of the ways AQH·* could lose its excess energy would be the emission of radiant energy, as depicted in eq. 4. The process described is one of chemiluminescence. Although irradiated solutions were observed to fluoresce green during photopotential measurements, this cannot be considered support for process 3a because the radical AQH· is fluorescent under the condition of excitation.[18]

We have assumed that the electroactive species is the monomeric radical AQH·. The possibility exists that the AQH· radical undergoes reaction with an unexcited AQ molecule to produce a radical dimer, or that AQH· radicals partially dimerize to produce an equilibrium mixture of monomeric radicals and dimer.

(17) R. Livingston and V. S. Rao, *J. Phys. Chem.*, **63**, 794 (1959).

(18) D. M. Hercules and J. J. Surash, to be published elsewhere. Investigation of the degree of chemiluminescence in the AQ system will be the subject of a continuing investigation.

The shape of the curve shown in Fig. 2 is readily understood if one assumes the mechanism given above to hold. Prior to irradiation, the predominant species in the vicinity of the electrode surface is AQ. Upon irradiation some of the AQ undergoes photochemical reaction to form AQH· which begins to accumulate at the electrode surface, changing the potential of the electrode. As irradiation proceeds, a steady-state is established and the potential becomes constant. When the radiation is interrupted, chemical reaction of AQH· and diffusion remove it from the electrode surface, and the potential slowly falls to a value near the starting potential.[19]

If one assumes the Nernst equation to hold for an electrode indicating the potential of the AQ/AQH· system, the fact that the potential of the irradiated electrode becomes more negative relative to the Ag/AgCl electrode is quite reasonable. The Nernst equation for this system would be

$$E = K + \frac{RT}{nF} \ln \frac{[AQ]}{[AQH\cdot]} \qquad (5)$$

When both AQ and AQH· are present in solution, the ratio [AQ]/[AQH·] will determine the potential of the electrode. During the course of irradiation, AQ is being converted into AQH·, which will make the ratio [AQ]/[AQH·] become smaller as a function of time. Such a behavior would tend to produce a negative potential according to eq. 5. When a steady-state concentration of AQH· is reached at the electrode surface, the ratio [AQ]/[AQH·] will be constant and the potential of the electrode will become constant as a function of time. When the radiation is extinguished, AQH· will be removed from the electrode surface (and AQ will diffuse into the previously irradiated area) causing the potential to become more positive.

The interpretation presented above is consistent with the observation that the electroactive species can be produced in the absence of an electrode, but will cause a change in the potential of an electrode brought into contact with the solution after the exciting radiation is extinguished (see discussion below). The interpretation also is consistent with the observation that a larger initial concentration of AQ gives a larger maximum potential.

The major difference between the results of Levin, *et al.*,[11-13] and the present study is that the former investigators obtained *positive* photopotentials while we obtained *negative* photopotentials. This discrepancy arises because Levin, *et al.*, measured photopotentials of solutions in equilibrium with atmospheric oxygen, while we measured solutions that had been purged with nitrogen. When we equilibrated our solutions with air, positive photopotentials were obtained, as shown in Table II. In the presence of air, it is quite probable that AQH· undergoes further reaction immediately after it is formed

$$AQH\cdot + O_2 \longrightarrow AQ + HO_2\cdot \qquad (6)$$

$$2HO_2 \longrightarrow H_2O_2 + O_2 \qquad (7)$$

(19) Since some AQ apparently is used up in a photochemical reaction, the final potential is more positive than the initial potential.

Therefore, in the presence of air the ratio of [AQ]/[AQH·] will not determine the potential of the electrode, but it probably will be determined by the O_2/H_2O_2 or the H_2O_2/H_2O couple. Apparently, the potentials of these couples are more positive than the initial potential of the platinum electrode. This was confirmed experimentally by the addition of small amounts of 3% H_2O_2 to an ethanolic solution of AQ (non-irradiated, in air) in the vicinity of the point electrode. The potential became more positive during addition of the H_2O_2. From this one may conclude that Levin, *et al.*, were really measuring the relative efficiencies of compounds to photoöxidize ethanol, and that their changes in potentials were largely due to peroxide formation.

TABLE II

EFFECT OF AIR ON PHOTOPOTENTIALS

Compound	Molar concn. in absolute ethanol	Photopotentials in mv.[a] Air[b]	Nitrogen
Acetophenone	0.01	+10	−434
4-Bromoacetophenone	.01	+60	−210
4-Methoxyacetophenone	.01	0	−350
9,10-Anthraquinone	.0005	+70	−395
Benzoin	.01	+47	−409
Benzophenone	.01	+60	−400

[a] Measured against Ag/AgCl reference electrode; reproducibility ±3%. [b] Same experimental arrangement was used as for the nitrogen-flushed samples except that a 50-ml. Pyrex beaker was used as the cell.

Effects of Variables on Photopotentials.—The effect of solute concentration on maximum photopotentials for AQ and diphenylamine is summarized in Table III. It is evident that the maximum photopotentials vary with concentration of solute, approaching a limiting value. On the basis of the proposed mechanism, it is reasonable to expect the maximum photopotential to increase with concentration due to the increased absorption of radiation in the more concentrated solutions and the corresponding increase in production of intermediate species per unit time. The limiting value of the photopotential probably occurs at the point of total absorption of the exciting radiation by the solution in the vicinity of the electrode.

TABLE III

EFFECT OF SOLUTE CONCENTRATION OF PHOTOPOTENTIALS

Compound	Molar concn. in absolute ethanol × 10^3	Photopotentials in mv.[a]
9,10-Anthraquinone	0.5	−395
9,10-Anthraquinone	.1	−285
9,10-Anthraquinone	.05	−225
9,10-Anthraquinone	.01	−200
9,10-Anthraquinone	.005	−195
9,10-Anthraquinone	.001	0[b]
Diphenylamine	10.0	−465
Diphenylamine	1.0	−465
Diphenylamine	0.1	−320
Diphenylamine	.05	−160
Diphenylamine	.01	− 15

[a] Measured against Ag/AgCl reference electrode; reproducibility ±3%. [b] Visual observation revealed the presence of a very small amount of yellow intermediate around the irradiated electrode, but the detection system was not sensitive enough to show any photopotential.

It was necessary to determine if photopotentials might be caused by accumulation of photoreduction products at the electrode surface. The benzophenone–benzopinacol system was chosen for this study because the photochemical synthesis of benzopinacol from benzophenone is well known. Photopotentials were recorded for solutions containing varying amounts of benzopinacol with constant amounts of benzophenone. The results are tabulated in Table IV. From these data it is apparent that benzopinacol had no effect on the photopotential of benzophenone.

TABLE IV

EFFECT OF BENZOPINACOL ON THE PHOTOPOTENTIAL OF 0.001 *M* BENZOPHENONE (IN ABSOLUTE ETHANOL)

Molar concn. of benzopinacol in absolute ethanol × 10^3	Photopotential in mv.[a] Filtered light (2400–4200 Å.)	Unfiltered light
0	−200	−305
0.1	−200	−300
0.5	−196	−305
1.0	−204	−310

[a] Measured against Ag/AgCl reference electrode; reproducibility ±3%.

Figure 4 illustrates the effect of viscosity on the photopotential–time curves for benzophenone in ethanol. It is apparent that the maximum photopotential decreases as a function of viscosity, and that the rate of decay of the photopotential decreases as viscosity increases. The latter phenomenon is readily explained if we assume diffusion to be the principal mechanism for removal of the intermediate from the electrode surface after the exciting radiation is extinguished.[20] The decrease in maximum photopotential with increasing solvent viscosity probably results from collision of the two radicals formed in eq. 3 within a Franck–Rabinowitch cage.[21] As the solvent viscosity increases, the radicals will encounter a slower rate of diffusion and an increased probability of recombination. This will tend to reduce the number of free radicals at the electrode surface.

Earlier investigators[12] attempted to correlate the magnitude of the photopotential with absorption of radiation by the compound. However, their data were not conclusive. Figure 4 shows that the photopotentials definitely follow the absorption spectrum for AQ. (Similar results were obtained for benzoin and benzophenone.) The first $\pi \rightarrow \pi^*$ absorption band was chosen for irradiation studies because the $n \rightarrow \pi^*$ band in AQ was too weak for study. It is reasonable to anticipate a correlation of photopotentials with the absorption spectrum because increased absorption results in a greater number of molecules being excited per unit time. These can produce a greater number of electroactive species at the electrode surface and consequently a larger photopotential.

In order to distinguish the photo-induced electrode potentials of the present study from a true

(20) This assumes diffusion is rapid relative to any chemical reaction by the intermediate.

(21) This type of process has been studied recently by L. Herk, M. Feld, and M. Szwarc, *J. Am. Chem. Soc.*, **83**, 2998 (1961), and R. K. Lyon and D. H. Levy, *ibid.*, **83**, 4290 (1961).

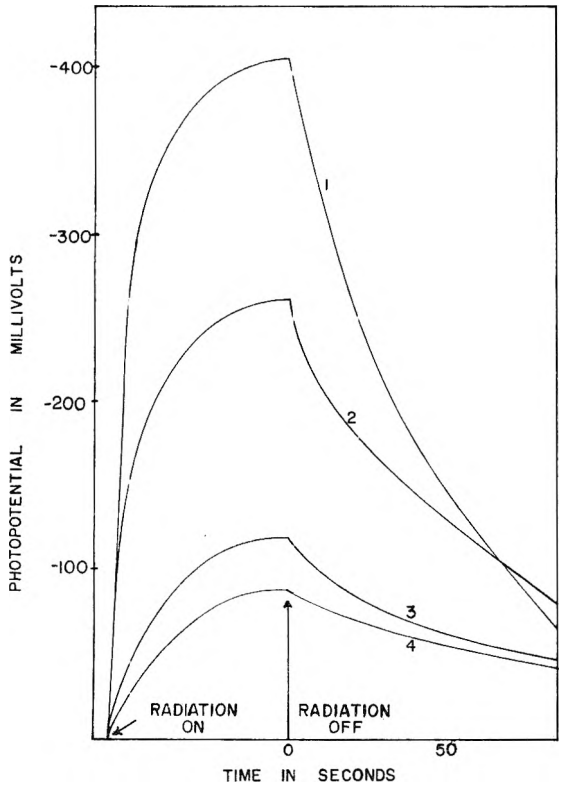

Fig. 4.—Effect of solvent viscosity on the decay curve of irradiated benzophenone solutions (0.01 *M*): curve 1, 100% absolute ethanol; curve 2, 80% absolute ethanol plus 20% glycerol; curve 3, 60% absolute ethanol plus 40% glycerol; curve 4, 40% absolute ethanol plus 60% glycerol.

photovoltaic effect, it was necessary to prove the electroactive species was produced in solution *independently* of the electrode surface, and if an electrode was placed in contact with the electroactive species in the absence of radiation, the electrode potential would become more negative. To accomplish this, the platinum point electrode was rotated 180° so it was not in the path of the incident radiation. With the recorder running, radiation was made incident on the cell. During several minutes of irradiation, no change in potential of the electrode was recorded, even though formation of the yellow intermediate was observed visibly. Then the exciting radiation was shut off, and immediately the platinum electrode was rotated 180° to its normal position against the cell wall in the area previously irradiated. The potential of the electrode became more negative, reaching a maximum value and decaying to a final potential very near the starting potential.

Nature of the Intermediate Species.—Although the intermediate giving rise to photopotentials was assumed to be a free radical, an attempt was made to acquire some direct evidence to support this assumption. Electron spin resonance studies on ethanolic solutions of the intermediate in the photoreduction of AQ were inconclusive, due to loading of the e.s.r. spectrometer cavity by the alcohol. However, other studies indicate that the intermediate is a free radical.

Upon irradiation of a solution of AQ in ethanol, a new diffuse band appears in the electronic absorption spectrum from 350 to 460 mμ. The maximum is at 380 mμ. When an alcoholic KOH solution of AQ is irradiated, an additional band appears having its maximum at 480 mμ. In their flash photolysis studies, Bridge and Porter[22] reported a group of bands at *ca.* 360–390 mμ which they attributed to the semiquinone radical and a band at 480 mμ which they attributed to the semiquinone ion. The maxima reported here, as well as those of Bridge and Porter, are consistent with the normal spectral shift that would accompany the ionization

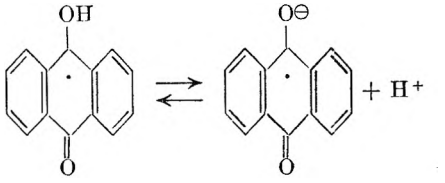

Studies have been reported on the photoreduction of eosin with accompanying potential measurements.[23–25] Electron spin resonance studies on the photoreduction intermediate indicated the presence of a free radical.[25] We have obtained typical photopotential curves for the systems studied by these investigators.

Additional evidence that the intermediate in the photoreduction of AQ is a free radical was provided by polymerization studies similar to those of Cooper, *et al.*[26] It was demonstrated that the yellow-colored intermediate could initiate polymerization of styrene and methyl methacrylate. Furthermore, photopolymerization of styrene has been initiated by benzoin,[27–29] while benzoyl peroxide[30,31] and phenazine[32] have been reported as sensitizers. All three compounds gave photopotentials in the present study.

Berg, *et al.*,[33] have postulated free radical intermediates for a number of compounds in their photopolarographic studies. They were concerned with irradiating a dropping mercury electrode and measuring the changes in limiting current produced. It is quite probable that the electroactive species in the work of Berg, *et al.*, are similar to those of the present investigation.

(22) N. K. Bridge and G. Porter, *Proc. Roy. Soc.* (London), **A244**, 259 (1958).

(23) V. F. T. Tsepalov and V. Ia. Shliapintokh, *Dokl. Akad. Nauk SSSR*, **116**, 641 (1957).

(24) V. F. T. Tsepalov and V. Ia. Shliapintokh, *Izv. Akad. Nauk SSSR, Otd. Khim. Nauk*, **4**, 737 (1959).

(25) N. N. Bubnov, L. A. Kibalko, V. F. Tsepalov, and V. Ia. Shliapintokh, *Opt. i Spektroskopiya*, **7**, 71 (1959).

(26) W. Cooper, G. Vaughan, S. Miller, and M Fielden, *J. Polymer Sci.*, **34**, 651 (1959).

(27) B. R. Chinmayanandam and H. W. Melville, *Trans. Faraday Soc.*, **50**, 73 (1954).

(28) R. M. Joyce, U. S. Patent 2,647,080, July 28, 1953.

(29) C. M. McCloskey and J. Bond, *Ind. Eng. Chem.*, **47**, 2125 (1955).

(30) S. G. Cohen, B. E. Ostberg, D. B. Sparrow, and E. R. Blout, *J. Polymer Sci.*, **3**, 264 (1948).

(31) M. Burnett and H. W. Melville, *Proc. Roy. Soc.* (London) **A189**, 456 (1947).

(32) G. A. Schroter, *Kunstoffe*, **41**, 291 (1951).

(33) (a) H. Berg, *Collection Czech. Chem. Commun.*, **25**, 3404 (1960); (b) H. Berg, *Naturwiss.*, **47**, 320 (1960); (c) H. Berg and H. Schmeiss, *ibid.*, **47**, 513 (1960); (d) H. Berg and H. Schmeiss, *Nature*, **191**, 1270 (1961).

THE EFFECT OF PRESSURE ON THE EQUILIBRIUM OF MAGNESIUM SULFATE[1]

BY F. H. FISHER

University of California, San Diego Marine Physical Laboratory of the Scripps Institution of Oceanography, San Diego 52, California

Received February 16, 1962

Conductivity at 25° of aqueous solutions of $MgSO_4$ has been measured as a function of pressure up to 2000 atm. for five concentrations from 0.0005 to 0.02 *M*. The effect of pressure on the dissociation constant was calculated with the equation used by Davies, Otter, and Prue. The difference of partial molal volumes between products and reactants, $\Delta\bar{V}^0$, was found to be -7.3 ± 0.4 cc./mole. The relation of this work to results of sound absorption measurements in $MgSO_4$ solutions is pointed out. Measurements of the effect of pressure on conductivity also were made for the following aqueous solutions: KCl, K_2SO_4, $MgCl_2$, and NaCl at 25° over the same concentration range. Values of equivalent conductivity at infinite dilution, Λ_p^0, were determined as a function of pressure for $MgSO_4$, KCl, K_2SO_4, and $MgCl_2$. Values of Λ_p/Λ_1 are given for $MgSO_4$, KCl, K_2SO_4, and $MgCl_2$ at each concentration. Since $V_2^0 = -6.4$ cc./mole for $MgSO_4$, the partial molal volume of the state which dissociates into ions is $\sim +1$ cc./mole.

The unusually high sound absorption of sea water, about 30 times greater than that of fresh water, is due to a small concentration of magnesium sulfate, approximately 0.02 *M*.[2] Tamm and Kurtze[3] found that other 2–2 sulfates exhibit similar high absorption and Eigen[4] has discussed their significance. Liebermann[5] showed how a pressure dependent chemical reaction could produce this sound absorption and Bies,[6] on the basis of pressure dependent dissociation, derived a theory by which he determined equilibrium constants of magnesium sulfate from sound absorption measurements at atmospheric pressure in water and dioxane–water solvents. Verma[7] has made a recent summary of sound absorption in electrolytes which includes measurements as a function of concentration, temperature, dielectric constant, pressure, and the effect of heavy water as solvent.

For any quantitative check of the theory of sound absorption based on pressure dependent dissociation reactions, it is vital to know the volume change upon dissociation into ions, that is $\Delta\bar{V}^0$ which appears in eq. 1.[8] It should, in principle, be possible to use the same ($\Delta\bar{V}^0$) and degree

$$\left(\frac{\partial \ln K_m}{\partial p}\right)_{T,m} = -\frac{\Delta\bar{V}^0}{RT} \qquad (1)$$

of dissociation (α) to describe results of density and conductivity measurements; if sound absorption is due to dissociation into ions, it should be possible, using the same ($\Delta\bar{V}^0$) and α, to account for it also. This has been done for a weak electrolyte in the case of ammonium hydroxide in work reported by Hamann and Strauss[9] and by Carnevale and Litovitz.[10]

Since $\Delta\bar{V}^0$ has not been determined experimentally for any of the 2–2 sulfates from conductivity measurements as a function of pressure, the object of this work is to do so at 25° to facilitate comparison with values of ΔV determined by Bies.[11] The molal dissociation constant K_m was calculated from equation 2, in which it is assumed that the activity coefficient of the associated salt is unity at all pressures and concentrations. The degree of dissociation was determined at 25° for magnesium sulfate by dividing the measured equivalent conductivity by the theoretical value determined from the equation

$$K_m = \frac{m\alpha^2 f_\pm^2}{1-\alpha} \qquad (2)$$

$$\Lambda = \Lambda^0 - \left[\frac{R\Lambda^0}{1 + B\mathring{a}\sqrt{I}/2} + E\right]\frac{\sqrt{I}}{1 + B\mathring{a}\sqrt{I}} \qquad (3)$$

used by Davies, Otter, and Prue.[12] The activity coefficients were calculated from the Debye–Hückel equation

$$-\log f_\pm = \frac{A|z_1 z_2|\sqrt{I}}{1 + B\mathring{a}\sqrt{I}} \qquad (4)$$

In both eq. 3 and 4 molar concentrations varying with pressure were used. In eq. 2 the rational activity coefficient is used for the molal activity coefficient. Tables I and II list constants for aqueous solutions useful in evaluating eq. 3 and 4.

The dielectric constant ϵ was calculated using the Owen and Brinkley[13] equation

$$\epsilon_p = \epsilon_1 \Big/ \left[1 - 0.4060 \log\left(1 - \frac{p+1}{B+1}\right)\right] \qquad (5)$$

where p is in atmospheres and the 25° value $B = 2885$ atm. from Gibson[14] is used. The viscosity

(1) This work represents results of research under joint sponsorship of the Office of Naval Research, Contract Nonr 2216 (05) and the Division of Physical Chemistry, Commonwealth Scientific and Industrial Research Organization, Melbourne, Australia. Contribution from Scripps Institution of Oceanography, New Series.

(2) R. W. Leonard, *J. Acoust. Soc. Am.*, **20**, 254 (1948).

(3) K. Tamm and G. Kurtze, *Acustica*, **3**, 33 (1953).

(4) M. Eigen, *Discussions Faraday Soc.*, **24**, 25 (1957).

(5) L. N. Liebermann, *Phys. Rev.*, **76**, 1520 (1949).

(6) D. A. Bies, *J. Chem. Phys.*, **23**, 428 (1955).

(7) G. S. Verma, *Rev. Mod. Phys.*, **31**, 1052 (1959).

(8) B. B. Owen and S. R. Brinkley, *Chem. Rev.*, **29**, 461 (1941).

(9) S. D. Hamann and W. Strauss, *Trans. Faraday Soc.*, **51**, 1684 (1955).

(10) (a) M. Eigen, *Z. Physik. Chem.* (Frankfurt), **1**, 176 (1954); (b) E. H. Carnevale and T. A. Litovitz, *J. Acoust. Soc. Am.*, **30**, 610 (1958).

(11) Because of an error in concentration $(\Delta V)^2$ reported by Bies was a factor of 10^3 low. The corrected value is $(\Delta V)^2 = 10$ (cc./mole)^2.

(12) W. G. Davies, R. J. Otter, and J. E. Prue, *Discussions Faraday Soc.*, **24**, 103 (1957).

(13) B. B. Owen and S. R. Brinkley, *Phys. Rev.*, **64**, 32 (1943).

(14) R. E. Gibson, *J. Am. Chem. Soc.*, **56**, 4 (1934).

data were interpolated graphically from the measurements of Bridgman[15] and the ratio of densities ρ_r was calculated from Dorsey.[16] The value $\alpha = 14.28$ at atmospheric pressure is that used by Robinson and Stokes[17]; it decreases as a function of pressure, varying inversely as the dielectric constant.

TABLE I

CONSTANTS FOR WATER AS A FUNCTION OF PRESSURE AT 25°

P, atm.	ϵ	ϵT	$(\epsilon T)^{1/2}$	$(\epsilon T)^{3/2} \times 10^{-6}$	η (poise)	ρ_r
1	78.54	23,417	153.0	3.583	0.008937	1.0000
500	80.81	24,094	155.2	3.739	.009014	1.0220
1000	82.88	24,712	157.2	3.885	.009132	1.0416
1500	84.80	25,284	159.0	4.020	.009314	1.0595
2000	86.57	25,812	160.7	4.148	.009604	1.0758

TABLE II

CONDUCTIVITY AND ACTIVITY COEFFICIENT EQUATION CONSTANTS AS A FUNCTION OF PRESSURE FOR AQUEOUS SOLUTIONS AT 25° IN THE EQUATIONS

$$\Lambda_p = \Lambda_p^0 - \left[\frac{R\Lambda_p^0}{1 + B\mathring{a}\sqrt{I/2}} + E\right]\frac{\sqrt{I}}{1 + B\mathring{a}\sqrt{I}}$$

$$-\log f = \frac{A|z_1 z_2|\sqrt{I}}{1 + B\mathring{a}\sqrt{I}}$$

P, atm.	R	E	B	A	$\mathring{a}$ $MgSO_4$
1	0.9157	120.64	0.3286	0.5092	14.28
500	.8775	117.9	.3239	.4880	13.88
1000	.8445	114.8	.3198	.4696	13.53
1500	.8161	111.4	.3162	.4538	13.23
2000	.7910	106.9	.3129	.4398	12.95

Experimental

Apparatus.—The apparatus was essentially that described by Ellis.[18] The conductivity cell consisted of a cylindrical Teflon tube closed at one end; a sliding Teflon plug inserted at the other end of the cell supported the electrodes, transmitted the pressure, and isolated the conductivity cell from white paraffin oil used in the pressure vessel. Heavy platinum wire pins were mounted parallel to the axis of the cylindrical plug and went all the way through it to provide electrical contact with the electrodes. Corrections to the cell constant as a function of pressure due to compression of the Teflon were obtained by comparing potassium chloride conductivity results. These were obtained with a sliding plug in which one electrode was supported by heavy platinum wire as above; the other electrode was supported by a glass rod located at the edge of both electrodes and whose axis was perpendicular to the plane of both electrodes and perpendicular to the axis of the cylindrical plug. A fine platinum wire provided electrical contact between the glass supported electrode and a shorter heavy platinum wire mounted in the sliding plug. Corrections for the solubility of the glass were made assuming the rate of solution or the change in conductivity $\Delta\kappa$ proportional to pressure and time, $\Delta\kappa = \Sigma\alpha Pt$, where α is assumed to be independent of pressure. A Wayne–Kerr universal bridge B221 was used for measuring conductance. The effects of series lead resistance and shunt resistance of the hydraulic oil as a function of pressure were measured; corrections for the 0.2 ohm series lead resistance were made where necessary. The temperature was 25 ± 0.05°.

Materials and Method.—Aqueous solutions of potassium chloride, potassium sulfate, magnesium chloride, and magnesium sulfate were prepared from analytical grade reagents. Conductivities of these salts were measured at three concentrations and for magnesium sulfate, for two additional concentrations. Solvent conductivity corrections were made using experimentally measured values. Measured equivalent conductivities and calculated values at infinite dilution as a function of pressure were obtained as follows.

1. **Water Conductivity Correction.**—Subtract water conductance measured in same cell at same pressure.

$$\kappa'_{salt} - \kappa'_{H_2O} = \kappa'_{salt - H_2O}$$

2. **Specific Conductivity.**—Multiply water corrected conductance by pressure dependent cell constant to get specific conductivity as a function of pressure; cell constant was measured for each concentration.

$$(\kappa'_{salt - H_2O})L_p = \kappa_p$$

Pressure dependence of cell constant for the Teflon cell was determined by comparing 0.02 M KCl data in the Teflon cell with 0.01 M KCl data for the cell with a glass bar. It is assumed that Λ_p/Λ_1 for KCl is independent of concentration.[19]

TABLE III

Λ_p/Λ_1 FOR AQUEOUS SOLUTIONS AT 25°

C is atmospheric pressure concentration in moles/l.

	$C \times 10^4$	P, atm. 500	1000	1500	2000
$MgSO_4$	5.000	1.025	1.033	1.030	1.021
	10.01	1.028	1.041	1.040	1.033
	20.00	1.033	1.050	1.055	1.050
	100.1	1.051	1.083	1.098	1.104
	200.0	1.058	1.094	1.116	1.126
K_2SO_4	5.000	1.015	1.016	1.007	0.995
	20.00	1.016	1.017	1.011	0.998
	220.6	1.021	1.029	1.026	1.018
$MgCl_2$	5.000	1.019	1.023	1.015	0.999
	20.000	1.021	1.024	1.019	1.005
	200.7	1.023	1.029	1.025	1.014
KCl	5.000	1.015	1.018	1.010	0.996
	20.00	1.015	1.016	1.008	.994
	99.99	1.016	1.018	1.010	.996
	200.0	1.016	1.018	1.012	.998

3. **Ratio of Equivalent Conductivities.**—Divide $(\kappa_p/\kappa_1) = (\Lambda_p\rho_r/\Lambda_1)$ by ρ_r to get (Λ_p/Λ_1) for each pressure at each concentration. Plot (Λ_p/Λ_1) for each pressure *vs.* the square root of the molality, extrapolate to find $(\Lambda_p^0/\Lambda_1^0)$, and multiply by respective conductivities at infinite dilution. For $MgSO_4$, calculate Λ_p^0/Λ_1^0 according to the equation

$$[\Lambda_p^0]MgSO_4 = [\Lambda_p^0]K_2SO_4 + [\Lambda_p^0]MgCl_2 - [\Lambda_p^0]KCl$$

where

$$\Lambda_p^0 = \Lambda_1^0(\Lambda_p^0/\Lambda_1^0)$$

Results

The values of Λ_p/Λ_1 for all the salts used are listed in Table III. Equivalent conductance for $MgSO_4$ is listed in Table IV and equivalent conductances at infinite dilution are presented in Table V. The dissociation constants, K_m, and degree of association $(1 - \alpha)$ calculated using eq. 2, 3, and 4 are shown in Tables VI and VII for each concentration as a function of pressure; the $\Delta\bar{V}^0$

(15) P. W. Bridgman, "Physics of High Pressure," Bell and Sons, 1949.

(16) E. N. Dorsey, "Properties of Ordinary Water Substance," Reinhold Publ. Co., New York, N. Y., 1940.

(17) R. A. Robinson and R. H. Stokes, "Electrolyte Solutions," Butterworths, London, 1955, p. 401.

(18) A. J. Ellis, *J. Chem. Soc.*, 3689 (1959).

(19) The deviations of Λ_p/Λ_1 in Table III are within the limits of experimental error.

values were obtained graphically from the slope of log K_m plotted against pressure and are listed in Table VI. Although the 0.0005 molar value of $\Delta\bar{V}^0$ is much less than the other values, it is included in the average $\Delta\bar{V}^0 = -7.3$ cc./mole.

Note the change in the concentration dependence of K_m as the pressure increases; the variations in K_m decrease as pressure increases and K_m shows a slight dip at the two highest pressures.

TABLE IV

Λ_p FOR AQUEOUS $MgSO_4$ SOLUTIONS AT 25°

C is atmospheric pressure concentration in moles/l.

	P, atm.				
$C \times 10^4$	1	500	1000	1500	2000
5.000	116.6[a]	119.5	120.4	120.1	119.0
10.01	109.6[a]	112.7	114.1	114.0	113.2
20.00	101.3[b]	104.6	106.4	106.9	106.4
100.1	78.6	82.6	85.1	86.3	86.8
200.0	69.0	73.0	75.5	77.0	77.7

[a] Taken from Dunsmore and James. [b] Av. between extrapolated value from Dunsmore and James and this work.

TABLE V

Λ_p^0 FOR AQUEOUS SOLUTIONS AT 25°

	P, atm.				
	1	500	1000	1500	2000
K_2SO_4	(153.52)	155.7	155.8	154.0	152.1
$MgCl_2$	(129.40)	131.6	132.2	130.7	128.4
KCl	(149.85)	152.2	152.5	151.3	149.3
$MgSO_4$	(133.07)	135.1	135.5	133.4	131.2

TABLE VI

MOLAL DISSOCIATION CONSTANT, K_m, AND $\Delta\bar{V}^0$ FOR AQUEOUS $MgSO_4$ AT 25°

C is atmospheric pressure concentration in moles/l.

ΔV^0,	C	P, atm.				
cc./mole	$\times 10^4$	1	500	1000	1500	2000
−8.5	5.000	0.0047	0.0054	0.0058	0.0078	0.0091
−7.0	10.01	.0048	.0055	.0062	.0075	.0086
−7.0	20.00	.0052	.0059	.0066	.0080	.0090
−7.3	100.1	.0063	.0073	.0083	.0097	.0111
−6.9	200.0	.0071	.0079	.0094	.0109	.0123
−7.3 Av.						

TABLE VII

DEGREE OF ASSOCIATION $(1 - \alpha)$ FOR AQUEOUS $MgSO_4$ AT 25°

C is atmospheric pressure concentration in moles/l.

	P, atm.				
$C \times 10^4$	1	500	1000	1500	2000
5.000	0.067	0.059	0.056	0.043	0.037
10.01	.107	.096	.089	.075	.068
20.00	.158	.144	.133	.115	.105
100.1	.314	.290	.271	.248	.230
200.0	.386	.360	.340	.315	.297

At the lowest concentration and the highest pressure, the value of $\Delta\bar{V}^0$ is very sensitive to the change in $\mathring{a}$ as a function of pressure because $(1 - \alpha)$ is very small, as shown in Table VII. Errors in the conductivity measurement, of course, have a large effect of the value of $(1 - \alpha)$, especially at the lowest concentration.

Original data and cell constants are listed in the Appendix. Results obtained in this work for 0.009999 M KCl are compared with those obtained by Ellis[18] in Table VIII. Results interpolated for 0.01 M K_2SO_4 from this work are compared with those obtained by Adams and Hall[20] in Table IX. Results obtained in this work for 0.01 KCl also are compared with values reported by Adams and Hall[20] in Table X. This work shows smaller differences with the results of Adams and Hall than with those of Ellis. The average deviation of these results from those of Adams and Hall is under 0.4% and with those of Ellis over 0.6%. The error in Λ shows up in the equilibrium constant almost completely in the $(1 - \alpha)$ term. For this type of experiment, Hamann estimated that accuracy was about ±0.3% in Λ_p/Λ_1.

For the 0.0005 M solution at 2000 atm., the effect of an error of ±0.4% in the conductivity will cause $\Delta\bar{V}^0$ to vary by approximately 1 cc./mole. The data at low concentration are not accurate enough to enable us to say anything about a possible concentration dependence of $\Delta\bar{V}^0$. The average of all five concentrations and the average deviation are

$$\Delta\bar{V}^0 = -7.3 \pm 0.4 \text{ cc./mole}$$

TABLE VIII

$\Lambda_p\rho_r/\Lambda_1$ FOR 0.009999 M KCl, 25°

P, atm.	Ellis	Fisher
500	1.031	1.038
1000	1.052	1.060
2000	1.068	1.072

TABLE IX

$\Lambda_p\rho_r/\Lambda_1$ FOR 0.01 M K_2SO_4, 25°

P, atm.	Adams and Hall	Fisher
500	1.0381	1.041
1000	1.0644	1.065
2000	1.0894	1.084

TABLE X

$\Lambda_p\rho_r/\Lambda_1$ FOR 0.02 M NaCl, 25°

P, atm.	Adams and Hall	Fisher
500	1.0343	1.039
1000	1.0566	1.060
2000	1.0727	1.070

Using the value $\bar{V}_2^0 = -6.4$ cc./mole for $MgSO_4$,[14] the partial molal volume of the state which dissociates into ions is $+0.9 \pm 0.4$ cc./mole.

Conclusions

The value $\Delta\bar{V}^0 = -7.3$ cc./mole does not agree by a factor of two with that deduced by Bies[6] on the assumption that a pressure dependent dissociation reaction is responsible for sound absorption.

It also disagrees with the values of $\Delta\bar{V}^0$ of −15 to −20 cc./mole quoted by Eigen, Kurtze, and Tamm.[21]

The authors indicate that $\Delta\bar{V}^0$ which appears in eq. 1 is not the same one which appears in the sound absorption equation. However, they say that for concentrations below 0.02 M, the difference between the two is less than 0.7 cc./mole. These authors explicitly showed the relationship

(20) L. H. Adams and R. E. Hall, *J. Phys. Chem.*, **35**, 2145 (1931).
(21) M. Eigen, G. Kurtze, and K. Tamm, *Z. Elektrochem.*, **57**, 114, 118 (1953).

between density and sound absorption data in terms of α and $\Delta\bar{V}^0$, but did not have conductivity data available to provide an independent measurement of $\Delta\bar{V}^0$.[22]

The reasons for the discrepancies are not clear at this time. Although hydrolysis corrections were not applied in determining equivalent conductivity for $MgSO_4$ as Owen and Gurry[23] did for $ZnSO_4$ and $CuSO_4$, the maximum values of their corrections are small at atmospheric pressure (0.2 and 0.8 conductance unit, respectively) and if relatively pressure independent, these corrections would not affect the $\Delta\bar{V}^0$ values significantly.

It may be, as Eigen[4] suggests, that observed sound absorption relaxation effects are due to intermediate reactions preceding dissociation into ions and that the lower relaxation frequency $f \sim 10^5$ c.p.s. which Bies[6] observed is associated with an intermediate chemical reaction. On the basis of another model, Fisher[24] calculated from density and sound absorption data values of degree of dissociation which agreed with conductivity data within 5%; one assumption was that the partial molal volume of the intermediate state preceding dissociation was zero, an assumption to which this work gives support.

Whatever the final interpretation of the mechanism of sound absorption, it is necessary to have quantitative values of partial molal volumes in order to check the theory.

The calculations of $\Delta\bar{V}^0$ made herein are based on a particular equation from electrolyte theory, the selection of the closest distance of approach of ions, and the assumption that it varies inversely with the dielectric constant as pressure increases. Changes in the theory will undoubtedly affect the value of $\Delta\bar{V}^0$. If the simpler Onsager–Debye–Hückel equation is used, the values of $\Delta\bar{V}^0$ are about -10 cc./mole and show no concentration dependence. However, new values can be calculated from the data presented here. Changes in α due to changes in closest distance of approach were shown by Davies, Otter, and Prue[13] to be very small, 0.4% at 0.0004 mole/l. as $\mathring{a}$ varied from 10 to 14 Å.[25]

The type of work reported here also will be of use in evaluating the theoretical equations giving the pressure dependence of activity coefficients.

Acknowledgment.—The author wishes to thank Dr. S. D. Hamman, Chief of the Division of Physical Chemistry of C.S.I.R.O., Fisherman's Bend, Melbourne, Australia, for his stimulating help and keen interest in this work and for his most generous coöperation in making his high pressure equipment available and ready for these measurements. Without his help it would not have been possible to do this work in the short time allotted. The author also wishes to thank the Office of Naval Research and the Director of the Marine Physical Laboratory, Dr. F. N. Spiess, for making it possible to do this work.

(22) M. Eigen and K. Tamm, *J. Phys. Chem.*, **66**, 93 (1962), propose a multistate dissociation model in which volume changes obtained acoustically and by conductivity methods are related but are not numerically the same.

(23) B. B. Owen and R. W. Gurry, *J. Am. Chem. Soc.*, **60**, 3074 (1938).

(24) F. H. Fisher, Marine Physical Laboratory Technical Memorandum 113, University of California, Marine Physical Laboratory of the Scripps Institution of Oceanography, 1960.

(25) At the highest concentration, $m = 0.02$, the effect of reducing the $\mathring{a}$-parameter by a factor of three resulted in a decrease of $\Delta\bar{V}$ from -6.9 to -9.4 cc./mole.

Appendix A

Cell Constants

To find cell constant, L_p, at pressure P multiply atmospheric pressure value L_1 by L_p*

P, atm.	L_p*
500	0.995
1000	.990
1500	.985
2000	.980

Salt	Concn., moles/l.	L_1
$MgSO_4$	0.0005000	0.686
	.001001	.719
	.002000	.723
	.01001	.719
	.02000	.732
K_2SO_4	.0005000	.696
	.002000	.699
	.02207	.732
$MgCl_2$	.0005000	.696
	.002000	.699
	.02007	.732

Appendix B

Copy of original conductivity data measured for electrolytes at 25° in aqueous solutions; Teflon cell without glass bar

	P, atm.					
	1	478	985	1495	2001	1[a]
0.02 *M* KCl, mmho	3.774	3.932	4.040	4.102	4.132	3.770
0.02 *M* $MgSO_4$, mmho	3.766	4.082	4.330	4.517	4.656	3.763
0.02207 *M* K_2SO_4, mmho	7.163	7.501	7.746	7.909	8.006	7.137
0.02007 *M* $MgCl_2$, mmho	5.699	5.981	6.6167	6.286	6.347	5.699
0.002 *M*						
KCl, μmho	404.6	421.5	433.0	439.9	443.1	404.0
$MgSO_4$	566.6	600.8	626.2	643.3	654.7	565.1
K_2SO_4	805.8	839.4	862.2	876.7	884.6	807.2
$MgCl_2$	684.5	716.2	738.2	751.0	757.3	682.7
0.0005 *M*						
KCl, μmho	108.8	113.6	117.2	119.5	120.8	108.9
$MgSO_4$	168.0	176.9	183.2	187.4	190.1	167.8
K_2SO_4	205.0	213.6	219.7	223.1	225.7	205.4
$MgCl_2$	174.4	182.5	188.3	191.6	193.3	174.5
0.01001 *M* $MgSO_4$, mmho	2.188	2.358	2.490	2.584	2.653	2.186
0.00100 *M* $MgSO_4$, μmho	308.2	325.4	337.7	346.0	351.1	3.082
Water, μmho	1.1	1.5	1.9	2.5	3.1	
Series lead resitance, ohm	0.2	0.2	0.2	0.2	0.2	

[a] The readings in this column were obtained the day after the pressure run was made.

Appendix C

Notation

$$A = \frac{1.8246 \times 10^6}{(\epsilon T)^{3/2}}$$

$$B = \frac{5.209 \times 10^9}{(\epsilon T)^{1/2}}$$

$$E = \frac{41.25(|z_1| + |z_2|)}{\eta(\epsilon T)^{1/2}}$$

$$R = \frac{2.801 \times 10^6 |z_1 z_2| q}{(\epsilon T)^{3/2}(1 + \sqrt{q})}$$

$\mathring{a}$ = 14.28, Bjerrum critical distance in Ångstroms for a 2:2 electrolyte in water at 25°. This varies as a function of pressure

c = concentration in moles/l.

m = concentration in moles of solute/kg. of solvent

q = $^1/_2$ for symmetrical electrolytes, $z_1 = z_2$; $z_1 = z_2 = 2$ for $MgSO_4$

I = $4c\alpha$, ionic strength of 2–2 salt

T = absolute temperature

α = degree of dissociation

ϵ = dielectric constant

η = viscosity

ρ_r = relative density of water

THE RADIOLYSIS OF SATURATED HYDROCARBONS

By T. J. Hardwick

Gulf Research & Development Company, Pittsburgh 30, Pennsylvania

Received February 21, 1962

The yields of primary products in the radiolysis of some twenty saturated hydrocarbons (C_5–C_{10}) have been measured. For all paraffins investigated, the yield of "molecular" hydrogen gas is approximately a constant fraction of the total hydrogen gas (0.40) despite changes in hydrocarbon structure and total hydrogen gas yield. Evidence is presented which indicates that this "molecular" hydrogen arises by a "hot" hydrogen atom mechanism rather than by a molecular detachment process. The balance of the hydrogen gas formed arises from the reaction of radiolytically produced chemical hydrogen atoms with the solvent. Congruent "molecular" unsaturation (olefins of the same carbon number produced in the presence of alkyl radical scavengers) ranges from 50–80% of the "molecular" hydrogen yield. Radicals produced by C–C bond scission interact within the cage of formation by disproportionation or recombination, or may escape from the cage to react with other radicals or solutes. Yields of such freely diffusing radicals have been measured, and a definite relation to chemical structure has been found. The results for all hydrocarbons studied are in complete agreement with the mechanism previously postulated for saturated hydrocarbon radiolysis. Determinations of free radical yields by e.p.r. give results in good agreement with other methods.

Introduction

From previous studies on the mechanism of the radiolysis of saturated hydrocarbons (hereinafter called paraffins, to include both alkanes and naphthenes), it appears that two types of processes occur, often giving identical products. The first forms stable, identifiable products by a mechanism which is uninfluenced by small concentrations (< 2%) of solute. The second forms hydrogen atom and/or alkyl radical intermediates, the subsequent reactions of which are controlled by diffusion processes and the types of added solute, if any. These radical intermediates may react with themselves, with irradiation products, or with added solutes, eventually giving stable products.

It is one purpose of this paper to distinguish between these two types of processes. For the first process, experiments are designed to investigate the mechanism. For the second process, measurements of the radical yields and some indication of their subsequent reactions will be given. This has been done for some twenty paraffins, normally liquid at room temperatures.

In a previous paper,[1] a sequence of reactions was postulated for the radiolysis of *n*-hexane, and as will be shown later, this reaction scheme is generally applicable to all liquid paraffins.

Three primary processes account for most of the initial radiolytic reactions[2]

$$RH \overset{G_1}{\rightsquigarrow} H_2 + \text{products} \qquad (1)$$

$$RH \overset{G_2}{\rightsquigarrow} H + R \qquad (2)$$

$$RH \overset{G_R}{\rightsquigarrow} R_a + R_b \qquad (R)$$

Reaction 1 produces hydrogen gas, plus other products, in yield G_1 by reactions unaffected by the presence of scavengers. Reaction 2, with yield G_2, is a simple C–H bond scission giving a freely diffusing hydrogen atom and an alkyl radical. In reaction R, C–C bond splitting gives two alkyl radicals. The interaction of these radicals with themselves and with solutes gives rise to stable products.

It has been shown that the hydrogen atom, produced by reaction 2, reacts competitively with solvent (RH) by hydrogen abstraction (3) or with solutes by addition (4) or hydrogen abstraction (5).

$$H + RH \overset{k_3}{\longrightarrow} H_2 + R \qquad (3)$$

$$H + S \overset{k_4}{\longrightarrow} HS \qquad (4)$$

$$H + S \overset{k_5}{\longrightarrow} H_2 + R' \qquad (5)$$

From the kinetics it is possible to determine the yields of reactions 1 and 2 (G_1 and G_2) from a measurement of the decrease in radiolytic hydrogen gas yield as a function of solute concentration.[1,3]

Experimental

Materials.—All paraffins were Phillips pure grade. They were further purified by prolonged stirring with con-

(1) T. J. Hardwick, *J. Phys. Chem.*, **64**, 1623 (1960).

(2) The nomenclature used in this paper is that employed previously.[1] Where necessary, new definitions of quantities have been made.

(3) T. J. Hardwick, *J. Phys. Chem.*, **65**, 101 (1961).

centrated sulfuric acid until the unsaturation content was sufficiently low for use. In all cases the unsaturation of the purified stock material was measured by bromination. An indication of the purity is found in the first column, Table II.

Aromatics were pure grade; olefins present in them were removed by silica gel. Other reagents used in solution make-up were the best grade available. For unsaturation analysis all materials were reagent grade.

Diphenylpicrylhydrazil (DPPH) was obtained from K and K Laboratories. Coppinger's radical (COP)[4] was kindly prepared by Dr. H. O. Strange of the Product Development Division. The e.p.r. rating agreed well with previous batches and measured 98–102% radical.

Hydrogen Yields.—The method for determining hydrogen gas yields has been described in detail previously.[1,3] Briefly, 100 ml. of deaerated solution was irradiated with X-rays to about 20 krads, and the hydrogen gas was removed, isolated, and measured on a McLeod gage. The energy absorbed by the samples was concurrently monitored using a Fricke dosimeter.

Unsaturation.—Irradiations were made in an all-stainless steel circulating loop of 400 ml. capacity, using a spot beam of electrons.[5] Samples were irradiated in an atmosphere of nitrogen. Unsaturation was measured by the uptake of bromine in acetic acid medium. Conversion of the excess bromine to iodine before titration enabled the excess to be measured by the more precise iodometric method.

"Initial" Unsaturation.—Measurements were made to determine the initial unsaturation yield arising from congruent olefins.[6] It was necessary, however, to remove lower boiling olefins resulting from C–C bond scission; otherwise, a spuriously high value would have been obtained. This was accomplished by fractional distillation, wherein a paraffin of appropriate boiling point was added to improve the separation of the two classes of olefin. The amount of unsaturation in the residue, measured by bromination, was taken as the yield of congruent olefins. Distillations were made in duplicate or triplicate, giving a reproducibility of measurement of ±2%. As an illustration of the efficiency of separation, no measurable olefin was found in the forerun of the following mixtures: (a) pentane–hexene-2–*n*-hexane, (b) hexane–2-methylhexene-1–2,4-dimethylpentane; furthermore, in both cases the measured olefin content of the residue corresponded to that present initially within ±1%.

Molecular Unsaturation.—In order to measure the molecular unsaturation, a scavenger was needed to remove all radical intermediates. Solutions of paraffin containing 1.25% methacrylic acid were irradiated in the circulating loop in the same manner as the pure paraffin. A small amount of fluffy precipitate was formed, but the inclusion of this in the sample did not alter results. The irradiated sample was fractionated in the same manner as before, but after removal of the light hydrocarbons, the contents of the still pot were added to a steam distillation unit, made alkaline with 4 *N* NaOH, and steam distilled. The unsaturation of the organic distillate layer, measured by bromination, was taken as a measure of the molecular unsaturation.

Methane Yields.—Samples of pure paraffin and paraffin containing 1% methyl methacrylate (MMA) were prepared and irradiated in a manner identical to that for hydrogen gas measurements. The evolved gas was pumped by a Toepler pump through a trap at −100° and collected in a sample flask. Mass spectrometric measurements were made on the CH_4/H_2 ratio, and from the measured hydrogen yields, known from previous experiments, the methane yields were calculated. At least two runs were made for each hydrocarbon.

E.p.r. Measurements.—All e.p.r. measurements were made with a Varian Associates X-Band spectrometer, with a 6-in. magnet and rectangular resonant cavity. Relative intensities of COP were measured by taking derivative peak heights and comparing such numbers with the intensity obtained from a standard solution of DPPH (1 m*M*) in benzene. The ratio of COP intensity to that of DPPH should represent the relative concentrations of unpaired electrons. The e.p.r. signal intensity of standard solutions of COP in benzene, measured under standard conditions, was linear with the molar concentration of the radical at least up to concentrations of 25 m*M*. Stringent removal of oxygen was necessary to obtain reproducible results.

It was found difficult to prepare a standard solution of COP in many paraffin solvents, presumably due to traces of reactive impurities. Where marked deterioration in a solvent was evident, further purification steps were taken. As a further test, all solutions were stored for at least 5 days after preparation and before e.p.r. measurements. If less than 5% decay of the radical was observed in the succeeding 5 days, the samples were used in the radiolysis experiments.

Samples were prepared in the following manner. About 17 mg. of COP was placed in tubes, shown in Fig. 1a. A 5-ml. volume of purified solvent was pipetted into these tubes, filling the lower bulb about three-quarters full. The solution was degassed and sealed from the atmosphere at B, giving a tube suitable for irradiations (with the solution in the bulb) and e.p.r. measurements (with the solution in the narrow tube) as shown in Fig. 1b. The outside diameter of the glass in the narrow portion of the tube was close to 4.8 mm., the diameter of a circular hole in the resonance cavity. Irradiations were made using X-rays from a Van de Graaff accelerator. The rate of energy absorption, about 200 krads/hr., was measured by the Fricke dosimeter solution. The necessary corrections for energy absorption were made by comparing the electron densities of the paraffin and the dosimeter solution.

Once the zero-order kinetics were confirmed, the usual irradiations were such as to remove about 70% of the initial radical signal. The time between the final pre-irradiation e.p.r. measurement and the corresponding post irradiation measurement was always less than 2 days.

Separate experiments showed that the low exposure received by the upper end of the irradiated tubes had no noticeable effect on the e.p.r. signal in the region of measurement. To overcome any drifts in the instrument sensitivity, all e.p.r. results were normalized using a standard sample of DPPH which tests had shown to be invariant over several months. After radiolysis, the tubes were opened at the bottom, cleaned, and the narrow part filled with a standard solution of DPPH. Variations in the diameter of the tubes, with corresponding effects in the signal intensity, thus were measured directly, and corrections were applied.

Net changes were obtained in units of spins/cc. × constant/Mrad absorbed. The method for subsequent treatment of the data is found in the Results.

Results

Hydrogen Gas Yields.—The yields of hydrogen gas from the purified compounds ($G_{H_{2(0)}}$) are found in Table I. The low olefin content of the stock solutions made unnecessary any corrections to the hydrogen yield. The values of G_2 were determined by measuring the yield of radiolytic hydrogen gas ($G_{H_{2(S)}}$) for paraffins containing a range (0.1–0.7%/vol.) of methyl methacrylate (MMA) scavenger. For all paraffins the kinetic plot $1/(G_{H_{2(0)}} - G_{H_{2(S)}})$ $(= 1/\Delta G_{H_2})$ *vs.* (RH)/(S) gave a straight line, from whose intercept G_2 was obtained. Values of G_2 found in this manner are given in column 3, Table I; values of G_1, obtained by difference $(G_{H_{2(0)}} - G_2)$, are listed in the preceding column.

Unsaturation.—In measuring the initial congruent unsaturation, it is necessary to account for olefin disappearing by reactions 4 and 5; otherwise, low values will be obtained. In practice, a compromise must be found between producing sufficient olefin for analysis and minimizing the amount of olefin reacting with hydrogen atoms. Fortunately, data are available to make reliable corrections in the latter case.

(4) G. Coppinger, *J. Am. Chem. Soc.*, **79**, 501 (1957).

(5) W. S. Guentner and T. J. Hardwick, *Intern. J. Appl. Radiation Isotopes*, **13**, 98 (1962).

(6) The term "congruent" is used when referring to olefins or radicals having the same number of carbon atoms as the solvent; *e.g.*, hexene and hexyl radicals are the congruent olefins and radicals in hexane radiolysis.

TABLE I

HYDROGEN YIELDS FROM IRRADIATED PARAFFINS

	$G_{H_2(0)}$	G_1	G_2	$G_1/G_{H_2(0)}$
		Molecule/100 e.v.		
n-Pentane	6.35	2.10	4.25	0.33
n-Hexane	5.28	2.12	3.16	.40
n-Heptane	6.06	2.36	3.70	.39
n-Octane	6.18	2.85	3.33	.46
n-Nonane	6.05	2.52	3.53	.42
n-Decane	4.90	1.70	3.20	.35
2-Methylbutane	4.24	1.66	2.59	.39
2-Methylpentane	4.47	1.61	2.86	.36
3-Methylpentane	4.56	1.60	2.96	.35
Cyclopentane	5.78	2.72	3.06	.47
Cyclohexane	5.56	2.43	3.13	.44
Methylcyclopentane	4.62	1.99	2.63	.43
Methylcyclohexane	4.76	2.05	2.71	.43
1,2-Dimethylcyclohexane	3.78	1.68	2.10	.44
2,3-Dimethylbutane	4.02	1.69	2.33	.42
2,4-Dimethylpentane	4.19	1.59	2.60	.38
2,3,4-Trimethylpentane	2.96	1.21	1.75	.41
2,2-Dimethylbutane	3.12	1.16	1.96	.37
2,2,4-Trimethylpentane	2.91	1.24	1.67	.43
2,2,5-Trimethylhexane	2.70	1.16	1.54	.43

As part of the determination of G_2, data are obtained from which the rate of reaction of H atoms with the solvent hydrocarbon (k_3) can be expressed in absolute terms.[3] In other work reported elsewhere,[7] the reactivity of hydrogen atoms with olefins in paraffin solution has been determined. From such results it has been shown that for olefins produced by radiolysis $k_4 = 6.0 \times 10^{11}$ cc. mole^{-1} sec.$^{-1}$, $k_5 = 1.2 \times 10^{11}$ cc. mole^{-1} sec.$^{-1}$.

Knowing k_3, k_4, and k_5, one can determine for a given olefin concentration the fraction of the hydrogen atoms reacting with paraffin and olefin (f_3, f_4, f_5 for reactions 3, 4, and 5). Reaction 4 will remove the olefin to form an alkyl radical: reaction 5 will produce an alkenyl radical. Since alkenyl radicals react mostly by addition to alkyl radicals,[1] an olefin is the stable product, and no olefin is lost from the system. Alkyl radicals are produced to the same extent regardless of whether reaction 3 or 4 takes place.

Summing up the possible reactions, it can be shown that, except for the negligible effect of reaction 5 to reduce the alkyl radical concentration, the net result of reaction 4 is to remove one olefin molecule. A summation of the value of f_4 for a series of olefin concentrations (1, 3, 5 mM, etc.) was made, using the appropriate length of sum to correct for the total olefin produced. Final olefin concentrations ranged from 7–14 mM for *ca.* 50 j./g. of energy absorbed. The corrections resulting from reaction 4 varied from 1.5% for 2,3-dimethylbutane to 11% for *n*-pentane. Values of the initial congruent olefin yield (G_u) corrected for this olefin loss and for initial olefin content are listed in column 3, Table II.

In the separation preceding analysis, olefins were found in the forerun of the distillation in yields of 0.1–0.7 molecule/100 e.v., indicating that olefins of lower carbon number are formed.

(7) T. J. Hardwick, *J. Phys. Chem.*, **66**, 291 (1962).

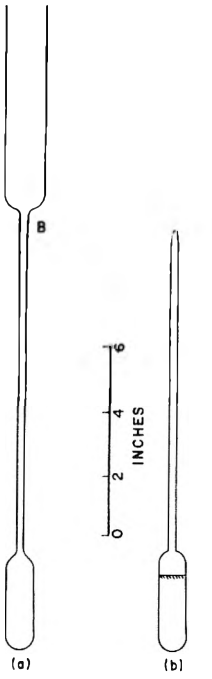

Fig. 1.—Cell for measuring the total radical yield by e.p.r.: (a) unfilled cell; (b) cell filled and sealed for radiolysis and measurement.

TABLE II

INITIAL AND "MOLECULAR" UNSATURATION IN IRRADIATED PARAFFINS

	Initial olefin content, mM	"Molecular" yield of congruent olefin (G_{1C})	Initial yield of congruent olefin (G_u)	$\frac{G_{1C}}{G_1}$	$\frac{(G_u - G_{1C})}{G_2}$
		Molecule/100 e.v.			
n-Pentane	0.11	1.42	4.07	0.68	0.62
n-Hexane	.10	1.47	3.30	.69	.58
n-Heptane	.12	1.51	3.43	.65	.52
n-Octane	.11	1.47	3.05	.52	.48
n-Nonane	.15	1.40	2.93	.55	.43
Isopentane	.16	1.27	3.35	.77	.80
2-Methylpentane	.09	1.12	2.78	.70	.58
3-Methylpentane	.18	0.87	2.11	.52	.42
2,4-Dimethylpentane	.31	1.24	2.62	.78	.53
2,3-Dimethylbutane	.23	1.09	2.52	.65	.61
2,2,4-Trimethylpentane	.31	1.00	1.92	.80	.55
Cyclopentane	.07	1.73	4.24	.64	.82
Methylcyclopentane	.21	1.67	3.89	.84	.84
Cyclohexane	.09	1.75	3.61	.72	.60
Methylcyclohexane	.18	1.15	3.09	.56	.56

Part of this congruent unsaturation is the so-called "molecular" unsaturation, the yield of which (G_{1C}) is unaffected by the presence of scavengers. The presence of a polymerizable monomer during paraffin radiolysis removes freely diffusing alkyl radicals which are normally precursors of olefins through disproportionation. Using acidic monomers, a steam distillation from alkaline solution separates the olefin from the monomer and polymer.

Preliminary experiments were made to determine the effect of type and concentration of monomer scavenger. Solutions of *n*-hexane containing 0.5, 1, 2, and 3%/vol. methacrylic acid (MAA) were irradiated to 100 j./g. After correcting for direct absorption of energy in the solute, G_{1C} was found to be 1.48 ± 0.03. Acrylic acid (AA) solutions in *n*-hexane, prepared and treated in the same way, gave G_{1C} = 1.45 ± 0.04. These results are in good agreement with those previously published using methyl methacrylate,[1] where G_{1C} = 1.47 ± 0.02. Methacrylic acid is preferred over the other monomers: separation is easier with an acid group, and less precipitate forms with MAA than with AA.

Irradiations were made with *n*-hexane–MAA solutions at doses ranging from 50–150 j./g. No change in G_{1C} was found. The low olefin concentration relative to that of the monomer makes a correction for olefin disappearance unnecessary. As standard procedure, 1.25%/vol. solutions of MAA in paraffin were irradiated.

In the preanalytical fractional distillations, olefin was found in the forerun in all cases, showing that olefins having fewer carbon atoms than the congruent one are formed by some process which is not associated with scavengeable free radicals. The yields of congruent unscavengeable olefins, G_{1C}, measured in this fashion are given in column 3, Table II.

Total Free Radical Yield (G_{TR}).—Preliminary tests made with four concentrations of COP in *n*-hexane showed that the free radical disappearance was truly zero order.

Our confidence in directly measuring the absolute concentration of COP in solution was not better than ±5%. Accordingly, an indirect method of measuring absolute yields (G_{-COP}) was required. Solutions of DPPH and COP in benzene and toluene were prepared and irradiated in the same manner as for paraffins.

In the case of the DPPH solutions, it was feasible to measure the change in DPPH concentration with good accuracy, and this result could be related to the absolute yield of the free radical disappearance (G_{-DPPH}). It was assumed that G_{-DPPH} is a true measure of the total radical yield. A comparison is made in Table III of the total radical yields (G_{TR}) in benzene and toluene determined by various experimental techniques. As can be seen, the values obtained in the present study agree well with previous results. Accordingly, considerable confidence has been placed in the e. p. r. method.

A further reasonable assumption was made: the disappearance of COP likewise measured G_{TR}. Experimentally one determines by e.p.r. some value proportional to the concentration of COP ($K \times$ [COP]). The change in concentration per Mrad $\Delta(K \times [COP])$/Mrad is related to the yield of COP disappeared (G_{-COP}). In comparing the change in COP concentration per Mrad for benzene and toluene, calibration factors cancel, and the ratio G_{-COP}(benzene)/G_{-COP}(toluene) (0.64) is in good agreement with the corresponding ratio for DPPH (0.626).

From such results the e.p.r. response for COP solutions could be related directly to the free radical concentration. Accordingly, G_{TR} could be determined directly for alkane solutions using COP as solute.

TABLE III

TOTAL RADICAL YIELD (G_{TR}) IN BENZENE AND TOLUENE RADIOLYSIS

Method of measurement	G_{TR} molecule/100 e.v.	Ref.
	Benzene	
Polymerization	0.74	8
	.78	9
Disappearance of DPPH (colorimetric)	.74	10
Reduction of ferric ion	.78	11
Disappearance of DPPH (e.p.r.)	.77	This work
	Toluene	
Polymerization	1.1	8
	1.2	12
Disappearance of DPPH (colorimetric)	1.1	13
Disappearance of DPPH (e.p.r.)	1.23	This work

Although hydrogen atoms react rapidly with COP ($k_4 = 1.0 \times 10^{13}$ mole^{-1} sec.$^{-1}$) a considerable fraction of them will react with the solvent. This, however, produces another radical, which in turn reacts with COP. This secondary formation of radicals has no effect on the net change of COP concentration as measured by the e.p.r. method.

Total radical yields (G_{TR}) for a series of paraffins are shown in Table IV. One striking result is that for the alkanes, the total number of radicals formed lies in a small range, 7.8–9.5, and is reasonably independent of structure. Cycloalkanes, as a group, show similar yields (6.7–7.7).

Scission of a C–H bond produces atomic hydrogen, and the yield of this intermediate has been accurately measured (G_2). The total yield of radicals from a C–H bond split is therefore $2G_2$, and values of this are shown in the second column of Table IV. The yield of radicals formed from a C–C bond scission ($2G_R$) is $G_{TR} - 2G_2$, and such values are shown in column 3, Table IV.

The paraffins listed in Table IV have been grouped according to general chemical structure, *n*-alkanes, singly branched methylalkanes, etc. The extent of radical formation from C–C bond scission is clearly related to the chemical structure. As has been suggested before,[14] the greater the branching, the greater the number of radicals formed by C–C bond scission.

The ratio $2G_R/G_{TR}$ (column 4, Table IV) is the fraction of the total radicals which are formed by C–C bond scission. The similarity of this ratio within each structural type is quite marked, and permits a more sensible grouping according to structure; *e.g.*, 1,2-dimethylcyclohexane is classed with 2,3-dimethylalkanes rather than with methylcycloalkanes. The agreement within each struc-

(8) A. Chapiro, *J. chim. phys.*, **47**, 747, 764 (1950).
(9) C. Cousin, Thesis, University of Paris, 1953.
(10) L. Bouby and A. Chapiro, *J. chim. phys.*, **52**, 645 (1955).
(11) E. A. Chermak, E. Collinson, F. S. Dainton, and G. M. Meaburn, *Proc. Chem. Soc.*, 54 (1958).
(12) W. H. Seitzer and A. V. Tobolsky, *J. Am. Chem. Soc.*, **77**, 2687 (1955).
(13) N. Gilson, reported by A. Chapiro, *J. Phys. Chem.*, **63**, 801 (1959).
(14) H. A. Dewhurst, *J. Am. Chem. Soc.*, **80**, 5607 (1958).

TABLE IV

TOTAL RADICAL YIELDS (G_{TR}) AS MEASURED BY E.P.R.

	G_{TR}	$2G_2$	$2G_R$	$2G_R/G_{TR}$	
	Molecule/100 e.v.				
n-Pentane	8.7	8.50	0.2		
n-Hexane	7.8	6.32	1.5	0.19	
n-Heptane	9.1	7.40	1.7	.19	0.20
n-Octane	8.3	6.66	1.6	.19	
n-Nonane	9.4	7.06	2.3	.23	
n-Decane	8.9	6.40	2.5	.28	
2-Methylbutane	7.9	5.18	2.7	.34	
2-Methylpentane	8.5	5.72	2.8	.33	0.33
3-Methylpentane	8.7	5.92	2.8	.32	
Methylcyclopentane	6.9	5.26	1.6	.23	0.23
Methylcyclohexane	6.9	5.42	1.5	.22	
2,4-Dimethylpentane	9.3	5.20	4.1	.44	
2,3-Dimethylbutane	9.2	4.66	4.5	.49	0.50
1,2-Dimethylcyclohexane	6.7	3.34	3.4	.51	
2,3,4-Trimethylpentane	8.1	3.50	4.5	.55	
2,2-Dimethylbutane	9.5	3.92	5.6	.59	
2,2,4-Trimethylpentane	8.9	3.34	5.6	.63	0.63
2,2,5-Trimethylhexane	8.9	3.08	5.8	.65	
Cyclopentane	6.5	6.12	0.4		
Cyclohexane	7.7	6.26	1.4		

tural group is quite striking, and provides a measure of the relative number of radicals arising from C–H and C–C bond ruptures which is independent of the total radical yield.

It should be remembered that the ratio $2G_R/G_{TR}$ refers to *free radicals* only, and not to the total number of bonds broken. The ratio offers assistance in establishing that paraffins of similar structure will break down in similar fashion during radiolysis.

Although the number of C–C bond ruptures are in the main consistent with structure, there are three cases which merit further comment. The value of $2G_R = 0.2$ for *n*-pentane is obviously wrong, but measurements of both the total radical yield and the hydrogen yields give consistent results. However, a recent measurement of the radical production in *n*-pentane, using a novel scavenging technique,[15] gives a total radical yield of 10.13/100 e.v.; $2G_R/G_{TR}$ is therefore 0.16 for *n*-pentane, in good agreement with the values for other *n*-alkanes.

Cyclopentane produces radicals by a C–C bond split ($G_R = 0.2$). Such a value would be consistent with a very low probability of ring opening on cyclopentane radiolysis. Cyclohexane, on the other hand, produces 1.6 radicals by C–C bond rupture. Evidence is accumulating[16] that hexene and other straight chain products are formed on radiolysis, presumably through an intermediate biradical. As such a biradical is the normal consequence of ring opening, it may be that each event in the net result accounts for the disappearance of two COP radicals. Both hexene-1 and cyclohexylhexene are found among the products of pure cyclohexane radiolysis. The yield is sufficient to account for about 80% of the observed radicals, if the intermediate entities are scavenged by COP.

Methane Yields.—The radiolytic methane yields for several pure C_6 paraffins are shown in the first column, Table V. The second column gives the methane yield when the solution contained initially 1.25%/vol. (117 m*M*) methyl methacrylate monomer. Preliminary experiments showed no variation in methane yield with 0.5–3.0%/vol. monomer, although both the hydrogen gas yield and the methane/hydrogen ratio varied over the concentration range. The methane formed with monomer present, therefore, is considered to originate in some process which does not involve freely diffusing methyl radicals. Methane formed from scavengeable free radicals would therefore be the difference of these two measurements, and such values are given in column 3, Table V.

TABLE V

METHANE YIELDS IN C_6 PARAFFINS, WITH AND WITHOUT RADICAL SCAVENGER

	Methane yield, molecule/100 e.v.			Methyl radical yield,[a] molecule/100 e.v.
	Pure paraffin	Paraffin +1.25% MAA	Decrease in G_{CH_4} due to scavenger	
Cyclopentane	<0.02	<0.02		
Cyclohexane	< .05	< .05		
n-Hexane	.11	.03	0.08	0.08
Methylcyclopentane	.11	06	.05	
2-Methylpentane	.40	.18	.22	.27
3-Methylpentane	.30	.16	.14	.16
2,3-Dimethylbutane	.64	.37	.37	.34
Neohexane	1.63	.76	.87	.96

[a] R. H. Schuler, private communication.

Both with and without scavenger present, the results show that increased branching, particularly when two methyl groups are on the same carbon atom, gives higher methane yields. As expected, cyclohexane and cyclopentane produce no significant amount of methane.

Discussion

There are two types of processes occurring in liquid paraffin radiolysis: "molecular" processes and those involving freely diffusing free radicals. Although in many instances the same products are formed in both processes, it is convenient to discuss them separately.

"Molecular" Processes.—The "molecular" process (or processes), as it is defined experimentally, is a process which is not affected by the presence of small amounts (<2%) of highly reactive materials, particularly free radical scavengers. It is generally considered not to involve freely diffusing free fadicals. Since by its very nature one is presented with a *fait accompli*, direct investigation by modifying such a process by various means cannot be made. One can argue only by inference and by analogy.

"Molecular" Hydrogen.—As applied to the production of "molecular" hydrogen, four processes have been postulated to explain this "molecular"

(15) R. Holroyd and G. W. Klein. Presented at the Thirteenth Pittsburgh Conference on Analytical Chemistry and Applied Spectroscopy, Pittsburgh, Pennsylvania, March, 1962.

(16) (a) A. C. Nixon and R. E. Thorpe, *J. Chem. Phys.*, **28**, 1004 (1958); (b) G. R. Freeman, *ibid.*, **33**, 71 (1960); (c) P. J. Dyne, private communication.

process. (1) Molecular hydrogen is detached from the same molecule, leaving a biradical or olefin. (2) A hydrogen atom can be ejected from an excited solvent molecule with sufficient energy to react on collision with a neighboring molecule. For alkanes, hydrogen abstraction to form hydrogen gas is the expected reaction. (3) An excited molecule, produced by charge neutralization or direct excitation, can react with a nearest neighbor to give hydrogen gas and products in a Stern–Vollmer type of reaction. (4) Under certain conditions ion–molecule reactions may occur, the net result being the production of hydrogen gas.

None of these processes is necessarily exclusive, nor is there any inherent reason why all could not occur to some extent at the same time.

Molecular detachment of hydrogen gas from one molecule has been suggested as a "molecular" process, and indication of such a mechanism in the liquid phase has been found in the case of cyclohexane–cyclohexane-d_{12} mixtures.[17,18] In the gas phase, molecular detachment resulting from both photochemical[19,20] and ionizing radiation sources[21–23] appears to occur.

In such a process, however, the remaining fragment on alkane radiolysis must be an olefin or a biradical, which may (a) revert to an olefin by internal rearrangement, (b) decompose into a lighter olefin and alkane, or (c) abstract hydrogen from a nearby solvent molecule to produce a pair of alkyl radicals. If an olefin is formed exclusively, or if the biradical becomes an olefin, the yield of unscavenged olefin must be equal to the molecular hydrogen. As is apparent in Table II, this is not the case, for G_{1C} is always less than G_1.

The decomposition of the biradical into an olefin plus an alkane may be possible at room temperature. In the radiolysis of cyclohexane, a carbon–carbon bond split gives a dihexyl radical. Apparently this is converted into a hexane, for hexene-1 is a significant product in cyclohexane radiolysis[15,16]; methane, ethane, and propane are not.[16,24]

If, on the other hand, the biradical were to abstract hydrogen from a nearest neighbor, two alkyl radicals would be produced in a cage. These radicals would most likely add or disproportionate giving stable products, one of which is an olefin. If such a mechanism were to occur, it would be indistinguishable from the hot atom mechanism (*vide infra*).

Although evidence in the liquid phase is lacking, it appears that, in the gas phase at least, internal rearrangement of a biradical into an olefin is the normal process.[19]

The hot atom process, adopted from photochemical experiments[25,26] by Burton[27] and further developed by the present author,[1] requires that some of the hydrogen atoms ejected from the excited molecules have sufficient energy to react with a nearest neighbor on first collision. In alkanes, a hydrogen abstraction will occur, producing a hydrogen molecule and leaving two alkyl radicals resident in a solvent "cage." Reaction of these radicals by addition or disproportionation will occur, and as these radicals are most likely secondary or tertiary in nature, disproportionation is the more probable event. The net effect is to produce hydrogen gas, plus an equivalent amount of olefin plus saturated dimer.

Production of hydrogen gas by a Stern–Vollmer reaction or an ion–molecule reaction is not considered to be an event of major occurrence in liquid paraffin radiolysis. The yield of other products associated with such reactions, even their nature, cannot be predicted *a priori* from our present knowledge. In both cases, a restriction is set by the requirement of exothermicity, and probabilities of their occurrence will be markedly affected by structure. Since 35–45% of the total hydrogen yield arises by "molecular" reaction (Table I) despite considerable variations in structure, it is unlikely that either Stern–Vollmer or ion–molecule reactions occur in general to any significant extent in paraffin radiolysis.

The "molecular" process would therefore most likely occur by a hydrogen molecule detachment, a hot atom process, or both. An examination of the data in Table II shows that the yield of unscavengeable congruent olefin is 50–75% of the "molecular" hydrogen. Molecular hydrogen elimination therefore cannot account for all the molecular process, but may contribute to part of it.

The results in Table II are completely in keeping with those expected from a hot hydrogen atom process. The olefin is formed in the yield appropriate for disproportionation of secondary or tertiary congruent radicals. In systems where appropriate measurements have been made, saturated dimer is found initially despite the presence of alkyl radical scavengers.[28]

This semiquantitative agreement with predicted values does not prove that the hot atom process occurs exclusively. If, however, a molecular detachment process is taking place simultaneously, it will contribute only a minor fraction of the "molecular" hydrogen gas.

The results in the last column, Table I, show the rather remarkable feature that the fraction of hydrogen arising from "molecular" processes is approximately the same for all paraffins. A more detailed grouping is possible, for the mean value of $G_1/G_{H_2(0)}$ for alkanes is 0.39 ± 0.035, while the corresponding value for cycloalkanes is 0.44 ± 0.015. These results are significant in that this ratio is constant, despite a range of $G_{H_2(0)}$ from 2.7–6.3, and despite the great differences of paraffin structure within the groups. It is therefore reasonable to assume that one process only contributes to the

(17) P. J. Dyne and W. M. Jenkinson, *Can. J. Chem.*, **38**, 539 (1960).
(18) P. J. Dyne and W. M. Jenkinson, *ibid.*, **39**, 2163 (1961).
(19) H. Okabe and J. R. McNesby, *J. Chem. Phys.*, **34**, 668 (1961).
(20) M. C. Sauer, Jr., and L. M. Dorfman, *ibid.*, **35**, 497 (1961).
(21) L. J. Stief and P. Ausloos, *J. Phys. Chem.*, **65**, 1560 (1961).
(22) L. M. Dorfman, *ibid.*, **62**, 29 (1958).
(23) H. A. Dewhurst, *J. Am. Chem. Soc.*, **83**, 1050 (1961).
(24) W. S. Guentner, R. P. Nejak, and T. J. Hardwick, *J. Phys. Chem.*, **30**, 601 (1959).
(25) R. A. Ogg, Jr., and R. R. Williams, *J. Chem. Phys.*, **13**, 586 (1945).
(26) H. A. Schwarz, R. R. Williams, and W. H. Hamill, *J. Am. Chem. Soc.*, **74**, 6007 (1952).
(27) J. P. Manion and M. Burton, *J. Phys. Chem.*, **56**, 560 (1952).
(28) H. A. Dewhurst, *ibid.*, **63**, 813 (1959).

formation of "molecular" hydrogen, and that such a process is not affected by the chemical structure of the paraffin molecule.

The probability of eliminating a hydrogen molecule directly from an excited paraffin molecule almost certainly is related to the molecular structure of the paraffin. One would not expect, for example, that the same fraction of the total hydrogen gas should be produced unimolecularly from both *n*-hexane and 2,3,4-trimethylpentane.

The hot hydrogen atom process is a part of the general concept of events following the scission of a C–H bond. As the excited molecules will have a range of energies, so will the ejected hydrogen atoms. Those with sufficient energy will react on first collision (hot atom process); those with less energy will be slowed to thermal energies, where they will eventually react with solvent or solute.

"Molecular" Methane Yields.—Although most attention has been given to "molecular" processes involving hydrogen gas, other "molecular" processes, involving C–C bond scission, take place. Despite the addition of free radical scavengers, there is a persistent amount of lower molecular weight alkanes formed on paraffin radiolysis. The results in column 2, Table V, show that radiolytic formation of methane is never completely suppressed, despite large amounts of free radical scavenger. Methane, therefore, arises from two sources: (a) reaction of methyl radical with another freely diffusing radical or with a solvent molecule, and (b) by some molecular process.

The unimolecular decomposition of alkane molecules to give methane is not normally considered a low temperature or liquid phase process. Methyl radical formation is much the preferred method of decomposition.

The "molecular" production of methane is considered to occur in a manner similar to the molecular formation of the congruent olefin. When an excited molecule breaks by C–C split, the fragments are necessarily formed within the same solvent cage. Subsequently they may (a) diffuse out of the cage to become freely diffusing radicals, or (b) add to, or (c) disproportionate with each other. Reaction (b) (addition) gives the parent paraffin and no net reaction is observed. Reaction (c) gives an alkane and an olefin, the sum of whose molecular weights is that of the solvent.

Methyl radicals produced in this fashion may be caged with primary, secondary, or tertiary radicals, depending whether the paraffin was normal (hexane), methyl substituted (2- and 3-methylpentane), or dimethyl substituted on the same carbon atom (neohexane). Wijnen[29] has summarized evidence to show that methyl radicals react with *n*-alkyl radicals by addition rather than by disproportionation. The yield of "molecular" methane from irradiated *n*-alkane is accordingly low.

Free Radical Production.—In this section the term alkyl radicals refers to those alkyl radicals which diffuse freely through the solution, in contrast to those which interact within their solvent cage of formation.

(29) M. H. J. Wijnen, *J. Am. Chem. Soc.*, **83**, 3752 (1961).

C–H Bond Scission.—The yields of freely diffusing hydrogen atoms, G_2, formed on the radiolysis of paraffins, are found in Table I. In general, the greater the branching, the fewer the C–H bond splits.

The total yield of alkyl radicals produced will be the sum of (1) alkyl radicals formed complementarily to hydrogen atoms, (2) alkyl radicals produced by the reaction of hydrogen atoms with the solvent, and (3) those formed by C–C bond scission (total = $2(G_2 + G_R)$ initially). At high dose rates, such as occur with electron bombardments, these radicals react entirely with one another, by addition or disproportionation, giving, among other products, congruent olefins. The net amount of congruent olefin so produced from irradiated paraffin will be the total congruent unsaturation minus the congruent "molecular" unsaturation.

The data in the last two columns of Table II compare the ratios "molecular" olefin/"molecular" hydrogen gas (G_{1C}/G_1), and olefin formed by the disproportionation of the freely diffusing congruent alkyl radicals/number of congruent alkyl radicals ($(G_u - G_{1C})/G_2$). Considering for the moment *n*-alkanes, where the production of congruent olefins is less complicated, we find that the diffusion process produces olefins in 15 ± 5% lower yield than are formed by the "molecular" process.

In the "hot atom" process for *n*-alkanes, it is anticipated that alkyl radicals formed as intermediates would be almost entirely secondary. Freely diffusing radicals, on the other hand, would be only about 84% secondary (*vide infra*), the rest being primary radicals generated in a C–C bond scission. In this latter case, some primary–secondary alkyl interreaction will occur, resulting in a decrease in the extent of disproportionation, and this is, in fact, what is observed. Extension of such calculations to branched alkane radiolysis is not justified, for the congruent radicals will be both secondary and tertiary, while those formed on C–C bond scission will be of all three types.

Corresponding to the olefins formed by disproportionation is the saturated dimer product formed by addition of congruent radicals. Data for the initial yields of dimer are known accurately for only cyclohexane, where values of G_{dimer} = 2.0[28,30] were obtained. In the same system, Waight and Walker[31] found $G_{C_{12}}$ saturates = 2.2 ± 0.2, and Horner and Swallow[32] found 4.2 molecules of cyclohexane converted to polymer for each 100 e.v. absorbed. More recently Dyne and Stone,[33] in a very careful study of initial yields, found G_{dimer} = 1.95. On the other hand, Muccini and Schuler found G_{dimer} = 1.35.[34]

If our picture of the "hot atom" mechanism is correct, "molecular" dimer should be formed in a yield $(1 - G_{1C}/G_1)G_1$; dimer from freely diffusing

(30) T. D. Nevitt and L. P. Remsberg, *J. Phys. Chem.*, **64**, 969 (1960).

(31) E. S. Waight and P. Walker, *J. Chem. Soc.*, 2225 (1960).

(32) P. J. Horner and A. J. Swallow, *J. Phys. Chem.*, **65**, 953 (1961).

(33) P. J. Dyne and J. A. Stone, *Can. J. Chem.*, **37**, 2381 (1961).

(34) G. A. Muccini and R. H. Schuler, *J. Phys. Chem.*, **64**, 1436 (1960).

alkyl radical sources should be $\{1-(G_u - G_{1C})/G_2\}G_2$; total dimer is therefore $G_1 + G_2 - G_u$. For cyclohexane, the calculated dimer yield is 1.95 molecules/100 e.v., in excellent agreement with most experimental results. With cyclopentane, however, the calculated yield ($G_{dimer} = 1.54$) is somewhat greater than the value reported by Muccini and Schuler.[34]

This calculation cannot be applied as easily to alkanes, for the presence of radicals other than congruent alkyl radicals complicates the calculation to an unpredictable degree.

C–C Bond Scission.—Breaking a C–C bond produces two alkyl radicals which may (1) interact in the "cage" of formation or (2) leave the site of generation and diffuse freely through the solution. Column 3, Table IV, lists the total yield of freely diffusing radicals formed in such a process. As expected, the greater the branching, the greater the number of radicals formed by C–C bond scission.

It is more interesting, however, to consider the fraction of the total radicals which are formed by C–C bond split (column 4, Table IV). In this case a definite relation to structure is found. In Table IV the paraffins are grouped according to structure: *n*-alkanes, monomethyl alkanes, monomethylcycloalkanes, polymethylparaffins with no quaternary carbon atoms, and polymethylalkanes with one quaternary carbon atom. Within each group the same fraction of radicals is formed by C–C bond split. Even within groups it can be seen that a higher local degree of branching provides a greater percentage of C–C bond scission (*cf.* the polymethylparaffins in the fourth group).

A measurement of the individual radical yields has been made in a few cases. Dewhurst[35] measured the individual alkyl iodide yields in irradiated hexane–iodine solutions. The fraction of bonds ruptured by C–C split $G_{C_1-C_5}$ iodide/$(2G_{C_6}$ iodide + $G_{C_1-C_5}$ iodide) was 1.50/(6.60 + 1.50) = 0.19. In a similar experiment, using a much lower conversion than Dewhurst, Green[36] found this fraction to be 0.20 for *n*-hexane, and 0.28 for 2-methylbutane, in good agreement with our results.

Methane Formation.—The results in Table V lead to the conclusion that methane is produced within a solvent cage by disproportionation (column 2) as well as from freely diffusing methyl radicals. This latter value, determined by difference (column 1 − column 2, Table V), should be proportional to the methyl radical yield. In column 4, Table V, are listed the methyl radical yields from these alkanes, as measured by Schuler,[37] using the iodine scavenging technique. The methyl radical yields calculated from the difference in methane production are in general only slightly less than those directly measured. The difference likely represents those freely diffusing methyl radicals which react by addition.

Number of Solvent Molecules Decomposed per 100 e.v.—This number is defined as the total number of solvent molecules in which bonds are rearranged or broken. The yield of such events for C–H bond scission is $G_{H_2(0)}$, and varies from 2.70 molecules/100 e.v. for 2,2,5-trimethylpentane to 6.35 molecules/100 e.v. for *n*-pentane.

The gross number of molecules decomposing by C–C bond scission is more difficult to determine. Radicals so formed which diffuse out of the cage of formation are easily measured. The extent of disproportionation within the germinate cage is markedly dependent on structure, and will of course be greatest where the radicals are secondary or tertiary in nature. As a result, the highest yields for molecular formation in C–C bond scission are found in paraffins such as 2,2-dimethylbutane and 2,2,5-trimethylhexane, but lowest for *n*-alkanes and cycloparaffins.

It is our estimate that about 8–10 molecules decompose for every 100 e.v. absorbed by the system. Germinate recombination of alkyl radicals formed by C–C bond rupture results in a lower measured value. It is likely that this number is a little smaller for cycloalkanes.

Comparison with Previous Work.—To compare results presented in this paper, representing various product yields for some twenty paraffins, with previously published values, would involve writing a review of all work on liquid paraffin radiolysis; furthermore, such detail would serve little purpose. It may, however, be fairly concluded that the experimental results reported here are in good agreement with those of other workers, although other interpretations have often been made.

With one apparent exception, on which comment is made below, the postulate of the mechanism of radiolysis expressed previously,[1] and reiterated in this paper, explains reasonably well results obtained by other authors on liquid paraffin radiolysis.

There is a diversity of opinion on the mechanism of paraffin radiolysis, particularly in the mode of production of "molecular" hydrogen gas. While we have maintained that such hydrogen gas arises from "hot" hydrogen atoms, an alternative explanation is that both hydrogen atoms derive from the same parent molecule, detaching as a unit in a single process.

Evidence for this latter view arises from measurements of G_{D_2} from cyclohexane–cyclohexane-d_{12} mixtures. The yield of D_2, calculated on the basis of energy absorbed in C_6H_{12}, does not extrapolate to zero at $[C_6D_{12}] = 0$, but to a value of 0.32–0.35 molecule D_2/100 e.v.[18] Such a value, it is implied, is the true "molecular" yield of hydrogen from cyclohexane. Clearly it is incompatible with our value of G_1 for cyclohexane (2.43 molecules/100 e.v.).

Further consideration, however, would lead us to cite such a result as evidence *for* the hot atom reaction. The ejection of a hot hydrogen atom would occur in a direction averaging normal to the carbon chain skeleton. In the peculiar case of cycloalkanes, a fraction of such hydrogen atoms will collide with the opposite side of the ring. As in the case of nearest neighbors, hydrogen will be abstracted to form hydrogen gas. In C_6D_{12} mixtures, this would lead to some D_2 always being

(35) H. A. Dewhurst, *J. Phys. Chem.*, **62**, 15 (1958).
(36) J. H. Green, private communication.
(37) R. H. Schuler, private communication.

produced. In cyclohexane, the extent of this would be $0.32/G_1 = 0.13$, a very reasonable value for the fraction of ejected hydrogen atoms which collide with the opposite side of the ring. In this connection, it is perhaps worth noting that values of $G_1/G_{H_2(0)}$ are about 13% higher for cycloparaffins as a group than they are for alkanes.

Positive yields of G_D, would be expected for mixtures of standard and deuterated cycloalkanes, but not in the corresponding case of alkanes. Such work using deuterated cycloparaffins is not necessarily evidence for the "hot" hydrogen atoms, but the results cannot be used as arguments against such a postulate.

Conclusions

Our conclusions are those expressed previously.[1] Irradiated liquid paraffins decompose into radicals by C–H and C–C bond scission. Hydrogen atoms produced in the first case will be "hot" or thermal; "hot" atoms react by hydrogen abstraction on first collision, thermal atoms react competitively with solvent and solute. "Molecular" unsaturation occurs by disproportionation of adjacent congruent radicals. C–C bond ruptures produce alkyl radicals within a cage. Some diffuse out, while others interact within this cage by disproportionation and recombination, the relative extent being related ultimately to the paraffin structure. At high dose rates, freely diffusing alkyl radicals recombine by addition or disproportionation.

Acknowledgment.—The author wishes to thank the Nuclear Applications Section for the operation of the Van de Graaff accelerator, and Mr. J. Itzel for e.p.r. calibration and analysis.

REACTIONS INITIATED BY β-DECAY OF TRITIUM. IV. DECAY AND β-LABELING

BY KANG YANG AND PRESTON L. GANT

Radiation Laboratory, Continental Oil Company, Ponca City, Oklahoma

Received February 23, 1962

The β-decay of tritium, $T_2 \rightarrow HeT^+ + e$, initiates the reactions forming tritiated hydrocarbons in the system initially composed of gaseous propane and tritium. The $L(X)$ (the labeling yield per decay) for tritiated methane, ethane, and propane increases linearly with increasing tritium concentration: $L(X) = a + b(T_2)$ (1) where a and b are constants and (T_2) denotes total β-activity in the sample. These yields decrease when T_2 is replaced by HT, but irradiation with an external gamma source increases them. Nitric oxide eliminates the term $b(T_2)$ in (1) but has no effect on the other term, a. A quantitative explanation is given for these effects based on the division of labeling processes into two parts: HeT^+ ion-initiated reactions and electron-initiated reactions.

Introduction

A widely used method for synthesizing tritiated compounds is the Wilzbach method[1-3] in which the compound to be labeled is exposed to gaseous tritium. In such systems, the initiating step is the β-decay

$$T_2 \longrightarrow HeT^+ + e$$

which produces two reactive species, namely, HeT^+ ion and electron. Subsequent reactions can be divided into three sets: those initiated by the HeT^+ ion, those initiated by the electrons, and those initiated by both the HeT^+ ion and the electron. It was suggested[4,5] to name the first decay labeling and the second β-labeling.[6] The third set may be called mixed labeling. As discussed later, mixed labeling is likely to be unimportant; and, if so, the experimental methods described in ref. 4 can be used for distinguishing the decay and β-labeling quantitatively.

Decay labeling seems to involve[4-6] gas phase ionic reactions with a simple ion, HeT^+, whose structural parameters have been estimated.[7] Detailed investigations on this decay labeling may yield the information on gas phase ionic reactions at atmospheric pressure and in the absence of electrical field which may supplement the previous data[8] (obtained by using a mass spectrometer) in elucidating some gas phase radiolysis mechanism. Before attempting such investigations, however, it seems desirable to consolidate further the previous methods used in distinguishing the decay yields from β-yields[4] because the only system in which the consistency of the decay yield estimated by different methods has been demonstrated is the ethylene–tritium system.

In the present paper, these methods are applied in investigating the kinetics of the propane–tritium system, this mixture being chosen as a model saturated hydrocarbon system. The result indicates that the decay yields for various tritiated compounds estimated by different methods are in good agreement.

Experimental

The T_2 gas purchased from the Oak Ridge National Laboratory contained tritiated methane as an impurity. To remove the methane, T_2 gas was passed through a Molecular Sieve (Linde 3A) column, which was maintained at the tem-

(1) K. E. Wilzbach, *J. Am. Chem. Soc.*, **79**, 1013 (1957).

(2) P. E. Riesz and K. E. Wilzbach, *J. Phys. Chem.*, **62**, 6 (1958).

(3) R. W. Ahrens, M. C. Sauer, Jr., and J. E. Willard, *J. Am. Chem. Soc.*, **79**, 3285 (1957).

(4) K. Yang and P. L. Gant, *J. Chem. Phys.*, **31**, 1589 (1959).

(5) P. L. Gant and K. Yang, *ibid.*, **32**, 1757 (1960). (See footnote 8.)

(6) T. H. Pratt and R. Wolfgang divide β-labeling into two parts in reporting an investigation of the methane–tritium system; see *J. Am. Chem. Soc.*, **83**, 10 (1961).

(7) M. Cantwell, *Phys. Rev.*, **101**, 1747 (1956).

(8) For a recent review, see F. W. Lampe and F. H. Field, *Tetrahedron*, **7**, 189 (1959).

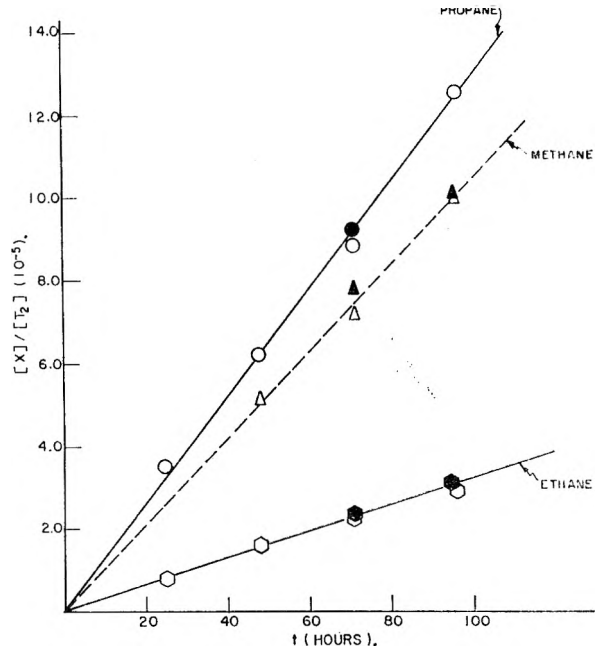

Fig. 1.—The rate of formation of tritiated products in propane–tritium systems at a total β-activity of 2.2 curies: O, △, ⬡, reaction vessel with stopcock; ●, ▲, ⬢, reaction vessel with breakoff seal.

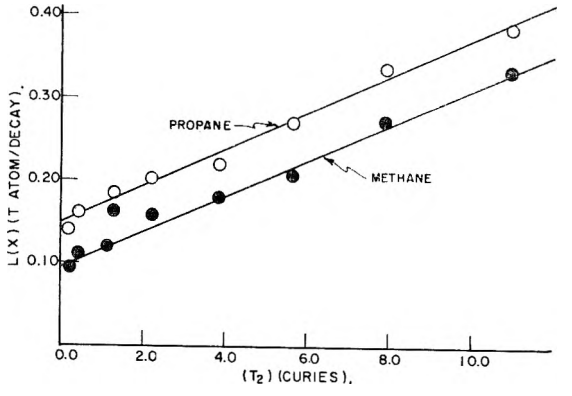

Fig. 2.—The labeling yield, $L(X)$, for tritiated methane and propane at various total β-activities.

perature of liquefied natural gas. In the purified T_2, the concentration of tritiated methane was less than 10^{-6} times that of T_2.

When allowed to stand in a Pyrex vessel, purified T_2 was rapidly recontaminated with tritiated methane. Attempts to prevent this by keeping the storage bulb at liquid nitrogen temperature or baking out the bulb prior to storage were not successful. Gas chromatographic analysis with a flame ionization detector showed the presence of a trace amount of untritiated methane in the purified T_2. This methane probably came from the β-radiolysis of stopcock grease in the process of T_2 transfer and might have been responsible for the tritiated methane. The rate data in the present paper do not contain any correction for the recontamination. The error attributable to this cause was probably small, because the reactions were started right after T_2 purification, and propane pressure was high enough to absorb practically all of the β-energy.

All experimental data were obtained at room temperature, 60 cm. of propane pressure, and with 150-cc. Pyrex vessels. Care was taken to minimize the contamination of the sample with mercury vapor by using a trap packed with glass wool and maintained at the temperature of a Dry Ice–acetone bath. About 1×10^4 curies of Co^{60} were used in irradiating some samples. The samples were analyzed using a programmed temperature chromatograph with the addition of a 10-cc. ion chamber in the gas outlet.

HT was prepared by sparking 1 to 1 mixtures of H_2 and T_2 with a Tesla coil. The resulting samples were analyzed by using a low-temperature chromatograph.[9] Other experimental details have been described previously.[4]

Results

Figure 1 shows the rates of formation of tritiated methane, ethane, and propane. The results of two different experiments are included. In one experiment, about 1.5% of the gas samples was withdrawn at successive reaction times through a stopcock attached to the reaction vessel. In the other experiment, the reaction vessel was sealed off at a capillary constriction after introducing propane and tritium. A single sample was taken through a breakoff seal after an appropriate reaction period. Analysis followed immediately. The two sets of data agree very well, showing that withdrawing samples through the stopcock does not affect the rate data.

These labeled products also were detected: *n*-butane (0.06), isobutane, ethylene (0.007), and propylene (0.004). The numbers in parentheses indicate initial $L(X)$, the number of T atoms incorporated per T decay, at $(T_2) = 2.2$ curies. With increasing reaction time, the rates of formation of ethylene and propylene decreased, and pentanes and hexanes, whose initial rates were nearly zero, became detectable. Both ethylene and propylene seem to undergo secondary reactions rapidly (possibly radical reactions), forming pentanes and hexanes.

By using figures similar to Fig. 1, we determined $L(X)$ values at different (T_2). Figure 2 shows the results for tritiated methane and propane. The results for tritiated ethane gave an equally good straight line. Least squares treatment of the data gives these equations

$$L(\text{Methane}) = (0.11 \pm 0.01) + (0.020 \pm 0.002)(T_2) \quad (1)$$

$$L(\text{Ethane}) = (0.020 \pm 0.003) + (0.014 \pm 0.001)(T_2) \quad (2)$$

$$L(\text{Propane}) = (0.15 \pm 0.01) + (0.022 \pm 0.001)(T_2) \quad (3)$$

where error ranges are indicated by using standard deviation.

Figure 3 shows the $L(X)$ values for tritiated *n*-butane and isobutane as functions of (T_2). As compared with Fig. 2, these data show more scattering. The formation of these compounds may involve some impurity-sensitive reactions such as ion–electron and radical–radical recombinations. This also may explain qualitatively the dependence of $L(X)$ on a power of (T_2) less than unity as is evident in Fig. 3.

Table I shows effects of replacing T_2 by HT. $L(X)$ values decrease.

Table II compares the $L(X)$ values in the presence and absence of an external radiation source. The energy input rate from the Co^{60} γ-source was

(9) P. L. Gant and K. Yang, *Science*, **129**, 1548 (1959).

TABLE I

THE LABELING YIELD, $L(X)$, IN T_2–C_3H_8 AND T_2–HT–C_3H_8 SYSTEMS AT A TOTAL β-ACTIVITY OF 1.2 CURIES

F^a	$L(X) \times 100$				
	Methane	Ethane	Propane	*i*-Butane	*n*-Butane
1.00	13.0	3.7	18.0	3.4	3.7
0.54	7.4	2.2	10.0	1.7	1.8
0.53	7.9	1.8	9.8	1.5	1.9

[a] The fraction of β-activity in T_2.

TABLE II

THE $L(X)$ AT $(T_2) = 2.2$ CURIES IN THE IRRADIATED AND UNIRRADIATED SYSTEMS

Expt.	$L(X) \times 100$				
	Methane	Ethane	Propane	*i*-Butane	*n*-Butane
Not irrad.	15	5.1	20	6.0	6.0
Irrad.[a]	21	10	29	14	17
Irrad.[a]	25	11	34	17	19

[a] 8.0×10^{-4} e.v./hr./molecule of ethylene estimated with an ethylene dosimeter.

8.0×10^{-4} e.v./hr./molecule of ethylene. Irradiation increases $L(X)$ values.

Table III shows the effect on $L(X)$ values of adding nitric oxide: $L(X)$ values are reduced, but the presence of a remainder not eliminated by nitric oxide is unmistakable.

TABLE III

THE $L(X)$ AT $(T_2) = 2.2$ CURIES IN THE PRESENCE AND ABSENCE OF NITRIC OXIDE

$[NO]/[C_3H_8]$	$L(X) \times 100$				
	Methane	Ethane	Propane	*i*-Butane	*n*-Butane
0.00	15	5.1	20	6	6
.02	13	2.4	13	0	1
.02	13	2.5	14	0	1

Discussion

Equations 1 to 3

$$L(X) = a + b(T_2)$$

where a and b are constants can best be explained by making these identifications

$$a = L(X)_d = b(T_2) = L(X)_\beta$$

where subscripts d and β signify the contributions from the decay and β-labeling. This linearity also indicates that the mixed labeling is not important. Various mechanisms are conceivable[6] which may lead to a complicated dependence of $L(X)$ on (T_2) as is the case in the formation of iso- and *n*-butane. In such cases, $L(X)_d$ may be estimated by extrapolating $L(X)$ to the zero value of (T_2).

The decrease, $-\Delta L(X)$, in the HT experiment (Table I) is likely to arise from the fact that HT decays to give HeH^+ ions but not HeT^+ ions. We assume that HeH^+ ions do not lead to tritiated products and also that $L(X)_\beta$ depends only on the total tritium atom concentration but not on the presence of a small amount of H atoms (as HT) or H_2 molecules; then

$$L(X)_d = -\Delta L(X)/(1 - F)$$

$$L(X)_\beta = L(X) - L(X)_d$$

where F denotes the fraction of β-activity in T_2.

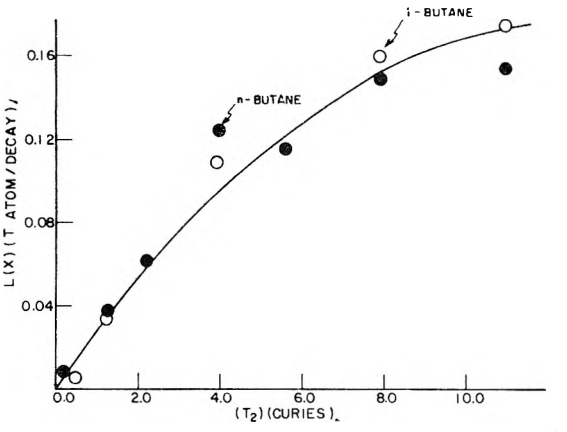

Fig. 3.—The labeling yield, $L(X)$, for tritiated *n*- and *i*-butane at various total β-activities.

The increase, $\Delta L(X)$, in the γ-irradiation experiment (Table II) is attributable to the increase in the rate of electron production. It can be shown that

$$L(X)_\beta = \Delta L(X)\left(\frac{\text{energy absorbed in system from } T_2 \text{ per unit time}}{\text{energy absorbed in system from } Co^{60} \text{ per unit time}}\right)$$

The decrease in the NO experiment (Table IV) is explainable based on the assumption that NO eliminates all the β-labeling without affecting the decay labeling. In some systems, this assumption is not correct,[4] and its validity must be tested by carrying out one of the experiments described above. Once this is done, the nitric oxide method is a simple and easy one for investigating the dependence of $L(X)_d$ or $L(X)_\beta$ on various modifications of experimental conditions.

The above arguments, when applied to the data of Tables I to III, yield two sets of $L(X)_d$ and $L(X)_\beta$. The average values are reported below.

As shown in Table IV, $L(X)_d$ values estimated by different methods agree very well. It is noteworthy

TABLE IV

THE $L(X)_d$ FROM DECAY LABELING ESTIMATED BY DIFFERENT METHODS

Method	$L(X)_d \times 100$				
	Methane	Ethane	Propane	*i*-Butane	*n*-Butane
Concn.	11	2.0	15	0	0
HT	12	3.7	17	4	4
Irrad.	12	2.7	15	2	1
NO	13	2.5	14	0	1
Av.	12 ± 1	2.7 ± 0.5	15 ± 1	2 ± 2	2 ± 2

TABLE V

THE $L(X)_\beta$ FROM β-LABELING AT $(T_2) = 2.2$ CURIES ESTIMATED BY DIFFERENT METHODS

Method	$L(X)_\beta \times 100$				
	Methane	Ethane	Propane	*i*-Butane	*n*-Butane
Concn.	4.4	3.1	4.8	6	6
HT	3	1	3	2	2
Irrad.	3.0	2.4	5.0	4	6
NO	2	3	6	6	5
Av.	3 ± 1	2 ± 1	5 ± 1	5 ± 2	5 ± 1

that decay labeling not only gives tritiated propane but also tritiated products whose formation required C–C bond rupture.

Table V compares $L(X)_\beta$ values estimated by different methods. Here, it is essential to specify (T_2) because $L(X)_\beta$ depends on (T_2). Since the largest number of experiments were carried out at $(T_2) = 2.2$ curies, the comparison was made at this total β-activity. Under these experimental conditions, accuracy in determinations of $L(X)_\beta$ was sacrificed for good estimates of $L(X)_d$; nevertheless, $L(X)_\beta$ values estimated by the different methods agree reasonably well.

Acknowledgment.—We express our appreciation to Dr. F. H. Dickey and L. O. Morgan for their valuable discussion and Mr. E. L. DeWitt and Mr. J. D. Reedy for helping with the experimental work.

γ-IRRADIATION OF ISOPROPYLBENZENE

BY ROBERT R. HENTZ

Socony Mobil Oil Company, Inc., Research Department, Princeton, N. J.

Received February 26, 1962

Cobalt-60 γ-irradiation of isopropylbenzene has been studied in the liquid phase at 36 and 145° and in the gas phase over the temperature range 163–385° at pressures of 0.5 and 1.0 atm. Maximum *G*-values are obtained in the gas phase at 385° and are as follows (*G*-values for liquid-phase irradiation at 36° are in parentheses): isopropylbenzene reacted, 16 (1.8); polymer, 9 (1.7); methane, 3.4 (0.090); benzene, 2.8 (0.05); C_6-benzene, 2.3; hydrogen, 2.1 (0.179); C_2-benzene, 1.5 (0.04); propene, 0.56 (0.010); propane, 0.51 (0.011); toluene, 0.5; ethene, 0.23 (0.002); ethane, 0.07 (0.004); and acetylene, 0.05 (0.004). Radiolysis is compared with catalytic and non-catalytic thermal cracking.

This study was undertaken to determine how radiation cracking of isopropylbenzene compares with catalytic and non-catalytic thermal cracking and whether a selective radiation dealkylation to benzene might be obtained with reasonably high radiation-energy yield (*G*) in the presence of a microporous solid which is a good catalyst for the thermal dealkylation. Isopropylbenzene was chosen for study because of the availability for comparison of thorough studies on the catalytic and non-catalytic thermal cracking of this compound.[1,2] This paper reports on the first phase of this study in which isopropylbenzene has been irradiated with cobalt-60 γ-rays over a wide range of experimental conditions. A communication to the editor on the γ-irradiation of isopropylbenzene adsorbed on microporous silica–alumina has been published,[3a] and a complete paper on this second phase of the work accompanies this article.[3b]

Experimental

Chemicals.—A volume of 1170 ml. of Eastman Kodak 1481 isopropylbenzene was distilled on a 100 theoretical-plate column under conditions giving 85 plates. A constant-boiling middle fraction of 223 ml. was used in all experiments: $n^{20}D$ 1.4913; $n^{20}D$ (lit.) 1.4914. Not more than two days prior to each experiment, 20 ml. of the distilled isopropylbenzene was passed through 10 ml. of Alcoa F-20 alumina in a 50-ml. buret with a Teflon stopcock at a rate of about 2 ml./min. for removal of isopropylbenzene hydroperoxide.[2]

Procedures.—Reagent was measured into a weighed bulb which then was reweighed. The bulb was attached to a high-vacuum line on which the isopropylbenzene was transferred into a tube which contained a sodium mirror. The reagent then was degassed by repeated freezing with liquid nitrogen, pumping, and thawing. The procedure was completed by transfer of the reagent into the reaction cell on the vacuum line and sealing off of the cell. Weighing of the reaction cell before and after filling gave a second weight of reactant and the average was used. Weights of 0.087–0.198 g. were used in gas-phase irradiations. In liquid irradiations, weights of 1–5 g. were used.

Gas-phase irradiations were carried out in cylindrical Pyrex cells about 3 cm. in internal diameter, 8–9 cm. in length, and 60 ml. in volume. The cells were equipped with a breakoff seal and a tube for filling. The volume of each cell was determined accurately so that the pressure could be calculated from temperature and weight of isopropylbenzene using the ideal gas law. Liquid irradiations were carried out in cylindrical Pyrex cells about 3 cm. in length and 2 cm. in internal diameter, also equipped with a breakoff seal and a tube for filling. These cells were designed to prevent any appreciable contribution from irradiation of the vapor. A new cell was used in each experiment.

The reaction cells were placed in a vertical cylindrical furnace surrounded by four cobalt-60 cylinders (about 2 kilocuries each) in vertical aluminum tubes at the corners of a square. Temperatures were measured with thermocouples attached to the cell; in high temperature experiments, the cobalt cylinders were protected from possible ill-effects of the heat by passing a stream of air through a manifold on the bottom of the irradiation unit and up through the supporting aluminum tubes. After irradiation the reaction cell was attached to a high-vacuum line. Total gas products were measured in a modified Saunders–Taylor apparatus[4] after separation from the liquid at the temperature of an ethyl bromide mush, −118°. Gas products were analyzed mass spectrometrically.

The condensed liquid after irradiation has a yellow color. The liquid was distilled from the reaction cell, after gas removal, into a weighed tube immersed in liquid nitrogen on the vacuum line. The tube, equipped with a breakoff seal, was sealed off and weighed to obtain the weight of liquid recovered. The distilled liquid was colorless, and on the walls of the reaction cell a yellow deposit was left which appeared to be a very viscous liquid. The distilled liquid and yellow residue were both analyzed mass spectrometrically except for the liquid product of the liquid-phase radiolysis, which was analyzed chromatographically.

The difference between initial weight of isopropylbenzene and weight of liquid recovered gives essentially the weight of yellow residue. *G*-(Residue) is based on molecules of isopropylbenzene converted to residue. The weight of liquid recovered with its percentage of isopropylbenzene gives *G*-(−Isopropylbenzene) and the percentage decomposition. The weights of residue and of isopropylbenzene lost are obtained as small differences. *G*-(Residue), *G*-(−Isopropylbenzene), and percentage decomposition in experiments two and three in Table I have a reliability of about ±10%. At

(1) C. J. Plank and D. M. Nace, *Ind. Eng. Chem.*, **47**, 2374 (1955).

(2) R. W. Maatman, R. M. Lago, and C. D. Prater, *Advan. Catalysis*, **9**, 531 (1957).

(3) (a) R. R. Hentz, *J. Phys. Chem.*, **65**, 1470 (1961); (b) R. R. Hentz, *ibid.*, **66**, 1625 (1962).

(4) K. W. Saunders and H. A. Taylor, *J. Chem. Phys.*, **9**, 616 (1941).

TABLE I

γ-IRRADIATION OF ISOPROPYLBENZENE

T, °C.	163	178	233	236	244	320	367	387[a]	385	385[b]	36[c]	36[c]	145[c]
P, atm.	0.51	0.69	1.10	0.47	1.03	0.97	1.04	1.01	0.96	0.96			
G (Hydrogen)[e]	0.49	0.43	0.70	1.01	0.89	1.65	1.88	0.15	2.23	2.08	0.179	0.185	0.203
G (Methane)	2.08	1.92	1.89	2.14	2.02	2.18	2.87	.13	3.50	3.37	.090	.088	.179
G (Acetylene)	0.21	0.15	0.11	0.18	0.18	0.10	0.05	0	0.05	0.05	.004	.004	.006
G (Ethene)	.13	.11	.16	.14	.11	.12	.16	0.01	.24	.23	.002	0	.003
G (Ethane)	.02	.01	.02	.01	.03	.04	.05	0	.07	.07	.004	0.001	.003
G (Propene)	.14	.09[d]	.08[d]	.10[d]	.10[d]	.15	.13[d]	0.02	.58	.56	.010[d]	.015[d]	.021[d]
G (Propane)	.08	.06	.08	.10	.13	.27	.18	.01	.52	.51	.011	.015	.061
G (−Isopropylbenzene)		5	5		6	7	7		16		1.8		
G (Residue)		4	4		5	5	3		9		1.7		
G (Benzene)	P	0.3	0.4		P	1.2	2.5		2.8		0.05		
G (C_2-Benzene)[f]	P	.6	.6		P	P	0.9		1.5		0.04		
G (C_6-Benzene)[g]	P					P	1.0		2.3				
G (Toluene)	P	.1	.2		P	P	0.4		0.5				

[a] Thermal blank (dose = 0) with apparent G-values based on the dose that would have been received for the reaction time and sample weight used. [b] G for radiolytic reaction assuming additivity of thermal and radiolytic reactions. [c] Liquid phase irradiations. [d] These values are a little low due to incomplete removal from the liquid. [e] G is the yield in molecules/100 e.v. [f] Definitely ethylbenzene in liquid radiolysis and probably also ethylbenzene in gas radiolyses. [g] Could be diisopropylbenzene or a hexylbenzene.

lower percentage decompositions these values have only order of magnitude reliability.

The liquid recovered contained from 97 to almost 100% isopropylbenzene. Consequently, the G-values given for liquid products are not of high accuracy, but are represented reasonably well by the figures given. Where amount of a product was too small for representation by a meaningful number, its presence is noted by the symbol P.

Dosimetry.—Energy absorbed in the gas phase is based on $G = 72$ for the acetylene dosimeter[5] and is corrected for the electron density of isopropylbenzene relative to acetylene. A dose rate of 1.08×10^{20} e.v./g./hr. was obtained with the acetylene dosimeter in the experimental geometry. Energy absorbed in the liquid phase is based on $G = 2.40$ for the ceric sulfate dosimeter[6] and is corrected for the electron density of isopropylbenzene relative to 0.4 M sulfuric acid solution. A dose rate of 0.94×10^{20} e.v./g./hr. was obtained with the ceric sulfate dosimeter in the experimental geometry. All doses are corrected for decay of the cobalt-60 source. Energy absorbed is based on the initial weight of isopropylbenzene.

In all gas-phase irradiations except those at 178 and 233°, the absorbed dose was within the range $2–5 \times 10^{20}$ e.v., corresponding to 1–5% decomposition of isopropylbenzene. At 178 and 233° the dose was increased to 13.0×10^{20} e.v. to give about 10% decomposition in order to obtain more reliable values of yields for loss, residue, and the liquid products. The G for total gas products is seen to be about 10% smaller at this higher dose. Doses in the liquid-phase irradiations at 36 and 145° for which liquid products are not reported were 7.4 and 9.4×10^{21} e.v., respectively, corresponding to about 0.6 and 1.1% decomposition. The liquid-phase irradiation at 36° for which liquid products are reported was at a dose of 12.1×10^{21} e.v., corresponding to about 4% decomposition. The slight decrease in gas yields at this higher % decomposition is within experimental error in this case.

Results and Discussion

Introduction.—The results are given in Table I. In irradiation of the gas phase, small amounts of butane, isobutane, butenes, pentenes, and isopentane also were detected. Mass spectrometric analysis of the yellow residue shows it to consist of a complex mixture with indications of several prominent aromatic systems based on correlations observed with the usual hydrocarbons found in petroleum. Phenanthrenes or anthracenes, pyrenes, and possibly acenaphthenes and naphthacenes, benzanthracenes, or chrysenes are all present both bare and substituted. No dimer of isopropylbenzene was detected; however, it may be present since the dimer parent peak sensitivity is very low. A prominent mass-224 peak suggests the presence of C_9H_{11}–C_8H_9. A maximum molecular weight of approximately 740 was recorded with an average of roughly 300–400. The dark yellow color may be attributable to naphthacene and higher polynuclear hydrocarbons. Previous work[7–10] on the yellow residue formed in irradiation of all aromatics also has shown it to consist largely of polymers of the parent compound having an average molecular weight of 395 in the case of toluene and an average molecular weight that increases to a maximum of 530 with increasing dose in the case of benzene.

It is apparent that γ-irradiation of isopropylbenzene yields a complex array of products. This certainly is not unexpected in view of the literature of hydrocarbon radiation chemistry[11] and the fact that the mass spectrometric fragmentation pattern of isopropylbenzene shows the formation of about 85 different ions.[12] Because of this complexity, it is futile to attempt a detailed discussion of the radiation chemistry of isopropylbenzene in terms of primary ionizations and excitations and subsequent reactions of the ions, excited molecules, and free radicals formed; discussion will be limited to some plausible processes that could be responsible for the more important observations.

Gas-Phase.—In the mass spectrum of isopropylbenzene the predominant ion is that formed by loss of a methyl radical. This ion accounts for about 40% of the total ionization. If 25 e.v. be assumed for the average energy required to form an ion pair in isopropylbenzene vapor, a $G = 1.6$ is ob-

(5) L. M. Dorfman and F. J. Shipko, *J. Am. Chem. Soc.*, **77**, 4723 (1955).

(6) D. E. Harmer, *Nucleonics*, **17**, No. 10, 72 (1959).

(7) R. R. Hentz and M. Burton, *J. Am. Chem. Soc.*, **73**, 532 (1951).

(8) W. N. Patrick and M. Burton, *ibid.*, **76**, 2626 (1954).

(9) S. Gordon, A. R. Van Dyken, and T. F. Doumani, *J. Phys. Chem.*, **62**, 20 (1958).

(10) A. R. Jones, *J. Chem. Phys.*, **32**, 953 (1960).

(11) W. H. Hamill, *Ann. Rev. Phys. Chem.*, **11**, 87 (1960).

(12) Unpublished mass-spectral fragmentation pattern.

tained for methyl radical production by this process alone. There are several other likely sources of methyl radicals. High-energy radiation produces excitation as well as ionization. Photochemically excited isopropylbenzene in the gas phase yields methyl radicals.[13] In addition, neutralization of the parent ion and of the predominant ion may result in splitting off of methyl radicals.

The benzene ring is a very effective free radical scavenger in the liquid phase at room temperature,[14] which may preclude methane formation *via* methyl radicals. It is reasonable to attribute some methane formation to "hot" methyl radicals and molecular elimination reactions (including ion–molecule), but to account for all methane in this way requires an explanation of the temperature dependence of the methane yield in terms of possible molecular elimination processes. Since the activation energy for abstraction of a hydrogen atom from isopropylbenzene should be considerably less than that for abstraction from benzene, it seems more reasonable to attribute some of the methane yield to thermal methyl radical abstraction reactions and to account for the temperature dependence in terms of competition between abstraction and ring-addition reactions. (Hardwick[15] has presented evidence that for reaction of hydrogen atoms with isopropylbenzene the rate-constant ratio for abstraction relative to ring addition is about 0.05 at 23°.) This argument is given some support by vapor-phase photolysis data at 150–160° and about 0.5 cm. pressure.[13] Ethane is the major gas product, exceeding methane by a factor of about two and hydrogen by a factor of about three. Clearly, all methyl radicals are not being scavenged by addition to the ring and combination is favored over abstraction at the low pressure of the photolysis.

Considerations similar to the foregoing would apply to most of the other products formed in the radiolysis. Of the 85 ions in the mass spectrum of isopropylbenzene only 10 have a relative abundance greater than 5. It is possible, but not particularly enlightening, to account for all products observed in terms of the 10 most abundant ionization processes and plausible secondary reactions of the ions and radicals formed. The increase in yield with increase in temperature of all products except acetylene may be accounted for as in the case of methane; however, a unique explanation is possible for the relatively large rates of increase in benzene, propene, and propane yields (by analogy to the mechanism for catalytic dealkylation which involves proton transfer from the catalyst) in terms of slightly endothermic proton transfers from positive ions in the system to isopropylbenzene with ultimate formation of benzene and a propyl radical (or propene and a hydrogen atom) on neutralization of $C_9H_{13}^+$ or of $C_3H_7^+$ after decomposition of $C_9H_{13}^+$.

Radiation cracking in the gas phase is similar to non-catalytic thermal cracking in that hydrogen and methane are major gas products; the ratio of methane to hydrogen varies from 4.2–1.3 as temperature goes from 163–385°. This ratio is 0.9 at 385° in non-catalytic thermal cracking as seen in column 8 of Table I and as reported by Plank and Nace.[1] As in catalytic thermal cracking, benzene is a major product of gas-phase radiation cracking; however, propene is not formed in equal amount. Whereas a unimolecular decomposition into benzene and propene is probably the only significant reaction in catalytic thermal cracking, such a decomposition is only one of many possible reactions which may ultimately yield benzene and propene or propane in radiation cracking. Very significant differences between radiation cracking and both catalytic and non-catalytic thermal cracking are seen in the multiplicity of radiolysis products obtained and, particularly, in the formation of a non-volatile, largely polymeric residue as the major product.

Liquid.—A twofold increase in pressure has a small effect on the gas-phase results (compare columns 4 and 5 of Table I). However, an almost sevenfold decrease in G for total gas occurs in going from irradiation of gas to liquid at about the same temperature (compare columns 1 and 13 of Table I). Significant decreases also occur in G-values of isopropylbenzene reacted and of liquid products. Manion and Burton[16] have observed a greater than threefold decrease in gas yield in electron irradiation of benzene in going from gas to liquid, but no decrease in the case of cyclohexane. It would appear that marked radiation resistance of aromatics relative to aliphatics may be characteristic only of the condensed state. Additional evidence is found in the $G(-C_6H_6) = 4.23$ reported by Huyskens and co-workers[17] for gas-phase irradiation of benzene as compared to G-(polymer) = 0.77 in liquid-phase irradiation.[16] The large change in yields with change in phase on irradiation of aromatics is most plausibly attributable to collisional deactivation processes in the liquid phase. Effects of excitation and ionization are assumed to be spread over many bonds in an aromatic. Consequently, in excited aromatic ions and molecules the time required for sufficient energy to concentrate in a particular bond is long enough that appreciable collisional deactivation can occur in the liquid state.

An additional factor in the decreased yields of the liquid state is evident in comparison of the hydrogen and methane yields in columns 1 and 13 of Table I. While G-(H_2) decreases by only a factor of 2.5, G-(CH_4) decreases by a factor of almost 12; thus hydrogen becomes the predominant gas product in irradiation of the liquid. Yields of all other products possibly derived from larger free radicals are also greatly reduced relative to hydrogen. This effect also has been observed in radiolyses of benzene and cyclohexane.[16] These observations are understandable in terms of the Franck–Rabino-

(13) T. J. Sworski, R. R. Hentz, and M. Burton, *J. Am. Chem. Soc.*, **73**, 1998 (1951).

(14) J. G. Burr and J. M. Scarborough, *J. Phys. Chem.*, **64**, 1367 (1960).

(15) T. J. Hardwick, *ibid.*, **66**, 117 (1962).

(16) J. P. Manion and M. Burton, *ibid.*, **56**, 560 (1952).

(17) P. Huyskens, P. Claes, and F. Cracco, *Bull. soc. chim. Belges*, **68**, 89 (1959).

witch[18] postulate of a cage effect which favors recombination of larger radicals with a resultant decrease in yield. The smaller hydrogen atom may escape the cage more readily, or hydrogen atoms may contribute much less to the gas-phase hydrogen yield than do methyl radicals to the methane yield. The observed general increase in liquid-radiolysis yields with increase in temperature and particularly the much greater increase in G-(CH_4) relative to G-(H_2) is consistent with an increased probability of escape from the cage or of hydrogen atom abstraction from the caging molecules.

(18) J. Franck and E. Rabinowitch, *Trans. Faraday Soc.*, **30**, 120 (1934).

IRRADIATION OF ISOPROPYLBENZENE ADSORBED ON MICROPOROUS SILICA–ALUMINA

BY ROBERT R. HENTZ

Socony Mobil Oil Company, Inc., Research Department, Princeton, N. J.

Received March 15, 1962

Irradiation with cobalt-60 γ-rays of a heterogeneous system consisting of isopropylbenzene and microporous silica–alumina has been studied over the entire range of isopropylbenzene electron fraction, F, and with two solids of different surface areas. G(benzene) increases markedly relative to yields of all other products as F decreases and passes through a sharp maximum at very low F; yields for benzene formation and isopropylbenzene decomposition are higher in the presence of solid than in the pure liquid at the same temperature, 36°, even though the radiation is absorbed overwhelmingly in the solid. Characteristic G-values for the major products at low electron fraction are as follows for $F = 0.0068$: isopropylbenzene reacted, 3.8; benzene, 1.05; hydrogen, 0.208; methane, 0.0042. Interpretation of the maximum as due to saturation of sites effective in isopropylbenzene dealkylation permits a calculation for both solids of effective site concentrations which are in good agreement. The unique behavior of benzene yields and the higher per cent conversion of decomposed isopropylbenzene to benzene suggest that isopropylbenzene is chemisorbed on those sites effective in thermal dealkylation; that radiation produces in the solid electronic excitation of relatively long lifetime at room temperature; and that this excitation energy is transferred to chemisorbed isopropylbenzene, where it is utilized (with greater efficiency than in the liquid) for the reaction of dealkylation to which the isopropylbenzene is predisposed on the chemisorption sites. A different mechanism is postulated for hydrogen formation.

This paper reports on the second phase of a study undertaken to determine how radiation cracking of isopropylbenzene compares with catalytic and noncatalytic thermal cracking and whether a selective radiation dealkylation to benzene might be obtained with reasonably high radiation-energy yield (G) in the presence of a microporous solid which is a good catalyst for the thermal dealkylation. A recent paper[1] on the first phase of this study reports results on the cobalt-60 γ-irradiation of pure isopropylbenzene over a wide range of experimental conditions. A communication to the editor has been published[2] on preliminary results obtained in γ-irradiation of isopropylbenzene adsorbed on microporous silica–alumina.

Experimental

Chemicals.—The same isopropylbenzene was used as in the earlier experiments,[1] and the same purification procedures were followed. The microporous silica–alumina (10% alumina) beads used were from 2–6 mm. in diameter with a surface area of 400 m.²/g., pore volume of 0.43 ml./g., and particle density of 1.15 g./ml. The low-surface silica–alumina was prepared by steam treatment (20 hr. at 700°) of the high-surface beads and had the properties: surface area, 169 m.²/g.; pore volume, 0.36 ml./g.; particle density, 1.25 g./ml.

Procedures.—Prior to use, the silica–alumina was placed in a muffle furnace at 550° for 20–70 hr. and then stored in a desiccator containing anhydrous magnesium perchlorate. This procedure resulted in a weight loss of about 7%. The desired amount of solid was weighed into a reaction cell of the type previously used in gas-phase irradiations[1]; the cell was attached to a vacuum line and placed in a furnace. The cell then was maintained at about 450° for approximately 22 hr. while evacuation proceeded to and was maintained at a pressure of 10^{-5}–10^{-6} mm. This treatment caused a further weight loss of less than 0.6%; therefore, the solid was not reweighed after each high temperature evacuation, but was allowed to come to room temperature under high vacuum. The desired weight of isopropylbenzene then was introduced as in gas-phase radiolyses, and the cell was sealed off. At least 2 hr. was allowed for attainment of a homogeneous distribution prior to irradiation. Weights of solid ranged from 0.2–40.0 g. and weights of isopropylbenzene from 0.01–2.0 g. A new cell and fresh reagents were used in each experiment, except as noted.

Irradiations were conducted in the same apparatus and in the same manner as previously described.[1] After irradiation the cell was attached to the vacuum line, usually after having stood overnight. The breakoff seal was broken and gas products were removed from the solid in the reaction cell at room temperature by repeated expansion through a trap at −118° (ethyl bromide mush) into the 556 ml. volume of a Saunders-Taylor[3] apparatus, followed by measurement in a 5.28 ml. volume, until no further gas could be removed. Liquid products then were removed from the solid by placing liquid nitrogen around the trap and a boiling water bath around the cell for about 4 hr. Any additional gas products (usually very little) then were removed before isolating the cell by means of a stopcock and again after stopcock closure by placing ethyl bromide mush around the trap containing the recovered liquid. This liquid was transferred by liquid nitrogen distillation into a weighed bulb on the vacuum line, and the bulb was sealed off and reweighed to obtain the weight of liquid recovered. When liquid recovery was likely to be very small, a weighed amount of pure isopropylbenzene was added to the weighed bulb and degassed prior to transfer of the liquid products into the bulb. Gas products were analyzed mass spectrometrically and liquid products chromatographically. Except for isopropylcyclohexane, products heavier than isopropylbenzene were not found in sufficient concentration in the recovered liquid to warrant routine determination. This may be due partially to limitations of the chromatographic equipment used but is more likely a result of inability to remove heavier products from the solid by the technique necessitated.

Since the silica–alumina solid used is a catalyst for thermal dealkylation of isopropylbenzene, it was found necessary to employ a temperature for liquid product recovery

(1) R. R. Hentz, *J. Phys. Chem.*, **66**, 1622 (1962).

(2) R. R. Hentz, *ibid.*, **65**, 1470 (1961).

(3) K. W. Saunders and H. A. Taylor, *J. Chem. Phys.*, **9**, 616 (1941).

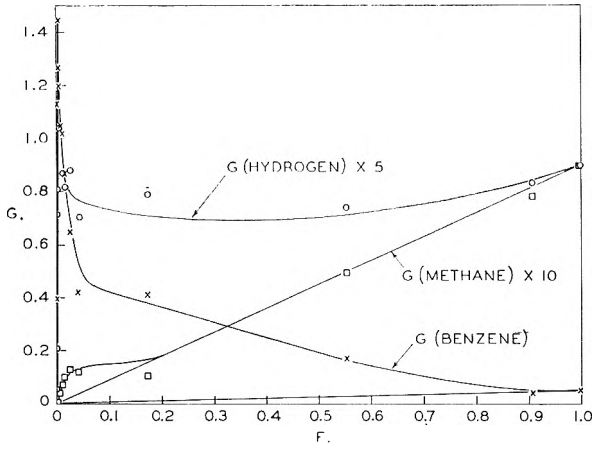

Fig. 1.—γ-Irradiation of isopropylbenzene and high-surface silica–alumina.

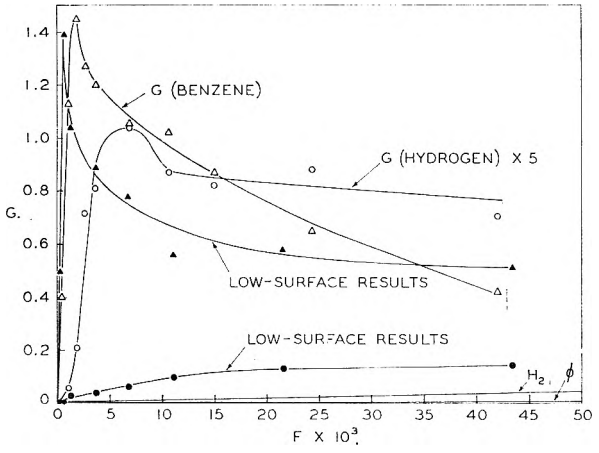

Fig. 2.—Comparison of high-surface and low-surface results at low F.

from the solid not much in excess of 100°. Blank experiments were performed in which benzene–isopropylbenzene mixtures and pure isopropylbenzene were adsorbed on the solid, allowed to stand overnight at room temperature (in one case after having been maintained at 102° for almost 4 hr.), and then removed by the procedure described. Recovery of benzene proved to be quantitative and isopropylbenzene decomposition negligible in all cases; however, recovery of isopropylbenzene (and most likely, therefore, heavier products) is far from quantitative at low weights of isopropylbenzene relative to weight of solid. Consequently, calculations of G(–isopropylbenzene) and per cent decomposition due to radiolysis are made by use of a rather large and not very reproducible correction for the amount of isopropylbenzene that remains adsorbed on the solid after the liquid recovery procedure. When weight of solid relative to that of isopropylbenzene is small enough for the correction to be negligible, an upper limit for G(–isopropylbenzene) and per cent decomposition is obtained by ignoring the correction. In any case, these values have only an approximate significance. As might be expected, the low-surface solid retains much less isopropylbenzene and, therefore, yields more reliable values for G(–isopropylbenzene). The fact that the low-surface values are consistently lower along with other observations suggests that irradiated solid may retain more isopropylbenzene than the unirradiated solid which, if true, would make the values for G(–isopropylbenzene) too large. Attempts to remove the liquid by saturation of the solid with pyridine followed by distillation from the solid at room temperature into a liquid nitrogen trap also gave quantitative benzene recovery but much poorer isopropylbenzene recovery; therefore, this more difficult procedure was not used.

A blank experiment was performed in which isopropylbenzene and an amount of propene equivalent to the amount of benzene that would be produced in an irradiation were adsorbed on and removed from the solid by the usual procedure. Only 0.3% of the propene was recovered, and very small amounts of diisopropylbenzenes accounting for less than 8% of the added propene were found in the liquid recovered; however, little recovery from the solid of diisopropylbenzenes might be expected even if present in the adsorbed isopropylbenzene at the theoretical 6% based on quantitative conversion of the propene. The significance of this result will be discussed later.

Blank irradiations of the solid in the absence of isopropylbenzene yielded no gas product.

Dosimetry.—Absorbed dose was determined with a ceric sulfate dosimeter as previously described,[1] with appropriate corrections for the electron density of the solid–isopropylbenzene system relative to 0.4 M sulfuric acid.

The results in Table I show that yields of all major products decrease with increasing absorbed dose. At the highest dose even the amounts (proportional to $G \times$ dose) of methane, propane, and benzene have decreased. It was necessary to obtain accurately measurable G-values for comparable conditions over the whole range of composition studied in order to observe the dependence of G-values on F (electron fraction of isopropylbenzene in the system) without undue influence of the effect of dose dependence. This required, within the experimental limitations of this work, that at the lower electron fractions the ratio of dose to weight of isopropylbenzene be kept approximately constant at a value near that of column 2, Table I. This value of the ratio, as shown by an average over many experiments, corresponds to approximately 20% decomposition of isopropylbenzene at the lower values of F. At values of F greater than about 0.01 for high-surface solid the per cent decomposition decreased to a value of 4% for pure isopropylbenzene. Consequently, G-values for values of F greater than 0.01 may, if anything, be a little high relative to those at lower values of F. Similar considerations apply to the low-surface solid. Nevertheless, Fig. 1 and 2 should represent quite well the important features of the dependence of G on F, especially in the low F region on which the interpretations are based. Obviously, as shown by the data of Table I, the G-values of Table II and of Fig. 1 and 2 are lower than the zero-dose values.

TABLE I

DOSE DEPENDENCE OF YIELDS IN IRRADIATION OF HETEROGENEOUS SYSTEM[a]

	Dose, e.v. × 10^{-21}				
	1.24	5.31	10.5	51.8	175
G[b](Hydrogen)	0.194	0.208	0.150	0.093	0.061
G(Methane)	.0051	.0042	.0036	.0024	.0003
G(Propene)	.0015	.0004	.0007	.0001	.0001
G(Propane)	.0044	.0033	.0033	.0013	.0003
G(Isobutane)	.0007	.0011	.0025	.0011	.0007
G(–Isopropylbenzene)	14	3.8	3.6	1.1	.4
G(Benzene)	2.3	1.05	0.74	0.18	.039
G(Ethylbenzene)		0.003	0.004	.002	.0007
G(Isopropylcyclohexane)	0.04	0.03		.009	.002
% decomposition	16	20	38	56	67

[a] High-surface solid at 36° and electron fractions of isopropylbenzene near 0.007 (about 0.2 g. of liquid to 30 g. of solid). [b] Yield in molecules/100 e.v. based on total absorbed energy.

In the experiment of column 4, Table II, the solid was pumped overnight on the vacuum line after gas and liquid products had been removed. Then fresh isopropylbenzene was introduced and the system was irradiated. The results are shown in column 5, Table II. The reduced yields, particularly of benzene, show that the decrease in yields with increased dose is due largely to products which are not removed from the solid, even by overnight pumping.

Results and Discussion

Introduction.—In addition to products shown in Table I much smaller amounts of the following products occasionally were observed in the presence of the solid: ethane, butane, butenes, isopentane, toluene, n-propylbenzene, and miscellaneous non-aromatics (C_6–C_{11}). Acetylene and

TABLE II

γ-IRRADIATION OF ISOPROPYLBENZENE AND HIGH-SURFACE SILICA–ALUMINA

	Temp., °C.				
	36	94	130	36	36[c]
F[a]	0.00683	0.00751	0.00730	0.0244	0.0218
G[b](Hydrogen)	.208	.201	.218	.176	.141
G(Methane)	.0042	.0078	.0087	.0127	.0086
G(Propane)	.0033	.0110	.0186	.0054	.0050
G(Isobutane)	.0011	.0020	.0071	.0020	.0006
G(Benzene)	1.05	1.28	1.66	.65	.2

[a] Electron fraction of isopropylbenzene. [b] Yield in molecules/100 e.v. based on total absorbed energy. [c] Irradiation of isopropylbenzene introduced to the solid of the experiment in the preceding column after liquid recovery.

ethylene were not found. Whether a yellow polymeric residue was produced as in pure isopropylbenzene radiolyses[1] could not be determined; however, a major fraction of the product is left behind on the solid in some form. Columns 1, 2, and 3 of Table II show that with the possible exception of the hydrogen yield there is a general increase in product yields with increase in temperature.

Plots of major product yields *vs.* F (electron fraction of isopropylbenzene in the system) for irradiations at 36° are shown in Fig. 1 and 2 along with corresponding "liquid lines" which represent the behavior expected if the absorbed radiation energy is initially partitioned between the two phases in proportion to their electron fractions (an explicit assumption in all that follows) and if adsorbed isopropylbenzene behaves exactly like the liquid without energy exchange or interaction with the solid.

Benzene Yield.—Figures 1 and 2 illustrate the unique behavior of the benzene yield. It is apparent that the mechanism of benzene formation is different from that for formation of other products. For high-surface solid the yield of methane does not greatly exceed the "liquid line" value at low F and very shortly merges with the "liquid line"; on the other hand, G(hydrogen) does not vary greatly from the pure liquid value as F decreases from unity to 0.00365–0.00683 when a sharp drop occurs; but, most significantly, the benzene yield very markedly increases relative to the yields of the other major products as F decreases. (Yields for all products in irradiation of the pure liquid are given in reference 1.) Indeed, benzene becomes the greatly predominant recovered product at low F whereas hydrogen predominates in radiolysis of the pure liquid, and the yields for benzene formation and isopropylbenzene decomposition (G = 1.8 for pure liquid[1]) are higher in the presence of the solid than in the pure liquid at the same temperature even though the radiation is absorbed overwhelmingly in the solid.

If 100% energy transfer from solid to adsorbate is assumed, then for the value of G(benzene) = 1.13 at F = 0.00106 the yield of benzene from total energy received by adsorbate also must be 1.13. If no energy transfer is assumed, then a yield of benzene based on only that radiation energy directly deposited in the adsorbate may be calculated as $G/F = 1.06 \times 10^3$, which gives a value of 0.09 e.v. ($100F/G$) of radiation energy directly deposited in adsorbate for each molecule of benzene formed. A comparison may be made with the energy requirements of the gas phase dealkylation of isopropylbenzene to benzene and propene for which $\Delta F^0 = 0.57$ e.v. and $\Delta H^0 = 1.0$ e.v. at 25°. The corresponding thermodynamic quantities are not known for this reaction on the solid surface; moreover, as will be discussed fully later, the stoichiometric reaction by which benzene is formed in the radiolysis has not been established. Consequently, arguments from energetic considerations that the solid must transfer energy to the adsorbate are not conclusive; however, such results as the foregoing strongly suggest that radiation energy deposited in the solid is converted to a form which is efficiently transferred to the adsorbed isopropylbenzene, where it is used for benzene formation with an efficiency considerably greater than in liquid phase radiolysis. Further, the persistence of high yield, 1.13, to such a low electron fraction, 0.00106, at which 99.9% of the radiation energy is initially absorbed in the solid and which corresponds to about 0.6% surface coverage (based on a 50 Å.^{2} cross section for isopropylbenzene) suggests that transfer of energy from solid to adsorbate is rapid relative to the decay time of the responsible transfer entity. The low-surface results of Fig. 2 support these conclusions.

Complete surface coverage corresponds to about F = 0.15 for the high-surface solid. At this electron fraction one might expect a linear decrease in G(benzene) with increasing F since the only feature of the system that is changing is the ratio of unimolecularly adsorbed to total isopropylbenzene and, therefore, the partition of energy between these two different states of isopropylbenzene, each with a characteristic G(benzene); however, Fig. 1 and 2 show that the benzene yield reaches a maximum of about 1.45 at F = 0.00177 for the high-surface solid, then decreases rapidly to a value of G(benzene) = 0.41 in the region F = 0.04–0.17, and then decreases slowly to the pure liquid value. This passage through a sharp maximum at low-surface coverage suggests saturation at the maximum of those surface sites which are effective in benzene formation so that above F corresponding to the maximum additional isopropylbenzene occupies sites which compete for the transferred energy but are relatively inefficient in benzene formation. The maximum occurs at 1.0% surface coverage and corresponds to 2.0×10^{16} sites/m.^{2}. Results for the low-surface solid tend to confirm this interpretation of the maximum. In this case, Fig. 2, a very sharp maximum occurs at about F = 0.000616, corresponding to 0.8% surface coverage and 1.7×10^{16} sites/m.^{2}. Agreement with the high-surface value is good. Oblad[4] has presented data for a similar catalyst (12.5% alumina) from which a value is obtained of 1.3×10^{17} sites/m.^{2} for quinoline chemisorption.

A mechanism is tentatively proposed as follows to account for the data on benzene formation. Isopropylbenzene is chemisorbed on those sites effective in thermal dealkylation. Radiation produces in the solid electronic excitation of relatively long lifetime at room temperature. As suggested

(4) G. A. Mills, E. R. Boedeker, and A. G. Oblad, *J. Am. Chem. Soc.*, **72**, 1554 (1950).

by Sutherland and Allen[5] in discussion of their data on radiolysis of pentane adsorbed on various solids, these excited states may be electrons and positive holes which migrate independently through the solid. One of these entities may be trapped by isopropylbenzene on the surface and subsequently neutralized by the other with release to the isopropylbenzene of the neutralization energy either as electronic excitation or as vibrational excitation of the ground state (equivalent to a high local temperature as a result of internal conversion of the neutralization energy into vibrational energy of neighboring atoms). Regardless of the detailed mechanism it is postulated that electronic excitation energy produced in the solid by irradiation is transferred to chemisorbed isopropylbenzene, where it is partially utilized to satisfy the energy requirements of the dealkylation reaction to which isopropylbenzene is predisposed on the chemisorption sites.

At higher temperatures (*cf.* Table II) the average energy of adsorbed isopropylbenzene molecules is closer to the activation energy; consequently, a smaller fraction of the solid excitation energy is required for activation, and the probability of transfer or conversion of the requisite energy may be larger. It has been postulated that at an electron fraction corresponding to saturation of chemisorption sites most effective in dealkylation, the benzene yield is a maximum since additional isopropylbenzene is adsorbed on sites at which excitation transfer occurs but with a lower probability of benzene formation. This may be due to a larger activation energy for dealkylation on these sites. The large decrease in yield of benzene with increasing dose may be attributed to a greater probability for transfer of solid excitation energy to certain products which dissipate the energy without chemical effect or without benzene formation.

In addition to Caffrey and Allen[6] and Sutherland and Allen[5] several other authors have invoked energy transfer from a solid to an adsorbed phase to account for results on radiolysis of a heterogeneous system. Two recent reviews are available.[7,8] Clingman[9] has reported a $G = 2.2$ for a more selective propane oxidation by X-ray irradiation in the presence of zinc oxide which absorbs essentially all the energy. He suggests that energy transfer by interaction of a positive hole with anionically adsorbed oxygen produces a new species of adsorbed oxygen that is a reactive intermediate in the altered reaction.

Hydrogen Yield.—Whereas the benzene yield on high-surface solid decreases sharply at F less than 0.00177, the hydrogen yield begins to fall sharply in the region $F = 0.00365$–0.00683. It is possible that hydrogen formation is a higher energy process that occurs *via* shorter lifetime, higher excited states of the solid; however, the greatly reduced hydrogen yields on a solid whose surface area has been reduced by only a factor of 2.4 is difficult to explain in such terms (*cf.* Fig. 2). Sutherland and Allen[5] have observed that replacement of 19% of the sodium ions of Linde Co. "Molecular Sieve 13X" with hydrogen ions resulted in a great increase of the hydrogen yield on irradiation of adsorbed pentane. These authors postulate that the hydrogen ions on the surface may trap electrons from the conduction band to form hydrogen atoms, which then may abstract hydrogen from pentane. A similar mechanism could account satisfactorily for the data on hydrogen yields from adsorbed isopropylbenzene. Without specification of the detailed mechanism for the bond rupture process, it is postulated that irradiation of the solid dissociates surface O–H bonds and that the hydrogen atoms migrate on the surface until they are recaptured by a surface valence, add to the ring of an isopropylbenzene molecule, or form hydrogen by abstraction from the β C–H bond of an isopropylbenzene molecule. The latter two processes would have fixed relative probabilities as composition is varied; however, at a sufficiently low electron fraction of isopropylbenzene, recapture of hydrogen atoms by the surface would become important relative to reaction with isopropylbenzene, and the hydrogen yield would decrease with decreasing F. Above the electron fraction at which hydrogen yields decrease sharply, from about $F = 0.00365$–1.0, the approximate constancy of G(hydrogen) can be explained if it is assumed that G-values for hydrogen atom production from solid and from isopropylbenzene do not differ appreciably.

Assuming one hydrogen atom from the solid per molecule of hydrogen produced by irradiation, the maximum number of hydrogen atoms obtained from a gram of solid in an experiment was 7×10^{18}. If the solid is assumed to retain only 1% by weight of water after the pretreatment procedures, there would be 7×10^{20} hydrogen atoms present in a gram of solid. Thus, only 1% of the solid's hydrogen atoms would have been removed in this experiment. In terms of the proposed mechanism for hydrogen formation, the much reduced yields of hydrogen from isopropylbenzene on low-surface solid are explained as due to destruction of labile O–H bonds by the surface reduction treatment.[10] The failure to obtain any hydrogen on irradiation of solid alone is consistent with this mechanism.

Other Products.—Caffrey and Allen[6] as well as Sutherland and Allen[5] have commented on the suppression of unsaturates in irradiation of pentane adsorbed on silica gel and the enhancement of branched products. In this work also nonaromatic unsaturates found in irradiation of the gas and liquid were either absent or considerably suppressed in the products recovered from the solid. Isobutane formation seems to be enhanced by the presence of the solid, and isopropylcyclohexane was found only in the presence of solid.

Selectivity.—The percentage of decomposed isopropylbenzene which has been converted to benzene (per cent conversion) may be calculated from values for G(–isopropylbenzene) and G(benzene); however, as discussed in the section on

(5) J. W. Sutherland and A. O. Allen, *J. Am. Chem. Soc.*, **83**, 1040 (1961).

(6) J. M. Caffrey, Jr., and A. O. Allen, *J. Phys. Chem.*, **62**, 33 (1958).

(7) M. Haissinsky, *Jaderna energie*, **7**, 73 (1961).

(8) R. Coekelbergs, A. Crucq, and A. Frennet, *Advan. Catalysis*, **13**, 55 (1961).

(9) W. H. Clingman, Jr., *Ind. Eng. Chem.*, **52**, 915 (1960).

(10) J. L. Weill, *Chim. mod.*, **5**, No. 37, 193 (1960).

experimental procedures, values for G(–isopropylbenzene) are not very reliable because of the large correction necessitated by incomplete recovery from the solid. In ten experiments with high-surface solid per cent conversion values ranged from 13–57%. Seven of the ten values lay between 21 and 41%, and the average of all ten was 29%. On low-surface solid the recovery of isopropylbenzene was much better, and no correction was used for isopropylbenzene retained; consequently, the values of G(–isopropylbenzene) used are too large and per cent conversions are minima. The range of per cent conversion from five experiments with low-surface solid was 29–36%, with an average of 37%. Application of a quite small correction (10-fold smaller than that measured for high-surface solid) for isopropylbenzene retention on the low-surface solid brings the average per cent conversion to near 50% and reduces the spread in values. It would appear that the per cent conversion on low-surface solid is appreciably higher than that for high-surface solid. The much lower values for G(hydrogen) add support to this view; however, it is possible that retention by irradiated high-surface solid is greater than the retention correction used and, therefore, that per cent conversions calculated for high-surface solid are low. Conversion in liquid radiolysis is about 3%, and the maximum value in gas radiolysis would appear to be about 18%.[1] There appears to be little doubt that presence of the solid has enhanced the selectivity of the radiolysis of isopropylbenzene considerably, as shown particularly by the results for per cent conversion with low-surface solid.

Low values for G(propene), about 0.2% of G(benzene), may be due to failure to produce propene or the inability to recover propene from the solid containing adsorbed isopropylbenzene, as discussed in the section on experimental procedures. Since thermodynamic equilibrium at 100°, the temperature used for recovery of liquid products, overwhelmingly favors isopropylbenzene relative to benzene and propene, observation of appreciable benzene yields is contingent on failure to produce equivalent amounts of propene or on conversion of propene to other products on the solid. Possible fates of propene are polymerization and formation of diisopropylbenzene. The possibility that propene is formed in an amount equivalent to benzene and subsequently disappears in isopropylbenzene alkylation would decrease the amount of G(–isopropylbenzene) attributable to side reactions and impose an upper limit on conversion of 50%; this value appears to be closely approached with low-surface solid. In the blank experiment (*cf.* Experimental Procedures) less than 8% of unrecovered propene was recovered as diisopropylbenzenes; however, this represents positive evidence for such a reaction. Thus, a radiation-induced, solid-catalyzed unimolecular split into benzene and propene with conversion of propene to diisopropylbenzene could be the major reaction occurrent.

The unique behavior of the benzene yields and the higher per cent conversion of isopropylbenzene to benzene on a solid which is a catalyst for thermal dealkylation suggest the possibility that a solid to some extent may direct absorbed radiation energy into that reaction for which it is a thermal catalyst. It is intended to test this speculation by the use of solids of varying catalytic activity, particularly a very pure silica of little or no catalytic activity.

AN ISOPIESTIC INVESTIGATION OF DI-(2-ETHYLHEXYL)-PHOSPHORIC ACID (DPA) AND TRI-*n*-OCTYLPHOSPHINE OXIDE (TPO) IN *n*-OCTANE[1]

BY C. F. BAES, JR.

Contribution from the Oak Ridge National Laboratory, Oak Ridge, Tennessee

Received February 28, 1962

Isopiestic measurements are presented in which octane solutions of di-(2-ethylhexyl)-phosphoric acid (DPA) and tri-*n*-octylphosphine oxide (TPO) are compared with triphenylmethane (TPM)–octane as the reference solution. In the range 0–0.2 m the results show deviations up to 10 and 20% from ideal solution behavior of DPA dimer and TPO monomer, respectively. While partial trimerization of DPA (in qualitative agreement with previous iron(III) extraction results for DPA) and partial dimerization of TPO (which is not supported by molar polarization results) can account in part for the results, it is evident that non-specific non-ideal behavior of the solutes also is involved. Practical activity coefficients were estimated on two separate assumptions: (1) $\gamma_{TPM} \equiv 1$, giving $\log \gamma_{(DPA)_2} = -0.5227m_{(DPA)_2}^{1/3} + 0.420m_{(DPA)_2}$ and $\log \gamma_{TPO} = -1.168m_{TPO} + 0.149m_{TPO}^2$; and (2) $\log \gamma_{(DPA)_2} \equiv -0.6432m_{(DPA)_2}^{1/3}$ (from iron(III) extraction results), giving $\gamma_{TPM} = -0.737m_{TPM}$ and $\log \gamma_{TPO} = -1.886m_{TPO} + 0.245m_{TPO}^2$.

The isopiestic measurements reported here were undertaken in connection with solvent extraction studies of di-(2-ethylhexyl)-phosphoric acid (DPA)[2-4] and tri-*n*-octylphosphine oxide (TPO).[5,6]

(1) This communication is based on work performed for the U. S. Atomic Energy Commission at Oak Ridge National Laboratory, Oak Ridge, Tennessee, operated by Union Carbide Corporation.

(2) (a) C. F. Baes, Jr., R. A. Zingaro, and C. F. Coleman, *J. Phys. Chem.*, **62**, 129 (1958); (b) C. F. Baes, Jr., and H. T. Baker, *ibid.*, **64**, 89 (1960).

(3) C. A. Blake, K. B. Brown, and C. F. Coleman, "The Extraction and Recovery of Uranium (and Vanadium) from Acid Liquors with Di-(2-ethylhexyl)-phosphoric Acid and Some Other Organophosphorus Acids," ORNL-1903, May 13, 1955, p. 106.

(4) C. A. Blake, D. J. Crouse, C. F. Coleman, K. B. Brown, and A. D. Kelmers, "Progress Report: Further Studies of the Dialkylphosphoric Acid Extraction (Dapex) Process for Uranium," ORNL-2172, Sept. 6, 1956, p. 110.

(5) H. T. Baker and C. F. Baes, Jr., "An Infrared and Isopiestic Investigation of the Interaction Between Di-(2-ethylhexyl)-phosphoric Acid and Tri-(*n*-octyl)-phosphine Oxide in Octane," paper presented at ACS Meeting, Chicago, Sept. 7–12, 1958, paper in preparation.

(6) C. A. Blake, K. B. Brown, and C. F. Coleman, "Solvent Extraction of Uranium (and Vanadium) from Acid Liquors with Trialkylphosphine Oxides," ONRL-1964, Aug. 26, 1955, p. 106.

The extent to which solvent extraction behavior can be understood often is limited by one's knowledge of the chemistry of the organic solutions involved. It therefore is desirable that studies of solvent extraction verify the solute species present and, if possible, permit estimation of their activity coefficients. In this study the species of DPA and TPO present in octane solution were confirmed by isopiestic measurements, and their activity coefficients were estimated.

The isopiestic method, which has long been used to determine activity coefficients in aqueous solutions,[7] has found but limited application to organic solutions.[2a,8] In the previously reported measurements on DPA–hexane solutions,[2a] the accuracy (~2%) was much poorer than that attained in aqueous solutions (~0.1%) and solute molecular weights only could be estimated. In making the present measurements, one purpose was to achieve sufficiently greater accuracy so that the results also would permit the estimation of activity coefficients.

From previous studies[2a,9-12] DPA is expected to form a stable dimer in octane solution. At 0.001 *M* no deviation from Beer's law was detectable in measurements[5] of the intensity of the infrared absorption band associated with the stretching of the H-bonded phosphoryl group of DPA in octane, and no band associated with the non-H-bonded phosphoryl group was found. It was concluded that no appreciable dissociation of the DPA dimer occurred at this low concentration. However, recent results[2b] on extraction of iron(III) by DPA in octane suggest that DPA may undergo partial trimerization with increasing concentration in this solvent. Uranium(VI) extraction measurements[2a] did not indicate a similar effect in hexane,[13] and the accompanying isopiestic measurements, though few and relatively inaccurate, did not show marked deviations from the expected dimer behavior. The present isopiestic measurements in octane provide a more direct comparison with the iron(III) extraction results.

The measurements on TPO were originally undertaken to check routine molecular weight measurements by freezing point in benzene, which were high for a series of purified samples.[14] The results are of interest because they confirm considerable positive deviation from Raoult's law even though association of TPO is not expected.

(7) R. A. Robinson and R. H. Stokes, "Electrolyte Solutions," Academic Press, Inc., New York, N. Y., 1955, p. 175 ff.

(8) E. N. Lassettre and R. G. Dickinson, *J. Am. Chem. Soc.*, **61**, 54 (1939); F. T. Wall and P. E. Rouse, Jr., *ibid.*, **63**, 3002 (1941); F. T. Wall and F. W. Banes, *ibid.*, **67**, 898 (1945).

(9) G. M. Kosolapoff and J. S. Powell, *J. Chem. Soc.*, 3535 (1950).

(10) D. F. Peppard, J. R. Ferraro, and G. W. Mason, *J. Inorg. Nucl. Chem.*, **4**, 371 (1957); **7**, 231 (1958).

(11) D. Dyrssen, *Acta Chem. Scand.*, **11**, 1771 (1957); D. Dyrssen and Liem Djiet Hay, *ibid.*, **14** 1091 (1960).

(12) C. J. Hardy and D. Scargill, *J. Inorg. Nucl. Chem.*, **11**, 128 (1959).

(13) A small deviation of the uranium(VI) extraction results from the expected second power dependence on DPA concentration was in the opposite direction, and it was tentatively suggested that this was caused by partial dissociation of the DPA dimer. In view of the evident stability of the dimer, this now seems unlikely.

(14) K. B. Brown, C. F. Coleman, D. J. Crouse, and A. D. Ryon, "Progress Report on Raw Materials for September, 1957," ORNL-2443, Jan. 7, 1958, p. 9.

Experimental

Apparatus and Procedure.—The isopiestic apparatus, incorporating many of the features described by Scatchard, Hamer, and Wood,[15] already has been described.[2a] It contains a mechanism, operated through a bellows, for covering and uncovering the sample cups while the apparatus is sealed.

Short-term temperature control of the oil thermostat was ±0.002° (read on a resistance thermometer). A solenoid valve (actuated by the thermoregulator and relay) was used to control the flow of cooling water. Sufficient heating was produced by the bath stirrer.

It was observed in preliminary runs on octane solutions, using the outgassing procedure previously described,[2a] that the time required for isopiestic equilibrium to be reached was generally longer than for hexane solutions and was extremely variable. It was concluded that the distillation rate was critically dependent on the partial pressure of air in the apparatus, the rate being greatly decreased by higher air pressures. Accordingly, the following, more thorough, outgassing procedure was adopted.

Before outgassing, the lower portion of the apparatus was immersed in a Dry Ice–ether bath. After 15 min. of cooling, which was sufficient to freeze the sample solutions, the apparatus was outgassed by repeatedly opening it to an evacuated 1-l. bulb. Upon several such expansions, the partial pressure of air in the apparatus was a few microns (read on a McLeod gage). The apparatus was then allowed to warm for 10 to 20 min., the sample cups were uncovered for a few minutes and then covered again, and the apparatus was cooled once more. The outgassing procedure was resumed until the indicated air pressure within the apparatus was 0.1 μ or less. The sample cups were then opened and the apparatus was placed in the thermostat. In runs at the lowest concentrations (0.01–0.05 *m*), the apparatus was removed from the bath after 1 day, cooled once more, and opened to the vacuum system. It was found that the partial pressure of air had increased to several microns, presumably as the result of degassing of the sample solutions. This gas was removed and the run was resumed. In runs at higher concentrations, this second outgassing step was omitted. By this procedure, usually less than 1 ml. of octane was removed from the apparatus.

Equilibration times of 10 days were sufficient for the lowest concentrations studied (0.01 *m*), decreasing to only 2 or 3 days for solutions more concentrated than 0.1 *m*.

In all the present measurements, anhydrous magnesium perchlorate was placed in the bottom of the apparatus. In a typical run, the same sample solution was placed in two cups and triphenylmethane (TPM) reference solution was placed in the two remaining cups. The ratio of the initial solution concentrations usually was near the expected equilibrium ratio. At the end of a run, duplicate sample concentrations usually agreed to within ±0.25%, the average for all the runs being ±0.14%.

Reagents.—Procedures used at this Laboratory for the preparation and purification of DPA[3,4,16] and TPO[6,14,17] have been described previously. The DPA used was 99.5% dioctyl phosphoric acid containing <0.1% monooctylphosphoric acid by potentiometric titration with standard sodium hydroxide. The remaining principal impurities were probably 2-ethylhexanol and the trioctyl phosphate ester. Their effect on the isopiestic results is expected to be no larger than the experimental uncertainty. The TPO was purified with special care, the final stage of purification involving repeated recrystallization from petroleum ether. The product contained <0.07% free and combined acid (as dioctylphosphinic and dioctylphosphinous acids). The TPM (Eastman Kodak White Label) was recrystallized from ethanol; *n*-octane, the solvent, was Phillips Petroleum Co. Pure Grade (99 mole % minimum).

(15) G. Scatchard, W. J. Hamer, and S. E. Wood, *J. Am. Chem. Soc.*, **60**, 3061 (1938).

(16) K. B. Brown, C. F. Coleman, D. J. Crouse, and A. D. Ryon, "Progress Report on Raw Materials for October, 1957," ORNL-2451, Jan. 29, 1958, p. 8.

(17) K. B. Brown, C. F. Coleman, D. J. Crouse, and A. D. Ryon, "Progress Report on Raw Materials for August, 1957," ONRL-2399, Oct. 30, 1957, p. 9.

Results

The ratio of triphenylmethane (TPM) molality, m_{TPM}, to the DPA dimer molality, $m_{(DPA)_2}$, at isopiestic equilibrium plotted against $m_{(DPA)_2}$ (Fig. 1) fell ~9% below unity in the range up to ~0.18 dimer molality and then rose sharply. The corresponding plot of the TPO results (Fig. 2) fell ~17% below unity, then rose sharply at about the same reference solute molality. Table I lists values of these ratios, given by the solid curves in the figures.

If these solutions contained only TPM monomer, TPO monomer, and DPA dimer species and all had unit activity coefficients, then all the observed isopiestic ratios would have been unity. The decrease of the ratios below unity are in the direction corresponding to association of DPA dimer and TPO monomer. It is difficult to decide, however, to what extent real association, leading to the formation of new chemical species, actually occurs in each case, as distinguished from less specific non-ideal behavior of the solute. The sharp rise in the ratios begins at ~0.18 *m* TPM in both cases and is presumably the result of increasing non-ideal behavior of the TPM–octane solutions as saturation (~0.27 *m*) is approached.

TABLE I

SMOOTHED MOLAL ISOPIESTIC RATIOS[a]

Temp. 25°

$m_{(DPA)_2}$	$(m_{TPM}/m_{(DPA)_2})$	m_{TPO}	(m_{TPM}/m_{TPO})
0	(1.000)	0	(1.000)
0.02	0.945	0.02	0.974
.04	.921	.04	.949
.06	.914	.06	.927
.08	.911	.08	.906
.10	.910	.10	.888
.12	.911	.12	.871
.14	.913	.14	.856
		.16	.842
		.18	.834
		.20	.844

[a] These results may be converted to the molarity scale by the following relations based on density measurements

$$M_{(DPA)_2} = 0.6986m_{(DPA)_2} - 0.3207m^2_{(DPA)_2} + 0.15m^3_{(DPA)_2}$$

$$M_{(TPO)} = 0.6986m_{(TPO)} - 0.2145m^2_{(TPO)} + 0.07m^3_{(TPO)}$$

$$M_{(TPM)} = 0.6986m_{(TPM)} - 0.1155m^2_{(TPM)} + 0.02m^3_{(TPM)}$$

In the case of the DPA results, the abrupt drop in the isopiestic ratio in the low concentration range strongly suggests, in agreement with the iron(III) extraction results,[2b] that association is occurring. The dashed curve represents the expected result assuming the trimerization reaction

$$3(DPA)_2 \rightleftarrows 2(DPA)_3;\ Q_t = \frac{[(DPA)_3]^2}{[(DPA)_2]^3} \quad (1)$$

with the quotient $Q_t = 1.2\ m^{-1}$ (1.7 M^{-1}). However, it is evident that this can be only a partial explanation of the results at higher concentrations.

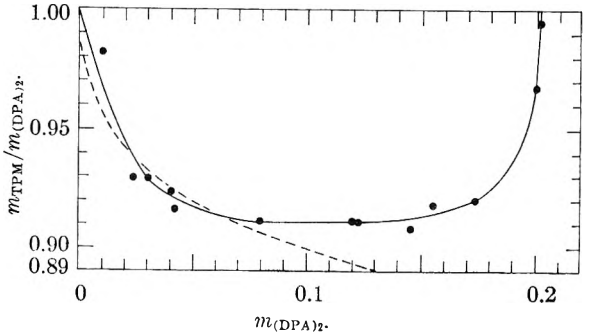

Fig. 1.—Change in ratio of triphenylmethane, TPM, molality to the DPA dimer molality in octane at isopiestic equilibrium with increasing DPA dimer molality. The dashed curve was calculated assuming partial trimerization of DPA ($Q_t = 1.2\ m^{-1}$) and ideal behavior of all solute species.

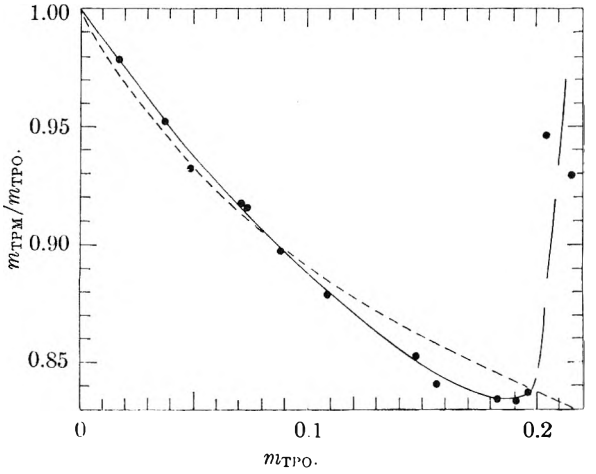

Fig. 2.—Change in ratio of triphenylmethane, TPM, molality to the TPO molality in octane at isopiestic equilibrium with increasing TPO molality. The dashed curve was calculated assuming partial dimerization of TPO ($Q_d = 1.8\ m^{-1}$) and ideal behavior of all solute species.

Also, this indicated trimerization quotient is much lower than was estimated from the iron(III) extraction results ($Q_t \sim 10\ M^{-1}$).

In the case of TPO, the results confirm the pronounced deviations indicated by the freezing point measurements in benzene.[12] They also show a good extrapolation to the expected limiting ratio of unity, thus yielding a molecular weight in agreement with the calculated value. Again the results can be partially accounted for if association is assumed. The dashed curve is the expected result for partial dimerization ($Q_d = 1.8\ m^{-1}$). Here such an interpretation must be regarded with some suspicion for two reasons. First, the deviation of the isopiestic ratio from unity is relatively smaller in the low concentration range and could well be in greater part the result of a non-specific solution effect. Secondly, while dimerization might be expected to result from dipole–dipole interaction involving the phosphoryl group $\gtrdot \overset{+}{P} \rightarrow \overset{-}{O}$, this was not supported by dielectric constant measurements,[18] which showed no appreciable change in the molar polarization of TPO with increasing concen-

(18) These measurements were made with the collaboration of W. J. McDowell, using the equipment described by W. J. McDowell and K. A. Allen, *J. Phys. Chem.*, **63**, 747 (1959).

tration (Table II). Absence of dipole–dipole association might well be predicted from the structure of TPO since the three long alkyl chains should screen the phosphoryl group rather effectively.

TABLE II

MOLAR POLARIZATION OF TPO IN OCTANE

Temp. 25° (measured at 960 kc.)

Concn. of TPO, Molarity	Concn. of TPO, Mole fraction	Density, g./ml.	Dielectric constant[a]	Molar polarization,[b] ml.
0	0	0.6986	1.9465	
0.0100	0.001638	.6994	1.9678	514
.0200	.003286	.7002	1.9878	499
.0300	.004943	.7010	2.0081	495
.0500	.008289	.7026	2.0497	493
.0700	.01168	.7042	2.0932	494
.1001	.01684	.7066	2.1616	498
.1499	.02560	.7105	2.2874	508
.2000	.03466	.7145	2.4333	523

[a] These values were calculated from

$$\epsilon - \epsilon_a = (c - c_a)(\epsilon_s - \epsilon_a)/(c_s - c_a)$$

where c denotes capacitance and ϵ denotes dielectric constant; the subscripts a and s refer to dry air and cyclohexane, which was used as the standard; ϵ_a and ϵ_s were taken as 1.0006 and 2.0173, respectively. [b] These values were calculated from

$$P_2 = \left(\frac{\epsilon - 1}{\epsilon + 2}\right)\left(\frac{x_1M_1 + x_2M_2}{d}\right)\Big/x_2 + P_1$$

where P is the molar polarization, x the mole fraction, M the molecular weight, and d the density; the subscripts 1 and 2 refer to octane and TPO, respectively.

Estimation of Activity Coefficients.—In view of the uncertainties of the above interpretations, it is more useful to express the observed non-ideal behavior in terms of the activity coefficients $\gamma_{(DPA)_2}$ γ_{TPO}, and γ_{TPM}, which refer to the hypothetical molal standard states of DPA dimer and TPO and TPM monomer.

The relation between the isopiestic ratio m_B/m_A for two solutes A and B and their activity coefficients γ_A and γ_B is given by Robinson and Stokes[7] as

$$\ln \gamma_A = \ln \gamma_B + \ln (m_B/m_A) + \int_0^{m_B} (m_B/m_A - 1)\, d \ln \gamma_B m_B \quad (2)$$

Since the present measurements did not extend below 0.01 m, this was the lower limit of the integration. Also, an equivalent form of this integral

$$\int \frac{(m_B/m_A - 1)}{\gamma_B m_B} d\gamma_B m_B$$

was found more convenient; it was evaluated by tabulation. Accordingly, the equations used in the present calculations were of the form

$$\ln (\gamma_A/c) = \ln \gamma_B + \ln (m_B/m_A) + \int_{m_B=0.01}^{m_B} \frac{(m_B/m_A - 1)}{\gamma_B m_B} d\gamma_B m_B \quad (3)$$

in which c arises from the integration constant; *i.e.*, $\ln c$ is the value of the integral between $m_B = 0$ and $m_B = 0.01$. In general, it will have a different value for each pair of solutes. It was determined by suitable graphical extrapolation of γ/c to $m = 0$.

If γ_{TPM} were known in octane, or if $\gamma_{(DPA)_2}$ or γ_{TPO} were known, the present results would yield by eq. 3 the activity coefficient of the other two solutes. Since no single set of γ values is known with certainty, however, two separate calculations of the results have been made based on different assumptions concerning the activity coefficient of one solute. In calculation I, γ_{TPM} was assumed to be unity throughout the range of measurements. From the ratios in Table I, $\gamma_{(DPA)_2}$ and γ_{TPO} were determined by appropriate substitutions in eq. 3. In calculation II, the $\gamma_{(DPA)_2}$ values given by the iron(III) extraction results[2b,19] were assumed correct for the present dry solutions. These values are listed in the fourth column of Table III. γ_{TPM} was evaluated first, and these values were used to calculate γ_{TPO}.

TABLE III

ESTIMATED ACTIVITY COEFFICIENTS AT 25°

m	γ_{TPM}, Calcn. II	$\gamma_{(DPA)_2}$ Calcn. I[a,b]	$\gamma_{(DPA)_2}$ Calcn. II[c]	γ_{TPO} Calcn. I[a]	γ_{TPO} Calcn. II
0.02	0.967	0.740	0.672	0.950	0.919
.04	.934	.689	.601	.903	.848
.06	.903	.661	.560	.861	.786
.08	.873	.643	.529	.824	.733
.10	.844	.630	.503	.790	.684
.12	.816	.620	.482	.761	.645
.14	.788	.613	.464	.734	.608
.16	.762	.608	.450	.709	.575
.18	.737		.436	.691	548
.20			.423	.685	.530

[a] Calculation I was based on the assumption that $\gamma_{TPM} = 1$. [b] These values are subject to a systematic uncertainty of 4% owing to uncertainty in the integration constant. [c] Calculation II was based on these $\gamma_{(DPA)_2}$ values, obtained from iron(III) extraction measurements.[2b]

By both calculations $\ln (\gamma_{TPO}/c)$ was found to be nearly a linear function of m_{TPO} and by calculation II $\ln (\gamma_{TPM}/c)$ was found to be a linear function of m_{TPM}. The integration constant therefore was determined in each case by direct extrapolation. However, a plot of $\ln (\gamma_{(DPA)_2}/c)$, by calculation I, *vs.* $m_{(DPA)_2}$ showed enough curvature that it could not be extrapolated with confidence. Instead, since a relation analogous to that found from the iron ex-

(19) The observed variation of the iron(III) extraction quotient

$$Q = \frac{[FeX_6H_3]_{org}[H^+]_{aq}^3}{[Fe^{+3}]_{aq}c^3_{(DPA)_2}}$$

with $c_{(DPA)_2}$, the DPA dimer molarity, is given by

$$Q^{1/3} = 152.4 - 0.3885\sqrt{Qc_{(DPA)_2}}$$

(A relation of this form is predicted if partial trimerization of DPA is assumed.) If the variation in Q is attributed to variation in the DPA dimer molar activity coefficient $y_{(DPA)_2}$, then the equilibrium constant $K = Q/y_{(DPA)_2}^3 = (152.4)^3$. Substitution of $Q = (152.4)^3 \times y_{(DPA)_2}$ into the above relation gives

$$y_{(DPA)_2} = 1 - 4.80y_{(DPA)_2}^{3/2}\, c_{(DPA)_2}^{1/2}$$

Activity coefficients from this relation, converted to the molality scale, are listed in Table II.

traction measurements (see footnote 19) might be expected in this case, $\gamma_{(DPA)_2}/c$ was plotted *vs.* $(\gamma_{(DPA)_2}/c)^{3/2}m_{(DPA)_2}^{1/2}$ for extrapolation. It was a relatively long extrapolation, and the resulting c value had an estimated uncertainty of ±4%. Consequently, the $\gamma_{(DPA)_2}$ values from calculation I are subject to the same large, though systematic, uncertainty.

The results of calculations I and II are compared in Table III. They are summarized within the precision of the calculations by the empirical expressions

	Calcn. I	Calcn. II
$\log \gamma_{TPM}$	= 0 (assumed)	= $-0.737m_{TPM}$
$\log \gamma_{(DPA)_2}$	= $-0.5227m_{(DPA)_2}^{1/3}$ + $0.42m_{(DPA)_2}$	= $-0.6432m_{(DPA)_2}^{1/3}$ (assumed)
$\log \gamma_{TPO}$	= $-1.168m_{TPO}$ + $0.149m_{TPO}^2$	= $-1.886m_{TPO}$ + $0.245m_{TPO}^2$

While they are not in agreement, both sets of γ values reflect the non-ideal behavior apparent from the observed isopiestic ratios, and for $\gamma_{(DPA)_2}$ and for γ_{TPO} the two sets of values are closer to each other than to unity.

Of the two separate assumptions made in these calculations, the assumption that $\gamma_{TPM} = 1$ (calculation I) is probably the more extreme. Indeed, it is to be expected from what is known of solutions of non-electrolytes that γ_{TPM} will decrease with increasing concentration. The magnitude of this decrease can be roughly estimated from a semi-empirical treatment given by Hildebrand and Scott,[20] which expresses deviations from ideal behavior in terms of the molar volumes (V_1 and V_2) of the two components and their solubility parameters, δ_1 and δ_2, which are related to their heats of vaporization. The activity coefficient of the solute at low concentrations is given by

$$\log \gamma_2 = \frac{M_1}{2.3 \times 1000}\left[-1 + \left(\frac{V_2}{V_1} - 1\right)^2 - \frac{2V_2^2}{V_1}\frac{(\delta_2 - \delta_1)^2}{RT}\right] m_2 \quad (4)$$

(20) J. H. Hildebrand and R. L. Scott, "The Solubility of Nonelectrolytes," Third Ed., Reinhold Publ. Corp., New York, N. Y., 1950. Their equation (eq. 47, p. 131) is of the form

$$\ln a_2 = \ln \phi_2 + \phi_1(1 - [V_2/V_1]) + [V_2\phi_1^2(\delta_2 - \delta_1)^2]/RT$$

where a_2 is the activity of component 2 referred to the pure liquid (in this case, the hypothetical supercooled liquid TPM at 25°) as the standard state and ϕ_1 and ϕ_2 are volume fractions. To convert to the hypothetical molal standard state, ($\ln a_2$) is replaced by $\ln(\gamma_2 m_2) + \Delta\bar{G}_2/RT$, wherein $\Delta\bar{G}_2$ denotes the chemical potential difference of component 2 in the two standard states. The quantity $\Delta\bar{G}_2/RT$ is determined from the above equation by the condition that $\gamma_2 \to 1$ as $m_2 \to 0$, giving

$$\Delta\bar{G}_2/RT = [\ln(\phi_2/m_2)]_{\lim,\, m_2\to 0} + (1 - [V_2/V_1]) + V_2(\delta_2 - \delta_1)^2/RT$$

Noting that

$$\phi_2 = (1 - \phi_1) = \frac{m_2M_1V_2}{1000V_2}\Big/\left(1 + \frac{m_2M_1V_2}{1000V_2}\right)$$

eq. 4 is obtained as the resulting expression for γ_2 at low concentrations of component 2.

where M_1 is the molecular weight of the solvent. Introducing the following numerical values for component 1 (octane) and component 2 (TPM)

$$M_1 = 114.22,\ V_1 = 164 \text{ ml.},\ \delta_1 = 7.55$$
$$V_2 = 237 \text{ ml.},\ \delta_2 = 10.06$$

eq. 4 gives

$$\log \gamma_{TPM} = -0.40m_{TPM} \quad (5)$$

The molar volume of TPM was estimated from the density measurements of TPM–octane solutions. The solubility parameter for TPM could best be determined from its heat of vaporization. Since no reliable value has been found, δ_{TPM} was instead estimated by the following procedure: TPM is known[21] to behave ideally in dilute benzene solutions; accordingly, using the molar volume of benzene (89 ml.) and its solubility parameter, 9.15,[20] δ_{TPM} was solved for by placing the right side of eq. 4 equal to zero.

Note that, while in principle eq. 5 is an independent evaluation of γ_{TPM}, it is too approximate to consider as another basis for estimating $\gamma_{(DPA)_2}$ and γ_{TPO}. The significance of this estimate is that it qualitatively supports the conclusions from analysis of the extraction data and lies between the results of calculations I and II.

The assumption on which calculation II is based, that $\gamma_{(DPA)_2}$ has the same value in dry solutions as was found in the water-saturated solutions of the iron(III) extraction measurements, also is open to some question. The solubility of water in DPA–octane solutions has been found to increase with the DPA concentration

$$m_{H_2O} = 0.0034 + 0.030m_{(DPA)_2}$$

where $m_{(DPA)_2} = 0$–0.08. This suggests a weak interaction between DPA and water, which might well alter the value of $\gamma_{(DPA)_2}$. It is likely that the principal species present in solution are the dimer and trimer. Of these, the trimer, owing to its more open structure

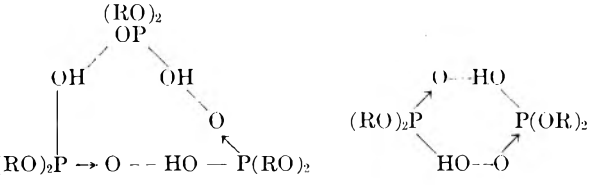

might be expected to interact more strongly with water. If this is true, $\gamma_{(DPA)_2}$ should be lower for wet solutions than for dry solutions.

From these arguments, it seems likely that the correct γ_{TPM}, $\gamma_{(DPA)_2}$, and γ_{TPO} values lie somewhere between those estimated by calculations I and II, and, in view of the non-ideal behavior expected for the reference solute, TPM (eq. 5), it is expected that they are nearer those given by calculation II.

In conclusion, it is the author's view that increased use of the isopiestic method in organic systems is much to be desired. The attention given thus far to binary organic solutions has been con-

(21) N. E. White and M. Kilpatrick, *J. Phys. Chem.*, **59**, 1044 (1955).

cerned largely with the full composition range from one pure component to the other. Little direct information is presently available for dilute solutions (below a few tenths molar), wherein it is commonly assumed in solvent extraction studies that activity coefficients of solute species are constant. The isopiestic method can readily be used to test this assumption. It seems clear from the present results and from eq. 5, based on the treatment of Hildebrand and Scott,[20] that such an assumption often is not justified. For example, it can be predicted that for 0.1, 0.2, and 0.3 *m* TPM in octane, $\gamma_{TPM} = 0.84, 0.71$, and 0.60 by calculation II and 0.91, 0.83, and 0.76 by eq. 5, respectively. These values are significantly below unity for a system in which no specific chemical effects have been assumed.

Acknowledgment.—It is a pleasure to acknowledge the valuable technical assistance of W. E. Oxedine in this investigation.

ELECTRIC MOMENTS OF SUBSTITUTED SUCCINIC ACIDS. THE LOW ELECTRIC MOMENT OF SUCCINIC ACID[1]

BY H. BRADFORD THOMPSON, LENNART EBERSON, AND JEANNE V. DAHLEN

Department of Chemistry, Gustavus Adolphus College, St. Peter, Minnesota, and the Division of Organic Chemistry, Draco, Lunds Farmacevtiska, Lund, Sweden

Received February 28, 1962

The electric moments of substituted succinic acids have been determined in order to explain the relatively low moment of succinic acid. Contrary to previous speculations, a low moment is associated with conformations in which carboxyl groups are separated, while structures involving internal hydrogen bonding show high moments.

Rogers[2] noted that the electric moment of succinic acid was 0.4 D. lower than that of other aliphatic dicarboxylic acids, and proposed that "a ring structure involving both carboxyl groups" might be responsible. He also noted that a similar low moment for diethyl succinate had been reported by Smyth and Walls.[3] This would appear to rule out hydrogen bonding as the basis for any such cyclic conformation.

Similar low moments for the four-carbon members have been reported in other series of α,ω-disubstituted alkanes,[4-5] and recently have been explained[6,7] without recourse to cyclic conformation. It seems advisable to consider more closely, then, the case of succinic acid. Accordingly, we report here electric moment studies of 2,3-disubstituted succinic acids, in some of which cyclic structures are sterically most unlikely.

Experimental

Electric moments were determined by Guggenheim's method[8]: the quantity $(\epsilon - n^2)/(\epsilon + 2)(n^2 + 2)$ was calculated for each of four or five solutions, and plotted against concentration in moles/cc. The slope (S) of the best straight line was taken equal to $4\pi N\mu^2/27kT$. The dielectric constants (ϵ) were determined using apparatus previously described.[9] Refractive indices were measured using a Bausch and Lomb dipping refractometer; after some practice readings were reproducible within 0.00004.

Preparation and purification of the substituted acids have been described previously.[10] Oxalic acid was sublimed at about 130° *in vacuo*. The remaining unsubstituted acids (Eastman) were recrystallized and dried *in vacuo* at 55–60° for at least 24 hr.

At least four solutions of each acid in dioxane were prepared, the most concentrated being in every case less than 0.005 mole fraction acid. Dioxane was purified by reflux with sodium for at least 24 hr.; reflux was continued until no further dulling of the shiny surface of the molten sodium spheres occurred. The dioxane then was fractionally distilled, and the fraction between 100.0 and 100.4° (at 730 mm.) collected and used within 24 hr. Less than 0.04% volatile impurity could be detected by vapor chromatography.

Results and Discussion

The Unsubstituted Acids.—Table I summarizes our results and those of Rogers for the unsubstituted dibasic acids. We, too, find a low moment for succinic acid. However, our moments and those of Rogers differ significantly, our values agreeing more closely with those of Beguin and Gaumann.[11] It appeared worthwhile to determine whether the discrepancy lies in the method, since we employed the procedure of Guggenheim[8] while Rogers used that of Halverstadt and Kumler.[12] Accordingly, we have used the latter method also, using Rogers' solution density data and our dielectric constants. Results are summarized in the last three columns of Table I. The disagreement would appear to stem from a difference in dielectric-constant data. A possible explanation might be found in the difference in drying procedures. In the case of oxalic acid, where purification procedures were nearly identical, close agreement was obtained.

Moments by the two methods seem to agree well when the same dielectric-constant data are used, with those according to Guggenheim slightly

(1) (a) This work was supported in part by the National Science Foundation, through a basic research grant and through an undergraduate research participation grant supporting J. V. D.; (b) presented before the Division of Physical Chemistry at the 139th National Meeting of the American Chemical Society, St. Louis, Mo., March, 1961.

(2) M. T. Rogers, *J. Phys. Chem.*, **61**, 1442 (1957).

(3) C. P. Smyth and W. S. Walls, *J. Am. Chem. Soc.*, **53**, 527 (1931).

(4) C. P. Smyth and W. S. Walls, *J. Chem. Phys.*, **1**, 200 (1933).

(5) P. Trunel, *Ann. chim.*, [11] **12**, 93 (1939).

(6) H. B. Thompson and S. L. Hanson, *J. Phys. Chem.*, **65**, 1005 (1961).

(7) R. P. Smith and J. J. Rasmussen, *J. Am. Chem. Soc.*, **83**, 3785 (1961).

(8) E. A. Guggenheim, *Trans. Faraday Soc.*, **45**, 714 (1949).

(9) H. B. Thompson and C. C. Sweeney, *J. Phys. Chem.*, **64**, 221 (1960).

(10) L. Eberson, *Acta Chem. Scand.*, **13**, 40 (1959).

(11) C. Beguin and T. Gaumann, *Helv. Chim. Acta*, **41**, 1376 (1958).

(12) I. F. Halverstadt and W. D. Kumler, *J. Am. Chem. Soc.*, **64**, 2988 (1942).

TABLE I

ELECTRIC MOMENTS OF UNSUBSTITUTED ACIDS

Acid	S	Moments—Here	Rogers	B. & G.[11]	H. & K. Calculations a	ϵ_1	μ
Oxalic	48.25	2.66	2.63		10.31	2.2091	2.71
Malonic	44.50	2.56	2.57	2.54	9.56	2.2099	2.62
Succinic	29.35	2.08	2.20	2.14	6.27	2.2103	2.11
Glutaric	41.48	2.47	2.64	2.37	8.67	2.2094	2.50
Adipic	36.06	2.30	2.60	2.30	7.79	2.2096	2.36

lower.[13] It appears that this method is as satisfactory as that of Halverstadt and Kumler for comparison of moments in this series.

Moments of Substituted Succinic Acids.—The electric moments of nine substituted succinic acids are summarized in Table II. Preliminary inspection shows that these fall sharply into two groups: moments of about 2.0 D. for two *meso* acids; and moments of 2.4 to 2.6 D. for the rest. Clearly the former group matches the unsubstituted succinic acid while the latter group resembles more closely the other dicarboxylic acids.

TABLE II

ELECTRIC MOMENTS OF SUBSTITUTED SUCCINIC ACIDS

Acid	Form	S	Moment
2,3-Di-*t*-butyl-	*meso*	28.16	2.03
	racemic	43.78	2.53
2,3-Diisopropyl-	*meso*	27.56	2.01
	racemic	45.20	2.57
2,3-Dimethyl-2,3-diethyl-	*meso*	44.35	2.55
	racemic	43.71	2.53
2,3-Dimethyl-2,3-dipropyl-	*meso*	38.78	2.39
	racemic	41.90	2.48
Tetraethyl		46.20	2.60

The *Diamond-Lattice model*[6,7,14] provides a convenient means of analyzing the steric interactions involved. In this model the C–C bonds are taken as equal in length, and the angles between them are assumed to be tetrahedral. In addition a staggered position with respect to each internal rotation is assumed. As a result, the carbon skeleton always can be superimposed upon a portion of a diamond lattice. The most important steric effect following this model is the virtual exclusion[6,15] of conformations in which the first and fourth C–C bonds of any five-carbon segment are parallel (providing any alternative conformation exists).

Most easily analyzed are the diisopropylsuccinic acids. Only the conformations in Fig. 1 should occur, since all others have "excluded" five-carbon segments. This is most easily seen by noting that rotation about the central bond must place both isopropyl groups *gauche* to hydrogens. Otherwise, a methyl group will be brought too close to either a carboxyl or an isopropyl. Thus the *meso* form, possessing the low electric moment, must have the

(13) Following the practice used by Rogers, no correction for atomic polarization was employed in the Halverstadt–Kumler calculation. If an atomic term equal to 10% of the molar refraction is assumed, the acid moments are, respectively, 2.69, 2.60, 2.09, 2.47, and 2.32. The Guggenheim moments are lower than these by an average of only 0.02 D.

(14) A. Tobolsky, R. E. Powell, and H. Eyring, in Ch. 5 of "The Chemistry of Large Molecules," R. E. Burk and O. Grummitt, Ed., Interscience Publishers, Inc., New York, N. Y., 1943, p. 157.

(15) R. P. Smith and E. M. Mortensen, *J. Chem. Phys.*, **35**, 714 (1961).

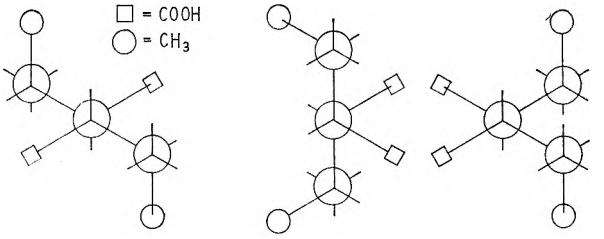

Fig. 1.—Conformations for 2,3-diisopropylsuccinic acid: a, *meso*- (left); b, *d*- or *l*- (right).

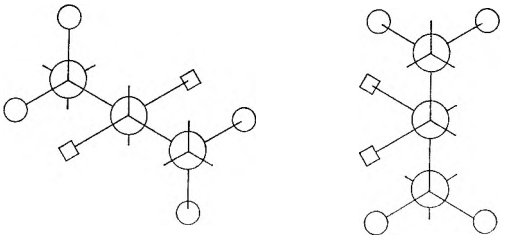

Fig. 2.—Conformations for 2,3-di-*t*-butylsuccinic acid: a, *meso*- (left); b, *d*- or *l*- (right).

carboxyl groups separated, while the high-moment *racemic* mixture must have them close together. There is, in fact, considerable experimental evidence[16,17] that intramolecular hydrogen bonding occurs in the *racemic* form but not in the *meso*. Of particular interest here will be the ratio of the first to the second ionization constant in 50% by weight alcohol solution. The log of this ratio (ΔpK) is 2.12 for the *meso* form and 7.78 for the *racemic*.[16]

The di-*t*-butylsuccinic acids are a more difficult case, since no conformations satisfy the model. The least difficulty would appear to arise when the butyl groups are mutually *trans* (Fig. 2), since a *gauche* position brings non-bonded carbon atoms within 1.6 Å. of one another. This again brings the acid groups together in the optically-active forms and keeps them apart in the *meso*. The steric difficulties between butyl and carboxyl groups can be relieved slightly in the former case by rotation about the central bond. This would bring the carboxyls even closer together than in the isopropyl, a fact that may be reflected in the very high ΔpK (9.54) reported previously.

In tetraethylsuccinic acid there is again no conformation meeting the requirements of the model. Here, however, there is no obvious choice for best rotational position about the central bond. All these have high ΔpK's.

For each of the remaining four acids examined, conformations with carboxyls *gauche* and with carboxyls *trans* are both possible within the model. From the electric moments it would appear that the *gauche* form is important here. The question thus arises: why are the moments for these acids greatly different from those for unsubstituted succinic acid? An attractive explanation is that the energy difference between *trans* and *gauche* states is higher in the unsubstituted than in the substituted acids. Such an energy term is important[6,7] in explaining the low moment of 1,4-

(16) L. Eberson, *Acta Chem. Scand.*, **13**, 211 (1959).

(17) L. Eberson, *ibid.*, **13**, 224 (1959); L. Eberson and S. Forsen, *J. Phys. Chem.*, **64**, 767 (1960).

dihalobutanes, and may apply equally for succinic acid. If the barrier is similar to that in butane, this energy may be as high as 770 cal./mole.[18] In the tetrasubstituted acids, however, the situation might be quite different. If the term in question depends primarily on the atoms immediately bonded to the carbons terminating the central bond, the *trans–gauche* energy should be zero.[19] Thus it seems quite reasonable that succinic acid favors the *trans* conformation to a much greater extent than do the tetraalkylsuccinic acids.

(18) W. G. Dauben and K. S. Pitzer, in "Steric Effects in Organic Chemistry," M. S. Newman, Ed., John Wiley and Sons, Inc., New York, N. Y., 1956.

(19) A more exact consideration might involve analysis of factors such as those considered by N. L. Allinger and V. Zalkow, *J. Org. Chem.*, **25**, 701 (1960). Analysis of the enthalpy and entropy factors involved in the ionizations of some of these acids is underway at Lund.

Conclusions

I. Cyclic structures and intramolecular hydrogen bonding in substituted succinic acids appear to be associated with high, rather than low, electric moments.

II. The electric moment of succinic acid is lower than that of homologous dicarboxylic acids as a result of steric effects similar to those active in the polymethylene dihalides and not because of a cyclic structure.

III. There is evidence that while the *trans* conformation is favored energetically in succinic acid itself, there is a much smaller (or zero) energy difference between rotomers in the tetraalkyl acids

---

THERMODYNAMIC PROPERTIES OF NITRYL FLUORIDE

BY E. TSCHUIKOW-ROUX

Jet Propulsion Laboratory, California Institute of Technology, Pasadena, California

Received March 3, 1962

The thermodynamic functions of FNO_2 have been calculated from 200 to 1200°K. from spectroscopic data using the rigid-rotator-harmonic-oscillator approximation. These functions, together with a recently communicated value for the heat of formation of nitryl fluoride, are used to evaluate the free energy, enthalpy, entropy, and equilibrium constants for several possible reactions of nitryl fluoride. The N–F and N–O bond energies in FNO_2 are calculated to be 44.7 and 61.3 kcal./mole, respectively.

Introduction

In connection with our current interest in the kinetics of several reactions of nitryl fluoride it was felt necessary to consider the thermochemistry of these reactions. Such thermochemical calculations were not possible until recently, since neither the heat of formation of nitryl fluoride nor its thermodynamic functions were available.

However, the infrared and Raman spectrum of nitryl fluoride has been studied by Dodd, Rolfe, and Woodward[1] and the microwave spectrum has been reported by Smith and Magnuson.[2] Using these spectroscopic data, the thermodynamic functions of nitryl fluoride were evaluated in the temperature range from 200 to 1200°K. at 100° intervals. Very recently, an approximate value for the standard heat of formation of FNO_2 ($\Delta H_f^0{}_{298} = -20 \pm 5$ kcal./mole) was reported by Anderson, MacLaren, and co-workers.[3] This value was subsequently revised to -19 ± 2 kcal./mole.[4] Using this value for the standard heat of formation of nitryl fluoride and the thermodynamic data from the literature for the species FNO, NO_2, NO, O, F, F_2, CO, CO_2, it was possible to calculate the standard enthalpies, free energies, entropies, and equilibrium constants for the reactions of interest. The bond dissociation energies for the N–F and N–O bonds in FNO_2 have been calculated and are compared with the corresponding bond dissociation energies of the N–Cl and N–O bonds in $ClNO_2$.

We shall be interested in the reactions

$$NO_2 + F_2 = FNO_2 + F \quad (1)$$

$$FNO_2 + F = NO_2 + F_2 \quad (2)$$

$$FNO_2 = NO_2 + {}^1/_2F_2 \quad (3)$$

$$FNO_2 = NO_2 + F \quad (4)$$

$$FNO_2 = FNO + O \quad (5)$$

$$FNO_2 + NO = FNO + NO_2 \quad (6)$$

$$FNO_2 + CO = FNO + CO_2 \quad (7)$$

$$NO + F_2 = FNO + F \quad (8)$$

Calculations.—The thermodynamic functions of nitryl fluoride were calculated according to the rigid-rotator-harmonic-oscillator approximation. Nitryl fluoride was assumed to be a perfect gas and the pressure was taken as one atmosphere. The molecular constants, determined from spectroscopic measurements, are summarized in Table I. The fundamental frequencies were taken from the reported infrared spectrum.[1] The moments of inertia and the corresponding molecular dimensions are based on the microwave spectrum.[2] The symmetry number, σ, is 2. Nitryl fluoride is a planar molecule with a C_{2v} axis of symmetry.[1,2] The ground state electronic degeneracy corre-

(1) R. E. Dodd, J. A. Rolfe, and L. A. Woodward, *Trans. Faraday Soc.*, **52**, 145 (1956).

(2) D. F. Smith and D. W. Magnuson, *Phys. Rev.*, **87**, 226 (1952).

(3) R. Anderson and R. O. MacLaren, 2nd Quarterly Technical Summary Report, Contract No. Nonr 3433(00); ARPA Order No. 184-61; United Technology Corporation, Sunnyvale, Calif., October, 1961.

(4) R. O. MacLaren, private communication.

sponding to this point group is unity, and thus the electronic contribution to the thermodynamic functions has been neglected. The results of these calculations are presented, in conventional form, in Table II.

TABLE I

MOLECULAR CONSTANTS FOR FNO_2

Fundamental freq., cm.$^{-1}$ Ref. 1	Moments of inertia, g. cm.^{2} Ref. 2	Molecular dimensions Ref. 2
ν_1 = 1312	I_a = 63.562 × 10^{-40}	r(N–F) 1.35 Å.
ν_2 = 822	I_b = 73.313 × 10^{-40}	r(N–O) 1.23 Å.
ν_3 = 460	I_c = 137.116 × 10^{-40}	
ν_4 = 1793		∢ONO 125°
ν_5 = 570	$I_aI_bI_c$ = 6.3895 × 10^{-115}	∢ONF 117.5°
ν_6 = 742	g.^{3} cm.^{6}	

TABLE II

THERMODYNAMIC FUNCTIONS OF NO_2F (CAL. MOLE^{-1} DEG.$^{-1}$)

T, °K.	C_p^0	$(H^0 - H_0^0)/T$	$-(F^0 - H_0^0)/T$	S^0
200	9.857	8.421	49.427	57.848
273.16	11.428	9.019	52.137	61.156
298.16	11.919	9.241	52.937	62.178
300	11.954	9.258	52.993	62.251
400	13.626	10.150	55.780	65.930
500	14.903	10.979	58.135	69.114
600	15.877	11.718	60.204	71.922
700	16.621	12.368	62.068	74.436
800	17.193	12.936	63.749	76.685
900	17.638	13.435	65.302	78.737
1000	17.988	13.874	66.741	80.615
1100	18.265	14.261	68.081	82.342
1200	18.487	14.604	69.338	83.942

In calculating the standard enthalpy, free energy, and entropy changes as well as the equilibrium constants for reactions 2 through 8 we have used the value of −19 kcal./mole for the standard heat of formation of nitryl fluoride at 298°K. and the thermodynamic functions from Table II. The thermodynamic data for all the other species in reactions 2 to 8 were taken from the literature. Thus the values used for the standard heat of formation of NO_2, NO, O, F, CO, and CO_2 were those tabulated by Pitzer and Brewer.[5] The heat of formation of FNO has been measured recently by calorimetry by Johnston and Bertin.[6] These authors report the value ΔH_f^0(NOF) = −15.8 kcal./mole at 298°K. The thermodynamic functions for fluorine atom and fluorine molecule have been computed by Potter,[7] while the functions for nitric oxide and carbon monoxide were obtained from ref. 8. The thermodynamic functions used for atomic oxygen and carbon dioxide were taken from ref. 9 and 5, respectively. For nitrogen dioxide and nitrosyl fluoride, the thermodynamic functions used were taken from papers by Altshuller[10] and Stephenson and Jones,[11] respectively.

The results of these calculations are presented in Tables IV and V. Table IV gives the standard enthalpy change at 0°K. and the enthalpy, free energy, and entropy changes of reactions 2 to 8 in their standard states at 298°K. Table V lists the logarithm of the equilibrium constant, log K_p, for said reactions as a function of temperature from 200 to 1200°K.

The standard heat of formation at 0°K. and the free energy and equilibrium constant of formation at 298°K. of FNO_2, all based on its reported $\Delta H_{f^0_{298}}$,[4] are presented in Table III.

TABLE III

STANDARD ENTHALPY, FREE ENERGY, AND EQUILIBRIUM CONSTANT OF FORMATION OF FNO_2 AND $ClNO_2$ AND HEATS OF DISSOCIATION OF THE N–X AND N–O BONDS AT 0 AND 298°K.

	FNO_2	Ref.	$ClNO_2$	Ref.
ΔH_{f0}^0 (kcal./mole)	−17.6	[a]	7.7	[a]
ΔH_f^0 (kcal./mole)	−19	4	6.5	[a]
ΔF_f^0 (kcal./mole)	− 8.9	[a]	16.5	[a]
log K_{eq}	6.51	[a]	−12.11	[a]
$\Delta H_0^0{}_{N-X}$ (kcal./mole)	44.7	[a]	29.5	12
$\Delta H^0{}_{N-X}$ (kcal./mole)	46.0	[a]	30.5	[a]
$\Delta H_0^0{}_{N-O}$ (kcal./mole)	61.3	[a]	64.2	[a]
$\Delta H^0{}_{N-O}$ (kcal./mole)	62.8	[a]	65.6	[a]

[a] Calculated, this work.

TABLE IV

CALCULATED THERMODYNAMIC DATA

Reaction	ΔH_0^0	ΔH_{298}^0 (kcal. mole^{-1})	ΔF_{298}^0	ΔS_{298}^0 (cal. deg.$^{-1}$ mole^{-1})
2	8.0	8.2	6.5	5.67
3	26.4	27.1	21.3	19.36
4	44.7	46.0	36.1	33.06
5	61.3	62.8	52.2	35.53
6	−10.4	−10.3	−11.5	4.04
7	−64.4	−64.4	−64.7	0.93
8	−18.4	−18.5	−18.0	−1.63

The enthalpy changes in reactions 4 and 5 represent the heat of dissociation of the N–F and N–O bonds in FNO_2. It was thought instructive to compare these values with the corresponding bond energies in $ClNO_2$. Cordes and Johnston[12] have reported the heat of the reaction

$$ClNO_2 = NO_2 + Cl \quad \Delta H_0^0 = 29.5 \text{ kcal./mole}$$

Using this value together with the thermodynamic functions for nitryl chloride[13] and nitrosyl chloride,[14] as well as the known heat of formation of nitrosyl chloride,[15] the heats of the reaction

$$ClNO_2 = ClNO + O$$

(5) G. N. Lewis and M. Randall, revised by K. S. Pitzer and L. Brewer, "Thermodynamics," McGraw-Hill Book Co., New York, N. Y., 1961.

(6) H. S. Johnston and H. J. Bertin, Jr., *J. Am. Chem. Soc.*, **81**, 6402 (1959).

(7) R. L. Potter, *J. Chem. Phys.*, **26**, 394 (1957).

(8) "Selected Values of Properties of Hydrocarbons," Natl. Bur. Stand. Circular C461, 1947.

(9) D. R. Stull and G. C. Sinke, "Thermodynamic Properties of the Elements," Advances in Chemistry Series, No. 18, American Chemical Society, Washington, D. C., 1956.

(10) A. P. Altshuller, *J. Phys. Chem.*, **61**, 251 (1957).

(11) C. V. Stephenson and E. A. Jones, *J. Chem. Phys.*, **20**, 135 (1952).

(12) H. F. Cordes and H. S. Johnston, *J. Am. Chem. Soc.*, **76**, 4264 (1954).

(13) G. Geiseler and M. Rätzsch, *Z. physik. Chem.*, **207**, 138 (1957).

(14) W. G. Burns and H. J. Bernstein, *J. Chem. Phys.*, **18**, 1669 (1950).

TABLE V
EQUILIBRIUM CONSTANTS

	log K_p						
T, °K.	Reaction 2	3	4	5	6	7	8
200	−7.72	−25.34	−42.96	.....	...	...	...
298.16	−4.77	−15.63	−26.48	−38.23	8.44	47.55	13.21
300	−4.73	−15.51	−26.28	−37.95	8.39	47.12	13.13
400	−3.25	−10.57	−17.88	−26.49	6.51	35.38	9.77
500	−2.38	− 7.61	−12.83	−19.60	5.38	28.34	7.76
600	−1.81	− 5.63	− 9.46	−14.99	4.62	23.65	6.43
700	−1.41	− 4.23	− 7.05	−11.70	4.07	20.29	5.48
800	−1.13	− 3.19	− 5.24	− 9.22	3.66	17.77	4.79
900	−0.89	− 2.36	− 3.83	− 7.30	3.34	15.81	4.23
1000	−0.72	− 1.71	− 2.71	− 5.75	3.08	14.25	3.80
1100	−0.58	− 1.18	− 1.79	− 4.50	2.87	12.97	3.44
1200	−0.46	− 0.74	− 1.02	− 3.45	2.68	11.90	3.15

have been calculated at 0 and 298°K. These data also are listed in Table III.

Discussion

In making the thermodynamic calculations our aim was to make a prediction of the feasibility of investigating the kinetics of some of these reactions. In particular we were interested in the thermal decomposition of nitryl fluoride and its reaction with nitric oxide. In the seemingly analogous case of nitryl chloride the thermal decomposition has been studied successfully.[12,16] At 250° and low pressures (order of a few mm.) the reaction proceeds at a comfortable rate *via* the mechanism

$$ClNO_2 = NO_2 + Cl \qquad (a)$$

$$ClNO_2 + Cl = NO_2 + Cl_2 \qquad (b)$$

with an over-all observed stoichiometry

$$ClNO_2 = NO_2 + {}^1/_2Cl_2 \qquad (c)$$

Reactions a, b, and c are analogous to our reactions 4, 2, and 3, respectively. Whereas in the case of nitryl chloride the equilibrium of reaction b lies on the right-hand side even at 1000°K.,[13] the equilibrium of reaction 2 lies on the side of the reactants. The equilibrium of the unimolecular decomposition of FNO_2, eq. 4, as compared to that of $ClNO_2$, eq. a, lies on the side of the reactants by at least 6 orders of magnitude at 500°K. and 2 orders of magnitude at 1000°K. As a result of this the equilibrium of the resulting stoichiometric reaction, eq. 3, is also to the left, *i.e.*, on the side of the reactant even at 1200°K. In contrast to this the equilibrium constant of reaction c is of the order 10^3 to 10^4 over the temperature range. We therefore must conclude that the homogeneous thermal decomposition, such as found in the case of nitryl chloride, cannot be studied in the case of FNO_2 at temperatures below 1200°K.

Benson[17] has suggested that the decomposition of FNO_2 might possibly occur through an N–O rather than an N–F bond rupture, eq. 5. Because of our calculated results, we must rule out this suggestion, since the N–O bond in FNO_2 appears to be stronger by some 15 kcal.

The equilibrium of the reaction between nitryl fluoride and nitric oxide, eq. 6, lies comfortably on the side of the reaction products. Here we note that the equilibrium shifts from right to left (toward the reactants) with increasing temperature. Reaction 6 finds its counterpart in the case of nitryl chloride, where the reaction $ClNO_2 + NO = ClNO + NO_2$ has been shown to be a fast, homogeneous, elementary bimolecular reaction.[18]

The oxidation of carbon monoxide to carbon dioxide by nitrogen dioxide has been studied quantitatively.[19] It was thought of interest to predict the possibility of a similar reaction between FNO_2 and CO, eq. 7. As may be seen from Table V, the equilibrium of this reaction lies overwhelmingly on the side of the reaction products. Here again, the equilibrium shifts toward the reactants with increasing temperature, nevertheless, even at 1200°K. the reaction is essentially 100% complete. One would expect the rate of this reaction to be extremely fast and probably of an explosive character.

The equilibrium constant for reaction 8, which is equal to the product of the equilibrium constants of reactions 1 and 6, decreases with increasing temperature; however, the equilibrium lies safely on the side of the reaction products throughout our temperature range. This reaction is of interest since it probably represents the initial step in the formation of nitrosyl fluoride from nitric oxide and elemental fluorine.

The kinetics of reaction 1, which is, of course, the reverse of reaction 2, have been studied.[20] A combination of the measured rate constant, k_1, with our calculated equilibrium constant for reaction 2 enables us to evaluate the rate constant k_2. If we write $k = A \exp(-E/RT)$, then

$$K_p = k_2/k_1 = Z \exp(-E_2 + E_1)/RT$$

from which it follows that

$$k_2 = A_1 Z \exp(-E_2/RT)$$

and

$$E_2 = E_1 + RT(\ln Z - \ln K_p)$$

(15) C. M. Beeson and D. M. Yost, *J. Chem. Phys.*, **7**, 44 (1939).
(16) H. J. Schumacher and G. Sprenger, *Naturwiss.*, **17**, 997 (1929); *Z. physik. Chem.*, **B12**, 115 (1931).
(17) S. W. Benson, private discussion.
(18) E. C. Freiling, H. S. Johnston, and R. A. Ogg, Jr., *J. Chem. Phys.*, **20**, 327 (1952).
(19) G. M. Calhoun and R. H. Crist, *ibid.*, **5**, 301 (1937).
(20) R. L. Perrine and H. S. Johnston, *ibid.*, **21**, 2205 (1953).

where Z is the ratio of partition functions, *i.e.*, $Z = Q_{NO_2}Q_{F_2}/Q_{FNO_2}Q_F$. At 300°K., assuming ideal gas behavior and pressures of 1 atm. for all species participating in the reaction, Z is found to be 11.612. Using this value, together with the corresponding K_p at 300°K. ($\log K_p = -4.73$) and the reported value for k_1 [$k_1 = 1.59 \times 10^{12} \exp(-10470/RT)$][20] we obtain the rate constant for reaction 2

$$k_2 = 1.85 \times 10^{13} \exp(-18{,}430/RT)$$

Turning our attention to Table III we observe that the nitrogen–halogen bond energy in FNO_2 is about 15 kcal. higher than in $ClNO_2$, whereas the nitrogen–oxygen bond energy is larger in the case of nitryl chloride by about 3 kcal.

It is interesting to note that the dissociation energy of 46.0 kcal. of the N–F bond in nitryl fluoride is about 9 kcal. less than the dissociation energy of the N–F bond in nitrosyl fluoride, 55.4 kcal.,[6] which in turn is about 9 kcal. less than the average single bond energy of 64.6 kcal. for the N–F bond in nitrogen trifluoride (one-third the energy for the dissociation of NF_3 into N and 3F). The N–F bond dissociation energy in FNO_2 is thus 18 kcal. less than the normal N–F single bond energy. We may attribute this difference to the "reorganization energy" of the NO_2 radical,[6,21] that is, the NO_2 radical in FNO_2 is less stable than is the free NO_2 molecule. Qualitatively speaking, the odd electron "used up" in the N–F bond forms a resonating three-electron bond in free NO_2, thus stabilizing the molecule with a gain of 18 kcal.

The energy values given for FNO_2 in Tables III and IV are, of course, approximate values with an inherent uncertainty of ±2 kcal. This uncertainty resides in the reported value for the standard heat of formation of nitryl fluoride, *i.e.*, −19 ± 2 kcal. The same uncertainty is carried over to the equilibrium constants in Table V. Thus the equilibrium constant could be off, in the worst case, by as much as about two orders of magnitude. The conclusions reached earlier, however, would remain essentially the same.

In conclusion we may note that all reactions 2 to 8 show a strong temperature dependence and the reaction which is promising for kinetic studies is reaction 6, *i.e.*, nitryl fluoride plus nitric oxide. The study of the kinetics of this reaction is presently being carried out at this Laboratory.

Acknowledgment.—The helpful discussions of this work with Dr. Hadley Ford are acknowledged.

(21) M. Szwarc and M. G. Evans, *J. Chem. Phys.*, **18**, 618 (1950).

DYNAMIC MECHANICAL PROPERTIES OF POLYVINYL CHLORIDE GELS[1]

BY STEPHEN D. MORTON AND JOHN D. FERRY

Department of Chemistry, University of Wisconsin, Madison, Wisconsin

Received March 5, 1962

The storage and loss compliances, J' and J'', have been measured between 0.05 and 160 cycles/sec. and between −40 and 45° for five gels of polyvinyl chloride: in di-2-ethyl hexyl phthalate (DOP) at polymer concentrations of 5, 7.5, and 10% by volume, and in two polyester plasticizers of high viscosity, G50 and G54, at 5% polymer by volume. The temperature dependence of viscoelastic properties was satisfactorily described by the method of reduced variables with shift factors calculated from the temperature dependence of the solvent viscosity, except for certain anomalies in G50 and G54. The monomeric friction coefficients in G50 and G54 were much smaller than would be calculated from that in DOP on the basis of direct proportionality to solvent viscosity, indicating that in the former solvents (molecular weights 2000–3000) the local effective viscosity is smaller than the macroscopic viscosity. The friction coefficient in DOP increased somewhat with polymer concentration. The relaxation spectra of the DOP gels exhibited unusual inflections which could be attributed to contributions from molecular strands with free ends; the latter contributions vanish at long times while some from the gel network persist.

Introduction

In some earlier studies,[2–4] the viscoelastic properties of a gel of polyvinyl chloride in dimethylthianthrene containing 10% polymer by volume were measured over a very wide range of time and frequency. Less extensive measurements[5] were made on a much more dilute gel of polyvinyl chloride in di-2-ethyl hexyl phthalate. The observed behavior was compared with the Bueche[6] theory for cross-linked systems, and the relation of relaxation times to the solvent viscosity was discussed.

The present studies were undertaken to provide some comparative data for polyvinyl chloride gels of different concentrations and in different solvents covering a range of viscosities. They provide some information on the dependence of monomeric friction coefficient on concentration and solvent viscosity, and reveal some unexpected phenomena which can be attributed to the presence in these gels of a substantial proportion of strands attached at only one end to the gel network.

Experimental

Materials.—The polyvinyl chloride (VYNV-1524) was kindly furnished by Mr. A. T. Walter of Union Carbide Chemicals Co. It was actually a copolymer with about 2.5% of polyvinyl acetate. It was subjected to a rough fractionation by dissolving in tetrahydrofuran and precipitating with water; a high cut of about 11% and a low one of about 22% were rejected. The remaining central fraction had an intrinsic viscosity at 25° in cyclohexanone of 1.71 dl./g.,

(1) Part XXXIX of a series on Mechanical Properties of Substances of High Molecular Weight.

(2) E. R. Fitzgerald and J. D. Ferry, *J. Colloid Sci.*, **8**, 1 (1953).

(3) J. D. Ferry and E. R. Fitzgerald, *ibid.*, **8**, 224 (1953).

(4) J. D. Ferry, D. J. Plazek, and G. E. Heckler, *J. chim. phys.*, **55**, 152 (1958).

(5) M. H. Birnboim and J. D. Ferry, *J. Appl. Phys.*, **32**, 2305 (1961).

(6) F. Bueche, *J. Chem. Phys.*, **22**, 603 (1954).

corresponding[7] to a molecular weight of 1.0×10^5. The Huggins constant was 0.39.

The solvents used for preparing gels were di-2-ethyl hexyl phthalate (DOP), also generously furnished by Union Carbide Chemicals Co., and Paraplex G50 and G54, manufactured by Rohm and Haas Co. The latter are polyesters of moderately low molecular weight. The molecular weights, densities (ρ), thermal expansion coefficients (α), and viscosities (η) at 25° are given in Table I.

TABLE I

PROPERTIES OF SOLVENTS

	Mol. wt.	ρ, 25°, g./cc.	α, deg.$^{-1}$ $\times 10^3$	η, 25°, poise	c_1	c_2, deg.
DOP	390	0.986	1.00	0.57	3.56	139
G50	2200	1.08	0.87	21.9	4.41	133
G54	3300	1.08	0.87	57.6	4.41	139

Viscosities of the solvents were measured by the falling sphere method, using spheres of steel and of synthetic ruby, over a temperature range from −25 to 25° for the DOP and 7.5 to 59° for the two others. The calculations were made by the Faxén equation. Identical results were obtained in a number of cases where different sphere sizes, or both steel and ruby, were used at the same temperature. The temperature dependence of the viscosity could be quite well represented for each solvent by an empirical equation of the WLF form[8]

$$\log (\eta/\eta_0) = c_1(T - T_0)/(c_2 + T - T_0) \quad (1)$$

where η_0 is the viscosity at a reference temperature T_0, chosen here as 25.0°. The values of c_1 and c_2 are included in Table I. Equation 1 fits the data for DOP over the entire temperature range; although the constants differ slightly from those derived from fitting previous capillary viscosimeter measurements[6] between 2 and 70°, the calculated viscosities in the overlap of the two temperature ranges agree very well. Equation 1 fits the data for G50 and G54 only at 12.5° and above. Below 12.5°, the viscosities of these liquids increase extremely rapidly with decreasing temperature.

Each gel was prepared by thoroughly mixing the finely divided polymer with solvent at room temperature and heating at 175° for 45 min. A stabilizer (Union Carbide Chemicals Co. D-22), in amount equal to 4% of the polymer present, was used to inhibit decomposition. The gels were molded into disks for transducer and torsion pendulum measurements. Densities were measured pycnometrically and agreed with calculated values assuming additivity of volumes with a polymer density of 1.41. Concentrations were chosen to correspond to volume percentages of polymer of 5, 7.5, and 10% in DOP, and of 5% in the other solvents. Molded samples were aged at room temperature for at least three days before making measurements.

Methods.—The Fitzgerald transducer[2] and Plazek torsion pendulum[9] methods were used to measure the storage and loss compliances, J' and J'', over a frequency range between 0.05 and 160 cycles/sec. The upper limit was severely restricted by the low rigidities, because of which the corrections for driving tube impedance[2] became too large for adequate precision above the limit cited.

Since changes of mechanical properties of polyvinyl chloride gels implying gradual structural changes with time have sometimes been observed,[5,10] check runs at 25° were made on every sample at the beginning, near the middle, and at the end of the sequence of measurements at different temperatures. The duration of the sequence was usually 10 to 15 days. In the transducer (15 to 160 cycles/sec.) the initial and final measurements always agreed; in the torsion pendulum (0.05 to 1.6 cycles/sec.), measurements at 25° before and after a sequence at higher temperatures agreed, but after a sequence at lower temperatures the storage and loss compliances usually were smaller by about 5%. This is well within the absolute accuracy of these measurements, and it can be concluded that there were no irreversible changes which significantly affected the results. An earlier, more detailed study of thermal history for a 10% gel in dimethylthianthrene led to the same conclusion.[2]

The disk-shaped samples are subjected to compressions of the order of 5 to 15% in installation in both instruments, and in gels the compressive stresses do not relax. A few measurements therefore were made at different degrees of compression in both instruments on 5% gels in DOP and G54. These indicated that both J' and J'' increased about 1.2% for a 1% decrease in sample thickness, without any significant change in their frequency dependences. Compressions in the torsion pendulum ranged from 5 to 12%; 5% appeared to be the minimum for ensuring good contact with the sample faces. No attempt was made to take the effect of compression into account within this range. In the transducer, compressions were somewhat greater, and the values of J' and J'' were in fact somewhat larger when matched to the torsion pendulum data after frequency reduction; the differences in magnitude were absorbed in an empirical correction applied to the transducer data as described below. Thus all the data reported refer to an average compression of about 8%.

To save space, the details of sample dimensions and temperature sequences which usually are given for such experiments[11] have been relegated to a more detailed unpublished report.[12] At least two samples of different shapes were measured for each gel in the torsion pendulum, and usually one pair of samples in the transducer. The values of J' and J'' calculated from different sample shapes in the torsion pendulum were generally in good agreement. The temperature sequence was usually 25° followed by a series at lower temperatures, check at 25°, series at higher temperatures, and finally check at 25°. The actual temperatures for the gels in DOP are listed in the legend of Fig. 1. For the 5% gel in G50, the torsion pendulum measurements ranged from −35 to 25°; transducer measurements are not reported because of uncertainty in the sample coefficient. For the 5% gel in G54, measurements in the torsion pendulum covered a temperature range from −40 to 45°, and in the transducer from 0 to 35°.

Results

The data, which are tabulated in detail elsewhere,[12] are shown here only after temperature reduction. For this purpose, the shift factors a_T were not determined in the usual empirical manner, because the curves for J' were in many cases too flat and the individual frequency ranges were rather small. Instead, it was assumed that in these rather dilute systems the shift factor would be governed by the ratio of solvent viscosities, η_s/η_{s0}, at the temperature of measurement (T) and the reference temperature of 298°K. (T_0). If the local friction is proportional to η_s, the shift factor should be $\eta_s T_0\rho_0/\eta_{s0}T\rho$, where ρ and ρ_0 are the gel densities at T and T_0, respectively. The results were quite satisfactory, as shown in Fig. 1 and 2. Here J' and J'', after multiplication by the usual magnitude factor $T\rho/T_0\rho_0$, are plotted logarithmically against $\omega_r = \omega\eta_s T_0\rho_0/\eta_{s0}T\rho$ for the three gels in DOP; ω is the radian frequency.

When originally plotted in this way, both torsion pendulum and transducer data reduced satisfactorily to give composite curves which for each gel overlapped over a substantial frequency range. The transducer values of logarithm of compliance were higher by an amount which was the same for both log J' and log J'' and equal to 0.15, 0.22, 0.22, and 0.21 for the 5, 7.5, and 10% DOP gels and the 5% G54 gel, respectively. The identity of the dis-

(7) F. Danusso, G. Moraglio, and S. Gazzera, *Chim. ind.* (Milan), **36**, 883 (1954).

(8) M. L. Williams, R. F. Landel, and J. D. Ferry, *J. Am. Chem. Soc.*, **77**, 3701 (1955).

(9) D. J. Plazek, M. N. Vrancken, and J. W. Berge, *Trans. Soc. Rheol.*, **2**, 39 (1959).

(10) A. T. Walter, *J. Polymer Sci.*, **13**, 207 (1954).

(11) R. F. Landel and J. D. Ferry, *J. Phys. Chem.*, **60**, 294 (1956).

(12) S. D. Morton, Ph.D. Thesis, University of Wisconsin, 1962.

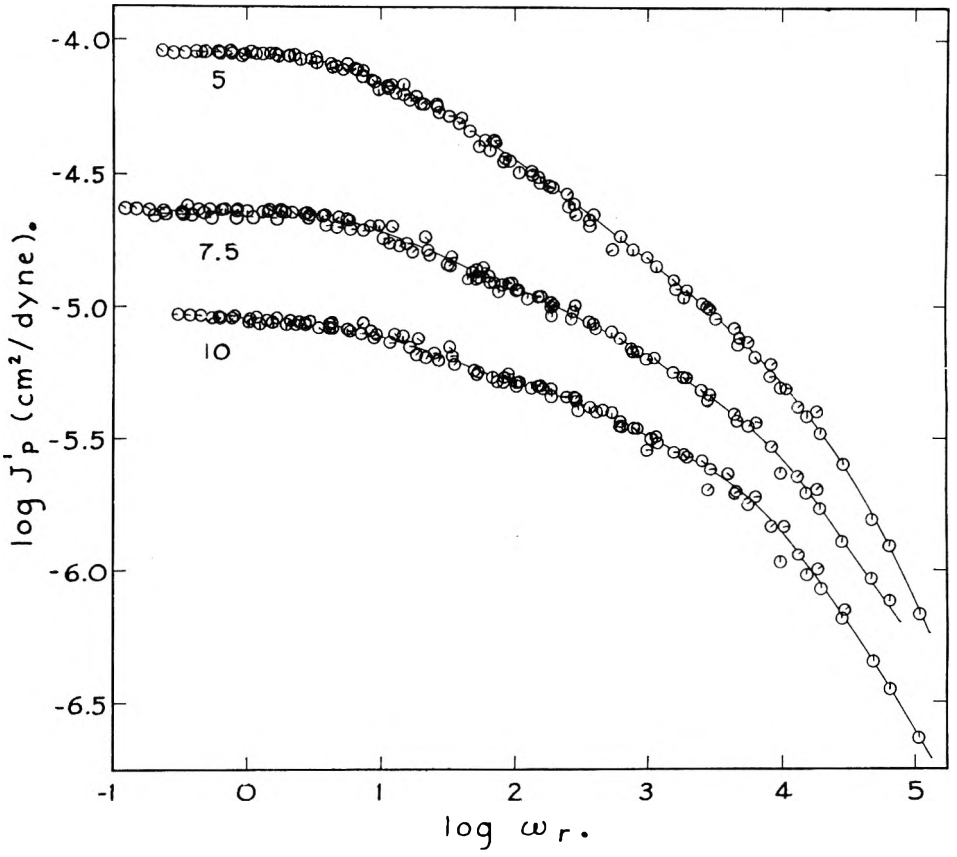

Fig. 1.—Storage compliance reduced to 25°, plotted logarithmically against reduced frequency, for three gels in DOP at concentrations (volume % polymer) indicated: 5%, pip up at highest frequency, −25.0°, successive 45° rotations clockwise correspond to −15.0, −10.0, −5.0, 5.0, 15.0, 25.0, and 35.0°; 7.5%, corresponding temperature sequence of −25.0, −15.0, −5.0, 5.0, 15.0, 25.0, 35.0, and 45.0°; 10%, corresponding temperature sequence of −25.0, −15.0, −5.0, 5.0, 15.0, 25.0, and 35.0°.

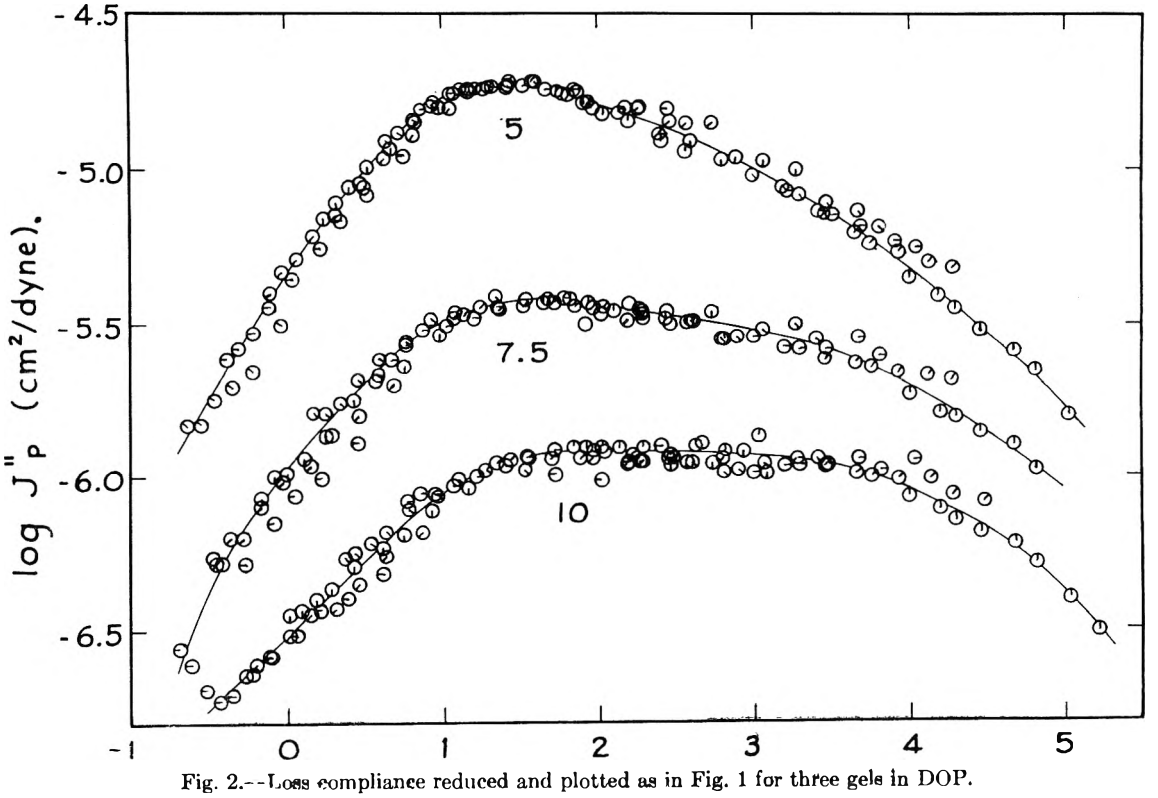

Fig. 2.--Loss compliance reduced and plotted as in Fig. 1 for three gels in DOP.

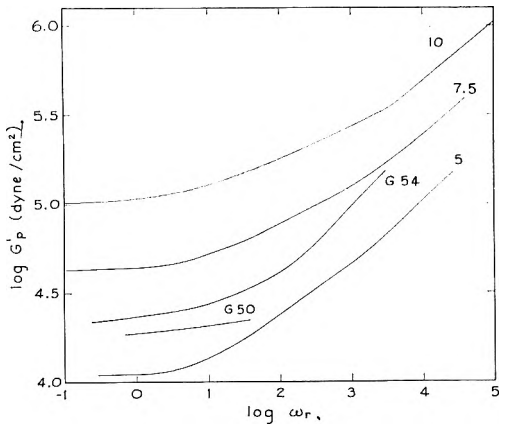

Fig. 3.—Storage modulus plotted logarithmically against reduced frequency at 25° for five gels: 5, 7.5, and 10 denote volume percentages in DOP; G50 and G54, 5% gels in those solvents.

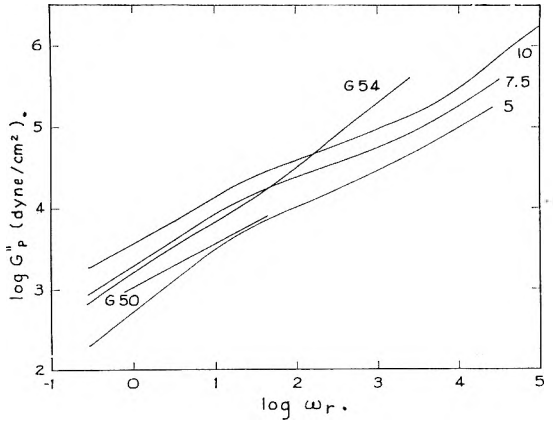

Fig. 4.—Loss modulus plotted as in Fig. 3 for five gels.

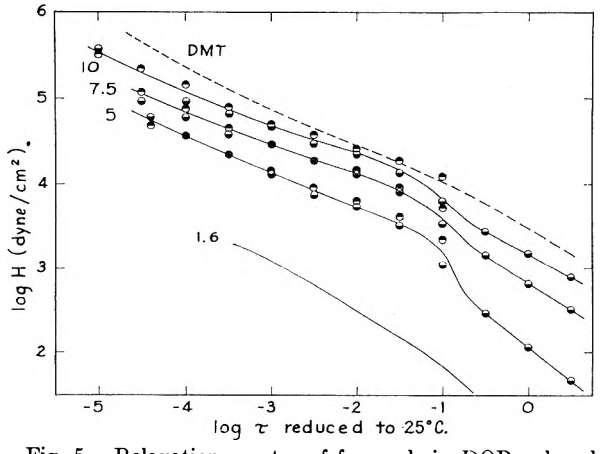

Fig. 5.—Relaxation spectra of four gels in DOP reduced to 25°. Numbers denote concentration of polymer in volume %; 1.6 is from ref. 5. DMT is 10% gel in dimethylthianthrene from ref. 3 and 4. Points top black, from G'; bottom black, from G''.

crepancy for J' and J'' indicates an error in sample coefficient, though the difference probably is due in part to differences in compression as described above. Since the transducer samples underwent more distortion (and were unequally compressed because of the weight of the floating mass cylinders), and the torsion pendulum data for different sample shapes agreed so well, the latter were assumed to be correct and the transducer data were empirically corrected by subtracting the logarithmic differences listed above. After this correction, the data all coincide very well as seen in Fig. 1 and 2. For example, for the 10% gel the region of log ω_r from 1.5 to 3.0 includes overlapping points from both experimental methods.

The reduced data for the gels of G50 and G54 are not shown. In these solvents, reduction in terms of the temperature dependence of solvent viscosity failed below 12.5°. The enormous increase in viscosity at lower temperatures evidently was not accompanied by a corresponding increase in relaxation times, since use of ω_r as calculated above resulted in an overcorrection. For G54, the reduction was nevertheless quite satisfactory above 12.5°, and even at lower temperatures the data could be superimposed by empirical a_T shifts. For G50, the reduction was not quite successful even above 12.5°, and only the data measured directly at 25° are used in subsequent comparisons. The anomalous behavior of these polymeric solvents is further discussed below.

Complex Modulus.—The components of the complex shear modulus, G'_p and G''_p, were calculated from J'_p and J''_p (where the subscript p indicates reduction to 298°K. by the factor $T\rho/T_0\rho_0$), and are plotted logarithmically in Fig. 3 and 4 for all five gels. The data comprise the pseudo-equilibrium zone, where marked differences in equilibrium modulus are evident, and the beginning of the transition zone where both G' and G'' rise substantially with frequency.

Relaxation Spectra.—The relaxation spectra (H) were calculated from the data of Fig. 3 and 4 by the Williams–Ferry approximation method[13]; in view of the unusual shapes of these functions for the DOP gels, calculations also were made in the range of log τ from -1.5 to -0.5 by the Schwarzl–Staverman and Fujita methods,[13] and all the methods agreed quite well. The results for the DOP gels are shown in Fig. 5. At long times, H can be obtained only from G'' because the frequency dependence of G' is too small. Curves for a 1.6% gel[5] (volume %) in DOP and a 10% gel in dimethylthianthrene[4] (DMT) are included for comparison. The curves for the two 10% gels lie near each other.

The spectra for the DOP gels show a curious inflection, especially marked at a volume concentration of 5%, which will be discussed further below. This cannot be ascribed to any artifact caused by the empirical correction applied to the transducer data, since it is entirely encompassed by data derived from the torsion pendulum. Its probable significance will be discussed below.

The relaxation spectra for the three 5% gels are compared in Fig. 6. They lie surprisingly close together, considering the wide range of solvent viscosities as seen in Table I.

Retardation Spectra.—The retardation spectra (L) were calculated from the data of Fig. 1 and 2, and similar data for the G50 and G54 solvents, by the Williams–Ferry method. The results for the

(13) J. D. Ferry, "Viscoelastic Properties of Polymers," John Wiley and Sons, New York, N. Y., 1961, Chapter 4.

DOP gels are shown in Fig. 7, where the maximum characteristic of network structures is apparent. It becomes markedly broader and flatter with increasing polymer concentration. The spectrum for a 10% gel in dimethylthianthrene,[4] included for comparison, lies close to that for the 10% gel in DOP.

The retardation spectra of the three 5% gels are compared in Fig. 8. In the polymeric solvents, the spectra are sharper than in DOP, and the maximum is more nearly symmetrical.

Monomeric Friction Coefficients.—By matching the logarithmic relaxation spectra to a slope of $-1/2$, choosing the region above the inflections in Fig. 5, the monomeric friction coefficient ζ_0 was calculated from the modified theory of Rouse,[14] in which the density ρ appearing in the equation for undiluted polymers is replaced by c, the polymer concentration in g./cc.

$$\log \zeta_0 = 2 \log H + \log \tau + \log (6/kT) + 2 \log (2\pi M_0/acN_0) \quad (2)$$

where M_0 is the monomer molecular weight, N_0 Avogadro's number, and a the root mean square end-to-end distance per square root of the number of monomer units, taken to be 6 Å. The results are given in Table II, the units of ζ_0 being dyne-sec./cm.

TABLE II

MONOMERIC FRICTION COEFFICIENTS AT 25°

Gel	log ζ_0	log ζ_0/η_s
5% DOP	−6.34	−6.09
7.5% DOP	−6.20	−5.95
10% DOP	−5.90	−5.65
5% G50	−6.04	−7.38
5% G54	−5.58	−7.34
10% DMT[4]	−5.36	−6.36
Stokes' law		−6.31

Relation of Local Friction to Solvent Viscosity.—At a concentration as low as 5%, it might be expected that the monomeric friction coefficient would be governed primarily by solvent viscosity and proportional to it. For the two polymeric solvents, G50 and G54, the ratio ζ_0/η_s is in fact almost the same, as shown in the third column of Table II. However, that for DOP is far larger. The discrepancy almost certainly means that the local effective viscosity in the polymeric solvents (even for molecular weight as low as 2000) is considerably smaller than the steady-flow viscosity, so that division by η_s gives an overcorrection. This effect is of course related to the failure of temperature reduction in terms of the solvent viscosity, where enormous viscosity increases with decreasing temperature below 12.5° are accompanied by much milder changes in local friction.

Comparing the two 10% gels, the ratio ζ_0/η_s is considerably higher in DOP than in dimethylthianthrene. However, at this concentration the polymer component is playing a bigger role in the local friction, so that direct proportionality of ζ_0 to η_s is not expected.

Relation of Local Friction to Polymer Concentration.—In the DOP series, there is a moderate

(14) Reference 13, p. 255.

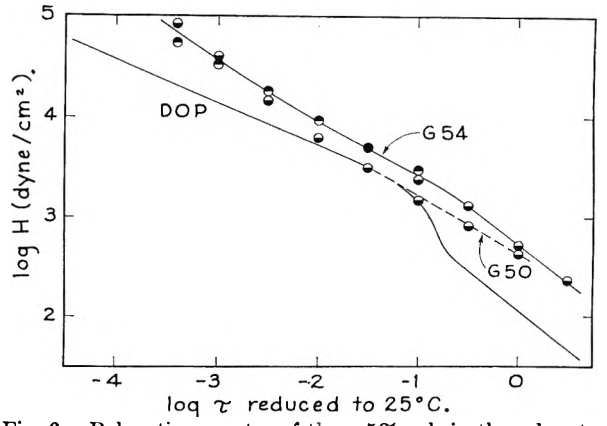

Fig. 6.—Relaxation spectra of three 5% gels in the solvents indicated.

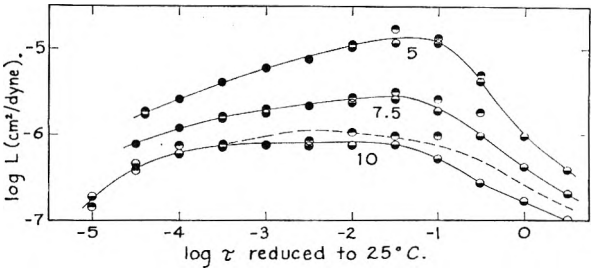

Fig. 7.—Retardation spectra of three gels in DOP at concentrations indicated. Dashed line is 10% gel in dimethylthianthrene as in Fig. 5. Points top black, from J'; bottom black, from J''.

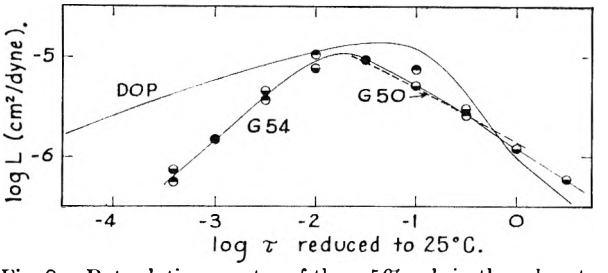

Fig. 8.—Retardation spectra of three 5% gels in the solvents indicated; points refer to G54.

increase in ζ_0 with polymer concentration, as would be expected since there is an increasing contribution to frictional resistance from neighboring polymer segments. The results, extrapolated to zero concentration, correspond to a value of log ζ_0/η_s of about −6.2. This is not far from the value calculated from Stokes' law on the basis of the radius (r) of a sphere with volume equal to that of a monomer unit: log $6\pi r$ = −6.31. No attempt is made at present to analyze the concentration dependence; it is probably related to the concentration dependence of effective local viscosity found in dynamic measurements on dilute uncross-linked polymer solutions.[15]

Analysis of Relaxation Spectrum in Terms of Contributions from Network and Free Ends.—The pseudo-equilibrium shear modulus, G_e, is given in Table III for each gel. If the average molecular weight between cross-links, M_c, is calculated by the simple formula of rubber-like elasticity (M_c =

(15) R. B. DeMallie, Jr., M. H. Birnboim, J. E. Frederick, N. W. Tschoegl, and J. D. Ferry, *J. Phys. Chem.*, **66**, 536 (1962).

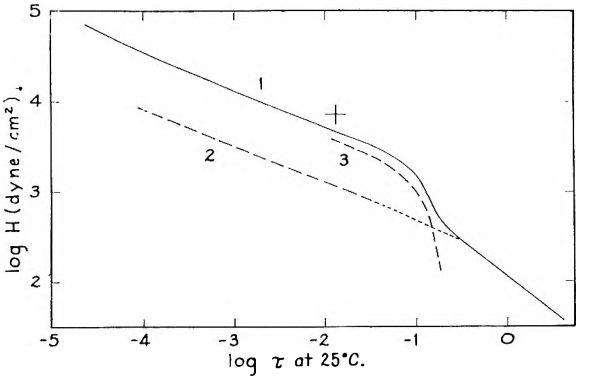

Fig. 9.—Analysis of relaxation spectrum of 5% gel in DOP: curve 1, observed H; curve 2, contribution of network, calculated as $H_m = 0.23H$ (long dashes) and extrapolated (short dashes); curve 3, contribution of free ends obtained by difference.

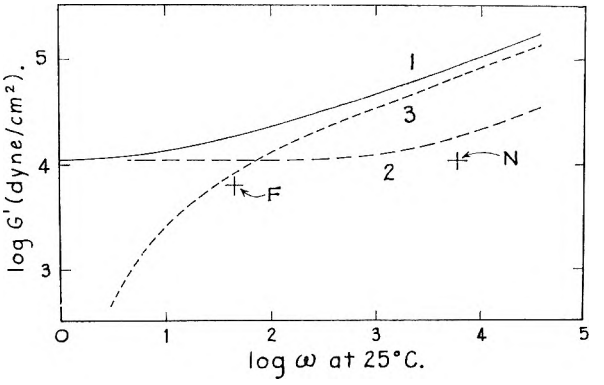

Fig. 10.—Analysis of storage modulus of 5% gel in DOP: curve 1, total observed G'; curve 2, contribution of network, from trifurcate branching formula of Blizard, fitted to log $G_e = 4.04$ at low frequencies and $G'_m = 0.23G'$ at high frequencies; curve 3, contribution of free ends obtained by difference; cross F, origin of dimensionless plot of Blizard free end theory matched to curve 3; cross N, origin of dimensionless plot of Blizard trifurcate network theory matched to curve 2.

cRT/G_e), meaninglessly large values are obtained which for the 5% gel in DOP actually exceed the polymer molecular weight. It is necessary to take into account the free ends and the sol fraction, w_s, in the system by the formula[16]

$$G_e = (1 - w_s)(cRT/M_c)(1 - 2M_c/M) \quad (3)$$

A rough estimate of the magnitude of w_s can be obtained from Flory's treatment[17] of post-gelation statistics even though the cross-links in polyvinyl chloride gels are not expected to have the tetrafunctionality on which his theory is based. For a polymer initially homogeneous with respect to molecular weight, the average number of cross-linked units per initial molecule in the gelled system is $\gamma = -\ln w_s/(1 - w_s)$; the average density of cross-links in the gel fraction is higher than this by a factor of $1 + w_s$. Accordingly, M_c can be estimated as $M/\gamma(1 + w_s)$. By combining these relations with eq. 3, we find for the 5% gel in DOP $w_s = 0.12$, $w_m = 0.23$, and $w_f = 0.65$. Here $w_m = (1 - w_s)(1 - 2M_c/M)$, the fraction of the network contributing to the pseudo-equilibrium modulus, and $w_f = 1 - w_s - w_m$, the fraction of the network in free ends.

Since w_s in this gel is small, and in the other gels smaller still, it has been lumped together with w_f in the subsequent calculations, and M_c has been obtained from eq. 3 with w_s assumed zero. The results are given in Table III. The proportion of polymer in the network is relatively small for the dilute gels, as expected.

TABLE III

WEIGHT FRACTION OF POLYMER IN NETWORK (w_m) AND AVERAGE MOLECULAR WEIGHT BETWEEN CROSS-LINKS

Gel	log G_e	w_m	M_c
5% DOP	4.04	0.23	38,000
7.5% DOP	4.63	.45	28,000
10% DOP	5.03	.60	20,000
5% G50	4.26	.34	33,000
5% G54	4.34	.38	31,000

As a first approximation, the closed network and the free ends are associated each with its own relaxation spectrum, as described in an early treatment by Blizard.[18] A crude attempt to separate them for the 5% gel is shown in Fig. 9. Curve 1 represents H, the experimentally determined total spectrum. At short times, the individual spectra should be identical in form and the magnitude of each proportional to the weight fraction of the corresponding component, since short-range configurational motions are oblivious of cross-links or free ends. Hence, at short times, $H_m = w_m H$, and this is drawn as curve 2 at the left in Fig. 9. At longer times, on the other hand, the spectrum for the free end component should vanish, while on the basis of experience with cross-linked systems, the spectrum for the network should persist so that at long times H becomes equal to H_m. This feature provides a plausible explanation for the inflection in H and the fact that its magnitude decreases with increasing polymer concentration (Fig. 5). Curve 2 therefore is extrapolated in the region of the inflection (short dashes) to join the experimental curve for H at long times. The difference, $H - H_m$, is plotted as curve 3 and represents the contributions of free ends.

For a quantitative analysis of the network contributions, it is better to use the storage modulus, since the theory of Blizard[18] predicts the frequency dependence of the different contributions in the form of continuous functions which serve to guide the separation procedure. Equation 17 of reference 18 is based on a model in which each network strand is linked to others through a series of trifurcate branchings, and the mechanical impedance of a single strand corresponds in molecular terms to the normal-mode model of Rouse.[19] A numerical evaluation of this equation has been made[20] on a high-speed computer and expressed in terms of dimensionless variables based on the Rouse theory, in the manner described recently for linear mole-

(16) P. J. Flory, "Principles of Polymer Chemistry," Cornell University Press, Ithaca, N. Y., 1953.

(17) P. J. Flory, *J. Am. Chem. Soc.*, **69**, 30 (1947).

(18) R. B. Blizard, *J. Appl. Phys.*, **22**, 730 (1951).

(19) P. E. Rouse, Jr., *J. Chem. Phys.*, **21**, 1272 (1953).

(20) S. E. Lovell, unpublished calculations. A table of values may be obtained on request.

cules.[21] The results can be expressed in dimensionless form

$$G'_{m}M_c/w_mcRT = G'_{mR}(\omega\tau_{1m}) \qquad (4)$$

where τ_{1m} is the terminal relaxation time for the viscoelastic contributions of the network.

In Fig. 10, curve 1 represents the observed total G' for the 5% gel in DOP. At high frequencies, G'_m should be simply w_mG' just as $H_m = w_mH$ at short times. Curve 2 is drawn as w_mG' above log $\omega = 4$. The remainder of curve 2 is the theoretical function, eq. 4, with its logarithmic scales adjusted to match w_mG' at high frequencies and the limiting value of log $G_e = 4.04$ at low frequencies. The cross N indicates the origin of the dimensionless function, eq. 4; its abscissa is therefore $-\log \tau_{1m}$ and its ordinate log w_mcRT/M_c.

Subtraction of G'_m from G' at all frequencies gives G'_f, which is plotted logarithmically as curve 3 in Fig. 10. It conforms quite closely in shape to the Blizard theory for free ends, calculated[20] from eq. 16 of reference 18. The cross F denotes the origin of the dimensionless plot for free ends, corresponding to eq. 4, matched to curve 3; its abscissa is $-\log \tau_{1s}$, the terminal relaxation time for the free ends, and its ordinate is log w_fcRT/M_f, where M_f is an effective molecular weight for the free ends. A similar analysis of G'' for the 5% DOP gel is impractical because G'' is dominated by the free ends throughout the frequency range.

The ordinate of cross N corresponds of course to $M_c = 38{,}000$ because it is determined by the value of G_e, from which the latter value was calculated in Table III. The abscissa gives log $\tau_{1m} = -3.67$. This may be compared with a value calculated on the basis of the Rouse theory, $\tau_{1m} = a^2Z^2_c\zeta_0/6\pi^2kT$. Here a^2 is the mean square chain length per monomer unit, taken as 6 Å., Z_c is the degree of polymerization between cross-links ($= M_c/62.5$), and ζ_0 is taken from Table II. The calculated value is log $\tau_{1m} = -2.60$. This is a rather large discrepancy, but there is some uncertainty about the numerical factor in the above expression applied to networks and also a distribution of strand lengths which the theory does not account for.

The ordinate of cross F corresponds to $M_f = 210{,}000$, which is much too large; it should be similar in magnitude to M_c. However, a small amount of sol fraction whose average molecular weight must be above 100,000 because of aggregation has been lumped with this component. The abscissa of the cross gives log $\tau_{1f} = -1.65$. If τ_1 is calculated from the equation in the preceding paragraph, with Z_c replaced by Z_f ($= M_f/62.5$), the result is log $\tau_{1f} = -2.11$.

It is puzzling that τ_{1f} is considerably larger than τ_{1m}, implying either that the free ends are longer than the strands of the closed network or that they participate in entanglement coupling. Better knowledge of the gel network topology is needed for clarification. It also should be pointed out that there are small additional network contributions to the relaxation spectrum beyond the nominal terminal relaxation time τ_{1m}, which appear in Fig. 5, 6, and 9 for log $\tau > 0$. Such contributions at very long times are observed in all cross-linked networks and are not yet explained by any theory.[22] They are not apparent in the storage modulus because their contributions to G' are very small compared with G_e.

Acknowledgments.—This work was supported in part by the Office of Naval Research under Contract N7onr28509, and in part by the Research Committee of the Graduate School of the University of Wisconsin from funds supplied by the Wisconsin Alumni Research Foundation. We are much indebted to Mrs. A. Rossol for assistance with calculations.

(21) S. E. Lovell and J. D. Ferry, *J. Phys. Chem.*, **65**, 2274 (1961).

(22) Reference 13, p. 189.

THE HEAT CAPACITY OF CUPROUS OXIDE FROM 2.8 TO 21°K.[1]

BY LAWRENCE V. GREGOR[2]

Department of Chemistry and Lawrence Radiation Laboratory, University of California, Berkeley, California

Received March 7, 1962

The heat capacity of Cu_2O has been measured from 2.8 to 21°K. Although no anomalous peaks are observed, there are similarities below 15°K. to the heat capacity of highly annealed Ag_2O, which is isostructural with Cu_2O. The observed heat capacity is lower than predicted by a Debye extrapolation from data above 14°K., and a revised value of 22.26 ± 0.5 cal. deg.$^{-1}$ was obtained for $S^0_{298.15}$.

Introduction

The only common metallic oxides which have the cuprite structure are Cu_2O and Ag_2O.[3,4] Although possessing cubic symmetry, the cuprite structure consists of atoms arrayed on two interpenetrating sublattices which are displaced from each other by a_0, the edge length of the cubic unit cell. Thus the atoms on one sublattice are situated in the voids of the second, and the two interlaced substructures are not connected by primary chemical bonds. A second unusual feature is the low degree of coördination. Each metal atom has two nearest-neighbor oxygen atoms linearly arranged and each oxygen is surrounded tetrahedrally by four metal atoms.[5]

(1) This work was supported by the U. S. Atomic Energy Commission.

(2) International Business Machines Corporation, Thomas J. Watson Research Center, Yorktown Heights, New York.

(3) R. W. G. Wyckoff, *Am. J. Sci.*, **3**, 184 (1922).

(4) P. Niggli, *Z. Krist.*, **57**, 253 (1922).

(5) R. W. G. Wyckoff, "Crystal Structures," Vol. I, Interscience Publishers, Inc., New York, N. Y., 1948, Chapter IV.

The symmetry of the crystal structures at room temperature indicates that the mean positions of the atoms on one sublattice are at the centers of the "holes" in the second. It is conceivable, however, that at low temperatures the vibrational frequencies of the lattice may be diminished to such an extent that the potential energy minima are shifted slightly off center. Thus a slight distortion of the crystal structure would produce a lowering of the free energy. There are several instances of this type of distortional behavior in ionic solids.[6] The anomalous "hump" between 20 and 50°K. in the heat capacity of unannealed Ag_2O, first observed by Pitzer and Smith,[7] apparently is associated with some sort of structure alteration and is a function of the size and perfection of the crystals of Ag_2O.[8,9] The heat capacity of Cu_2O has been measured by Hu and Johnston[10] from 14 to 300°K., and no anomalous behavior was observed comparable to that of Ag_2O. The present research was undertaken to extend the range of heat capacity observations on Cu_2O to lower temperatures.

Experimental

Cu_2O was prepared by the reduction of warm Fehling's solution with dextrose. Fehling's solution, made by dissolving reagent grade $CuSO_4 \cdot 5H_2O$ and $NaKC_4H_4O_6$ (1:2 mole ratio) in 2 l. of distilled water and adding reagent grade NaOH until the turbidity disappeared, was warmed to 50° and stirred while small portions (15–25 ml.) of 2 *M* dextrose solution were added every few minutes. The precipitation was complete in 1 hr. After "aging" in the warm, stirred supernatant liquid for ten hours, the precipitate was filtered, washed several times with hot distilled water, and dried in an oven at 110° for 12 hr.

The dried sample was a finely divided red powder. Titrimetric analysis gave 88.3 ± 0.2% Cu^+ (theoretical 88.82%). Since no significant impurities were detected, the sample was assumed to be 99.4% Cu_2O with the rest as CuOH or CuO. The calorimetric sample weighed 44.27 g. (0.309 mole). The cryostat, calorimeter, and experimental procedures were those employed in similar measurements on Ag_2O, and have been described elsewhere.[8,11]

Results

The heat capacity of Cu_2O was measured between 2.8 and 21°K. in two runs. First, the sample was cooled to 2.8° and measurements made to 21° (run 1). Because of apparatus difficulties, a gap was left between 17 and 20°. The sample then was cooled to 16° and more observations were made (run 2). This served to cover the gap and also to determine if there were any supercooling effects detectable in the heat capacity; such effects had been noticed in unannealed Ag_2O.[7] The data are given in Table I. The uncertainty in a given measurement is estimated as ±2% below 20°K.

The measurements of Hu and Johnston at their lowest temperatures are considerably higher than that observed here. This may be due to the increasing uncertainty of their data below 20°K. The two sets of data agree at 19°K.; the disagreement above this point may be due to the decreasing sensitivity above 20° of the carbon resistance thermometer used in the present measurements. For this reason, no data were obtained above 21°K.

TABLE I

MOLAR HEAT CAPACITY OF Cu_2O

T_{av}, °K.	C_p, cal. deg.$^{-1}$ mole^{-1}	T_{av}, °K.	C_p, cal. deg.$^{-1}$ mole^{-1}
	Run 1		
2.794	0.00451	8.778	0.1364
3.087	.00595	9.269	.1554
3.375	.00922	9.811	.1880
3.635	.01102	10.385	.2106
3.937	.01363	11.019	.2416
4.107	.01352	11.723	.2910
4.406	.01901	12.462	.3330
4.662	.02284	13.196	.3927
4.943	.02694	14.951	.5432
5.313	.03506	15.975	.7070
5.671	.04149	17.076	.8355
6.384	.05747	20.207	1.476
6.760	.06654	21.090	1.611
7.138	.07895	Run 2	
7.496	.08767	16.423	0.7648
7.910	.1049	17.793	0.9901
8.335	.1173	19.081	1.1185

The entropy of Cu_2O, $S^0_{298.15}$, was determined by Hu and Johnston from their heat capacity observations and a Debye extrapolation below 16°K. Since the experimentally determined heat capacity below 19° is less than that given by the Debye approximation, S^0 was re-evaluated by graphical integration of C_p/T *vs.* T from 2.8 to 19°K., and the previous observations of Hu and Johnston above 19°K. were added to give a slightly revised value of $S^0_{298.15}$ for Cu_2O. The results are given in Table II.

TABLE II

MOLAR ENTROPY OF Cu_2O(s)

T, °K.	S^0, cal. deg.$^{-1}$ mole^{-1}
Hu and Johnston[10]	
0–16	0.41 ± 0.04
16–19	0.17
19–298.15	21.86 ± 0.03
298.15	22.44 ± 0.07
This study	
0–19	0.40 ± 0.02
19–298.15	21.86 ± 0.03
298.15	22.26 ± 0.05

Discussion

It has been established that unannealed Cu_2O has no anomalous heat capacity "hump," at least above 2.8°K., analogous to the region of high heat capacity observed for unannealed Ag_2O between 20 and 50°K. The Ag_2O "hump" has been tentatively attributed to a transition from a slightly distorted low-temperature state to a more symmetric high-temperature state, associated in some manner with

(6) For a recent review, see J. D. Dunitz and L. H. Orgel, "Advances in Inorganic Chemistry and Radio-Chemistry," Vol. II, edited by H. J. Emeléus and A. G. Sharpe, Academic Press, New York, N. Y., 1960, Chapter I.

(7) K. S. Pitzer and W. V. Smith, *J. Am. Chem. Soc.*, **59**, 2633 (1937).

(8) L. V. Gregor and K. S. Pitzer, *ibid.*, **84**, 2664 (1962).

(9) R. E. Gerkin and K. S. Pitzer, *ibid.*, **84**, 2662 (1962).

(10) J. H. Hu and H. L. Johnston, *ibid.*, **73**, 4450 (1951).

(11) L. V. Gregor, Ph.D. Dissertation, University of California, Berkeley, May, 1961.

the low degree of coördination and the absence of primary chemical bonding between the interpenetrating substructures comprising the cuprite lattice.[8] This transition hypothesis also is encouraged by the observation of a high-pressure transition in Ag_2O between 4000 and 8000 kg./cm.^{2} at 30° by Bridgman.[12] However, Cu_2O showed no such transition up to 12,000 kg./cm.^{2}.

High-temperature annealing of Ag_2O under high O_2 partial pressure has a considerable effect on the heat capacity. The anomaly disappears,[9] and there are other similarities to the heat capacity of Cu_2O. The variation of the Debye characteristic temperatures θ_D is given in Fig. 1. There is a qualitative similarity and a resemblance, perhaps fortuitous, to the θ_D *vs.* T curve calculated by Blackman[13] for a square two-dimensional lattice with nearest and next-nearest neighbor interactions. Also, there are short temperature intervals over which the heat capacity increases approximately as T^2 for both substances, 4–8°K. for Cu_2O and 2–7°K. for Ag_2O.

Both Ag_2O and Cu_2O are highly covalent, being more stable by about 130 and 100 kcal./mole, respectively (Born–Haber cycle), than calculated on the basis of the observed interatomic distanc s and simple ionic bonding.[14] Cu_2O appears to be slightly more ionic than Ag_2O, which may account for its greater thermal stability. On this basis alone, it would be expected that Cu_2O would have a greater tendency to achieve a higher effective degree of coördination by a structure alteration. This is not observed, an indication that the phenomenon in unannealed Ag_2O is not a simple second-order structure change. Both compounds are semiconductors, Cu_2O being well known as p-type, indicating a slight deficiency of Cu. However, Ag_2O is undoubtedly n-type, for it has a slight excess of Ag. The excess Ag atoms probably are accommodated interstitially, with consequent localized disturbance of the regularity of the crystal structure. It is possible that the presence of interstitial Ag atoms is responsible for the occurrence of the structure change responsible for the heat capacity anomaly in unannealed Ag_2O. If so, then Cu_2O would not undergo a similar change readily since its characteristic defects are lattice vacancies, rather than interstitial atoms. The behavior of highly annealed Ag_2O then is explained by the removal of structural defects and the decrease in the number of excess interstitial Ag atoms during the annealing process.

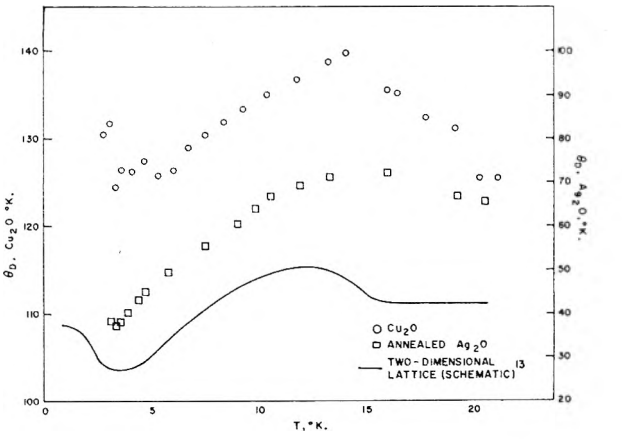

Fig. 1.—Variation of θ_D with temperature for Ag_2O and Cu_2O. Solid curve is schematic with arbitrary θ_D and T axes.

From these considerations, it appears that the cuprite lattice itself is not primarily responsible for the transition in Ag_2O, though it probably is conducive to the transition. Further elucidation of the role of this structure in the lattice heat capacity might be obtained by investigation of lead suboxide, Pb_2O, which is reported to have the cuprite structure, $\alpha_0 = 5.38$ Å.[5] The relative instability and greater interatomic distances might lead to an anomalously high heat capacity in unannealed Pb_2O; if annealing is possible without decomposition, annealed Pb_2O might be expected to have a T^2 heat capacity dependence and a variation in θ_D similar to Ag_2O and Cu_2O.

Acknowledgment.—The author is indebted to Professor K. S. Pitzer for valuable discussions and encouragement.

(12) P. W. Bridgman, *Rec. trav. chim.*, **51**, 827 (1932).
(13) N. Blackman, *Proc. Roy. Soc.* (London), **A149**, 117 (1937).
(14) J. Sherman, *Chem. Rev.*, **11**, 93 (1932).

ELECTRON IMPACT SPECTROSCOPY OF SULFUR COMPOUNDS. I. 2-THIABUTANE, 2-THIAPENTANE, AND 2,3-DITHIABUTANE[1]

BY BRICE G. HOBROCK AND ROBERT W. KISER

Department of Chemistry, Kansas State University, Manhattan, Kansas

Received March 8, 1962

The appearance potentials of the principal ions in the mass spectra of 2-thiabutane, 2-thiapentane, and 2,3-dithiabutane are reported. Assignments of the probable processes of ionization and dissociation are made consistent with the observed energetics. Heats of formation for the various ions are computed and tabulated. From appearance potential data, (1) the ionization potentials of 2-thiabutane, 2-thiapentane, and 2,3-dithiabutane are 8.70 ± 0.10, 8.80 ± 0.15, and 9.1 ± 0.2 e.v., respectively; (2) the proton affinities of H_2S and CH_3SH are −195 ± 7 and −201 ± 10 kcal./mole, respectively; and (3) the derived ionization potentials of S_2 and CH_3S_2 are 11.0 ± 0.2 and 9.5 ± 0.5 e.v., respectively.

Introduction

Organic sulfur compounds are of considerable interest in petroleum technology. The electron impact study of such molecules can provide significant information concerning these sulfur compounds and their gaseous ions. Gallegos and Kiser[2,3] recently have reported ionization potentials and heats of formation for a number of ions formed from various saturated heterocyclic sulfur compounds. The ionization potentials for a few of the straight-chain sulfides and disulfides have been reported, but no detailed investigation of the appearance potentials and heats of formation of the various ionic products of the ionization and dissociation process has been made. We have, therefore, initiated a program to study a number of the sulfur compounds by electron impact methods.

In this paper we report information obtained in a study of three sulfur-containing molecules: 2-thiabutane, 2-thiapentane, and 2,3-dithiabutane. We have determined mass spectral cracking patterns for these compounds and find good agreement with the data reported in the API tables.[4] (Serial numbers 473, 476, 496, 498, 588, and 913.) Ionization and appearance potential data were determined for the principal ions formed from these three sulfur compounds. The measured ionization potentials are compared to those calculated using a group orbital treatment and interaction parameters previously given.[3] From the experimental data, the proton affinities of hydrogen sulfide and methanethiol are calculated.

Experimental

The experimental data reported here were obtained using a time-of-flight mass spectrometer with an analog output system. The instrumentation has been described previously.[5]

The samples of 2-thiabutane and 2,3-dithiabutane were obtained from Eastman Organic Chemicals. The 2-thiapentane was obtained from Aldrich Chemical Co. Gas–liquid partition chromatographic analysis of 2-thiabutane and 2,3-dithiabutane revealed no impurities. The analysis of 2-thiapentane revealed approximately 2 mole % impurity of higher molecular weight. It is believed that this small impurity affected neither the mass spectral cracking pattern determinations nor the appearance potential measurements.

Mass spectra were obtained at nominal electron energies of 70 e.v. The voltage scale in the determination of ionization and appearance potentials was calibrated using xenon mixed intimately with the compound under investigation. The extrapolated voltage difference method[6] was used for determining appearance potentials. Ionization potentials also were determined using the technique of Lossing, Tickner, and Bryce,[7] and were checked by means of the energy compensation method.[8]

Results

The mass spectral cracking patterns and appearance potential data for the three compounds investigated are given in Tables I–III. The relative abundance of the principal ions formed at 70 e.v. is given in column 2. The measured appearance potentials are summarized in column 3 and the probable processes for the formation of the ions are given in column 4. The heats of formation consistent with the proposed processes for the various ions are given in the last column.

The heats of formation of the sulfur-containing molecules were determined by the U. S. Bureau of Mines workers and were employed consistently in all of the thermochemical calculations. The heats of formation for 2-thiabutane,[9] 2-thiapentane,[10] and 2,3-dithiabutane[11] are −14.22, −19.51, and −5.75 kcal./mole, respectively. The heats of formation of various radicals involved in the dissociation processes were taken from those summarized by Gallegos.[12]

Discussion

Ionization Potentials.—The ionization potentials determined for the three molecules investigated are shown in Table IV, where a comparison with other experimental results and calculations using

(1) This work was supported by the U. S. Atomic Energy Commission under contract No. AT(11-1)-751 with Kansas State University. A portion of a dissertation to be presented by B. G. Hobrock to the Graduate School of Kansas State University in partial fulfillment of requirements for the degree of Doctor of Philosophy; presented at the 141st National Meeting of the American Chemical Society, Washington, D. C., March 20–29, 1962.

(2) E. J. Gallegos and R. W. Kiser, *J. Phys. Chem.*, **65**, 1177 (1961).

(3) E. J. Gallegos and R. W. Kiser, *ibid.*, **66**, 136 (1962).

(4) "Mass Spectral Data," American Petroleum Institute Research Project 44, National Bureau of Standards, Washington, D. C.

(5) E. J. Gallegos and R. W. Kiser, *J. Am. Chem. Soc.*, **83**, 773 (1961).

(6) J. W. Warren, *Nature*, **165**, 811 (1950).

(7) F. P. Lossing, A. W. Tickner, and W. A. Bryce, *J. Chem. Phys.*, **19**, 1254 (1951).

(8) E. J. Gallegos and R. W. Kiser, *J. Phys. Chem.*, **66**, 947 (1962).

(9) W. N. Hubbard and G. Waddington, *Rec. trav. chim.*, **73**, 910 (1954).

(10) W. N. Hubbard, W. D. Good, and G. Waddington, *J. Phys. Chem.*, **62**, 614 (1958).

(11) W. N. Hubbard, D. R. Douslin, J. P. McCullough, D. W. Scott, S. S. Todd, J. F. Messerly, I. A. Hossenlopp, A. George, and G. Waddington, *J. Am. Chem. Soc.*, **80**, 3547 (1958).

(12) E. J. Gallegos, "Mass Spectrometric Investigation of Saturated Heterocyclics," Doctoral Dissertation, Kansas State University, Manhattan, Kansas, January, 1962.

TABLE I

MASS SPECTRUM AND APPEARANCE POTENTIALS OF THE PRINCIPAL IONS OF 2-THIABUTANE

m/e	Relative abundance	Appearance potential (e.v.)	Process	ΔH_f^+, kcal./mole
15	7.8	17.6 ± 0.5	$C_3H_8S \rightarrow CH_3^+$ (?)	
26	9.7	17.8 ± .5	$\rightarrow C_2H_2^+ + CH_3 + SH + H_2$	332
			$\rightarrow C_2H_2^+ + CH_3 + H_2S + H$	315
27	42.4	16.0 ± .4	$\rightarrow C_2H_3^+ + CH_3S + H_2$	316
29	21.9	14.1 ± .2	$\rightarrow C_2H_5^+ + CH_3 + S$	225
34	3.5			
35	16.4	15.1 ± .2	$\rightarrow H_3S^+ + CH_2 + C_2H_2 + H$	160
41	5.8			
44	4.2			
45	24.4	15.9 ± .4	$\rightarrow CHS^+ + C_2H_4 + H + H_2$	287
46	11.6	13.6 ± .3	$\rightarrow CH_2S^+ + C_2H_5 + H$	225
47	36.5	14.7 ± .2	$\rightarrow CH_3S^+ + CH_3 + CH_2$	226
48	55.6	11.8 ± .2	$\rightarrow CH_4S^+ + C_2H_2 + H_2$	204
49	5.8	12.0 ± .3	$\rightarrow CH_5S^+ + C_2H_2 + H$	157
57	2.6			
58	4.8			
59	6.7	13.4 ± .4	$\rightarrow C_2H_3S^+ + CH_3 + H_2$	262
			$\rightarrow C_2H_3S^+ + CH_4 + H$	260
60	3.1			
61	100.0	11.8 ± .2	$\rightarrow C_2H_5S^+ + CH_3$	225
62	4.0			
63	4.4			
75	3.8			
76	58.4	8.70 ± 0.10	$\rightarrow C_3H_8S^+$	186
77	3.6			
78	2.5			

TABLE II

MASS SPECTRUM AND APPEARANCE POTENTIALS OF THE PRINCIPAL IONS OF 2-THIAPENTANE

m/e	Relative abundance	Appearance potential (e.v.)	Process	ΔH_f^+, kcal./mole
15	8.8	16.6 ± 0.5	$C_4H_{10}S \rightarrow CH_3^+ + (?)$	
26	3.3			
27	34.7	15.8 ± .4	$\rightarrow C_2H_3^+ + C_2H_4 + H_2S + H$	285
29	7.0	15.3 ± .5	$\rightarrow C_2H_5^+ + C_2H_2 + H_2S + H$	233
			$\rightarrow C_2H_5^+ + CH_3 + SCH_2$	235
35	10.5	15.6 ± .3	$\rightarrow H_3S^+ + CH_2 + C_3H_4 + H$	174
39	17.9	18.4 ± .5	$\rightarrow C_3H_3^+ + CH_2S + H + 2H_2$	277
40	3.3			
41	36.6	14.8 ± .2	$\rightarrow C_3H_5^+ + CH_2 + SH + H_2$ (?)	223
42	13.5	12.5 ± .4	$\rightarrow C_3H_6^+ + CH_4 + S$	234
43	27.0	12.3 ± .4	$\rightarrow C_3H_7^+ + CH_3S$	226
45	22.2	15.2 ± .4	$\rightarrow CHS^+ + C_3H_6 + H + H_2$	274
46	10.2	14.1 ± .3	$\rightarrow CH_2S^+ + C_3H_5 + H + H_2$	222
			$\rightarrow CH_2S^+ + CH_3 + C_2H_5$	252
47	21.7	14.0 ± .2	$\rightarrow CH_3S^+ + C_2H_5 + CH_2$	214
48	45.5	11.3 ± .2	$\rightarrow CH_4S^+ + C_2H_2 + CH_4$	205
49	23.7	11.0 ± .2	$\rightarrow CH_5S^+ + C_2H_2 + CH_3$	147
58	4.1			
59	3.4			
61	100.0	11.9 ± .2	$\rightarrow C_2H_5S^+ + C_2H_5$	233
62	8.7			
63	4.7			
75	12.0	11.7 ± .2	$\rightarrow C_3H_7S^+ + CH_3$	219
89	1.1			
90	47.7	8.8 ± .15	$\rightarrow C_4H_{10}S^+$	184
91	3.3			
92	2.3			

the group orbital method[13] is made. It is seen that the ionization potential we determined for 2-thiabutane is in good agreement with the other result reported in the literature and with the calculated value. The ionization potential for 2-

(13) J. L. Franklin, *J. Chem. Phys.*, **22**, 1304 (1954).

TABLE III

MASS SPECTRUM AND APPEARANCE POTENTIALS OF THE PRINCIPAL IONS OF 2,3-DITHIABUTANE

m/e	Relative abundance	Appearance potential (e.v.)	Process	ΔH_f^+, kcal./mole
15	14.0	15.7 ± 0.3	$C_2H_6S_2 \rightarrow CH_3^+$ (?)	
44	3.5			
45	58.6	15.5 ± .3	$\rightarrow CHS^+ + CH_4S + H$	299
46	39.5	12.2 ± .2	$\rightarrow CH_2S^+ + CH_4 + S$	240
47	27.4	13.0 ± .4	$\rightarrow CH_3S^+ + CH_3S$	255
48	14.8	11.5 ± .2	$\rightarrow CH_4S^+ + CS + H_2$	205
49	5.3	11.9 ± .2	$\rightarrow CH_5S^+ + CS + H$	175
61	16.7	10.9 ± .2	$\rightarrow C_2H_5S^+ + SH$	213
64	9.6	15.4 ± .3	$\rightarrow S_2^+ + 2CH_3$	285
78	3.1			
79	54.3	12.1 ± .2	$\rightarrow CH_3S_2^+ + CH_3$	240
80	2.6			
81	4.9			
93	1.9			
94	100.0	9.1 ± .2	$\rightarrow CH_3SSCH_3^+$	204
95	5.6			
96	9.3			

thiapentane agrees with the calculated value. No previous experimental determination of the ionization potential of 2-thiapentane has been made.

Our value of 9.1 ± 0.2 e.v. for the ionization potential of 2,3-dithiabutane does not agree very well with the experimental result of 8.46 e.v. determined by the photoionization method.[14] Using Watanabe's value of 8.46 e.v., we calculate an S–S interaction parameter of 1.14 e.v., and using this, we further calculate an ionization potential of 8.36 e.v. for 3,4-dithiahexane. This calculated value agrees with the 8.27 e.v. reported by Watanabe.[14] (We note that d(S–S) = 1.32 if 8.27 e.v. for 3,4-dithiahexane is used to evaluate d; this leads to I(2,3-dithiabutane) = 8.34 e.v.) Since the electron impact ionization potentials correspond to vertical transitions according to the Franck-Condon principle, it would be better to compare our results to values determined by others using mass spectrometric methods. A value of 8.53 e.v. for the ionization potential of 2,3-dithiabutane has been reported by Varsel, *et al.*,[15] using the electron impact method with argon as the calibrant gas. We could not, however, obtain a value lower than 8.9 e.v. for the ionization potential in any determination. We do not have an explanation for this apparent discrepancy.

TABLE IV

MOLECULAR IONIZATION POTENTIALS OF SOME SULFUR COMPOUNDS

Molecule	Ionization potential (e.v.) Calcd.	Measd.		
b	1.55[a]			
c	1.99[b]			
d	1.14			
e	13.31[a]			
f	10.46[c]			
CH_3SH	(9.44)	9.44[d]		
CH_3–S–CH_2CH_3	8.65	8.55[d]	8.70[e]	
CH_3–S–CH_2–CH_2CH_3	8.64	8.80[e]		
CH_3–S–S–CH_3	(8.46)	8.46[d]	8.53[f]	9.1[e]
CH_3CH_2–S–S–CH_2CH_3	8.36	8.27[d]		

[a] These parameters are given by Franklin.[13] [b] See ref. 2. [c] K. Watanabe, *J. Chem. Phys.*, **26**, 542 (1957). [d] See ref. 14. [e] Data reported in this work. [f] See ref. 15.

m/e = **15.**—In each of the three molecules studied, the m/e = 15 ion is CH_3^+. We have determined and reported in Tables I–III the appearance potentials of the m/e = 15 ion in each case, but we are not able to arrive at a singular process for their formation since energetic considerations indicate that a number of processes may contribute.

m/e = **26.**—From 2-thiabutane, the only ion of m/e = 26 that could be formed is $C_2H_2^+$ and we find that two processes could be involved in its formation. The processes are those shown in Table I. The first involves the formation of the neutral fragments CH_3 + SH + H_2 and thus $\Delta H_f^+(C_2H_2)$ = 332 kcal./mole. The second process provides for the formation of CH_3 + H_2S + H and has $\Delta H_f^+(C_2H_2)$ = 315 kcal./mole. Both are in fair agreement with the value of 317 kcal./mole given by Field and Franklin[16] and it is not possible to differentiate between the two processes.

m/e = **27.**—The ion of m/e = 27 is $C_2H_3^+$ and is believed to be accompanied from 2-thiabutane by the neutral fragments CH_3S + H_2. The heat of formation of this ion for this process is 316 kcal./mole. This is high in comparison to the literature value of 280 kcal./mole,[16] but it is the most reasonable process for the formation of this ion from 2-thiabutane, as is shown by the energetics.

From 2-thiapentane, this ion is observed with the accompanying formation of C_2H_4 + H_2S + H, according to the energetics. $\Delta H_f^+(C_2H_3)$ = 285 kcal./mole is calculated. This agrees with the value determined for this ion from 2-thiabutane.

m/e = **29.**—The formation of $C_2H_5^+$ from 2-thiabutane appears to occur by the process shown in Table I. The heat of formation of this ion according to the proposed process is 225 kcal./mole. This is in good agreement with the literature value of 224 kcal./mole.[16]

In the study of 2-thiapentane, the energetics indicate two equally plausible processes for the formation of the m/e = 29 ion. These are shown in Table II. Another possible process would be $C_4H_{10}S \rightarrow C_2H_5^+ + CH_2 + CH_3S$. Considering the uncertainty assigned to the determined appearance potential, the average $\Delta H^+(C_2H_5)$ = 234 kcal./mole, calculated, is in good agreement with the literature[16] and the value determined from 2-thiabutane.

m/e = **35.**—The ion of m/e = 35 can only be H_3S^+, analogous to H_3O^+, and must be formed as a result of rearrangement. The neutral fragments formed from 2-thiabutane are believed to be CH_2 + C_2H_2 + H; therefore $\Delta H_f^+(H_3S)$ = 160 kcal./mole.

From the 2-thiapentane study, the appearance potential of 15.6 ± 0.3 e.v. for this ion leads to $\Delta H_f^+(H_3S)$ = 174 kcal./mole if the neutral frag-

(14) K. Watanabe, T. Nakayama, and J. Mottl, "Final Report on Ionization Potentials of Molecules by a Photoionization Method," December, 1959. Department of Army #5B99-01-004 ORD-#TB2-001-00R-#1624. Contract No. DA-04-200-ORD 480 and 737.

(15) C. J. Varsel, F. A. Morrell, F. E. Resnik, and W. A. Powell, *Anal. Chem.*, **32**, 182 (1960).

(16) F. H. Field and J. L. Franklin, "Electron Impact Phenomena and the Properties of Gaseous Ions," Academic Press, Inc., New York, N. Y., 1957.

ments are $CH_2 + C_3H_4 + H$. The results are in reasonably good agreement; an experimental heat of formation of this ion has not been reported previously. The ionization efficiency curves for this ion from both molecules were found to resemble closely an ionization efficiency curve for a parent molecule-ion, each having a small "foot." The average $\Delta H_f^+(H_3S)$ is 167 kcal./mole. This leads to a proton affinity of H_2S of 195 ± 7 kcal./mole, using $\Delta H_f^+(H) = 367$ kcal./mole and $\Delta H_f(H_2S) = -4.8$ kcal./mole. Lampe and Field[17,18] have studied the reaction of the H_2S^+ ion with both H_2S and CH_4 to form H_3S^+. Assuming that these reactions have a zero heat of reaction, one calculates the heat of formation of H_3S^+ to be equal to or less than 186 kcal./mole. This substantiates our average value of 167 kcal./mole. Lampe and Field also give an approximate value of >175 kcal./mole for the proton affinity of H_2S. This tends to substantiate our value of 195 ± 7 kcal./mole. The determination of a more accurate value from additional data is presently underway in our Laboratories, and hopefully will lead to a reliable proton affinity for hydrogen sulfide.

m/e = **39.**—The $C_3H_3^+$ ion was observed in sufficient quantity to allow an appearance potential determination only in the 2-thiapentane spectrum. Energetic considerations lead to a choice of $CH_2S + H + 2H_2$ as neutral fragments, and therefore we calculate a value of $\Delta H_f^+(C_3H_3) = 277$ kcal./mole, in reasonable agreement with other determinations.[13]

m/e = **41.**—$C_3H_5^+$ also was observed only in the 2-thiapentane spectrum in quantities sufficient for appearance potential measurements. The process given in Table II is considered reasonable, leading to $\Delta H_f^+(C_3H_5) = 223$ kcal./mole; however, another process which is possible is the formation of this ion accompanied by $CS + 2H_2 + H$ as the neutral fragments, leading to $\Delta H_f^+(C_3H_5) = 217$ kcal./mole.

m/e = **42.**—The spectrum of 2-thiapentane in the region of *m/e* = 40 indicates that the *m/e* = 42 ion is due to $C_3H_6^+$. Assuming the neutral fragments to be $CH_4 + S$, $\Delta H_f^+(C_3H_6) = 234$ kcal./mole, in agreement with the literature.[16] Although the processes involving neutral fragments of $CH_3S + H$ and $CH_2S + H_2$ seemed more reasonable, energetic considerations cause us to eliminate them as probable processes.

m/e = **43.**—Taking CH_3S as the singular neutral fragment involved in the formation of $C_3H_7^+$ from 2-thiapentane, a $\Delta H_f^+(C_3H_7) = 226$ kcal./mole is calculated. Although this value is higher than the "best value" of 190 kcal./mole listed by Field and Franklin,[16] better agreement is obtained if the error assigned to the appearance potential is considered.

m/e = **45.**—If the formation of CHS^+ from 2-thiabutane is accompanied by the neutral fragments $C_2H_4 + H + H_2$, $\Delta H_f^+(CHS)$ is calculated to be 287 kcal./mole, in fair agreement with the heat of formation for this ion obtained by Gallegos and Kiser[2] from various sulfur-containing heterocyclics. $\Delta H_f^+(CHS) = 299$ and 274 kcal./mole are calculated from the studies of 2,3-dithiabutane and 2-thiapentane, respectively, as shown in Tables II and III.

m/e = **46.**—This ion is CH_2S^+ and is believed to be formed by the processes indicated in Tables I–III. We calculate $\Delta H_f^+(CH_2S) = 222$–241 kcal./mole, about the same as values given by Gallegos and Kiser.[2] However, the energetics eliminate other processes, although the formation of accompanying neutral fragments of $CH_3 + C_2H_5$ from 2-thiapentane is considered possible.

m/e = **47.**—Heats of formation of 226 and 214 kcal./mole are determined for CH_3S^+ from the appearance potentials of 2-thiabutane and 2-thiapentane, respectively, employing the processes given in Tables I and II. These results are in near agreement with those reported by Franklin and Lumpkin.[19] However, the value of $\Delta H_f^+(CH_3S)$ determined from 2,3-dithiabutane is 255 kcal./mole, and essentially reflects a difference of 1.6 e.v. in the appearance potentials for the same ion and process reported by us and by Franklin and Lumpkin. Using the average $\Delta H_f^+(CH_3S) = 220$ kcal./mole and $\Delta H_f(CH_3S) = 35$ kcal./mole (essentially the same value obtained by Franklin and Lumpkin) we calculate that the appearance potential of CH_3S^+ from 2,3-dithiabutane would be 11.3 e.v., in agreement with that reported by Franklin and Lumpkin.[19] We can offer no explanation for our apparent failure to determine correctly the appearance potential for CH_3S^+ from 2,3-dithiabutane.

m/e = **48.**—A value of 204 kcal./mole is calculated for $\Delta H_f^+(CH_4S)$ assuming that $C_2H_2 + H_2$ are formed as the neutral fragment from 2-thiabutane. $\Delta H_f^+(CH_4S) = 205$ kcal./mole is calculated if the neutral fragment of the dissociation in the case of 2-thiapentane is $C_2H_2 + CH_4$. Both of these values are only slightly lower than the value of 212 kcal./mole calculated from $I(CH_3SH) = 9.440$ e.v.[14] and $\Delta H_f^+(CH_3SH) = -5.56$ kcal./mole.[20] $\Delta H_f^+(CH_4S) = 190$ kcal./mole was determined in the 2,3-dithiabutane study. It is apparent from energetic considerations that the process in the latter case must be written as $CH_4S^+ + CS + H_2$.

m/e = **49.**—The heat of formation of the very interesting ion CH_5S^+ has not been reported previously. We calculate from the 2-thiabutane study a $\Delta H_f^+(CH_5S) = 157$ kcal./mole, taking the neutral fragments to be $C_2H_2 + H$.

Assuming that a similar process occurs in each of the other two molecules studied, the neutral fragments $C_2H_2 + CH_3$ and $CS + H$ should be formed in the dissociation processes in the cases of 2-thiapentane and 2,3-dithiabutane, respectively. These are the processes shown in Tables II and III. From the appearance potentials, $\Delta H_f^+(CH_5S) = 147$, 157, and 175 kcal./mole. The internal agreement is fairly good. We shall take $\Delta H_f^+(CH_5S) = 160 \pm 10$ kcal./mole. From this

(17) F. W. Lampe and F. H. Field, *J. Am. Chem. Soc.*, **79**, 4244 (1957).

(18) F. W. Lampe and F. H. Field, *ibid.*, **80**, 5583 (1958).

(19) J. L. Franklin and H. E. Lumpkin, *ibid.*, **74**, 1023 (1952).

(20) J. P. McCullough and W. D. Good, *J. Phys. Chem.*, **65**, 1430 (1961).

result, and using $\Delta H_f^+(H) = 367$ kcal./mole and $\Delta H_f^+(CH_3SH) = -5.56$ kcal./mole, we calculate the proton affinity of methanethiol to be -201 kcal./mole.

m/e = **59.**—This ion, which is $C_2H_3S^+$, is rather small in the mass spectrum of 2-thiabutane and is believed to be formed by the processes shown in Table I. The two processes are thought to have about equal probability. They lead to $\Delta H_f^+(C_2H_3S) = 262$ and 260 kcal./mole, with the accompanying formation of the neutral fragments $CH_3 + H_2$ and $CH_4 + H$, respectively.

m/e = **61.**—$\Delta H_f^+(C_2H_5S) = 225$ and 233 kcal./mole, as determined from the appearance potentials of $m/e = 61$ from 2-thiabutane and 2-thiapentane, respectively. (See Tables I and II for the processes involved.) These results agree fairly well with the value of 213 kcal./mole listed by Field and Franklin.[16] The $\Delta H_f^+(C_2H_5S) = 213$ kcal./mole determined from the appearance potential of $m/e = 61$ from 2,3-dithiabutane is in excellent agreement. The process shown in Table III is the only one possible for this ion, based on the observed energetics, and this process involves a somewhat unusual rearrangement. It would be of special interest to study the analogous ions in other alkyl disulfides.

m/e = **64.**—The appearance potential of $m/e = 64$ from 2,3-dithiabutane leads to a $\Delta H_f^+(S_2) = 285$ kcal./mole. The neutral fragments are two methyl groups. This result for $\Delta H_f^+(S_2)$ is in agreement within the experimental error with a value of $\Delta H_f^+(S_2) = 279$ kcal./mole[16] determined directly from the ionization potential of $S_2(g)$.[21] Our result leads to an ionization potential of S_2 equal to 11.0 ± 0.2 e.v., which agrees with 10.8 ± 0.3 e.v. reported by Blanchard and LeGoff.[22]

m/e = **75.**—The $C_3H_7S^+$ ion originates by cleavage of the CH_3–S bond in $C_4H_{10}S^+$. The appearance potential of this ion, given in Table II, leads to $\Delta H_f^+(C_3H_7S) = 219$ kcal./mole.

m/e = **76.**—This is the 2-thiabutane parent molecule-ion, $C_3H_8S^+$. Using the heat of formation of the gaseous molecule and the observed ionization potential, a value of 186 kcal./mole is calculated for the heat of formation of this ion.

m/e = **79.**—$CH_3S_2^+$ originates by ionization and a subsequent S–CH_3 bond cleavage in 2,3-dithiabutane. The appearance potential of 12.1 ± 0.2 e.v. gives $\Delta H_f^+(CH_3S_2) = 240$ kcal./mole. From an estimated $\Delta H_f(CH_3S_2) = 21$ kcal./mole, we calculate the ionization potential of CH_3S_2 to be 9.5 ± 0.3 e.v.

m/e = **90.**—This ion was observed only in thiapentane and is the parent molecule-ion. From the ionization potential of 8.80 ± 0.15 e.v., we calculate $\Delta H_f^+(C_4H_{10}S) = 184$ kcal./mole.

m/e = **94.**—From our studies, the ionization potential of 2,3-dithiabutane is 9.1 e.v. This gives $\Delta H_f^+(C_2H_6S_2) = 204$ kcal./mole. If the value of 8.46 e.v.[14] is taken for the ionization potential, $\Delta H_f^+(C_2H_6S_2) = 189$ kcal./mole.

Acknowledgments.—The authors wish to acknowledge the very helpful comments of Dr. J. L. Franklin and to express their appreciation for his kind suggestions for improvement.

(21) H. D. Smyth and J. P. Blewett, *Phys. Rev.*, **46**, 276 (1934).

(22) L. B. Blanchard and P. LeGoff, *Can. J. Chem.*, **35**, 89 (1957).

ELECTRON IMPACT SPECTROSCOPY OF SOME SUBSTITUTED OXIRANES[1]

BY YASUO WADA AND ROBERT W. KISER

Department of Chemistry, Kansas State University, Manhattan, Kansas

Received March 29, 1962

Appearance potentials and relative abundances are reported for the principal positive ions in the mass spectra of 3,4-epoxy-1-butene, 1,2-epoxy-3-methoxypropane, epichlorohydrin, and epibromohydrin. Probable ionization and dissociation processes are given consistent with computed energetics from the electron impact data. The heats of formation are tabulated for the various ions as derived from the energetics. Molecular ionization potentials are calculated using the group orbital method and the results are used to calculate heats of formation for some of the parent molecule-ions.

Introduction

We have determined the mass spectral cracking patterns and the appearance potentials of the principal ions from 3,4-epoxy-1-butene, 1,2-epoxy-3-methoxypropane, epichlorohydrin, and epibromohydrin. The results for these derivatives of ethylene oxide are compared to information reported for various oxacycloalkanes[2,3] in the literature in an attempt to determine the fragmentation processes occurring at electron energies at or slightly above the appearance potentials.

Experimental

The mass spectra and the appearance potentials of positive ions reported here were obtained using a time-of-flight mass spectrometer. The instrumentation has been described.[2,4] Mass spectra were determined at nominal electron energies of 70 e.v. Appearance potentials were determined from the ionization efficiency curves using the technique of extrapolated differences described by Warren[5] and the critical slope method given by Honig.[6] Krypton or xenon, mixed with the compounds being investigated, was used to calibrate

(1) This work was supported by the U. S. Atomic Energy Commission under Contract No. AT(11-1)-751 with Kansas State University. It is taken in part from a thesis submitted by Y. Wada to the Graduate School of Kansas State University in partial fulfillment of the requirements for the M.S. degree, January, 1962.

(2) E. J. Gallegos and R. W. Kiser, *J. Am. Chem. Soc.*, **83**, 773 (1961).

(3) E. J. Gallegos and R. W. Kiser, *J. Phys. Chem.*, **66**, 136 (1962).

(4) E. Gallegos and R. W. Kiser, *ibid.*, **65**, 1177 (1961).

(5) J. W. Warren, *Nature*, **165**, 811 (1960).

(6) R. E. Honig, *J. Chem. Phys.*, **16**, 105 (1948).

the ionizing voltage scale. Known spectroscopic values for the ionization potential of krypton and xenon were used for calibration.[7]

3,4-Epoxy-1-butene was obtained from Matheson Coleman and Bell. No significant impurities were noted either in the mass spectrum or during gas chromatographic analyses. Similarly, the 1,2-epoxy-3-methoxypropane, obtained from K & K Laboratories, showed no significant impurities.

Epichlorohydrin and epibromohydrin were obtained from Eastman Organic Chemicals. The mass spectra and gas chromatographic analyses showed no gross amounts of impurities using a Fisher–Gulf model 150 partitioner; consequently, the compounds were used as received.

Results

The results of the determinations of the mass spectral cracking patterns and appearance potentials of various ions from 3,4-epoxybutene-1,1,2-epoxy-3-methoxypropane, epichlorohydrin, and epibromohydrin are summarized in Tables I to IV. In the first two columns are given the principal ions formed by 70 v. electrons from each compound and their relative abundances. In the next two columns are listed the appearance potentials and the probable processes by which the various ions were formed, consistent with measured and extrapolated energetics. The calculated heats of formation of the ions are given in the last column.

In the thermochemical calculations, NBS[8] values of the heats of formation for various molecules and radicals were used where available. The value of $\Delta H_f(C_3H_5OCl)(g) = -27$ kcal./mole employed was evaluated from the reported[9] heat of combustion at 20° for the liquid compound, 423.0 ± 0.1 kcal./mole, determined with a moving bomb calorimeter (to give $HCl \cdot 600H_2O$ in an excess of water); this agrees satisfactorily with an estimated value of −22 kcal./mole calculated by the method of Franklin.[10] The values of $\Delta H_f(C_3H_5OBr)(g) = -6$ kcal./mole, $\Delta H_f(C_4H_8O_2)(g) = -43$ kcal./mole, and $\Delta H_f(C_4H_6O)(g) = 10$ kcal./mole were evaluated by the method of Franklin.[10] Other heats of formation employed are: C_2H_3, 64 kcal./mole[11]; C_3H_2, 87 kcal./mole[11]; and C_2H_3O, −11 kcal./mole.[12]

Discussion

Mass Spectra.—The 70 e.v. mass spectra of these compounds are shown in Fig. 1. Each of these compounds has three dominant groups in its mass spectrum. The mass spectrum of epichlorohydrin is quite similar to that of epibromohydrin. In these two halogen-containing compounds, the most abundant specie is formed by the removal of the halogen from the parent molecule and cleavage of the oxacyclic group. However, in the mass spectra of the 3,4-epoxy-1-butene the dominant ionic species are formed by breaking the oxacyclic

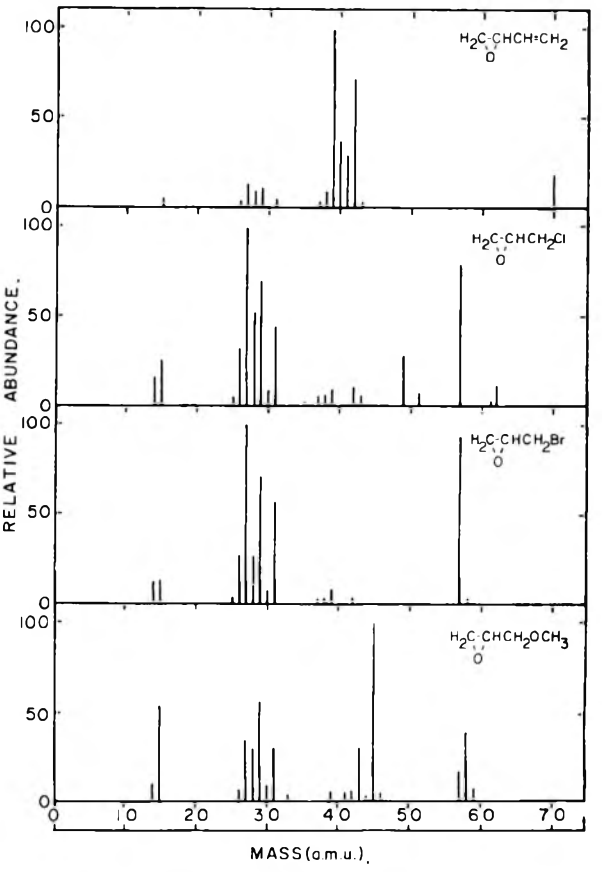

Fig. 1.—Mass spectral cracking patterns of some substituted oxiranes.

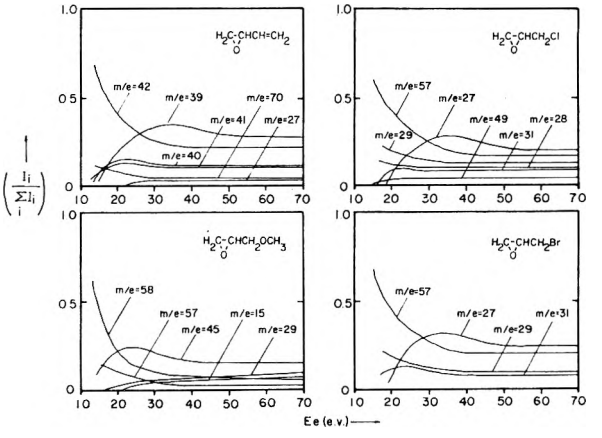

Fig. 2.—Ion abundance as a function of the electron energy for some substituted oxiranes.

group and by cleavage of the vinyl group from the molecule.

In both epichloro- and epibromohydrin, the ion abundances of the species formed by the removal of the halogen atom are large and the parent ion abundances are very small. However, 3,4-epoxy-1-butene has a significant parent-molecule-ion peak. These data suggest that in the case of epichlorohydrin and epibromohydrin, the halogen atom is removed first and then the oxacyclic group is dissociated. The greater relative abundance of $m/e = 57$ in the epibromohydrin mass spectrum compared to that in the epichlorohydrin

(7) C. E. Moore, "Atomic Energy Levels," Natl. Bur. Std. Circ. 467, Vol. III, 1958.

(8) F. D. Rossini, D. D. Wagman, W. H. Evans, S. Levine, and I. Jaffe, "Selected Values of Chemical Thermodynamic Properties," Natl. Bur. of Std. Circ. 500, U. S. Govt. Printing Office, Washington, D. C., 1952.

(9) L. Bjellerup and L. Smith, *Kgl. Fysiograf. Sallskap. Lund, Förh.*, **24**, 21 (1954).

(10) J. L. Franklin, *Ind. Eng. Chem.*, **41**, 1070 (1949).

(11) F. H. Field and J. L. Franklin, "Electron Impact Phenomena and the Properties of Gaseous Ions," Academic Press, Inc., New York, N. Y., 1957.

(12) P. Gray and A. Williams, *Chem. Rev.*, **59**, 239 (1959).

TABLE I

APPEARANCE POTENTIALS AND HEATS OF FORMATION OF THE PRINCIPAL IONS OF 3,4-EPOXY-1-BUTENE

m/e	Relative abundance	Appearance potential (e.v.)	Process	ΔH_f^+ (kcal./mole)
26	5.2	13.8 ± 0.3	$C_4H_6O \rightarrow C_2H_2^+ + C_2H_2 + H_2O$	332
27	14.1	12.6 ± .3	$\rightarrow C_2H_3^+ + C_2H_3O$	293
28	11.4			
29	12.4	12.9 ± .6	$\rightarrow CHO^+ + C_3H_4 + H$	210
31	5.8	13.3 ± .5	$\rightarrow CH_3O^+ + C_3H_2 + H$	178
38	10.4	15.8 ± .5	$\rightarrow C_3H_2^+ + CH_2O + H_2$	402
			$\rightarrow C_3H_2^+ + CHO + H_2 + H$	325
39	100.0	13.5 ± .3	$\rightarrow C_3H_3^+ + CO + H_2 + H$	297
			$\rightarrow C_3H_3^+ + CH_2O + H$	297
40	39.0	11.3 ± .3	$\rightarrow C_3H_4^+ + CO + H_2$	298
			$\rightarrow C_3H_4^+ + CH_2O$	298
41	32.4	11.1 ± .2	$\rightarrow C_3H_5^+ + CO + H$	241
42	74.1	9.8 ± .4	$\rightarrow C_2H_2O^+ + C_2H_4$	224
43	6.2	10.5 ± .2	$\rightarrow C_2H_3O^+ + C_2H_3$	188
70	19.6	9.7 ± .3	$\rightarrow C_4H_6O^+$	234

TABLE II

APPEARANCE POTENTIALS AND HEATS OF FORMATION OF THE PRINCIPAL IONS OF 1,2-EPOXY-3-METHOXYPROPANE

m/e	Relative abundance	Appearance potential (e.v.)	Process	ΔH_f^+ (kcal./mole)
14	9.5	21.3 ± 0.5	$C_4H_8O_2 \rightarrow CH_2^+ + C_2H_3O + CHO + 2H$	339
15	55.0	16.0 ± .3	$\rightarrow CH_3^+ + C_2H_3O + CHO + H$	269
26	9.3	16.2 ± .3	$\rightarrow C_2H_2^+ + CHO + CH_3O + H_2$	323
27	34.9	16.3 ± .2	$\rightarrow C_2H_3^+ + 2CHO + H_2 + H$	287
			$\rightarrow C_2H_3^+ + CH_3O + CHO + H$	274
28	30.7	13.5 ± .2	$\rightarrow C_2H_4^+ + CHO + CH_3O$	261
			$\rightarrow C_2H_4^+ + 2CHO + H_2$	274
			$\rightarrow CO^+ + C_2H_4 + CH_3OH$	305
			$\rightarrow CO^+ + C_2H_4O + CH_4$	299
29	58.2	14.4 ± .2	$\rightarrow CHO^+ + C_2H_2 + CH_2O + H + H_2$	211
30	10.1	10.9 ± .2	$\rightarrow CH_2O^+ + C_2H_4 + CH_2O$	224
31	30.4	13.9 ± .4	$\rightarrow CH_3O^+ + C_2H_2 + CH_2O + H$	199
39	7.3	15.9 ± .4	$\rightarrow C_3H_3^+ + CHO + OH + H_2 + H$	264
			$\rightarrow C_3H_3^+ + CHO + O + 2H_2$	267
41	6.6	13.0 ± .3	$\rightarrow C_2HO^+ + CH_3 + CH_2O + H_2$ (?)	252
42	8.3	12.3 ± .3	$\rightarrow C_2H_2O^+ + CH_3 + CH_3O$	198
			$\rightarrow C_2H_2O^+ + CH_3 + CHO + H_2$	211
43	33.4	13.1 ± .2	$\rightarrow C_2H_3O^+ + CH_3 + CHO + H$	177
			$\rightarrow C_2H_3O^+ + CH_2 + CH_3O$	181
45	100.0	12.1 ± .15	$\rightarrow C_2H_5O^+ + CHO + CH_2$	170
57	19.9	11.2 ± .2	$\rightarrow C_3H_5O^+ + CH_3O$	205
58	42.9	10.2 ± .2	$\rightarrow C_3H_6O^+ + CH_2O$	220
88	2.2		$\rightarrow C_4H_8O_2^+$	

TABLE III

APPEARANCE POTENTIALS AND HEATS OF FORMATION OF THE PRINCIPAL IONS OF EPICHLOROHYDRIN

m/e	Relative abundance	Appearance potential (e.v.)	Process	ΔH_f^+ (kcal./mole)
14	15.2	21.6 ± 0.5	$C_3H_5OCl \rightarrow CH_2^+ + CO + CH_2 + H + Cl$	350
15	24.9	14.6 ± .5	$\rightarrow CH_3^+ + CO + CH_2 + Cl$	241
26	30.2	16.6 ± .1	$\rightarrow C_2H_2^+ + CH_2O + H + Cl$	303
27	100.0	14.0 ± .4	$\rightarrow C_2H_3^+ + CH_2O + Cl$	295
28	52.1	13.6 ± .4	$\rightarrow C_2H_4^+ + CHO + Cl$	259
29	68.3	12.0 ± .5	$\rightarrow CHO^+ + C_2H_4 + Cl$	208
			$\rightarrow CHO^+ + C_2H_4Cl$	226
31	43.0	13.4 ± .2	$\rightarrow CH_3O^+ + C_2H_2 + Cl$	199
42	10.3	12.1 ± .1	$\rightarrow C_2H_2O^+ + CH_3 + Cl$	191
49	22.8	12.5 ± .1	$\rightarrow CH_2Cl^+ + CO + CH_3$	256
			$\rightarrow CH_2Cl^+ + C_2H_3O$	226
57	79.7	11.4 ± .3	$\rightarrow C_3H_5O^+ + Cl$	207
92	0.4		$\rightarrow C_3H_5OCl^+$	
94	0.2		$\rightarrow C_3H_5OCl^+$	

TABLE IV

APPEARANCE POTENTIALS AND HEATS OF FORMATION OF THE PRINCIPAL IONS OF EPIBROMOHYDRIN

m/e	Relative abundance	Appearance potential (e.v.)	Process	ΔH_f^+ (kcal./mole)
14	10.7	21.4 ± 0.5	$C_3H_5OBr \rightarrow CH_2^+ + CO + H + CH_2 + Br$	369
15	13.8	15.6 ± .5	$\rightarrow CH_3^+ + CO + CH_2 + Br$	287
26	26.4	16.7 ± .6	$\rightarrow C_2H_2^+ + CH_2O + H - Br$	328
27	100.0	14.4 ± .2	$\rightarrow C_2H_3^+ + CH_2O + Br$	327
29	71.8	11.8 ± .2	$\rightarrow CHO^+ + C_2H_4 + Br$	227
			$\rightarrow CHO^+ + C_2H_4Br$	230
31	56.8	12.5 ± .2	$\rightarrow CH_3O^+ + C_2H_2 + Br$	201
57	93.0	10.8 ± .1	$\rightarrow C_3H_5O^+ + Br$	216
136	0.05		$\rightarrow C_3H_5OBr^+$	
138	0.05		$\rightarrow C_3H_5OBr^+$	

spectrum reflects a somewhat smaller dissociation energy for a C–Br bond compared to that for a C–Cl bond. Figure 2 shows how the ion abundance varies with energy for a number of the ions of each of the compounds studied. This figure indicates how a given ion may further fragment to form a new ion, but we note that this does not necessarily correspond to the process at the threshold.

Molecular Ionization Potentials.—The calculated and observed ionization potential for 3,4-epoxy-1-butene and the calculated ionization potentials for 1,2-epoxy-3-methoxypropane, epichlorohydrin, and epibromohydrin are given in Table V. Theoretical treatments similar to those employed by Hall[13–15] and Franklin[16] were employed for the calculations. The calculated value of 9.3 e.v. for the ionization potential for 3,4-epoxy-1-butene is in fair agreement with our experimental value of 9.7 ± 0.2.

TABLE V

IONIZATION POTENTIALS OF $H_2C(O)CH-X$

X =		$-CH=CH_2$	$-CH_2OCH_3$	$-CH_2Cl$	$-CH_2Br$
Parameters[a] (e.v.)	e	10.57	10.57	10.57	10.57
	f	10.51	10.00	11.28	10.52
	b	1.23	1.02	1.14	1.11
Obsd. I.P. (e.v.)		9.7 ± 0.3	...	...	...
Calcd. I.P. (e.v.)		9.3	9.2	9.7	9.4
ΔH_f^+ (parent) (kcal./mole)		234	169	196	218

[a] The second row, f, gives the parameters due to Franklin[16]; the first and third rows assume that the $-CHCH_2O$ unit may be treated as a group and other parameters are those given by Franklin[16] and in the Tables of Ionization Potentials.[17]

3,4-Epoxy-1-butene. *m/e* = **26.**—The ion corresponding to *m/e* = 26 is $C_2H_2^+$. If C_2H_2 and H_2O are the neutral products accompanying the ionization and dissociation of the parent compound, $\Delta H_f^+(C_2H_2)$ = 332 kcal./mole. This is considerably higher than the value of 303 kcal./mole determined from epichlorohydrin, and slightly larger than 323 kcal./mole determined from 1,2-epoxy-3-methoxypropane, and 328 kcal./mole determined from epibromohydrin, and other reported values.[2,11]

m/e = **27.**—$\Delta H_f^+(C_2H_3)$ is calculated to be 293 kcal./mole, considering C_2H_3O to be the neutral fragment. This value is in agreement with other reported values.[11]

m/e = **29.**—This ion is CHO^+. From the energetics, the neutral products are C_3H_4 and H, leading to a $\Delta H_f^+(CHO)$ = 210 kcal./mole. This value is in agreement with reported values,[11] but lower than the values reported from the ethylene oxide and propylene oxide studies.[2]

m/e = **31.**—From the similarities in the spectra and from the appearance potential, this ion is CH_3O^+. Considering the neutral fragments to be C_3H_2 + H, $\Delta H_f^+(CH_3O)$ = 178 kcal./mole, in agreement with literature values.[2,11]

m/e = **38.**—This ion must be $C_3H_2^+$. But the energetics cannot distinguish between neutral fragments of $CH_2O + H_2$ and $CHO + H_2 + H$. $\Delta H_f^+(C_3H_2)$ is calculated to be 402 and 325 kcal./mole, respectively; 360 kcal./mole has been reported.[11]

m/e = **39.**—This ion is the dominant one in the mass spectrum: $C_3H_3^+$. The energetics do not allow us to distinguish between CO + H + H_2 and CH_2O + H as neutral products. $\Delta H_f^+(C_3H_3)$ = 297 kcal./mole.

m/e = **40.**—The neutral groups accompanying the formation of $C_3H_4^+$ may be either CO + H_2 or CH_2O. Both processes give 298 kcal./mole for $\Delta H_f^+(C_3H_4)$. This value is in fair agreement with literature values.[11]

m/e = **41.**—This ion is $C_3H_5^+$, and very likely the allyl ion. The energetics suggest that the neutral products are CO + H rather than CHO. $\Delta H_f^+(C_3H_5)$ calculated from the observed appearance potential is then 241 kcal./mole. This is slightly higher than other reported values.[11]

m/e = **42.**—This ion might be either $C_2H_2O^+$ or $C_3H_6^+$. However, since the ion has such a large abundance in the mass spectrum and the appearance potential is only 9.8 e.v., it is concluded that the ion is $C_2H_2O^+$. The neutral product then is C_2H_4 and $\Delta H_f^+(C_2H_2O)$ is calculated to be 224 kcal./mole.

m/e = **43.**—The value of $\Delta H_f^+(C_2H_3O)$ = 188 kcal./mole determined from the appearance potential of the *m/e* = 43 ion according to the process shown in Table I is in good agreement with the values of 199 and 188 kcal./mole determined by Gallegos and Kiser from studies of propylene oxide[2] and tetrahydrofuran,[3] respectively.

(13) G. G. Hall, *Proc. Roy. Soc.* (London), **A205**, 541 (1951).
(14) G. G. Hall, *Trans. Faraday Soc.*, **49**, 113 (1953).
(15) G. G. Hall, *ibid.*, **50**, 319 (1954).
(16) J. L. Franklin, *J. Chem. Phys.*, **22**, 1304 (1954).
(17) R. W. Kiser, "Tables of Ionization Potentials," U. S. Atomic Energy Commission, *TID-6142*, June 20, 1960.

m/e = 70.—This ion could only result from ionization without further dissociation of the compound. Therefore, $\Delta H_f^+(C_4H_6O)$ is 234 kcal./mole.

1,2-Epoxy-3-methoxypropane. m/e = 14.—Although there are other possible combinations of neutral fragments which might accompany the formation of CH_2^+ in the ionization and dissociation of 1,2-epoxy-3-methoxypropane, the process shown in Table II satisfies the energetic requirements and leads to a value of $\Delta H_f^+(CH_2)$ = 339 kcal./mole.

m/e = 15.—A value of $\Delta H_f^+(CH_3)$ = 269 kcal./mole is obtained from the appearance potential of the m/e = 15 ion with the process shown in Table II. Other processes are possible; this process was chosen because of the similarity to the process for the m/e = 14 ion.

m/e = 26.—From the proposed process and the energetics, $\Delta H_f^+(C_2H_2)$ = 323 kcal./mole, in reasonable agreement with the literature.[11]

m/e = 27.—Two processes are considered nearly equally probable for the formation of the m/e = 27 ion, as shown in Table II. Energetics alone will not allow a differentiation to be made.

m/e = 28.—The appearance potential of the ion suggests the possibility that this ion is due to CO^+; either of the processes shown in Table II agree with literature values of $\Delta H_f^+(CO)$. We note, however, that on energetic grounds we cannot dismiss the possibility that m/e = 28 also may be due to $C_2H_4^+$.

m/e = 29.—$\Delta H_f^+(CHO)$ is calculated to be 212 kcal./mole, assuming that the neutral products are C_2H_5 + CHO + H. The energetics do not allow us to distinguish the neutral fragments from the possible fragmentation to give C_2H_2 + CH_2O + H_2 + H, which would lead to $\Delta H_f^+(CHO)$ = 211 kcal./mole.

m/e = 30.—The appearance potential of 10.9 e.v. for m/e = 30 suggests that this ion is CH_2O^+. $\Delta H_f^+(CH_2O)$ is calculated to be 224 kcal./mole, assuming the neutral products to be C_2H_4 + CH_3O. This value is in agreement with Field and Franklin.[11]

m/e = 31.—The relative abundance of this ion at 70 e.v. rules out any significant contribution from $C^{13}H_2O$, as does also the appearance potential. Thus the ion is considered to be CH_3O^+. This suggests that the neutral products are either C_2H_3 + CHO + H or C_2H_2 + CH_2O + H. $\Delta H_f^+(CH_3O)$ = 199 kcal./mole is calculated using the latter group of neutral fragments.

m/e = 39.—This ion is $C_3H_3^+$. Assuming that the neutral products are CHO + OH + H + H_2, $\Delta H_f^+(C_3H_3)$ is calculated to be 264 kcal./mole. However, the neutral fragments CHO + O + $2H_2$, considered unlikely, would lead to $\Delta H_f^+(C_3H_3)$ = 267 kcal./mole.

m/e = 41.—This ion may be C_2HO^+, assuming CH_3 + CH_2O + H_2 to be the neutral fragments. This ion may also possibly be $C_3H_5^+$, but by analogy with the m/e = 42 ion, $C_2H_2O^+$, it is believed that C_2HO^+ is the more reasonable assignment for the m/e = 41 ion. The energetics then give $\Delta H_f^+(C_2HO)$ = 252 kcal./mole.

m/e = 42.—The appearance potential of the ion with m/e = 42 indicates that this ion is $C_2H_2O^+$. Then, $\Delta H_f^+(C_2H_2O)$ is calculated to be either 198 or 211 kcal./mole, as indicated in Table II; therefore, the energetics do not allow us to distinguish between the two possible processes.

m/e = 43.—$\Delta H_f^+(C_2H_3O)$ is found to be 177–181 kcal./mole. This value is in agreement with values for $C_2H_3O^+$ given in Field and Franklin.[11]

m/e = 45.—This ion is $C_2H_5O^+$. $\Delta H_f^+(C_2H_5O)$ is 170 kcal./mole, in agreement with literature values.[11]

m/e = 57.—The neutral product accompanying the formation of the $C_3H_5O^+$ ion is CH_3O. $\Delta H_f^+(C_3H_5O)$ is 205 kcal./mole.

m/e = 58.—This ion is likely produced by the rupture of the oxacyclic group, rather than by cleavage of a CH_3O group and H atom transfer. We calculate $\Delta H_f^+(C_3H_6O)$ = 220 kcal./mole, a value somewhat greater than that found from the study of propylene oxide.[2]

Epichlorohydrin and Epibromohydrin.—m/e = 14.—This ion is CH_2^+. From the epichlorohydrin data, $\Delta H_f^+(CH_2)$ = 350 and from the epibromohydrin data, $\Delta H_f^+(CH_2)$ = 369 kcal./mole, using identical fragmentation processes.

m/e = 15.—The methyl ion is abundant in the spectra of both epichlorohydrin and epibromohydrin. Using similar ionization and dissociation processes, $\Delta H_f^+(CH_3)$ = 241 and 287 kcal./mole, as determined from the reported energetics for epichlorohydrin and epibromohydrin, respectively. It is possible that other processes may be written as well.

m/e = 26.—The ion corresponding to m/e = 26 is apparently $C_2H_2^+$. Neutral products are C-H_2O + H + halogen. $\Delta H_f^+(C_2H_2)$ is calculated to be 303 kcal./mole from the epichlorohydrin data and 328 kcal./mole from the epibromohydrin data. These values are in fair agreement with the literature.[2,11]

m/e = 27.—The ion is $C_2H_3^+$. $\Delta H_f^+(C_2H_3)$ is calculated to be 295 kcal./mole (from epichlorohydrin) and 327 kcal./mole (from epibromohydrin); the latter value is not in good agreement with other workers.[11]

m/e = 28.—This ion from epichlorohydrin is $C_2H_4^+$. Assuming neutral products of CHO and Cl, $\Delta H_f^+(C_2H_4)$ is 259 kcal./mole. This is in good agreement with values in the literature.[2,11] The appearance potential for m/e = 28 was not determined in the study of epibromohydrin.

m/e = 29.—The large abundance of this ion in the spectra of both epichlorohydrin and epibromohydrin indicates that the ions are identical, and that it is CHO^+. However, the energetics do not allow us to distinguish between C_2H_4 + Cl and C_2H_4Cl, and between C_2H_4 + Br and C_2H_4Br as neutral fragments. $\Delta H_f^+(CHO)$ calculated from the appearance potentials is 208–230 kcal./mole. This is in agreement with values reported from ethylene oxide and propylene oxide,[2] and given by Field and Franklin.[11]

m/e = 31.—The only possible ion for this mass from epichlorohydrin and epibromohydrin is CH_3O^+. $\Delta H_f^+(CH_3O)$ calculated from the ap-

pearance potentials are 199 and 201 kcal./mole, respectively. These values are higher than that of 173 kcal./mole,[11] but agree with those determined from the ethylene oxide and propylene oxide study[2] and the above study of 1,2-epoxy-3-methoxypropane.

m/e = **42.**—$C_2H_2O^+$ is formed from epichlorohydrin with the neutral products CH_3 + Cl. $\Delta H_f^+(C_2H_2O)$ is calculated to be 191 kcal./mole. This is somewhat lower than values reported in the literature.[2,11]

m/e = **49.**—The only possible ion is CH_2Cl^+, since from Fig. 1 it can be seen that the ratio of I_{49}/I_{51} is about 3. But the energetics do not distinguish between the neutral products CO + CH_3 and C_2H_3O. $\Delta H_f^+(CH_2Cl)$ is calculated to be 226–256 kcal./mole. For the present, we tend to favor the greater value. The heat of formation for this ion, to our knowledge, has not been reported previously. The corresponding ion in epibromohydrin was not observed.

m/e = **57.**—This ion is formed by removal of halogen from the parent molecule-ion in both epichlorohydrin and epibromohydrin. $\Delta H_f^+(C_3H_5O)$ are 207 kcal./mole for epichlorohydrin and 216 kcal./mole for epibromohydrin. Although in fair agreement, these values are a little higher than that reported from a study of propylene oxide.[2]

THERMODYNAMIC PROPERTIES AND PHASE RELATIONS IN THE SYSTEM HYDROGEN–HAFNIUM[1,2]

BY RUSSELL K. EDWARDS AND EWALD VELECKIS[3]

Department of Chemistry, Illinois Institute of Technology, Chicago 16, Illinois

Received March 10, 1962

Isothermal equilibrium pressure measurements were carried out as a function of composition for the hydrogen–hafnium system in the temperature range 251 to 872° and up to a pressure of one atmosphere. The proposed partial phase diagram indicates the existence of three homogeneous phases. In the primary solid solution phase (α) the solubility of hydrogen reaches nearly 11 atom % hydrogen at the highest temperature investigated but decreases considerably toward the lower temperatures. Conformance to Sieverts' law was established throughout the α-phase; the temperature variation of the Sieverts' law constant can be expressed by the equation $\log(\sqrt{P_{mm}}/N_H) = 3.820 - 1964T^{-1}$, where P_{mm} is the pressure of hydrogen and N_H is the atom fraction of hydrogen in the condensed phase. The second phase (δ) is homogeneous from a minimum composition of 24% at the highest temperature to a maximum of about 64% at lower temperatures. In the pressure range studied this latter boundary remains essentially constant with temperature. A very narrow two-phase region separating the δ-phase and a third phase (ϵ) is inferred with the latter extending to $HfH_{1.97}$ for our lowest temperature. The extrapolated phase boundaries show a good correlation with the room temperature X-ray studies of Sidhu and McGuire. The relative partial molal and integral heats and entropies are presented for the composition range 0 to 57 atom % hydrogen. The heat and entropy of the $\alpha \rightarrow \delta$ reaction are -15.66 ± 0.84 kcal./g.-atom H and -12.34 ± 0.28 cal./deg. g.-atom H; for the $\delta \rightarrow \epsilon$ reaction the respective quantities are -13.39 ± 0.21 kcal./g.-atom H and -20.64 ± 0.16 cal./deg. g.-atom H.

Introduction

The system hydrogen–hafnium has been studied by Sidhu and co-workers,[4] who made a thorough investigation of phase and structural relations by metallographic and by X-ray and neutron diffraction techniques at room temperature. A hexagonal primary solid solution was found to transform into a tetragonal (deformed cubic) phase in the range from <2.25 to 60.5 atom % hydrogen. At this latter composition the tetragonal phase gradually deformed into a face-centered cubic phase which extended to 64.8%. A second tetragonal phase, homogeneous from 65.3%, extended up to the dihydride composition.

More recently, Espagno, *et al.*,[5] studied the system by dilatometric and X-ray methods. Analogous to Sidhu's findings, their X-ray patterns revealed a tetragonal (deformed cubic) phase at 50 atom % hydrogen and a face-centered cubic structure at 62.2%. The transition from the tetragonal to the cubic structure could be effected either by increasing the hydrogen content or by raising the temperature. This latter behavior was completely reversible between 85 and 100°. They also obtained a solubility isobar at 1 atm. from which they inferred the existence of two heterogeneous regions, one at 950° between 16.7 and 33.3 atom % hydrogen and the other at ~400° in the vicinity of 63%.

The purpose of the work reported here was to obtain thermodynamic data and to elucidate the phase relations in the unexplored regions of the hydrogen–hafnium phase diagram.

Experimental

Apparatus.—The modified Sieverts' apparatus used in this research is described in detail elsewhere.[1] The hafnium sample, contained within a small porcelain thimble, was placed in a Vycor reaction tube which was connected to a calibrated volumetric bulb used for the introduction of known quantities of hydrogen into the reaction zone and to an adjustable level mercury manometer for recording equilibrium hydrogen pressures. The sample could be heated by means of a large pot furnace using liquid lead (above 350°) and Wood's metal (below 350°) as the heat exchange media. A porcelain protection tube, suspended in the metal bath to a depth of 15 in., was employed to prevent direct contact between the liquid metal and Vycor. The temperature of

(1) Based on a thesis by Ewald Veleckis submitted to Illinois Institute of Technology in partial fulfillment of the requirements for the M.S. degree, January, 1957.

(2) Presented at the April, 1957, Meeting of the American Chemical Society.

(3) Both authors now at Argonne National Laboratory, Chemical Engineering Division, Argonne, Illinois.

(4) S. S. Sidhu and J. C. McGuire, *J. Appl. Phys.*, **23**, 1257 (1952); S. S. Sidhu, *J. Chem. Phys.*, **22**, 1062 (1954); S. S. Sidhu, *Acta Cryst.*, **7**, 447 (1954); S. S. Sidhu, L. Heaton, and D. D. Zauberis, *ibid.*, **9**, 607 (1956).

(5) L. Espagno, P. Azou, and P. Bastien, *Compt. rend.*, **250**, 4352 (1960).

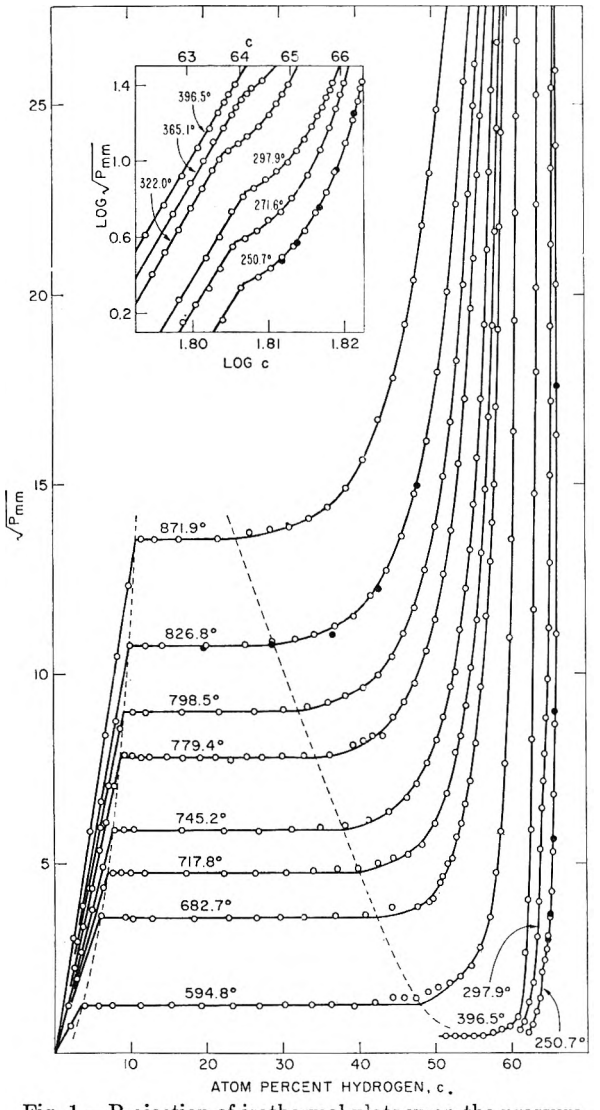

Fig. 1.—Projection of isothermal plots upon the pressure–composition plane for the system hydrogen–hafnium. Dashed curves indicate the extent of the ($\alpha + \delta$) coexistence region. Inset shows an enlarged portion of the graph at higher hydrogen concentrations plotted on a double logarithm scale: O, absorption measurements; ●, desorption measurements.

the sample (measured with a Chromel–Alumel thermocouple located just opposite the sample outside the Vycor reaction tube) could be controlled within less than 1° for any desired period of time.

Materials.—The hafnium metal was hot-rolled sheet of 0.25 mm. thickness. Vacuum fusion analyses showed oxygen and nitrogen contamination of 0.035% each. The major impurity was zirconium at 1.0 ± 0.5% by weight based on gravimetric analyses. A corrected molecular weight of the sample was used in calculating hydrogen concentrations, assuming zirconium to be equivalent to hafnium in its reactions with hydrogen.

The hydrogen used was obtained from the National Cylinder Gas Co. Before being admitted to the system, it was passed over shredded 5% platinized asbestos heated at 230° to reduce any oxygen, then through a liquid nitrogen trap to collect any water formed, and finally over zirconium turnings heated at 800° to remove any remaining reactive impurities. Generally, it was stored within the zirconium turnings and portions as needed were driven off by raising the temperature of the turnings.

Argon, supplied by the Matheson Co., was used in residual volume calibrations. It was purified by passing through a carbon tetrachloride–Dry Ice trap and then over hot zirconium turnings in the same manner as for hydrogen.

Procedure.—A typical run was made as follows. Approximately 6 g. of hafnium strips was abraded with Armour's emery polishing paper 3/0. The sample was degassed to less than 10^{-5} mm. at about 800° in a separate furnace arrangement so connected to the vacuum system as to yield higher pumping rates. The sample then was saturated with hydrogen several times by repeated sorption and desorption. It then was cooled *in vacuo* to room temperature and was transferred to the reaction system in the liquid bath which had been preheated to the desired temperature. It was once more degassed at the temperature of the experiment until a vacuum of at least 10^{-5} mm. was obtained. With this pretreatment, rapid reaction rates prevailed at temperatures as low as 250°. Otherwise, the rates were slow at low temperatures (*e.g.*, 60 min. or more was required to reach equilibrium at 300°) although they were rapid at higher temperatures (10 min. for temperatures above 500°).

Next, a calibration of the residual volume surrounding the hafnium sample and extending to a constant level arm of the manometer was carried out using argon. Successive amounts of hydrogen then were admitted to the reaction zone and the respective equilibrium hydrogen pressures were measured.

Due to an on–off control arrangement, the temperature of the bath oscillated with a period of about 2 min. accompanied by a slight oscillation of the hydrogen pressure. Pressure readings were taken at the moment of the precise temperature selected for the run. The Chromel–Alumel thermocouple was calibrated several times during the course of the study as some drift in its properties was noted.

It is interesting to note that a direct observation of the exothermic nature of the reaction of hydrogen with hafnium was easily possible in that one could observe an immediate rise in the sample temperature when a fresh portion of hydrogen was introduced. Likewise, an immediate temperature decrease could be noted if vacuum pumping was used to remove hydrogen.

Results

The pressure–temperature–composition data are shown in Fig. 1 as $\sqrt{P_{mm}}$ *vs.* composition isotherms ranging from 250.7 to 871.9°. Above 594.8° the isotherms are comprised of two rising portions that are separated by horizontal lines. The composition ranges of the first and second rising sections correspond to homogeneous phases designated α and δ, respectively; constant pressure plateaus define the ($\alpha + \delta$) coexistence region. Throughout the α-phase the isotherms are linear. This is in accordance with Sieverts' general law for metal hydrogen systems

$$\sqrt{P_{H_2}} = kN_H$$

where P_{H_2} is the pressure of hydrogen, N_H is the atom fraction of hydrogen in the condensed phase, and k is a temperature dependent factor peculiar to the system under investigation. When the hydrogen pressure is expressed in mm., the variation of the Sieverts' law constant with temperature (°K.) may be given by the equation

$$\log k = 3.820 - 1964T^{-1} \ (\pm 0.015, \text{ std. dev.})$$

In the ($\alpha + \delta$) two-phase region, the plateau pressures vary with temperature according to the equation

$$\log \sqrt{P_{mm}} = 4.137 - 3423T^{-1} \ (\pm 0.010, \text{ std. dev.})$$

Due to the knowledge of more exact $\sqrt{P}$ *vs.* composition relationships in the α-phase, the precision in delineating the boundaries on the left of the horizontal portion of the isotherms is appreciably better than for the boundaries on the right.

Reversibility of the reaction of hydrogen with hafnium was confirmed by desorption measurements as indicated by the additional points on the 826.8 and 250.7° isotherms of Fig. 1.

To preserve clarity three isotherms (at 365.1, 322.0, and 271.6°) were omitted from the main Fig. 1. However, they are included in the low temperature data alternatively presented in the inset of Fig. 1 as log $\sqrt{P_{mm}}$ *vs.* log c plots, where c is the atom % hydrogen in the condensed phase. Discernible in these plots are significant changes in the pressure–composition relationships that are indicative of phase transformations or distortions in the vicinity of 64 atom % hydrogen (a similar observation was made by Espagno, *et al.*,[5] at about 63%). No truly horizontal sections are apparent in these isotherms. The inflections in the curves could indicate that a two-phase region exists here but is too narrow for direct observation, or that such a region exists at temperatures somewhere below 250° and the inflections are typical of isotherms just above the critical temperature. We have proposed a tentative partial phase diagram, shown in Fig. 2, which assumes the first of these interpretations. The composition range of the two-phase region was inferred from our single boundary and from the X-ray diffraction results of Sidhu, *et al.*[4] Thus at a composition of about 64%, the δ-phase begins to undergo a transformation into a new phase (ε) which becomes homogeneous from about 65% and extends to 66.3% for our lowest temperature and a pressure of 1 atm. The shoulder points in the inset of Fig. 1 ("plateau pressures") of the (δ + ε) field conform surprisingly well to the equation

$$\log \sqrt{P_{mm}} = 5.950 - 2926T^{-1} \ (\pm 0.005, \text{ std. dev.})$$

in spite of the fact that they do not occur at exactly the same composition.

Phase boundary points at room temperature reported by Sidhu, *et al.*,[4] also are shown in Fig. 2. Their point at 2.25 atom % hydrogen (obtained from a metallographic examination) corresponds to the lowest composition for which two solid phases

TABLE I

COMPOSITIONS[a] OF THE PHASE BOUNDARIES IN THE HYDROGEN–HAFNIUM SYSTEM

Temp., °C.	$\alpha - (\alpha + \delta)$ ±3%	$(\alpha + \delta) - \delta$ ±5%	$\delta - (\delta + \epsilon)$ ±1%	Isobar at 1 atm. ±1%
871.9	10.64	23.9	..	52.1
826.8	9.95	28.9	..	55.1
798.5	9.29	32.2	..	56.4
779.4	8.69	34.4	..	57.3
745.2	7.55	38.0	..	58.5
717.8	6.92	40.1	..	59.3
682.7	6.15	42.3	..	59.9
594.8	3.55	47.8	..	61.5
396.5	..	56.2	..	64.0
365.1	..	..	64.2	64.5
322.0	..	..	63.7	65.1
297.9	..	..	64.2	65.9
271.6	..	..	64.0	66.1
250.7	..	..	64.2	66.3

[a] Compositions in atom % hydrogen.

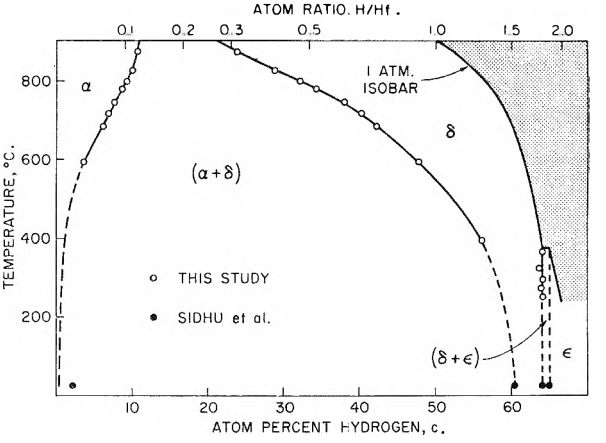

Fig. 2.—Partial phase diagram of hydrogen–hafnium system represented as a non-isobaric projection upon the temperature–composition plane. A portion of an isobar at 1 atm. is shown on the right. The shaded area indicates the unexplored region in which the hydrogen pressure exceeds 1 atm.

were found to coexist; thus one may make the interpretation that the primary solid solution phase extends to some lower composition. The phase boundary compositions are listed in Table I.

The shaded area in Fig. 2 represents an uninvestigated region in which hydrogen pressures exceed 1 atm. The boundary line between the shaded and unshaded areas then corresponds to the solubility of hydrogen at a pressure of 1 atm. On the average, our values (listed in the last column of Table I) are 2.5% higher than those reported by Espagno, *et al.*[5]

The thermodynamic data are presented in Table II. Throughout the α-phase and in the (α + δ) two-phase region such data may readily be calculated from the knowledge of the temperature dependence of the Sieverts' law constant and from the variation of plateau pressures with temperature. In the δ-phase, the relative partial molal data were also of sufficient quality so that the Gibbs–Duhem equation could be used to obtain the related quantities reported.[6]

The standard heat and entropy of formation, ΔH_f and ΔS_f, correspond to the formation of one gram atom of solution from solid hafnium and gaseous diatomic hydrogen at a pressure of 1 atm.

The data beyond 57 atom % hydrogen are considered too uncertain from a standpoint of phase boundaries and from an exceedingly sensitive pressure variation to warrant reporting of the complete thermodynamic results.

Discussion

The phase diagrams of the systems H–Ti and H–Zr are regarded[7] to be of the eutectoid type. The H–Hf system would be expected to show an analogous behavior. The partial phase diagram of Fig. 2 does not exclude the possibility of having a eutectoid transformation outside the temperature

(6) For a discussion of the methods involved in the evaluation of similar thermodynamic data see, *e.g.*, C. Wagner, "Thermodynamics of Alloys," Addison–Wesley Press, Inc., Cambridge, Mass., 1952, Chap. I.

(7) A review of literature on the H–Ti and H–Zr systems may be found in M. Hansen and K. Anderko, "Constitution of Binary Alloys," McGraw–Hill Book Co., Inc., New York, N. Y., 1958, pp. 799, 808.

TABLE II

THERMODYNAMIC QUANTITIES FOR THE SYSTEM HYDROGEN–HAFNIUM

Atom % H	$-(\bar{H}_H - \frac{1}{2}H^0_{H_2})$, kcal./g.-atom H	$-(\bar{S}_H - \frac{1}{2}S^0_{H_2})$, cal./deg. g.-atom H	$-\Delta H_f$,[c] kcal./g.-atom		$-\Delta S_f$,[c] cal./deg. g.-atom	
0.00	8.99 ± 0.8	$-\infty$	0		0	
2.00	8.99 ± .8	3.12 ± 0.3	0.180		0.023	
4.00	8.99 ± .8	4.49 ± .3	.359		.102	
6.00	8.99 ± .8	5.30 ± .3	.539	± 9.5%	.202	± 7.0%
8.00	8.99 ± .8	5.87 ± .3	.719		.317	
8.69[a]	8.99 ± .8	6.04 ± .3	.781		.359	
..	15.66 ± .8[d]	12.34 ± .3[d]	...		...	
34.40	15.19 ± 1.2	11.95 ± .5	4.97		3.73	
37.00	15.69 ± 1.1	12.45 ± .4	5.39		4.07	
38.00	15.88 ± 1.1	12.65 ± .4	5.55		4.20	
39.00	16.13 ± 1.0	12.90 ± .4	5.72		4.34	
40.00	16.42 ± 1.0	13.20 ± .4	5.89		4.48	
41.00	16.73 ± 0.9	13.51 ± .4	6.07		4.63	
42.00	17.03 ± .9	13.83 ± .4	6.25		4.78	± 2.6%
43.00	17.32 ± .9	14.14 ± .4	6.44		4.94	
44.00	17.62 ± .9	14.48 ± .4	6.64		5.11	
45.00	18.86 ± .9	15.67 ± .3	6.84	± 5.6%	5.29	
46.00	19.15 ± .8	16.01 ± .3	7.06		5.48	
47.00	19.50 ± .8	16.41 ± .3	7.29		5.68	
48.00	19.79 ± .8	16.78 ± .3	7.52		5.88	
49.00	20.02 ± .6	17.11 ± .2	7.76		6.10	
50.00	20.19 ± .8	17.39 ± .3	8.00		6.32	
51.00	20.29 ± .9	17.63 ± .3	8.25		6.54	
52.00	20.56 ± .7	18.08 ± .3	8.50		6.77	
53.00	20.26 ± .8	18.00 ± .3	8.74		7.00	
54.00	20.14 ± .7	18.13 ± .2	8.98		7.23	
55.00	20.42 ± .8	18.70 ± .3	9.22		7.48	
56.00	20.43 ± 1.3	19.05 ± .6	9.47		7.73	
57.00	20.75 ± 2.0	19.82 ± 1.0	9.73		8.00	

[a] Concentration at the $\alpha - (\alpha + \delta)$ boundary for an arbitrarily selected temperature, 1052°K. [b] Concentration at the $(\alpha + \delta) - \delta$ boundary for the same temperature. [c] In the single phase regions the integral heats and entropies show no variation with temperature within the experimental error. However, because of the temperature dependence of the phase boundaries, due regard must be paid in the application of these data for temperatures other than 1052°K. [d] It is to be noted that, whereas the second and third columns list relative partial quantities, the particular numbers 15.66 and 12.34 reported for the two phase region correspond instead to the heat and entropy for the reaction

$$\frac{1}{r'' - r'}\,HfH_{r'} + \frac{1}{2}\,H_2 \longrightarrow \frac{1}{r'' - r'}\,HfH_{r''}$$

where r' and r'' are the atom ratios (H/Hf) at the $\alpha - (\alpha + \delta)$ and $(\alpha + \delta) - \delta$ boundaries, respectively. The numbers were left in the table for convenience.

range of this study (Espagno, *et al.*,[5] *e.g.*, found evidence for a phase transformation at ~100°). The closure of the $(\alpha + \delta)$ miscibility gap, suggested by the rapid increase in mutual solubilities of the α and δ-phases with temperature, is not likely because of the presumably different crystalline structures of these two phases.

The two-phase region at 950° extending from 16.7 to 33.3 atom % hydrogen reported by Espagno, *et al.*,[5] is wider than would be expected from an extrapolation of our data to that temperature. In view of a perceptible temperature dependence of composition in the plateau portion of their isobar, we feel that their data would permit narrower limits. The second heterogeneous region observed by Espagno, *et al.*,[5] in their 1 atm. isobar (~400° and ~63 atom % hydrogen) is in good agreement with our phase diagram (376° and ~64%).

The extrapolation of the phase boundaries toward the lower temperatures is rather arbitrary. Nevertheless, the correspondence with the room temperature limits of Sidhu, *et al.*,[4] is reasonable and aids in the structural identification of the intermediate phases. Thus the α-phase would have the hexagonal structure of the primary solid solution of hydrogen in α-hafnium. The δ-phase would correspond to the tetragonal (deformed cubic) or the face-centered cubic structures, assuming that these two structures actually represent a single phase of continuous distortion.[4] The ϵ-phase would correspond to the face-centered tetragonal structure.

Neutron diffraction studies of metal–hydrogen solid phases have gone far in clarifying the sometimes ambiguous interpretation of the role of hydrogen in metals. Rundle's[8] stressing of the importance of metal–metal bonds in the interstitial compounds points also to similar considerations in the metal–hydrogen systems. Sidhu, *et al.*,[4] have shown that significant structural changes take place in the hafnium metal lattice as hydrogen is introduced. It is clear that the

(8) R. E. Rundle, *J. Am. Chem. Soc.*, **69**, 1719 (1947).

entrance of hydrogen brings about disturbances of the M–M bonds. Some of the changes show lengthening of some M–M bond classes along with a shortening of other M–M bond classes. The hexagonal structure of pure hafnium is of non-ideal axial ratio. Since initial directional preferences are present in the pure metal, it is not surprising to see the distortion which is met in the face-centered cubic structure. One can infer that the distortion of the M–M bonds by hydrogen is itself endothermic since the sign of the relative partial molal enthalpy of hafnium is positive.

Both deformation and energetics indicate that the process is much more than a simple filling of interstitial holes. The fact that diatomic hydrogen enters a number of metals exothermally while at the same time undergoing dissociation has always seemed somewhat startling from an energetic point of view to those thinking in terms of a simple "solution" of a gas in a solid. The bonding of a hydrogen atom to its surrounding metal atoms is thus even stronger than its covalent bonding to another hydrogen atom in diatomic hydrogen. Sidhu, *et al.*,[4] have stated that the M–H bonds are stronger than M–M bonds, but this is misleading. The important factor is that the hydrogen atoms within the interstitial positions yield additional bonding beyond the normal M–M bonding. That is, due to the small size of the hydrogen atom, one gains M–H bonding while retaining most of the M–M bonding. If the assumption is made that the hydrogen bonding energy is divided among four bonds associated with its four nearest metal neighbors, use of the thermodynamic data here obtained, the dissociation energy of diatomic hydrogen, and the sublimation energy of hafnium leads to a greater energy for the M–M bond than for the M–H bond.

Acknowledgment.—The support of the ONR and AFOSR during the course of this study is gratefully acknowledged. We wish to thank Prof. S. E. Wood for valuable discussions.

MERCURY(II) HALIDE MIXED COMPLEXES IN SOLUTION. V. COMPARISON OF CALCULATED AND EXPERIMENTAL STABILITY CONSTANTS[1]

BY Y. MARCUS AND I. ELIEZER

Israel Atomic Energy Commission Laboratories, Rehovoth, Israel

Received March 10, 1962

The equilibrium constants for the formation of mercury(II) halide ternary (mixed ligand) complexes from the parent binary complexes have been calculated on the basis of a "polarized ion" model. The values obtained agree fairly well with the experimental results available.

Introduction

The stability of ternary complexes MA_iB_j as compared with that of the binary complexes MA_n and MB_n, where $n = i + j$, has not been studied much as yet but the basis for its theoretical treatment was laid by Bjerrum in his study of the ratio between consecutive formation constants of binary complexes.[2] Bjerrum divided the factors influencing the complex formation constants into a "statistical effect" and a "ligand effect" further subdividing the latter into an "electrostatic effect" and a "rest effect." Of late Kida has discussed some of the above factors.[3]

The mixed complexes of mercury(II) with Cl, Br, and I have been thoroughly investigated by one of us,[4-7] while very recently Hume and Spiro[8] studied spectrophotometrically the uncharged mixed mercury halides confirming the results obtained in ref. 5. We have tried to ascertain to what an extent the experimental results can be explained by applying theoretical considerations along the lines mentioned above.[9]

Theory. a. Definitions.—We can write for the formation of the mixed complex from the parent complexes

$$\frac{i}{n}\,MA_n + \frac{j}{n}\,MB_n \rightleftarrows MA_iB_j$$

equilibrium constant K_M (I)

Using the conventional[10] over-all stability constants β one obtains

$$K_M = \beta_{ij} \times \beta_{no}^{-i/n} \times \beta_{on}^{-j/n} \quad \text{(II)}$$

Let us now analyze K_M somewhat similarly to Bjerrum's ideas. We can write

$$\log K_M = \log K_{stat} + \log K_{el} + \log K_R \quad \text{(III)}$$

where K_{stat} = the value of K_M if formation of the mixed complex proceeds statistically; K_{el} = the stabilization constant of the mixed complex due to the electrostatic effect; K_R = any additional stabilization, which Bjerrum calls the rest effect.

(1) Presented at the 7th International Conference on Coördination Chemistry, Stockholm, June, 1962.

(2) J. Bjerrum, "Metal Ammine Formation in Aqueous Solution," P. Haase & Sons, Copenhagen, 1957.

(3) S. Kida, *Bull. Chem. Soc. Japan*, **34**, 962 (1961).

(4) Y. Marcus, *Acta Chem. Scand.*, **11**, 329 (1957).

(5) Y. Marcus, *ibid.*, **11**, 599 (1957).

(6) Y. Marcus, *ibid.*, **11**, 610 (1957).

(7) Y. Marcus, *ibid.*, **11**, 811 (1957).

(8) T. G. Spiro and D. N. Hume, *J. Am. Chem. Soc.*, **83**, 4305 (1961).

(9) Y. Marcus, *Bull. Res. Council Israel*, **10A**, No. 3, 2 (1961).

(10) J. Bjerrum, G. Schwarzenbach, and L. G. Sillén, "Stability Constants," The Chemical Society, London, 1958.

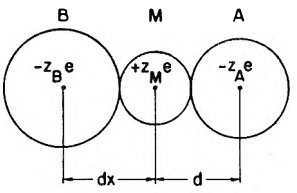

Figure 1.

We shall now discuss each of these in turn.

b.—K_{stat} can be evaluated as follows: Let us assume that M has N coördination positions. Let us denote the probability of a ligand A or ligand B to be found at a coördination position by a or b, respectively, which are assumed to be independent. Then the probability of a solvent molecule S being at the coördination position will be $1 - a - b$ and the number of molecules $MA_iB_jS_{N-n}$ will be proportional to

$$\frac{a^i b^j (1 - a - b)^{N-i-j} N!}{i!\, j!\, (N - i - j)!} = \frac{a^i b^j (1 - a - b)^{N-n} N!}{i!\, j!\, (N - n)!}$$

Writing similar expressions for the number of MA_n and MB_n molecules and introducing them into the expression for the stability constant (I), we obtain

$$K_{stat} = \frac{n!}{i!\, j!} = \binom{n}{i} \qquad \text{(IV)}$$

that is K_{stat} is independent of the coördination number, of the occupation of coördination positions by solvent molecules, and of the affinity of the ligands for the central metal ion. The number of complexes for which the experimental value of K_M is found identical with K_{stat} is rather small. Usually $K_M > K_{stat}$.

c. **The Electrostatic Effect.**—The model on which the following treatment is based is depicted in Fig. 1 for the case of the MAB linear ternary complexes. The following symbols will be used:

ΔE_{el} = difference in electrostatic energy of interaction between the ternary complex and the binary complexes, thus $\ln K_{el} = \Delta E_{el}/kT$

z_M, z_A, z_B = charges on the metal cation and anion A and B (in units of electron charge)

d, dx = distance between the centers of the ions M–A, and M–B, respectively

ϵ = dielectric constant

We shall write + for attraction and − for repulsion.

The molecule will be treated[11–16] as a system of point charges and point dipoles at the center of the ions given by $\mu = \alpha F$ where F is the field strength at the center of the ion in which μ is induced and α its polarizability. We then obtain for the ion–dipole interaction energy

$$W = {}^1/_2\mu F = {}^1/_2\alpha F^2$$

The energy for dipole–dipole interaction was found to be quite small and therefore we shall neglect it in the following treatment. We shall assume the dipoles at the anion centers to be due solely to the cation charge.

We shall deal first with the linear[17–21] uncharged complexes as shown in Fig. 1.

ΔE_{el} will be given by

$$\Delta E_{el} = E_{el}(MAB) - {}^1/_2E_{el}(MA_2) - {}^1/_2E_{el}(MB_2) = \left[\frac{z_Az_M}{d} + \frac{z_Bz_M}{dx} - \frac{z_Az_B}{d(x+1)} + \frac{\alpha_Az_M^2}{2d^4} + \frac{\alpha_Bz_M^2}{2(dx)^4} + \frac{\alpha_M}{2}\left(\frac{z_A}{d^2} - \frac{z_B}{(dx)^2}\right)^2 - \left(\frac{z_Az_M}{d} - \frac{z_A^2}{4d} + \frac{\alpha_Az_M^2}{2d^4} + \frac{z_Bz_M}{dx} - \frac{z_B^2}{4dx} + \frac{\alpha_Bz_M^2}{2(dx)^4}\right)\right]\frac{e^2}{\epsilon} = \left[\frac{z_A^2}{4d} + \frac{z_B^2}{4dx} - \frac{z_Az_B}{d(x+1)} + \frac{\alpha_M}{2}\left(\frac{z_A}{d^2} - \frac{z_B}{(dx)^2}\right)^2\right]\frac{e^2}{\epsilon} \qquad \text{(V)}$$

In the case of the halides $z_A = z_B = 1$ so that we obtain finally

$$\frac{\epsilon\Delta E_{el}}{e^2} = \frac{(x-1)^2}{4dx(x+1)} + \frac{\alpha_M(x^2-1)^2}{2(dx)^4} \qquad \text{(VI)}$$

In the case of the tetrahedral complexes of the type MA_3B we obtain

$$\frac{\epsilon\Delta E_{el}}{e^2} = \frac{3}{2}\sqrt{\frac{3}{2}}\left(\frac{z_A^2}{2d} + \frac{z_B^2}{2dx}\right) - \frac{3z_Az_B}{d\sqrt{1 + x^2 + \frac{2}{3}x}} + \frac{\alpha_M}{2}\left(\frac{z_A}{d^2} - \frac{z_B}{(dx)^2}\right)^2 \qquad \text{(VII)}$$

Neglecting polarization effects and putting $x = 1$ and $\epsilon = 1$ we obtain

$$\frac{\Delta E_{el}}{e^2} = \frac{3\sqrt{6}}{8d}(z_A - z_B)^2$$

which is the expression obtained by Kida in his discussion of the problem.[3] For the case of the mercury halides ($z_A = z_B = 1$) we obtain

$$\frac{\epsilon\Delta E_{el}}{e^2} = \frac{3}{d}\left(\frac{1+x}{4x}\sqrt{\frac{3}{2}} - \frac{1}{\sqrt{1 + x^2 + \frac{2}{3}x}}\right) + \frac{\alpha_M(x^2-1)^2}{2(dx)^4} \qquad \text{(VIII)}$$

The same expression, of course, holds for the MAB_3 complexes. For the MA_2B_2 complexes we obtain

(11) E. S. Rittner, *J. Chem. Phys.*, **19**, 1030 (1951).
(12) S. A. Rice and W. Klemperer, *ibid.*, **27**, 573 (1957).
(13) K. P. Lawley, *Trans. Faraday Soc.*, **57**, 1809 (1961).
(14) G. M. Rothberg, *J. Chem. Phys.*, **34**, 2069 (1961).
(15) K. S. Krasnov, *Dokl. Akad. Nauk SSSR*, **128**, 326 (1959).
(16) C. J. F. Bottcher, "Theory of Dielectric Polarization," Elsevier, 1952, pp. 143, 150.
(17) P. A. Akishin, V. P. Spiridonov, and A. N. Hodchenkov, *Zh. Fiz. Khim.*, **33**, 20 (1959).
(18) C. L. van P. van Eck, Thesis, Leyden, 1958.
(19) J. D. E. McIntyre, *Dissertation Abstr.*, **22**, 754 (1961).
(20) A. R. Tourky and H. A. Rizk, *Can. J. Chem.*, **35**, 630 (1957).
(21) A. R. Tourky, H. A. Rizk, and Y. M. Girgis, *J. Phys. Chem.*, **64**, 565 (1960).

$$\Delta E_{el}(MA_2B_2) = \frac{4}{3}\Delta E_{el}(MA_3B) \quad (IX)$$

Assuming for the MA_2B complexes a pyramidal structure such that the metal is at the center of a tetrahedron three of the corners of which are occupied by the halide ions we obtain

$$\Delta E_{el}(MA_2B) = \Delta E_{el}(MAB_2) = \frac{2}{3}\Delta E_{el}(MA_3B) \quad (X)$$

Comparison with the Experimental Results.—In order to calculate numerically the stabilization constant, values have to be chosen for the dielectric constant, the distances between the metal and the halide ions, and the polarizability of the metal ion. For our calculations we put $\epsilon = 1$, which seems not unreasonable. For the distances between the various atoms we chose Akishin's values obtained from electron diffraction,[17] which seem to be the most accurate and which are in good agreement with previous values.[18,22] They are

$$d_{Hg-Cl} = 2.29\ \text{Å}.;\ d_{Hg-Br} = 2.41\ \text{Å}.;\ d_{Hg-I} = 2.59\ \text{Å}.$$

From these the appropriate values for x were calculated in each case.

For the polarizability of Hg^{2+} there is no generally accepted value. We chose two rather different values: 1.244×10^{-24} cm.^{3} [23] and 2.45×10^{-24} cm.^{3} [24] and calculated a separate set of results for each. The reasons for this will be discussed later.

The results of the calculations are given in Table I.

TABLE I

Complex	log K_{stat}	log K_{el} α_M = 1.244	log K_{el} α_M = 2.45	log K_M (calcd.) α_M = 1.244	log K_M (calcd.) α_M = 2.45	log K_M (obsd.) Marcus[4-7]	log K_M (obsd.) Hume[8]
HgClBr	0.30	0.09	0.13	0.39	0.43	0.6	0.57
HgClI	.30	.45	.70	.75	1.00	1.0	.68
HgBrI	.30	.14	.22	.44	0.52	0.54	.54
$HgBr_2I^-$	.48	.24	.30	.72	.78	.99	..
$HgBrI_2^-$	.48	.24	.30	.72	.78	.81	..
$HgBr_3I^{2-}$	.60	.37	.44	.97	1.04	1.3	...
$HgBrI_3^{2-}$	.60	.37	.44	.97	1.04	1.10	..
$HgBr_2I_2^{2-}$	.78	.49	.59	1.27	1.37	1.80	..

(22) D. W. Allen and L. E. Sutton, *Acta Cryst.*, **3**, 46 (1950).

(23) E. A. Moelwyn-Hughes, "Physical Chemistry," 2nd Ed., Pergamon, 1961, p. 400.

(24) J. A. A. Ketelaar, "Chemical Constitution," 2nd Ed., Elsevier, 1958, p. 91.

I together with the experimental results available.[4-8]

Discussion

From Table I we can see that there is a large measure of agreement between the theoretical and experimental values. However the following points should be noted.

The theoretical considerations include many simplifications. The "polarized-ion" model used (Fig. 1; ref. 11–16) cannot take the partly covalent nature of the bonding fully into account. Some secondary effects, which would make the calculations very tedious, have been neglected.

The effects of the solvent have not been introduced explicitly, but some are implicit in the value of α. The distances are strictly applicable only to the gaseous neutral molecules, and they were assumed to apply also to the complexes in solution.[18] That an effect of the solvent exists may be shown by the differences in stability of the ternary complex in aqueous and benzene solutions.[6] Hume and Spiro[8] report E. L. King's suggestion that this is due to the interaction of the dipole of the ternary complex with the solvent. As long as such interactions cannot be calculated explicitly, they might be included in a "rest effect."

There is no agreement on the value of α_M for mercury. The value 1.244 obtained by Pauling[25-27] has been criticized by Fajans[28] and a value approximately twice as large suggested by him was arrived at also by Ketelaar.[24] Recently, Murgulescu[29] gave the value 3.18, while Berry[30] thinks 1.0 to be still too high. Fortunately, the calculated values of K_{el} are not too sensitive to the value of α_M (Table I).

Calculations on other metal–ligand systems are now in progress.

Although there is obviously much room for improvement of the theory and removal of the various approximations and assumptions, this would seem of doubtful value unless at the same time more accurate experimental data become available.

Acknowledgment.—We thank Prof. L. G. Sillén for helpful discussions.

(25) L. Pauling, *Proc. Roy. Soc.* (London), **A114**, 181 (1927).

(26) J. H. Van Vleck, "Electric and Magnetic Susceptibilities," Oxford, 1932, p. 225.

(27) A. Heydweiller, *Physik. Z.*, **26**, 526 (1925).

(28) K. Fajans, *et al.*, *Z. Physik*, **13**, 1 (1924); *Z. physik. Chem.*, **B24**, 103 (1934); *J. Am. Chem. Soc.*, **64**, 3023 (1942).

(29) J. G. Murgulescu and E. Latiu, *Rev. chim. Acad. rep. populaire Roumaine*, **2**, 27 (1954).

(30) R. S. Berry, *J. Chem. Phys.*, **30**, 286 (1959).

INFRARED STUDY OF THE INTERACTION OF CARBON MONOXIDE AND HYDROGEN ON SILICA-SUPPORTED IRON

BY G. BLYHOLDER AND LAURENCE D. NEFF

Chemistry Department, University of Arkansas, Fayetteville, Arkansas

Received March 10, 1962

Infrared spectra of surface complexes formed when CO and H_2 are exposed at 20 and 180° to silica-supported iron have been obtained. The results are interpreted as indicating that: (a) no interaction takes place at 20°; (b) complexes of the type H OH \ / R—C—M are formed; (c) the surface is about 75% free to chemisorb CO even after 15 hr. of reaction at 180°; (d) CO is in rapid dynamic equilibria between the surface and gas phases; and (e) there is physically adsorbed as well as chemisorbed CO on the surface at 180°. These findings are in accord with the proposal that alcoholic intermediates are important in Fischer–Tropsch synthesis.

Introduction

The interaction of CO and H_2 on solid catalysts is most familiar as the Fischer–Tropsch synthesis.[1,2] This reaction has been the subject of many studies, including kinetic, radioactive tracer, and adsorption studies. In spite of the great effort, the mechanism remains uncertain. Recently, infrared techniques have been applied to the study of adsorbed molecules. It is our purpose to examine the results of an infrared study of the interaction of CO and H_2 on silica-supported iron. Fischer and Tropsch[3] originally proposed that the reaction proceeded by the formation of a carbide, which was hydrogenated to methylene group, which in turn polymerized. Storch, Golumbic, and Anderson[2] proposed oxygenated intermediates containing mainly OH groups. Emmett and co-workers,[1,4,5] in a series of tracer experiments on the incorporation of alcohols in the synthesis products, have found evidence supporting the idea of oxygenated intermediates. An infrared study can give information as to whether an appreciable number of oxygen containing complexes are on the surface at various conditions. The question always arises as to what, if anything, observed surface complexes have to do with the reaction. The reaction may proceed through a small number of active sites, in which case observed complexes are not involved directly in the reaction. However, the reaction also may proceed through the commonest species on the surface. With this difficulty in mind, caution should be exercised in drawing conclusions about reaction mechanisms from infrared studies. In any case, valuable information can be gained about the nature of adsorbed species and this information can be used to help understand reaction mechanisms.

A number of workers[6-8] have found that in experiments from −80 to +97° on various iron, nickel, and cobalt catalysts, preadsorption of a small amount of CO enhances the quantity of H_2 subsequently adsorbed, while a large CO pre-adsorption inhibits H_2 adsorption. The enhancement effect has led to the proposal that complexes H_2 such as M–C–OH are formed on the surface. Eischens,[9] in an investigation of the effect of hydrogen on CO chemisorbed on silica-supported iron, found no infrared bands in the 2 to 7.5 μ range which could be attributed to such complexes.

In this study we have examined the spectra obtained when CO and H_2 are present over an iron catalyst at 20 and 180°, this latter temperature being in the range of temperatures used for Fischer–Tropsch synthesis.

Experimental

The experimental technique, cells, sample preparation, gas purification, and reduction procedures have previously been described[10] in detail. Essentially, $Fe(NO_3)_3$ is dispersed on silica (Cab-O-Sil[11]), pressed into a disk, and the disk placed in a vacuum cell. After evacuation (which took 6–9 hours to assure complete evacuation and removal of any contaminants), hydrogen, at 1 atm. pressure, was passed through the purification system, into the vacuum system, and then through the cell. The initial flow rate was about 500 ml./min. After the hydrogen was allowed to flow for 1–2 min. the heating coils were warmed up to about 280°. This flow rate and temperature were used for about the first hour. After the first hour, the flow rate was reduced to about 100 ml./min. and the temperature increased to about 320°. Then after another 2 hr., the flow rate was reduced to 20–50 ml./min. and the temperature increased to 380°. This process was continued for about 15 hr. After the reduction process was completed, the sample was cooled in a hydrogen atmosphere and then evacuated. After cooling, the cells were completely evacuated, removed from the vacuum system, and then placed in the spectrophotometer. After this was accomplished, a vacuum system for handling gases was attached to the sample cell *via* a movable arm. Then background spectra of the two samples were recorded using the "differential" technique described earlier. Because the silica only transmits infrared radiation from 2.5 to 7.6 μ, only this range can be used. After the background spectrum was recorded, the gas was introduced into the cell. Then, depending on what information was desired, the cells were kept at room temperature or heated up to 180°. By recording spectra at various time intervals, the desired information was obtained.

When the experiment was finished, the gas phase material was pumped out while the cells were either hot or cold. The

(1) P. H. Emmett, Ed., "Catalysis," Vol. IV, Reinhold Publ. Corp., New York, N. Y., 1956.

(2) H. H. Storch, N. Golumbic, and R. B. Anderson, "The Fischer–Tropsch and Related Synthesis," John Wiley and Sons, Inc., New York, N. Y., 1951.

(3) F. Fischer and H. Tropsch, *Brennstoff-Chem.*, **7**, 97 (1926).

(4) J. T. Kummer, H. H. Podgurski, W. B. Spencer, and P. H. Emmett, *J. Am. Chem. Soc.*, **73**, 5641 (1951).

(5) (a) J. T. Kummer and P. H. Emmett, *ibid.*, **75**, 5177 (1953); (b) W. K. Hall, R. J. Kokes, and P. H. Emmett, *ibid.*, **79**, 2983 (1957); (c) R. J. Kokes, W. K. Hall, and P. H. Emmett, *ibid.*, **79**, 2989 (1957).

(6) C. W. Griffin, *ibid.*, **59**, 2431 (1937).

(7) M. V. C. Sastri and T. S. Viswanathan, *ibid.*, **77**, 3967 (1955).

(8) S. Brunauer and P. H. Emmett, *ibid.*, **62**, 1732 (1942).

(9) R. P. Eischens, "Advances in Catalysis," Vol. X, Academic Press, New York, N. Y., 1958.

(10) G. Blyholder and L. D. Neff, *J. Phys. Chem.*, **66**, 1464 (1962).

(11) Donated by Godfrey L. Cabot, Inc., Boston, Mass.

same materials appeared to be present no matter which path was followed, but the relative amounts of the materials were not the same in each case.

For experiments in which only chemisorbed carbon monoxide and gas phase hydrogen were present in the cell, the CO was added to the cell first. A pressure of 1 cm. of CO was introduced into the cell and allowed to remain in the cell for a few minutes. After this time, the gas phase CO was pumped out and the desired amount of hydrogen was introduced.

For those experiments in which an excess of CO and H_2 were present in the cell, the gases were introduced in one of two ways. Either the desired amounts of the gases were measured out and allowed to mix thoroughly within the manifold before introduction to the cell, or the CO was added first, followed by immediate introduction of the hydrogen.

Results and Assignments

When CO and H_2 are added to a sample of iron at 20°, no interaction is observed. Various amounts of H_2 and CO were added to the cell and allowed to stand for several hours. In those cases where CO was added to the cell before the H_2 was admitted, a larger chemisorbed CO peak resulted than if the gases were mixed prior to introduction to the cell. This is shown in Fig. 1. There is some question as to the reality of this effect, as surfaces can hardly be reproduced within 5% of each other and differences in CO intensities vary as much as 5% from each other. Each adsorption must be on a new sample, as the heating necessary to remove chemisorbed CO considerably deactivates the surface. This experiment was carried out several times with the same qualitative result each time. Chemisorbed CO here refers to CO which is not removed by evacuation for 5 min. at 20°. On our samples, CO which does not desorb immediately upon evacuation at 20° is found to be stable for at least several days.

When the gas mixture is admitted to a clean iron surface and the temperature increased to 180°, interaction of CO and H_2 is observed. Curve c of Fig. 2 shows the spectrum recorded 30 min. after the cell heaters were turned on, starting with 8 cm. of CO and 14 cm. of H_2 in a closed cell. The cell is within a few degrees of its final temperature of 180° after 10 min. As well as the usual bands for gas phase, physically adsorbed, and chemisorbed CO at 4.5 to 5.5 μ, an increase in the OH stretching band at 2.8 μ, and the appearance of 3 bands near 3.3 μ in the C–H stretching region are noted. The background OH band is from the silica support. The three bands near 3.3 μ correspond rather exactly to the published[12] spectrum of gas phase methane and so are assigned as gas phase methane. The spectrum recorded 1 hr. after turning on the heaters is shown as curve d of Fig. 2. The principal difference here, aside from the disappearance of CO, is the growth of a band at 3.4 μ. When the gas phase was pumped out and the spectrum immediately recorded on this sample, all CO bands disappeared, the OH band remained more intense than the background had been, and a small band at 3.4 μ remained. Using Bellamy's assignments[13] which Eischens'[9] work has indicated are valid for chemisorbed hydrocarbons, the 3.4 μ band is assigned to

(12) R. H. Pierson, A. N. Fletcher, and E. St. Clair Grantz, *Anal. Chem.*, **28**, 1218 (1956).

(13) L. J. Bellamy, "Infrared Spectra of Complex Molecules," Methuen and Co., Ltd., London, 1958.

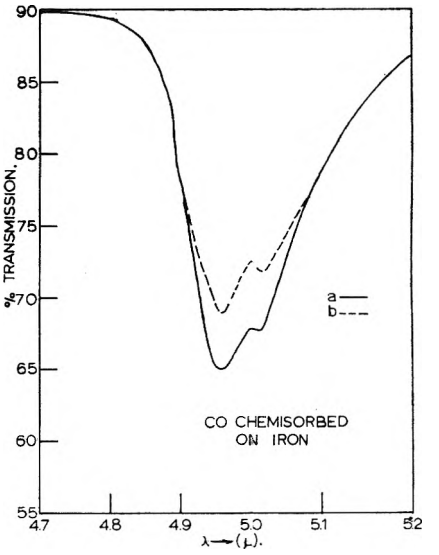

Fig. 1.—Spectra of CO chemisorbed on silica-supported iron at 20°: (a) CO admitted before H_2; (b) CO and H_2 mixed before admission to the cell.

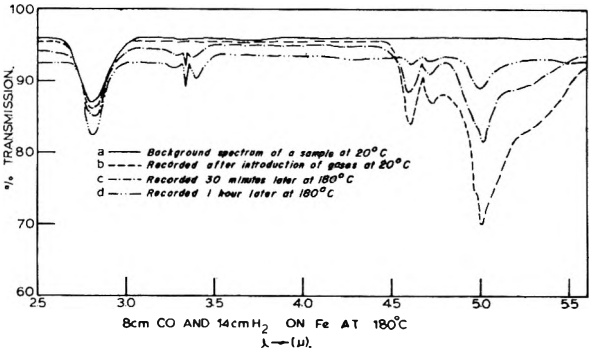

Fig. 2.—Spectra recorded before and while heating a closed cell which started with 8 cm. of CO and 14 cm. of H_2 over silica-supported iron.

a C–H stretching mode where the carbon is saturated and has two or three hydrogen atoms bonded to it. In particular here, we wish to distinguish between the carbon atom being unsaturated, in which case a band around 3.3 μ should have appeared, and its being saturated, in which case a band at 3.4 μ is expected. With the Q branch of methane to key from, there seems little doubt that the band is at 3.4 μ and consequently represents a saturated carbon atom.

The result of heating a sample for 6 and 11 hr. is shown as curves b and c, respectively, of Fig. 3. In this experiment, the manifold of the vacuum system was filled with 10 cm. of CO and 18 cm. of H_2 and the cell was left open to the manifold so that reaction did not seriously change the CO partial pressure. This time the OH and C–H bands are larger and a small band at 4.31 μ indicates the presence of CO_2 in the spectrum recorded after 11 hr.

In Fig. 4 the full range of the spectrum permitted by the silica support from 2 to 7.5 μ is shown for this sample after 15 hr. of heating. Two distinct bands at 6.4 and 6.96 μ, which began to develop appreciably after 5 hr., are shown. When this sample is evacuated at 180°, the CO and CO_2

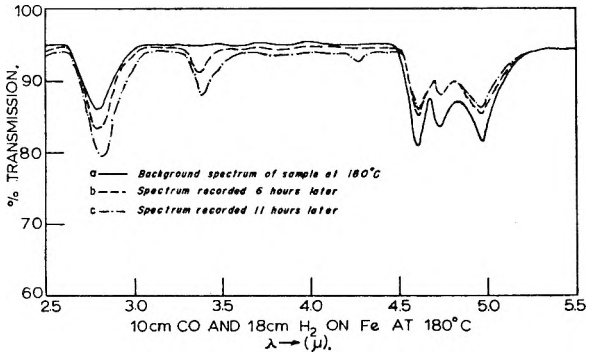

Fig. 3.—Spectra recorded before and while heating 10 cm. of CO and 18 cm. of H_2 over silica-supported iron at 180°. The cell is open to a large reservoir so the CO and H_2 pressures remain fairly constant. The background spectrum was recorded with the CO and H_2 in the cell just after it had reached 180°.

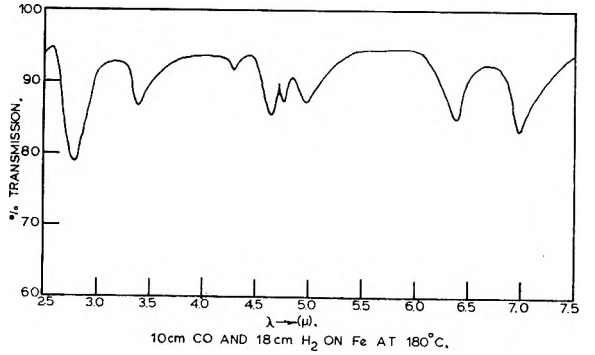

Fig. 4.—Spectrum of sample shown in Fig. 3 after 15 hr. of heating at 180°.

bands disappear while the others remain in part or entirely. A band at 6.4 μ has been found[10] to develop when CO_2 or a mixture of CO and O_2 are heated over a silica-supported iron catalyst. In that study this band was tentatively assigned to CO_2 chemisorbed by a metal–carbon bond to form a carboxylate type structure. No combination of heating oxides of carbon either alone or with O_2 was found[10] to produce a band near 7 μ. Although one does not usually find the C–H deformation band more intense than the C–H stretching band, for lack of anything else and because it is in the right place, part of the 6.96 μ band might be tentatively assigned as a C–H deformation band. One difficulty with assigning much of this band to carbon–hydrogen bending is the fact that while the 6.4 and 6.96 μ bands remain unchanged upon pumping out the cell at 180°, the intensity of the 3.4 μ band is reduced to about one-half its former value. Even after 2 hr. of evacuation at 180°, the 6.4 and 6.96 μ bands are unchanged.

It is possible that a carbide structure contributes to the bands at 6.4 and 6.96 μ since nothing is known about the infrared spectra of carbides. However, it has been shown[10] that heating CO_2 or CO and O_2 at 180° over silica-supported iron produces a band at 6.4 μ, whereas heating CO alone at 180° over the same samples produces no band in this region. It has been demonstrated[1] that heating CO over iron catalysts at 200 to 270° carbides the catalyst. It therefore appears more likely that at least the band at 6.4 μ is due to an oxide rather than a carbide structure.

Several experiments were performed to see if hydrogen would interact with CO chemisorbed on the surface with no gas phase CO present. In these experiments CO was chemisorbed, the gas phase CO was pumped out, and then H_2 was admitted to the cell. No interaction was observed at 20 and 150°. When this technique was used at 180°, a tiny amount of C–H formation was observed, but at this temperature CO immediately desorbs so that it is not possible to say that H_2 reduced chemisorbed CO.

Discussion

In agreement with Eischens,[9] we find no interaction between CO and H_2 to the extent of C–H or O–H bond formation at or near room temperature. In fact, no interaction was found until the iron surface was hot enough to desorb chemisorbed CO rapidly.

The infrared spectra obtained can be interpreted as giving evidence for the existence of oxygenated complexes on the surface. This arises from the fact that bands indicating the presence of C–H and O–H bands in species on the surface are observed. It has been shown[10] that water or mixtures of water and hydrogen do not give O–H bands on silica-supported iron at either 20 or 180°. Therefore, the O–H groups are presumed to be attached to carbon atoms. The spectra may be accounted for by the assumption of surface complexes such as

R–C—M, where R can be a hydrogen atom or an alkane group. As well as this structure, there

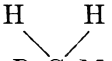

may be complexes such as R–C–M, where R is, as before, contributing to the C–H band at 3.4 μ. There is no evidence in our spectra as to whether or not R is bonded to the surface at any place other than the carbon atom shown. There also could be contributions to the C–H band of carbon, hydrogen, and oxygen complexes attached to the surface by oxygen–metal bonds as suggested by Blyholder and Emmett.[14] There may, of course, be all kinds of interesting intermediate reaction complexes in quantities too small to detect.

The size of the chemisorbed CO band in Fig. 4 has some interesting implications with regard to the nature of the surface after 15 hr. reaction. The intensity of this band is about three-quarters of that formed by the same amount of CO over a clean iron surface at 180°. This indicates that the surface is still largely free. From the study[10] of chemisorbed CO on iron, it is known that the chemisorbed CO at 180° is in rapid dynamic equilibrium with the gas phase. It also is noted that the three bands observed[10] for interaction of oxygen with an iron surface are absent. The shape of the gas phase CO bands at 4.6 and 4.7 μ indicates[15] the presence of physically adsorbed CO on the iron surface.

(14) G. Blyholder and P. H. Emmett, *J. Phys. Chem.*, **63**, 962 (1959).

(15) G. Blyholder and L. D. Neff, *J. Chem. Phys.*, **36**, June (1962).

While the exact nature of the surface structure represented by the bands at 6.4 and 6.96 μ is somewhat of a mystery, their outstanding characteristic is their inertness. We therefore assume that they are too stable to be part of the reaction path. This assumption belongs to the pragmatic philosophy that "if you don't understand it, ignore it," which we may live to regret.

At this point it seems appropriate to consider the course of the reaction. With the reservations expressed in the Introduction, it is assumed that oxygenated intermediates indicated by our spectra belong to the main course of the reaction. Most of the reactive oxygenated intermediates originally proposed by Storch, Golumbic, and Anderson[1,2] contained double bonds between the carbon and the surface. Our study indicated the presence only of saturated intermediates. Considering all of their intermediates to be saturated results in no fundamental change in their proposed mechanism. There are some differences in conditions and catalysts which will raise the question of the applicability of our observations to the usual Fischer–Tropsch synthesis. While our silica-supported iron is not the usual Fischer–Tropsch catalyst, it should be quite similar to singly promoted catalysts which contain no alkali but are promoted with stable oxides like SiO_2, Al_2O_3, and ThO_2. The gas pressures used in this study are about one-third of an atmosphere, whereas the usual synthesis is at one atmosphere or higher. Offhand, we see no reason why these differences should change the mechanism.

In one of the early experiments which lent support to the idea of oxygenated intermediates, Kummer, *et al.*,[4] observed the incorporation of radioactive methanol in the synthesis products. The increasing radioactivity of the products indicated participation of the methanol or its derivative in the chain growth step, but a question arises as to whether the methanol is dehydrogenated to CO before incorporation. The gas phase CO was found to contain too little radioactivity for it to account for the activity of the products. However, if it is assumed that radioactive CO can be formed from the methanol and does not readily desorb from the surface, the incorporation of methanol could proceed *via* CO formation rather than through an alcoholic intermediate. However, our experiments indicating that the surface CO is in rapid dynamic equilibrium with the gas phase suggests that dehydrogenation of methanol to CO would result in the gas phase CO being radioactive, which was observed not to be the case, so the methanol seems likely to have added *via* an alcoholic intermediate as Kummer, *et al.*, assumed.

In view of the fact that methanol was much better at chain initiation than chain growth, the question still remains as to whether physically adsorbed CO, chemisorbed CO, and alcoholic species, or all, are the species added in chain growth. The small chain growth caused by added methanol could be interpreted as indicating CO is one of the principal adding species. The pattern of Kummer's[4,5] chain growth steps proceeds unaltered with the assumption of hydrogenation of the chain adding species after rather than before addition.

In the experiment which produced Fig. 2, methane is observed to be the primary product. This is believed not to be particularly significant with regard to Fischer–Tropsch synthesis because a small amount of reaction greatly reduced the CO pressure. This resulted in there being little CO for chain building, so the principal reaction was reduction of surface complexes to methane.

In the previously proposed mechanisms it has generally been assumed that the chain and chain adding species are adsorbed on adjacent metal atoms. While this is entirely possible, it also is possible that they are bonded by different d orbitals of the same metal atom on the surface either in their initial states before reaction or in the transition state. In this case the reaction would have many considerations in common with substitution reactions of coördination compounds. This, however, is a subject in itself and will be dealt with in a subsequent publication.

Acknowledgment.—Acknowledgment is made to the donors of the Petroleum Research Fund, administered by the American Chemical Society, for partial support of this research. We also wish to express our thanks to the Research Corporation for a grant which partially supported this research.

CALORIMETRIC INVESTIGATIONS OF LIQUID SOLUTIONS OF THE ALKALINE EARTH NITRATES IN THE ALKALI NITRATES

BY O. J. KLEPPA

Institute for the Study of Metals and Department of Chemistry, University of Chicago, Chicago 37, Illinois

Received March 14, 1962

Some new calorimetric data are presented for the solutions of strontium and barium nitrate in liquid sodium, potassium, rubidium, and cesium nitrates. It is shown that the limiting heats of solution of the alkaline earth nitrates in the alkali nitrates obey semi-empirical relations of the type already found for calcium nitrate: $\Delta\bar{H}_{Me(NO_3)_2} \cong A - 225[(r_{++/2} - r_{+/1})/(d_1 + d_2)]^2$ kcal./mole. In this expression r_{++} and r_+ are the ionic radii of the two cations (which have charges +2 and +1), while d_1 and d_2 are the sums of the ionic radii in each of the two solution partners. The parameter A depends on the choice of reference state, and varies from solute to solute. For undercooled, liquid calcium nitrate at 350° $A \cong 0.3$ kcal./mole. The corresponding values for strontium and barium nitrates at 450° are approximately +0.6 and +0.8 kcal./mole, respectively.

In recent communications we have reported some new thermochemical information on the various binary liquid systems formed among the alkali metal nitrates,[1,2] silver nitrate,[3] and thallium nitrate.[4] Since all cations have the same charge in these salts, there probably is no profound structural change associated with the formation of the mixture from the two pure components. In the liquid mixtures considered in the present work, on the other hand, there is an asymmetry in the charge structure of the two solution partners. This introduces an element of complexity which is absent in the simpler systems explored previously.

It is an unfortunate fact that the nitrates of the divalent metals usually decompose more readily at elevated temperatures than do the corresponding monovalent nitrates. For example, we have noted that in calcium nitrate, which melts at about 560°, significant thermal decomposition already sets in between 350 and 400°. In strontium and barium nitrates, with nominal melting points of 645 and 590°, respectively, decomposition starts between 450 and 500°. In view of these complications, we have been unable to study the complete liquid range from pure monovalent nitrate to pure divalent nitrates, and we have confined our attention to liquid solutions which contain up to 30–50 mole % of the alkaline earth nitrates.

Recently we gave a first report on some of this work.[5] This covered the solutions of calcium nitrate in lithium, sodium, potassium, and rubidium nitrates at 350°. In the present paper we consider the solutions of strontium and barium nitrates in sodium, potassium, rubidium, and cesium nitrates at 450°. The higher operating temperature was chosen because of the lower solubility and higher stability of the strontium and barium salts. Unfortunately, lithium nitrate is thermally unstable at 450°. Therefore, we have no information on the solutions of barium and strontium nitrates in this salt.

Experimental and Chemicals

In the course of the present investigation we carried out two types of calorimetric measurements.

(1) **Solid–Liquid Mixing Experiments.**—In these we measured the heats of formation of various liquid mixtures from liquid monovalent nitrate plus solid divalent nitrate.

(2) **Dilution Experiments.**—After a more concentrated mixture had been formed in the preceding solid–liquid experiment, the solution was diluted in the calorimeter with a known amount of the pure liquid monovalent nitrate. These experiments provide direct information on the heats of dilution for a moderately wide range of compositions. Due to a lack of adequate experimental precision we were unable to extend these experiments into the very dilute range.

Details of experimental equipment and procedures have been reported elsewhere.[1,5] The monovalent nitrates used were obtained from the same sources and were of the same quality as the salts used in our earlier work. The strontium and barium nitrates were Mallinckrodt Analytical Reagents. They were used without further purification after appropriate drying.

The calorimetric data reported below are based on calibration by the "drop method," *i.e.*, on the heat content equation for gold as given by Kelley.[6]

Results

Our experimental results are presented in graphical form in Fig. 1 and 2. In these graphs we have plotted the mole fraction of the alkaline earth nitrate along the abscissa, and the quantity $\Delta H^M/X$ along the ordinate axis. ΔH^M is the molar enthalpy change associated with formation of a liquid mixture of mole fraction X from pure liquid alkali nitrate and solid alkaline earth nitrate. The function, $f(X) = \Delta H^M/X$, and its derivative are particularly useful for calculating partial molal heat quantities.[5] Direct experimental information on df/dx (actually on $\Delta f/\Delta X$) is provided by the dilution experiments. These data are given in separate inserts in the figures.

The two limiting values of $\Delta H^M/X$ at $X = 0$ and at $X = 1$ are of special interest. The value at $X = 0$ is the partial molal enthalpy associated with the transfer of one mole of alkaline earth nitrate from the pure crystalline state into the pure liquid alkali nitrate at the considered temperature. The (extrapolated) value at $X = 1$ represents the heat of fusion of the salt at 450°.

Although all our experimental results refer to solutions with solute mole fractions $X \gtrsim 0.5$, the data for the binaries involving a single alkaline earth nitrate permit us to extrapolate our several curves for $\Delta H^M/X$ to $X = 1$ with reasonable confidence. In this manner we have obtained the values 10.65 and 9.95 kcal./mole for the heats of fusion of strontium and barium nitrates at 450°.

(1) O. J. Kleppa, *J. Phys. Chem.*, **64**, 1937 (1960).

(2) O. J. Kleppa and L. S. Hersh, *J. Chem. Phys.*, **34**, 351 (1961).

(3) O. J. Kleppa, R. B. Clarke, and L. S. Hersh, *ibid.*, **35**, 175 (1961).

(4) O. J. Kleppa and L. S. Hersh, *ibid.*, **36**, 544 (1962).

(5) O. J. Kleppa and L. S. Hersh, *Discussions Faraday Soc.*, **32**, 99 (1961).

(6) K. K. Kelley, "Contributions to the Data on Theoretical Metallurgy," Bureau of Mines Bull. No. 584, 1960.

These figures should be compared with our earlier value of 5.7 kcal. for calcium nitrate 350°.[5] The significance of these results is discussed elsewhere.[7]

Discussion

Our earlier work on the binary alkali nitrates showed that the following approximate relation holds for the dependence of the heat of mixing on the size of the two cations

$$\Delta H^M \cong -140X(1 - X)\delta^2 \text{ kcal./mole} \quad (1)$$

Here X and $(1 - X)$ are the mole fractions of the two components. The size parameter $\delta = (d_1 - d_2)/(d_1 + d_2)$, where d_1 and d_2 are the sums of the Pauling ionic radii in the two salts. Since the ionic radius of the anion cancels in the numerator, we may also write $\delta = (r_1 - r_2)/(d_1 + d_2)$, where r_1 and r_2 are the ionic radii of the two cations.

In our study of the alkali nitrate–calcium nitrate solutions we found an empirical expression for the limiting heats of solution of calcium nitrate in the alkali nitrates

$$\Delta\bar{H}_{Ca(NO_3)_2}(s, 350°) = 6.0 - 225\delta'^2 \text{ kcal./mole} \quad (2)$$

Here the parameter $\delta' = (r_{++}/2 - r_+/1)/(d_1 + d_2)$; r_{++} are r_+ and the ionic radii of the two cations (which have charges of +2 and +1, respectively). Correcting for the heat of fusion of calcium nitrate (5.7 kcal.) we obtained for the limiting heats of solution of undercooled, liquid calcium nitrate in the considered salts

$$\Delta\bar{H}_{Ca(NO_3)_2}(l, 350°) = 0.3 - 225\delta'^2 \text{ kcal./mole} \quad (3)$$

Figures 1 and 2 contain the experimental information which is required in order to check whether relations similar to (2) and (3) hold also for the considered strontium and barium nitrate systems. For this purpose we have in Fig. 3 plotted the observed limiting heats of solution of calcium, strontium, and barium nitrates *vs.* the square of the size-charge parameter δ'.

These three salts have different heats of fusion. Therefore the curves plotted in Fig. 3 cannot superpose. However, it is apparent that the three curves have very similar slopes. Thus, we find that all the data contained in Fig. 3 can be represented to a good approximation by a general empirical expression

$$\Delta\bar{H}_{Me(NO_3)_2} = A - 225\delta'^2 \text{ kcal./mole} \quad (4)$$

The parameter A varies from system to system, and depends on the reference state adopted for the solute. When the reference state is the pure, undercooled liquid solute (at the considered temperatures) the experimental values of A are +0.3, +0.6, and +0.8 kcal./mole for calcium, strontium, and barium nitrates, respectively.

So far we have been unable to give any really satisfactory theoretical justification for this relation. Its principal merit rests in the fact that for the special case where the charge on the two cations is the same, the size-charge parameter δ' reduces to the pure size parameter δ of eq. 1. This latter parameter occurs in several different theoretical approaches to the problem of the heat of mixing in simple fused salt systems.[2,8,9]

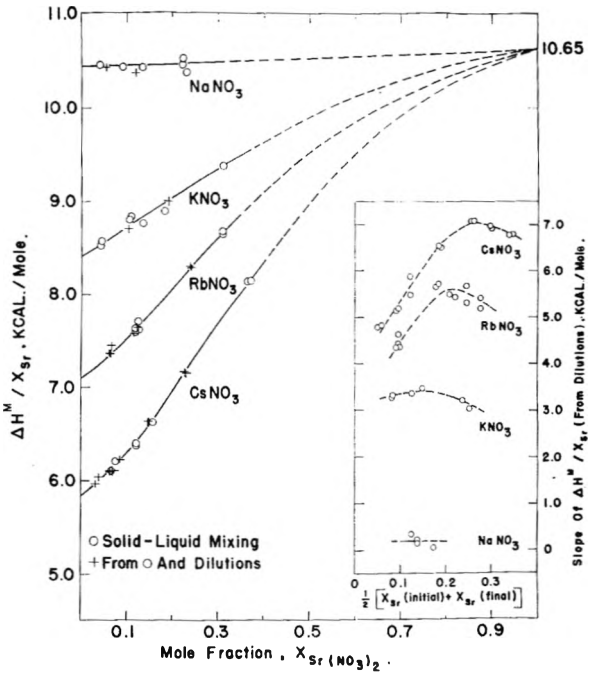

Fig. 1.—Heat data for solutions of strontium nitrate in the alkali nitrates at 450°.

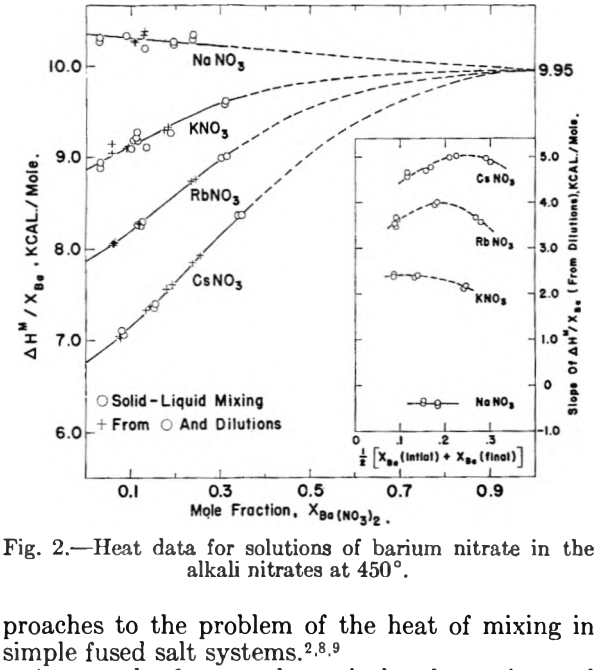

Fig. 2.—Heat data for solutions of barium nitrate in the alkali nitrates at 450°.

As a result of recent theoretical and experimental work on simple fused salt mixtures, it is believed that the following three factors make the most significant contributions to the enthalpy of mixing.

(a) There is a *negative* contribution arising to a large extent from the reduction in second nearest neighbor Coulomb repulsion.[2]

(b) Similarly, there is a *negative* contribution which is due to the polarization of the common anion. This polarization is in the main caused by

(7) O. J. Kleppa, *J. Phys. Chem. Solids*, **23**, 819 (1962).

(8) H. Reiss, J. L. Katz, and O. J. Kleppa, *J. Chem. Phys.*, **36**, 144 (1962).

(9) J. Lumsden, *Discussions Faraday Soc.*, **32**, 138 (1961).

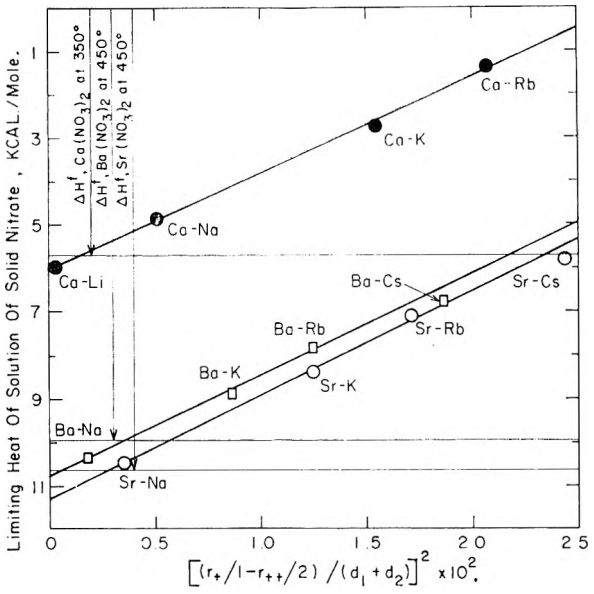

Fig. 3.—The dependence of the magnitude of the limiting heat of solution (of calcium, strontium, and barium nitrates in the alkali nitrates) on the parameter $(r_+/1 - r_{++}/2)/(d_1 + d_2)$.

the unsymmetrical field produced by the neighboring cations.[9]

(c) Finally, there is a positive contribution which is related to the change in van der Waals energy on mixing. This term probably is largely caused by changes in the second nearest neighbor populations.[9,10]

All the binary alkali nitrate systems exhibit negative enthalpies of mixing. Thus, the contributions from (a) and (b) outweigh those of (c). On the other hand, in mixtures of monovalent nitrates involving the more highly polarizable cations Ag^+ and Tl^+, one sometimes finds positive and sometimes negative enthalpies of mixing. Positive values are common for systems with relatively small values of δ, *i.e.*, in the cases where (c) outweighs the combined negative effects of (a) and (b).

So far our discussion has completely neglected possible structural factors. This perhaps may be justified in mixtures of salts of similar charge structure which have a common anion. However, it seems obvious that in the type of solution system covered in the present work we must consider, in addition to the interionic forces, the possible influence of the charge asymmetry on the mixing enthalpy. Here our results demonstrate that for systems with large negative enthalpies of mixing, the magnitude of the limiting heat of solution is determined largely by the square of the difference $(r_+/1 - r_{++}/2)$. This quantity is simply related to the difference between the "ionic potentials" (Z_i/r_i) of the two cations.

In a qualitative sense we believe that the negative term in eq. 4 may be given the following tentative interpretation. When we mix two fused salts which have a common anion, a certain structural rearrangement must occur unless the two cations happen to be identical. In the first approximation, this structural rearrangement presumably involves the local organization of the anions around the cation with the higher ionic potential. If this view is correct, we might expect the structural organization of the mixture to be dominated by the high field cation, and this should be the case even in mixtures where the two salts have the same charge structure. In all the systems considered in the present work, the higher ionic potential of the divalent ion is believed to represent the organizing force. When the difference in ionic potential becomes sufficiently large, the structural organization centered on the high field ion may be considered to take on the character of "complex" formation. It is noteworthy that the heat of solution rapidly becomes more exothermic with increasing size of the lower charged ion. This is consistent with similar trends frequently observed in the inorganic chemistry of ionic salts, *e.g.*, in the stability of double salts.

Associated with the structural reorganization there will be a negative change in enthalpy. Due to the long range nature of the Coulombic forces, it is difficult to attribute this enthalpy change to a particular mode of interaction, such as nearest neighbor, second nearest neighbor, polarization, etc.

We turn next to the positive term A in eq. 4. It will be noted that when the solutes are in the undercooled, liquid state, the magnitude of this term increases in a regular manner as the size of the divalent cation increases. In fact, there is a reasonable correlation between this term and the polarizability of the divalent cation.[11]

This suggests that the term A may be related to the change in van der Waals energy on mixing. In view of the structural difference between the solution partners it is difficult to make quantitative numerical estimates. This difficulty is compounded by the fact that this energy contribution, due to the r^{-6} dependence on distance, is extremely sensitive to the proper choice of interionic separation. However, the magnitude of A is consistent with estimates of the contribution of the van der Waals energy to the heat of mixing in structurally simpler systems.[9,10]

It remains to consider briefly the heat of dilution data. The most striking feature of these data is the pronounced maximum in $\Delta H^M/X$ found in all systems which exhibit strong interaction. This maximum is particularly evident for the solutions of strontium and barium nitrates in rubidium and cesium nitrates. Previously, we found similar maxima in the calcium–potassium and calcium–rubidium nitrate systems.[5]

It should be recognized that the maximum in $\Delta H^M/X$ corresponds to a maximum in the second derivative of ΔH^M, *i.e.*, in the curvature of the ΔH^M–X curve. This suggests that the mixture at this composition has a special stability compared to mixtures of other compositions. Frequently such a curvature maximum occurs at or near the composition of the enthalpy *minimum* for the homogeneous

(10) M. Blander, *J. Chem. Phys.*, **36**, 1092 (1962).

(11) J. H. Van Vleck, "The Theory of Electric and Magnetic Susceptibilities," Oxford University Press, 1932.

(*i.e.*, liquid–liquid) mixing process. However, this does not seem to be the case for the mixtures considered in the present work. Thus, we see from Fig. 1 and 2 that the curvature maximum appears to fall at solute mole fractions of the order of 0.2 to 0.3. There is some doubt about the location of the enthalpy minima. However, they probably all occur at significantly higher solute concentrations. It should be noted also that for a given solute (*e.g.*, strontium nitrate) the curvature maximum tends to shift to a higher solute concentration as the liquid–liquid mixing enthalpy becomes more negative.

Previously we attempted to relate the location of this maximum to the existence of a solid state double salt at the same composition.[5] In the light of the information now available we have some doubts about this relation. On the other hand, all the systems with heat of dilution maxima appear to have solid state double salts at some composition.

Finally, we should like to mention that the magnitude of the heat of dilution of course is related to the limiting heat of solution and to the size-charge parameter δ'. However, the extent and quantitative character of these correlations are very sensitive to the actual choice of solute concentration.

Acknowledgments.—This work has been supported by the Office of Naval Research under Contract No. Nonr 2121(11) with the University of Chicago, and by the National Science Foundation under grant No. G 19513.

THE THERMAL ISOMERIZATION OF VINYLCYCLOPROPANE

BY C. A. WELLINGTON[1]

Department of Chemistry, University of Rochester, Rochester, N. Y.

Received March 19, 1962

The gas phase thermal isomerization of vinylcyclopropane has been studied in a static system between 324.7 and 390.2°. It has been found to be a first-order unimolecular process at pressures above 8 mm., giving cyclopentene as the major product (~96%) with small amounts (~1% each) of 1,4-pentadiene, *cis*- and *trans*-1,3-pentadiene, but no isoprene. The effect of small additions of nitric oxide and the effect of increasing the surface/volume ratio by a factor of 27 are discussed, the former having no significant effect while the latter increased the rate of reaction by a small extent. From experiments with initial pressures of 10–11.5 mm., the two most important processes, the over-all reaction and the formation of cyclopentene, were found to have activation energies of 50.0 ± 0.3 and 49.7 ± 0.3 kcal./mole, respectively, and the rate constants (sec.$^{-1}$) could be expressed by k(over-all) = (5.3 ± 0.1) × 10^{13} exp(−50,000/RT) and k(cyclopentene) = (4.09 ± 0.05) × 10^{13} exp(−49,700/RT). Under the same conditions, the activation energies (kcal./mole) and rate constants (sec.$^{-1}$) for the formation of the minor products were: 1,4-pentadiene, 57.3 ± 1.0, k = (2.7 ± 0.2) × 10^{14} exp(−57,300/RT); *trans*-1,3-pentadiene, 53.6 ± 0.8, k = (1.01 ± 0.06) × 10^{12} exp(−53,600/RT); and *cis*-1,3-pentadiene, 56.2 ± 0.8, k = (8.0 ± 0.5) × 10^{13} exp(−56,200/RT).

Introduction

Previous work on the pyrolysis of vinylcyclopropane had indicated that the main product was cyclopentene. Vogel[2] has stated that vinylcyclopropane and 1-phenyl-1-vinylcyclopropane isomerize thermally into the corresponding cyclopentenes. He discusses the similarity between a double bond and a cyclopropane ring and he draws an analogy between the vinylcyclopropane isomerization and the reversible isomerization of cyclopropanecarboxaldehyde to 2,3-dihydrofuran. Furthermore, the pyrolysis in a flow system at 500–520° of a solution of 3 g. of a mixture of 68% vinylcyclopropane, 31% cyclopentene, and 0.3% 1,4-pentadiene in 15 ml. of acetic acid gave 70% cyclopentene, 28% vinylcyclopropane, and 3% 1,4-pentadiene.[3] This indicated that the vinylcyclopropane had been converted to cyclopentene and perhaps to a little 1,4-pentadiene.

However, passage of vinylcyclopropane over kieselguhr at 120–150° produced piperylene, the catalyst losing its activity after one pass.[4] Since in this latter experiment the reaction took place on the surface, it probably would not be of great significance in the decomposition in the gas phase. Thus an investigation of the gas phase reaction was undertaken with a view to determining if the ring expansion reaction was a homogeneous gas phase process and determining the kinetic parameters of all the processes that occur.

While this work was in progress, Flowers and Frey[5] reported that vinylcyclopropane undergoes a first-order thermal isomerization to cyclopentene. Investigation at four temperatures in the range 339–391° gave a good Arrhenius plot from which they obtain k = $10^{13.5}$ exp(−49,600/RT) sec.$^{-1}$. At 390.5° they report that 1% of the product was a mixture of 1,4-pentadiene, isoprene, and *cis*- and *trans*-1,3-pentadiene.

Experimental

Materials.—Vinylcyclopropane was obtained from the National Bureau of Standards, Washington 25, D.C., and the physical properties quoted for the sample were: m.p. −109.82°; n^{20}D 1.4138; d^{20} 0.72105 g./ml. The purity of the sample was tested by gas chromatography using two different columns, diisodecyl phthalate on celite, and dimethyl sulfolane on firebrick. In both cases no peak other than that due to vinylcyclopropane could be detected, showing that the sample contained less than 1 part in 10,000 of impurity.

Cyclopentene and 1,4-pentadiene were obtained from the National Bureau of Standards and were used without further purification. The impurity of each was checked by gas chromatography and found to conform to the quoted values of 0.034 ± 0.021 and 0.07 ± 0.05 mole %, respectively.

(1) Shell Foundation Postdoctoral Research Fellow.

(2) E. Vogel, *Angew. Chem.*, **72**, 4 (1960).

(3) C. G. Overberger and A. E. Borchert, *J. Am. Chem. Soc.*, **82**, 4896 (1960).

(4) B. A. Kazanskiĭ, M. Yu. Lukina, and L. G. Cherkashina, *Izvest. Akad. Nauk S.S.S.R. Otdel. Khim. Nauk*, 553 (1959); *Chem. Abstr.*, **53**, 21701^{d} (1959).

(5) M. C. Flowers and H. M. Frey, *J. Chem. Soc.*, 3547 (1961).

trans-1,3-Pentadiene was obtained from Columbia Organic Chemicals Co. Inc., Columbia, S. C. It was found by gas chromatography to contain no *cis* isomer, but about 4% cyclopentene as impurity. The sample was purified using a 2 m. silver nitrate/glycol chromatographic column at room temperature.

cis-1,3-Pentadiene was obtained from Phillips 90% piperylene using a 2-m. silver nitrate/glycol chromatographic column at low flow rate and room temperature.

Isoprene was used only to determine its retention time under the various analytical conditions used on the vapor phase chromatograph and a sample (Eastman Kodak Co.) was distilled and dried.

Apparatus and Procedure.—The apparatus has been described previously.[6] In the apparatus the stopcocks in the vicinity of the reaction vessel were replaced by mercury cut-offs of the float valve type to avoid any absorption of the reactants and products in stopcock grease.

The following procedure was used. In order that up to three experiments could be conducted at the same initial pressure, vinylcyclopropane was first metered out into a nest of three sample tubes with equal (±1%) volumes. The reactant vapor in one of the tubes was then condensed on a small cold finger in the mercury cut-off section in the immediate vicinity of the reaction vessel. The reaction was commenced by evaporating the reactant condensed on the cold finger by means of a bath of boiling water. The pressure in the reaction vessel was measured on a wide bore mercury manometer using a vernier telescope. The pressure was essentially constant during the course of the reaction, on occasion showing an increase of not more than 1 part in 3000. The reaction was stopped by opening the contents of the reaction vessel to a trap immersed in liquid nitrogen, where rapid condensation took place. All the products were condensable, no permanent gas being produced during the reaction. The condensate then was transferred to a sample tube immersed in liquid nitrogen and kept therein until it was condensed into the gas sampling section of a gas chromatographic apparatus.

Analysis of the Products.—Two packed columns were used separately and successively to analyze the products. The mixture was first run through a 2-m. silver nitrate/ethylene glycol column at room temperature and at low flow rate. By comparison with the retention times for the pure compounds under the same conditions, it was found that with this column it was possible to detect and estimate isoprene, *trans*-1,3-pentadiene, and *cis*-1,3-pentadiene, but 1,4-pentadiene, vinylcyclopropane, and cyclopentene could not be separated from one another. When a 4 m. column of dimethyl sulfolane on firebrick was used, it was possible to separate and estimate 1,4-pentadiene, cyclopentene, and vinylcyclopropane from each other. However, *cis*- and *trans*-1,3-pentadiene had retention times very similar to that of cyclopentene and could not be separated from the latter. The products of the reaction were analyzed as follows. The whole sample from the reaction vessel was introduced into the gas chromatograph and analyzed using the 2 m. silver nitrate/ethylene glycol column. Thus the amounts of *cis*- and *trans*-1,3-pentadiene and the total amount of 1,4-pentadiene, cyclopentene, and vinylcyclopropane were measured using a Perkin-Elmer printing integrator. The fraction containing 1,4-pentadiene, cyclopentene, and vinylcyclopropane was collected in a long, efficient, glass spiral immersed in liquid nitrogen and connected to the exit tube from the Perkin-Elmer vapor fractometer, Model 154D. Within the accuracy of analysis complete quantitative condensation of the fraction was achieved. This latter fraction then was reintroduced into the gas chromatograph. The three components could be separated and analyzed quantitatively by the use of the 4 m. dimethylsulfolane column at medium flow rate.

By this procedure no peak corresponding to that for isoprene was detected. Since the formation of isoprene has been reported previously,[5] special steps were taken to ascertain whether it was present in the products in this work. At 393° a sample at 12 mm. pressure was taken to at least 90% decomposition. The products were run on the gas chromatograph and no peak corresponding to isoprene could be detected. In a second experiment the products of a decomposition were divided into two portions. The first portion was analyzed in the usual way on the silver nitrate/ethylene glycol column, while to the second portion a small amount of isoprene was added and then the mixture was analyzed in the same way as the first portion. On comparing the two chromatographs, the second showed the peak due to isoprene which was quite distinct and well separated from the rest of the products, with a retention time a little less than that of *trans*-1,3-pentadiene. The first, however, showed no trace of a corresponding isoprene peak. Thus, isoprene could not be detected in the products of the decomposition of vinylcyclopropane under the conditions used for the experiments in this work.

However, peaks corresponding to the other compounds mentioned above always were present. Two other small peaks were often noted but these were not estimated, since each constituted an amount of less than 1 part in 10,000 of that of the products. One of these peaks, appearing at long retention time, also appeared when a pure sample of cyclopentene was left in the reaction vessel at the highest temperature employed in this work for many hours and then analyzed. Again its amount was negligible compared with that of the pure cyclopentene used. This peak was the only peak, other than that of the cyclopentene itself, that appeared in the analysis, showing that no vinylcyclopropane had been produced from cyclopentene. Thus, it seems that no equilibrium occurs between vinyl cyclopropane and cyclopentene as exists between cyclopropane carboxaldehyde and 2,3-dihydrofuran.[2,7]

The presence of 1,4-pentadiene and cyclopentene in the products was confirmed by collecting the fractions from the gas chromatographic analyses corresponding to each compound and taking an infrared spectrum of each, using a 1-m. gas cell. The two spectra obtained corresponded exactly to the respective spectra in the literature[8] and were quite different from those of the isomers of the two compounds.

The isomerization of vinylcyclopropane can thus be represented by eq. 1

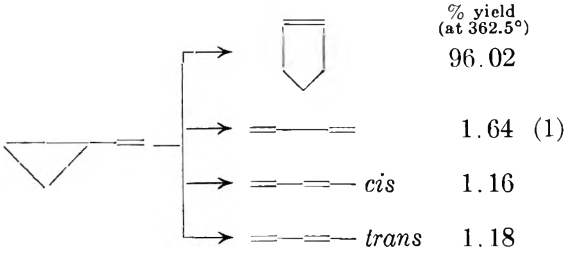

The printing integrator and the gas chromatograph were calibrated for each of the products of the reaction, using standard mixtures of the pure compounds. The relative response of the intruments compared with that for vinylcyclopropane were: cyclopentene, 1.00; 1,4-pentadiene, 0.98; *trans*-1,3-pentadiene, 1.01; *cis*-1,3-pentadiene, 1.01. With these values, the fractions of 1,4-pentadiene and cyclopentene in the mixture of these compounds and vinylcyclopropane were calculated from the results on the dimethyl sulfolane column. With this information, together with the results for the silver nitrate/ethylene glycol column, the fractions of *cis*- and *trans*-1,3-pentadiene in the products could be calculated. The over-all fraction of reaction then was computed and also the fraction of each product of the total products. The over-all rate constant and the relative rate constants for the formation of each product were calculated. In many cases also, the over-all rate constant was obtained from results at different durations (but all other conditions being the same) by plotting $-\log(1 - \text{fraction reacted})$ against the time of reaction. This plot always produced a good straight line, showing the reaction was of first order (as indicated by Table I) and from the slope of the straight line the rate constant was obtained.

In order that the system of analysis, which involved the condensation of a major part of the product and all of the unchanged reactant, might be well checked as to its accuracy, two identical experiments were performed. The products of the first experiment were analyzed by the same two-column sequential procedure already described and the

(6) C. A. Wellington and W. D. Walters, *J. Am. Chem. Soc.*, **83**, 4888 (1961).

(7) C. L. Wilson, *ibid.*, **69**, 3002 (1947).

(8) American Petroleum Institute, Catalog of Infrared Spectra Data (1959), No. 450, 362, and 456.

over-all rate constant calculated. The products of the second reaction were analyzed on the dimethyl sulfolane column only. In this latter case small amounts of *cis*- and *trans*-1,3-pentadienes contributed to the cyclopentene peak. However, the response of the chromatograph was almost the same (1%) toward the 1,3-pentadienes as to cyclopentene, and so from the size of this composite peak and that of the peak for 1,4-pentadiene, the total amount of product was estimated and the rate constant calculated. The difference between the over-all rate constants from the two methods of analysis was only 1 part in 2,000, which showed that the method used for analysis was adequate.

Results

Order of the Reaction.—A number of experiments at five different temperatures in the range 332.6 to 375° were conducted at different reaction durations at initial pressures of 4.6 to 12 mm. Some of the results of these experiments are given in Table I where, in the fourth column, the values of the rate constants calculated assuming first-order kinetics are given. At each temperature the first-order rate constants are constant within experimental error at increasing times of reaction, showing the decomposition to be first order.

TABLE I

ORDER OF REACTION OF VINYLCYCLOPROPANE

Temp. (°C.)	Duration (sec.)	% Reaction	$10^5 \times k$ (over-all) (sec.$^{-1}$)
332.7	3601	15.9	4.80
	7200	28.9	4.73
344.6	1569	15.3	10.59
	2826	26.0	10.66
350.2	1080	15.0	15.01
	2160	27.8	15.06
361.5	300.0	8.70	30.5
	1080.0	27.8	30.2
375.0	312.0	19.6	69.8
	595.8	35.1	70.1
	903.0	46.9	70.0

On varying the initial pressure of vinylcyclopropane from 24 to 0.14 mm. at 361.5° the fall-off in the first-order rate constant, as expected for a unimolecular reaction, was observed and the results are given in Table II.

TABLE II

FALL-OFF OF FIRST-ORDER RATE CONSTANT

Initial pressure (mm.)	$10^5 \times k$ (over-all) (sec.$^{-1}$)
24.7	3.06
8.13	3.05
8.01	3.02
4.57	3.03
1.17	2.88
0.43	2.64
0.14	2.30

The fall-off curve of $\log(k/k_\infty)$ against $\log p_0$ followed closely that of methylcyclobutane.[9]

Effect of Temperature.—The effect of temperature from 324.7 to 390.2° on the reaction was studied at initial pressures in the range 10–11.5 mm. in the unpacked reaction vessel in order to determine the activation energies and pre-exponential factors for each of the processes occurring in the reaction. The Arrhenius plots of $(-\log k)$ *vs.* $1/T$ are shown in Fig. 1 for the over-all isomerization (plot A) and for the formation of cyclopentene (plot B), and in Fig. 2 for the formation of 1,4-pentadiene (C) and *cis*- (E) and *trans*-pentadienes (D). The Arrhenius plots for all five processes show good straight lines, the greater spread of

(9) Experiments conducted by W. D. Walters and A. Pataracchia in these Laboratories.

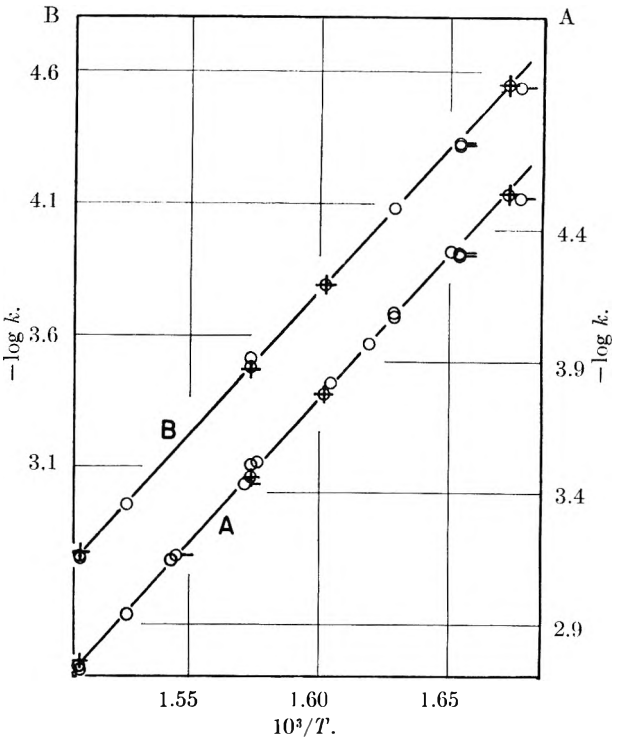

Fig. 1.—Temperature dependence of the first-order rate constants: A, over-all isomerization; B, formation of cyclopentene; O, no additive; +, NO added; O–, packed bulb.

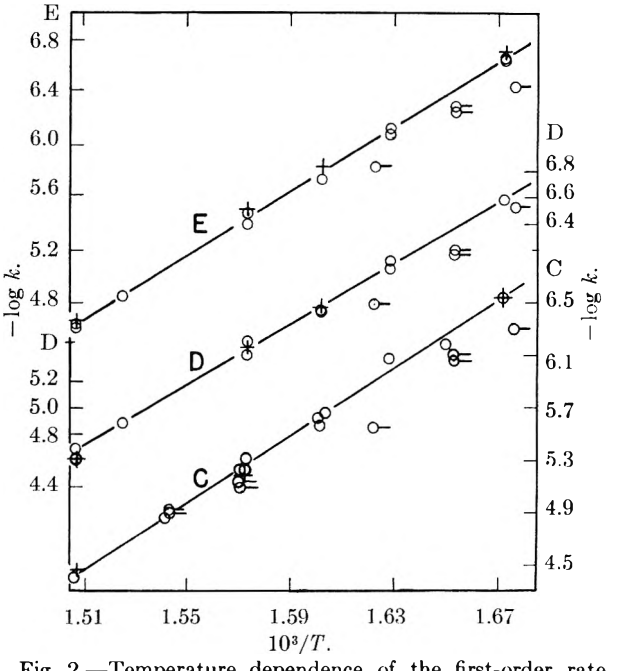

Fig. 2.—Temperature dependence of the first-order rate constants: C, formation of 1,4-pentadiene; D, formation of *trans*-1,3-pentadiene; E, formation of *cis*-1,3-pentadiene; O, no additive; +, NO added; O--, packed bulb.

points for the latter three compounds being due to the difficulty of measuring accurately the very small amount of each formed in the reaction. A least squares analysis of each set of data was performed on an I.B.M. 650 computer to determine the activation energy. The activation energies (kcal./mole) were found to be: over-all process, 50.0 ± 0.3; formation of cyclopentene, 49.7 ± 0.3; 1,4-pentadiene, 57.3 ± 1.0; *cis*-1,3-pentadiene 56.2 ± 0.8; *trans*-1,3-pentadiene, 53.6 ± 0.8. With these activation energies, the rate constants (sec.$^{-1}$) with the corresponding standard deviations for the various processes could be expressed by: over-all process, $(5.3 \pm 0.1) \times 10^{13} \exp(-50{,}000/RT)$; formation of cyclopentene, $(4.09 \pm 0.05) \times 10^{13} \exp(-49{,}700/RT)$; 1,4-pentadiene, $(2.7 \pm 0.2) \times 10^{14} \exp(-57{,}300/RT)$; *cis*-1,3-pentadiene, $(8.0 \pm 0.5) \times 10^{13} \exp(-56{,}200/RT)$; *trans*-1,3-pentadiene, $(1.01 \pm 0.06) \times 10^{13} \exp(-53{,}600/RT)$.

Effect of Nitric Oxide and Surface.—Since the parent compound was itself unsaturated, it seemed probable that if radicals were present during the reaction, addition to the unsaturated linkage would take place. However, no product of molecular weight higher than that of the parent compound was found on analyzing the products by gas chromatography and by mass spectrometry on a Consolidated 21/620 instrument. On addition of small and large amounts of nitric oxide at four different temperatures, the over-all rate was not affected. The relative rates of formation of the various products also were unaffected. The results are shown in Fig. 1 and 2. It was concluded that there was no effective radical participation in the reaction.

On studying the reaction in a Pyrex reaction vessel packed with thin-walled Pyrex tubing (resulting in an increased surface to volume ratio of about 27), a significant increase in the over-all reaction rate was observed when no conditioning of the packed vessel was made. The increase in the over-all reaction rate did not seem to decrease significantly on doing four successive experiments and was not reproducible. However, after three decompositions of 3,4-dihydro-2H-pyran, which yield acrolein and ethylene, had been carried out in the vessel, it was found that the reaction rate of vinylcyclopropane was reproducible and only slightly greater than that in the unpacked vessel which previously had been used to study the decomposition of 3,4-dihydro-2H-pyran. The results are shown in Fig. 1 and 2. It was concluded from these results that the contribution from a surface reaction in those experiments in the unpacked vessel was negligible.

Discussion

The foregoing results show that the isomerization of vinylcyclopropane is a unimolecular, first-order, essentially homogeneous process which is unaffected by additions of nitric oxide and yields mainly cyclopentene together with very small amounts of 1,4-pentadiene and *cis*- and *trans*-1,3-pentadiene. It has been shown that cyclopentene does not form vinylcyclopropane under the conditions of this work and so the isomerization of vinylcyclopropane is not complicated by an equilibrium between vinylcyclopropane and cyclopentene as exists between cyclopropane carboxaldehyde and 2,3-dihydrofuran.[7] No isoprene could be found under the conditions of the present investigation. If isoprene is not a product, the minor products do not necessarily result from the usual rupture of the cyclopropane ring as has been suggested,[5] but may result from a process involving a transition state in which the π-orbital of the vinyl group interacts with the partial delocalized electron cloud associated with the cyclopropyl ring in the vicinity of the two bonds of the ring adjacent to the vinyl group.[1] This probably is not possible with the third bond which probably is too far removed from the π-bond. The possibility of this type of transition state may be the reason why this compound can isomerize at temperatures much lower than those associated with the isomerizations of cyclopropane and the alkyl cyclopropanes. The relative ease with which vinylcyclopropane isomerizes may be due to the fact that for the formation of the main product, cyclopentene, hydrogen migration is not necessary and moreover for those products where it is necessary, namely the pentadienes formed, the activation energies are significantly higher than that for cyclopentene formation.

While in the addition of methylene radicals to butadiene, Trotman-Dickenson, *et al.*,[10] reported no cyclopentene as a product, Frey[11] has more recently reported that cyclopentene is formed from the decomposition of the excited vinylcyclopropane produced. The results of Frey show that, although the decomposition of the latter species also produces 1,4-pentadiene and *cis*- and *trans*-1,3-pentadiene, no isoprene is produced. This is consistent with the results of the present work and with the mechanism suggested above, and so the results of the decomposition of vinylcyclopropane may not be directly applicable to a consideration of the decomposition of cyclopropane and methylcyclopropane.

NOTE ADDED IN PROOF.—The small entropy of activation of 0.28 cal./deg. mole at 390° for the formation of cyclopentene indicates that the difference in rigidity between the normal and activated states of the molecule may be less than for the isomerization of cyclopropane. This is consistent with the mechanism for the isomerization suggested in the Discussion.

Acknowledgments.—The author wishes to thank Professor W. D. Walters for his great interest in this work and also Mr. Carl Whiteman, Jr., for making infrared measurements and least squares calculations.

(10) B. Grzybowska, J. H. Knox, and A. F. Trotman-Dickenson, *J. Chem. Soc.*, 4404 (1961).

(11) H. M. Frey, *Trans. Faraday Soc.*, **58**, 516 (1962).

THE STABILITY CONSTANT OF THE $H_2SO_4 \cdot HSO_4^-$ ION AND ITS MOBILITY IN ACETONITRILE[1]

BY I. M. KOLTHOFF AND M. K. CHANTOONI, JR.

School of Chemistry, University of Minnesota, Minneapolis 14, Minn.

Received March 21, 1962

From the electrical conductance at 25° of mixtures of tetraethylammonium bisulfate and sulfuric acid in acetonitrile (AN) a value of 65 for the mobility at infinite dilution of the conjugate ion, $H_2SO_4 \cdot HSO_4^-$, has been derived. From the solubility in AN of sodium bisulfate in the presence of various concentrations of sulfuric acid, the solubility product of sodium bisulfate and the stability constant of the conjugate ion have been calculated to be 3×10^{-7} and 1.0×10^3, respectively. Knowing the mobility of the conjugate ion, a value of 1.0×10^3 for the stability constant was calculated from conductance data in pure sulfuric acid solutions in AN. The value of 1.0×10^3 is in excellent agreement with the value 1.15×10^3 obtained from indicator equilibria in solutions of sulfuric acid.[2]

Introduction

Spectrophotometric and conductometric studies in acetonitrile of the dissociation of uncharged weak acids[2] have been interpreted on the basis of self-conjugation, *i.e.*, association of an anion with its conjugate acid.

$$HA + A^- \rightleftarrows A \cdot HA^-$$

For sulfuric acid

$$K_{AHA^-} = \frac{[H_2SO_4 \cdot HSO_4^-] f_{H_2SO_4 \cdot HSO_4^-}}{[H_2SO_4][HSO_4^-] f_{HSO_4^-}} = \frac{[H_2SO_4 \cdot HSO_4^-]}{[H_2SO_4][HSO_4^-]} \quad (1)$$

assuming $f_{H_2SO_4 \cdot HSO_4^-} = f_{HSO_4^-}$. The value of the stability constant, K_{AHA^-}, of sulfuric acid (eq. 1) was calculated from spectrophotometric data; only an approximate value could be derived from conductometric data because the mobility of the $H_2SO_4 \cdot HSO_4^-$ ion is not known. In the present paper, the electrical conductance of solutions of tetraethylammonium bisulfate in the presence of sulfuric acid has been determined and from these data the mobility of $H_2SO_4 \cdot HSO_4^-$ has been calculated.

This enabled us to calculate K_{AHA^-} from the conductance data of solutions of sulfuric acid[2] and to compare this value with those obtained spectrophotometrically and from the solubility of sodium bisulfate in sulfuric acid solutions.

The solubility of sodium bisulfate in solutions of sulfuric acid in acetonitrile increases with increasing concentration of added sulfuric acid.

$$NaHSO_4 \rightleftarrows Na^+ + HSO_4^-$$

$$HSO_4^- + H_2SO_4 \rightleftarrows H_2SO_4 \cdot HSO_4^-$$

$$NaHSO_4 + H_2SO_4 \rightleftarrows Na^+ + H_2SO_4 \cdot HSO_4^-$$

From the solubility data, the solubility product of sodium bisulfate and K_{AHA^-} could be calculated.

Finally, the conductance of solutions saturated with sodium bisulfate in the presence of varying concentrations of sulfuric acid has been determined.

Solubility of Sodium Bisulfate in Solutions of Sulfuric Acid.—The solubility product of sodium bisulfate is

$$K_{sp} = [Na^+][HSO_4^-] f^2 \quad (2)$$

in which $f = f_{Na^+} = f_{HSO_4^-}$.

In any solution of sodium bisulfate in the presence of sulfuric acid, the electroneutrality rule states

$$[Na^+] + [H^+] = [HSO_4^-] + [H_2SO_4 \cdot HSO_4^-] \quad (3)$$

The dissociation of sulfuric acid is greatly repressed by the presence of bisulfate, hence $[H^+] << [Na^+]$ (see Table I). Under this condition we find from eq. 1, 2, and 3

$$f^2[Na^+]^2 = K_{sp}\{1 + K_{AHA^-}[H_2SO_4]\} \quad (4)$$

where $[Na^+] = s - [NaHSO_4]$, s being the solubility and $[NaHSO_4]$ the concentration of undissociated sodium bisulfate in saturated solutions. An effort has been made to determine the dissociation constant of sodium bisulfate by measuring the

$$K_d = \frac{[Na^+][HSO_4^-] f^2}{[NaHSO_4]} = \frac{K_{sp}}{[NaHSO_4^-]}$$

conductance of a set of dilutions of the saturated solution. Unfortunately, some disproportionation of the bisulfate ion in the saturated solution without added sulfuric acid prevented a simple interpretation of the solubility data. No disproportionation was found when the analytical concentration of sulfuric acid added was equal to or greater than 0.01 M. Fortunately, the correction for $[NaHSO_4]$ is small and almost negligible at the higher concentrations of sulfuric acid added. Assuming a reasonable value of K_d of sodium bisulfate of the order of 5×10^{-4}, a correction for $[NaHSO_4]$ could be calculated.

It is shown in Table I that the average value of K_{sp} changes very little only when the assumed value for $[NaHSO_4]$ in the saturated solution is varied from 2.5×10^{-4} to 7×10^{-4} M.

As a first but close approximation we can write

$$[H_2SO_4] = c_a - s$$

assuming that all bisulfate ions are present in conjugated form AHA^-. At c_a greater than 0.02

(1) This research was supported by the U. S. Air Force through the Air Force Office of Scientific Research of the Air Research and Development Command, under Contract No. AF49-(638)519. Reproduction in whole or in part is permitted for any purpose of the U. S. Government.

(2) I. M. Kolthoff, S. Bruckenstein, and M. K. Chantooni, Jr., *J. Am. Chem. Soc.*, **83**, 3927 (1961).

TABLE I

SOLUBILITY OF SODIUM BISULFATE IN ACETONITRILE IN PRESENCE OF SULFURIC ACID

H_2SO_4 added (moles/l.)	Total acidity (moles/l.)	Solubility ($M \times 10^3$)	$[H^+]^a$ ($M \times 10^5$), calcd.	$[HSO_4^-]^a$ ($M \times 10^4$), calcd.	$[H_2SO_4 \cdot HSO_4^-]^a$ ($M \times 10^3$), calcd.	$K_{sp} \times 10^7$ $[NaHSO_4] = 2.5 \times 10^{-4}$ M	$K_{sp} \times 10^7$ $[NaHSO_4] = 5 \times 10^{-4}$ M	$K_{sp} \times 10^7$ $[NaHSO_4] = 7 \times 10^{-4}$ M
0.018	0.0131	2.34	0.36	1.92	1.88	2.8	2.2	1.7
.0237	.0264	3.92	0.93	1.74	3.50	4.2	3.5	3.2
.0470	.0490	4.57	3.5	1.00	4.27	2.7	2.4	2.2
.0964	.0976	7.45	11.2	0.81	7.25	3.2	3.0	2.9
.248	.251	12.4	55.6	0.51	12.14	2.9	2.9	2.8
						Av. 3.1	2.8	2.6 ($\times 10^{-7}$)

[a] Values calculated using $K_{AHA^-} = 1.0 \times 10^3$ and $[NaHSO_4] = 2.5 \times 10^{-4}$.

M the error thus introduced becomes smaller than 5%.

A plot of f^2s^2 *vs.* $c_a - s$ was made and tentative values of K_{sp} and K_{AHA^-} were obtained from the intercept and slope of the best straight line (see eq. 4).

The activity coefficient, f, in eq. 4 was calculated from the limiting Debye–Hückel relation, $-\log f = 1.52\sqrt{\mu}$ in acetonitrile at 25°, where μ = ionic strength = $[Na^+] \cong s$.

After finding the approximate values of K_{AHA^-} and K_{sp}, a new plot was made of $f^2\{s - [NaHSO_4]\}^2$ *vs.* $[H_2SO_4]$ taking

$$[H_2SO_4] = c_a - s + [NaHSO_4] \qquad (5)$$

The values of K_{AHA^-} and K_{sp} thus found did not need further correction.

Mobility of $H_2SO_4 \cdot HSO_4^-$ from Conductance of Mixtures of Tetraethylammonium Bisulfate and Sulfuric Acid.—In such mixtures the electroneutrality rule is

$$[Et_4N^+] + [H^+] = [HSO_4^-] + [H_2SO_4 \cdot HSO_4^-] \qquad (6)$$

Under our experimental conditions sulfuric acid was in large excess over tetraethylammonium bisulfate and all bisulfate was essentially present as $H_2SO_4 \cdot HSO_4^-$ (see Table II), hence

$$[H_2SO_4] = c_a - c_s \qquad (7)$$

where c_a and c_s denote the analytical concentrations of acid and salt, respectively. Because tetraethylammonium bisulfate is extensively dissociated in the concentration range studied,[2] $[Et_4N^+]$ was taken equal to c_s in eq. 6. In a few instances it was necessary to take $Et_4N^+ \cdot HSO_4^-$ formation into account, using the constant[2]

$$K_d' = \frac{[Et_4N^+][HSO_4^-]f^2}{[Et_4N^+ \cdot HSO_4^-]} = 1.4 \times 10^{-3}$$

Substituting eq. 1 and 7 into eq. 6 yields

$$[H_2SO_4 \cdot HSO_4^-] = \frac{\{[H^+] + c_s\}\{c_a - c_s\}K_{AHA^-}}{1 + K_{AHA^-}\{c_a - c_s\}} \qquad (8)$$

Introducing the relations in (7) and (8) into eq. 1 yields eq. 9

$$[HSO_4^-] = \frac{\{[H^+] + c_s\}}{1 + K_{AHA^-}\{c_a - c_s\}} \qquad (9)$$

From

$$K_{2(HA)} = \frac{[H^+][H_2SO_4 \cdot HSO_4^-]f^2}{[H_2SO_4]^2} = 5.5 \times 10^{-5\ 2} \qquad (10)$$

and eq. 7, $[H^+]$ is calculated, assuming $[H_2SO_4 \cdot HSO_4^-] = c_s$ as a first approximation. For the calculation of $[H_2SO_4 \cdot HSO_4^-]$ and $[HSO_4^-]$ from eq. 8 and 9, respectively, a value of $K_{AHA^-} = 1.0 \times 10^3$ (see sections on Experimental Results and Discussion) was used. The calculated values of $[H^+]$, $[HSO_4^-]$, and $[H_2SO_4 \cdot HSO_4^-]$ are given in Table II.

Equation 11 is found from Kohlrausch's law of independent ion migration

$$1000L_{obsd.} = \lambda_{H^+}[H^+] + \lambda_{Et_4N^+}[Et_4N^+] + \lambda_{HSO_4^-}[HSO_4^-] + \lambda_{H_2SO_4 \cdot HSO_4^-}[H_2SO_4 \cdot HSO_4^-] \qquad (11)$$

where $L_{obsd.}$ and λ with the appropriate subscript refer to the specific conductance of the solution and equivalent conductance of a given ion at the prevailing ionic strength, respectively. The equivalent conductance of the solvated proton at infinite dilution is 80,[3] of tetraethylammonium ion, 86.1,[4] and of bisulfate ion, 90.[2] The value of the equivalent conductance of each ion at a given ionic strength was calculated from the Onsager relation[5]

$$\lambda = \lambda_0 - [0.735\lambda_0 + 115]\sqrt{c} \qquad (12)$$

the constants of which were calculated using the values of 36[4] and 0.345 cp.[4] for the dielectric constant and viscosity of acetonitrile, respectively, at 25°.

From the difference between $1000L_{obsd.}$ and the sum of the first three terms on the right hand side of eq. 11, $\lambda_{H_2SO_4 \cdot HSO_4^-}$ was found at the known ionic strength. With the aid of the Onsager relation, the value at infinite dilution, $\lambda_{0H_2SO_4 \cdot HSO_4^-}$, was calculated. The conductance of the mixtures then was calculated and the values obtained compared with the experimental data in Table II.

Conductance of Solutions Saturated with Sodium Bisulfate and Containing Various Concentrations of Sulfuric Acid.—The conductivity of

(3) I. M. Kolthoff and J. F. Coetzee, *J. Am. Chem. Soc.*, **79**, 6110 (1957).

(4) P. Walden and E. J. Birr, *Z. physik. Chem.*, **144**, 269 (1929).

(5) L. Onsager, *Physik. Z.*, **27**, 388 (1926); **28**, 277 (1927).

TABLE II

CONDUCTANCE OF MIXTURES OF SULFURIC ACID AND TETRAETHYLAMMONIUM BISULFATE

Series[a]	c_s, $M \times 10^3$	c_a, $M \times 10^2$	$[H^+]$, $M \times 10^4$	$[H_2SO_4 \cdot HSO_4^-]$, $M \times 10^3$	$[HSO_4^-]$, $M \times 10^5$	$[Et_4N^+]$, $M \times 10^3$	Specific conductance (ohm^{-1} cm.$^{-1}$ $\times$ 10^5) Calcd.	Obsd.	Δ^b in %
I	2.04	2.0	0.13	1.92	12.3	1.93	27.85	29.0	+4.1
	2.04	5.0	0.92	2.10	5.0	2.00	29.40	30.0	+2.0
	2.04	8.0	2.41	2.25	3.3	2.02	31.33	31.5	+0.5
II	1.02	2.0	0.24	0.98	5.9	0.97	14.51	14.5	0.0
	1.02	5.0	1.06	1.09	2.6	1.00	15.81	15.1	−4.4
III	0.204	0.51	0.066	0.170	4.1	0.20	3.14	3.10	−1.3
	0.204	1.0	0.27	0.207	2.4	0.20	3.45	3.36	−3.2

[a] In series I, λ_{H^+}, λ_{AHA^-}, λ_{A^-}, and $\lambda_{Et_4N^+}$ equal 72.5, 57.6, 81.8, and 78.0, respectively; series II, 74.9, 59.8, 84.3, and 80.4; series III, 77.9, 62.7, 87.5, and 83.6. [b] $\Delta = \left[\frac{L_{obsd.} - L_{calcd.}}{L_{calcd.}}\right] \times 100$.

saturated solutions of sodium bisulfate containing various amounts of added sulfuric acid was measured. From the known solubility and eq. 8, 9, and 10, the concentrations of $H_2SO_4 \cdot HSO_4^-$, simple bisulfate ion, and hydrogen ion were calculated, taking $c_s = s - [NaHSO_4]$, $[NaHSO_4] = 2.5 \times 10^{-4}$, and $K_{AHA^-} = 1.0 \times 10^3$. Mobilities of the ions were calculated as before. $\lambda_{0H_2SO_4 \cdot HSO_4^-}$ and λ_{0Na^+}[4] were taken equal to 65.0 and 69.8, respectively. From the difference between the observed conductance of the saturated solution and the sum of the first, third, and fourth terms on the right hand side of eq. 11, the sodium ion concentration was calculated (sodium ion replaces tetraethylammonium ion in eq. 11).

Experimental

Reagents and Chemicals.—Acetonitrile was purified and dispensed as described previously.[2]

Sulfuric Acid and Tetraethylammonium Bisulfate.—These were prepared and purified as described previously.[2]

Sodium Bisulfate.—The Merck Reagent Grade product was recrystallized from water and dried at 100° *in vacuo* for 4 hr. Assay by alkalimetric titration was 99.7%.

Conductivity Cell and Bridge.—A conductivity cell having a cell constant of 0.224, with unplatinized electrodes and mercury leads 10 cm. apart, was used for all conductance measurements. The cell was placed in a light kerosene oil bath, maintained at 25.00 ± 0.05°. The conductance was determined with the Industrial Instruments, Inc. 1R-C conductivity bridge.[2]

Determination of Solubility of Sodium Bisulfate.—Approximately 50 mg. of dry sodium bisulfate (ground in an agate mortar) was placed in a 5-ml. volumetric flask. Four ml. of a freshly prepared solution of sulfuric acid in AN of known concentration was pipetted into the flask. In a separate sample, the sulfuric acid concentration was determined by alkalimetric titration after flooding with 20 volumes of conductivity water.

The flask and contents were shaken at 29° for 12 hr. and then at 25° for 4 hr. in a mechanical shaker operating at 260 oscillations/min. After centrifuging at 1500 r.p.m. for 10 min., duplicate 1-ml. portions of the saturated solution were pipetted into 1-ml. porcelain crucibles and taken to dryness under an infrared lamp. The residue was treated with 1.5 ml. of water and 4 drops of 6 *M* aqueous ammonium hydroxide (DuPont Reagent Grade, distilled at atmospheric pressure) and the solution was taken to dryness.

The crucible with residue was gradually heated to 600° over a Tirrill burner and held at that temperature for 10 min. After allowing to cool, the residue was dissolved in a 30% ethanol–70% water mixture and transferred to the conductivity cell described above.

Increments of aqueous standard barium chloride solution were added from a 1-ml. buret calibrated in 0.010-ml. divisions. The conductivity of the solution[6] was measured 3 to 5 min. after addition of each increment. Volume corrections were made whenever necessary. No thermostat is required, provided room temperature does not vary more than 1° during the titration. The end-point was determined in the conventional way.

In the above procedure 2 moles of sodium bisulfate yield 1 mole of sodium sulfate after ignition.

Blanks were run with 1-ml. samples of 0.00940 *M* aqueous sodium bisulfate solutions pipetted in 1-ml. crucibles. Sufficient concentrated sulfuric acid (98%) was added to make the solution 0.08 *M* in sulfuric acid and the contents were taken to dryness under an infrared lamp. The residue was treated with 0.7 ml. of acetonitrile, taken to dryness, and treated further as in the above procedure beginning with the treatment with aqueous ammonia.

The total acidity in saturated sodium bisulfate solutions in the presence of sulfuric acid was determined by pipetting a 1-ml. aliquot into 20 ml. of water and titrating to the phenolphthalein end-point with standard sodium hydroxide. The total acidity, a_t, expressed in molar concentration of sulfuric acid is equal to the molar concentration of free sulfuric acid plus 1.5 times the solubility of sodium bisulfate in moles/l., all bisulfate being considered to be present in the form $H_2SO_4 \cdot HSO_4^-$. Alternatively, the free sulfuric acid concentration was calculated from eq. 5.

Experimental Results

Solubility of Sodium Bisulfate.—Solubility data of sodium bisulfate in sulfuric acid solutions in AN are presented in Table I. The slope and intercept of the plot of $f^2\{s - [NaHSO_4]\}^2$ *vs.* $c_a - s + [NaHSO_4]$ are 3.1×10^{-4} and 3.0×10^{-7}, respectively, from which K_{AHA^-} is found to be 1.0×10^3, taking $[NaHSO_4]$ equal to 2.5×10^{-4} *M*. Since the intercept, K_{sp}, is very small, the solubility product was calculated from the solubility at each concentration of sulfuric acid added, assuming three different values of $[NaHSO_4]$. The results are found in the last three columns of Table I. It is seen that the average value of K_{sp} changes only from 3.1×10^{-7} to 2.6×10^{-7} when $[NaHSO_4]$ is assumed to vary from 2.5×10^{-4} to 7×10^{-4} *M* in solutions saturated with the salt.

Conductance of Mixtures of Tetraethylammonium Bisulfate and Sulfuric Acid.—Using a value of 1.0×10^3 for K_{AHA^-}, the concentrations of the various ionic species in mixtures of tetraethylammonium bisulfate and sulfuric acid are calculated and listed in Table II. Satisfactory agreement between calculated and observed conductance of the mixtures given in Table II was obtained when $\lambda_{0H_2SO_4 \cdot HSO_4^-}$ was taken equal to 65.0.

Conductance of Solutions Saturated with Sodium Bisulfate in Presence of Sulfuric Acid.—The sodium ion concentrations as calculated from the conductivity of saturated sodium bisulfate

(6) I. M. Kolthoff and T. Kameda, *Ind. Eng. Chem., Anal. Ed.*, **3**, 129 (1931).

solutions in presence of sulfuric acid were found to agree within 5% with the values obtained from solubility determinations.

Discussion

Knowing the mobility at infinite dilution of the $H_2SO_4 \cdot HSO_4^-$ (AHA^-) ion to be 65, and that of the proton, 80,[3] we find a value of $\Lambda_{0H^+AHA^-} = 145$. It is now possible to obtain K_{AHA^-} and the first dissociation constant of sulfuric acid, K_{HA}, from previously[2] determined conductance data of pure sulfuric acid in AN using the plot of $\Lambda - \sqrt{c\{1 + 1/K_{AHA^-}\}}$ *vs.* c. This plot yields a value for K_{AHA^-} of 1.03×10^3 and for K_{HA} of 5.0×10^{-8}, in excellent agreement with the values of 1.15×10^3 and 4.8×10^{-8} obtained from spectrophotometrically determined[2] equilibrium data of indicators in solutions of sulfuric acid in AN. The value of 1.0×10^3 for K_{AHA^-} obtained in the present paper from solubility data of sodium bisulfate in solutions of sulfuric acid in AN lends strong support to the claim that the assumptions made in the calculations are justified.

The stability constant of 1.0×10^3 for $H_2SO_4 \cdot HSO_4^-$ is considerably greater than those of 1.7×10^2 and 2.8×10^2 for hydrochloric and hydrobromic acids, respectively.[2] Presumably, strong hydrogen bonding between bisulfate and sulfuric acid occurs in acetonitrile as well as in nitromethane.[7]

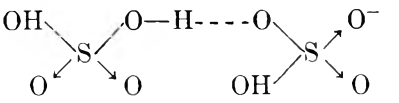

In a discussion of bilateral triple ion formation

$$3AB \rightleftarrows ABA^+BAB^-$$

in solutions of tetraisoamylammonium nitrate in water–dioxane mixtures, Fuoss[8] estimates that $\lambda_{0ABA^-} + \lambda_{0BAB^+}$ is equal to one-third to one-half of Λ_{0AB}. This estimate may be valid when dealing with the large size complex ions he used, but it is clear that his estimation should not be generalized for ions of much smaller size. As a matter of fact, the difference between the mobilities of HSO_4^- (80) and $H_2SO_4 \cdot HSO_4^-$ (65) is remarkably small in acetonitrile.

(7) H. Van Looy and L. P. Hammett, *J. Am. Chem. Soc.*, **81**, 3872 (1959).

(8) R. M. Fuoss, *ibid.*, **56**, 1857 (1934).

KINETICS OF THE REACTION OF PYRIDOXAL AND ALANINE[1]

BY GEORGE M. FLECK[2] AND ROBERT A. ALBERTY

Department of Chemistry, University of Wisconsin, Madison, Wisconsin

Received March 22, 1962

Kinetics of the reaction of pyridoxal and alanine in aqueous solution have been studied at 25° by observing the changes in visible and ultraviolet absorbancy and optical rotation which occur following mixing of the reactants. When the initial alanine concentration is much greater than the initial pyridoxal concentration, the absorbancy, A_t, due to pyridoxal, intermediates, and products, is given as a function of time by $A_t = B_0 + B_1e^{-m_1t} + B_2e^{-m_2t} + B_3e^{-m_3t}$, where m_1, m_2, and m_3 are pseudo first-order constants in the order of decreasing magnitude. Detailed studies are reported of the dependence of one of these pseudo first-order rate constants on pH, initial reactant concentrations, and ionic strength. It is concluded that at least three compounds which are distinguished spectrophotometrically are formed by the reaction.

Introduction

Pyridoxal reacts with amino acids in a variety of biologically important enzymatic reactions, and analogous non-enzymatic reactions have been reported. It is believed that the aldehyde group of pyridoxal reacts with the α-amino group of the various amino acids to form imines, with subsequent rearrangement of the imines.[3] Several investigators[4] have reported absorbancy changes with half-lives of a few minutes when pyridoxal and certain amines are mixed or when the pH of the resulting solutions is changed.

The present kinetic study of the reaction of pyridoxal and alanine was conducted to gain information regarding the mechanism of the non-enzymatic reaction. Reported in this paper are results of investigations on this reaction, in aqueous solution at 25.0°, studied by observing changes in visible and ultraviolet absorbancy and optical rotation.

Experimental

Reagents.—All water used had been redistilled from alkaline permanganate solution in a Barnstead still. The redistilled water was boiled in glass to drive off dissolved gases just before being used to prepare solutions, and precautions were taken to exclude carbon dioxide.

For studies of the variation of pseudo first-order rate constant m_2 with alanine concentration, ionic strength, and pH, C.P. D,L-α-alanine from Pfanstiehl Chemical Co. was used. Alanine from five different lots was separately recrystallized from 1 volume of 95% ethanol and 3 volumes of water. The mother liquor was yellow. These recrystallized products were pooled and twice recrystallized from 7 volumes of ethanol and 3 volumes of water. The crystals were washed with ethanol and then dried in a vacuum desiccator over phosphorus pentoxide.[5] Alanine for all other spectrophotometric measurements was D,L-α-alanine from Mann Research Laboratories. This product was recrystallized

(1) From a thesis submitted in partial fulfillment of the requirements for the degree of Doctor of Philosophy at the University of Wisconsin, 1961. This research was supported by grants from the National Science Foundation, the National Institutes of Health, and the Research Committee of the University of Wisconsin from funds supplied by the Wisconsin Alumni Research Foundation.

(2) William H. Danforth Graduate Fellow, 1956–1961.

(3) E. E. Snell, *Vitamins Hormones*, **16**, 77 (1958).

(4) J. B. Neilands and V. Williams, *Arch. Biochem. Biophys.*, **53**, 56 (1954); D. E. Metzler, *J. Am. Chem. Soc.*, **79**, 485 (1957); H. N. Christensen, *ibid.*, **80**, 99 (1958).

(5) F. J. Gutter and G. Kegeles, *ibid.*, **75**, 3893 (1953); P. K. Smith and E. R. B. Smith, *J. Biol. Chem.*, **121**, 607 (1937).

from 1 volume of ethanol and 3 volumes of water and yielded a colorless mother liquor. The material was then recrystallized from 7 volumes of ethanol and 3 volumes of water, washed with ethanol, and dried over phosphorus pentoxide. For polarimetric measurements, A grade L-α-alanine was purchased from California Corporation for Biochemical Research. This alanine was twice recrystallized from ethanol and water and dried over phosphorus pentoxide.

Pyridoxal was obtained as the hydrochloride from California Corporation. It was recrystallized and prepared in the neutral form by dissolving in water, adjusting the pH to 6 with sodium hydroxide, and letting the neutral product crystallize overnight. The crystals were washed with cold water, dried in a vacuum desiccator over phosphorus pentoxide, and stored in a brown glass bottle at room temperature.[6]

Measurement of pH was made with a Leeds and Northrup line-operated pH meter. Standardization of the meter was made at pH 9.18 at 25° with freshly prepared borate buffer and at pH 7.00 at 25° with phosphate buffer. A series of alanine solutions could be adjusted separately with dropwise addition of sodium hydroxide to a pH value reproducible to within 0.02 of the nominal value.

Kinetic Measurements by Absorbancy Change.—Three successive changes in visible and ultraviolet absorbancy occur following mixing of an aqueous pyridoxal solution with an alanine solution. If the initial pyridoxal concentration is much less than the alanine concentration, the temporal course of the absorbancy in the wave length range 3500 to 4500 Å. is given by

$$A_t = B_0 + B_1e^{-m_1t} + B_2e^{-m_2t} + B_3e^{-m_3t} \quad (1)$$

where A_t is the absorbancy at time t, and m_1, m_2, and m_3 are pseudo first-order rate constants in the order of decreasing magnitude, which are functions of pH, ionic strength, and alanine concentration at constant temperature.

Under the reaction conditions employed, there exist time intervals in which the absorbancy changes can be described by equations of the form

$$\ln |A_{t+\tau} - A_t| = -m_rt + \text{constant} \quad (2)$$

where $A_{t+\tau}$ is the absorbancy at a time $t + \tau$, τ being an arbitrary constant time interval.[7]

In experiments for the determination of m_3, solutions were prepared containing pyridoxal, alanine, and sodium acetate, adjusted to the appropriate pH with sodium hydroxide. The reaction solution was filtered through a previously sterilized Morton bacterial filter[8] and transferred to spectrophotometer cells which were then closed with ground-glass stoppers. The all-Pyrex Morton filter assembly and the cells were sterilized by heating for 3 hr. at 160°.

When at least 30 min. had elapsed after mixing, the absorption spectrum of the contents of each cell was determined from 3000 to 5000 Å. using a Cary Model 14 recording spectrophotometer. The spectral changes associated with pseudo first-order rate constants m_1 and m_2 occurred before the first absorbancy measurement was made. The cells then were placed in closely-fitting cylindrical openings of a brass constant-temperature storage block. The cells were returned to the spectrophotometer and the spectra recorded at intervals of about 24 hr. The cells were kept in total darkness except when being transferred to and from the spectrophotometer.

The brass storage block was maintained at 25.00 ± 0.02° by circulating water from a constant temperature bath. The sample compartment of the spectrophotometer was at 25.0 ± 0.01°. Temperature measurements were made with mercury-in-glass immersion thermometers which were individually calibrated at 25° against a National Bureau of Standards calibrated thermometer.

In all experiments the ratio of molar concentrations of alanine to pyridoxal was at least 5×10^3 so that the concentration of alanine can be considered constant throughout the course of the reaction. Even at the highest concentrations used, alanine solutions are essentially transparent in the wave length range in which measurements of absorbancy were made.

For the determination of m_2, a thermostated mixing device was built to fit in the Cary spectrophotometer sample compartment, and both the mixing device and the sample compartment were thermostated by circulating water from a constant temperature bath. Stock solutions of pyridoxal and of alanine and sodium acetate, both adjusted to the same pH with sodium hydroxide, were stored in the bath in volumetric flasks. The flask containing the pyridoxal solution was shielded from direct illumination. In later experiments, a red Pyrex low actinic volumetric flask was used to filter radiation of less than 5000 Å.

In a typical experiment, a 25-ml. aliquot of a solution of alanine and sodium acetate was pipetted into the glass chamber of the mixing device and allowed to equilibrate thermally for a timed interval of 10 min. A 1.5-v. electric motor was turned on to rotate a Teflon stirring rod, 1 ml. of pyridoxal solution was added, and a Teflon plug was lifted to allow the mixed solution to flow down into a cylindrical quartz absorption cell of 10 cm. path length in the sample light beam of the spectrometer.

Measurements of absorbancy at various times at a fixed wave length were made with a Cary Model 14 recording spectrophotometer with a double-pen scale which records absorbancy from 0.0 to 0.1 and 0.1 to 0.2. To utilize the full range of the expanded absorbancy scale, the pen was arbitrarily set at an end of the scale at the beginning of the reaction. Hence absolute absorbancy readings were not obtained. Since only differences of absorbancies were used in the calculations, the unknown additive constant always vanished.

Both the effects of varying alanine concentration and of varying ionic strength at a fixed pH were investigated in a single series of experiments. Experiments at pH 9.20 and 10.40 demonstrated that the experimental value of m_2 is independent of the wave length of light employed for the measurements over the range from 3500 to 4500 Å.

All experiments to determine the dependence of m_2 on alanine concentration were performed using recrystallized Pfanstiehl alanine. Control experiments at pH 10.40 to verify the independence of observed m_2 on wave length were performed using recrystallized Mann alanine. These experiments permit a check for comparative purity of the two products. Identical values of m_2 were obtained.

Kinetic Measurements by Optical Rotation Changes.—The optical rotation of a solution of L-alanine is substantially increased by the addition of pyridoxal. The rotation of the resulting solution decreases slowly with time. If the concentration of pyridoxal is small compared with the concentration of alanine, this decrease is described by the equation

$$\ln (\alpha_t - \alpha_{t+\tau}) = -m_at + \text{constant} \quad (3)$$

where α_t is the observed rotation at time t, $\alpha_{t+\tau}$ is the rotation at time $t + \tau$, and m_a is a pseudo first-order rate constant.

Measurements of optical rotation were made with a Rudolph Model 200S spectropolarimeter equipped with a Hanovia quartz mercury arc, a Beckman monochromator, an oscillating polarizer, and a modified Photovolt photometer. Readings were taken by the symmetrical-angle method. Deviation from the mean of three readings averaged about 0.002°. A minimum time of 1 min. was required to make a single measurement of rotation. The instrument was kept in a room maintained at 25 ± 1° to minimize error due to differential expansion of various components of the polarimeter.

Solutions were sterilized by filtration through a Morton bacterial filter. Rotation of each solution in a 40-cm. tube was determined at 5461 Å. at intervals of about 10 hr. The sample was kept in complete darkness between readings.

Results

Determination of m_3 and m_2 require reaction times of the order of weeks. The dependence of these pseudo first-order rate constants on alanine concentration at ionic strength 0.05, pH 8.00, was investigated. Detailed studies of the dependence of m_2 on alanine concentration, pH, and ionic strength have been made. Due to the higher rate of reaction, rather limited information

(6) D. E. Metzler and E. E. Snell, *J. Am. Chem. Soc.*, **77**, 2431 (1955).
(7) E. A. Guggenheim, *Phil. Mag.*, [7] **2**, 538 (1926).
(8) H. E. Morton, *J. Bacteriol.*, **47**, 379 (1944).

about m_1 could be obtained. Some data at pH 8.00 are reported.

Calculation of m_2.—The quantity $\ln |A_{t+\tau} - A_t|$ was plotted *vs.* time. Values of both A_t and $A_{t+\tau}$ were read directly from the spectrophotometer recorder chart. At almost all wave lengths employed, the relative absorbancy indices are such that a rapid decrease in absorbancy is associated with pseudo first-order rate constant m_1 followed by a slower increase in absorbancy associated with m_2. The plot of absorbancy *vs.* time therefore has a minimum early in the reaction, a few seconds after mixing. In determinations of m_2, no absorbancy readings were recorded until after this minimum.

The magnitude of the arbitrary constant time interval τ was chosen small enough so that no correction had to be made for absorbancy changes associated with m_3. It was ordinarily possible for τ to be equal to at least two half-lives of the reaction.

At low pH values, the fastest absorbancy change produced a detectable downward curvature in some of the plots of $\ln |A_{t+\tau} - A_t|$ *vs.* time during the first 10% of the time period. A substantially greater departure from linearity in the same direction was observed at pH 8.00 at the highest alanine concentration, 0.17 *M*, indicating that difficulty in separating these two absorbancy changes would be expected in extending the experiments to lower values of pH and to higher values of alanine concentration.

To obtain a measure of the deviation of the data from linearity in plots of $\ln |A_{t+\tau} - A_t|$ *vs.* time, the deviation of each point was computed in terms of uncertainty in the readings of absorbancy. The average of the computed absorbancy uncertainties for a kinetic run is termed ΔA. At pH 8.80, ionic strength 0.10, the average value of ΔA for 15 kinetic runs was 0.0003; at pH 9.20, ionic strength 0.10, ΔA averaged 0.0006 for 15 runs. The smallest division on the recorder chart corresponds to an absorbancy of 0.001 and intermediate values of absorbancy can be estimated to about ± 0.0001.

All determinations were performed in sets of three or four identical runs, and the deviation from mean values of m_2 averaged 2.8% for 300 experiments at seven pH values.

At each value of pH and of ionic strength studied, m_2 can be represented by an equation of the form

$$m_2 = a_2(\mathrm{A})_0 + b_2 \qquad (4)$$

where $(\mathrm{A})_0$ is the initial alanine concentration, and a_2 and b_2 are pH-dependent parameters. Values at seven pH values are given in Table I.

Deviations from linearity of plots of m_2 *vs.* $(\mathrm{A})_0$ at ionic strength 0.05 at each pH value were calculated as average deviations of experimental points from a straight line, and comparison was made with the average of mean deviations in sets of identical kinetic runs and with the average uncertainty arising from an uncertainty of ± 0.02 in adjustment of pH. In each case it was shown that the plots are linear within the limits of experimental error.

The experimental value of m_2 was verified as being independent of initial pyridoxal concentration in the range 10^{-5} to 10^{-4} *M* at pH 9.20.

Dependence of both a_2 and b_2 on pH was determined with pH adjusted by addition of sodium hydroxide. Both kinetic parameters increase with increasing pH in the pH range studied, as shown in Table I.

TABLE I

DEPENDENCE OF THE KINETIC PARAMETERS a_2 AND b_2 ON IONIC STRENGTH AND pH

pH	Ionic strength	a_2, M^{-1} sec.$^{-1}$	b_2, sec.$^{-1}$	$(\mathrm{A})_0$ range. *M*
10.40	0.050	1.17	0.065	0.0086 to 0.059
10.00	.050	0.63	.041	.0090 to .064
9.60	.14	.53	.022	.020 to .093
	.10	.50	.021	
	.075	.49	.021	
	.050	.46	.021	
9.20	.10	.26	.0122	.0096 to .087
	.075	.26	.0106	
	.050	.28	.0093	
	.025	.27	.0091	
8.80	.10	.083	.0083	.019 to .13
	.075	.080	.0078	
	.050	.079	.0072	
	.025	.072	.0068	
8.40	.10	.038	.0045	.030 to .15
	.075	.034	.0046	
	.050	.036	.0041	
	.025	.037	.0038	
	.0075	.034	.0044	
8.00	.10	.023	.0031	.030 to .17
	.075	.016	.0034	
	.050	.017	.0034	
	.025	.019	.0032	
	.0075	.020	.0033	

The effect on the kinetic parameters a_2 and b_2 of changing ionic strength was studied at five values of pH from 8.00 to 9.60 with ionic strength adjusted by addition of sodium acetate. Results are shown in Table I. Any effects due to changing ionic strength are in most cases less than the experimental error in determining the kinetic parameters. The only trends apparent are seen in values of b_2 at pH 9.20 and 8.80, where b_2 shows an increase with increasing ionic strength.

Calculation of m_3.—The quantity $\ln |A_{t+\tau} - A_t|$ was plotted *vs.* time. The constant time interval τ was taken to be more than two half-lives of the slow reaction; its magnitude is arbitrary, but in the event that no subsequent reaction occurs, the plot is most accurate when τ is large compared with the half-life.[7] Separate plots were made from data at each of four different wave lengths. Values of m_3 obtained at various initial alanine concentrations are shown in Table II.

Several complications enter into an analysis of these data. The plots used to calculate m_3 are concave downward, with only slight deviation from linearity appearing at the lowest alanine concentrations, more marked deviations appearing at the higher alanine concentrations. The observed

TABLE II

VARIATION OF m_3 WITH $(A)_0$ AT pH 8.00, IONIC STRENGTH 0.05

$(A)_0$, M	Wave length, Å.	$m_3 \times 10^6$, sec.$^{-1}$
0.172	4400	2.7
	4100	2.6
	3800	2.6
	3200	2.4
.213	4400	4.6
	4100	4.7
	3800	4.2
	3200	3.9
.254	4400	6.3
	4100	6.6
	3800	6.1
	3200	5.6
.290	4400	7.8
	4100	8.2
	3800	8.3
	3200	6.0

value of m_3 determined at 3200 Å. is consistently lower than values determined at higher wave lengths, and the difference becomes greater at higher alanine concentrations.

Previous investigators have reported instability of aqueous pyridoxal solutions under certain conditions.[9] In conjunction with experiments on the determination of m_3, controls revealed that a sterilized pyridoxal solution at pH 8.00 undergoes spectral changes over periods of days, even in total darkness. The magnitudes of the changes were not reproducible with duplicate samples. The total magnitude of these absorbancy changes per mole of pyridoxal at wave lengths being used to determine m_3 was about 5% of the changes observed when alanine also was present at concentrations of about 0.2 M.

Estimation of m_1.—The existence of the spectral change associated with m_1 can be demonstrated using the Cary Model 14 spectrophotometer at pH values lower than 9.20. However, the reaction is too fast for detailed study using manual mixing techniques.

An experiment was performed at pH 8.00, initial alanine concentration 1.5×10^{-4} M, initial pyridoxal concentration 4×10^{-5} M, 25.0°. The quantity $\ln |A_{t+\tau} - A_t|$ was plotted *vs.* time. The average of eight determinations at eight wave lengths from 3100 to 4100 Å. was $m_1 = 0.11 \pm 0.04$ sec.$^{-1}$.

Calculation of m_a.—Determination of m_a from measurements of optical rotation was made by plotting $\ln (\alpha_t - \alpha_{t+\tau})$ *vs.* time. Values obtained at pH 8.00, ionic strength 0.05, are recorded below at several initial concentrations of alanine: 0.176 M, 2.1×10^{-6} sec.$^{-1}$; 0.274 M, 1.0×10^{-6} sec.$^{-1}$; 0.488 M, 2.8×10^{-6} sec.$^{-1}$; 0.772 M, 5.4×10^{-6} sec.$^{-1}$.

No optical rotatory changes were detected corresponding to spectral changes associated with pseudo first-order rate constant m_2.

(9) E. Cunningham and E. E. Snell, *J. Biol. Chem.*, **158**, 491 (1945); L. Davis, F. Roddy, and D. E. Metzler, *J. Am. Chem. Soc.*, **83**, 127 (1961); D. Heyl, S. A. Harris, and K. Folkers, *ibid.*, **70**, 3429 (1948); H. N. Christensen, *ibid.*, **80**, 99 (1958).

Optical rotation changes occurring in these solutions could not reasonably be anticipated to be due entirely to a racemization of uncomplexed alanine in solution, since a residual rotation equal to that expected for alanine alone remained after the reaction characterized by m_a had passed through several half-lives. A control experiment was performed in which a sterilized solution of alanine at pH 8.00 was placed in a one-decimeter tube and optical rotation readings taken over a period of one month. No significant change in rotation was detected during this time.

Discussion

Existence of the three spectral relaxation times requires that the chemical mechanism involve, in addition to pyridoxal and alanine, a minimum of three other species. One of the most reasonable of such mechanisms can be formulated as

$$A + P \underset{k_{-1}}{\overset{k_1}{\rightleftharpoons}} X_1$$

$$X_1 \underset{k_{-2}}{\overset{k_2}{\rightleftharpoons}} X_2$$

$$X_2 \underset{k_{-3}}{\overset{k_3}{\rightleftharpoons}} X_3$$

Here A and P are alanine and pyridoxal. Suggestions about the chemical nature of X_1, X_2, and X_3 will be made below. The integrated rate equation for this mechanism can readily be obtained for the case where initial alanine concentrations are much greater than pyridoxal concentrations so that one has a set of first-order and pseudo first-order reactions. If the small changes which do occur in the concentration of alanine are not detectable spectrophotometrically, one obtains[10] the following equation for the absorbancies

$$A_{t+\tau} - A_t = \sum_{r=1}^{3} B_r' e^{-m_r t} \qquad (5)$$

where B_r' is a function of τ, initial reactant concentrations, absorbancy indices, and rate constants for the mechanism. The set of pseudo first-order rate constants is related to the rate constants of the mechanism by the equations

$$m_1 + m_2 + m_3 = k_1(A)_0 + k_{-1} + k_2 + k_{-2} + k_3 + k_{-3}$$

$$m_1m_2 + m_1m_3 + m_2m_3 = (A)_0 [k_1(k_2 + k_{-2} + k_3 + k_{-3})] + k_{-1}k_{-2} + k_{-1}k_3 + k_{-1}k_{-3} + k_2k_3 + k_2k_{-3}$$

$$m_1m_2m_3 = (A)_0[k_1(k_2k_3 + k_2k_{-3} + k_{-2}k_{-3})] + k_{-1}k_{-2}k_{-3} \qquad (6)$$

(10) For methods employed in this derivation, see: A. Rakowski, *Z. physik. Chem.* (Leipzig), **57**, 321 (1907); T. M. Lowry and W. T. John, *J. Chem. Soc.*, **97**, 2634 (1910); E. A. Guggenheim, *Phil. Mag.*, [7] **2**, 538 (1926); F. A. Matsen and J. L. Franklin, *J. Am. Chem. Soc.*, **72**, 3337 (1950).

If a time interval exists during which changes in the quantity $(A_{t+\tau} - A_t)$ are due to contributions of but one term of the right member of eq. 5, then eq. 2 will be valid in that time interval and it will be possible to determine m_r from the slope of plots such as have been described in this paper. Having obtained a set of m's, one can in principle get unique values for all rate constants of the mechanism by plotting each of the quantities $(m_1 + m_2 + m_3)$, $(m_1m_2 + m_1m_3 + m_2m_3)$, and $(m_1m_2m_3)$ *vs.* $(A)_0$. The three slopes and three intercepts suffice to determine the six rate constants.

For the case in which $m_1 >> m_2 >> m_3$, one can readily obtain the equation

$$m_2 = \frac{a_2(A)_0 + b_2}{c_2(A)_0 + 1} \qquad (7)$$

where

$$a_2 = \frac{k_1(k_2 + k_{-2} + k_3 + k_{-3})}{k_{-1} + k_2 + k_{-2} + k_3 + k_{-3}}$$

$$b_2 = \frac{k_{-1}(k_{-2} + k_3 + k_{-3}) + k_2(k_3 + k_{-3})}{k_{-1} + k_2 + k_{-2} + k_3 + k_{-3}}$$

$$c_2 = \frac{k_1}{k_{-1} + k_2 + k_{-2} + k_3 + k_{-3}}$$

The observed concentration dependence of m_2 within the range of initial alanine concentration employed, given by eq. 4, is consistent with eq. 7 if $c_2(A)_0$ is small compared to unity. An upper limit for c_2 thus is established at each value of pH listed in Table I.

The dependence of m_2 on $(A)_0$ is not an effect of changing activity coefficient. The experiments were performed at constant ionic strength, and since the major anionic species contributing to the ionic strength are the alaninate and acetate ions, the requirement of constant ionic strength is equivalent to the requirement of constant total carboxylate concentration. The fact that neither a_2 nor b_2 is strongly dependent on ionic strength adjusted with sodium acetate is evidence that the dependence of m_2 on $(A)_0$ is due neither to changes in ionic environment of the reactants nor to a specific dependence on carboxylate ion or sodium ion concentration. Activity coefficient data[11] for the zwitterion form of alanine in aqueous solution demonstrate that alanine solutions show no significant departures from ideality at concentrations used in these kinetic experiments. It therefore appears justifiable to seek an explanation of the observed dependence using a chemical reaction mechanism written in terms of molar concentrations.

Structures of species X_1, X_2, and X_3 in the above mechanism cannot be determined from these experiments. However, previous studies of this and related reactions provide rationale for suggestions regarding the chemical nature of the three compounds. The first step is similar to one proposed for analogous reactions by Jencks,[12] and X_1 may be an addition compound of the structure

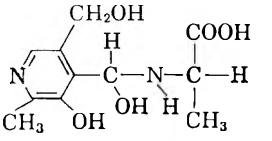

Heyl, Harris, and Folkers[13] have reported isolation of a compound formed from potassium alaninate and pyridoxal in ethanol, giving evidence for the structure

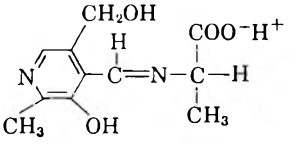

It therefore seems reasonable that X_2 may be formed from X_1 by the loss of water to give a carbon–nitrogen double bond. Loss of optical activity in the final step of the reaction suggests that asymmetry is lost at the α-carbon, possibly by X_3 having the structure

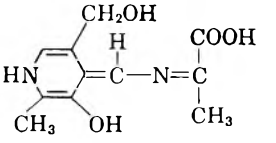

According to this mechanism, the pseudo first-order rate constant determined from optical rotation experiments should be equal to one of the pseudo first-order rate constants from absorbancy measurements. However, m_a and m_3 do not show the same dependence on $(A)_0$. Water has not been included in the formal mechanism, since these kinetic experiments could not detect the participation of water in any of the steps.

Acknowledgment.—The authors are indebted to Drs. E. L. King and L. Peller for helpful discussions.

(11) P. K. Smith and E. R. B. Smith, *J. Biol. Chem.*, **121**, 607 (1937); R. A. Robinson, *ibid.*, **199**, 71 (1952).

(12) W. P. Jencks, *J. Am. Chem. Soc.*, **81**, 475 (1959); B. M. Anderson and W. P. Jencks, *ibid.*, **82**, 1773 (1960).

(13) D. Heyl, S. A. Harris, and K. Folkers, *ibid.*, **70**, 3429 (1948).

KINETICS OF DISCHARGE OF THE ALKALI METALS ON THEIR AMALGAMS AS STUDIED BY FARADAIC RECTIFICATION

BY HIDEO IMAI[1] AND PAUL DELAHAY

Coates Chemical Laboratory, Louisiana State University, Baton Rouge, Louisiana

Received March 24, 1962

The kinetics of discharge of the alkali metals on their amalgams was studied at 24 ± 0.6° by faradaic rectification from 0.25 to 3 megacycles sec.$^{-1}$ in 0.498 *M* MCl + 0.002 *M* MOH. The metal was generated *in situ* ($C_M \ll C_{M^+}$ at electrode surface), and *no* supporting electrolyte (tetraalkylammonium salt) was added to avoid interference with kinetics. Standard rate constants were corrected for the double layer structure. Correction for Cs is very approximate because specific adsorption of Cs^+ was neglected. It was concluded from previous work and from polarograms of 2.5 m*M* MCl without supporting electrolyte that hydrogen evolution did not interfere to an appreciable extent with metal ion discharge except possibly for Li. Transfer coefficients from Li to Cs: 0.65, 0.61, 0.59, 0.58, 0.57. Apparent standard rate constants: 0.09, 0.2, 0.05, 0.05, 0.09 cm. sec.$^{-1}$. Standard rate constants: 0.02, 0.04, 0.01, 0.01, (0.02) cm. sec.$^{-1}$ (Gouy–Chapman theory); 0.002, 0.01, 0.005, 0.005, (0.007) cm. sec.$^{-1}$ (Brodowski–Strehlow theory).

The method of faradaic rectification for the study of fast electrode processes[2,3] is applied in this paper to the kinetics of discharge of the alkali metals on their amalgams. These electrode processes were studied by faradaic impedance by Randles and Somerton[4] for Na, K, and Cs in 1 *M* tetramethylammonium hydroxide. Only approximate apparent standard rate constants ($k_a^0 \approx 0.4$, 0.1, and 0.2 cm. sec.$^{-1}$ for Na, K, and Cs, respectively) were obtained, as the upper limit of rate constants was reached which could be measured by faradaic impedance with the equipment used by these authors. Further, discharge kinetics was undoubtedly complicated by adsorption of tetramethylammonium ion and the resulting coverage of the electrode and influence on the double layer structure. The present study was undertaken for the following reasons: (a) Values of k_a^0 are of interest in establishing correlations between kinetic parameters and atomic and ionic properties for the series Li to Cs, especially since appreciable complex formation and ionic association can be ruled out, at least for chloride medium in water.[5] (b) Correction of k_a^0 for the double layer structure allows comparison of the Gouy–Chapman theory of the diffuse double layer with the recently developed treatment of Brodowski and Strehlow[6] at very cathodic potentials, at which the two theories give significantly different results. (c) Data on k_a^0 for Li to Cs are indirectly of interest in the elucidation of the not yet fully understood mechanism of hydrogen evolution in the electrolysis of alkali hydroxide solutions.[7] (d) The kinetic study of these processes should show the usefulness of faradaic rectification. A novel feature in this work is the elimination of supporting electrolyte and the concomitant interference by tetraalkylammonium ion.

Experimental

Solutions.—The alkali chloride solutions were prepared from analytical reagents. The hydroxides were obtained by decomposition of electrolytically prepared amalgams by water. Distilled water which had been redistilled over $KMnO_4$ was used. Solutions were treated with activated charcoal as recommended by Barker,[8] and charcoal was removed by centrifugation. High area platinum black might have been better than charcoal, as noted by the reviewer of this paper, to avoid contamination by dissolution in alkaline solution of oxidation products of charcoal. Oxygen was removed by nitrogen which was purified by pyrogallol, vanadous sulfate, and activated charcoal at Dry Ice temperature.

Cell.—The microcell previously described[2c] was used with a capillary length of 35 mm. The electrode area was approximately 0.01 cm.^{2} at the time the a.c. pulse was applied. This area was not so large as to make power consumption too high for the a.c. signal generator, but it was large enough to correspond to a cell resistance of approximately 100 ohms with the solutions being used, *i.e.*, below the resistance for for which stray capacity interfered. The non-resistive component of the cell impedance was nearly proportional to frequency up to 6 Mc., and consequently the effect of stray capacity was negligible.

Faradaic Rectification.—Rectification voltages were determined indirectly by compensation with a voltage step by means of equipment previously described.[2b,c] Ringing in the network of the low-pass filter prevented observations for the first 50 μsec. Compensation was not achieved for approximately 100 μsec. because the transient characteristics of the compensation circuit were not the same as for the rectification process. Perfect compensation was achieved for $t > 100$ μsec. (Fig. 1).

Double Layer Measurements.—Equipment for differential capacity measurements and determination of electrocapillary curves was quite conventional and was previously described.[9] Differential capacities of the double layer at the potential at which rectification voltages were determined were extrapolated from values at less negative potentials at which there is practically no metal deposition. Extrapolation was satisfactory because of slow variation of the double layer differential capacity with potential. The following values were used: 16.8, 16.9, 16.8, 17.6, and 18.0 μf. cm.$^{-2}$ from Li to Cs.

Polarographic Measurements.—A Sargent polarograph, model XXI, which had been fitted with a 1-sec. full scale deflection pen-and-ink recorder, was used according to

(1) Postdoctoral research associate 1960–1962; on leave from Minami College, Hiroshima University, Hiroshima.

(2) (a) P. Delahay, M. Senda, and C. H. Weis, *J. Am. Chem. Soc.*, **83**, 312 (1961); (b) M. Senda, H. Imai, and P. Delahay, *J. Phys. Chem.*, **65**, 1253 (1961); (c) H. Imai and P. Delahay, *ibid.*, **66**, 1108 (1962); (d) for a review, *cf.* P. Delahay in "Advances in Electrochemistry and Electrochemical Engineering," P. Delahay, editor, Interscience Publishers, New York, N. Y., 1961, pp. 279–300.

(3) See also related papers: (a) M. Senda and P. Delahay, *J. Am. Chem. Soc.*, **83**, 3763 (1961); (b) M. Senda and P. Delahay, *J. Phys. Chem.*, **65**, 1580 (1961).

(4) J. E. B. Randles and K. W. Somerton, *Trans. Faraday Soc.*, **48**, 951 (1952).

(5) J. Bjerrum, G. Schwarzenbach, and L. G. Sillén, "Stability Constants. Part II, Inorganic Ligands," The Chemical Society, London, 1958, p. 93.

(6) H. Brodowski and H. Strehlow, *Z. Elektrochem.*, **63**, 262 (1959); **64**, 891 (1960).

(7) For a recent review, *cf.* A. N. Frumkin in "Advances in Electrochemistry and Electrochemical Engineering," Vol. 1, P. Delahay, Ed., Interscience–Wiley, New York, N. Y., 1961, pp. 65–121.

(8) G. C. Barker, "Transactions of the Symposium on Electrode Processes, Philadelphia 1959," E. Yeager, Ed., John Wiley and Sons, New York, N. Y., 1961, pp. 325–365.

(9) K. Asada, P. Delahay, and A. K. Sundaram, *J. Am. Chem. Soc.*, **83**, 3396 (1961).

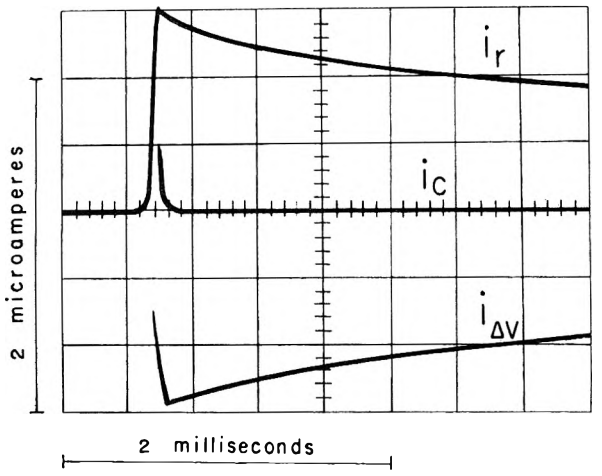

Fig. 1.—Tracings of current–time curves in the determination of rectification voltages by compensation for discharge of Na^+ in 0.498 M NaCl, 0.002 M NaCl at 24 ± 0.6°: i_r, rectification current; $i_{\Delta V}$, compensating current for voltage step $\Delta V = -1$ mv.; and i_c, current after compensation. Equilibrium potential −1.95 v. *vs.* pool, $f = 2$ Mc.; amplitude of cell voltage, 4.52 v.; amplitude of current density, 3.74 amp. cm.$^{-2}$.

standard procedure. Maximum currents at the end of drop life were measured.

Generation *in Situ*.—Metals were generated *in situ* because dropping amalgam electrodes for the alkali metals plug very easily and are not reliable, as noted by Randles and Somerton.[4] The cell circuit was the same as that used in previous work on rectification by the double layer.[2c] The generation circuit was open with a relay, which was synchronized by the signal operating the magnetic hammer 5 msec. before drop fall and was closed 0.1 sec. after drop fall. Continuous variation of the capillary characteristics resulted when generation was not interrupted.

The concentrations of alkali metal were calculated from polarographic theory by reckoning that the current includes a migration component but that diffusion is the sole mass transfer process for metal M. It was assumed that the current for hydrogen evolution was negligible (see below, however). Thus

$$i = KD_M^{1/2}C_M \qquad (1)$$

where K represents all the coefficients in the Ilkovic equation[10] except for concentration and diffusion; C_M is the alkali metal concentration in the amalgam at the electrode surface; D_M the diffusion coefficient of M in the amalgam; and i is the current. Diffusion coefficients[11] D_M, except for Rb, were taken from Schwarz[12] and are based on the experimental values of Wogau.[13] We took $D_{Rb} = D_{Cs}$ at 25° since these diffusion coefficients are nearly the same at 10° according to Wogau and the temperature coefficient should not vary much from Rb to Cs. (This coefficient is relatively small, anyhow.) Concentrations C_M are listed in Table I. The concentration C_{Rb} is only approximate because of interference by H_2 evolution (see below), and the value in Table I was estimated from the metal concentrations calculated below from the Nernst equation. Thus, $C_{Rb} = (C_{Rb}'/C_M')C_M$ where the (C')'s are from the Nernst equation, C_M is calculated from the current as indicated above, and M ≡ Li, Na, K, Cs. The average value of C_{Rb} was taken. No correction was attempted for any possible abnormal concencentration of the metal at the interface. (This possible error was pointed out by the reviewer of this paper.)

(10) This is only approximate because the Ilkovic equation holds for diffusion toward an expanding sphere, whereas there is diffusion of metal M toward the center of the drop. This approximation is usually made in the theory of polarography.

(11) We did not use the values of D_M from A. Vlcek, *Collection Czech. Chem. Commun.*, **20**, 413 (1955), which were calculated from Stokes' law (0.82, 0.68, 0.51, 0.49, and 0.45 × 10^{-5} cm.^{2} sec.$^{-1}$ for Li to Cs) for two reasons: (a) Application of Stokes' law is not rigorous and (b) D_{Na} in Table I agrees well with the more recently determined value (0.80 ± 0.04) × 10^{-5} cm.^{2} sec.$^{-1}$ at 22°, from M. v. Stackelberg and V. Toome, *Z. Elektrochem.*, **58**, 226 (1954).

(12) K. Schwarz, *ibid.*, **39**, 553 (1933).

(13) M. v. Wogau, *Ann. Physik*, [4] **23**, 345 (1907).

TABLE I

DATA FOR CALCULATION OF ALKALI METAL CONCENTRATIONS AT ELECTRODE SURFACE AT 24 ± 0.6°

Metal	E_e, v. *vs.* pool[a]	i,[b] μa.	$D_M \times 10^{-5}$, cm.^{2} sec.$^{-1}$	C_M, mM
Li[d]	−2.16	1.26	0.92	0.87
Na	−1.95	1.70	.86	1.2
K	−1.94	0.98	.77	0.74
Rb	−1.96	..	.63	(0.76)[e]
Cs	−1.97	1.36	.63	1.1

[a] E of pool *vs.* s.c.e., +0.048 v. [b] Pronounced interference by H_2 evolution for Rb. [c] See section on generation *in situ*. [d] See discussion of the possibility of hydrogen evolution.

The concentrations C_M were also estimated from the potential on the assumption that the Nernst equation can be applied.[11] (Electrode processes are fast enough.) These values of C_M were not used because the calculation appeared more uncertain than application of eq. 1 because of uncertainty on the standard potentials and activities of the amalgam for Li, Rb, and Cs.

Description and Discussion of Results

Rectification Data and Kinetic Parameters.—Results are summarized in Fig. 2, and the corresponding kinetic parameters are listed in Table II. The data of Fig. 2 were analyzed by means of the general equation for the rectification voltage previously derived.[2a] One has for charge transfer without complication for $C_{M^+} >> C_M$ and ctn $\theta >> 1$ (θ is phase angle between current and potential)

$$\frac{RT}{nF}\frac{\Delta\bar{E}_\infty}{V_A^2} = \frac{2\alpha - 1}{4} - \frac{(1-\alpha)I_a^0}{2^{3/2}nFC_MD_M^{1/2}}\frac{1}{\omega^{1/2}} \qquad (2)$$

where $\Delta\bar{E}_\infty$ is the rectification voltage; V_A is the amplitude of the alternating voltage across the electrode impedance; α is the transfer coefficient;

TABLE II

KINETIC DATA FOR DISCHARGE OF THE ALKALI METALS ON THEIR AMALGAMS AT 24 ± 0.6°[a]

Metal	E, v. *vs.* s.c.e.	α	I_a^0, ma. cm.$^{-2}$	k_a^0, cm. sec.$^{-1}$	$k^{0,b}$ cm. sec.$^{-1}$	$k^{0,c}$ cm. sec.$^{-1}$
Li[e]	−2.11	0.65	72	0.09	0.022	0.002
Na	−1.90	.61	219	.18	.040	.009
K	−1.89	.59	53	.052	.011	.005
Rb	−1.91	.58	57	.052	.011	.005
Cs	−1.92	.57	123	.087	(.016)[d]	(.007)[d]

[a] See values of C_M in Table I. Solution composition: 0.498 M MCl, 0.002 M MOH. [b] Double layer correction by Gouy–Chapman theory. [c] Double layer correction by Brodowski–Strehlow theory. [d] Double layer correction is quite approximate because specific adsorption of Cs^+ was not considered. [e] See discussion of the possibility of hydrogen evolution.

I_a^0 is the apparent exchange current density, *i.e.*, not corrected for the double layer structure; $\omega = 2\pi f$, f being the frequency; and n, F, R, T are as usual. V_A was calculated from the amplitude of the cell current and the differential capacity of the double layer. This was feasible since, except for 0.25 Mc. (note slight curvation in plots of Fig. 2),

the double layer impedance was much smaller than the faradaic impedance. It was assumed on the basis of previous experimental results[2c] that the double layer capacity was frequency-independent. Values of I_a^0 in Table II were converted to the apparent standard rate constant k_a^0 by

$$I_a^0 = nFk_a^0 C_{M^+}^{1-\alpha} C_M^{\alpha} \qquad (3)$$

The k^0's in Table II for Na, K, and Cs are somewhat smaller than the values reported by Randles and Somerton,[4] namely, 0.4, 0.1, and 0.2 cm. sec.$^{-1}$, but our k^0's are almost in the same ratio of 4:1:2 as the data of these authors. It should be noted that, in their case, k^0's were measured in 1 M tetramethylammonium hydroxide.

Double Layer Correction.—One has on the assumption of no specific adsorption

$$k^0 = k_a^0 \exp[(\alpha n - z)F\Delta\varphi/RT] \qquad (4)$$

where k^0 is standard rate constant; z (= +1) the ionic valence of the discharged species; and $\Delta\varphi$ the difference of potential across the diffuse double layer from the plane of closest approach to solution. One has here $(\alpha n - z)\Delta\varphi > 0$, $k_a^0 > k^0$, and the double layer effect accelerates the discharge process. Specific adsorption is negligible for Li^+ to Rb^+ but must be considered for Cs^+ as pointed out by Frumkin and co-workers.[14] Standard rate constants are listed in Table II for values of $\Delta\varphi$ calculated[15] by the Gouy–Chapman theory (G.C.) and the modified form of this theory by Brodowski and Strehlow[6] (B.S.). Data for the calculation of $\Delta\varphi$ are given in Table III.[16,17] It is seen that the double layer correction is relatively large and that the discharge of alkali metals is not particularly rapid, especially if one considers the k^0's corrected by the B.S. theory. Further, values of $\Delta\varphi$, and consequently of k^0, obtained by this theory and the G.C. theory differ markedly for a given metal. The G.C. and B.S. theories yield much closer values of $\Delta\varphi$ for ionic radii of 2–3 Å. at potentials not as cathodic as those prevailing in the discharge of the alkali metals. Note that k^0, as corrected by the B.S. theory, for Li has the lowest value of the series while this is not so for k^0 with correction by the G.C. theory. Sodium has the highest k^0—an observation which will not be interpreted here.

Possibility of Interference by Hydrogen Evolution.—Reduction of water with hydrogen evolution at an appreciable rate would interfere because the calculation of the concentration of metal for generation *in situ* would be seriously in error and faradaic rectification measurements would be affected. Interference, except possibly for Li, however, appears to be negligible on the basis of two arguments: (a) The current density for hydro-

(14) For a review of evidence for Cs^+ adsorption on Hg, see A. N. Frumkin, *Electrochim. Acta*, **5**, 265 (1961).

(15) Ionic association, which must be considered in the calculation of $\Delta\varphi$ (*cf.*, P. Delahay and A. Aramata, *J. Phys. Chem.*, **66**, 1194 (1962)), was neglected for LiOH and NaOH because of the low concentration of hydroxide in comparison with the chloride. There is no evidence of ionic association for KOH, RbOH, and CsOH according to ref. 5, p. 2.

(16) For radii of solvated ions, see C. B. Monk, "Electrolytic Dissociation," Academic Press, New York, N. Y., 1961, p. 271.

(17) Dielectric constants calculated according to J. B. Hasted, D. M. Ritson, and C. H. Collie, *J. Chem. Phys.*, **16**, 1 (1948).

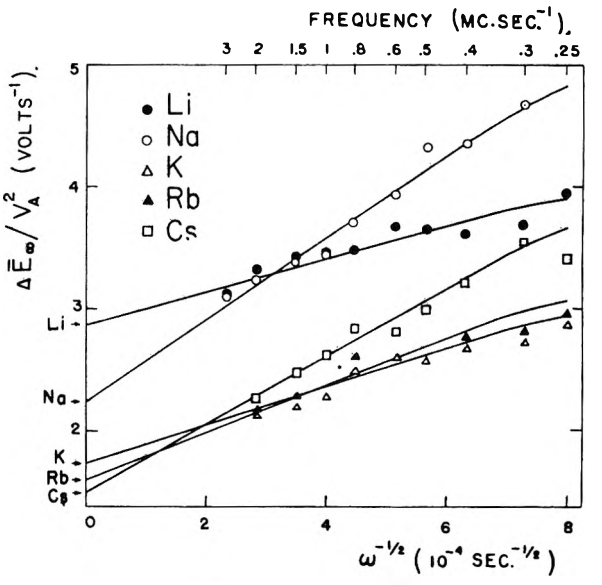

Fig. 2.—Plot of $\Delta\bar{E}_\omega/V_A^2$ against $\omega^{-1/2}$ for discharge of alkali metals on their amalgams for 0.498 M MCl, 0.002 M MOH at 24 ± 0.6°.

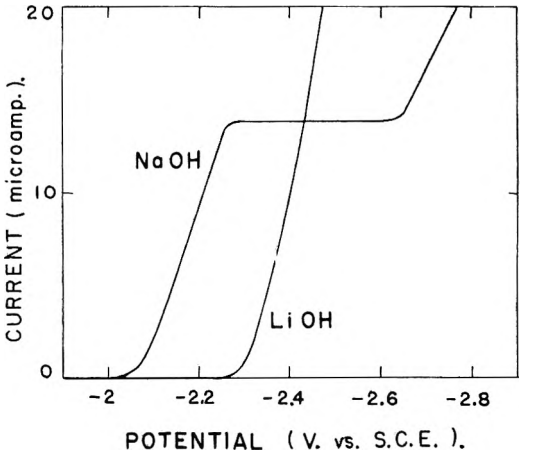

Fig. 3.—Polarograms of 2.5 mM LiOH and 2.5 mM NaOH without supporting electrolyte at 24°. Potentials are corrected for ohmic drop; cell resistance, 25,500 ohms for LiOH; 14,700 ohms for NaOH; drop time with magnetic hammer, 3.33 sec.; rate of flow of mercury, 0.68 (LiOH) and 0.95 (NaOH) mg. sec.$^{-1}$; current corrected for residual current.

TABLE III

DATA FOR THE CALCULATION OF $\Delta\varphi$

Metal	E, v. *vs* s.c.e.	q,[a] μcoulombs cm.$^{-2}$	r,[b] Å.	ϵ[c]	$\Delta\varphi$,[d] v.	$\Delta\varphi$,[e] v.
Li[h]	−2.11	30.1	2.50	71.5	−0.103	−0.275
Na	−1.90	28.5	2.17	73.0	− .100	− .193
K	−1.89	26.7	1.75	73.5	− .097	− .149
Rb	−1.91	27.9	1.75	73.5	− .099	− .152
Cs	−1.92	29.0	1.53	(73.5)[f]	(− .101)[g]	(− .158)[g]

[a] Charge on the electrode. [b] Radius of solvated ion according to Monk.[16] [c] Dielectric constant of 0.5 M MCl solution calculated according to ref. 17. [d] Gouy–Chapman theory. [e] Brodowski–Strehlow theory. [f] Taken as being the same as for RbCl. [g] Not corrected for specific adsorption of Cs^+. [h] See discussion of the possibility of hydrogen evolution.

gen evolution in KOH solution at the potential used in this work (Table I) is much smaller than the current density for metal deposition. Calculations were based on the data of Kaptsan and Iofa[7,18] for the Tafel line. (b) Polarograms for dilute solutions of MOH (Fig. 3) exhibit a well defined plateau except for LiOH, and it is concluded that reduction of H_2O at current densities of the order of those used for metal deposition in generation *in situ* requires appreciably more negative potentials than the potentials prevailing in faradaic rectification measurements.[19] Evidence for lithium is not conclusive, and the data in Tables I to III for this metal should be regarded as tentative. There was some evidence of H_2 evolution for Rb, and this is why the method used in the calculation of the concentration C_{Rb} at the electrode was devised (see Experimental). It should be noted that the k^0's for Li and Rb are not out of line with respect to the other metals.

Acknowledgment.—This investigation was supported by the National Science Foundation.

(18) O. L. Kaptsan and Z. A. Iofa, *Zh. Fiz. Khim.*, **26**, 193, 201 (1952).

(19) It must be noted that the solution composition was not the same in the polarographic and faradaic rectification measurements. Further, the OH^- concentration at the electrode increases with the current for H_2 evolution in the polarographic experiments.

A GENERALIZED RELATION BETWEEN REDUCED DENSITY AND TEMPERATURE FOR LIQUIDS WITH SPECIAL REFERENCE TO LIQUID METALS[1]

BY P. J. McGONIGAL[2]

Research Institute of Temple University, Philadelphia 44, Pennsylvania

Received March 29, 1962

A correlation exists among various liquids in regard to their reduced density *vs.* temperature behavior. The dimensionless quantity Δ is defined. When the reduced variable Δ_{red} is plotted against reduced temperature, a series of quite similar curves is obtained. The correlation is shown for fifteen liquid metals and seven other liquids. A method for estimating critical densities is described.

The density *vs.* temperature behavior of liquid metals has recently been the subject of extensive investigation at this Institute. A consideration of the results obtained from these investigations as well as those reported by other workers shows that there is a broad spread in the densities of different liquid metals as well as in the values of the temperature coefficient of density. To date there has been no general correlation among the density data for different metals.

In an attempt to produce such a correlation, use was made of the reduced properties of metals. It has been shown by Grosse[3] that reasonable estimates of the critical temperatures of metals can be made by application of the law of corresponding states to the entropies of vaporization. Critical densities may be estimated if reliable liquid density data are available by evaluation of the equation of the rectilinear diameter at the critical temperature. In many cases the density *vs.* temperature behavior of a metal between its melting point and normal boiling point can be represented by a straight line well within the limit of experimental error. The equation of the rectilinear diameter is then one-half of the density *vs.* temperature equation. In cases where the density *vs.* temperature behavior is best represented by a curve, the rectilinear diameter may be constructed by using one-half the sum of the liquid and vapor densities at various temperatures. Critical densities then may be obtained by evaluating the rectilinear diameter equation at the critical temperature.

If reliable estimates of the critical temperatures and critical densities are available, the density *vs.* temperature behavior of liquids may be compared on the basis of reduced variables. Such a comparison is most conveniently made by utilizing the reduced rectilinear diameters, since these are straight lines which all begin at the point $(D\,\delta)_{red} = 1$, $T_{red} = 1$, where $(D\,\delta)_{red}$ is the reduced rectilinear diameter and T_{red} is the reduced temperature. The variation in the slopes of these lines for different liquid metals is considerable. In a previous publication[4] the density of magnesium at the normal boiling point and the density at the critical point, as well as the slope of the density *vs.* temperature line between the melting point and the normal boiling point, were predicted with a fair degree of accuracy (relative to the values of these quantities as determined by experiment and extrapolation of experimental data) by using an average reduced rectilinear diameter based on data for six metals. The use of such a method is, of course, justifiable only in the absence of experimental data or, as in the case of magnesium, in cases where available experimental data disagree to a very large extent.

The concept of the reduced rectilinear diameter, as such, does not indicate the general relation be-

(1) (a) This work was supported by the National Science Foundation under grant 18829; (b) presented before the Division of Physical Chemistry, 142nd National Meeting of the American Chemical Society, Atlantic City, N. J., September, 1962.

(2) A report of this work will constitute a portion of a dissertation to be submitted by the author to the Graduate Council of Temple University in partial fulfillment of the requirements for the degree of Doctor of Philosophy.

(3) A. V. Grosse, *J. Inorg. Nucl. Chem.*, **22**, 23 (1961).

(4) P. J. McGonigal, A. D. Kirshenbaum, and A. V. Grosse, *J. Phys. Chem.*, **66**, 737 (1962).

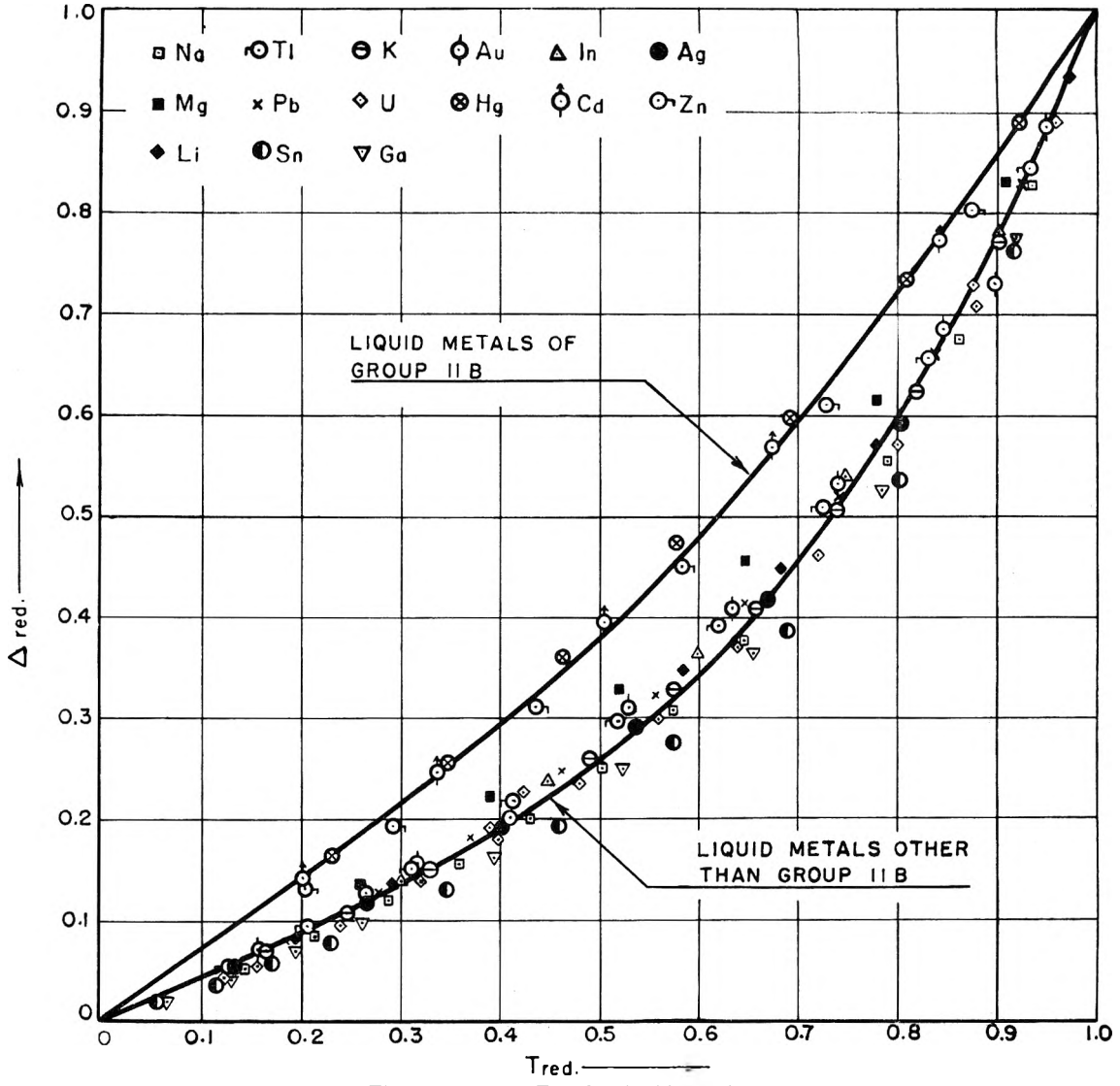

Fig. 1.—$\Delta_{red.}$ *vs.* $T_{red.}$ for liquid metals.

tween reduced density and temperature that exists for liquids. This relation was arrived at by use of the dimensionless variable $(dD\,\delta/dT)(T/D\,\delta)$ which is termed Δ (by analogy to the π of Codegone,[5] who proposed a dimensionless expression relating the temperature and pressure of saturated vapors). The use of the rectilinear diameter permits the eval-

TABLE I

SUMMARY OF PERTINENT DATA FOR LIQUID METALS

Metal	a, g./cm.^{3}	$-b \times 10^4$, g./cm.^{3}-°K.	T_c, °K.	D_c, g./cm.^{3}	$-\Delta c$	Ref.
Ag	5.232	4.534	7460	1.85	1.83	6
Na	0.510	1.234	2780	0.17	2.05	7
Tl	6.094	7.67	4830	2.39	1.55	8
K	0.454	1.194	2440	1.63	1.79	7
Au	9.44	6.00	9460	3.76	1.51	9
In	3.658	3.400	6680	1.39	1.63	10
Mg	0.917	1.324	3850	0.41	1.24	4
Pb	5.734	6.587	5400	2.18	1.63	11
U	9.678	5.164	12500	3.22	2.00	12
Hg	7.19	14.38	1733	4.70	0.53	13, 14
Cd	4.33	5.37	2970	2.75	0.58	7
Zn	3.78	4.61	3430	2.20	0.72	15
Li	0.273	0.4125	4110	0.10	1.64	7
Sn	3.642	3.00	8720	1.03	2.55	16
Ga	3.12	2.88	7620	0.93	2.36	17

(5) C. Codegone, *Allgem. Waermetech.*, **9**, 58 (1959).

(6) A. D. Kirshenbaum, J. A. Cahill, and A. V. Grosse, *J. Inorg. Nucl. Chem.*, **22**, 33 (1961).

(7) "Liquid Metals Handbook," 2nd Ed., R. N. Lyon, Editor-in-chief, sponsored by the Committee on the Basic Properties of Liquid Metals, Office of Naval Research, Department of the Navy, in Collaboration with the Atomic Energy Commission and the Bureau of Ships, Department of the Navy, Washington, D. C., June, 1952, NAVEXOS P-733 (Rev.).

(8) A. Schneider and G. Heymer, *Z. anorg. allgem. Chem.*, **286**, 111 (1958).

(9) W. Krause and F. Sauerwald, *ibid.*, **181**, 347 (1929).

(10) P. J. McGonigal, J. A. Cahill, and A. D. Kirshenbaum, *J. Inorg. Nucl. Chem.*, in press, 1962.

(11) A. D. Kirshenbaum, J. A. Cahill, and A. V. Grosse, *ibid.*, in press, 1962.

(12) A. V. Grosse, J. A. Cahill, and A. D. Kirshenbaum, *J. Am. Chem. Soc.*, **83**, 4665 (1961).

(13) J. Bender, *Physik. Z.*, **16**, 246 (1915).

(14) J. Bender, *ibid.*, **19**, 440 (1918).

(15) P. Pascal and A. Jouniaux, *Compt. rend.*, **158**, 414 (1914).

(16) A. L. Day, R. B. Sosman, and J. C. Hostetter, *Am. J. Sci.*, **37**, 1 (1914).

(17) W. H. Heather, *Proc. Phys. Soc.* (London), **48**, 699 (1936).

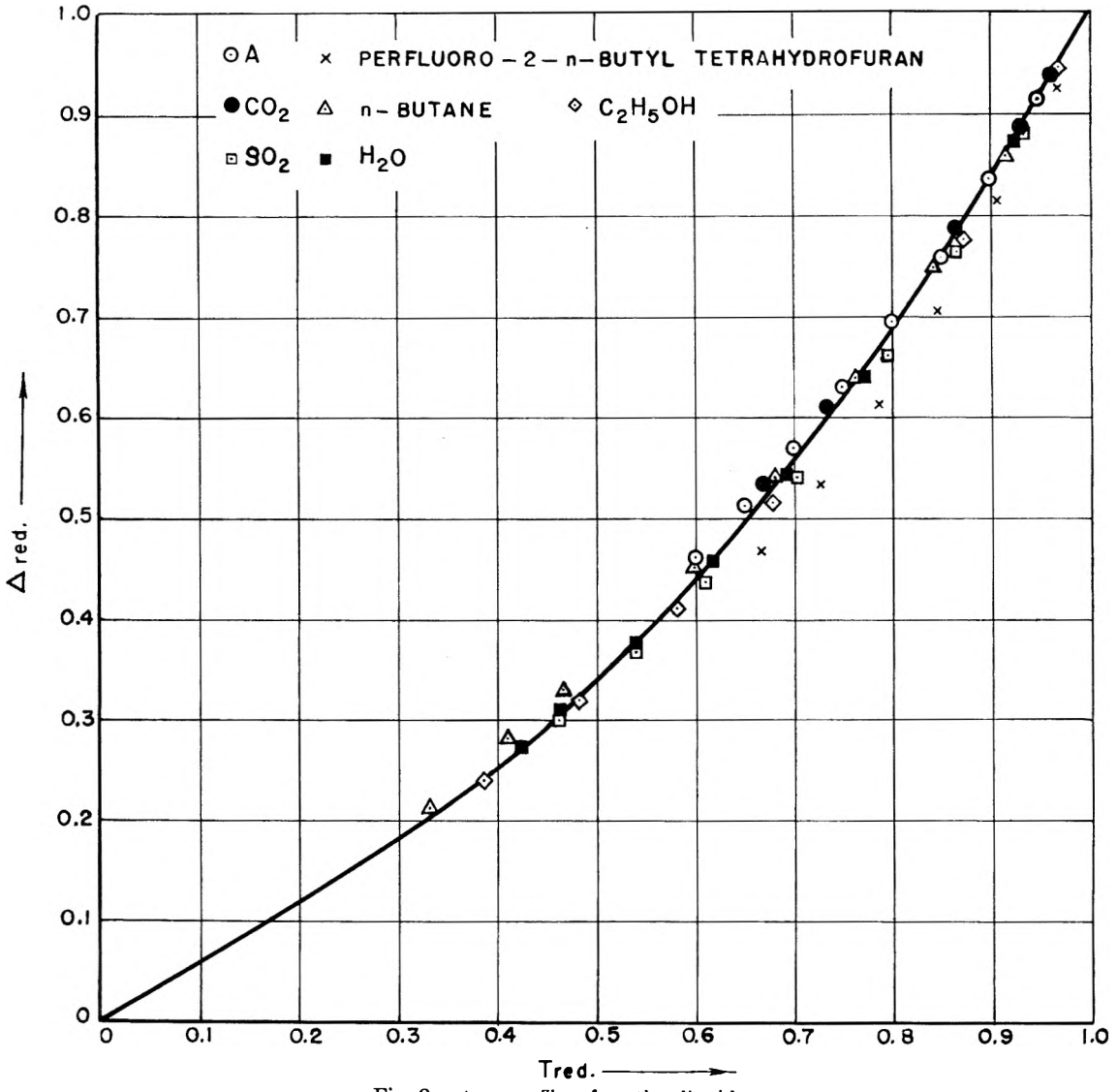

Fig. 2.—$\Delta_{red.}$ *vs.* $T'_{red.}$ for other liquids.

TABLE II

SUMMARY OF PERTINENT DATA FOR OTHER LIQUIDS

Liquid	a, g./cm.³	$-b \times 10^4$, g./cm.³-°K.	T_c, °K.	D_c, g./cm.³	$-\Delta c$	Ref.
SO_2	1.059	12.45	430.4	0.523	1.025	18
n-Butane	0.408	4.30	426	.225	0.814	18
CO_2	.815	11.40	304.3	.468	.740	18
H_2O	.632	4.75	647.4	.324	.949	18
C_2H_5OH	.546	5.23	516.2	.276	.978	18
Perfluoro-2-*n*-butyltetrahydrofuran	1.358	15.4	500.21	.588	1.309	19

uation of Δ at the critical point, whereas the actual density *vs.* temperature curve would have an infinite slope at the critical point. In order to compare the behavior of different liquids, the quantity Δ_{red} is plotted against T_{red}. Δ_{red} is simply $\Delta/\Delta c$ where Δc is the value of Δ at the critical point. Figure 1 shows Δ_{red} *vs.* T_{red} plots for liquid metals and Fig. 2 shows the plots for several other liquids. Table I is a collection of numerical values pertinent to this work for liquid metals and Table II gives similar information for several other liquids. The a and b refer to the constants in equations of the form

$$D\,\delta\,(\text{g./cm.}^3) = a - bT(^\circ\text{K.})$$

The literature references are for density data. Critical temperatures for the metals were estimated according to the method described by Grosse with the exception of that for mercury, which was experimentally determined.[20] Rectilinear diameter equations for the metals were calculated as necessary from the original data.

The data for argon are omitted from Table II since Δ and Δ_{red} were calculated from the reduced density equation of Guggenheim.[21] The references in Table II are for tables of thermodynamic func-

(18) "Handbook of Chemistry and Physics," 35th Ed., Chemical Rubber Publishing Co., Cleveland, O.

(19) R. M. Yarrington and W. B. Kay, *J. Chem. Eng. Data*, **5**, 24 (1960).

(20) F. Birch, *Phys. Rev.*, **41**, 641 (1932).

(21) E. A. Guggenheim, *J. Chem. Phys.*, **13**, 253 (1945).

tions or density data from which the rectilinear diameter equations were calculated.

The agreement shown in Fig. 1 among the liquid metals is considered good since, with the single exception of mercury, the critical temperatures are estimated and evaluation of the critical densities involves extrapolations which are large compared with the temperature range over which experimental measurements were made. Two curves are shown in Fig. 1 since the behavior of the group IIB metals, although internally consistent, appears to be rather different from that of the other metals. The agreement in Fig. 2 is better since the critical temperatures and critical densities for these liquids have been experimentally determined.

The correlation illustrated in Fig. 1 and 2 may be presumed valid for other metals and liquids in general, at least in the absence of experimental evidence to the contrary. The Δ_{red} *vs.* T_{red} curve may be used to estimate critical densities for those metals and other substances for which adequate experimental data are not available. Since the curve for the group IIB metals is so distinct, it is considered reasonable not to refer to it in making the estimates.

If the density of a liquid is known at only a single point between its melting point and normal boiling point, its critical density may be determined to a first approximation from the average value of Δ_{red} at T_{red} corresponding to the temperature at which the density is known. Knowledge of the two density values permits estimation of the slope of the rectilinear diameter and hence that of the density *vs.* temperature line between the melting point and the normal boiling point.

As an example of the application of the method described herein, the critical densities, densities at the normal boiling points, and slopes of the density *vs.* temperature lines have been calculated for rubidium and cesium, two metals for which reliable density data are available only at the melting points.[7] Results of experimental measurements on the densities of liquid rubidium and cesium will be reported in a subsequent publication from this Institute. The calculated values, which agree rather closely with those predicted by Grosse[22] on the basis of an average ratio of density at the normal boiling point to critical density for several metals,[3] are shown in Table III. The recent values of Weatherford[23] in Table III were taken from a density *vs.* temperature plot for the alkali metals, apparently constructed with the assumption that the slopes for rubidium and cesium would be quite similar to the slopes for sodium and potassium. The true situation is more complicated, however, since even in the case of elements in the same group of the periodic table, comparisons should be made only on the basis of reduced properties.

TABLE III

DENSITY DATA FOR RUBIDIUM AND CESIUM

Metal	M.p., °K.	$D_{M.P.}$, g./cm.³	B.p., °K.	$D_{B.P.}$, g./cm.³ This work	$D_{B.P.}$, g./cm.³ Weatherford	T_c, °K.	D_c, g./cm.³	$-dD/dT \times 10^4$, g./cm.³. °K.
Rb	312	1.475	974	1.16	1.33	2190	0.29	4.8
Cs	301	1.84	958	1.44	1.68	2150	0.36	6.0

Acknowledgment.—The author gratefully acknowledges the encouragement and guidance of Dr. A. V. Grosse.

(22) A. V. Grosse, "The Liquid Range of Metals and Some of Their Physical Properties at High Temperatures," Paper No. 2159, A.R.S., Space Flight Report to the Nation, New York, N. Y., Oct. 9–15, 1961.

(23) W. D. Weatherford, Jr., paper presented at the Symposium on High Temperature Properties and Applications of Liquid Metals, Fifty-fourth Annual Meeting, A.I.Ch.E., New York, N. Y., Dec. 2–7 1961.

KINETICS OF THE REVERSIBLE HYDRATION OF 2-HYDROXYPTERIDINE

BY Y. INOUE[1] AND D. D. PERRIN

Department of Medical Chemistry, Institute of Advanced Studies, Australian National University, Canberra, Australia

Received March 29, 1962

Rapid-reaction methods have been used to study the kinetics of reversible hydration of 2-hydroxypteridine across the $C_{(4)}$, $N_{(3)}$ double bond. The reaction is acid–base catalyzed and, over the pH range 4.55 to 12.4, times of half-completion at 20° range from 0.5 to 375 sec. A possible reaction mechanism is suggested.

Introduction

Although reversible hydration across C=O bonds, for example in aldehydes and some ketones, is well known, similar reactions involving C=N bonds have been much less investigated. Known examples where such hydration occurs include pteridine (cation and neutral molecule),[2] 2-hydroxy- and 6-hydroxypteridine (neutral molecule and anion),[3–5] 2-mercaptopteridine (neutral molecule and anion),[6] 1,4,6-triazanaphthalene (cation and neutral molecule),[5,7] and quinazoline (1,3-diazanaphthalene) (cation and neutral molecule),[8,9] as well as some of their methyl and other derivatives. In each case, the first of the forms given in parentheses exists mainly as the hydrate while the second form is mainly anhydrous.

Covalent hydration and dehydration of 6-hydroxypteridine (across positions 7 and 8) proceeds

(1) Australian National University Scholar.
(2) D. D. Perrin, *J. Chem. Soc.*, 645 (1962).
(3) A. Albert, *ibid.*, 2690 (1955).
(4) D. J. Brown and S. F. Mason, *ibid.*, 3443 (1956).
(5) D. D. Perrin and Y. Inoue, *Proc. Chem. Soc.*, 342 (1960).
(6) Y. Inoue and D. D. Perrin, *J. Chem. Soc.*, 2600 (1962).
(7) A. Albert and C. Pedersen, *ibid.*, 4683 (1956).
(8) A. R. Osborn, K. Schofield, and L. N. Short, *ibid.*, 4191 (1956).
(9) A. Albert, W. L. F. Armarego, and E. Spinner, *ibid.*, 5267 (1961).

sufficiently slowly in neutral or weakly alkaline solutions that a hysteresis loop can be demonstrated by rapid potentiometric titration with alkali followed, after some minutes, by rapid back-titration with acid.[10] 2-Hydroxypteridine behaves similarly,[5] adding water across positions 3 and 4.[4] Until now, the kinetics of such hydration reactions have not been studied except for qualitative observations that dehydration of the hydrated form of 6-hydroxypteridine is catalyzed by hydroxyl ion,[5] and hydration–dehydration of pteridine shows acid–base catalysis.[2,11] The present paper describes the results of potentiometric and spectrophotometric studies at 20° of the reversible hydration of 2-hydroxypteridine (which exists in solution predominantly as the amide (lactam) tautomer (I) rather than the enol (lactim) form[4]) to give 3,4-dihydro-2,4-dihydroxypteridine (II).

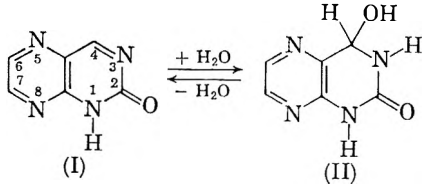

(I) (II)

Experimental

Materials.—2-Hydroxypteridine[12] was generously provided by Professor A. Albert. All other reagents were of C.P. grade. Buffer solutions in the pH range 3.4–6.2 were prepared by mixing 0.05 *M* sodium borate and 0.05 *M* succinic acid solutions. Similarly, in the ranges pH 6.3–9.2 and 9.4–10.6, 0.05 *M* sodium borate was added to 0.1 *M* potassium dihydrogen phosphate and 0.1 *M* sodium carbonate, respectively. Above pH 10.6, 0.1 *M* sodium hydroxide was added to 0.1 *M* disodium hydrogen phosphate.

Methods.—Potentiometric titrations were carried out under nitrogen in a magnetically-stirred, thermostated reaction vessel using a Vibron model 33B Electrometer pH meter (Electronic Industries Ltd.) fitted with a saturated calomel electrode and an internally shielded glass electrode. The output of the pH meter was applied directly to a Rectiriter recording milliammeter (Texas Instrument Co.). Standard 0.100 *M* acid or alkali (carbonate-free) was added by micrometer syringe.

Ultraviolet spectra were recorded continuously on either a Perkin–Elmer Spectracord or a Shimadzu model RS 27 recording spectrophotometer, the optical density scales of which were calibrated against standard potassium chromate solutions. Into the cell compartment of each instrument was fitted a 1-cm. silica cell attached to a modified Chance[13] rapid reaction apparatus which consisted essentially of two 10-ml. nylon syringes connected to a perspex tap, in the barrel of which a mixing chamber had been constructed. The syringes and cell were water-jacketed in metal blocks to maintain solutions at 20 ± 0.05°. Each of the syringes could be filled independently of the other. One of them contained an approximately 9×10^{-5} *M* 2-hydroxypteridine solution in either 0.004 *M* hydrochloric acid or 0.008 *M* potassium hydroxide (depending on whether the initial species was to be mainly hydrated or anhydrous); the other syringe held a buffer solution to which the corresponding amount of alkali or acid, respectively, had been added. The barrels of the two syringes were depressed simultaneously by a metal plunger, so that the reactant solutions were mixed in the mixing chamber and placed in the cell. Using a "stopped flow" technique, optical density readings at a selected wave length could be recorded continuously from about 1 sec. after mixing. The region near 370 mμ was convenient because both anhydrous 2-hydroxypteridine and its anion absorbed strongly, whereas its hydrated species had negligible absorption. The pH's of the final solutions were checked against the standards, freshly-prepared 0.05 *M* potassium hydrogen phthalate (pH 4.00 at 20°) and 0.05 *M* sodium borate (pH 9.23 at 20°). Extinction coefficients and maxima of stable or only slowly changing species were checked on a Hilger Uvispeck spectrophotometer. Replicate kinetic experiments gave first-order rate constants agreeing within ±5%.

Calculation of Reaction Velocities.—The equilibria in 2-hydroxypteridine solutions can be summarized by the scheme

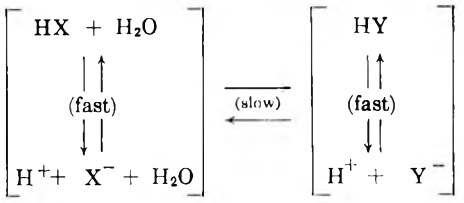

where HX is (anhydrous) 2-hydroxypteridine and HY is the hydrated form. (Lactam–lactim tautomerism, involving only a proton transfer between a nitrogen and an oxygen atom, is probably too fast to be detected by the methods used in this work.) At any given pH the ratios $[HX]/[X^-]$ and $[HY]/[Y^-]$ are constant and equal to $(a_{H^+})/K_a^X$, $(a_{H^+})/K_a^Y$, respectively, where K_a^X and K_a^Y are "practical" acid dissociation constants. Also, X^- and HX are in dynamic equilibrium, and so are Y^- and HY. Under these conditions, the system can be treated as if it were

$$A + H_2O \underset{k_d}{\overset{k_h}{\rightleftarrows}} B$$

where $[A] = [X^-] + [HX]$, and $[B] = [Y^-] + [HY]$. Assuming that the forward- and back-reactions obey first-order rate equations, the composite constants, k_h and k_d, in the equation

$$-d[A]/dt = k_h[A] - k_d[B] = d[B]/dt \quad (1)$$

can be evaluated as described below.

Because $[A] + [B] = [A]_{eqm} + [B]_{eqm}$, eq. 1 can be written as

$$-d[A]/dt = (k_h + k_d)[A] - k_d([A]_{eqm} + [B]_{eqm})$$

$$-d[B]/dt = (k_h + k_d)[B] - k_h([B]_{eqm} + [A]_{eqm})$$

But, at constant wave length and constant pH, the optical density, *D*, of the system is given by $D = \alpha[A] + \beta[B]$, where α and β are constants. Making use of the values of $d[A]/dt$ and $d[B]/dt$ given above, it may readily be deduced that

$$-dD/dt = k_{obs}(D - D_{eqm})$$

where $k_{obs} = k_h + k_d$. Also, because $k_d/k_h = [A]_{eqm}/[B]_{eqm}$, it can further be deduced that

$$k_h = k_{obs}\left(\frac{K_2(a_{H^+}) + K_1K_a^X}{(K_2 + 1)(a_{H^+}) + (K_1 + 1)K_a^X}\right) \quad (2)$$

$$k_d = k_{obs}\left(\frac{(a_{H^+}) + K_a^X}{(K_2 + 1)(a_{H^+}) + (K_1 + 1)K_a^X}\right) \quad (3)$$

where the constants $K_1 = [Y^-]_{eqm}/[X^-]_{eqm}$, $K_2 = [HY]_{eqm}/[HX]_{eqm}$, and $K_a^X = (a_{H^+})[X^-]/[HX]$. As discussed elsewhere,[5,6] these constants can be evaluated from rapid- and

(10) A. Albert, D. J. Brown, and G. Cheeseman, *J. Chem. Soc.*, 1620 (1952).

(11) J. Komenda and D. Laskafeld, *Collection Czech. Chem. Commun.*, **27**, 199 (1962).

(12) A. Albert, D. J. Brown, and G. Cheeseman, *J. Chem. Soc.*, 474 (1951).

(13) B. Chance, "Rates and Mechanisms of Reactions," "Technique of Organic Chemistry," Vol. VIII, Ed. S. L. Friess and A. Weissberger, Interscience Publishers, Inc., New York, N. Y., 1953, p. 690.

equilibrium-titration data (or, alternatively, they can be obtained from analysis of rapid-flow and equilibrium absorption spectra).

Confirmation that the hydration–dehydration reaction of 2-hydroxypteridine obeys a first-order rate equation over at least the first nine-tenths of the reaction is provided by typical results shown in Fig. 1, where the plots of log $((D - D_{eqm})/D_{eqm})$ *vs.* time are good straight lines.

Results

Table I shows the pH-dependence of rates for the reversible hydration of 2-hydroxypteridine at 20°. The primary salt effect on k_{obs} was small and no attempt was made to extrapolate values to zero ionic strength. Thus, over the pH range 7.9 to 11.8, increasing the ionic strengths listed in Table I (0.054 to 0.087) to 0.100 by addition of sodium chloride gave no perceptible change in k_{obs}. Between pH 6.4 and 7.6 log k_{obs} increased by about 0.05. Differences became greater at lower pH values. The rate constants for hydration and dehydration, k_h and k_d, were obtained from k_{obs} by using eq. 2 and 3, respectively, and values of $K_1 = 0.14$, $K_2 = 320$, $K_a^X = 2.0 \times 10^{-8}$, and $K_a^Y = 9.0 \times 10^{-12}$.[6]

TABLE I

VELOCITY CONSTANTS FOR HYDRATION AND DEHYDRATION OF 2-HYDROXYPTERIDINE IN BUFFER SOLUTIONS AT 20°

pH	Ionic strength	k_{obs}[a]	k_h[b]	k_d[b]
4.55	0.017	1.43	1.43	0.00447
4.79	.019	1.01	1.01	.00316
4.93	.021	0.700	0.696	.00218
5.16	.024	.483	.481	.00150
5.39	.028	.293	.292	.000913
5.60	.030	.189	.188	.000590
5.89	.032	.108	.108	.000343
6.18	.038	.0532	.0530	.000171
6.43	.053	.0420	.0418	.000138
6.62	.059	.0326	.0324	.000110
6.82	.062	.0248	.0246	.0000870
7.02	.063	.0179	.0177	.0000669
7.23	.067	.0124	.0123	.0000513
7.48	.070	.00864	.00861	.0000432
7.63	.071	.00682	.00676	.0000391
7.89	.075	.00568	.00562	.0000448
8.31	.076	.00342	.00341	.0000541
8.46	.075	.00278	.00271	.0000572
8.56	.074	.00265	.00257	.0000661
8.70	.071	.00228	.00219	.0000751
8.84	.070	.00235	.00225	.000104
8.98	.066	.00221	.00208	.000130
9.16	.060	.00216	.00198	.000183
9.29	.054	.00185	.00165	.000203
9.76	.056	.00376	.00280	.000967
10.32	.059	.00305	.00145	.00161
10.59	.063	.00241	.000857	.00156
10.84	.077	.00267	.000722	.00195
11.28	.080	.00354	.000647	.00289
11.44	.082	.00439	.000725	.00366
11.76	.087	.00814	.00117	.00697
12.01	.093	.0122	.00164	.0105
12.38	.044	.0293	.00375	.0256

[a] k_{obs} = first-order velocity constant, in sec.$^{-1}$, from rate of change of spectrum. [b] k_h, k_d = composite rate constants for hydration and dehydration reactions, respectively, in sec.$^{-1}$.

From results in Table II, the reaction is catalyzed by borax buffer: at constant ionic strength and (approximately) constant pH, k_{obs} increases with the concentration of borax buffer. As discussed below, specific catalysis by boric acid is involved.

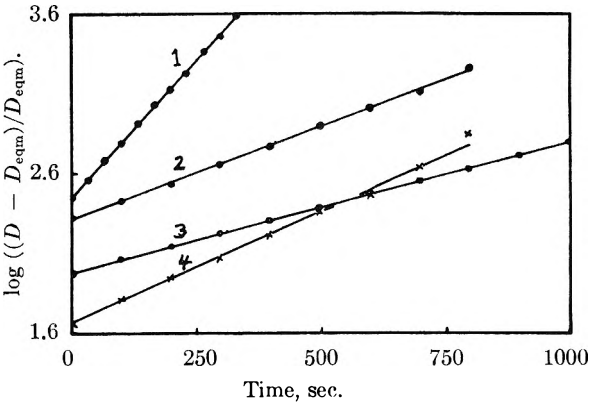

Fig. 1.—Representative plots of log $((D - D_{eqm})/D_{eqm})$ *vs.* time for hydration of 2-hydroxypteridine at 20° in buffers: 1, pH 7.58; 2, pH 8.43; 3, pH 9.25; 4, pH 10.19. Wave length, 370 mμ.

TABLE II

VARIATION OF VELOCITY CONSTANT WITH CONCENTRATION OF BORAX BUFFER[a]

B[b]	0.01	0.02	0.03	0.04	0.06	0.07	0.09
pH	9.16	9.20	9.21	9.23	9.27	9.29	9.34
$10^3 k_{obs}$, sec.$^{-1}$	2.0	3.5	4.0	4.6	5.2	5.6	6.3

[a] Ionic strength constant at 0.200 by addition of NaCl. [b] Total concentration of boric acid and borax, expressed as $Na_2B_4O_7$, in moles/l.

Discussion

The pH-dependence of k_h and k_d suggests that they are composite constants for the following simultaneous reactions which represent catalysis of hydration of HX and X^- and dehydration of HY and Y^- by solvent and by hydronium and hydroxyl ions.

$$HX + H_2O + H_3O^+ \underset{k_{-1}}{\overset{k_1}{\rightleftharpoons}} HY + H_3O^+$$

$$\left.\begin{array}{l} HX + H_2O + H_2O \xrightarrow{k_2} \\ X^- + H_2O + H_3O^+ \xrightarrow{k_3} \end{array}\right] \rightleftharpoons \left[\begin{array}{l} \xleftarrow{k_{-2}} HY + H_2O \\ \xleftarrow{k_{-3}} Y^- + H_3O^+ \end{array}\right]$$

$$\left.\begin{array}{l} HX + H_2O + OH^- \xrightarrow{k_4} \\ X^- + H_2O + H_2O \xrightarrow{k_5} \end{array}\right] \rightleftharpoons \left[\begin{array}{l} \xleftarrow{k_{-4}} HY + OH^- \\ \xleftarrow{k_{-5}} Y^- + H_2O \end{array}\right]$$

$$X^- + H_2O + OH^- \underset{k_{-6}}{\overset{k_6}{\rightleftharpoons}} Y^- + OH^-$$

The rate constants for reactions 2 and 3, and 4 and 5, cannot be evaluated separately because of the dynamic equilibrium between neutral species and their anions. Further reactions can be written to take account of catalysis by other species such as buffer ions. Thus, at very low reaction rates, ca-

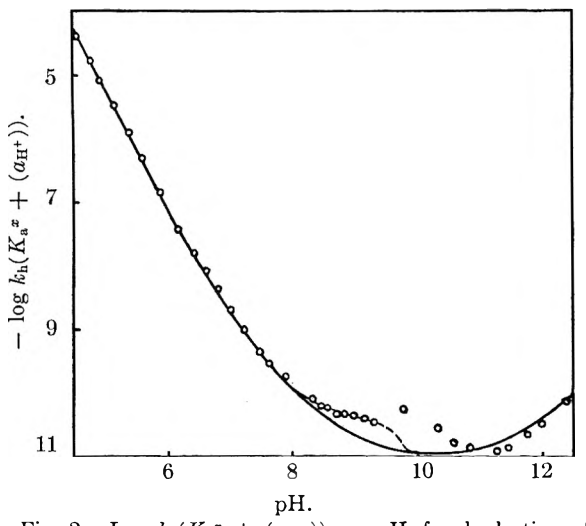

Fig. 2.—Log $k_h(K_a^x + (a_{H^+}))$ *vs.* pH for hydration of 2-hydroxypteridine: solid curve, eq. 5; dashed line, eq. 5 + $4.3 \times 10^{-10}[H_3BO_3]$.

talysis by boric acid and bicarbonate ion is significant.

Rearranging the equation for k_h, and substituting

$$[X^-] = K_a^X([X^-] + [HX])/(K_a^X + (a_{H^+}))$$

$$[HX] = (a_{H^+})([X^-] + [HX])/(K_a^X + (a_{H^+}))$$

gives

$$k_h(K_a^X + (a_{H^+})) = k_1(a_{H^+})^2 + (k_2 + k_3K_a^X)(a_{H^+}) + (k_4K_w + k_5K_a^X)[H_2O] + k_6K_a^XK_w/(a_{H^+}) \quad (4)$$

Values of log $k_h(K_a^X + (a_{H^+}))$ from the results in Table I are plotted against pH in Fig. 2. Over the pH ranges 4.5 to 8.5, 10.6 to 12.4, $k_h(K_a^X + (a_{H^+}))$, which varies by a factor of 3×10^6, can be well represented by the equation

$$k_h(K_a^X + (a_{H^+})) = 6.3 \times 10^4(a_{H^+})^2 + 1.1 \times 10^{-2}(a_{H^+}) + 1.0 \times 10^{-11} + 3.0 \times 10^{-23}/(a_{H^+}) \quad (5)$$

The deviations between pH 8.5 and 10.6 can be explained quantitatively if the additional terms, $4.3 \times 10^{-10}[H_3BO_3] + 2.8 \times 10^{-9}[HCO_3^-]$, are included in eq. 5. That specific catalysis by boric acid, and not borate ion, is involved in the reaction is supported by the absence of any correlation between the extent of the deviation and the borate concentration of the buffer solutions used. Similarly, for solutions where bicarbonate ion is present (pH 9.8 to 10.6 in Fig. 2), deviations correlate with bicarbonate, but not with carbonate, concentration. Below about pH 8.5 the effect of boric acid is swamped by hydrogen ion catalysis, and above pH 10 boric acid is largely ionized to borate (pK_a = 9.2). The highest point for the borax buffers in Table II gives $k_h(K_a^X + (a_{H^+})) = 1.15 \times 10^{-10}$, in fair agreement with the value calculated from eq. 5 only if the term for boric acid is included (7.8×10^{-11} as against 1.6×10^{-11}).

By equating coefficients in eq. 4 and 5, and taking $[H_2O] = 55.5\ M$, we obtain (in sec.$^{-1}$), $k_1 = 6.3 \times 10^4$, $k_6 = 0.22$, $k_2 + 2 \times 10^{-8}k_3 = 1.1 \times 10^{-2}$, $k_4 + 3 \times 10^6k_5 = 27$. Hence, at 20°, the rate constants for the hydration of 2-hydroxypteridine and its anion are given by

$$k_h = 6.3 \times 10^4(a_{H^+}) + \leq 2 \times 10^{-4}[H_2O] + \leq 1.5 \times 10^3(a_{OH^-}) \quad \text{(for HX)}$$

$$= \leq 5.5 \times 10^5(a_{H^+}) + \leq 9 \times 10^{-6}[H_2O] + 0.22(a_{OH^-}) \quad \text{(for } X^-\text{)}$$

The corresponding constants for the dehydration reaction are obtained by dividing by 320 and multiplying by 7.1, respectively.

Because the pyrimidine portion of the nucleus appears in 2-hydroxypteridine, as in pteridine itself,[2] to have little aromatic character, considerable charge localization is likely in the bond joining $N_{(3)}$, and $C_{(4)}$.[2] It is known that $C_{(4)}$ has a sufficiently large net positive charge to facilitate attack by nucleophilic reagents (so that 2-hydroxypteridine readily undergoes Michael addition reactions[14]) whereas $N_{(3)}$ can add electrophilic reagents. A comparable situation exists for the carbon and oxygen atoms of the carbonyl group in acetaldehyde and, as a tentative hypothesis, we suggest that the acid–base catalyzed hydration of 2-hydroxypteridine proceeds by a mechanism similar to that for acet-

Acid-catalyzed reaction

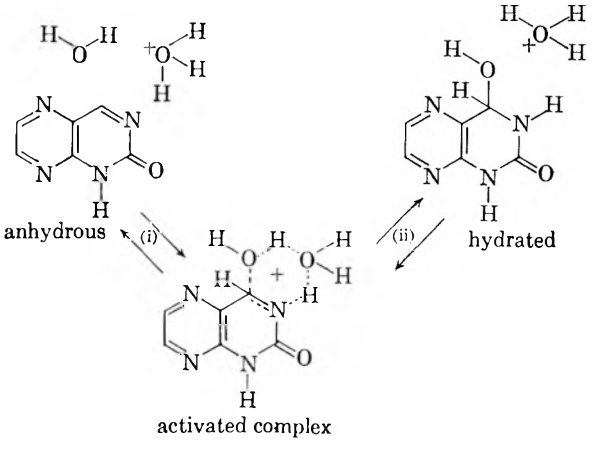

Base-catalyzed reaction

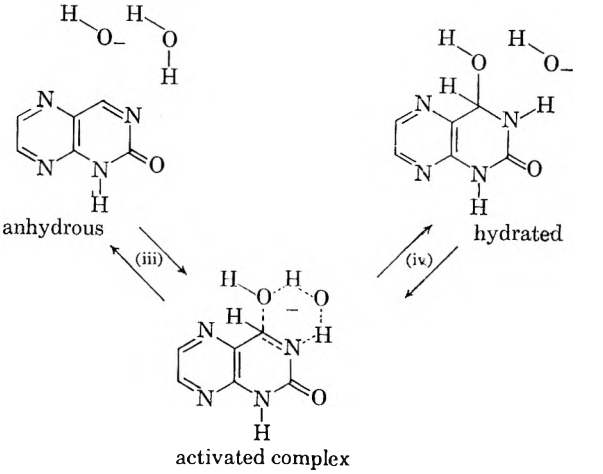

(14) A. Albert and C. F. Howell, *J. Chem. Soc.*, 1591 (1962).

aldehyde,[15] and also that the structures of the activated complexes from 2-hydroxypteridine are analogous to those postulated[16] for the acid–base catalyzed hydrolysis of esters and amides. Thus, the reactions for the neutral molecule with hydronium and hydroxyl ions would be as set out below. The steps (ii) and (iv) involve simple proton transfers to and from oxygen atoms and would be very fast, so that the steps (i) and (iii), which require more extensive structural rearrangements, would become rate-determining. The reversible acid–base catalyzed hydration of pteridine[2,11] and 2-hydroxypteridine across their 3:4 double bonds would be expected to involve similar mechanisms and analogous activated complexes. This accords with the view that the oxygen atom of 2-hydroxypteridine is not directly involved in the formation of the activated complex.

(15) R. P. Bell and W. C. E. Higginson, *Proc. Roy. Soc.* (London), **A197**, 141 (1949).

(16) K. J. Laidler and P. A. Landskroener, *Trans. Faraday Soc.*, **52**, 200 (1956).

TEMPERATURE DEPENDENCE OF THE KNIGHT SHIFT OF THE SODIUM–AMMONIA SYSTEM

By J. V. Acrivos

Lawrence Radiation Laboratory, Berkeley 4, California

and K. S. Pitzer

Department of Chemistry, Rice University, Houston 1, Texas

Received March 29, 1962

The Knight shift of Na^{23} and N^{14} in sodium–ammonia solution was measured over the temperature interval -33 to $+22°$ and in the concentration range corresponding to mole ratio 5.7 to 700 (NH_3/Na). The results in the dilute region, $R \geq 300$, were interpreted in terms of the equilibrium constants K_1 and K_2 for the reactions Na(am) = Na^+(am) + e^-(am) and Na(am) = $^1/_2Na_2$(am). The effective Knight shifts, k_0 for Na^{23} in Na(am) and k_1' for N^{14} in e^-(am) were found to be $k_0 = (0.034 \pm 0.005)T^{-1}$ and $k_1' = (13.5 \pm 1)T^{-1}$. The measured standard enthalpy and entropy of reaction for the dissociation and the dimerization equilibria are, respectively, ΔH_1^0 (298°) $\cong -6.6$ and $\Delta H_2^0 = -7.3 \pm 1$ kcal./mole and ΔS_1^0 (298°) $\cong -34$ and $\Delta S_2^0 = -24.1 \pm 3$ cal./deg. mole. The change in enthalpy for the dissociation equilibrium was temperature dependent and indicated that a large negative change in heat capacity accompanied the reaction. The electron densities at the Na^{23} nucleus were $\rho_1(Na^{23}) = 0.071\ a_0^{-3}$ and $0.00098\ a_0^{-3}$ for the concentrated ($R \cong 5.7$) and dilute solutions ($R \geq 300$), respectively.

The study of the electromagnetic properties of the alkali and alkaline earth metals in liquid ammonia has supplied a great deal of information about the chemical nature of these solutions. As a result of conductivity measurements, Kraus[1] has proposed that there exist, present in solution, solvated atoms, positive ions, and electrons. The presence of paramagnetic species was indeed verified by Huster[2] and Freed and Sugarman[3] from the static magnetic susceptibility, χ, and by Hutchison and Pastor[4] from the paramagnetic absorption by means of e.s.r. The main conclusions to be drawn from these measurements are: (a) the magnetic susceptibility of the metal in ammonia solution always lies below the expected Curie value, which is approached asymptotically only as the dilution increases to infinity, and (b) the $1/T$ temperature dependence of χ is not obeyed. Becker, Lindquist, and Alder[5] explained these results by assuming the existence of four different species, solvated metal dimers, atoms, and positive ions and electrons in the dilute solutions, and then proceeded to evaluate the chemical equilibrium constants for the dissociation and dimerization of the solvated metal atoms or monomers from the e.s.r. data.[4] These reactions may be written

$$\text{Na(am)} = \text{Na}^+\text{(am)} + \text{e}^-\text{(am)} \quad (1)$$

$$\text{Na(am)} = {}^1/_2\text{Na}_2\text{(am)} \quad (2)$$

with the combined reaction

$${}^1/_2\text{Na}_2\text{(am)} = \text{Na}^+\text{(am)} + \text{e}^-\text{(am)} \quad (3)$$

where the respective equilibrium constants are K_1, K_2, and K_3. The Knight shift (KS) data of McConnell and Holm[6] for the Na^{23}–$N^{14}H_3$ solutions at room temperature in the concentration range R = 5–500 supported these views. Pitzer[7] and Blumberg and Das[8] were able to explain some of the features of the KS data[6] by calculating the distribution of electron densities in the solvated paramagnetic species. Moreover, both Dye, Smith, and Sankuer[9] and Evers and Frank[10] derived sets of equilibrium constants from conductance measurements of Kraus[1] at $t = -33°$ together with transference number data. Their respective results are in fair agreement.

(1) C. A. Kraus, *J. Am. Chem. Soc.*, **43**, 749 (1921); for review work also see *J. Chem. Educ.*, **30**, 83 (1953).

(2) E. Huster, *Ann. Physik*, **33**, 477 (1938).

(3) S. Freed and N. Sugarman, *J. Chem. Phys.*, **11**, 354 (1943).

(4) C. A. Hutchison, Jr., and R. C. Pastor, *ibid.*, **21**, 1959 (1953).

(5) E. Becker, R. H. Lindquist, and B. J. Alder, *ibid.*, **25**, 971 (1956).

(6) H. M. McConnell and C. H. Holm, *ibid.*, **26**, 1517 (1957).

(7) K. S. Pitzer, *ibid.*, **29**, 453 (1958).

(8) W. D. Blumberg and T. P. Das, *ibid.*, **30**, 251 (1959).

(9) J. L. Dye, R. F. Sankuer, and G. E. Smith, *J. Am. Chem. Soc.*, **82**, 4797, 4803 (1960).

(10) E. C. Evers and P. W. Frank, *J. Chem. Phys.*, **30**, 61 (1959).

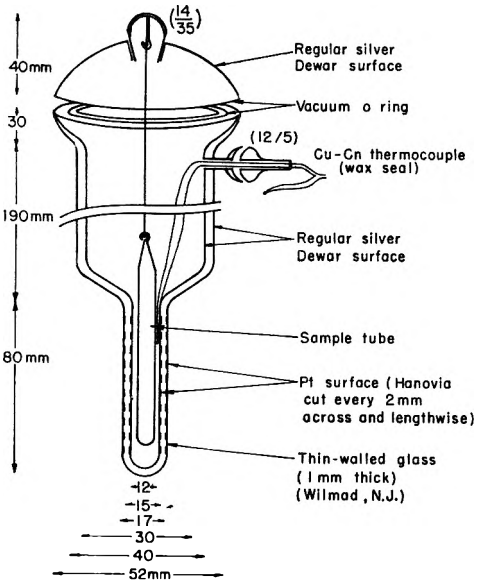

Fig. 1.—Rf. permeable dewar flask.

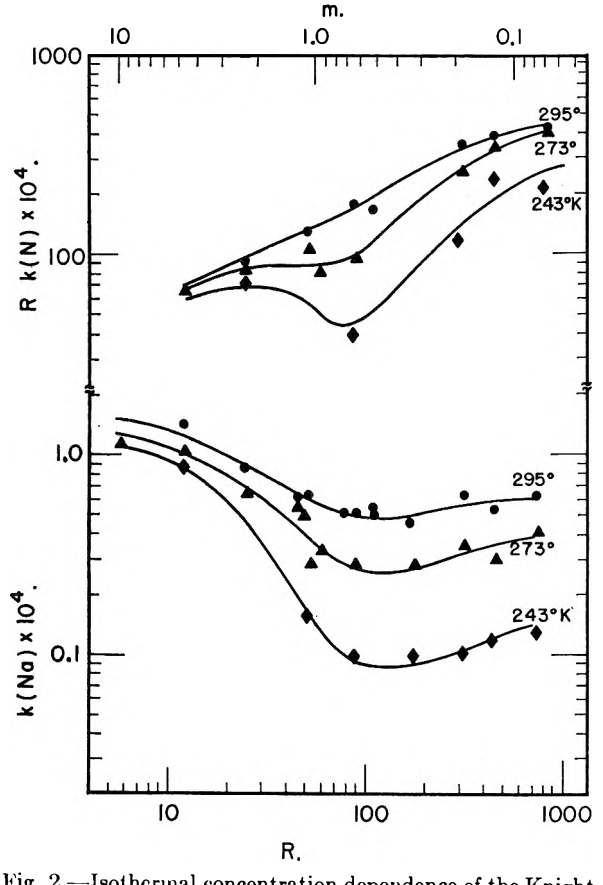

Fig. 2.—Isothermal concentration dependence of the Knight shift in the Na–NH_3 solutions.

The vapor pressure studies of Dewald[11] and the calorimetric results of Gunn and Green[12] also support the proposed equilibria of Becker, *et al.*[5] However, the equilibrium constants K_1 and K_2 as obtained from e.s.r.[5] are larger, by a factor of three, than those computed from the conductance experiments.[9,10] However, K_3 has substantially the same value from either source. In this work, the KS of Na^{23} and N^{14} in the Na–NH_3 solutions has been determined in the temperature interval −40 to 22°. In the concentration range where the chemical equilibria given in eq. 1 and 2 are valid, the constants K_1 and K_2 are evaluated from the KS data together with the activity coefficient of the charged species obtained from the Debye–Hückel theory. Although the relative accuracy of the measurements is very low at −33°, fair agreement is obtained with the values obtained from the conductance measurements.[1,9,10]

Experimental Results

The KS's of the Na–NH_3 solutions with respect to a standard of 0.5 *m* NaCl in NH_3 were measured with a Varian V-4200 wide line n.m.r. spectrometer operating at 10.0 and 2.77 Mc./sec. for Na^{23} and N^{14} resonance, respectively, in a constant magnetic field of 8881 oersteds.

The stabilities of the magnetic field and radiofrequency were the determining factors in the experimental accuracy. The radiofrequency was determined with a Hewlett–Packard counter No. 524B to ±2 c.p.s. while the field, stable to ±5 p.p.m., was swept with a linear potentiometer. The spectra were recorded by means of the sideband technique[13] with a modulation frequency ν_M = 412 c.p.s. The separation between the sidebands of 824 c.p.s. was then used to calibrate the potentiometer reading.

The temperature of the samples was measured to ±0.5°, by means of a copper–constantan thermocouple in contact with the sample tube. The sample tubes were immersed in a freezing mixture and contained in a dewar flask which allowed the rf. to penetrate. The constant temperatures were obtained as follows: 0° with an ice–water mixture, −15.3° with a solid–liquid mixture of benzyl alcohol, −30.6° with a solid–liquid mixture of bromobenzene, and below −33° with acetone–Dry Ice mixtures. The samples then were allowed to attain the equilibrium temperature inside the closed dewar. The dewar flask is shown in Fig. 1. The tip which contained the samples was not silvered but was covered with a thin layer of Pt (Hanovia) in which a cross and lengthwise grill was cut at 2 mm. intervals in such a manner that the inner and outer surfaces would be concentric so as to allow perfect rf. penetration.

The Na–NH_3 samples were prepared *in vacuo* by first distilling a known weight of Na into the side arm of a sample tube and then distilling the required volume of NH_3 from a Na–NH_3 solution. The sample tubes were first aged in dilute HCl, then passed through hot cleaning solution, and finally steamed and dried in the absence of dust. No decomposition was noticed when warming the samples to room temperature for long periods, as shown by the reproducibility of the n.m.r. measurements within the expected accuracy. The samples were stored in liquid nitrogen when not in use. The concentration of the Na–NH_3 solution is reported in terms of the mole ratio, *R*, or the sodium molality, *m*.

$$R = \frac{[NH_3]}{[Na]} = \frac{58.7}{m} = 1.35\,\frac{V_{NH_3} \times \rho_{NH_3}}{w_{Na}}$$

where *V* is the volume of ammonia determined before the solution was made, ρ its density at that temperature (see, for instance, Yost and Russell[14]), and *w* is the weight of sodium. For the more dilute samples, a chemical analysis for total sodium was carried out after the measurements were finished. For *R* = 730, the nuclear resonance signal to noise ratio at room temperature for Na^{23} was barely unity but rose to 10 at −33°. The KS data are given in Table I. Figure 2 shows the isothermal concentration dependence of the KS, according to the data given in Table I. The

(11) J. F. Dewald, Ph.D. Thesis, California Institute of Technology, 1948.

(12) R. S. Gunn and L. R. Green, *J. Chem. Phys.*, **36**, 363, 368 (1962).

(13) J. V. Acrivos, *ibid.*, **36**, 1097 (1962).

(14) D. M. Yost and H. Russell, Jr., "Systematic Inorganic Chemistry," Prentice-Hall, New York, N. Y., 1948, p. 138.

TABLE I

KNIGHT SHIFT OF Na^{23} AND N^{14} IN $Na–NH_3$ SOLUTIONS WITH RESPECT TO 0.5 MOLAL NaCl IN NH_3[a]

Sample no.	R	m	t (°C.)	k(Na) × 10^4 ±0.10	k(N) × 10^4 ±0.10	Rk(N) × 10^4
1	5.7	10	9.5	1.40	[a]	[a]
			0	1.25		
20	12.2	4.8	22	1.45	..	..
			0	1.06	5.58	68.07
			−27	1.00	..	..
			−46	0.94	..	..
18	25	2.4	22	.87	3.62	91
			0	.68	3.46	87
			−27	.63	2.78	70
			−30	.35[b] / .78	..	..
			−31	..	2.82	71
			−60		0.26[d]	7[d]
10	46	1.3	22.5	.61	[a]	[a]
			0	.56		
15	49	1.2	0	.51	[a]	[a]
25	52	1.1	26.3	.68	..	..
			22	..	2.55	133
			14	.48	..	..
			5	..	2.23	116
			0	.29	2.05	107
			−15	.16	1.61	84
			−31.2	.06	..	..
			−47	..	0.28	15
9	60	0.98	0	.34	1.54	80
			−19.5	..	1.40	84
			−24	.27	..	..
			−65	..	.40	24
			0	..	1.20[c] / 1.73	72 / 104
12	78	.75	22	.52	[a]	[a]
			− 7	.31	..	..
26	90	.66	25.1	.55	..	..
			23	..	1.87	168
			15.5	.50	..	..
			4	..	1.14	103
			0	.27	1.06	95
			−12	..	0.82	74
			−22	.13	.47	42
			−39	.07	..	..
			−56	.03	.20	18
11	110	.53	22	.56	[a]	[a]
17	111	.53	22	.51	1.66	184
			− 7	.26	..	..
			−19.5	..	.89	99
			−24	.21	..	..
7	118	.50	22	.46	[a]	[a]
			10	.37	..	..
			0	.29	..	..
			−46	.03	..	..
13	210	.28	− 7	.28	..	..
31	323	.18	22.8	.64	..	..
			21	..	1.11	358
			13.5	..	1.14	368
			9	.42	..	..
			4.5	..	0.90	291
			0	.35	.81	262
			− 9	..	.46	149
			−22	.15	..	..
			−27.5	..	.44	142
			−31	..	.37	120
			−52	..	.29	94
14	450	.13	22	.53	.83	374
			0	.31	.78	351
			− 7	.30	..	..
			−17	..	.48	216
			−24	.20	..	..
					..	..
			−29	..	.55	247
			−44	.07	..	..
			−46	.07	..	..
			−63	..	.10	45
37	730	.080	18.5	.62	.53	387
			11.5	.53	.60	438
			4.2	.49	.57	416
			0	.42	..	..
			−20	.18	..	..
			−22	..	.43	314
			−28.5	.18	..	..
			−30.5	..	.30	219
			−34	..	.13	95
			−43	..	.02	15
			−51	.02	..	..

[a] Poor annealing of the glass led to cracks at liquid nitrogen temperature and not all the runs could be completed. [b] Here the Na^{23} resonance shows two absorption lines. Although the temperature is above the critical value, the cause may be a different phase adsorbed on the surface of the sample tube. The N^{14} absorption gave a single line at this temperature. [c] Here the N^{14} resonance shows two absorption lines. Shaking the sample produced no effect; however, upon refreezing and warming up to 0° only one absorption was observed. The Na^{23} absorption was a single line at this temperature. [d] Measured for the dilute phases in the two-phase region.

isotherm at 243°K. was obtained by interpolating or extrapolating the data in Table I. The values at room temperature are in agreement, within the experimental accuracy, with the results of McConnell and Holm,[6] when a correction is made for the chemical shift of Na^+(am) with respect to Na^+(aq) of 17 p.p.m.

Knight Shift

The value of the effective field at the nucleus under observation, $\mathbf{H}_e$, is in general different from that of the externally applied one, $\mathbf{H}_0$. Thus,

$$\mathbf{H}_e = \mathbf{H}_0 + \mathbf{H}_s + \mathbf{H}_d + \mathbf{H}_c \qquad (4)$$

where $\mathbf{H}_s$ is the contribution due to the magnetization, $\mathbf{M}$[15,16]

$$\mathbf{H}_s = \left(\frac{4}{3}\pi - \alpha\right)\mathbf{M} + q\mathbf{M}$$

Here the Lorentz cavity field, $(4\pi/3)\mathbf{M}$, arises from the induced dipoles on the surface of a microscopic hypothetical sphere which contains the nucleus, α is the bulk diamagnetic correction factor, $\alpha = 4\pi/3$ or 2π, respectively, for a sample shaped as a sphere or an infinite cylinder. For $\chi \approx 10^{-7}$,[4] and infinite cylinder sample shape, the first term is of the order of 0.1 p.p.m. q is a steric factor which depends on the anisotropy of the electronic g factor of any paramagnetic species present in solution.

$$q = (16\pi/45)(b/a)^3 \frac{(g_\perp^2 - g_\parallel^2)}{g^2}$$

(15) N. Bloembergen and W. C. Dickinson, *Phys. Rev.*, **79**, 179 (1950).

(16) W. C. Dickinson, *ibid.*, **81**, 717 (1951).

where b is the radius of the paramagnetic species and a is its distance from the nucleus under observation, $g_\parallel$ and $g_\perp$ are, respectively, the g-factors in the directions parallel and perpendicular to the applied field. The g-factor for the Na–NH_3 solutions is $g = 2.0012$, which is lower than the free electron value of 2.0025. Since $g^2 = (1/3)(2g_\perp{}^2 + g_\parallel{}^2)$ in solution, if one assumes $g_\perp = 2.0025$, the anisotropy in the g factor gives a negligible contribution, $q\mathbf{M} \sim 0.003$ p.p.m. $\mathbf{H}_d$ is the field due to the orbital motion of the electrons in the individual species. For Na^+(am) it may be assumed that $\mathbf{H}_d$ is constant and independent of the anion as is the case for aqueous solutions of different sodium salts.[17] However, the diamagnetic correction for Na_2(am) and Na(am) is likely to be different from that for Na^+(am) and the estimate of this value is probably the largest source of error. The diamagnetic contribution from the electrons in expanded orbitals in the Na(am) and Na_2(am) species is thus (see for instance Pople, Bernstein, and Schneider[18])

$$-\frac{H_d}{H_0} = \frac{e^2}{3mc^2}\int \frac{\rho_1}{\epsilon r}\,d\tau$$

where ρ_1 is the electron density and ϵ the dielectric constant, which is larger than unity but smaller than the value for the bulk material. If $\langle(1/\epsilon r)\rangle \sim 0.1a_0{}^{-1}$, the diamagnetic shift at the central atom is of the order 2 p.p.m. for each electron, and zero at the coördinated NH_3 molecules. $\mathbf{H}_c$ is the field at the nucleus due to the Fermi contact term[19] in the paramagnetic species. Thus

$$\mathbf{H}_c = (8\pi/3)g\beta\rho_1(\mathbf{r}_n)\,\langle\mathbf{S}^z\rangle,\ \{\rho_1(\mathbf{r}_n) = \langle|\psi_e(\mathbf{r}_n)|^2\rangle\}$$

where

$$\langle S^z\rangle = \frac{1}{2}\left[\exp\left(\frac{g\beta H_0 S^z}{kT}\right) - \exp\left(-\frac{g\beta H_0 S^z}{kT}\right)\right]$$

$$= \chi^{mol}\frac{H_0}{N_0}(g\beta)$$

ψ_e is the unpaired electron wave function and N_0 is Avogadro's number. This term is now assumed to give the leading contribution to $\mathbf{H}_e$ in addition to $\mathbf{H}_0$. Thus, the field shift with respect to NaCl in NH_3

$$k = \frac{H_e - H_0}{H_0} \cong \frac{H_c}{H_0} = \frac{8\pi}{3}\frac{\chi^{mol}}{N_0}\rho_1(\mathbf{r}_n) \quad (5)$$

is the KS[20] and in the case where the chemical species containing the nucleus, n, under observation undergoes fast chemical exchange it can be shown that[21]

$$k(\mathrm{n}) = \sum k_i x_i \quad (6)$$

where k_i and x_i are the mole fraction and KS of the corresponding species.

Chemical Equilibria

In the concentration range where the chemical equilibria 1 and 2 are valid, $R \geqq 150$, the observed KS obey the relationships

$$k(Na^{23}) = x_0k_0$$

$$R \times k(N^{14}) = (x_0k_0' + x_1k_1')$$

$$= k_1'((k_0'/k_1')x_0 + x_1) \quad (7)$$

where k_0 is the KS for Na^{23} in Na(am), and k_0' and k_1' are the KS for N^{14} in the individual species Na(am) and e^-(am), respectively. The mole fractions of Na(am), e^-(am), and Na_2(am) within the solute are, respectively, x_0, x_1, and x_2. The volumetric and optical spectral properties of Na(am) and of Na^+(am) + e^-(am) are practically identical. Gold, Jolly, and Pitzer[22] concluded from these facts that Na(am) probably consisted of ion pairs of solvated sodium ions and electrons. From this model one would expect the KS for N^{14} to be substantially unchanged by this ion pair association and we shall hereafter assume $k_0' = k_1'$.

The room temperature value of k_1' is obtained by extrapolating $[R \times k(\mathrm{N})]$ to infinite dilution; see Fig. 3.

$$k_1' = \lim\,[R \times k(\mathrm{N})],\ \text{as } R \to \infty$$

$$\cong 500 \times 10^{-4}$$

or

$$k_1' = 14.6/T \quad (8)$$

when the Curie temperature dependence of the susceptibility is introduced. In order to determine k_0, the functional dependence of k(Na) with respect to m must be known. Thus, if the solutions obey the equilibrium relationships given by eq. 1 and 2

$$K_1' = \frac{K_1}{\gamma_\pm{}^2} = \frac{mx_1{}^2}{x_0}$$

$$K_2{}^2 = \frac{x_2}{mx_0{}^2}$$

$$x_0 + x_1 + 2x_2 = 1 \quad (9)$$

it follows that

$$\left(\frac{\partial \ln x_0}{\partial \ln m}\right)_{\gamma_\pm,T} = \frac{x_1 - 4x_2}{1 + x_0 + 6x_2}$$

$$\left(\frac{\partial \ln (x_1 + x_0)}{\partial \ln m}\right)_{\gamma_\pm,T} = -x_2\frac{\left(4 + \dfrac{2x_1}{x_1 + x_0}\right)}{1 + x_0 + 6x_2} \quad (10)$$

where $\gamma_\pm$ is the activity coefficient for the charged species. Hence, if one assumes that the value of

(17) J. E. Wertz and O. Jardetzky, *J. Chem. Phys.*, **25**, 357 (1956).

(18) J. A. Pople, W. G. Schneider, and H. J. Bernstein, "High Resolution Nuclear Magnetic Resonance," McGraw-Hill Book Co., Inc., New York, N. Y., 1959, p. 175.

(19) E. Fermi, *Z. Physik*, **60**, 320 (1930).

(20) C. H. Townes, C. Herring, and W. D. Knight, *Phys. Rev.*, **72**, 852 (1950).

(21) H. S. Gutowsky, D. W. McCall, and C. P. Slichter, *J. Chem. Phys.*, **21**, 279 (1953).

(22) M. Gold, W. L. Jolly, and K. S. Pitzer, *J. Am. Chem. Soc.*, **84**, 2264 (1962).

the activity coefficient will not vary appreciably with concentration, the value of k_0 may be determined when $k(\mathrm{Na})$ attains a maximum value. Thus, from eq. 9 and 10

$$k_0 = \left(\frac{[k(\mathrm{Na})] \times k_1'}{3[R \times k(\mathrm{N})] - 2k_1'}\right)_{k(\mathrm{Na})_{max}}$$

$$\left(\frac{\partial \ln [R \times k(\mathrm{N})]}{\partial \ln m}\right)_{\gamma_\pm, T, k(\mathrm{Na})_{max}} = -2x_2\left(1 + \frac{2x_2}{1 - 2x_2}\right) \quad (11)$$

At room temperature, $(\mathrm{d}k(\mathrm{Na})/\mathrm{d}m) = 0$, for $R \cong 700$; see, for instance, Fig. 2. Thus according to eq. 11

$$k_0 = 1.2 \pm 0.2 \times 10^{-4} = \frac{0.035 \pm 0.005}{T} \quad (12)$$

and

$$\left(\frac{\partial \ln [R \times k(\mathrm{N})]}{\partial \ln m}\right)_{\gamma_\pm, T, k(\mathrm{Na})_{max}} = -0.19$$

is to be compared with the mean slope

$$\frac{\Delta \ln [R \times k(\mathrm{N})]}{\Delta \ln m} = -0.16$$

between $R = 450$ and 730.

Here the error in k_0 is due to the uncertainty of the value of $[Rk(\mathrm{N})]$ when $k(\mathrm{Na})$ attains its maximum value. In addition, the values of k_0 and k_1' were determined by comparison of the KS data interpolated or extrapolated to $-33°$ with the average values of the equilibrium constants at this temperature[9,10]

$$K_1 = 0.013 \text{ (moles/kg.)}$$

$$K_2 = 19.0 \text{ (moles/kg.)}^{-1/2}$$

Thus, at $t = -33°$

$$k_0 = 1.4 \times 10^{-4}$$

$$k_1' = 508 \times 10^{-4}$$

or

$$k_0 = 0.034/T$$

$$k_1' = 12.3/T \quad (13)$$

Here the activity coefficients were evaluated from the Debye–Hückel theory, making use of the dielectric constant[23] and the density of pure ammonia[14] together with the distance of nearest approach of 5.5 Å., as chosen by Dye, *et al.*[9] Hence, the agreement of the room temperature and $-33°$ values of k_0 and k_1' justifies the assumption that $k_0' = k_1'$. The equilibrium constants for eq. 1 and 2 in the temperature interval 22 to $-33°$ are now obtained from the KS data together with the average values

(23) "Table of Dielectric Constants of Pure Liquids," NBS Circular 514 (1951).

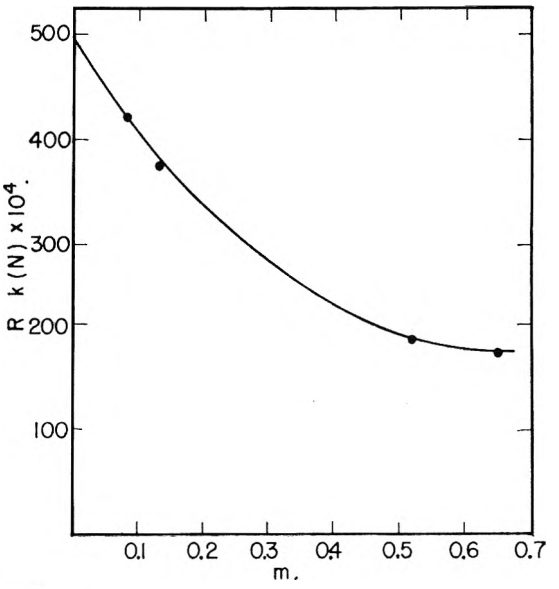

Fig. 3.—Extrapolation of the N^{14} Knight shift to infinite dilution.

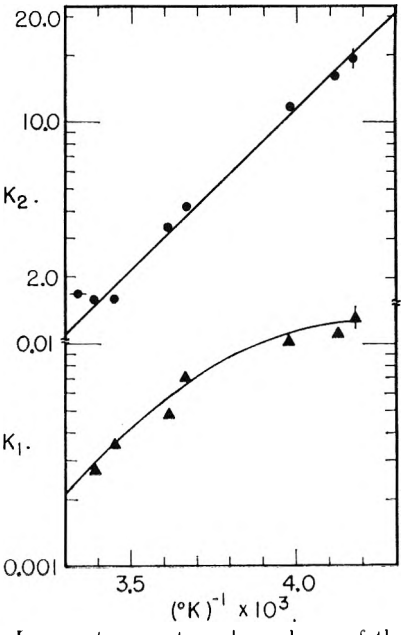

Fig. 4.—Inverse temperature dependence of the dissociation and dimerization equilibrium constants of Na(am) in the Na–NH_3 solutions. Values of K_2 and K_1 obtained by other authors are indicated as follows: (-●-) vapor pressure measurements of Dewald[11]; (▲, ●) conductance and other measurements by Dye, *et al.*,[9] and Evers, *et al.*[10]

$$k_1' = (13.5 \pm 1)/T$$

$$k_0 = (0.034 \pm 0.005)/T \quad (14)$$

They are given in Table II. Figure 4 shows the temperature dependence of the equilibrium constants.

The chemical equilibria 1, 2, and 3 are not satisfied for $R \leqq 111$; however, in this concentration range higher order sodium polymers, leading to a minimum in the KS, start to appear. As the concentration increases, $R \leqq 90$, the appearance of a metallic state is evidenced by an increase in the KS, which for Na^{23} tends to the limiting value of $k =$

TABLE II

EQUILIBRIUM CONSTANTS FOR THE DISSOCIATION AND DIMERIZATION OF Na(am) IN Na–NH_3

T	K_1 (moles/kg.)	K_2 (moles/kg.)$^{-1/2}$	$K_3 \times 10^2$ (moles/kg.)$^{3/2}$
295	0.0027 ± 0.001	1.6 ± 0.2	1.7
290	.0035	1.6	2.2
277	.0049	3.4	1.4
273	.0070 ± .0005	4.2	1.7
252	.010	12.2 ± 0.5	0.84
244	.011	15.8	0.67
240[a]	.013 (0.045)[b]	19 (67)[b]	0.69 (0.65)[b]

[a] The values of the equilibrium constants at this temperature are taken from the analysis of the conductance data of Kraus,[1] by Dye, Smith, and Sankuer,[9] and Evers and Frank.[10] [b] The equilibrium constants obtained from the e.s.r. data[4] by Becker, Lindquist, and Alder[5] are given for comparison.

1.5×10^{-4} for the saturated solution at room temperature.

Energy Calculations

The standard heats of reaction for the chemical equilibria 1, 2, and 3 are obtained from the temperature dependence of the respective equilibrium constant; thus, from Fig. 4

$$\Delta H_1^0\ (298) \cong -6.6 \text{ kcal./mole}$$

$$\Delta H_2^0 = -7.3 \pm 1 \text{ kcal./mole}$$

$$\Delta H_3^0\ (298) = \Delta H_1^0\ (298) - \Delta H_2^0 \cong 0.7 \text{ kcal./mole} \quad (15)$$

Here ΔH_2^0 is found to be constant throughout the temperature interval whereas ΔH_1^0 and consequently ΔH_3^0 are not. The value of ΔH_3^0 at room temperature is in agreement with the heat of dilution determined by Gunn and Green,[12] $\Delta H_3 = 1.2$ kcal./mole. Also, the temperature dependence of ΔH_1^0 indicates that a large negative change of heat capacity ΔC_p^0,[24,25] of the order of -100 cal./mole deg., accompanies the dissociation reaction.

The changes in entropy for the dissociation and dimerization reactions are found to be

$$\Delta S_1^0 \cong -34 \text{ cal./deg. mole at } T = 298°\text{K.}$$

$$\Delta S_2^0 = -24.1 \pm 3 \text{ cal./deg. mole}$$

Electron Densities

The parameters k_0 and k_1' in eq. 7 are, respectively, measures of the KS for Na^{23} and N^{14} in the single species Na(am) and e^-(am). Thus, the electron densities at the respective nuclei may be evaluated according to eq. 5 if one assumes χ^{mol} to be the theoretical susceptibility for $S = 1/2$. In the concentrated region, the density at the sodium nucleus was obtained from the KS making use of the combined Pauli spin susceptibility for a free electron gas with the Fermi energy evaluated from the metal electronic heat capacity.[26] The measured electron densities are given in Table III together with the values for the sodium-free atom[27] and the metal.[26]

TABLE III

ELECTRON DENSITIES IN THE Na–NH_3 SOLUTIONS IN UNITS OF a_0^{-3}

	$\rho_1(Na^{23})$					$\rho_1(N^{14})$
	Na–NH_3: R		Na	Na	Na^+	Na–NH_3
	5.7	≧300	(atom)	(metal)	(F-ctr.)	$R \geqq 300$
Exptl. value	0.071	0.00098	0.7525[c]	0.54[d]	0.014 to 0.009[e]	0.39
Theor. value		.066[a]				2.1[a]
		.014[a]				1.0[a]
		.016[b]				0.02[f]

[a] From two different solutions of the wave equation for the free electron in Na·6NH_3 (Blumberg and Das[8]). [b] From the solution of the wave equation for e^-(am) + Na^+(am) (Jortner[30]) where the distance between the ions is 7.2 a_0. [c] From atomic beam measurements (Kusch and Taub[27]). [d] From KS measurements (Knight[26]). [e] From the observed line widths in NaF and NaCl, F-centers (Lord[28]). [f] From the solution of the wave equation for the electron in $e^-\cdot NH_3$ (Pitzer[7]).

In conclusion, the variation of the electron density at the Na^{23} nucleus, from 9% of the value for the free atom in the concentrated region, $R = 5.7$, to 0.13% of the value for the free atom in the dilute region, $R \geqq 300$, indicates in the same manner as the conductance measurements of Kraus[1] the existence of two different types of Na–NH_3 solutions. The concentrated solutions possess properties characteristic of a metal, but in the dilute solutions the unpaired electrons are not closely associated with the sodium nuclei and therefore must occupy expanded orbitals in the dielectric medium. This also is evidenced by the high electron density observed for $N^{14}H_3$ in the dilute solutions. Here $\langle\rho_1(N^{14})\rangle$ is the sum of the densities at the nitrogen nuclei of each of the ammonia molecules coördinated to the paramagnetic species, and since the unpaired electron moves in an expanded orbital, it will contribute to the density at several layers of coördination shells in the same manner that the electron in an F-center contributes to the density at nuclei removed several lattice distances from the vacancy.[28,29] The electron densities cannot be explained on the basis of the Na·6NH_3 species, assumed by Blumberg and Das,[7] since the values of $\rho_1(Na^{23})$ obtained from this model are larger than the observed ones by more than an order of magnitude; see Table III. On the other hand, although the models proposed by Pitzer,[7] Jortner,[30] and Gold, *et al.*,[22] are more plausible, the solution of the wave equation for the unpaired electron has to be refined to determine the extension of the expanded orbitals in the dielectric medium, in order to obtain more accurate values of the electron density.

Acknowledgment.—This work was performed under the auspices of the U. S. Atomic Energy Commission.

(24) K. S. Pitzer, *J. Am. Chem. Soc.*, **59**, 2365 (1937).
(25) H. S. Harned and N. D. Embree, *ibid.*, **56**, 1042, 1050 (1934).
(26) W. D. Knight, "Solid State Physics," Vol. 2, Academic Press, Inc., New York, N. Y., 1956, p. 93.
(27) P. Kusch and H. Taub, *Phys. Rev.*, **75**, 1477 (1949).
(28) N. W. Lord, *Phys. Rev.*, **105**, 756 (1957).
(29) G. Feher, *ibid.*, **103**, 834 (1956); **105**, 1122 (1957).
(30) J. Jortner, *J. Chem. Phys.*, **30**, 839 (1959); **34**, 678 (1961).

CATALYTIC POLAROGRAPHIC CURRENTS FOR THE REDUCTION OF VANADIUM(III) IN THE PRESENCE OF VANADIUM(IV)[1]

BY JOHN W. OLVER[2] AND JAMES W. ROSS, JR.

Department of Chemistry and Laboratory for Nuclear Science, Massachusetts Institute of Technology, Cambridge 39, Mass.

Received April 3, 1962

Polarographic catalytic currents have been treated for the case where the primary reduction product of the diffusing electroactive species is produced *via* a second reduction path at the electrode surface. The precursor species for the second path is assumed to be present at high, constant concentration. Rate constants for the reaction V(II) + V(IV) → 2V(III) have been calculated from catalytic currents for the polarographic reduction of vanadium(III) in the presence of vanadium(IV) in sulfate media.

Introduction

Equations describing polarographic catalytic currents have been developed by several workers using a linear diffusion approximation to the dropping mercury electrode.[3-5] Koutecký[6,7] has treated the same problem using a more rigorous expanding sphere approximation. Reaction rate constants which are in good agreement with those calculated by independent experimental methods may be calculated from catalytic currents using Koutecký's solution, provided the following conditions are met. The reaction must follow the path

$$O + ne^- \longrightarrow R \text{ at the electrode}$$

$$R + Z \longrightarrow O \text{ in the solution phase}$$

In addition, the second step must be pseudo-unimolecular with respect to species R, *i.e.*, Z must be present at high, constant concentration in the electrode vicinity.

We have recently examined several inorganic systems giving rise to catalytic currents in which the species Z is reduced irreversibly to R when Z is present in sufficiently high concentration to ensure unimolecular regeneration of O. In the present paper we have developed a method for correcting catalytic currents for the reduction of Z and have used the method in calculating rate constants for the oxidation of vanadium(II) by vanadium(IV) in sulfate media.

Theoretical

The reaction scheme considered here is

$$O + n_1e^- = R \quad \text{at the electrode} \quad (1)$$

$$R + Z \xrightarrow{k} {}_aO \quad \text{in the soln. phase} \quad (2)$$

$$Z + n_2e^- = R \quad \text{at the electrode} \quad (3)$$

We assume the concentration of Z is much larger than O so that reaction 2 may be considered pseudo-unimolecular in R and concentration polarization may be neglected in reaction 3. k is the unimolecular rate constant for reaction 2.

Koutecký[6,7] has tabulated values of i_o/i_d as a function of k for the case where Z is not reduced directly. i_o and i_d are the experimentally observed currents for the reduction of O in the presence and in the absence of Z, respectively. In the present case we consider the expression

$$\frac{i_o'}{i_d} = \frac{i_T - i_z - f(i_z)}{i_d} \quad (4)$$

where i'_o is the current due to the reduction of O which would be obtained for our reaction scheme if the direct electroreduction of Z did not take place. i_T is the experimentally observed total current due to the simultaneous reduction of both O and Z. i_z is the experimentally observed current for the reduction of Z in the absence of O. $f(i_z)$ is the enhancement of the total current due to the increased rate of regeneration of O when Z is reduced directly at the electrode. All currents are assumed to be measured at the same potential.

Attempts to extend Koutecký's treatment to include the effect of reaction 3 were abandoned due to the complexity of the mathematics. We have chosen instead to use the simpler linear diffusion approximation to calculate $f(i_z)$. Rate constants, however, are calculated from Koutecký's tables using our values of i'_o/i_d.

The boundary value problem which applies to our model, assuming the diffusion coefficients D of O and R are equal, is

$$x > 0, t > 0 \qquad \frac{\partial C_O}{\partial t} = D\frac{\partial^2 C_O}{\partial x^2} + akC_R$$

$$\frac{\partial C_R}{\partial t} = D\frac{\partial^2 C_R}{\partial x^2} - kC_R$$

$$x \to \infty, t = 0 \qquad C_O = C_O^*, C_R = 0$$

$$x = 0, t > 0 \qquad C_O = 0$$

$$D\frac{\partial C_O}{\partial x} + D\frac{\partial C_R}{\partial x} - \frac{i_z}{n_2FA} = 0$$

C_O^* is the bulk solution concentration of O, F the faraday, and A the electrode area. Except for the boundary condition at $x = 0$ this problem is identical with that solved by Delahay and Stiehl.[3] The

(1) Taken in part from the Ph.D. thesis of John W. Olver, Massachusetts Institute of Technology, June, 1961. Presented in part at the September, 1961 National Meeting of the American Chemical Society. This work was supported in part by the U. S. Atomic Energy Commission under Contract AT(30-1)905.

(2) American Chicle Co. Fellow, 1959–1960. National Science Foundation Summer Fellow, 1960.

(3) P. Delahay and G. Stiehl, *J. Am. Chem. Soc.*, **74**, 3500 (1952).

(4) Z. Pospisil, *Collection Czech. Chem. Commun.*, **18**, 337 (1953).

(5) S. L. Miller, *J. Am. Chem. Soc.*, **74**, 4130 (1952).

(6) J. Koutecký, *Collection Czech. Chem. Commun.*, **18**, 311 (1953).

(7) J. Koutecký and J. Čižek, *ibid.*, **21**, 1063 (1956).

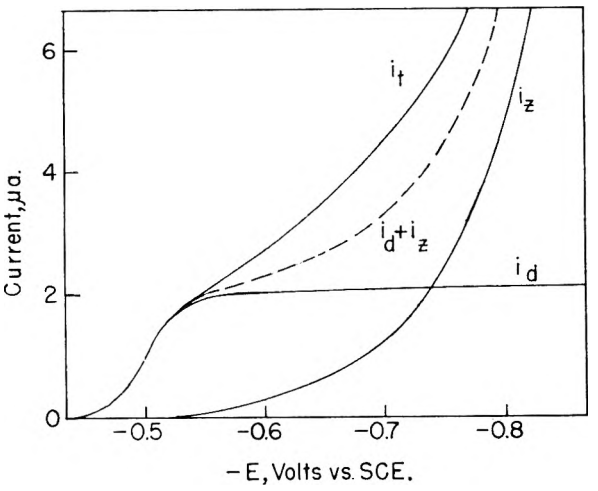

Fig. 1.—Vanadium polarograms in sulfate medium: i_d = 1.0×10^{-3} M vanadium(III); i_z = 0.010 M vanadium(IV); i_T = 1.0×10^{-3} M vanadium(III) and 0.010 M vanadium(IV). All polarograms obtained in 0.4 M H_2SO_4 and 0.15 M $NaHSO_4$.

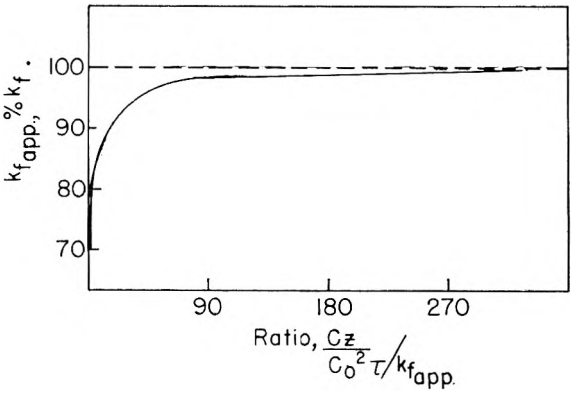

Fig. 2.—$k_{f\,app}$ as a function of the dimensionless parameter $C_z/C_0^2 \tau k_{f\,app.}$, showing the approach to pseudo-unimolecular behavior.

solution is readily obtained by a Laplace transformation yielding

$$\left.\frac{\partial C_O}{\partial x}\right|_{x=0} = \left.\frac{\partial C_O}{\partial x}\right|_{x=0}^{i_z=0} + \frac{i_z a}{2n_2 FA}\, g(kt) \quad (5)$$

where $g(kt) = \{1 - \exp(kt/2)[I_0(kt/2) + I_1(kt/2)]\}$. $I_0(kt/2)$ and $I_1(kt/2)$ are modified Bessel functions, tables of which are readily available.[8] The quantity

$$\left.\frac{\partial C_O}{\partial x}\right|_{x=0}^{i_z=0}$$

is identical to the gradient of concentration of O at the electrode surface if Z were not reduced.

Following Delahay and Stiehl[3] we transpose this result to the case for the dropping mercury electrode by multiplying (5) by the factor $(7/3)^{1/2}$ and replacing t by the drop time τ. Since

$$i_T - i_z = n_1 FAD \left.\frac{\partial C_O}{\partial x}\right|_{x=0}^{t=\tau}$$

we have

$$i_T - i_z = i_o' + \frac{n_1 i_z a}{2n_2}\left(\frac{7}{3}\right)^{1/2} g(k\tau) \quad (6)$$

The last term in (6) represents the enhancement $f(i_z)$ evaluated at the end of the drop life. Substitution in (4) yields

$$\frac{i_o'}{i_d} = i_T - \frac{\left[1 + \frac{n_1 i_z a}{2n_2}\left(\frac{7}{3}\right)^{1/2} g(k\tau) i_z\right]}{i_d} \quad (7)$$

The unimolecular rate constant k may be calculated from (7) by first assuming $g(k\tau)$ is zero and determining a trial k from Koutecký's tables. Using this trial k the bracketed terms in (7) may be evaluated and k recalculated from the corrected value of i_o'/i_d. In the present work one or two cycles were sufficient to define k to within experimental error.

Experimental

Reagents and Apparatus.—Electrolyte solutions were prepared from reagent grade sodium sulfate, sodium bisulfate, and sulfuric acid to give the desired pH values in the range 0 to 2 while maintaining the ionic strength of the electrolyte at 0.6.

A stock solution approximately 0.5 M in vanadium(IV) and 1 M in sulfuric acid was prepared from reagent grade vanadyl sulfate. A stock solution approximately 0.5 M in vanadium(III) and 1 M in sulfuric acid was prepared from the vanadium(IV) solution by controlled potential electrolysis until a polarogram of the solution showed no vanadium(IV) or vanadium(II). Both vanadium stock solutions were standardized by potentiometric titration with potassium permanganate.

Because vanadium(III) solutions are oxidized by air, precautions were taken to minimize air oxidation of the main V(III) stock solution although the presence of a small amount of vanadium(IV) in the vanadium(III) stock solutions was not detrimental to the kinetic interpretation.

All solutions were deaerated with prepurified tank nitrogen and were thermostated to ±0.2° in a water bath before polarograms were determined.

All polarograms were obtained using an E. H. Sargent and Co. Model XXI polarograph without damping. The Brown recorder had a full-scale deflection time of 10 sec. All currents were measured at the maximum deflection of the recorder pen.

The capillary used had a 6-sec. drop time and an m of 0.92 mg./sec. over the potential range covered in this work.

Experimental Method.—Typical polarograms required for a single determination of the unimolecular reaction rate are shown in Fig. 1. The difference between curves $i_T - i_z$ and i_z represents the catalytic portion of the total current due to the regeneration reaction

$$V(II) + V(IV) \xrightarrow{k_f} 2V(III) \quad (8)$$

The formal second-order reaction rate constant $k_f = k/C^*_{V(IV)}$ may be determined from these polarograms as outlined in the Theoretical section, provided the $C^*_{V(IV)}$ is sufficiently high to ensure pseudo first-order kinetics in (8). This condition is satisfied when vanadium(IV) is not reduced at the electrode, and the following condition holds[6]

$$\frac{C^*_{V(IV)}}{C^{*2}_{V(III)}} >> 0.665 k_f$$

Since vanadium(IV) is reduced in the present case, this condition is undoubtedly not sufficiently stringent.

In order to establish that reaction 8 meets the pseudo-first order restriction, apparent rate constants $k_{f\,app}$ were determined in each electrolyte used for different ratios of $C^*_{V(IV)}/C^*_{V(III)}$. As expected, $k_{f\,app}$ values increased with increasing $C^*_{V(IV)}/C^*_{V(III)}$, approaching a limiting value at

(8) Janke, Emde, and Lösch, "Tables of Higher Functions," 6th Ed., F. Lösch, Editor, McGraw-Hill Book Co., New York, N. Y., 1960.

large ratios. When plotted as shown in Fig. 2 all the experimental values of $k_{f\,app}$ in the various electrolytes fell in the same curve. At values of

$$\frac{C^*_{V(IV)}}{C^*_{V(III)^2}\,\tau k_{f\,app}}$$

greater than 30, $k_{f\,app}$ is equal to 0.95 of its limiting value k_f. All k_f values reported in this work were obtained under conditions where the limiting value is approached to within the experimental error of 5%.

The validity of the linear diffusion approximation used in the derivation of $f(i_z)$ was tested by determining k_f as a function of i_z. k_f is independent of potential although both i_T and i_z increase with increasing potential. If calculated values of k_f are independent of potential, it may be assumed that the correction term $f(i_z)$ is a good approximation to the enhancement caused by reaction 3. The results are shown in Table I.

TABLE I

VARIATION OF CALCULATED RATE CONSTANTS WITH POTENTIAL

E, v. *vs.* s.c.e.	i_T, μa.	i_z, μa.	i_d, μa.	k_f, l. mole^{-1} sec.$^{-1}$
−0.68	3.20	0.86	1.23	14.9
− .70	3.59	1.15	1.24	15.3
− .72	4.04	1.51	1.24	15.5
− .74	4.60	2.00	1.25	15.5
− .76	5.30	2.66	1.25	15.

Although current i_z varies from 0.86 to 2.66 μa. over this range, the calculated values of k_f are constant to within experimental error. At potentials outside the range, there is considerable scatter in calculated values of k_f because of the lower precision when measuring currents in steeply rising portions of the i_T wave.

Results

Kinetic Results.—The order of reaction 8 with respect to each of the reacting species was determined by measuring the magnitude of the catalytic contribution to the total current as a function of the concentration of one reacting species while holding the concentration of the other species constant. The reaction was first order with respect to both vanadium(II) and vanadium(IV) over 10-fold concentration ranges.

Rate constants obtained at various temperatures and pH values are summarized in Table II.

Discussion of Kinetic Results.—From published hydrolysis data for vanadium(III) and vanadium(IV),[9] between pH values of 0 and 2, aquovanadium(III) and VO^{+2} greatly predominate. Therefore the several-fold change in the magnitude of the reaction rate constant over that pH range cannot be explained by the formation of higher hydrolyzed species at higher pH values. Furthermore, the difference in sulfate ion concentration between the two solutions of lowest pH is practically negligible, thereby indicating that the variation in rate constant is not a function of sulfate ion concentration. On the other hand, the variation in bisulfate ion concentration between the two solutions of lowest pH is large (0.99 *M* at pH 0 and 0.54 *M* at pH 0.2). Also, the concentration of bisulfate ion becomes quite small at a pH value of 2 where the reaction rate is nearly independent of pH.

TABLE II

EFFECT OF pH AND TEMPERATURE ON RATE CONSTANTS (in l. mole^{-1} sec.$^{-1}$)

	Temperature, °C.			
pH	18	25	33	43
0	3.0	6.4	13	28
0.2		10	19	
.6	6.6	15	25	
.8	7.7			
1.3	8.9	18	37	
2.0	9.5	19	45	

In view of the above facts, the data can be explained adequately by postulating the existence of a vanadium(IV)–bisulfate complex, the stability constant of which is only of the order of 1. The proposal that the VO^{+2} is being complexed is supported by the fact that the $E_{1/2}$ for VO^{+2} shifts anodically with increase in HSO_4^- or H^+. The rate constant for the reaction path involving the bisulfate complex probably is small compared with that for the simple hydrolyzed species. Such a view would be reasonable if one of the hydroxy groups in the vanadium(IV) species were replaced, since usually a dihydroxy complex reacts much more rapidly than a monohydroxy complex of the same central species.

A rate expression for the reaction between V(II) and V(IV) in acidic sulfate media can be postulated as

$$\text{Rate} = k_f^1(VO^{+2})(V^{+2}) + k_f^2\,(VOHHSO_4^{+2})(V^{+2})$$

In order to say anything more definite about the rate expression for this reaction, knowledge of the nature and stability of all possible sulfate or bisulfate complexes of the reacting species would be required.

(9) J. Bjerrum, G. Schwarzenbach, and L. G. Sillén, "Stability Constants," Part I, The Chemical Society, London, 1957.

EVIDENCE FROM NUCLEAR MAGNETIC RESONANCE FOR MALATE COMPLEXES OF ALKALI METAL CATIONS[1]

BY LUTHER E. ERICKSON AND R. A. ALBERTY

Department of Chemistry, University of Wisconsin, Madison, Wisconsin

Received April 4, 1962

A pronounced concentration dependence is observed in the high-resolution proton n.m.r. spectra of D_2O solutions of all five of the alkali metal malates. By contrast, the spectrum of tetramethylammonium malate is independent of concentration. These observations suggest that there is appreciable ion association in the alkali metal malate solutions. From the magnitude of the concentration effects on spin–spin coupling constants and chemical shifts, the dissociation constant of the complex, CM^- (where C is any alkali metal ion), is estimated to be about 10 *M*.

Introduction

The great sensitivity of n.m.r. chemical shifts to molecular environments provides still another method for determining the nature of the ionic species present in aqueous solutions. Li, Johnson, and Shoolery[2] recently reported that added $ZnCl_2$ or $MgCl_2$ produced a decrease in the CH_2 proton chemical shifts of glycylglycinate and glycineamide in D_2O solution. The magnitude of the effect is greater for Zn^{+2} than for Mg^{+2} and apparently is closely related to the relative stabilities of the corresponding complexes formed between the metal ion and the proton-containing ligand. The striking dependence of the F^{19} chemical shifts of AlF^{+2} and AlF_2^+ on Na^+ and K^+ concentrations probably also reflects appreciable ion association.[3] Hammes, *et al.*,[4] have concluded that the adenine portion of ATP probably is not involved in the complexing of Mg^{+2} and Ca^{+2} by ATP, since the chemical shifts of the ring protons are not affected by added Mg^{+2} and Ca^{+2}.

On the basis of observed increases in the Na^{23} n.m.r. line widths with concentration, Wertz and Jardetzky[5] concluded that several α- and β-hydroxy carboxylic acid anions (among them malate) form complexes with Na^+ in concentrated aqueous solutions. These authors concluded that chloride, acetate, formate, and benzoate do not form complexes with sodium ion, since the Na^{23} line widths for aqueous solutions of sodium salts of these anions are identical and are independent of concentration.

Our studies of the concentration effects on the high-resolution proton spectra of alkali metal and tetramethylammonium (TMA) malates confirm Wertz and Jardetzky's conclusions and indicate, furthermore, that *all* of the alkali metal ions form complexes with malate in aqueous D_2O solutions, while tetramethylammonium ion does not. Failure to recognize the possibility of the existence of alkali metal complexes can lead to serious errors. Tate and Jones[6] recently have demonstrated the magnitude of the effect of the complexing by alkali metal ions by comparing the stability "constants" for $CdNO_3^+$ in the presence of a variety of electrolytes, including $LiNO_3$ and $NaNO_3$.

Experimental

The alkali metal malate (abbreviated Na_2M, K_2M, etc.) samples were prepared by neutralization of recrystallized L-malic acid with the carbonate or hydroxide of the corresponding metal. The samples were dried under vacuum and solutions of the desired concentration were prepared in D_2O. Reagent grade chemicals were used in all cases. Saturated aqueous solutions of the alkali metal carbonates were filtered to remove heavy metal impurities as hydroxides.

Cesium carbonate was prepared from Trona CsCl by treatment with H_2SO_4 and evaporation of HCl followed by precipitation of the sulfate with $Ba(OH)_2$ and conversion to the carbonate with CO_2. The CsCl was purified initially by conversion to $CsCl_2I$ with Cl_2 and I_2. This was recrystallized three times from 6 *N* HCl[7] and subsequently thermally decomposed to CsCl.

Samples of the alkali metal malates were placed in the inner of two coaxial tubes with benzene, used as a reference for chemical shift measurements, in the annular space between the tubes. All spectra were recorded at 40 Mc. using a Varian Associates V4300 n.m.r. spectrometer and accessories as described earlier.[8,9] In each case parameters based on averages of 3–5 sweeps are reported.

The notation used to refer to particular protons and chemical shifts is in agreement with that used earlier.[8] It should be noted, however, that subsequent work[10] requires that the subscripts b and c refer to methylene protons which Alberty and Bender designated as c and b, respectively. The subscript a refers to the methine proton.

Results

The changes observed in the proton n.m.r. spectra of the alkali metal malates resulting from an increase in concentration are in the same direction as the changes observed in going from the completely neutralized salt to the partially protonated species. In general, as the concentration is increased, the spectrum becomes less spread out. As shown in Fig. 1, this is particularly evident in the 2–3, 7–8, and 9–10 separations which change noticeably with concentration.[11] These changes

(1) This research was supported by grants from the National Science Foundation and the Research Committee of the Graduate School of the University of Wisconsin (from funds from the Wisconsin Alumni Research Foundation). A portion of the work was included in the thesis submitted by L. E. Erickson to the Graduate School of the University of Wisconsin in partial fulfillment of the requirements for the Ph.D. in Chemistry, 1959.

(2) N. C. Li, L. Johnson, and J. Shoolery, *J. Phys. Chem.*, **65**, 1902 (1961).

(3) R. E. Connick and R. E. Poulson, *ibid.*, **62**, 1002 (1958).

(4) G. G. Hammes, G. E. Maciel, and J. S. Waugh, *J. Am. Chem. Soc.*, **83**, 2394 (1961).

(5) J. E. Wertz and O. Jardetzky, *Archiv. Biochem. and Biophys.*, **65**, 569 (1956).

(6) J. F. Tate and M. M. Jones, *J. Phys. Chem.*, **65**, 1661 (1961).

(7) P. Bender and R. A. Strehlow, *J. Am. Chem. Soc.*, **70**, 1995 (1948).

(8) R. A. Alberty and P. Bender, *ibid.*, **81**, 542 (1959).

(9) The $(TMA)_2M$ spectra were recorded under similar conditions but at Pennsylvania State Univ. during the summer of 1961. Since only relative chemical shifts are required to reach the conclusion drawn, no external standard was included.

(10) O. Gawron, A. J. Glaid, III, and T. P. Fondy, *J. Am. Chem. Soc.*, **83**, 3634 (1961); F. A. L. Anet, *ibid.*, **82**, 994 (1960).

(11) Compare with Fig. 1 and 2 of reference 8.

reflect changes both in chemical shifts and in spin–spin coupling constants. Calculations of spin–spin coupling constants and chemical shifts are based on the ABX approximation[12] and are summarized in Table I. All chemical shifts are expressed in p.p.m. relative to a low field reference peak; *i.e.*, $\delta_i = 10^6(\nu_i - \nu_r)/\nu_r$ where ν_i and ν_r are the resonance frequencies of the sample and standard, respectively. An increase in the chemical shifts then represents increased shielding.

In every case the difference in the chemical shift of the two methylene protons increases with dilution. Similarly, the average chemical shift of the two methylene protons measured with respect to the methine proton increases with increasing dilution. This change is in the direction of the trend observed in going from H_2M (2 *M*) to K_2M (2 *M*) and reflects an increase in the difference in the magnetic environments of the two methylene protons as the solution is diluted.

Linear extrapolation of the chemical shifts of all of the alkali metal malates to infinite dilution resulted in a common value (within ±0.3 c.p.s. at 40 Mc.) for *each* of the chemical shifts of *all* of the five alkali metal malates (Table I). (The apparent large differences in proton chemical shifts for the different alkali malates can be accounted for almost entirely by the differences in bulk magnetic susceptibilities and the use of an external standard.)

TABLE I

CONCENTRATION AND CATION EFFECTS ON PROTON CHEMICAL SHIFTS AND SPIN–SPIN COUPLING CONSTANTS FOR MALATE SALTS[a]

Salt	Concn., *M*	δ_a ±0.01	δ_b ±0.01	δ_c ±0.01	A_{ab} ±0.2	A_{ac} ±0.2	A_{bc} ±0.2
Li_2M	0.49	2.16	4.09	3.80	10.4	2.7	15.3
	1.46	2.12	4.03	3.77	9.7	3.0	15.4
	2.45	2.09	3.97	3.74	9.4	2.9	15.3
Na_2M	0.50	2.14	4.08	3.79	10.2	2.8	15.3
	1.47	2.12	4.03	3.76	10.0	2.9	15.5
	2.50	2.08	3.93	3.72	9.2	3.1	15.4
K_2M	0.60	2.15	4.06	3.78	9.9	3.1	15.5
	1.50	2.11	3.99	3.74	9.8	3.1	15.3
	3.00	2.05	3.89	3.65	9.0	3.5	15.6
Rb_2M	0.50	2.15	4.04	3.76	10.1	2.8	15.5
	1.00	2.10	3.96	3.72	9.7	3.1	15.4
	2.00	2.02	3.86	3.64	9.3	3.5	15.3
Cs_2M	0.40	2.14	4.03	3.75	9.8	3.0	15.4
	1.20	2.04	3.89	3.65	9.7	3.0	15.4
	2.00	1.96	3.79	3.58	9.4	3.0	15.5
(+0.96CsCl)	0.48	2.06	3.92	3.68	9.7	3.1	15.3
(+2.50CsCl)	0.50	1.94	3.79	3.56	9.5	3.1	15.4
M^{-2}	0	0[b]	1.94[b]	1.64[b]	10.3	2.8	15.3
$(TMA)_2M$	0.95–1.90	0	1.94	1.64	10.4	2.6	15.2
H_2M	2.00	0.17[c]	1.92[c]	1.82[c]	7.1	4.4	17.1

[a] Chemical shifts of alkali metal malates are in p.p.m. relative to external benzene and are uncorrected for bulk susceptibility differences of sample and reference. A larger positive number corresponds to an upfield shift. [b] Obtained by extrapolation to infinite dilution and referred to $\sigma_a = 0$. [c] Chemical shifts in p.p.m. relative to external water.

The changes in spin–spin coupling constants with concentration are similar in magnitude. Of the three spin–spin coupling constants, A_{bc} is virtually independent of concentration (15.3 c.p.s.). On the other hand, A_{ab} increases (from 9.4 to 10.0 c.p.s.) and A_{ac} decreases slightly (from 3.2 to 2.9 c.p.s.) upon dilution from 2.5 to 0.5 *M*. Similarly $A_{ab} + A_{ac}$ (which is just the 1–4 separation and is susceptible to direct measurement) increases upon dilution. When the spin–spin coupling constants for all five alkali metal malates were plotted

(12) J. A. Pople, W. G. Schneider, and H. J. Bernstein, "High-resolution Nuclear Magnetic Resonance," McGraw-Hill Book Co., Inc., New York, N. Y., 1959, p. 132.

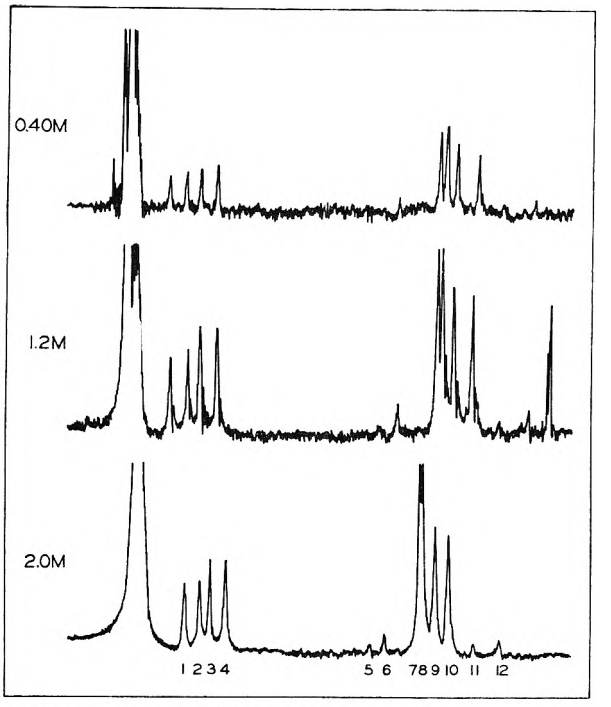

Fig. 1.—Concentration dependence of proton n.m.r. spectrum of D_2O solutions of Cs_2M at 40 Mc. The magnetic field increases from left to right. Lines 1–4 arise from the methylene proton, lines 5–12 from the methylene protons. Note changes in relative line spacings with concentration (especially 2–3, 7–8, and 9–10 separations).

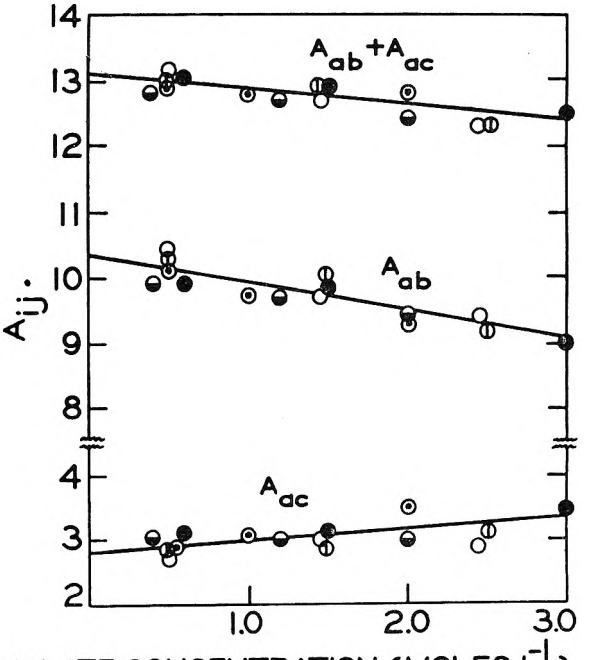

Fig. 2.—Concentration dependence of proton spin–spin coupling constants of alkali metal malates: Li_2M, ○; Na_2M, ◑; K_2M, ●; Rb_2M, ⊙; Cs_2M, ◒.

against concentration (Fig. 2), there appeared to be no systematic differences among the metals. The best straight line drawn through all the points was used to obtain the spin–spin coupling constants at infinite dilution (Table I).

By contrast, the chemical shifts and coupling constants for $(TMA)_2M$ are independent of concentration and are equal to those expected for the alkali metal malates at infinite dilution. An inspection of the proton spectrum of 1.9 or 0.95 *M* $(TMA)_2M$ reveals the increased spreading (again especially in the 2–3, 7–8, and 9–10 separations) which would be expected for more dilute solutions on the basis of the trends indicated in Fig. 1.[13] The spectra of 0.95 and 1.90 *M* $(TMA)_2M$ are the same. Average chemical shifts and spin–spin coupling constants (based on eight sweeps—four at each concentration) are compared in Table I with the corresponding quantities obtained by extrapolation of the data for the alkali metal malates.

Furthermore, the spectrum of 0.95 *M* $(TMA)_2M$ to which NaCl had been added to the extent of 2 *M* differs sharply from that of 0.95 *M* $(TMA)_2M$ and is virtually identical (apart from the TMA^+ proton signal) to that of 0.95 *M* Na_2M. Similar effects were observed when CsCl was added to a 0.5 *M* Cs_2M solution (Table I).

Discussion

The significant concentration dependence of the alkali metal malate proton n.m.r. spectra, in contrast to the insensitivity of the $(TMA)_2M$ spectrum to concentration changes, strongly suggests that a significant amount of ion association involving the malate anion and alkali metal cation occurs in these solutions.

The n.m.r. spectrum of $(TMA)_2M$ (or the common spectra of the alkali metal malates obtained by extrapolation) is that of the free malate anion. Karplus[14] has calculated the dependence of proton–proton spin–spin coupling constants for H–C–C–H on the dihedral angle, ϕ, between the protons as seen along the C–C bond. According to this calculation, the increase in A_{ab} and decrease in A_{ac} with dilution result from an increase in the proportion of molecules in the conformation in which the carboxyl groups are *trans*. This conclusion depends only on the theoretically calculated dependence of $A_{HH'}$ on ϕ ($A_{HH'}$ maximum at $\phi = 180°$) and does not depend on the less certain numerical values of $A_{HH'}$. It is reasonable that the mutual repulsion of the negatively charged carboxyl groups should be the most important factor in determining the conformation of the divalent malate anion in solution. The increase in the difference of the chemical shifts of the two methylene protons ($\delta_b - \delta_c$) with dilution is consistent with this interpretation.

For the complex ions (as for the undissociated acids), the proportion of molecules in which the carboxyl groups (and the two protons H_a and H_b) are *trans* is less than for the divalent anion. The observed coupling constant A_{ab} (averaged over all conformations) is then less than that of the anion. This reflects a greater contribution from species in which the two protons H_a and H_b are not *trans* ($\phi < 180°$) as would be expected to result from the complexing with a cation.

It would be very desirable to be able to determine the stability constants for the alkali metal malate complexes from the observed changes in the chemical shifts or spin–spin coupling constants which accompany the addition of complexing cation to ligand. Accurate determinations would require the characteristic parameters of the complexed species. However, some idea of the *order of magnitude* of the dissociation constant of the complex CM^- (where C is any alkali metal cation) can be obtained by noting that ($\delta_b - \delta_c$) and A_{ab} for a 2 *M* solution of any of the alkali metal malates is about $^1/_4$ of the way between the values for M^{-2} and H_2M. If we assume that these parameters change linearly with % neutralization (at least approximately true[8]) and that the chemical shifts and spin–spin coupling constants of HM^- are very similar to those of CM^-, this would correspond to about $^1/_4$ of the malate in the associated form, or a dissociation constant, *K*, for CM^- of $\sim$10 *M*. This is considerably higher than the dissociation constants of Ca^{+2}, Ba^{+2}, Mg^{+2}, and Sr^{+2} complexes with malate ($2–5 \times 10^{-2}$).[15] In this connection, a comparison of dissociation constants of several relatively weak metal–ligand complexes reveals that Na^+ and K^+ complexes usually have dissociation constants at least 100 to 1000 times greater than Ca^{+2} or Mg^{+2} complexes.[16–18]

The conclusion that TMA^+ is much less strongly bound than the alkali metal cations is consistent with results reported by other workers for such widely differing complexing agents as EDTA and ATP.[19,20] However, in the above cases Li^+ and Na^+ complexes are more stable than the other alkali metal complexes. Attempts to correlate the stability of alkali metal and alkaline earth complexes with the ratio e^2/r (where e is the charge on the cation and r is its ionic radius) have met with some success.[21] The failure of TMA^+ to form significant complexes with malate then can be attributed to its low e^2/r ratio. In view of the fact that TMA^+ is not bound by fairly good chelating agents, it is particularly valuable as an internal standard in n.m.r. chemical shift measurements in aqueous solutions (as used by Loewenstein and Roberts[22]).

(13) The strong TMA^+ proton signal lies between the methine and methylene proton signals ($\sim$0.6 p.p.m. below the center of the CH_2 octet) so that it does not interfere in the interpretation of the spectrum.

(14) M. Karplus, *J. Chem. Phys.*, **30**, 11 (1959).

(15) R. K. Cannan and A. Kibrick, *J. Am. Chem. Soc.*, **60**, 2314 (1938).

(16) G. Schwarzenbach, E. Kampitsch, and R. Steiner, *Helv. Chim. Acta*, **29**, 364 (1946).

(17) G. Schwarzenbach, E. Kampitsch, and R. Steiner, *ibid.*, **28**, 828 (1945).

(18) T. O. Denney and C. B. Monk, *Trans. Faraday Soc.*, **47**, 992 (1951).

(19) G. Schwarzenbach and H. Ackermann, *Helv. Chim. Acta*, **30**, 1798 (1947).

(20) R. M. Smith and R. A. Alberty, *J. Phys. Chem.*, **60**, 180 (1956).

(21) A. E. Martell and M. Calvin, "Chemistry of the Metal Chelate Compounds," Prentice-Hall, Inc., Englewood Cliffs, N. J., 1952, p. 191.

(22) A. Loewenstein and J. D. Roberts, *J. Am. Chem. Soc.*, **82**, 2705 (1960).

It provides a single peak (actually a poorly resolved triplet due to weak spin–spin interaction with N^{14}) that can be detected readily at low concentrations and apparently is chemically inert. An internal standard is especially valuable when small effects on chemical shifts must be measured accurately and bulk susceptibility corrections are too uncertain.

Acknowledgments.—The authors are indebted to Prof. Paul Bender for assistance in obtaining n.m.r. spectra under optimum operating conditions. One of us (L.E.E.) wishes to express his appreciation to the Petroleum Research Fund for support and to Pennsylvania State University and Prof. R. W. Taft for use of facilities for the completion of this work.

AN EFFUSION STUDY OF THE SIMULTANEOUS VAPORIZATION AND DECOMPOSITION OF SOLID IRON(III) CHLORIDE

BY R. R. HAMMER AND N. W. GREGORY

Department of Chemistry at the University of Washington, Seattle, Wash.

Received April 5, 1962

Estimates of the condensation coefficients for the vaporization of Fe_2Cl_6 ($\alpha = 10^{-2}$) and for the concomitant release of chlorine ($\alpha = 10^{-6}$) from solid $FeCl_3$ between 120 and 150° have been made from effusion data.

Vaporization characteristics of solid $FeCl_3$ between 200 and 300° have been investigated by a number of workers.[1-8] These results have been compared and additional data provided, which also extend down to 160°, in a recent paper from this Laboratory.[9] We now wish to report an effusion study of $FeCl_3$. The vaporization processes of interest are

$$2FeCl_3(s) = Fe_2Cl_6(g) \qquad (1)$$

and

$$2FeCl_3(s) = 2FeCl_2(s) + Cl_2(g) \qquad (2)$$

(The work of Kangro and Bernstorff[10] and of Schafer[11] indicates that the partial pressure of monomeric $FeCl_3(g)$ is less than 1% of that of the dimer in the equilibrium vapor in the range of effusion experiments.) Extrapolation of results at higher temperatures[1-9] suggests that at *ca.* 150°, (1) and (2) can be studied simultaneously in the same effusion experiment. Inasmuch as equilibrium data already are available, the principal objective of the work was to compare condensation coefficients, calculated from the dependence of steady state effusion pressures on cell dimensions following a method described earlier.[12] Also, the applicability of the effusion method for the study of decomposition reactions such as (2) has been a question of particular interest in this Laboratory. It has been shown, for example, that effusion is not at all suitable for determination of equilibrium water vapor pressures in the system $Mg(OH)_2 \rightarrow MgO + H_2O$.[13]

Experimental

Eastman practical anhydrous $FeCl_3$ and, alternately, material prepared by reaction of analytical grade iron wire and commercial tank chlorine, were used. Samples were resublimed twice under high vacuum, with the sublimate finally condensed directly into the Pyrex effusion cells (described previously[12]). Cell characteristics are

Cell	$a_0 \times 10^3$, cm.^{2}	$a_0 \times 10^3/a_s$	K
3	24.2	2.5	0.99
5	16.7	13.5	.96
6	4.23	0.6	.97

where a_0 is the orifice area, a_s the cross-section area of the cell, and K the Clausing factor[14] for the cell orifice.

Runs were initiated by placing a preheated furnace around the effusion cell which was attached to the high vacuum system. The temperature was measured with two Chromel–Alumel thermocouples, one near the orifice and the other at the opposite end of the cell. A potentiometric controller held the temperature within ±1° during the 8–30-hr. effusion periods.

The effused ferric chloride vapor condensed on a glass insert tube, *ca.* 25 mm. o.d., which fitted snugly against the wall of the vacuum line and extended from the room temperature zone into the furnace to the glass wall containing the orifice. At the conclusion of the run, the cell was cooled, an inert gas (dry air was also found satisfactory) admitted, the collecting tube quickly replaced, and the system reevacuated. The ferric chloride washed from the collector was determined either by titration with standard potassium dichromate, sodium diphenylamine sulfonate indicator,[15] or colorimetrically as the tris-(1,10-phenanthroline)-iron-(II) complex ion.[16]

Effused chlorine was trapped either on a liquid nitrogen cooled finger which extended to within *ca.* 3 cm. of the orifice or in a conventional trap which could be isolated from the effusion cell by closing a fluorocarbon-lubricated stopcock. Both methods gave similar results. The chlorine sample was dissolved in KI solution and the liberated iodine was determined by the amperometric dead-stop end-point method.[17]

(1) C. Maier, U. S. Bur. Mines Tech. Paper 360, 1925.
(2) E. Stirnemann, *Neues Jahrb. Mineral., Geol., Palaeont.*, **52A**, 334 (1925).
(3) K. Jellinek and R. Koop, *Z. physik. Chem.*, **145A**, 305 (1929).
(4) K. Sano, *J. Chem. Soc. Japan*, **59**, 1073 (1938).
(5) H. F. Johnstone, H. C. Weingartner, and W. E. Winsche, *J. Am. Chem. Soc.*, **64**, 241 (1942).
(6) O. E. Ringwald, Doctoral Dissertation, Princeton Univ., 1949.
(7) W. Kangro and E. Petersen, *Z. anorg. allgem. Chem.*, **261**, 157 (1950).
(8) H. Schafer and E. Oehler, *ibid.*, **271**, 206 (1953).
(9) L. E. Wilson and N. W. Gregory, *J. Phys. Chem.*, **62**, 433 (1958).
(10) W. Kangro and H. Bernstorff, *Z. anorg. allgem. Chem.*, **263**, 316 (1950).
(11) H. Schafer, *ibid.*, **259**, 53 (1949).
(12) J. H. Stern and N. W. Gregory, *J. Phys. Chem.*, **61**, 1226 (1957).
(13) E. Kay and N. W. Gregory, *ibid.*, **62**, 1079 (1958).
(14) P. Clausing, *Ann. Physik*, **12**, 961 (1932).
(15) I. M. Kolthoff and E. B. Sandell, "Textbook of Quantitative Inorganic Chemistry," Revised Ed., The Macmillan Co., New York, N. Y., 1947, pp. 493–494, 600, 608–609.
(16) W. B. Fortune and M. G. Mellon, *Ind. Eng. Chem. (Anal. Ed.)*, **10**, 60 (1938).
(17) G. Wernimont and F. J. Hopkinson, *ibid.*, **12**, 308 (1940).

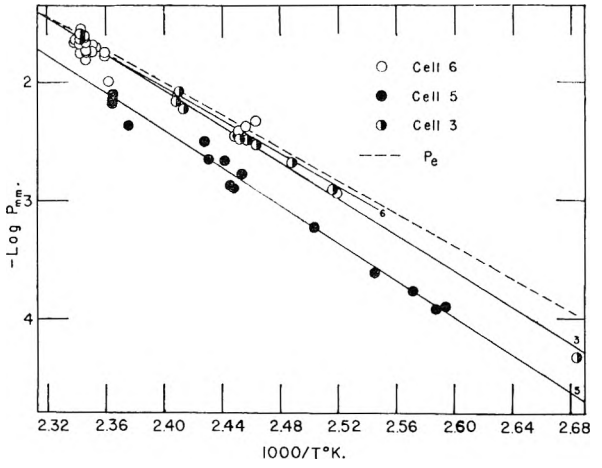

Fig. 1.—Fe_2Cl_6(g).

Steady state pressures of each species were calculated from the usual effusion equation

$$P_{mm} = \frac{17.14n(MT)^{1/2}}{a_0tK}$$

where n is the number of moles of effusate, M the molecular weight of the species in question, T the absolute temperature of the effusion vessel, and t the effusion time in seconds.

Results and Discussion

$2FeCl_3(s) = Fe_2Cl_6(g)$.—Fe_2Cl_6 effusion pressures were dependent on cell geometry, Fig 1. Steady state pressures, P_{ss}, from cell 6 are not significantly different from values predicted by extrapolation of the equation reported in ref. 9. A least squares treatment of data from each cell was used to establish the lines shown; corresponding constants in equations of the form log P(mm.) $= -AT^{-1} + B$ are listed in Table II. Data from the three cells were correlated by the equation[12]

$$P_e = P_{ss}(1 + f/\alpha) \qquad (3)$$

where P_e is the equilibrium pressure, f the ratio orifice area over cell cross-section area, and α the condensation coefficient. At each of the four temperatures listed, Table I, values of P_{ss} for each cell were calculated from the smoothed line (Fig. 1) and a least squares treatment based on (3) was used to obtain values of P_e and α.

TABLE I

EQUILIBRIUM PRESSURES AND CONDENSATION COEFFICIENTS FOR Fe_2Cl_6 OVER SOLID $FeCl_3$ FROM EFFUSION DATA

t, °C.	$P_e \times 10^3$ (mm.)	$\alpha \times 10^3$
120	1.0	5.2
130	2.7	6.4
140	7.1	7.7
150	18	9.3

TABLE II

EFFUSION STEADY STATE PRESSURES OF Fe_2Cl_6 OVER SOLID $FeCl_3$

Cell	$f \times 10^4$	$-A$	B
5	135	7790	16.27
3	25	7600	16.15
6	6.0	6902	14.51
Predicted equil. pressure effusion data and (3)		6887	14.52
Ref. 9		7142	15.11

Log P_e values predicted from effusion results are about 3% higher than those calculated from the equation given in ref. 9. α values calculated from eq. 3 and P_e values from ref. 9 are about 25% larger than those listed in Table I.

Results in Table I indicate $d\alpha/dT$ to be positive for Fe_2Cl_6. The treatment described in ref. 12 leads to values for a standard enthalpy and standard entropy of activation for vaporization at 135° of 38 kcal. mole^{-1} and 61 e.u., respectively; ΔH^0 is 33 kcal. and ΔS^0 56 e.u. for sublimation. In earlier work $d\alpha/dT$ was found to be negative for iodine,[12] which gave activation enthalpy and entropy less than the sublimation values. The different behavior may be associated with the fact that Fe_2Cl_6 molecules must be removed from an "infinite sandwich-layer-type crystal" of $FeCl_3$ in which each ferric ion is surrounded by six halogen ions, whereas the iodine crystal is composed of molecular units of the same type as those in iodine vapor.

Even though the condensation coefficient of Fe_2Cl_6 is rather small, steady state effusion pressures, when extrapolated to zero orifice area, are in reasonably good agreement with equilibrium vapor pressures extrapolated from measurements by other methods at higher temperatures.

$2FeCl_3(s) = 2FeCl_2(s) + Cl_2(g)$.—Steady state chlorine pressures are shown in Fig. 2. These points, with the exception of some runs with cell 5 for which insufficient chlorine for analysis was collected, correspond to the same experiments from which Fe_2Cl_6 pressures plotted in Fig. 1 were determined. Data shown for cell 6 were collected from 10 independent samples; usually about six successive measurements at various temperatures were made with each sample. The first values, indicated by symbols of the form ♀, in such a series were invariably much lower than subsequent values; the latter were used to fix the position of the line drawn in Fig. 2. It will be observed that pressures corresponding to this line are only *ca.* 1% of the equilibrium values (dotted line) predicted by extrapolation of data quoted in ref. 9.

The unusually low value in the initial run for each series might be associated with the initial small particle size of $FeCl_2$. In the equilibrium case at least, chlorine pressures for (2) with $FeCl_2$ in a microcrystalline state would be less than the value when $FeCl_2$ crystals are large enough for surface free energy effects to be negligible. This argument does not necessarily apply to the steady state pressures, however. In one series of measurements, corresponding data labeled o-, *ca.* 10 mole % of $FeCl_2$ was introduced before the $FeCl_3$ was sublimed into the cell; the initial point, as well as subsequent values in this series, was in general agreement with the cell 6 line. Solubility of $FeCl_2$ in $FeCl_3$ would be expected to make initial chlorine pressures high; actually, no evidence for appreciable solid solution between $FeCl_2$ and $FeCl_3$ has been observed.[3] In a number of cases in the present work, effusion was continued until virtually all of the volatile material had sublimed from the cell; other than the effect discussed above, no depend-

ence of pressures on the relative amounts of $FeCl_3$ and $FeCl_2$ was observed.

Fe_2Cl_6 pressures did not show a corresponding anomalous behavior for the initial measurements. One might expect that as cracks and crevices and roughening of the $FeCl_3$ crystals develop, the rate of the decomposition reaction would increase. The effect of such surface changes might be more readily observed in the case of the decomposition pressures, which are far below equilibrium values, than for the Fe_2Cl_6 pressures, which are moderately close to equilibrium.

Results from cell 3 are lower than those from cell 6 by another factor of *ca.* ten. Pressures shown, Fig. 2, were obtained from a single sample. Again the first measured value lies appreciably below the line drawn through the others. The order in which the temperature was changed between measurements was varied randomly.

A satisfactory set of steady state pressures was not obtained from cell 5. The capacity of this cell is small, which made it inconvenient to use large samples of $FeCl_3$; usually the sample was exhausted after three or four measurements; sufficient chlorine for analysis was obtained only at the highest temperatures and these results were widely scattered. In contrast, Fe_2Cl_6 data from this cell were quite consistent, however (see Fig. 1).

If P_e is extrapolated from data at higher temperatures[9] and eq. 3 applied, both cell 3 and 6 data give a very small condensation coefficient, 7×10^{-7} and 4×10^{-6}, respectively. Even though these values are in reasonable agreement, the effusion method does not seem well suited as an independent means of establishing the equilibrium pressure in such a case. With α of the order of 10^{-6}, the assumption that the surface area can be approximated by the cross-section of the cell is of questionable validity; some change in P_{ss} as the reaction progresses is observed and variation in the effective value of a_s from one sample to another is suggested by the relatively large scatter of results.

A number of additional experiments with cell 6 were conducted in which chlorine pressures, but not ferric chloride pressures, were determined. This permitted a series of successive measurements to be made without exposing the sample in the cell to dry air or to an inert gas, as the collecting trap for chlorine was isolated from the cell by a fluorocarbon-lubricated stopcock. The size of the $FeCl_3$ sample initially placed in the cell also was varied by a factor of the order of ten. Results of these experiments were similar in every respect to those shown in Fig. 2; steady state pressures showed no definite correlation with initial sample size but, as in earlier measurements, the first measured chlorine pressure was appreciably lower than subsequent values.

The chlorine steady state pressure dependence on temperature is not sufficiently well defined to draw quantitative conclusions about the dependence of the condensation coefficient on temperature. However, the slopes (Fig. 2) appear similar to that of the equilibrium line, *i.e.*, α does not appear to change materially with temperature, which suggests the small value of α is due mainly to probability rather than energetic factors.

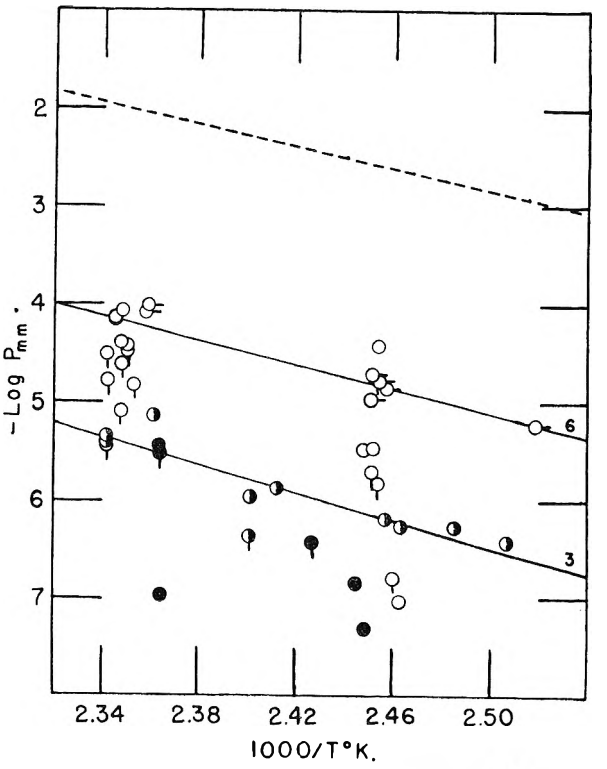

Fig. 2.—Cl_2 effusion pressures: ○, cell 6; ●, cell 5; ◑, cell 3; – – – –, P_e, Wilson and Gregory.

The value of α for reaction 1 is about ten thousand times larger than that for (2). Since both processes originate on the $FeCl_3$ crystal surface, the large difference between steady state pressures and equilibrium values must be attributed to a difference in the kinetics of the two processes rather than some factor such as the temperature of the crystal surface or geometric characteristics of the effusion cells or vacuum system.

In earlier work the reaction $2FeCl_2(s) + Cl_2(g) \rightarrow Fe_2Cl_6(g)$ was studied between 160 and 430° by the transpiration method.[9] Equilibrium constants were obtained from data between 220 and 430° but the rate of combination of chlorine with $FeCl_2(s)$ between 160 and 220° was so slow that equilibrium was not established even at a small flow rate when approached from the high chlorine pressure side. Neither of the dynamic methods, effusion or transpiration, is well suited for the study of reaction 2 at temperatures of the order of 150°.

Acknowledgment.—We are pleased to acknowledge financial assistance from the National Science Foundation.

PROPERTIES OF BASES IN ACETONITRILE AS SOLVENT. II. THE AUTOPROTOLYSIS CONSTANT OF ACETONITRILE

BY J. F. COETZEE[1] AND G. R. PADMANABHAN

Department of Chemistry, University of Pittsburgh, Pittsburgh 13, Pennsylvania

Received April 5, 1962

A conventional general purpose glass electrode responds reversibly to hydrogen ion activity in picric acid–tetraethylammonium picrate and 1,3-diphenylguanidine–diphenylguanidinium perchlorate buffers in acetonitrile as solvent. From glass electrode measurements in these buffers, and from the dissociation constants of picric acid and 1,3-diphenylguanidine in acetonitrile, determined before by conductometric and spectrophotometric methods, the autoprotolysis constant of acetonitrile is found to be equal to 3×10^{-27}. It is shown that a conventional agar–potassium chloride salt bridge is not suitable for precise potential measurements in acetonitrile.

Introduction

It is well known that acetonitrile is an excellent differentiating solvent for acid–base titrations. The main cause of the strongly differentiating nature of acetonitrile is the fact that the basic and particularly the acidic[2] properties of this solvent are very weak. The effect of the magnitude of its dielectric constant (36.0) will be considered later. In view of the numerous empirical and several theoretical acid–base studies that have already been carried out in acetonitrile, the value of the autoprotolysis constant of this solvent would be of considerable interest. However, a reliable value of this constant has not yet been reported.

In a previous communication[2] it was pointed out that several investigators had encountered the complication that conventional hydrogen ion indicator electrodes did not respond reversibly in solutions of acids in "anhydrous" acetonitrile as solvent. This limitation constituted a serious drawback for exact, quantitative acid–base studies in acetonitrile, and such studies had to be carried out almost entirely by means of conductometric[2,3] and spectrophotometric[3] methods. However, several authors (notably Hall[4]) obtained results of a semiquantitative nature by using the glass electrode, usually in conjunction with the aqueous saturated calomel electrode as reference electrode.

In this communication we report that the response of a conventional, "general purpose" type glass electrode is reversible both in picric acid–tetraethylammonium picrate and in 1,3-diphenylguanidine–diphenylguanidinium perchlorate buffers in anhydrous acetonitrile as solvent. From glass electrode measurements in these two types of buffer solutions, in conjunction with the results of conductometric studies of solutions of 1,3-diphenylguanidine[2] and conductometric as well as spectrophotometric studies of picric acid solutions,[3] the autoprotolysis constant of acetonitrile is calculated.

Experimental

Purification of the Solvent.—Sohio acetonitrile was purified by 3 different methods. **Method A** involved preliminary drying, first with silica gel, and then with phosphorus pentoxide, followed by two fractional distillations from fresh phosphorus pentoxide. **Method B** consisted of preliminary drying, first with silica gel, and then with calcium hydride, followed by two fractional distillations, first from phosphorus pentoxide, and then from calcium hydride. **Method C** was developed to remove traces of unsaturated nitriles from the solvent, and involved, successively, refluxing with a small amount of aqueous 1% potassium hydroxide solution (1 ml./l. of solvent), fractional distillation, drying with calcium hydride, and then two fractional distillations, one from phosphorus pentoxide and finally one from calcium hydride.

The water content of acetonitrile prepared by method A is generally between 1 and 2 mM, and that from methods B and C below 1 mM. The relative advantages of these three methods will be discussed elsewhere. In the present study, batches of solvent prepared by these three methods gave virtually identical results.

Buffer Components and Other Chemicals.—Baker and Adamson picric acid was recrystallized twice from acetone and dried at 80° in a vacuum oven. Eastman White Label 1,3-diphenylguanidine was recrystallized twice from toluene and dried at 40° in a vacuum oven. Tetraethylammonium picrate was prepared by titrating a 0.05-M (saturated) aqueous solution of picric acid with a 10% aqueous solution of tetraethylammonium hydroxide (Eastman) to just beyond the equivalence point (detected with a glass electrode), followed by evaporation until crystallization occurred. The product was recrystallized twice, first from water and then from 95% ethanol, and finally was dried at room temperature over phosphorus pentoxide in a vacuum desiccator. Tetraethylammonium perchlorate was prepared as described elsewhere.[5] Perchloric acid solutions were prepared by dissolving Baker and Adamson 70% aqueous perchloric acid in acetonitrile. Perchloric and picric acid and diphenylguanidine solutions always were used immediately after preparation.

Potential Measurements.—Electromotive force measurements with low resistance cells were made with a Leeds and Northrup volt potentiometer (Cat. No. 8687), and with a Beckman Model G pH meter for cells containing glass electrodes. Several Beckman "general purpose" No. 1190-80 glass electrodes were used, both with and without "conditioning" in acetonitrile for several months, which seemed to have little effect. A silver electrode was prepared by silver plating a platinum wire electrode in 0.05 M aqueous potassium argentocyanide solution (free of excess cyanide).

An H-type cell was constructed, with two 10-mm. diameter fritted glass disks of fine porosity inserted 5 cm. apart in the horizontal (salt bridge) section of the cell. Between the two disks a vertical inlet–outlet tube was provided for the introduction or removal of salt bridge solution. All three sections of the cell were stoppered to avoid absorption of moisture and carbon dioxide.

Resistance Measurements.—Resistance measurements were carried out with an Industrial Instruments Inc. Model RC-16B2 conductance bridge operated at a frequency of 1000 cycles.

Results and Discussion

The Reference Electrode.—In preliminary experiments, an aqueous saturated calomel electrode

(1) Address all correspondence to J. F. Coetzee.

(2) Part I of the series: W. S. Muney and J. F. Coetzee, *J. Phys. Chem.*, **66**, 89 (1962).

(3) I. M. Kolthoff, S. Bruckenstein, and M. K. Chantooni, Jr., *J. Am. Chem. Soc.*, **83**, 3927 (1961).

(4) H. K. Hall, Jr., *J. Phys. Chem.*, **60**, 63 (1956).

(5) I. M. Kolthoff and J. F. Coetzee, *J. Am. Chem. Soc.*, **79**, 870 (1957).

(s.c.e.) was used as the working reference electrode, together with a device (described before for voltammetric measurements in acetonitrile)[5] intended to prevent accidental introduction of water into the buffer solutions. This device consisted of a conventional aqueous potassium chloride–agar salt bridge dipping into a 0.1-*M* solution of tetraethylammonium perchlorate in acetonitrile contained in a fritted sealing tube, which in turn dipped into the buffer solution under investigation. However, in cells in which this assembly served as salt bridge, the glass electrode appeared to give drifting potentials. The cause of the drift was traced to the interface between the agar salt bridge and the acetonitrile solution, as shown by the following two experiments.

For the first experiment, one working (vertical) compartment of the H-cell described above contained an Ag/(0.01 *M* $AgNO_3$ in acetonitrile) electrode as reference (described before by Pleskov[6]). The remaining two compartments contained a 0.1-*M* solution of tetraethylammonium perchlorate in acetonitrile, with the agar–potassium chloride salt bridge of an s.c.e. dipping into the second working compartment. The e.m.f. of this cell increased with time. Representative e.m.f. and resistance data for several series of experiments are presented in Table I. It is evident that

TABLE I

APPARENT POTENTIAL OF AQUEOUS SATURATED CALOMEL ELECTRODE *vs.* PLESKOV REFERENCE ELECTRODE IN ACETONITRILE

	Expt. A[a]		Expt. B[b]		Expt. C[c]	
Time, min.	$-E$, mv.	R, ohms × 0.1	$-E$, mv.	R, ohms × 0.1	$-E$, mv.	R, ohms × 0.1
0	291.0	465	293.5	435	297.7	425
2	291.0	467	293.5	440	299.5	428
4	294.0	474	293.3	442	300.0	435
6	302.3	489	293.3	450	302.0	450
8	311.5	550	297.0	468	310.0	473
10	319.0	598	304.4	483	323.5	525
12	321.3	635	309.7	505	329.1	550
15	322.5	660			329.1	550
22	324.3	665				
30	323.5	695				
35	328.5	710				
40	333.2	710				

[a] For description of cell, see text. [b] Agar–KCl salt bridge removed, dipped into aqueous saturated KCl solution for 5 min., rinsed first with water, then with acetonitrile, and then returned to the cell for a repetition of experiment A. [c] Same as for experiment B, but in addition 0.1 *M* H_2O added to cell compartment receiving agar bridge.

the increase in e.m.f. is caused neither by a change in the Pleskov reference electrode (since all three experiments were carried out without changing the silver nitrate solution), nor by the effect of water extracted by the acetonitrile (since addition of a large amount of water had a comparatively slight effect). It is seen that the increase in e.m.f. is accompanied by an increase in cell resistance. We attribute the drift in e.m.f. to gradual deposition of a plug of solid potassium chloride and/or dehydrated agar at the tip of the salt bridge. Formation of such a plug, creating a constrained diffusion boundary, could change the liquid junction potential appreciably.

A second experiment was carried out, in which all three compartments of the H cell contained a 0.1-*M* solution of tetraethylammonium perchlorate in acetonitrile, with the agar–potassium chloride salt bridges of two saturated calomel electrodes dipping into the two working compartments. After measuring the cell e.m.f. (which was virtually zero), one salt bridge was left in position, while the other was reconditioned by the series of operations described for experiment B in Table I. After returning the reconditioned salt bridge, the cell e.m.f. was remeasured. The above sequence was repeated a number of times. Once again, it was found that the potential of the s.c.e. with the stationary salt bridge gradually became more negative, with a total drift of approximately 40 mv. in 30 min.

The aqueous saturated calomel electrode has been used extensively as a convenient working reference electrode for non-aqueous voltammetry, and its more general use in such studies has been advocated.[7] The use of the s.c.e. for such purposes is based on the implicit assumption that the liquid junction potential introduced will not change significantly during a given experiment, and will be reproducible (at least to within ±10 mv.) from one experiment to another in the same solvent. It was recognized before[5] that an aqueous agar–potassium chloride salt bridge should not be kept immersed unduly long in a solvent such as acetonitrile, because formation of a plug would increase the cell resistance and therefore the "*iR*-drop" in voltammetric measurements. To this must now be added that unless such measurements are completed very quickly (within 5 or 6 min.), potential values may be in error by as much as 0.04 v. or more, even after proper correction for the increased *iR*-drop in the cell.[8]

It can be concluded that even for those potential measurements for which an accuracy of ±10 mv. will suffice (*e.g.*, the majority of voltammetric studies), an aqueous agar–potassium chloride salt bridge should be used in acetonitrile with extreme caution. For more accurate potentiometric studies, such a salt bridge definitely should not be used in acetonitrile.[9]

All further measurements reported in this communication were made in an all-acetonitrile cell with the Pleskov Ag/(0.01 *M* $AgNO_3$ in acetonitrile) electrode as reference, and with a 0.1-*M* solution of tetraethylammonium perchlorate in acetonitrile serving as salt bridge between the two working compartments of the H-type cell described before. It was realized that this salt bridge would not eliminate the liquid junction potential between the two working compartments, because the mobilities of tetraethylammonium and perchlorate

(6) V. A. Pleskov, *Zh. Fiz. Khim.*, **22**, 351 (1948).

(7) R. C. Larson, R. T. Iwamoto, and R. N. Adams, *Anal. Chim. Acta*, **25**, 371 (1961).

(8) In the voltammetric studies in acetonitrile as solvent reported by Kolthoff and Coetzee, *J. Am. Chem. Soc.*, **79**, 870, 1852, 6110 (1957), all measurements were made as quickly as possible, generally within 5 min.

(9) An aqueous agar salt bridge containing sodium or tetraethylammonium perchlorate, rather than potassium chloride, may be more satisfactory in acetonitrile.

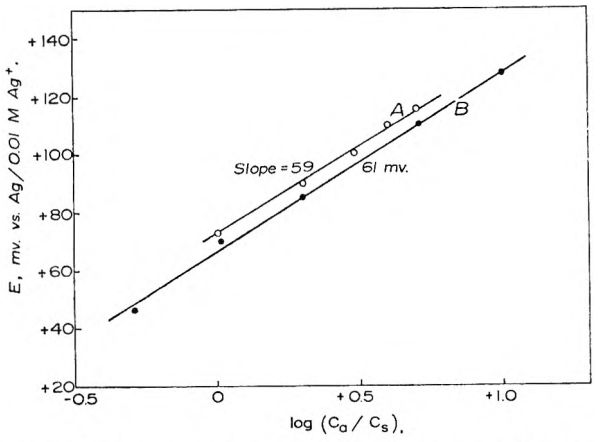

Fig. 1.—Response of glass electrode in picric acid–tetraethylammonium picrate buffers in acetonitrile. A and B: tetraethylammonium picrate concentration constant at 10^{-2} and 10^{-3} M, respectively.

ions in acetonitrile differ considerably. Limiting equivalent conductivity values for several ions in acetonitrile, recalculated in part from Walden and Birr's[10] results by using the revised values for the tetrabutylammonium and several other ions obtained by Berns and Fuoss,[11] are the following: Me_4N^+, 92.5; Et_4N^+, 83.0; Li^+, 56.2; Na^+, 66.7; K^+, 82.9; Ag^+, 81.6; Cl^-, 91.9; Br^-, 98.8; I^-, 104.1; ClO_4^-, 107.6; and picrate, 80.8. It is seen that the mobilities of common anions are generally higher than those of cations in acetonitrile. Tetramethylammonium chloride is only moderately soluble in acetonitrile. Furthermore, for the present purpose it was advisable to avoid the use of anions with appreciable basic properties. Hence a perchlorate salt was used, on the assumption that the liquid junction potential introduced would remain essentially constant.

Calibration of the Glass Electrode in Picric Acid Buffers.—In principle, many weak acid–salt combinations should be suitable as buffers in acetonitrile as solvent. Perchloric acid is the only strong (completely dissociated) acid in acetonitrile. However, the dissociation of only a few weak acids has been studied quantitatively in acetonitrile as solvent. Such studies are much more complicated than in water-like solvents.[3] In particular, in more concentrated solutions complexation (hydrogen bonding) between the anion and undissociated acid may lead to over-all dissociation reactions such as

$$2HA + \text{solvent} \rightleftharpoons H^+_{\text{solvated}} + (HA)A^- \quad (K_2)$$

or even

$$3HA + \text{solvent} \rightleftharpoons H^+_{\text{solvated}} + (HA)_2A^- \quad (K_3)$$

However, in sufficiently dilute solutions simple dissociation occurs

$$HA + \text{solvent} \rightleftharpoons H^+_{\text{solvated}} + A^- \quad (K_1)$$

The dissociation constant of picric acid in acetonitrile, for simple dissociation in dilute solution (pK_1 = 8.9), has been determined by Kolthoff, Bruckenstein, and Chantooni,[3] using conductometric and spectrophotometric methods.

Not many salts are completely dissociated in acetonitrile up to moderate concentrations (10^{-3} to 10^{-2} M).[10] Although incompletely dissociated salts could be used in buffer solutions, calculation of the hydrogen ion activity of such solutions would require knowledge of an additional equilibrium constant, namely the dissociation constant of the salt (in addition to the simple dissociation constant of the acid, K_1, as well as the formation constants of any anion–undissociated acid complexes that may be formed, given by K_2/K_1 or K_3/K_1).

The use of picric acid–tetraethylammonium picrate buffers seemed most promising for the present purpose. Picric acid undergoes simple dissociation up to relatively high concentrations,[3,12] and tetraethylammonium picrate is one of the strongest of the large number of electrolytes studied by Walden and Birr[10] (experimental slope of Λ *vs.* $C^{1/2}$ plot = 373; Onsager slope = 351); this salt is virtually completely dissociated up to 10^{-2} M concentrations.

For picric acid undergoing simple dissociation, it follows that

$$a_{H^+} = K_1 \cdot \frac{[HPi]}{[Pi^-]} \times \frac{f_0}{f_1} \qquad (1)$$

where all symbols have their customary meaning. At constant ionic strength the activity coefficient ratio, f_0/f_1, should remain essentially constant. Hence, if the glass electrode measures hydrogen ion activity reversibly, it follows from eq. 1 and the Nernst equation that a plot of the potential of the electrode as a function of the quantity log ([HPi]/[Pi$^-$]) should be linear with a slope of 59 mv. at 25° (provided junction potentials remain essentially constant).

Three glass electrodes used in several series of buffers came to equilibrium in a relatively short time (within 5 to 30 min.). The results obtained with one of the electrodes in two series of buffers, one at a constant concentration of tetraethylammonium picrate of 10^{-2} M and the other at 10^{-3} M, are represented in Fig. 1 by lines A and B, respectively. The quantities C_a and C_s refer to the total (analytical) concentrations of acid and salt, respectively, and were varied only within that region where the effect of the additional complicating reactions described above would be insignificant.

It can be concluded that the response of the glass electrode in picric acid–tetraethylammonium picrate buffers in acetonitrile as solvent is reversible.

The hydrogen ion activity of the buffer solutions used (at least for the series at ionic strength 10^{-3}) can be calculated from eq. 1 and the "reduced"[13] Debye–Hückel equation, which becomes for 25°

$$\log f_i = -355 z_i^2 D^{-3/2} S^{1/2} \qquad (2)$$

For a singly-charged ion in acetonitrile (dielectric constant D = 36.0) at an ionic strength S = 1.0 ×

(10) P. Walden and E. J. Birr, *Z. physik. Chem.*, **144**, 269 (1929).

(11) D. S. Berns and R. M. Fuoss, *J. Am. Chem. Soc.*, **82**, 5585 (1960).

(12) Unpublished results from this Laboratory (G. Cunningham).

(13) The extended form of the Debye–Hückel equation could not be used, since ion size parameters for acetonitrile as solvent are not yet available.

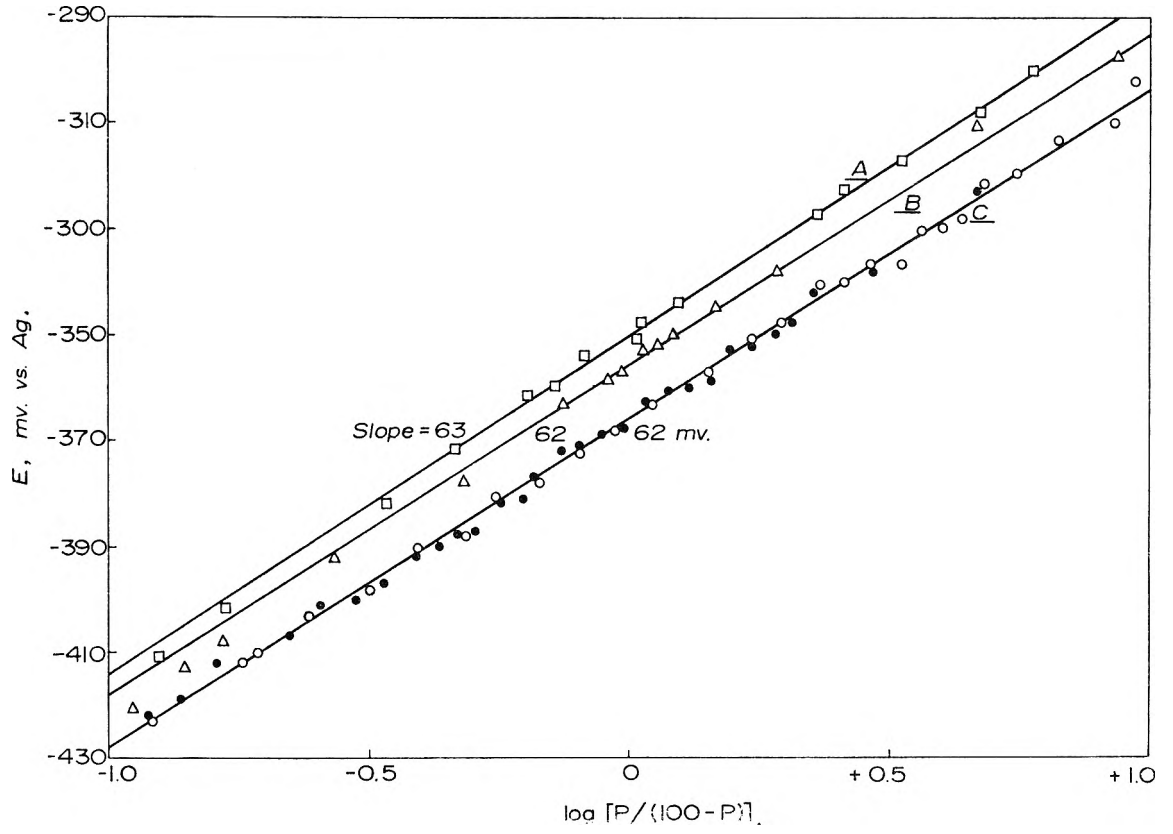

Fig. 2.—Response of glass electrode during titration of 1,3-diphenylguanidine (DPG) with perchloric acid in acetonitrile. A, 6.3×10^{-3} *M* DPG with 7×10^{-2} *M* $HClO_4$; B, 2.0×10^{-2} *M* DPG with 2.5×10^{-1} *M* $HClO_4$; C, 4.0×10^{-3} *M* DPG with 4×10^{-2} *M* $HClO_4$; closed circles, 0.1 *M* Et_4NClO_4 added; open circles, 0.2 *M* H_2O added.

10^{-3}, it follows that the activity coefficient $f_1 = 0.89$. Substituting $K_1 = 1.26 \times 10^{-9}$, and assuming that $f_0 \sim 1$, eq. 1 gives for $S = 10^{-3}$

$$a_{H^+} = 1.41 \times 10^{-9} C_a/C_s \qquad (3)$$

From line B in Fig. 1, the potential of the glass electrode *vs.* the Ag/0.01 *M* $AgNO_3$ reference electrode at $C_a/C_s = 1$ was equal to +67 mv.[14] Hence the following equation represents the response of the particular glass electrode used

$$E_{glass} \text{ (in mv. } vs. \text{ Ag ref. el.)} = 590 + 59 \log a_{H^+} \qquad (4)$$

The same electrode then was used in buffers of the type B + $BH^+ClO_4^-$.

Response of the Glass Electrode in Diphenylguanidine Buffers.—Several solutions of 1,3-diphenylguanidine were titrated with perchloric acid in acetonitrile as solvent. After each addition of titrant, the electrode came to equilibrium very quickly. The shape of the titration curves was that expected for a typical weak base–strong acid titration.

Since perchloric acid behaves as a strong (completely dissociated) electrolyte in acetonitrile, its reaction with 1,3-diphenylguanidine (B) can be represented by the simple equation

$$B + CH_3CNH^+ \rightleftharpoons BH^+ + CH_3CN \qquad (5)$$

For a base as strong as diphenylguanidine, the equilibrium lies very far to the right. Results presented later indicate that for solutions as dilute as those titrated, $BH^+ClO_4^-$ ion pair formation need not be considered. The dissociation constant, K_{BH^+}, of the protonated base is given by

$$K_{BH^+} = \frac{[B]}{[BH^+]} \times \frac{f_0}{f_1} \times a_{H^+} \qquad (6)$$

It follows from eq. 6 and the Nernst equation that a plot of the potential of the glass electrode *vs.* the quantity log $[P/(100 - P)]$, where P = percentage of B titrated, should be linear with a slope of 59 mv., provided (a) the electrode responds to hydrogen ion activity in a reversible manner, (b) neither B nor BH^+ is involved in additional reactions, (c) the ratio f_0/f_1 does not change significantly during the titration, and (d) the algebraic sum of all liquid junction potentials involved does not change significantly during the titration. Several such plots are shown in Fig. 2.

It has been shown by conductance measurements that in acetonitrile, hydrogen bonding occurs between 1,3-diphenylguanidine and its protonated form, resulting in the species BHB^+ with a formation constant of 20.[2] The effect of this complexation reaction will be to increase the slope of the E *vs.* log $[P/(100 - P)]$ plot to values greater than 59 mv. However, for solutions as dilute as those titrated the effect will be small. For example,

(14) The difference between corresponding potential values obtained at ionic strength values of 10^{-3} and 10^{-2} (67 and 73 mv., respectively, at $C_a = C_s$) is in good agreement with the 7 mv. difference predicted by eq. 2, which can give only very approximate results for an ionic strength as high as 10^{-2} in a solvent such as acetonitrile.

consider the titration of 6.3×10^{-3} M B with 7×10^{-2} M perchloric acid.

At 9.1% Titrated.—

$$[BH^+] + [BHB^+] = 5.7 \times 10^{-4}$$

$$[B] + [BHB^+] = 5.7 \times 10^{-3}$$

$$\frac{[BHB^+]}{[B][BH^+]} = 20$$

Solving, $[BHB^+] = 6 \times 10^{-5}$, $[BH^+] = 5.1 \times 10^{-4}$, and $[B] = 5.6 \times 10^{-3}$, so that $[B]/[BH^+] = 11$, rather than the value of 10 which would apply if the species BHB^+ were not formed.

At 50% Titrated.—$[B]/[BH^+] = 1$, whether or not BHB^+ is formed.

At 90.9% Titrated.—$[B]/[BH^+] = 1/11$. Hence, the slope of the plot between 9 and 91% titrated $= (\log 11) \times 59$ mv. $= 61$ mv.

A second type of hydrogen bonding reaction also must be considered, namely that which stabilizes the ion pairs of the salts of incompletely substituted ammonium bases in a non-hydrogen bonding solvent such as acetonitrile, which (unlike water-like solvents) does not mask this effect. It can be shown that such an ion-association reaction will decrease the slope of the E *vs.* log $[P/(100 - P)]$ plot. However, since addition of a common ion (as 0.1 M tetraethylammonium perchlorate) did not cause a significant change in the slope of the plot (line C in Fig. 2), it seems that 1,3-diphenylguanidinium perchlorate is extensively dissociated in acetonitrile.

Finally, it is to be expected that if the ionic strength increases significantly during the titration (lines A and B in Fig. 2), the activity coefficient ratio f_0/f_1 will increase; hence eq. 6 predicts that the slope of the E *vs.* log $[P/(100 - P)]$ plot will decrease. However, the liquid junction potential may also change. In the titration represented by line C in Fig. 2, the activity coefficient ratio, as well as the liquid junction potential, should have remained constant. It is concluded that the response of the glass electrode was reversible.

Since the titrant was prepared from 70% aqueous perchloric acid, it introduced appreciable amounts of water into the systems studied.[15] For example, in the titration of 6.3×10^{-3} M base, 7×10^{-3} M water had been introduced at the "half-neutralization" point, in addition to the approximately 1×10^{-3} M water originally present in the solvent. However, line C in Fig. 2 shows that addition of even much larger amounts of water has little influence on the slope of the line and only a moderate effect on the "half-neutralization" potential.

The Autoprotolysis Constant of Acetonitrile.—Acetonitrile is a comparatively inert amphiprotic solvent, with relatively weak basic and very weak acidic properties.[2] Hence its self-ionization will be very limited, and is assumed to occur by the reaction

$$2CH_3CN \rightleftharpoons CH_3CNH^+ + CH_2CN^- \quad (7)$$

Its autoprotolysis constant is then given by

$$K_s = a_{CH_3CNH^+} \times a_{CH_2CN^-} \quad (8)$$

and can now be calculated as follows. The over-all ionization constant of 1,3-diphenylguanidine, determined conductometrically,[2] is given by

$$K_B = a_{BH^+} \times a_{CH_2CN^-}/a_B = 2 \times 10^{-11} \quad (9)$$

In the titration of 6.3×10^{-3} M 1,3-diphenylguanidine with 7×10^{-2} M perchloric acid, the "half-neutralization" potential is equal to -350 mv. (Fig. 2, line A). From eq. 4 the corresponding hydrogen ion activity equals 1.3×10^{-16}. The ionic strength at this point is equal to 3×10^{-3} M. Hence, from eq. 2, $f_{BH^+} = f_1 = 0.81$, and from eq. 6, assuming that $f_B = f_0 \sim 1$

$$K_{BH^+} = a_B \times a_{H^+}/a_{BH^+} = 1.6 \times 10^{-16} \quad (10)$$

The product of eq. 9 and 10 gives the autoprotolysis constant of acetonitrile

$$K_B K_{BH^+} = K_s = 3 \times 10^{-27} \quad (11)$$

A value for the autoprotolysis constant of acetonitrile has been reported before by Römberg and Cruse,[16] from the results of the titration of various nitrogen bases with several weak acids, using mainly a glass electrode as hydrogen ion indicator electrode. The autoprotolysis constant of the solvent was calculated from the equivalence point potentials of those acid–base pairs which gave symmetrical titration curves. Römberg and Cruse's value of $K_s = 3.5 \times 10^{-20}$ is 7 powers of 10 larger than ours.[17]

The autoprotolysis constants of several solvents are listed in Table II. It is seen that the value for acetonitrile is much smaller than that of any other solvent listed. The value of the autoprotolysis constant of a given solvent depends on the strength of its acid as well as its basic properties, and also on the magnitude of its dielectric constant. The weaker the acid–base properties are and the lower the dielectric constant is, the smaller the autoprotolysis constant becomes. The dielectric constant of acetonitrile is somewhat higher than that of methanol, yet its autoprotolysis con-

(15) There is as yet no simple and convenient method available to prepare anhydrous solutions of perchloric acid in acetonitrile without introducing additional (more or less undesirable) substances. Anhydrous solutions of perchloric acid in acetic acid as solvent can be used for certain studies in acetonitrile, but are obviously not applicable for the present purpose. Generation of perchloric acid directly in acetonitrile by treating a solution of silver perchlorate with hydrogen chloride gas is not completely satisfactory, because the solubility of silver chloride in acetonitrile (particularly if excess chloride is present) is appreciable, owing to the stability of silver chloride complexes in acetonitrile. Likewise, on addition of anhydrous sulfuric acid to an equivalent amount of barium perchlorate in acetonitrile, a considerable amount of bisulfate is formed, since sulfate ion is a relatively strong base in acetonitrile.

(16) E. Römberg and K. Cruse, *Z. Elektrochem.*, **63**, 404 (1959).

(17) Römberg and Cruse calibrated their glass electrode in unbuffered solutions of picric acid in acetonitrile. However, on changing the picric acid concentration by a factor of 10, the potential changed by 64 mv., rather than by the 30 mv. associated with reversible response to simple dissociation (but if unilateral triple ion formation is predominant, the change would be 59 mv.). Furthermore, the value used for the (simple) dissociation constant of picric acid (2.5×10^{-7}) was much larger than that accepted by us (1.26×10^{-9}). The dissociation of weak acids in acetonitrile increases with time. Römberg and Cruse's value might have been determined for aged solutions.

stant is smaller by 10 powers of 10. This large difference is caused by the fact that acetonitrile is a weaker base and a much weaker acid than methanol.

TABLE II

AUTOPROTOLYSIS CONSTANTS OF VARIOUS SOLVENTS

Solvent	Dielectric constant (25°)	pK_s (25°)[a]
Water	78.5	14.0
Formic acid	58.5	6.2
Acetonitrile	36.0	26.5
Methanol	32.6	16.7
Ethanol	24.3	19.1
Acetic acid	6.1	14.5

[a] All values except for acetonitrile were taken from I. M. Kolthoff and S. Bruckenstein in "Treatise on Analytical Chemistry," Part I, Vol. 1, Interscience Publ., Inc., New York, N.Y., 1959, p. 484.

The titration of a strong acid (perchloric acid) with a solution of the lyate ion of acetonitrile (CH_2CN^-) should give a very large potential break at the equivalence point (over 1,000 mv. for 0.1 *M* solutions, as compared to 350 mv. in water). However, attempts to prepare such lyate ion solutions in sufficiently high concentrations for practical purposes (*e.g.*, by treatment of acetonitrile with sodium or lithium metal) only results in polymerization of the solvent. Likewise, essentially anhydrous solutions of tetraalkylammonium hydroxides in acetonitrile are not stable, at least not at ordinary temperatures. This lack of availability of a really strong base constitutes one of the major limitations of acetonitrile as a medium for acid–base reactions.

The over-all ionization constants of amines are approximately 8 powers of 10 smaller in acetonitrile than in water.[2] However, the autoprotolysis constant of acetonitrile is from 12 to 13 powers of 10 smaller than that of water. Hence, titration of amines with perchloric acid gives a potential break at the equivalence point which is from 250 to 300 mv. larger in acetonitrile than in water, and very weak bases can be titrated. Finally, it should be possible to titrate virtually all anion bases which are soluble in acetonitrile. For example, even chloride ion (pK of HCl = 8: ref. 3) is a relatively strong base in acetonitrile.

THERMODYNAMIC PROPERTIES OF INORGANIC SUBSTANCES. IV. THE HIGH TEMPERATURE HEAT CONTENTS OF TeO_2 AND Na_2TeO_4[1]

BY REIJI MEZAKI AND JOHN L. MARGRAVE

Department of Chemistry, University of Wisconsin, Madison, Wisconsin

Received April 6, 1962

The heat contents of TeO_2 and Na_2TeO_4 contained in gold capsules have been measured in a drop-type calorimeter over the ranges 446–1146 and 421–804°K., respectively. The heat of fusion of TeO_2 is 6.95 ± 0.10 kcal./mole.

Reliable high temperature thermodynamic data have not been available previously for TeO_2 or Na_2TeO_4. Estimates for TeO_2 have been given by Kubaschewski and Evans[2] based on analogies with other oxides. No information has been available for Na_2TeO_4.

Experimental Techniques and Material

The calorimeter used in this work has been described previously.[1] The apparatus has been calibrated electrically and, in addition, samples of synthetic sapphire from the National Bureau of Standards have been run for comparison purposes. The accuracy of the calorimeter is ±0.5%, while the reproducibility of a given measurement is slightly better. Several drops also were made with empty pure gold capsules at various temperatures since the heat content must be corrected for the containing capsule. The measured heat content may be compared with calculated values from Kelley[3] and in 43 runs the observed average deviations were ±1% over the range 400–700°K. and ±0.5% over the range 700–1200°K.

The TeO_2 samples studied were spectroscopically pure from Johnson, Matthey, and Co., Ltd., and showed only traces (a few p.p.m.) of Ag, Ca, Na, Si, and Mn. In the original runs with TeO_2 sealed in an argon atmosphere, some darkening was observed in the sample, but only TeO_2(s) showed in the X-ray pattern and gold was present in trace amounts. The darkening apparently was elementary Te from the disproportionation of TeO which formed as TeO_2 lost some oxygen at high temperatures. Later runs with TeO_2 sealed under O_2 did not show this darkening.

The anhydrous Na_2TeO_4 sample was procured from E. H. Sargent and Co., Inc. Spectrographic analysis showed Ca < 0.1% and traces of Ag and Al. An X-ray powder diffraction pattern of Na_2TeO_4 had the strongest lines at 5.20, 4.60, 3.00, and 2.55 Å., but no standard comparison pattern is available. At 615–635°, Na_2TeO_4 was observed to melt with some decomposition, so measurements were not extended to higher temperatures.

Results

Data from the calorimeter were processed on an IBM-650 computer as described by Mezaki[4] and the experimental results are presented in Tables I and II. A least squares fit of the experimental data provided the smoothed thermodynamic functions given in Tables III and IV.

From the data around the melting point of TeO_2, 1006°K., one can determine the heat of fusion as 6.95 ± 0.10 kcal./mole. The value 6 ± 2 kcal./mole may be derived from the slopes of vapor pressure curves for TeO_2(s) and TeO_2(l) as reported by Ueno,[5] by Soulen, Sthapitanonda, and Mar-

(1) For earlier papers in this series see: I. J. L. Margrave and R. T. Grimley, *J. Phys. Chem.*, **62**, 1436 (1958); II. M. S. Chandrasekharaiah, R. T. Grimley, and J. L. Margrave, *ibid.*, **63**, 1505 (1959); III. R. T. Grimley and J. L. Margrave, *ibid.*, **64**, 1763 (1960).

(2) O. Kubaschewski and E. Evans, "Metallurgical Thermochemistry," John Wiley and Sons, Inc., New York, N. Y., 1956.

(3) K. K. Kelley, U. S. Bureau of Mines Bulletin 584 (1960).

(4) R. Mezaki, M.S. Thesis, University of Wisconsin, 1961.

(5) K. Ueno, *J. Chem. Soc. Japan*, **62**, 990 (1941).

TABLE I

EXPERIMENTAL RESULTS FOR TeO_2

Temperature, °K.		Enthalpy, cal. mole^{-1}	
Sample (T_1)	Calorimeter (T_2)	$H_{T_1} - H_{T_2}$	$H_{T_1} - H_{298.16}$
445.16	298.85	2,297	2,308
551.56	298.90	4,190	4,202
761.46	298.97	7,762	7,775
867.06	298.95	9,703	9,715
877.66	299.09	10,040	10,054
960.36	299.19	11,472	11,488
1018.46	298.91	19,601	19,613
1085.26	298.98	21,472	21,485
1146.56	299.21	23,114	23,130

TABLE II

EXPERIMENTAL RESULTS FOR Na_2TeO_4

Temperature, °K.		Enthalpy, cal. mole^{-1}	
Sample (T_1)	Calorimeter (T_2)	$H_{T_1} - H_{T_2}$	$H_{T_1} - H_{298.16}$
421.16	298.82	4,062	4,081
459.66	298.85	5,341	5,360
548.46	298.85	8,427	8,446
803.76	299.02	16,780	16,805

grave,[6] and by Zlomanov, Novoselova, Paskinkin, Simanov, and Semenenko.[7]

More complete thermodynamic data for TeO_2(s) and Na_2TeO_4(s) are not available presently because of the lack of low temperature heat capacity measurements or reliable equilibrium studies to establish S^0_{298}. From an approximate fitting of the high temperature heat contents with a Debye equation, one estimates S^0_{298} (TeO_2) = 14 ± 2 e.u. and S^0_{298} (Na_2TeO_4) = 18.5 ± 2 e.u.[4] Kubaschewski[2] has estimated 16.8 ± 1 e.u. for TeO_2(s).

Acknowledgments.—The authors wish to acknowledge the financial support of this work by the American Smelting and Refining Company, the Selenium–Tellurium Development Committee, and the Wisconsin Alumni Research Foundation. Machine computations were carried out in the University of Wisconsin Numerical Analysis Laboratory.

(6) J. Soulen, P. Sthapitanonda, and J. Margrave, *J. Phys. Chem.*, **59**, 132 (1955).

(7) V. Zlomanov, A. Novoselova, A. Paskinkin, Y. Simanov, and K. Semenenko, *Zhur. Neorgan. Khim.*, **3**, 1473 (1958); *Chem. Abstr.*, **53**, 17615h (1959).

TABLE III

HIGH TEMPERATURE THERMODYNAMIC FUNCTIONS FOR TeO_2

Temp., °K.	$H_T - H_{298.16}$, cal. mole^{-1}	C_p, cal. mole^{-1} deg.$^{-1}$	$S_T - S_{298.16}$, cal. mole^{-1} deg.$^{-1}$
300	28	15.28	0.09
400	1,607	16.22	4.63
500	3,261	16.83	8.32
600	4,970	17.33	11.43
700	6,725	17.77	14.14
800	8,522	18.17	16.54
900	10,359	18.56	18.70
1000	12,234	18.94	20.67
1006.16(c)	12,351	18.96	20.79
1006.16(l)	19,297	27.44	33.10
1100	21,874	27.49	35.55
1200	24,625	27.54	37.95

TeO_2(c)

$$H_T - H_{298.16} = 15.58T + 1.74 \times 10^{-3}T^2 + 1.20 \times 10^5T^{-1} - 5203$$

(±1.8%, 446–960°K.)

$$C_p = 15.58 + 3.48 \times 10^{-3}T - 1.20 \times 10^8T^{-2}$$

$$\Delta H_{1006.16}(\text{fusion}) = 6946$$

TeO_2(l)

$$H_T - H_{298.16} = 26.92T + 0.26 \times 10^{-3}T^2 - 8049$$

(±0.2%, 1018–1146°K.)

$$C_p = 26.92 + 0.52 \times 10^{-3}T$$

TABLE IV

HIGH TEMPERATURE THERMODYNAMIC FUNCTIONS FOR Na_2TeO_4

Temp., °K.	$H_T - H_{298.16}$, cal. mole^{-1}	C_p, cal. mole^{-1} deg.$^{-1}$	$S_T - S_{298.16}$, cal. mole^{-1} deg.$^{-1}$
300	61	33.18	0.20
400	3,381	33.22	9.76
500	6,706	33.26	17.17
600	10,034	33.30	23.24
700	13,366	33.34	28.38
800	16,702	33.38	32.83

$$H_T - H_{298.16} = 33.07T + 0.20 \times 10^{-3}T^2 - 9877$$

(±1.9%, 421–804°K.)

$$C_p = 33.07 + 0.40 \times 10^{-3}T$$

ORTHO–PARA-HYDROGEN CONVERSION BY METAL SURFACES AT 21°K.

BY J. T. KUMMER

Scientific Laboratory, Ford Motor Company, Dearborn, Michigan

Received April 10, 1962

Ortho–para-hydrogen conversion has been used at 21°K. to study the magnetic properties of Cu, Ni, Fe, Au, Cu–Ni, and FeAu surfaces, and oxidized Ni and Fe surfaces. Copper and gold surfaces exhibit a slight paramagnetism, the origin of which is not known. It can be described in terms of an equivalent surface containing two unpaired electrons per 100 surface atoms in the case of copper and one unpaired electron per 100 surface atoms in the case of gold. The surfaces of nickel and copper–nickel alloys show a surface paramagnetism which is the same as that found for copper. No evidence was found for localized moments on the surface of the highest copper–nickel alloy used (~6% Ni) or on nickel itself other than the description given above for copper. Iron surfaces exhibit strong localized moments as do iron atoms in a gold–iron alloy surface. Oxidation produces strong moments on the surfaces of both nickel and iron.

Introduction

The conversion of ortho to para-hydrogen is generally recognized to occur by two different mechanisms. The first involves dissociation of hydrogen molecules and recombination of the atoms. The second is purely physical in nature and is induced by an inhomogeneous magnetic field such as exists as a result of the paramagnetism of unpaired electrons, or of nuclear moments. The magnetic conversion in a homogeneous phase is understood, as a result of Wigner's[1] work, in terms of the time spent within the perturbing field. The heterogeneous conversion on surfaces has been observed in a qualitative way by many workers, but rarely under conditions permitting quantitative interpretation and where a clear distinction is possible between the magnetic and dissociative mechanism. In recent years the work of Sandler,[2] Harrison and McDowell,[3] and Cunningham and Johnston[4] has made substantial progress in the understanding of the kinetics of the magnetic mechanism on surfaces. As a consequence, the study of the ortho–para-hydrogen conversion induced by perturbing inhomogeneous magnetic fields present in solid surfaces is a potentially powerful tool for improving our understanding of the magnetic properties and composition of such surfaces. Particularly important is the conversion at liquid hydrogen temperatures where the possible interference of the dissociative mechanism is virtually non-existent, and the over-all kinetics are simple by virtue of the presence of a complete monolayer of nearly 100% ortho-hydrogen on the surface.

The present work was undertaken to extend the application of the magnetic ortho–para-hydrogen conversion at liquid hydrogen temperatures to the study of metal–alloy surfaces.

Following the line of reasoning put forth by Harrison and McDowell,[3] one can visualize a surface as composed of c paramagnetic sites per cm.^{2} of magnetic moment μ_s. When this surface is covered by adsorbed hydrogen, the rate of para-hydrogen production in cc. S.T.P./min./cm.^{2} of surface is given by the expression

$$R = \left\{\frac{Kt^2}{r^8}\right\}(n)(c) \qquad (1)$$

where Kt^2/r^8 is the Wigner probability that an ortho-hydrogen molecule will be converted to para-hydrogen as it passes over a paramagnetic site. r is the distance of the molecule from the site paramagnetic moment and t is the time of interaction with the site. n is the number of hydrogen molecules passing over each site per unit time and c is the number of sites per cm.^{2} of surface. n can be expressed as n^*a where n^* is the number of ortho molecules passing over each cm.^{2} per unit time and a is the site area. Again following Harrison and McDowell[3] we can write

$$t = b/v \qquad (2)$$

where b is the root mean square of all the paths through the paramagnetic site area, and v is the velocity of lateral motion of the adsorbed hydrogen molecules along the surface.

Using Wigner's expression for K

$$K = A\mu_s^2 \qquad (3)$$

where A is a constant and μ_s is the effective magnetic moment of the paramagnetic site in Bohr magnetons, one can write for the rate

$$R = A\mu_s^2 c\left\{\frac{b^2 a n^*}{v^2 r^8}\right\} \qquad (4)$$

If one works at one temperature only and under conditions where the surfaces are covered with at least one monolayer of adsorbed hydrogen, then n^* and v in the expression will be constant. If the site has a diameter d and if this d changes as it will when one measures the conversion rate produced by different metals, then b^2a will vary as d^4. If one-half of r varies as d(r = radius of hydrogen molecule + radius of site) then r^8 also varies as d^4 for small variations in d. Because of this and because of the difficulty in estimating b, a, and r, we have assumed that part of (4) in the brackets to be constant at any one temperature, and have used the expression

$$R = B\mu_s^2 c \qquad (5)$$

for interpretation of our results. We have worked exclusively at 21.5° (vapor press. of H_2 = 1000 mm.) and at hydrogen pressures over our sample

(1) E. Wigner, *Z. physik. Chem.*, **B23**, 28 (1933).

(2) Y. L. Sandler, *J. Chem. Phys.*, **20**, 1050 (1952); *ibid.*, **21**, 2243 (1953); *Can. J. Chem.*, **32**, 249 (1954); *J. Phys. Chem.*, **58**, 54 (1954); *ibid.*, **63**, 1101 (1959).

(3) L. G. Harrison and C. A. McDowell, *Proc. Roy. Soc.* (London), **A220**, 77 (1953).

(4) C. M. Cunningham and H. L. Johnston, *J. Am. Chem. Soc.*, **80**, 2377 (1958).

of from 0.3 to 0.7 the vapor pressure at 21.5°K. so that the surface will be covered[5] with at least one monolayer of hydrogen. The hydrogens in the second layer are not converted due to the large dependence on distance. The rate has been found to be independent of total pressure in this range. It has been shown[5,6-8] that ortho-hydrogen is preferentially adsorbed over para-hydrogen, so that during an experimental ortho–para conversion run where the gas phase ortho-hydrogen may vary from 75% to as low as 30%, the surface remains very nearly completely covered with ortho-hydrogen so that the rate of para production, R, is constant with time. Since the equilibrium per cent para is ~99.7% at 21.5°K., one can neglect the back reaction in the range 75 to 30% ortho. This means that if one measures the total cumulative cc. S.T.P. of para made in an experiment in a given time, as the gas phase ortho concentration varies from 75 to ~30%, the rate of para production R that we want to use in eq. 5 is just the cc. of para made divided by the time of the experiment.

Although the constant B in eq. 5 can in principle be calculated, we have used the data of Johnston and Cunningham[4] for the conversion of ortho to para-hydrogen at liquid hydrogen temperature over surfaces with known Cr^{+3} content for this purpose. From their data for 20 Cr–Al in which they have 231×10^{-5} g. atom of Cr^{+3} on the surface and an initial rate of 1960 cc. S.T.P. of para produced/min., one can calculate using $\mu = 3.87$ Bohr magnetons that $B = 0.94 \times 10^{-19}$.

With this value of B in eq. 5 one can find $\mu^2 c$ for a metal surface if one has measured R, the rate of ortho–para-hydrogen conversion over the surface at liquid hydrogen temperatures. If there is available additional information on either μ or c, the other can be obtained. If no additional information is available, one can characterize the surface in terms of an equivalent one in which $\mu = 1.73$ and express it in terms of so many unpaired electrons per cm.^{2} or per 100 surface atoms.

Shallcross and Russell[9] have measured the ortho–para-hydrogen conversion rate over similar samples of Cu and Ni and alloys at 77°K. and above and report activation energies of 6–15 cal./mole for the reaction (chemical mechanism). Their rate data extrapolated to 21°K. give a value much too low to be measured, so that at 21°K. we are measuring a rate due to the magnetic mechanism only.

Experimental

The hydrogen used was freed of oxygen by hot copper (360°) and passed through a charcoal trap at 77°K. in order to remove any nitrogen that may have been present. The gold was made by reduction of gold chloride in acid solution by hydrazine. The iron–gold alloy was made by melting the two metals together in silica in a hydrogen atmosphere followed by quenching. After annealing, the X-ray diffraction lines were very sharp, giving a lattice parameter of 4.064 Å. for the 2 wt.% iron in gold alloy. This sample was filed up into ~50 μ particles and boiled with concentrated nitric acid to remove any contamination from the file. Although this treatment removes iron atoms from the gold–iron alloy surface, the surface again becomes populated with iron atoms after 16 hr. reduction at 530°, since under these conditions the surface and bulk are in diffusional equilibrium. The copper and nickel samples were reduced from the oxides. The copper oxide (Johnson Matthey) contained ~20 p.p.m. metallic impurities, principally silicon, iron, and calcium. The copper–nickel alloys were made by reduction of the co-precipitated carbonates. There is good evidence from the literature[10] that reduction of the co-precipitated carbonates gives a homogeneous alloy. The metals, after hydrogen treatment as specified in the tables, were treated with a stream of helium purified by charcoal at 77°K. flowing at 100 cc./min. for 0.5 hr. at reduction temperatures in order to desorb hydrogen from the surface, and the samples then were cooled in helium to 21.5°K. This temperature was maintained by the presence of liquid hydrogen in equilibrium with 1000 mm. of hydrogen pressure on the outside of the sample bulb (~7 cc. volume). The helium was evacuated at 21.5°K. and hydrogen was added to 740 mm. at the start of a run. Small samples were removed after intervals of time and analyzed for para-hydrogen by thermal conductivity. The plot of cumulative cc. of para made against time is a straight line for the first 50% conversion, the slope of which is the desired rate. The surface areas of the samples were measured by krypton adsorption at −195° using 20.8 Å.^{2} per Kr atom. The sample was protected from stopcock grease by liquid nitrogen traps and the Apiezon grease used was mixed with colloidal silver in an effort to remove sulfur compounds.

Results and Discussion

Figure 1 shows plots of some of the data. As can be seen from the graph, the rate is zero order in ortho-hydrogen as expected[4,6,7] since 25 cc. of para-hydrogen represents progress about one-half the way to equilibrium. Table I summarizes the data for copper and copper–nickel alloys, Table II contains the data obtained for nickel, Table III contains data for iron, and Table IV for an iron–gold alloy.

TABLE I

COPPER–NICKEL DATA

Sample	Redn. temp., °C.	Surface area, m.^{2}/g.	Conversion rate R, cc. of para/min./cm.^{2}
Cu	360	0.19	0.080×10^{-4}
Above sample + H_2 at 25°, 41 hr.	...	.19	$.0065 \times 10^{-4}$
Cu, CO pre-treated at 25° to remove Fe + Ni	300	.19	$.091 \times 10^{-4}$
Cu + 0.64% Ni	270	.72	$.108 \times 10^{-4}$
	430	.19	$.096 \times 10^{-4}$
Cu + 1.26% Ni	360	.27	$.102 \times 10^{-4}$
	430	.18	$.093 \times 10^{-4}$
	550	.16	$.087 \times 10^{-4}$
Cu + 6.4% Ni	450	.28	$.085 \times 10^{-4}$

It has been known since the work of Bonhoeffer[11] that the surfaces of diamagnetic solids can convert ortho to para-hydrogen. It has been proposed by Couper and co-workers[12] that this may be due to a surface lattice of unpaired electrons produced as a result of the projection of a free valency into space. Our results for copper show a conversion rate

(5) A. Van Itterbeek and J. Borghs, *Z. physik. Chem.*, **B50**, 128 (1941).

(6) Y. L. Sandler, *J. Phys. Chem.*, **58**, 58 (1954).

(7) D. White and E. N. Lassettre, *J. Chem. Phys.*, **32**, 72 (1960).

(8) E. Cremer, *Z. physik. Chem.*, **B49**, 245 (1941); **B28**, 383 (1935).

(9) P. B. Shallcross and W. W. Russell, *J. Am. Chem. Soc.*, **81**, 4132 (1959).

(10) W. K. Hall and L. Alexander, *J. Phys. Chem.*, **61**, 242 (1957).

(11) K. F. Bonhoeffer, A. Farkas, and K. W. Rummel, *Z. physik. Chem.*, **B21**, 225 (1933).

(12) A. Couper, D. D. Eley, M. J. Hulatt, and D. R. Rossington, *Bull. soc. chim. Belges*, **67**, 343 (1958).

TABLE II

NICKEL DATA

Sample	Reduction temp., °C.	Surface area, m.²/g.	Conversion rate R, cc. of para/min./cm.² of surface	Area/Ni atom,[a] Å.²
Baker's analyzed Ni	360	1.60	0.096×10^{-4}	11.6
Above sample + H_2 at 25°	..	1.60	$.050 \times 10^{-4}$	
Ni spec. pure	480	0.14	$.21 \times 10^{-4}$	
Further reduction	550	.12	$.32 \times 10^{-4}$	
Above sample + H_2 at 25°	..	.12	$.23 \times 10^{-4}$	
Further reduction	500	.12	$.41 \times 10^{-4}$	14.1
Above sample after dilute HNO_3 wash	360	.12	$.16 \times 10^{-4}$	11.9
	570	.10	$.26 \times 10^{-4}$	
Ni, oxide covered	..	.14	2.23×10^{-4}	

[a] From CO chemisorption at −78° assuming 1 CO/nickel atom.

TABLE III

IRON DATA

	Surface area	Rate, cc. of para produced/min./cm.²	μ_{eff} calcd.
Johnson Matthey iron sheet dissolved and reprecipitated			
Reduced 490°, 16 hr.	7300 cm.²/g.	5.5×10^{-4}	2.0
Above + O_2 at 25°	7300 cm.²/g.	19×10^{-4}	4.3
Johnson Matthey sponge			
Reduced 16 hr., 490°	2100 cm.²/g.	6.5×10^{-4}	2.2
Above + oxygen	2100 cm.²/g.	16×10^{-4}	3.9
Reduced 16 hr., 490°	1900 cm.²/g.	5.9×10^{-4}	2.1
Cooled in hydrogen	1900 cm.²/g.	2.6×10^{-4}	1.4

For J. M. Sponge CO chemisorption gives 13.6 Å.² per atom (one CO molecule per Ni atom), H_2 chemisorption gives 13.3 Å.² per atom (one H atom per Ni atom).

R of $\sim 0.09 \times 10^4$ cc. of para produced per minute per cm.² of surface when the surface is completely covered with ortho-hydrogen. This would give $\mu^2 c$ of 9.6×10^{13} and if we assume sites of a moment of one unpaired electron, then there would be 3.2×10^{13} of these paramagnetic sites. If we assume an average area of a copper atom of 7 Å.², then there are 1.4×10^{15} atoms/cm.², or one copper atom in 50 would have a moment of one unpaired electron. Our results also could be interpreted as each copper atom having a moment of 0.26 of a Bohr magneton, if this were possible, but not by nuclear moments of the surface copper atoms or of the ortho-hydrogen (homogeneous liquid phase conversion), since these would be too small. Exposure of the copper to hydrogen at room temperature for 41 hr. resulted in a rate of conversion of $^1/_{10}$ that for the sample as normally prepared by helium treatment at reduction temperatures. Apparently, the sites that cause ortho–para-hydrogen conversion can also chemisorb hydrogen. The activation energy for this is high enough (Kwan[13]) so that this does not take place at 21°K. The nature of the paramagnetic site on the copper surface that is responsible for the conversion is not known. It may be of interest to note that the lowest value of rate we found on our hydrogen poisoned copper is similar to that found by Cunningham and Johnston for pure γ-Al_2O_3, which converts 0.0052×10^{-4} cc. of para/min./cm.² of surface.

(13) T. Kwan, *Bull. Chem. Soc. Japan*, **23**, 73 (1950).

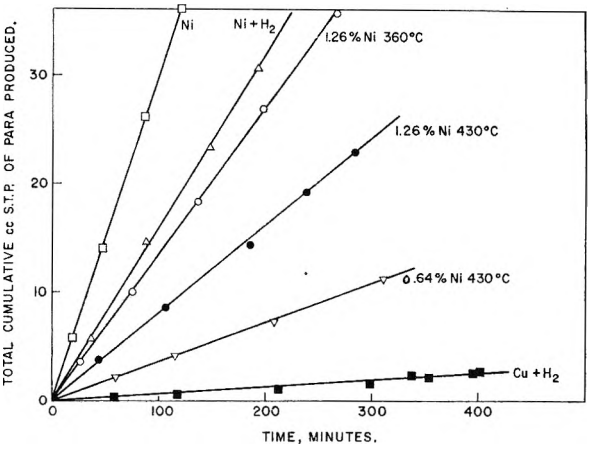

Fig. 1.—Ortho–para-hydrogen conversions over copper–nickel samples. The ordinate gives the total cumulative amount of para-hydrogen made for samples of varying weights. Ni and Ni + H_2 = 1.95 g., 1.26% Ni = 4.90 g., 0.64% Ni = 1.80 g., Cu + H_2 = 5.56 g. The temperatures given are the reduction temperatures.

The conversion rates over the Cu–Ni alloys per unit area are not much different from the value for pure copper. If each surface nickel atom had a localized moment of one unpaired electron and if the surface concentration of nickel were the same as the bulk composition and the nickel existed as an isolated atom in the surface (without pairing), then one would expect for the 6% nickel alloy a rate per unit area three times that for the copper (the copper rate corresponded to two unpaired electrons per 100 surface atoms). Since this is not observed, we have concluded that, within the limitations given above, the surface nickel atoms do not possess localized moments. We have assumed that a surface nickel atom in a copper matrix does not chemisorb hydrogen at 21°K. This will be discussed below with the nickel results.

We were interested in seeing what we might find out about the magnetic inhomogeneity of a nickel surface using ortho–para-hydrogen conversion. Our principal concern was the possibility of hydrogen chemisorption at 21°K. Although Beeck[14] has shown that evaporated nickel films chemisorb hydrogen at 20°K. and above, other experience has shown that hydrogen reduced powders chemisorb hydrogen slowly at 77°K. Schuit and de-Boer[15] have shown that the amount of hydrogen chemisorbed on nickel at 77°K. is a function of the temperature of reduction, being low for reduction at 300° and approaching total coverage after 500° reduction. Accordingly, we have measured the ortho–para conversion rate over nickel after various reduction temperatures in order to see if there were any evidence for a lowering of the rate after high temperature reduction due to hydrogen chemisorption. None was found, so we concluded that hydrogen does not chemisorb on

(14) O. Beeck, J. W. Givens, and A. W. Ritchie, *J. Colloid Sci.*, **5**, 141 (1950).

(15) G. C. A. Schuit and N. H. deBoer, *Rec. trav. chim.*, **70**, 1067 (1951).

our reduced nickel at 21°K. The effect of a small amount of oxygen left on the surface would be, as shown below, to increase the rate.

As can be seen from Table II, the nickel made by reducing Baker's analyzed NiO gave a rate similar to copper, indicating little magnetic inhomogeneity of the surface. The rate over nickel made by reducing spec. pure NiO to a very small surface area material increased somewhat with increasing reduction time, which leads us to suspect that some paramagnetic impurity insoluble in the nickel was accumulating on the very small surface of this sample (such as NiS). When this sample was washed with 0.01 N HNO_3 in conductivity water and then re-reduced, the rate was lower, which would be expected from removal of surface impurities (see Table II). CO chemisorption also suggests removal of surface impurity. If each nickel atom possesses a moment of 0.6 unpaired electron or ~1 effective Bohr magneton as judged from the saturation magnetic moment at 20°K., one would expect a rate of $\sim 1 \times 10^{-4}$ cc./min./cm.^{2}, which is 10 times the rate found for the high area nickel. The effect of chemisorbed hydrogen is very much less in the case of nickel than in the case of copper.

An oxide was formed on the nickel surface by exposure to oxygen at room temperature followed by heat treatment *in vacuo* at 200° for 15 min. in order to remove any remaining oxygen. As expected (Table II), the conversion rate over this sample was very fast due to the presence of localized moments of the Ni^{+2} ions. After the heat treatment, the surface probably was covered with patches of NiO and patches of oxygen chemisorbed on the nickel surface. If all the nickel were divalent, we would expect a rate of $\sim 7.5 \times 10^{-4}$ cc. S.T.P./min. from eq. 1, instead of the value 2.23 as found. The difference either reflects the inaccuracy of eq. 1 or our method of measuring surface area, or that the nickel atoms on the surface under the chemisorbed oxygen have a μ less than 2.83.

The conversion rate over iron is very fast. In fact, one could easily work with single crystals of iron of ~10 cm.^{2} surface area, particularly if one worked at p/p_0 of 0.3 and at a lower temperature so as to lower the amount of gas in the sample bulb. If one assumes a value of 1.4×10^{15} iron atoms/cm.^{2} of surface, which would seem reasonable, one can calculate an effective moment for each iron atom of 2–2.2 Bohr magnetons. This is lower than the effective moment of bulk iron of 3.1 magnetons. If, however, one uses the concentration of iron atoms on the surface as measured by CO and H_2 chemisorption[16] of 7.5×10^{14}/cm.^{2}, one obtains a μ_{eff} of ~2.8 for each iron atom, which is in better agreement with the bulk value. For the oxidized sample if one uses 10^{15} ferric ions per cm.^{2}, which seems reasonable, one calculates a moment of ~4 Bohr magnetons, which again is smaller than the value of 5.90 for ferric ion. The lowering of the rate due to chemisorbed hydrogen may be a result of the involvement of the unpaired electrons in the chemisorbed bond or it may be a steric effect.

(16) Assuming one CO molecule per nickel atom or one hydrogen atom per nickel atom.

In general, however, one can say that iron gives high conversion rates in approximate agreement with eq. 5 and that failure to find agreement in the case of nickel would indicate that the nickel surface does not possess localized moments.

The data for gold (Table IV) show that the surface paramagnetism per unit area of the high area gold is considerably higher than for the low area gold. It is not known whether this is due to the physical structure of the surface (a large number of edge and corner atoms) or whether this is due to some surface impurity. If it were due to an impurity, then this impurity must have been removed or altered by hydrogen reduction at 500° since this treatment resulted in a much lower surface paramagnetism per unit area. This latter surface can be described as in the case of copper as an equivalent surface of one unpaired electron per 100 gold surface atoms.

TABLE IV

Au, Fe–Au DATA

	Area	Rate: cc. of para/min./cm.^{2}
High area gold reduced 1 hr., 200°	6800 cm.^{2}/g.	0.52×10^{-4}
Gold sample above reduced 2 hr., 500°	230 cm.^{2}/g.	$.036 \times 10^{-4}$
6.3 atom % Fe–Au reduced 530°, 16 hr.	110	$.59 \times 10^{-4}$
Reduced + CO − 78.5°	110	$.44 \times 10^{-4}$
Reduced + H_2 − 78.5°	110	$.50 \times 10^{-4}$
Reduced + O_2 at 25°	110	3.8×10^{-4}

The iron–gold alloy after 530° reduction shows a high ortho–para conversion rate as compared to pure gold after reduction at a similar temperature. If one uses 3.1 Bohr magnetons for the effective moment of the iron atom on the gold surface, then using eq. 5 one finds that there are 6×10^{13} iron atoms/cm.^{2}. If one assumes 9 Å.^{2} per gold atom on the surface, then there are 1.1×10^{15} gold atoms/cm.^{2} and the atom % iron on the surface is 5.5 atom %. This is in favorable agreement with the bulk composition of 6.3 atom % iron. By carbon monoxide chemisorption, it was found that the atom % iron on the surface was 6.5 ± 0.5%, again assuming 9 Å.^{2} per gold atom.

The effect of CO and H_2 chemisorption was much less than expected since it was thought that both of these would involve bonds using the unpaired electrons responsible for the magnetic moment of the iron atom.

The gold–iron alloy after reduction and treatment with helium was exposed to oxygen at 25° for ~1 hr. and then the oxygen was evacuated. The conversion rate over this surface increased as for pure iron. In the case of iron, one undoubtedly forms an iron oxide lattice perhaps 20 Å. thick by O_2 treatment at room temperatures, the surface of which would contain the required ferric ions for conversion. In the iron–gold alloy case, the structure of the final product is not known, but from the rate observed one can say that the ferric ion is

not sterically hindered from interaction with the hydrogen molecules any more than in the case of iron oxide itself.

In summary, one can say that for the diamagnetic metals copper and gold one observes a small surface paramagnetism of unknown origin. For the transition metals, nickel and iron, one finds the existence of strong moments at each surface iron atom but no evidence for any at each surface nickel atom. Upon oxidation, each surface nickel or iron atom undergoes an increase in magnetic moment. For the binary alloy copper–nickel, there is no evidence for local moments at the surface nickel atoms, whereas for the binary alloy iron–gold, the experiment indicates that each iron atom has a moment of ~3 Bohr magnetic units. This method of measuring surface paramagnetism can be used to measure the surface composition of those binary metal alloys where one of the constituents possesses an isolated magnetic moment and the other does not.

KINETICS OF CHLORINE EXCHANGE BETWEEN CHLORIDE AND CHLOROACETATE IONS[1]

By F. J. Johnston

Department of Chemistry, University of Georgia, Athens, Georgia

Received April 10, 1962

In aqueous solutions containing chloride and chloroacetate ions, exchange of chlorine between the two species occurs simultaneously with hydrolysis of the latter. In acetate buffered systems, the exchange rate is first order with respect to each of the chloride and chloroacetate concentrations and may be described by the expression $R_x(t) = 2.26 \times 10^{11} \exp[(-26{,}400 \pm 400)/RT](Cl^-)(CH_2ClCOO^-)$ moles $l.^{-1}$ $sec.^{-1}$. The corresponding entropy of activation evaluated for 80° is −8.9 cal. $mole^{-1}$ $deg.^{-1}$. The simultaneous hydrolysis reaction was described by a pseudo-first-order behavior with the rate given by the expression $R_h(t) = 3.83 \times 10^{11} \exp[(-27{,}900 \pm 600)/RT](CH_2ClCOO^-)$ moles $l.^{-1}$ $sec.^{-1}$.

Introduction

In aqueous solutions at temperatures above 70°, chloroacetate ion undergoes hydrolysis at a measurable rate with the production of chloride and glycolate ions. With chloride labeled with chlorine-36 present in the system, it is observed that exchange with chloroacetate occurs under virtually the same conditions as the hydrolysis. This article reports the results of a kinetics study of the simultaneous exchange and hydrolysis reactions. The terminology and equations used are discussed below.

For the hydrolysis reaction

$$CH_2ClCOO^- + HOH \longrightarrow CH_2OHCOO^- + H^+ + Cl^- \quad (A)$$

$$\frac{d(Cl^-)}{dt} = -\frac{d(MCA^-)}{dt} = R_h(t) \quad (1)$$

$$(Cl^-)_t = \int_0^t R_h(t)dt = a + \rho(t) \quad (2)$$

$$(MCA^-)_t = b - \rho(t) \quad (3)$$

For the exchange reaction

$$CH_2ClCOO^- + Cl^{-*} \longrightarrow CH_2Cl^*COO^- + Cl^- \quad (B)$$

the rate is

$$R_x(t) = k_x(Cl^-)^m(MCA^-)^n \quad (4)$$

and

$$\frac{d(MCA^-)^*}{dt} = R_x(t)\left[\frac{(Cl^-)^*}{(Cl^-)} - \frac{(MCA^-)^*}{(MCA^-)}\right] - R_h(t)\frac{(MCA^-)^*}{(MCA^-)} \quad (5)$$

or[2,3]

$$\frac{d \ln (1 - F_t)}{dt} = \frac{R_x(t)(a + b)}{[a + \rho(t)][b - \rho(t)]} \quad (6)$$

F_t is the ratio of specific activity of chloroacetate ion at time t to that of total chlorine in the system at exchange equilibrium. a and b refer to initial concentrations, (MCA^-) is the monochloroacetate concentration, and the asterisk refers to labeled species.

If the exchange reaction is first order with respect to each of the exchanging species, eq. 6 becomes, upon integration

$$\ln (1 - F_t) = -k_x(a + b)t \quad (7)$$

As reaction A progresses, some undissociated chloroacetic acid is formed by association of the protons with chloroacetate ions. A kinetic study of the system then would be complicated by the change in concentration of the chloroacetate ion and by the reactions

$$CH_2ClCOOH + HOH \longrightarrow CH_2OHCOOH + H^- + Cl^- \quad (C)$$

and

(1) Presented before the division of Physical Chemistry at the March, 1962 National Meeting of the American Chemical Society in Washington, D. C.

(2) C. P. Luehr, G. E. Challenger, and B. J. Masters, *J. Am. Chem. Soc.*, **78**, 1314 (1956).

(3) R. A. Kenney and F. J. Johnston, *J. Phys. Chem.*, **63**, 1426 (1959).

TABLE I

DATA SUMMARY FOR EXPERIMENTS AT 81.5°

Set I. $(CH_2ClCOO^-)_0 = 0.0530$, $(Cl^-)_0 = 0.0077$, $(CH_3COO^-)_0 = 0.0530$
Total $C/m = 1662$

Time hr.	(CH_2ClCOO^-), M	(Cl^-), M	$C/m_{(MCA^-)}$	F	k_h (hr.$^{-1}$)	k_x (l. mole^{-1} hr.$^{-1}$)
0	0.0530	0.0077	0.8	...	.....	....
49.1	.0337	.0270	111	0.120	0.00922	0.0429
73.2	.0271	.0336	133	.179	.00916	.0444
98.7	.0212	.0395	139	.239	.00928	.0456
119.2	.0180	.0427	141	.286	.00906	.0467
				Av.	.00918	.0452

Set. II. $(CH_2ClCOO^-)_0 = 0.02500$, $(Cl^-)_0 = 0.0211$, $(CH_3COO^-)_0 = 0.0683$
Total $C/m = 1364$

0	0.0250	0.0211	0.0	...	.....	....
23.9	.0204	.0256	28.8	0.048	0.00865	0.0445
47.8	.0164	.0298	41.6	.086	.00890	.0408
72.0	.0132	.0330	50.3	.126	.00895	.0417
96.0	.0108	.0354	54.9	.173	.00882	.0428
119.8	.0088	.0373	57.0	.219	.00875	.0447
				Av.	.00881	.0429

Set III. $(CH_2ClCOO^-) = 0.0399$, $(Cl^-)_0 = 0.0206$, $(CH_3COO^-)_0 = 0.0500$
Total $C/m = 2632$

0	0.0399	0.0206	0.7	...	.....	....
24.0	.0324	.0281	87.0	0.062	0.00870	0.0439
48.0	.0263	.0341	138	.120	.00869	.0439
72.0	.0203	.0401	162	.183	.00935	.0465
96.0	.0169	.0436	171	.232	.00895	.0455
117.8	.0134	.0471	169	.290	.00916	.0479
				Av.	.00897	.0455

$$CH_2ClCOOH + Cl^{-*} \longrightarrow CH_2Cl^*COOH + Cl^- \quad (D)$$

(The hydrolysis and exchange reactions C and D have been described in a previous paper.[3]) For this reason the chloroacetate–chloride system was studied in the presence of sodium acetate. With acetate present, chloroacetic acid formation is diminished and the total ionic concentration is very nearly constant throughout the reaction.

Experimental

Sodium chloroacetate was prepared by titration of chloroacetic acid which had been fractionally crystallized from benzene. Sodium chloride-36 was prepared by titration of stock chlorine-36 labeled hydrochloric acid, as obtained from Oak Ridge Isotope Sales Department. Reagent Grade sodium acetate was used without further purification.

Groups of reaction cells of desired composition were prepared from stock solutions of known concentrations. Ten-ml. aliquots were introduced into cleaned Pyrex reaction cells, degassed, and sealed off *in vacuo*. If not reacted immediately, cells were stored at −78° until used.

Reactions were carried out by immersing the cells in an oil thermostat controlled at 71.5 ± 0.05°, and at 99.3 ± 0.10°. Following exposure, the cells were opened and the contents titrated potentiometrically with silver nitrate. The solution was allowed to stand for 24 hr., filtered, diluted to a predetermined volume, and an aliquot taken for counting. Control experiments showed that negligible exchange was induced by this procedure. Chloroacetate fractions were counted as liquid samples of 1 ml. In all cases a sufficient number of samples was counted to achieve an expected standard deviation for the net counting rate of less than 2%. The total counting rate for a cell of a given set was obtained directly by counting an aliquot of the original reaction mixture.

The fraction of equilibrium exchange at time t, F_t, was calculated as

$$F_t = \frac{(\text{specific activity of } CH_2ClCOO^-)_t}{(\text{specific activity of total Cl})_{t=\infty}}$$

Results and Discussion

Rate constants for the exchange process were evaluated from eq. 7. Rate constants for the hydrolysis reaction were calculated assuming a pseudo-first-order behavior, *i.e.*

$$k_h = \frac{1}{t} \ln \frac{b}{b - \rho(t)} \quad (8)$$

As typical of the data, the results at 81.5° are summarized in detail in Table I. The average rate constants for exchange and hydrolysis at the several temperatures studied are listed in Table II.

The exchange reaction is satisfactorily described by the second-order rate law at all concentrations and temperatures studied. In the one series at 99.3° in which no acetate buffer was added, apparent rate constants for the exchange increased with extent of reaction due to the formation of chloroacetic acid. The latter species undergoes chlorine exchange with chloride more readily than does chloroacetate ion. The reaction rate constants for this series which are listed in Table II were obtained by an extrapolation of the apparent constants to zero reaction time. (The apparent hydrolysis constants in this series decreased with time corresponding to a slower hydrolysis rate for the acid molecule. These constants were not included in the averages.)

Since the exchange reaction involves two nega-

TABLE II
SUMMARY OF RATE CONSTANTS FOR EXCHANGE AND HYDROLYSIS

Temp., °K.	$(CH_2ClCOO^-)_0$, mole l.$^{-1}$	$(Cl^-)_0$, mole l.$^{-1}$	$(CH_3COO^-)_0$, mole l.$^{-1}$	k_h, hr.$^{-1}$	k_x, l. mole^{-1} hr.$^{-1}$
372.5	0.1260[a]	0.0169	....	0.0668	0.278
	.1133	.0144	0.1133	.0767	.280
	.0567	.0130	.0567	.0760	.280
	.0464	.0333	.0336	.0677	.287
	.0232	.0166	.0731	.0784	.289
			Av.	0.0747	0.286
362.5	0.0232	0.0220	0.0690	0.0215	0.098
	.0399	.0206	.0500	.0218	.102
	.0212	.0048	.0125	.0204	.102
	.0332	.0156	.0208	.0210	.106
			Av.	0.0212	0.102
354.7	0.0399	0.0206	0.0500	0.00897	0.0455
	.0250	.0211	.0683	.00881	.0429
	.0530	.0077	.0530	.00918	.0452
			Av.	0.00898	0.0445
344.6	0.0250	0.0211	0.0683	0.00267	0.0148
	0.0530	0.0077	0.0530	0.00283	0.0158
			Av.	0.00275	0.0153

[a] Since this series involved a non-buffered system, the k's were obtained by extrapolation to zero reaction time. These were not included in the averages.

tively charged ionic species, it is expected that the rate constants would depend significantly upon ionic strength. The low specific activity of available chlorine-36 and the relatively longer half-times for the exchange compared to that for hydrolysis prevented the experiments from being carried out under concentration conditions where the Debye–Hückel limiting law is valid. In most of the experiments, the concentrations were adjusted so that the total ionic concentration was 0.114 mole l.$^{-1}$. The four series, the first and second at 99.3° and the third and fourth at 89.3° in Table II, studied at different ionic strengths gave rate constants not significantly different from those at 0.114. The results suggested that over these limited concentration ranges (corresponding to a change in μ from 0.114 to 0.241 at 99.3° and from μ = 0.039 to 0.114 at 89.3°), ionic strength effects were within experimental variations.

The hydrolysis reaction is adequately described at the lower temperatures by the pseudo-first-order relationship. At the highest temperature studied, 99.3°, the results suggest that this is an oversimplification. Note that despite the unsatisfactory behavior of the hydrolysis constants, the exchange constants are in good agreement.

Activation energies and Arrhenius factors for both reactions were evaluated in the usual way from a plot of log k *vs.* $1/T$ (Fig. 1). (The hydrolysis results at 99.3° were given less weight in making the plot.) It was found that $k_x = 2.26 \times 10^{11} \exp[(-26{,}400/RT)]$ l. mole^{-1} sec.$^{-1}$ and $k_h = 3.83 \times 10^{11} \exp[(-27{,}900/RT)]$ sec.$^{-1}$. The uncertainties in the activation energies for exchange and hydrolysis are ±400 and ±600 cal. mole^{-1}, respectively. The entropy of activation for exchange, as defined by the expression $k_x = kt/h \exp[-\Delta S^*/R] \exp[-\Delta H^*/RT]$ with $\Delta H^* = E_a - RT$, is −8.9 cal. mole^{-1} at 80°.

(4) H. M. Dawson and E. R. Pycock, *J. Chem. Soc.*, 153 (1936).

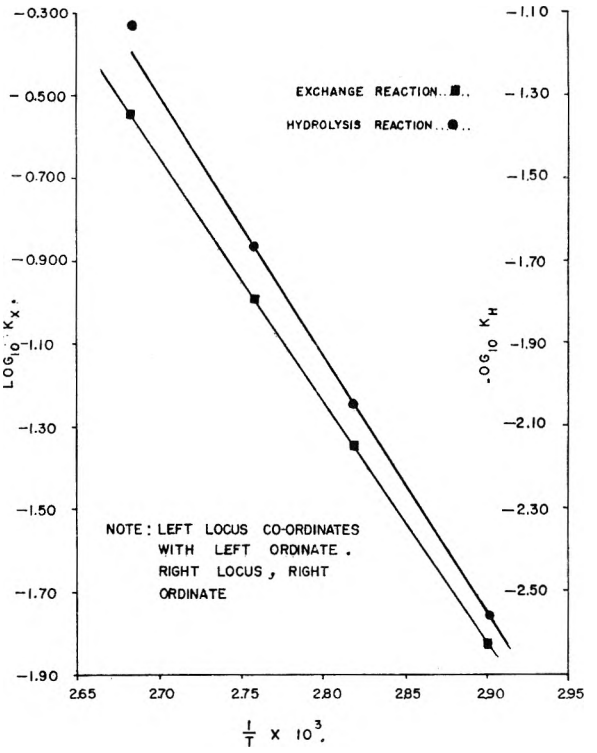

Fig. 1.—Plot of log k *vs.* $1/T$ for the exchange and hydrolysis reactions of chloroacetate ion.

Dawson and Pycock[4] suggest that the hydrolysis rate of chloroacetate ion in neutral solutions is given by the sum of three terms, one a pseudo-first-order expression, the second a bimolecular term involving the square of the chloroacetate concentration, and the third a bimolecular term involving the product of the chloroacetate and glycolate concentrations. That is, the rate expression would be

$$\text{rate} = k_1[b - \rho(t)] + k_2[b - \rho(t)]^2 + k_3[b - \rho(t)]\rho(t) \quad (9)$$

From their data at 25 and 45°

$$k_1 = 8.9 \times 10^{10} \exp(-27{,}000/RT) \text{ sec.}^{-1}$$

$$k_2 = 2.3 \times 10^{10} \exp(-25{,}300/RT) \text{ l. mole}^{-1} \text{ sec.}^{-1}$$

These constants were determined from initial rates so k_3 was not measured.

The exchange experiments were not carried out over a sufficiently wide range of chloroacetate concentrations to permit a significant estimation of the k's in (9). Assuming the above expressions for k_1 and k_2 are valid at 81.5°, the bimolecular term involving k_2 would contribute between 5 and 12% to the hydrolysis reaction at the concentrations studied. The agreement, at the lower temperature, of the pseudo-first-order hydrolysis constants obtained in the exchange studies probably reflects an insensitivity of the integrated first-order rate expression to the presence of additional fairly important terms of different order in the over-all rate equation.

In Table III are summarized the rate constants for chlorine exchange and the apparent pseudo-first-order hydrolysis constants for the chloroacetic

TABLE III

COMPARISON OF EXCHANGE AND HYDROLYSIS CONSTANTS FOR CHLOROACETATE ION AND CHLOROACETIC ACID

Reacting molecule	k_h (sec.$^{-1}$)	k_x (l. mole^{-1} sec.$^{-1}$)
CH_2ClCOO^-	$3.83 \times 10^{11} \exp(-27{,}900 \pm 600)/RT$	$2.26 \times 10^{11} \exp(-26{,}400 \pm 400)/RT$
$CH_2ClCOOH$[a]	$2.11 \times 10^{9} \exp(-24{,}800 \pm 500)/RT$	$0.95 \times 10^{11} \exp(-24{,}500 \pm 400)/RT$

[a] R. A. Kenney and F. J. Johnston, *J. Phys. Chem.*, **63**, 1426 (1959).

acid and chloroacetate systems. In the chloroacetic acid system, activation energies for exchange and hydrolysis were experimentally indistinguishable; in the chloroacetate system they are significantly different.

Pre-exponential factors for both exchange reactions are within a factor of two of that predicted on the basis of gas phase collision theory. The difference in the activation energies for the exchanges (1900 ± 800 cal. mole^{-1}) is consistent with electrostatic effects. A value of 1900 cal. mole^{-1} is equivalent to the work done in water at 80° in bringing together from an infinite distance two unit charges of like sign to a distance of 2.7 Å. apart.

The slightly smaller negative entropy of activation for the reaction involving the two ions (ΔS^* for exchange of the molecule is −10.6 e.u.) is not readily explainable. (The uncertainty in both entropy changes is approximately 1.6 e.u.)

The results are consistent with the assumption that chlorine exchange in both the chloroacetic acid–chloride and chloroacetate–chloride systems occurs by a simple bimolecular displacement type reaction. The results obtained in this work indicate that the hydrolysis and exchange reactions occur quite independently of each other.

Acknowledgment.—This work has been supported by AEC contract AT(40-1)2826.

THE CONDUCTANCE OF SYMMETRICAL ELECTROLYTES. I. POTENTIAL OF TOTAL FORCE

BY RAYMOND M. FUOSS AND LARS ONSAGER

Contribution No. 1691 from the Sterling Chemistry Laboratory, Yale University, New Haven, Connecticut

Received April 13, 1962

By means of a multiplicative expansion of the distribution functions which describe local ionic concentrations, the 1932 Onsager–Fuoss equation of continuity can be integrated with explicit retention of the Boltzmann factor, instead of approximating the latter by a truncated power series. The result is expressed in terms of the potential μ_{ji} of total force acting on a given ion: the present approximation to $\nabla\mu_{ji}$ includes the external field, the forces due to neighboring ions and to the asymmetry of the ionic atmospheres, and the virtual forces due to local concentration gradients. The differential equations which will lead to the forces from the velocity field also have been derived.

The Fuoss–Onsager conductance equation[1]

$$\Lambda = \Lambda_0 - Sc^{1/2} + Ec \log c + Jc \qquad (1)$$

precisely reproduces experimental data for dilute solutions of symmetrical electrolytes in solvents of high dielectric constant.[2-6] When combined with the hypothesis of ion association[7-9] to pairs, it leads to the more general conductance function

$$\Lambda = \Lambda_0 - Sc^{1/2}\gamma^{1/2} + Ec\gamma \log c\gamma + Jc\gamma - K_A c\gamma f^2 \Lambda \qquad (2)$$

which successfully describes observed values of conductance up to moderate concentrations ($\kappa a \approx 0.2$) in a wide variety of systems[10-17] covering the range of dielectric constant down to about 12, below which ionic interactions higher than pairwise become significant. As frequently happens in the feedback between theory and experiment, experiments designed to test the generality of the theory underlying (2) revealed some limitations, which in turn have suggested further theoretical studies.

The functional form of (2) appears to be correct, in that no systematic deviations between calculated and observed conductances appear within the claimed range of validity ($0 \leqslant \kappa a < 0.2$) of the equation. Problems have, however, arisen in the interpretation of the constants. The equation involves three arbitrary constants: Λ_0, J, and K_A. From each of these, one can compute the center-to-center contact distance a between the charged spheres which are used to represent the ions.[18-21]

(1) R. M. Fuoss and L. Onsager, *J. Phys. Chem.*, **61**, 668 (1957).
(2) J. E. Lind, Jr., J. J. Zwolenik, and R. M. Fuoss, *J. Am. Chem. Soc.*, **81**, 1557 (1959).
(3) J. E. Lind, Jr., and R. M. Fuoss, *ibid.*, **83**, 1828 (1961).
(4) J. E. Lind, Jr., and R. M. Fuoss, *J. Phys. Chem.*, **65**, 999 (1961).
(5) J. E. Lind, Jr., and R. M. Fuoss, *ibid.*, **65**, 1414 (1961).
(6) R. L. Kay, *J. Am. Chem. Soc.*, **82**, 2099 (1960).
(7) R. M. Fuoss, *ibid.*, **79**, 3301 (1957).
(8) R. M. Fuoss and C. A. Kraus, *ibid.*, **79**, 3304 (1957).
(9) R. M. Fuoss, *ibid.*, **81**, 2659 (1959).
(10) F. Accascina, A. D'Aprano, and R. M. Fuoss, *ibid.*, **81**, 1058 (1959).
(11) F. Accascina, S. Petrucci, and R. M. Fuoss, *ibid.*, **81**, 1301 (1959).
(12) E. Hirsch and R. M. Fuoss, *ibid.*, **82**, 1018 (1960).
(13) D. S. Berns and R. M. Fuoss, *ibid.*, **82**, 5585 (1960).
(14) F. Accascina and G. Craia, *Sci. Tec.*, **3**, 11 (1959).
(15) F. Accascina and L. Antonucci, *Ric. Sci.*, **29**, 1391 (1959).
(16) F. Accascina and S. Petrucci, *ibid.*, **29**, 1633 (1959); **30**, 808, 1164 (1960).
(17) F. Accascina, *J. Am. Chem. Soc.*, **81**, 4995 (1959).
(18) R. M. Fuoss, *ibid.*, **80**, 5059 (1958).
(19) R. M. Fuoss, *Proc. Natl. Acad. Sci. U.S.*, **45**, 807 (1959).
(20) R. M. Fuoss and E. Hirsch, *J. Am. Chem. Soc.*, **82**, 1013 (1960).
(21) D. S. Berns and R. M. Fuoss, *ibid.*, **83**, 1321 (1961).

For an electrolyte which conforms to the behavior theoretically predicted for the model of charged spheres, one would expect the equality

$$a_\Lambda = a_J = a_K \qquad (3)$$

where the subscripts indicate the source of the a-values.[22] It has been found that condition (3) is satisfied for a variety of electrolytes in mixed solvents down to dielectric constants of about 20, where a_J begins to increase quite rapidly, while a_Λ and a_K remain constant and equal. The precision with which J can be determined decreases as D decreases, because the association term increases exponentially, thereby masking the J-term, and making the value of a_J somewhat uncertain. Nevertheless, the trend is unmistakable, and has been observed in systems as different as potassium chloride–water–dioxane[4] and tetraalkylammonium tetraphenylborides–acetonitrile–carbon tetrachloride.[21] These observations, in our opinion, rule out any attempt to salvage the theory by changing the model *via* selective solvation to account for a variable a_J. Also, such an *ad hoc* hypothesis would lead to a new dilemma: why should solvation only affect a_J and not a_K and a_Λ? In the range of high dielectric constants, on the other hand, a_K gets into difficulties; according to theory, a plot of log K_A against D^{-1} should be linear. The plots are indeed nicely linear for $K_A > 10$, but run concave-down in the range below 10, and the computer has even delivered *negative* values of K_A for systems in solvents of high dielectric constant. Again, these values of K_Λ are uncertain, because here the J-term now masks the association term, but the trend is clearly observable.[4,5]

These two problems, variable a_J at low D and variable a_K at high D, have one element in common. To first approximation, both the J- and K_A-terms of (2) are linear in concentration. This suggests that the solution of the problems might be found in a re-examination of the approximations which lead to the linear terms in (1). Furthermore, the present theory is mathematically inelegant, in that the *ad hoc* hypothesis of ion association must be invoked in order to convert (1) into (2). Since ion-pairing is assumed to be a consequence of electrostatic forces alone,[23] it should be possible to deduce a conductance equation in which K_A does not appear as an arbitrary constant.

The purpose of the present series of papers is to develop a more general theory of the conductance of dilute solutions of symmetrical electrolytes. We shall use the same model as before[1,24] to represent the system: charged spheres in a continuum. The previous theory is based on the following approximation[25] for the Boltzmann factor

$$e^\zeta \approx 1 + \zeta + \zeta^2/2 \qquad (4)$$

where ζ is the ratio of electrostatic potential energy of one ion in the field of another to the thermal energy kT. In the present treatment, e^ζ will be retained explicitly in the integration of the equation of continuity. Anticipating the final result, it will be found that K_A is replaced by an explicit function of a, which has as its asymptotic limit the value previously assigned to K_A; in other words, the conductance function is reduced to one involving only two parameters, Λ_0 and a. In this paper, we present the integration of the equation of continuity, in order to obtain the potential of the total force acting on a reference ion, and in subsequent papers, we shall use the result to obtain the various terms of a revised conductance equation.

1. Statement of Problem.—The starting point for the theoretical study is the Onsager–Fuoss equation of continuity[26]

$$\mathrm{div}_1 (f_{ij}\mathbf{v}_{ij}) + \mathrm{div}_2 (f_{ji}\mathbf{v}_{ji}) = 0 \qquad (1.1)$$

where[27]

$$f_{ji}(\mathbf{r}_{21}) = n_j n_{ji}(\mathbf{r}_{21}) = n_i n_{ij}(\mathbf{r}_{12}) = f_{ij}(\mathbf{r}_{12}) \qquad (1.2)$$

are the symmetrical distribution functions used before and $\mathbf{v}_{ij}$ is the velocity of a j-ion in the vicinity of an ion of species i. The distribution functions and the potentials are related through the Poisson equations[28]

$$n_j \Delta\psi_j = -(4\pi/D)\Sigma_i \epsilon_i f_{ji} \qquad (1.3)$$

In order to save space, we shall take as given the material in chapters 8, 9, 10, and 13 of ref. 23. The velocities which appear in (1.1) are determined by the external field and the internal forces. The primary observable is specific conductance, which, as the ratio of current density to field strength, depends explicitly on ionic mobilities. Consequently, the problem of calculating conductance as a function of concentration reduces in principle to the mathematical problem of solving the differential eq. 1.1 and 1.3, subject to the appropriate boundary conditions.[29]

The previous attack[1,24] began by an additive expansion of the distribution functions ($f_{ji} = f^0_{ji} + f'_{ji}$); here, in order to keep the Boltzmann factor in $f^0_{ji} = n_j n_i e^\zeta$ explicit instead of approximating it by a truncated series,[25] we now make a multiplicative expansion as

$$f_{ji}(\mathbf{r}_{21}) = f^0_{ji}(r)[1 + \chi_{ji}(\mathbf{r}_{21})] \qquad (1.4)$$

where

$$f^0_{ji}(r) = n_j n_i \exp(-\epsilon_i\psi_j/kT) = n_j n_i e^\zeta \qquad (1.5)$$

is the distribution function[30] for zero external field and χ_{ji} is the perturbation produced in the spherically symmetrical f^0_{ji} by the external field X.

(22) H. Sadek and R. M. Fuoss, *J. Am. Chem. Soc.*, **81**, 4507 (1959).

(23) R. M. Fuoss and F. Accascina, "La Conducibilità Elettrolitica," Edizioni dell' Ateneo, Rome, 1959; "Electrolytic Conductance," Interscience Publishers, New York, N. Y., 1959, Chapter XVI. This reference will be cited here frequently as a source of previously derived equations; the notation FA. 3.29, for example, means eq. 29 of Chapter III.

(24) R. M. Fuoss and L. Onsager, *Proc. Natl. Acad. Sci. U.S.*, **41**, 274, 1010 (1955).

(25) FA. 12.23; FA.9.17.

(26) L. Onsager and R. M. Fuoss, *J. Phys. Chem.*, **36**, 2689 (1932); Equation 2.2.4; FA. 9.6. Further citations from this reference will be given as OF. 2.2.4, etc.

(27) OF. 2.1.6; FA. 8.3, 8.7, 8.10.

(28) OF. 2.4.2.; FA. 8.8.

(29) FA. X.

(30) FA. 9.13 and 9.15.

We shall assume as before that the field X is below that corresponding to a detectable Wien effect[31,32] and shall therefore drop all terms of quadratic or higher order in the field.

The potentials are expanded as

$$\psi_j(\mathbf{r}_{21}) = \psi^0{}_j(r) + \psi'{}_j(\mathbf{r}_{21}) \quad (1.6)$$

where $\psi^0{}_j(r)$ is the potential in the absence of an external field and $\psi'{}_j$ is the perturbation, assumed to be proportional to X. The latter is related to the corresponding term in the distribution function by the Poisson equations

$$n_j\Delta\psi_j' = -(4\pi/D)\Sigma_i\epsilon_i f^0{}_{ji}\chi_{ji} \quad (1.7)$$

The asymmetry potentials are assumed proportional to the charges by introduction of the function $\theta(r,\vartheta)$; specializing to the case of a simple electrolyte ($j = 1$, $i = 2$; $\epsilon_1 = \epsilon = -\epsilon_2$; $n_1 = n = n_2$)

$$\psi_1'(\mathbf{r}) = \epsilon_1\theta(r,\vartheta) \quad (1.8)$$

$$\psi_2'(\mathbf{r}) = -\epsilon_2\theta(r,\vartheta) \quad (1.9)$$

In terms of θ, the Poisson equations become

$$n_1\epsilon_1\Delta\theta = 4\pi\epsilon_2 f^0\chi_{21}/D \quad (1.10)$$

$$n_2\epsilon_2\Delta\theta = 4\pi\epsilon_1 f^0\chi_{21}/D \quad (1.11)$$

on expanding the sums in (1.7) and using the symmetry properties

$$\chi_{ij}(-\mathbf{r}) = -\chi_{ij}(\mathbf{r}) = \chi_{ji}(\mathbf{r}) \quad (1.12)$$

$$\chi_{jj}(\mathbf{r}) = 0 \quad (1.13)$$

$$\psi_i'(\mathbf{r}_{12}) = \psi_i'(-\mathbf{r}) = -\psi_i'(\mathbf{r}) \quad (1.14)$$

where

$$\mathbf{r}_{21} = \mathbf{r} = -\mathbf{r}_{12} \quad (1.15)$$

Equations 1.10 and 1.11 can be combined by multiplying the first by $n_2\epsilon_2\omega_2$ and the second by $n_1\epsilon_1\omega_1$ and then adding. The result is simplified by introducing a constant γ^2 defined as

$$\gamma^2 = (4\pi/DkT)(n_1\epsilon_1{}^2\omega_1 + n_2\epsilon_2{}^2\omega_2)/(\omega_1 + \omega_2) \quad (1.16)$$

which, for a binary electrolyte, becomes

$$\gamma^2 = q^2\kappa^2 = \kappa^2/2 \quad (1.17)$$

where κ^2 is the familiar Debye–Hückel parameter

$$\kappa^2 = (4\pi/D\dot{k}T)(n_1\epsilon_1{}^2 + n_2\epsilon_2{}^2) = 8\pi n\epsilon^2/DkT \quad (1.18)$$

The result of the above steps is

$$\epsilon_1\epsilon_2\Delta\theta = \gamma^2 kTe^{\zeta}\chi_{21} \quad (1.19)$$

Once χ_{21} has been determined by integration of (1.1), integration of (1.19) will give θ, and thence the relaxation field

$$\Delta X = -\nabla_x\psi_1'(a) = -\epsilon_1(\partial\theta/\partial x)_a \quad (1.20)$$

(31) L. Onsager, *J. Chem. Phys.*, **2**, 599 (1934).
(32) H. C. Eckstrom and C. Schmelzer, *Chem. Rev.*, **24**, 367 (1939).

The velocity is given by[33]

$$\mathbf{v}_{ji}(\mathbf{r}) = \mathbf{v}_i(\mathbf{r}) + \omega_i[\mathbf{K}_{ji}(\mathbf{r}) - kT\nabla \ln f_{ji}(\mathbf{r})] \quad (1.21)$$

and congruently for $\mathbf{v}_{ij}(\mathbf{r}_{12})$. Assuming superposition of the asymmetric parts of the ionic atmospheres, the force[34] $\mathbf{K}_{ji}(\mathbf{r})$ in turn is given by

$$\mathbf{K}_{ji}(\mathbf{r}) = \epsilon_i X\mathbf{i} - \epsilon_i\nabla_2\psi_i'(a) - \epsilon_i\nabla_2\psi_j(\mathbf{r}) \quad (1.22)$$

A parenthetic comment on the second term on the right is necessary. It represents the force on an i-ion due to its own atmosphere and is small compared to the third term which represents the force on the i-ion due to a neighboring j-ion and the atmosphere of the latter. Formally, the second term is $[-\epsilon_i\nabla_2\psi_i(\mathbf{r}_{12})]$, calculated at $r = a$; since a central force can produce no motion, the term $\psi_i{}^0$ in ψ_i drops out here, leaving $[-\epsilon_i\nabla_2\psi_i'(-\mathbf{r})]_a$. By the symmetry properties[35] (1.14), this is $[\epsilon_i\nabla_2\psi_i'(\mathbf{r})]_a$; hence the result above where

$$\nabla_2\psi_i'(a) \equiv [\nabla_2\psi_i'(\mathbf{r})]_a \quad (1.23)$$

The following steps combine the relevant functions to give the starting point for the mathematical analysis. The force vector (1.22) is substituted into (1.21) and the result into the equation of continuity (1.1). The expansions (1.4) and (1.6) for distribution functions and potentials are next introduced, and the various products are expanded, dropping terms of order X^2. All differentiations[36] are reduced to differentiations with respect to the coordinates of $\mathbf{r}_{21}$: $\nabla_2 = \nabla = -\nabla_1$; $\Delta_1 = \Delta = \Delta_2$. The final result of these manipulations is

$$\nabla\cdot\{e^{\zeta}[(\epsilon_1\omega_1 - \epsilon_2\omega_2)X\mathbf{i} - (\epsilon_1\omega_1\nabla\psi_2' - \epsilon_2\omega_2\nabla\psi_1') - (\omega_1 + \omega_2)kT\nabla\chi_{21} + [\epsilon_1\omega_1\nabla\psi_1'(a) - \epsilon_2\omega_2\nabla\psi_2'(a)] + (\mathbf{v}_1 - \mathbf{v}_2)]\} = 0 \quad (1.24)$$

On introducing $\theta(r,\vartheta)$ from (1.8) and (1.9), (1.24) becomes

$$\nabla\cdot[e^{\zeta}(\epsilon_1 X\mathbf{i} - \epsilon^2\nabla\theta - kT\nabla\chi_{21} + \epsilon^2\nabla\theta(a) + \mathbf{v}_1 - \mathbf{v}_2)] = 0 \quad (1.25)$$

It will be noted that the Boltzmann factor e^{ζ} appears explicitly as a multiplier *after* the divergence operator. In the earlier work, e^{ζ} was approximated by the first few terms of its series at this stage of the analysis, and disappeared from subsequent equations. The validity of the previous result for solvents of high dielectric constant and the eventual failure at low dielectric constants both thus become clear. The term in $\nabla\theta(a)$ is a constant which we shall temporarily absorb as a correction in the external field X (without change of notation); it will be calculated later and inserted.

It has been shown[37] that $\mathbf{v}_j$ is proportional to ϵ_i; therefore

(33) OF. 2.3.1.; FA. 9.11.
(34) OF. 2.5.4; FA. 9.35.
(35) FA. 9.38–42.
(36) FA. 9.37.
(37) FA. 13.124; R. M. Fuoss, *J. Phys. Chem.*, **63**, 633 (1959).

$$\mathbf{v}_1 - \mathbf{v}_2 = -2\mathbf{v}_1 = -2\mathbf{v} \qquad (1.26)$$

Since the velocity is divergence-free, and since ζ depends only on r (*i.e.*, is independent of $\cos\vartheta = x/r$), (1.25) rearranges to

$$\nabla\cdot e^{\zeta}(\epsilon_1 X\mathbf{i} - \epsilon^2\nabla\theta - kT\nabla\chi_{21}) = 2e^{\zeta}(v_x\cos\vartheta + v_r)(\mathrm{d}\zeta/\mathrm{d}r) \qquad (1.27)$$

We now require the solution of (1.27) and (1.19), subject to the boundary conditions[29]

$$\theta(\infty,\vartheta) = 0 \qquad (1.28)$$

$$[r(\partial\theta/\partial r) - \theta]_a = 0 \qquad (1.29)$$

$$\mathbf{Y}_{21}(\infty,\vartheta) = \epsilon_1 X\mathbf{i} \qquad (1.30)$$

$$(\mathbf{r}\cdot\mathbf{Y}_{21})_a = 0 \qquad (1.31)$$

where

$$\mathbf{Y}_{21} = \epsilon_1 X\mathbf{i} - \epsilon^2\nabla\theta - kT\nabla\chi_{21} \qquad (1.32)$$

2. Integration of the Equation of Continuity.—First, we define a function Z_{21} by

$$Z_{21} = -\chi_{21} - (\epsilon^2/kT)\theta \qquad (2.1)$$

which simplifies (1.27) to

$$\nabla\cdot e^{\zeta}(\epsilon_1 X\mathbf{i} + kT\nabla Z_{21}) = V(r) \qquad (2.2)$$

where we have abbreviated the inhomogeneous term of (1.27) as $V(r)$. The Poisson equation becomes

$$\Delta\theta - \gamma^2 e^{\zeta}\theta = (\gamma^2 kT/\epsilon^2)e^{\zeta}Z_{21} \qquad (2.3)$$

Next, define μ_{21} by

$$\mu_{21} = -\epsilon_1 Xx - kTZ_{21} \qquad (2.4)$$

so that (2.2) simplifies to

$$\nabla\cdot(e^{\zeta}\nabla\mu_{21}) = V(r) \qquad (2.5)$$

The symbol μ_{21} is used in (2.4) as a reminder that the quantity there defined is the potential of the total force acting on an ion of charge ϵ_1; it includes the external potential Xx, the potential due to neighboring ions and to the asymmetry in the ionic atmosphere produced by the external field, and the potential of the virtual forces arising from local concentration gradients which are expressed by χ_{21}, the perturbation of the distribution function. The Boltzmann coefficient e^{ζ} of $\nabla\mu_{21}$ in (2.5), which becomes large when pairwise distances become small or the dielectric constant becomes low ($\zeta \sim 1/rD$), explicitly takes into account the large pairwise interactions at short distances which were discarded as fluctuation terms by the previous series expansion of e^{ζ}, and which had to be restored by use of the mass action hypothesis in order to attain a usable conductance function for systems in solvents of lower dielectric constant.

Integration of (2.5) will be carried out in two steps. From our previous work,[1] we know that $V(r)$ gives rise to terms of order c log c and c in the final conductance equation. We first write μ_{21} as the sum of two terms

$$\mu_{21} = \mu_{21}' + \mu_{21}'' \qquad (2.5')$$

and define these terms as solutions of the equations

$$\nabla\cdot e^{\zeta}\nabla\mu_{21}' = 0 \qquad (2.6)$$

$$\nabla\cdot e^{\zeta}\nabla\mu_{21}'' = V(r) \qquad (2.7)$$

Here, we shall consider only (2.6), solution of which will give the leading $c^{1/2}$ term in the relaxation field, part of the c log c term, the pseudo-mass action term, and a relatively small linear term. Treatment of (2.7) will be deferred until later.

Expansion of (2.6) gives

$$\Delta\mu_{21}' + \nabla\zeta\cdot\nabla\mu_{21}' = 0 \qquad (2.8)$$

Now (2.8) is a homogeneous equation of second order; we therefore need two independent solutions, both of which satisfy the boundary conditions for $r = a$, and which reduce to the asymptotic value $(-\epsilon_i Xx)$ for large distances. The complete solution then will be a linear combination of these two, with coefficients chosen so that the final expression for μ'_{21} also conforms to the boundary conditions. The following procedure yields two independent approximate solutions which will give results valid through terms of order c in the final conductance equation. The largest part of μ'_{21} is the contribution from the external field, because the other term of (2.4) is an effect resulting from the external field as cause; we therefore approximate μ'_{21} in the second term on the left of (2.8) by

$$-\mu_{21}' \approx \epsilon_1 Xx = \epsilon_1 Xr\cos\vartheta \qquad (2.9)$$

In ζ, we use the Debye–Hückel limiting approximation for ψ_j^0

$$\zeta = -\epsilon_1\psi_2^0/kT = -\epsilon_1\epsilon_2 e^{-\kappa r}/rDkT \qquad (2.10)$$

The abbreviation

$$\beta = \epsilon^2/DkT \qquad (2.11)$$

simplifies (2.10) to

$$\zeta = \beta e^{-\kappa r}/r \qquad (2.12)$$

For later use, we define at this point the Bjerrum parameter b

$$b = \epsilon^2/aDkT = \beta/a \qquad (2.13)$$

Using the approximation (2.9) and the above symbols, (2.8) becomes

$$\Delta\mu_{21}' = \beta\epsilon_1 X\,\partial(e^{-\kappa r}/r)/\partial x \qquad (2.14)$$

A particular integral of (2.14) is found[38] to be

$$\mu_p = -(\beta\epsilon_1 X/\kappa^2)[\partial(e^{-\kappa r}/r)/\partial x] \qquad (2.15)$$

which, when combined with the solutions of the homogeneous equation $\Delta\mu'_{21} = 0$ gives a complete solution

$$\mu_{21}' = -\epsilon_1 X[(A_1 r + B_1/r^2)\cos\vartheta + \mu_p] \qquad (2.16)$$

From the condition that $\mu'_{21}(\infty,\vartheta) = -\epsilon_1 Xr\cos\vartheta$,

(38) For the method of obtaining particular integrals of equations of the type (2.14), see equations (43)–(60) of Chapter XIV of ref. 23 and the relevant discussion.

we see that $A_1 = 1$, and requiring that μ'_{21} remain finite for vanishing concentration, we find $B_1 = -\beta/\kappa^2$ by series expansion of the exponential in μ_p and inspection of the result

$$B_1/r^2 + (\beta/\kappa^2 r^2)(1 - \kappa^2 r^2/2 + \kappa^3 r^3/3 \ldots) \neq \infty \quad (2.17)$$

at $\kappa = 0$, provided B_1 has the above value. We thus have one solution of (2.8)

$$\mu_{21,1}' = -\epsilon_1 X[r - (\beta/\kappa^2 r^2) g_1(r)] \cos \vartheta = -\epsilon_1 X R_1(r) \cos \vartheta \quad (2.18)$$

where

$$g_1(r) = 1 - e^{-\kappa r}(1 + \kappa r) \quad (2.19)$$

To find a second solution, we try $e^{-\zeta} v$; again using (2.9) to give an inhomogeneous equation, and applying the above methods, we find

$$v = -\epsilon X[r - (\beta/\kappa^2 r^2) g_2(r)] \cos \vartheta = -\epsilon X R_2(r) \cos \vartheta \quad (2.20)$$

where

$$g_2(r) = 1 - e^{-\kappa r}(1 + \kappa r + \kappa^2 r^2) \quad (2.21)$$

whence

$$\mu_{21,2}' = -\epsilon_1 X e^{-\zeta}[r - (\beta/\kappa^2 r^2) g_2(r)] \cos \vartheta \quad (2.22)$$

Combining (2.18) and (2.22), the solution of (2.6) then is

$$\mu_{21}' = -\epsilon_1 X R(r) \cos \vartheta \quad (2.23)$$

where

$$R(r) = A R_1(r) + B e^{-\zeta} R_2(r) \quad (2.24)$$

The constants A and B must be evaluated next. Boundary condition (1.30) immediately gives

$$A + B = 1 \quad (2.25)$$

Boundary condition (1.31) becomes

$$(\mathbf{r} \cdot \nabla \mu_{21}')_a = [r(dR/dr)]_a = 0 \quad (2.26)$$

which, after a tedious but elementary calculation, leads to

$$A + B T_1(b) = 0 \quad (2.27)$$

where

$$T_1(b) = e^{-b}(1 + b + b^2/2) + O(\kappa a) \quad (2.28)$$

The terms in T_1 indicated by $O(\kappa a)$ are terms of order κa and higher, which came from the series expansion of $e^{-\kappa a}$ in evaluating (2.26); they would lead to terms of order $c^{3/2}$ in Λ and are therefore dropped. Solution of (2.25) and (2.27) immediately gives

$$A = -T_1/(1 - T_1) \quad (2.29)$$

$$B = 1/(1 - T_1) \quad (2.30)$$

Summarizing the results, we find for μ_{21}'

$$\mu_{21}' = -\epsilon_1 X[A R_1(r) + B e^{-\zeta} R_2(r)] \cos \varphi \quad (2.31)$$

where the constants are given by (2.29) and (2.30) and the functions in the brackets by (2.18), (2.19), (2.20), and (2.21).

For later treatment of the electrophoresis, we shall also need μ_{jj}, the potential of the total force on an ion of a given species when the reference ion at the origin is of the *same* species. Since $\chi_{jj} = 0$, and

$$f^0_{jj} = n^2 e^{-\zeta} \quad (2.32)$$

in this case, eq. 1.27 becomes

$$\nabla \cdot e^{-\zeta}(\epsilon_j X \mathbf{i} - \epsilon^2 \nabla \theta) = 0 \quad (2.33)$$

Then μ_{jj} is the solution of

$$\nabla \cdot e^{-\zeta} \nabla \mu_{jj} = 0 \quad (2.34)$$

where

$$\mu_{jj} = -\epsilon_j X x - \epsilon^2 \theta \quad (2.35)$$

By methods exactly parallel to those used to solve (2.6), the solution of (2.34) is found to be

$$\mu_{jj} = -\epsilon_j X P(r) \cos \vartheta \quad (2.36)$$

$$= -\epsilon_j X[M P_1(r) + N e^{\zeta} P_2(r)] \cos \vartheta \quad (2.37)$$

where

$$P_1(r) = r + (\beta/\kappa^2 r^2) g_1(r) \quad (2.38)$$

$$P_2(r) = r + (\beta/\kappa^2 r^2) g_2(r) \quad (2.39)$$

$$M = T_2/(T_2 - 1) \quad (2.40)$$

$$N = -1/(T_2 - 1) \quad (2.41)$$

and

$$T_2(b) = e^b (1 - b + b^2/2) \quad (2.42)$$

To summarize, integration of the equation of continuity (1.1), with explicit retention of the Boltzmann factor $e^{\zeta} = \exp(-\epsilon_i \psi_j^0/kT)$, gives (2.31) and (2.37) for the purely electrostatic part of the potential of total force acting on a given ion when an external field is applied to an electrolytic solution, (2.31) valid for unlike charges on the specified ion and the reference ion, and (2.37) for the case of like charges. The force $\nabla \mu_{ji}''$ due to the velocity field remains to be computed by integration of (2.7). Then, given the potentials μ_{ji}, μ_{jj}, the relaxation field and the electrophoresis can be obtained. We may expect the leading terms, $Sc^{1/2}$ and $Ec \log c$, of eq. 1 to remain unchanged, because those come from long range interactions of ions; we also expect the coefficient of the linear term Jc to appear with an entirely new functional dependence on a, part of which will be through e^b due to the presence of e^{ζ} in the Poisson equation (1.19), because e^{ζ} becomes e^b at $r = a$.

CONDUCTANCE OF THE ALKALI HALIDES. IV. RUBIDIUM BROMIDE IN DIOXANE–WATER MIXTURES

BY JOHN E. LIND, JR.,[1] AND RAYMOND M. FUOSS

Contribution No. 1692 from the Sterling Chemistry Laboratory, Yale University, New Haven, Connecticut

Received April 16, 1962

The conductance of rubidium bromide was measured at 25° in dioxane–water mixtures, the dielectric constants of which cover the range from 13.01 to 78.54. The data are fitted by the Fuoss–Onsager conductance equation within the experimental precision of 0.006–0.05%. Association is negligible down to a dielectric constant of 30.43 where $K_A = 13 \pm 2$. As in the cases of potassium chloride and cesium iodide, the contact distance a_J increases (from 3.1 to 5.5 Å.) with decreasing dielectric constant.

In this paper we present the conductance in dioxane–water mixtures of rubidium bromide, the third member of the group of isoelectronic alkali halides. Previously, the conductances of potassium chloride[2] and cesium iodide[3] have been reported in this solvent system. The data for these systems were fitted within an error of 0.01 to 0.05% by the equation[4,5]

$$\Lambda = \Lambda_0 - Sc^{1/2}\gamma^{1/2} + Ec\gamma \log c\gamma + J(a)c\gamma + J_2(c\gamma)^{3/2} - K_A c\gamma f^2\Lambda \quad (1)$$

where K_A, a, and Λ_0 are arbitrary constants. For all these systems, the contact distance a_J obtained from J increases systematically with decreasing dielectric constant, the hydrodynamic radii derived from Λ_0 seem unreasonably small, and K_A deviates slightly from its predicted dependence on the dielectric constant. The variation of a_J with dielectric constant is probably the consequence of other linear terms which are not included in the present theoretical treatment; the slight curvature of the log K_A–D^{-1} plots also probably arises from approximations made in the derivation of (1). The unrealistic (smaller than half the sum of lattice radii) values of the hydrodynamic radii are almost certainly a consequence of the failure of the sphere-in-continuum model for small ions in water. As might be expected, the properties of the rubidium bromide system in general lie between the properties of the potassium chloride and cesium iodide systems.

Experimental

Rubidium carbonate, purchased from A. D. MacKay Co., was analyzed by means of a flame photometer; the impurities in wt. % cation were 0.75% potassium, 0.02% sodium, and 1.2% cesium. In order to remove cesium impurity, an aqueous solution of the carbonate (20 g./10 ml.) was converted to the sulfate by titration with sulfuric acid. After recrystallizing the rubidium sulfate (23.1 g./33 ml.) three times from distilled water by evaporating to one-half the original volume and cooling, the cesium ion concentration in the remaining 12.1 g. of salt was less than 0.1%. In order to reduce the potassium impurity, 10.1 g. of rubidium sulfate was converted to the bromate in 120 ml. of water by addition of a slight deficiency of barium bromate (13.4 g.). The barium bromate was prepared by precipitation in aqueous solution from Baker's Reagent Grade barium hydroxide (29.1 g./49 ml.) and a slight excess of Mallinckrodt sodium bromate (53.0 g. slurried in 65 ml.). The barium bromate (61.8 g./1300 ml.) was recrystallized twice from water; the resulting 34.6 g. of crystals had only 0.01% by weight of cation of sodium by flame analysis. After forming the rubidium bromate and digesting it for 3 hr., the barium sulfate which had precipitated was filtered off. The rubidium bromate (7.0 g./39 ml.) was recrystallized four times from water by evaporating the solution to half its original volume and cooling until the excess rubidium sulfate had been removed, and the potassium impurity had been reduced. A slurry of 2.9 g. of rubidium bromate in 10 ml. of water was then reduced to the bromide catalytically by hydrogen with 50 mg. of platinum oxide catalyst. After reduction, 2.1 g. of salt was obtained by evaporation of the solution. Several drops of Baker's Analyzed hydrobromic acid, which had been distilled previously, were added to ensure complete conversion to the bromide. (Total conversion could not be carried out by the acid since it contained 0.02% hydrochloric acid, and accumulation of this impurity would have added a large chloride impurity to the rubidium bromide.) Since rubidium bromate forms the tribromide upon addition of hydrobromic acid, the tribromide was decomposed by heating to 50°. The 2.1 g. of salt was then recrystallized from 80 ml. of methanol, and the resulting 1.8 g. was dried to constant weight *in vacuo* at 45°. The pH of a solution of the salt indicated that, to within less than 0.01%, there is no acid present in the rubidium bromide. Flame photometer analysis on the purified rubidium bromide gave the following results expressed in wt. % of the bromide: 0.01% NaBr, 0.13% KBr, and 0.05% CsBr.

Dioxane was purified as described in the previous article,[2] and the apparatus and experimental technique were the same. The cell constants of the conductance cells are 2.4447, 1.0109, 0.39122, 0.12446, and 0.073286. The properties of the solvent mixtures are summarized in Table I and the conductance data are listed in Table II. The symbols in the tables are defined as: w = weight % dioxane in the mixture, ρ = solvent density, D = dielectric constant, η = viscosity, κ_0 = solvent conductance, c = salt concentration in equivalents/l. of solution, and $\Delta\Lambda$ = [Λ(obsd.) − Λ(calcd.)] where Λ(calcd.) is the conductance calculated from the theoretical equation. The concentration c was calculated from the experimental weight concentration m in moles/kg. of solvent by the relation $c/m = \rho - \beta m$, where β was determined experimentally for the whole range of solvent compositions to be 0.040 for rubidium bromide as compared to 0.060 for cesium iodide and 0.027 for potassium chloride.

TABLE I

PROPERTIES OF SOLVENTS

No.	w	ρ	D	$100\,\eta$	$10^6\kappa_0$
1	0.0	0.99707	78.54	0.8903	1.14
2	22.2	1.01577	60.26	1.330	0.76
3	45.6	1.03118	39.84[a]	1.835	.130
4	56.4	1.03530	30.43	1.972	.702
5	63.0	1.03614	24.81	1.983	.081
6	70.2	1.03675	19.07[a]	1.923	.151
7	78.7	1.03564	13.01	1.758	.108

[a] Calculated from wt. % dioxane by using previous data.[2,3]

(1) Du Pont Postdoctoral Research Fellow 1960–1962.

(2) J. E. Lind, Jr., and R. M. Fuoss, *J. Phys. Chem.*, **65**, 999 (1961).

(3) J. E. Lind, Jr., and R. M. Fuoss, *ibid.*, **65**, 1414 (1961).

(4) R. M. Fuoss and F. Accascina, "Electrolytic Conductance," Interscience Publishers, Inc., New York, N. Y., 1959. Symbols used in this paper are defined in Chapters 15 and 17.

(5) D. S. Berns and R. M. Fuoss, *J. Am. Chem. Soc.*, **82**, 5585 (1960).

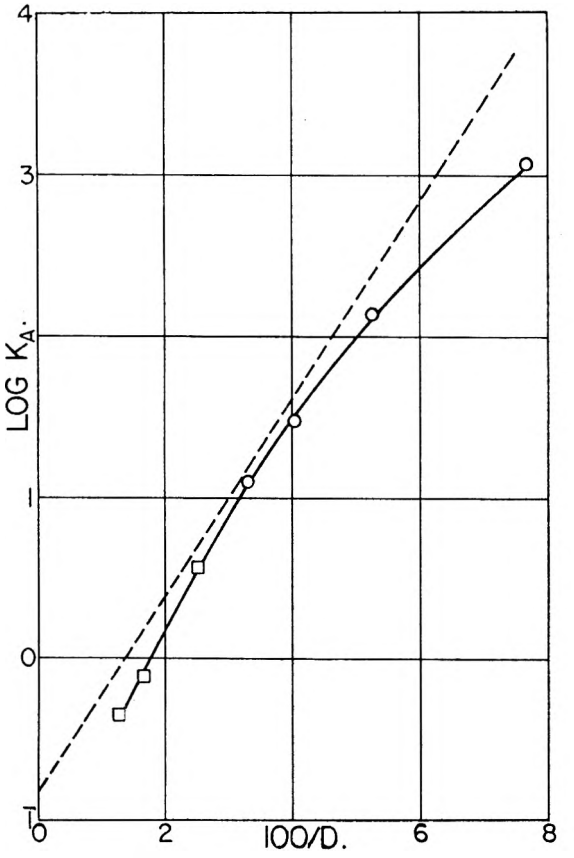

Fig. 1.—Dependence of association constant on the reciprocal of dielectric constant. Dashed line—theoretical dependence for $\mathring{a} = 4.0$.

TABLE II

CONDUCTANCE OF RUBIDIUM BROMIDE IN DIOXANE-WATER MIXTURES AT 25°

10^4c	Λ	$10^3\Delta\Lambda$	10^4c	Λ	$10^3\Delta\Lambda$
D = 78.54			D = 24.81		
102.728	146.487	− 3	30.835	43.823	− 2
80.993	147.370	− 7	24.330	44.753	+ 3
61.229	148.341	+11	18.287	45.799	+ 2
41.201	149.524	+ 5	12.413	47.069	− 4
20.200	151.216	− 8	6.1271	48.930	+ 2
D = 60.26			D = 19.07		
75.039	96.288	− 9	26.058	34.823	− 7
59.181	96.976	+10	20.585	35.992	+11
44.935	97.678	0	15.551	37.339	+ 6
29.940	98.597	− 5	10.462	39.117	−15
15.049	99.852	0	5.2133	41.801	+ 5
D = 39.84			D = 13.01		
50.219	61.958	− 3	15.829	21.371	−26
39.484	62.652	− 2	14.425	21.866	+ 4
30.300	63.357	+ 7	12.422	22.662	+18
20.497	64.256	+ 6	9.311	24.214	+ 2
9.6136	65.593	− 7	6.286	26.347	−28
			3.101	30.049	+ 6
D = 30.43					
38.026	50.554	− 5			
30.266	51.339	+ 9			
23.013	52.197	+ 3			
15.244	53.336	−10			
7.8260	54.832	+ 4			

Discussion

The data in Table II were analyzed on the IBM computer, using a modified form of Kay's program[6] for eq. 1. At dielectric constants below 30.43, the equation was fitted to the data by using all three adjustable parameters, Λ_0, a, and K_A. At higher dielectric constants, the association was so slight that the linear terms in concentration could not be separated into J and K_A terms. Therefore, K_A was set equal to zero ($\gamma = 1$) and Λ_0 and a were used to fit the equation to the data. The results of this analysis are given in Table III along with the standard deviations of the data points from values given by the equation. The standard deviations for these runs, in which the maximum concentration was always less than that corresponding to $\kappa a = 0.2$, increases from 0.006% in water to about 0.05% at the lowest dielectric constant.

TABLE III

CONSTANTS FOR RUBIDIUM BROMIDE IN DIOXANE-WATER MIXTURES AT 25°

D	Λ_0	a_J	K_A	σ
13.01	39.92 ± 0.14	5.47 ± 0.17	1119 ± 35	0.02
19.07	47.77 ± .06	4.70 ± .15	135 ± 6	.02
24.81	52.94 ± .01	4.16 ± .08	30 ± 1	.002
30.43	58.34 ± .04	4.12 ± .33	13 ± 2	.011
39.81	68.494 ± .007	2.89 ± .02	0	.007
60.26	103.048 ± .009	3.21 ± .02	0	.008
78.54	155.48 ± .01	3.13 ± .02	0	.009

The contact distance a_J increases, as was noted for the potassium chloride and cesium iodide systems, as the dielectric constant decreases. The value of a_J varies from 3.13 in water to 5.5 in the solvent with a dielectric constant of 13.01. There is a slight decrease of a_J as the dielectric constant is decreased from 78.54 to 39.81, but this is caused by the assumption that the association constant is zero. When there is a small amount of association, the value of J and consequently a_J should be increased to compensate for the term containing K_A which is opposite in sign to J. Since the variation of a_J probably is due to still missing linear terms which were excluded by approximations made in the present theory, a_J for those data for which K_A can be determined was extrapolated as a function of $1/D^4$ to infinite dielectric constant, yielding $a_J = 4.0$.

The graph of log K_A *vs.* $1/D$, shown in Fig. 1, is slightly concave downward and also is displaced downward from the graph corresponding to the following equation[7] in which $\mathring{a} = 4.0$

$$K_A = (4\pi Na^3/3000)\exp(e^2/aDkT) \quad (2)$$

The open circles represent data which could be analyzed for both K_A and a. However, the squares represent data for which K_A and a_J could not be determined directly and where $\mathring{a}_J$ was set equal to 4.0. The use of an ion size of 4.0 rather than the value in Table II does not appreciably change the fit of the conductance equation to the data when K_A is nearly zero. The vertical dis-

(6) R. L. Kay, *J. Am. Chem. Soc.*, **82**, 2099 (1960).
(7) R. M. Fuoss, *ibid.*, **80**, 5059 (1958).

placement of the graph could correspond to an ion–solvent interaction energy E_s, as defined by Gilkerson,[8] of the order of $(-kT)$.

The limiting conductance of rubidium bromide in water is 155.42; it was obtained from the experimental value of 155.48 by applying a correction of −0.06 conductance unit to allow for the impurities in the salt. The conductance of this purified salt also was compared to another sample of rubidium bromide received from A. D. MacKay Co. which was used without further purification beyond recrystallization from methanol and drying. This salt contained the following impurities in wt. % as measured on the flame photometer: 0.00% NaBr, 0.04% KBr, and 0.18% CsBr. The corrected value of the limiting conductance is 155.30, which is 0.08% lower than the conductance of the salt purified in this Laboratory. The ion size parameters for the two salts are comparable, 3.20 for this salt and 3.13 for the purified material.

From the conductance of the purified salt and the limiting conductance for the bromide ion[9] of 78.17, the limiting conductance of the rubidium ion is 77.25. While this does not agree well with Voisinet's value[9,10] of 77.81 from rubidium chloride, it is in good agreement with Kunze's[11] value of 77.20, which was obtained from the conductance of the chloride.

The Walden product for rubidium bromide is a monotonic function of the solvent composition, as shown in Fig. 2. The Stokes radii are calculated by assuming that the transference numbers in a solvent mixture are the same as in water. In Fig. 2 the Stokes radius of the rubidium ion is plotted as a function of $1/D$. The curve for the bromide ion lies about 0.02 Å. lower than the curve for the rubidium ion. When the four radii in the approximately linear portion of the graph ($19 \leq D \leq 40$) are fitted by a linear equation, these Stokes radii are given within 1% by the equations

$$10^8 R\ (\mathrm{Rb}^+) = 0.8565 + 17.79/D$$

$$10^8 R\ (\mathrm{Br}^-) = 0.8471 + 17.59/D$$

The limiting value for the sum of the radii a_Λ at infinite D is small, but if the Sutherland coefficient of $4\pi\eta$ replaces the Stokes coefficient of $6\pi\eta$, in order to correct for slippage of the solvent past the surface of the ion, δ_Λ becomes 2.56. This value is still much smaller than the sum of the crystallographic radii, which is 3.45 Å.

The ion size parameters for rubidium bromide, however, do lie between those for potassium chloride and cesium iodide; their sequence therefore is consistent with the sequence of the crystallographic dimensions. The fact that the contact distance of RbBr should lie between those of KCl and CsI also is reflected by the graphs of log K_Λ *vs.* $1/D$ which at $D = 20$, for example, predict association constants of 135, 100, and 63 for KCl, RbBr, and CsI, respectively. The association constant for CsI should be lowest, since the electrostatic interaction at contact is smallest because the ions are larger.

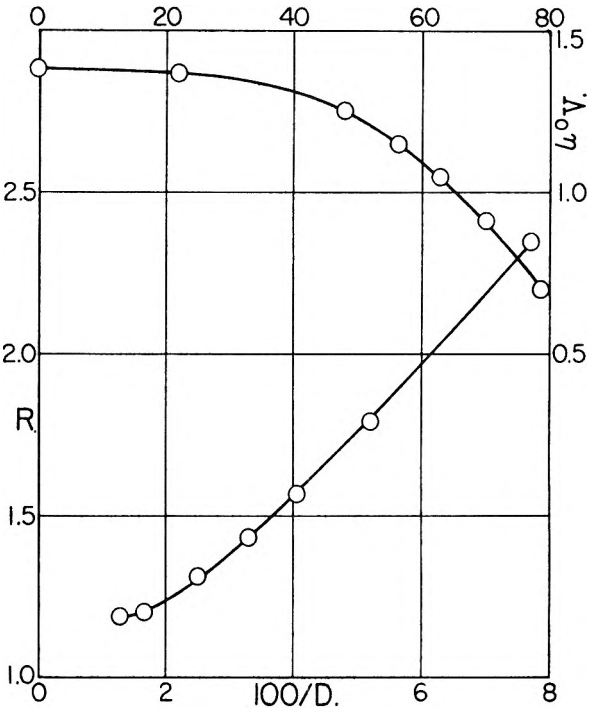

Fig. 2.—Walden product as a function of wt. % dioxane in solvent mixtures (top and right scales). Stokes radius of the rubidium ion as a function of reciprocal dielectric constant (left and bottom scales).

(8) W. R. Gilkerson, *J. Chem. Phys.*, **25**, 1199 (1956).
(9) B. B. Owen, *J. chim. phys.*, **49**, C-72 (1952).
(10) W. E. Voisinet, Dissertation, Yale University, 1951.
(11) R. W. Kunze, unpublished observations.

RADIOCARBON-LABELLED COMPOUNDS PRODUCED BY THE NEUTRON IRRADIATION OF CRYSTALLINE ACETAMIDE[1]

BY THOMAS W. LAPP AND ROBERT W. KISER

Department of Chemistry, Kansas State University, Manhattan, Kansas

Received April 28, 1962

An investigation has been made into the nature and relative amounts of the radiocarbon activities produced by dissolution in water of pile-neutron irradiated acetamide. The largest amounts of the activity isolated were present in propionamide, acetamide, acetylacetone, malonamide, and succinamide. Possible paths are suggested which lead to the final products observed in solution.

Introduction

During the neutron irradiation of nitrogen-containing compounds, a carbon-14 atom is produced with a recoil energy of 40,000 e.v. The kinetic energy imparted to the carbon atom is sufficient to cause complete bond rupture and projection of the recoil carbon-14 atom into its surroundings. This excess kinetic energy is dissipated to the surroundings in a period of about 10^{-13} sec., during which time free radicals and ions are formed in the regions near the recoil path. The fragmentation and recombination processes, including the processes involving the recoil carbon-14 atom, result in a complex mixture of both unlabelled and carbon-14-labelled products. Only one labelled product is formed by each recoil event. In view of the energy available at the site of entrapment, a variety of compounds can be formed. This is evidenced by the observed diversity of products produced in the neutron irradiations.

Numerous approaches to the determination of the reactions and the ultimate fates of the carbon-14 recoil atoms are possible. The investigation of specific products and the degree of labelling present in each product may be carried out; in addition, a complete product analysis may be made. The investigation of specific types or classes of compounds produced as a result of the irradiation is also valuable in attempting to elucidate the processes occurring during the recombination period.

Wolf and co-workers[2] have investigated the formation of carbon-14-labelled acetamide, propionamide, and acetone in the neutron irradiation of crystalline acetamide. The degree of labelling at various positions in each of the products also was studied. Tachikawa and Tsuchihashi[3] recently have investigated carbon-14-labelled products produced by the neutron irradiation of solid propionamide. However, in the latter study, the degree of position-labelling of the propionamide, butyramide, isobutyramide, and methyl ethyl ketone products studied was not ascertained.

In this study, the approach taken has been twofold: first, to separate propionamide, propionic acid, acetamide, and acetic acid and to determine the activity present in each of these products; and second, to study the presence of carbon-14 atoms in the "simpler" compounds. In the present investigation, the target compound was dissolved in water prior to analysis. The two specified objectives have been realized, and are found to aid in arriving at an improved understanding of the recombination processes.

The results obtained in this study are in agreement with those reported by Wolf and co-workers. In addition, information also has been obtained concerning the activity incorporated in a number of "simpler" compounds, as well as other more complex compounds, produced by the neutron irradiation of crystalline acetamide. The term "simpler" compounds is employed to designate those compounds, containing either one or two carbon atoms, which could be produced by dissociation of the acetamide molecule. The specific techniques employed and a discussion of our experimental results are presented below.

Experimental

Sample Preparation and Irradiation.—Acetamide (Eastman Red Label) was dried for approximately 24 hr. in a desiccator (sulfuric acid drying agent). A sample weighing 4.251 g. was placed in a quartz ampoule which was then attached to a vacuum system. Oxygen was rigorously excluded from the sample by repeatedly flushing the ampoule and its contents thoroughly with argon and evacuating to pressures of less than 1 μ. The quartz ampoule subsequently was sealed off under vacuum with a hand torch. The irradiations were carried out at Oak Ridge National Laboratories in the graphite reactor; pertinent data are as follows: neutron flux, approximately 5×10^{11} cm.$^{-2}$ sec.$^{-1}$; irradiation time, 670 hr.; γ-ray flux, 4.9×10^{5} r. hr.$^{-1}$; maximum sample temperature, 80°. The sample was stored for 22 months following irradiation; upon opening the ampoule, the contents were transferred to a Pyrex storage bottle under an argon atmosphere. Since acetamide is somewhat hygroscopic, the sample was kept in the desiccator during the entire course of the experimental study.

Preliminary Experiments.—Each carrier or its derivative isolated was dissolved either directly or by use of a suitable solvent into a scintillator solution. All activity measurements were made using a Packard Tri-Carb Liquid Scintillation Spectrometer. The counting efficiency and scintillator solution have been described previously.[4] The total carbon-14 activity of the irradiated sample was determined by dissolution of known portions in water. Aliquots were taken and the total activity was determined by liquid scintillation counting; the average value for two determinations made over a period of two months was 5.50 $\pm$ 0.06 μc. for the total sample; *i.e.*, 1.26 $\pm$ 0.01 μc./g.

In order to establish the distribution of the carbon-14 activity among the various species likely to result upon dissolution of the irradiated sample in water, solutions of irradiated acetamide samples were subjected to analysis for the chemical species listed in Table I. The apparatus

(1) This work was supported in part by the U. S. Atomic Energy Commission under Contract No. AT(11-1)-751 with Kansas State University. A portion of a dissertation to be presented by T. W. Lapp to the Graduate School of Kansas State University in partial fulfillment for the degree of Doctor of Philosphy in Chemistry.

(2) A. P. Wolf, C. S. Redvanly, and R. C. Anderson, *J. Am. Chem. Soc.*, **79**, 3717 (1957).

(3) E. Tachikawa and G. Tsuchihashi, *Bull. Chem. Soc. Japan*, **34**, 770 (1961).

(4) T. W. Lapp and R. W. Kiser, *J. Phys. Chem.*, **66**, 152 (1962).

used in the dissolution of the samples has been described in detail elsewhere.[4]

Chemical Separations.—Analyses usually were made for one carrier in each solution of the target sample; in a few cases, two or three carriers were added and analyzed per solution of target sample. The principal problem encountered in the procedures employed was the separation of the various activities free from contamination. Therefore, all compounds and derivatives isolated were purified to constant specific activity by repeated crystallizations or distillations in our attempt to achieve radiochemical purity.

Separation techniques for carbon dioxide, hydrogen cyanide, formaldehyde, formic acid, methylamine, and urea have been described.[4] We note briefly here only those analytical procedures which are new and germane to this study.

Acetic Acid and Acetone.—Acetone and acetic acid were removed by distillation and directly, but separately, dissolved into the scintillator solution.

Acetamide.—Acetamide was converted to the corresponding acetonitrile by heating with phosphorus pentoxide in diethylbenzene. The acetonitrile was removed by distillation and a purified sample was dissolved directly into the liquid scintillator.

Propionic Acid.—This was dissolved directly into the scintillator solution following distillation.

Propionamide.—Propionamide was converted to propionitrile with phosphorus pentoxide in diethylbenzene. The propionitrile was removed by distillation and dissolved directly into the scintillator solution.

Diacetamide.—Extraction with diethyl ether of an aqueous solution of the irradiated acetamide, containing added amounts of diacetamide, was followed by partial evaporation of the ether layer and then cooling to 0°, thereby carrying out the radio-labelled diacetamide. The diacetamide was recrystallized from Skelly C and dissolved directly into the scintillator solution.

Methanol.—Methanol was removed by distillation and dissolved directly into the scintillator solution.

Ethanol.—Ethanol was dissolved directly into the scintillator solution following removal by distillation.

Malonamide.—Malonamide was separated by repeated reerystallizations from 95% ethanol. Dissolution into the scintillator solution was accomplished by dissolving the malonamide in a known amount of water and adding an aliquot to the scintillator solution.

Succinamide.—Succinamide was separated by multiple recrystallizations from water. A portion of the recrystallized succinamide was dissolved in a known quantity of water and an aliquot of the aqueous solution added to the scintillator solution.

Results of Analysis.—The results obtained by the procedures described above are given in Table I. In all cases the data reported are based on specific activity measurements. The percentage activity is based on the total activity of aliquots of aqueous solutions of the original irradiated acetamide sample.

The total activity isolated in this study was 34.3% of the total carbon-14 activity induced in the acetamide sample by pile neutron irradiation. Malonamide, propionamide, 2,4-pentanedione, acetamide, and succinamide were found to contain the majority of the activity isolated in this study (75% of the total activity isolated).

TABLE I

CARBON-14 DISTRIBUTION AMONG VARIOUS COMPOUNDS RESULTING FROM PILE NEUTRON IRRADIATION OF ACETAMIDE

Fraction	% of Total activity Av.	Values obtained
CO_3^{-2} + HCN	0.0	0.1, 0.0, 0.0
HCHO	1.4	1.7, 1.4, 1.3, 1.2
HCOOH	0.4	0.7, 0.3, 0.2
CH_3OH	0.0	0.2, 0.0, 0.0
CH_3NH_2	0.0	0.0, 0.0
CH_3CH_2OH	0.0	0.0, 0.0
$CH_3C(O)CH_3$	0.5	0.8, 0.4, 0.2
$CH_3C(O)NH_2$	3.6	4.2, 3.6, 2.9
CH_3COOH	2.0	3.1, 1.5, 1.4
$(NH_2)_2CO$	0.0	0.0, 0.0
CH_3CH_2COOH	1.0	1.4, 1.0, 0.7
$CH_3CH_2C(O)NH_2$	5.0	6.0, 4.8, 4.2
$CH_3C(O)NHC(O)CH_3$	3.0	4.6, 2.8, 1.5
$CH_3C(O)CH_2C(O)CH_3$	4.2	4.5, 3.9
$NH_2C(O)CH_2C(O)NH_2$	6.1	6.9, 6.0, 5.3
$NH_2C(O)CH_2CH_2C(O)NH_2$	7.1	6.5, 7.6

Discussion

The relatively small amount of radiocarbon-labelling produced in the "simpler" compounds by the neutron irradiation of solid acetamide has provided an interesting insight into the species produced as a result of the recoiling carbon-14 atom and the associated γ-radiation effects.

In this investigation we have considered only the final form of the chemical species incorporating the recoil carbon-14 atom. Yankwich[5] previously has suggested that many chemical forms of the carbon-14 recoil atom are present within the solid matrix following irradiation. These matrix-stabilized forms undergo decomposition, rearrangement, or further reactions when the irradiated compound is dissolved in water. Since only the final form assumed by the recoil carbon-14 atom is actually determined, the matrix-stabilized species can, at best, be estimated only by a critical analysis of the results obtained from a particular study and the proposition of reasonable intermediates to yield the products actually observed.

An important and interesting result of this study is that the recoil carbon-14 atom in acetamide does not appear to be stabilized within the solid matrix as a "simple" chemical specie or in a form that would undergo rearrangement or decomposition in the presence of water to produce a "simple" compound. This is demonstrated by the low percentage of the total activity present in the lower alcohols, acids, and amides. This low percentage of activity in the "simple" compounds suggests that two possibilities may exist with regard to the solid matrix-stabilized radicals or ions. First, the recoil carbon-14 atom, when its energy has been reduced to where it becomes stable toward recombination, undergoes reactions with the solid matrix to produce complex, but stable, chemical species. Second, the recoil atom may undergo reactions with the solid matrix to produce unstable chemical species which, upon dissolution in water, react either with acetamide or with other chemical species to produce the complex compounds observed. The extensive γ-radiation damage (5–10%) may significantly influence the results as well.

Wolf and co-workers[2] reported an average value of 7.1% of the total activity present in acetic acid and 5.8% of the total activity in the form of propionic acid. Following their method of analysis, any carbon-14-labelled acetamide and propionamide present in the sample also would be expected to be hydrolyzed to the corresponding acids (or salts of the acids) and therefore would be included in the percentages reported for the two acids. In this study, we have successfully separated acetamide, propionamide, acetic acid, and propionic

(5) P. E. Yankwich and W. R. Cornman, Jr., *J. Am. Chem. Soc.*, **77**, 2096 (1955).

acid individually by using analytical procedures entirely different from those employed by Wolf, *et al.*, and determined the activity present in each of the chemical species. The results from Table I show the combined activity present in propionamide and propionic acid to be 6.0% of the total activity. This is in very good agreement with the value of 5.8% reported by Wolf, *et al.*[2] The combined activity present in acetamide and acetic acid was found to be 5.6% of the total activity, also in fair agreement with the values reported in the earlier study.[2] On the basis of this study, it appears that in the mechanism proposed by Wolf, Redvanly, and Anderson[2] for the formation of propionamide and propionic acid, the formation of propionamide is more dominant than the formation of the corresponding acid. In the case of acetic acid and acetamide, it appears that the two chemical species are formed in approximately equal amounts, although the amide form is still dominant.

Tachikawa and Tsuchihashi,[3] in their study of the (n,p) process on propionamide, recently reported an average value of 3.3% of the total activity present in propionamide and 2.1% of the total activity present in the synthesis product, butyramide. A value of 1.7% of the total activity was reported in the additional synthesis product studied, isobutyramide. As a result of their study, Tachikawa and Tsuchihashi have suggested that the formation of carbon-14-labelled butyramide and isobutyramide occurs by two processes. First, the recoiling carbon-14 atom abstracts hydrogen atoms from its surroundings to form radiocarbon-labelled methyl radicals, methylene radicals, and methyl ions. Butyramide and isobutyramide then are formed by the simple replacement of a hydrogen atom on the propionamide molecule by a radiocarbon-labelled methyl radical. Since the butyramide and isobutyramide were found to contain a low percentage of the total activity, it appears reasonable to expect that perhaps some of the radiocarbon-labelled methyl and methylene radicals remain trapped within the solid matrix. Upon dissolution in water, however, these species would be expected to form methanol and formaldehyde, respectively. The results of our study show that this does not occur with acetamide, and by extrapolation, we believe it probably would not occur with propionamide.

We found radiocarbon-labelled succinamide to contain the highest percentage of the total activity isolated in this study. The formation of the succinamide may be postulated to occur by eq. 1 and

$$CH_3\overset{\overset{O}{\|}}{C}NH_2 \xrightarrow[C^{14}\text{ recoil atom}]{\gamma\text{-ray or}} \cdot CH_2\overset{\overset{O}{\|}}{C}NH_2 + H\cdot \qquad (1)$$

$$\text{recoil carbon-14} + \cdot CH_2\overset{\overset{O}{\|}}{C}NH_2 \longrightarrow \cdot C^{14}H_2\overset{\overset{O}{\|}}{C}NH_2 \text{ and/or } \cdot CH_2C^{14}\overset{\overset{O}{\|}}{C}NH_2 \qquad (2)$$

2. The carbon-14-containing $\cdot CH_2CONH_2$ radicals might dimerize with other $\cdot CH_2CONH_2$ radicals, produced by the γ-radiation, to form succinamide. This postulate is supported by the results obtained by Miyagawa and Gordy[6] in the study of the production of free radicals in crystalline acetamide by X-irradiation. These latter authors have shown from their electron spin resonance studies that the principal free radical produced is the $\cdot CH_2CONH_2$ radical. The mechanism postulated for the formation of succinamide is similar to that proposed by Wolf, Redvanly, and Anderson.[2]

The results of this study have shown that the neutron irradiation of crystalline acetamide does not effect incorporation of carbon-14 into the "simpler" molecules. We would suggest that the incorporation of the recoil carbon-14 atom into the more complex chemical species occurs in many instances *via* "knock-on" reactions of carbon-14-containing radicals with new chemical species which result from γ-radiation damage. A future study of the (n,p) process on acetamide in the absence of large γ-fluxes would enable further clarification of this suggestion.

Acknowledgments.—The initial stage of this research was supported in part by a grant from the Petroleum Research Fund administered by the American Chemical Society. Grateful acknowledgment hereby is made to the donors.

(6) I. Miyagawa and W. Gordy, *J. Am. Chem. Soc.*, **83**, 1036 (1961).

THE PARTIAL SPECIFIC VOLUME AND THE DENSITY OF MICELLES OF ASSOCIATION COLLOIDAL ELECTROLYTES[1]

BY PASUPATI MUKERJEE[2]

Department of Chemistry, University of Southern California, Los Angeles 7, California

Received May 11, 1962

Density data of aqueous solutions of association colloidal electrolytes are analyzed. Methods are suggested for deriving the true partial specific volume of the micelles and also the true specific volume and the density. The assumptions involved are examined in detail and the associated probable errors shown to be small. The method is applied to several anionic and cationic association colloidal electrolytes for which precise experimental data are available in the literature and it can be extended readily to other charged colloidal particles. The final results show that little error (~4%) is made on using the experimental partial specific volume for the true volume when counterions are small and monovalent. With heavy and highly charged counterions, however, much larger errors are possible. Giant micelles show curious abnormalities.

A knowledge of the density of a charged colloid or macromolecule in solution, aside from its intrinsic importance, provides an important part of the bridge leading from weight concentration and mass to volume fraction and volume. The former are accessible directly and by light scattering, while the latter are of importance in the interpretation of diffusion, ultracentrifugation, viscosity, electrophoresis, and many other methods of study. The estimation of this density involves the typical difficulties associated with all solutes. To obtain the true density of the anhydrous solute from the experimentally accessible partial volumes,[3] allowance must be made for solute–solvent interactions, since the partial volumes can be looked upon as the sum of the true volumes of the ions themselves and of the associated volume changes of the solvent.

The present paper attempts to estimate the true partial specific volume and then the density of micelles of association colloidal electrolytes (ACE's) from the density of micellar solutions by the application of our existing knowledge regarding the structure of micelles and some recent investigations on the interaction of small ions with water. ACE's are one of the simplest and best characterized colloid systems now available and therefore one of the most tractable. The values derived in this paper can be used immediately for a large number of interpretations.

The currently accepted picture of micelles in water or salt solutions of not too high concentrations is basically that of Hartley.[4,5] A large number (30–100) of monomeric ions are aggregated into a compact spheroidal body on the surface of which the charged heads remain exposed to the water. Strong electrical interactions cause about two-thirds of the counterions to be firmly bound to the surface of this aggregate, which may be rough.[6] The remaining third is in the diffuse double layer surrounding the aggregate. The colloidal kinetic particle consists of the aggregate of the amphipathic ions, the firmly bound counterions, and the water of hydration.

Thus we can distinguish the following entities: (1) the anhydrous and electrically neutral micellar component, *i.e.*, the micelle with an equivalent amount of counterions; (2) the anhydrous micelle, which includes only the firmly attached counterions; and (3) the hydrated micelle, which includes the firmly attached counterions and the firmly attached water. In this paper we are concerned with the partial volume of the first, the partial and true volume of the second, and the electrostriction of the surrounding water, but not with the volume of the third one.

Method of Calculation

A typical plot of specific volumes against concentration of an ACE in water shows a more or less obvious change of slope at the critical micelle concentration (c.m.c.) and an almost linear variation above it (Fig. 1).[7] From the slope above the c.m.c. we get the partial specific volume of the micellar component, $\bar{V}_s$, on the assumption that the monomer concentration remains constant. This assumption has frequently been justified theoretically[8,9] and also experimentally.[10] Moreover, the partial specific volume of the ACE below the c.m.c. is generally within 5% or less of $\bar{V}_s$, so that a small variation in the monomer concentration introduces negligible error.

From $\bar{V}_s$, multiplying by the formula weight, we obtain $\bar{V}_m$, the partial molal volume of the micellar component which includes the free counterions. If the degree of dissociation is x and the partial molal volume of the counterions $\bar{V}$, then for the micelle proper, $\bar{V}_m'$, the partial volume of 1 mole of amphipathic ions and $1 - x$ mole of counterions is given by $\bar{V}_m - x\bar{V}$. The corresponding partial specific volume $\bar{V}_s'$ is the quantity truly representative of the micelle.

The value of x has been derived to be close to 0.3 for several systems.[10,11] We use this value and note than an error of 0.1 in it causes an error of less than 1% for our systems. For $\bar{V}$ values we use some recent estimates at infinite dilution,[12] −5.7 and 22.3 ml./mole for Na^+ and Cl^-, respectively. Two assumptions are involved here: (a) the effect of the finite concentrations in the non-micellar liquid is negligible; and (b) the potential drop in the diffuse double layer contributes nothing to the volume changes. Considering that only x mole of one ion is involved and that from infinite dilution to 0.1 M concentration 1:1 electrolytes show a

(1) This work was supported in part by the Office of Naval Research and presented at the 132nd National Meeting of the American Chemical Society in New York, September, 1957. Reproduction in part or in whole for purposes of the U. S. Government is permitted.

(2) Department of Physical Chemistry, Indian Association for the Cultivation of Science, Calcutta 32, India.

(3) E. A. Guggenheim, "Thermodynamics," North-Holland Publishing Co., Amsterdam, Third Edition, 1957.

(4) G. S. Hartley, "Aqueous Solutions of Paraffin-chain Salts," Hermann, Paris, 1936.

(5) G. S. Hartley, *Ann. Rep. Chem. Soc., London*, **45**, 33 (1948).

(6) D. Stigter and K. J. Mysels, *J. Phys. Chem.*, **59**, 45 (1955).

(7) K. A. Wright and H. V. Tartar, *J. Am. Chem. Soc.*, **61**, 544 (1939).

(8) R. C. Murray and G. S. Hartley, *Trans. Faraday Soc.*, **31**, 183 (1935).

(9) K. J. Mysels, *J. Colloid Sci.*, **10**, 507 (1955).

(10) K. J. Mysels and C. I. Dulin, *ibid.*, **10**, 461 (1955).

(11) I. M. Kolthoff and W. F. Johnston, *J. Am. Chem. Soc.*, **73**, 4563 (1951).

(12) P. Mukerjee, *J. Phys. Chem.*, **65**, 740 (1961).

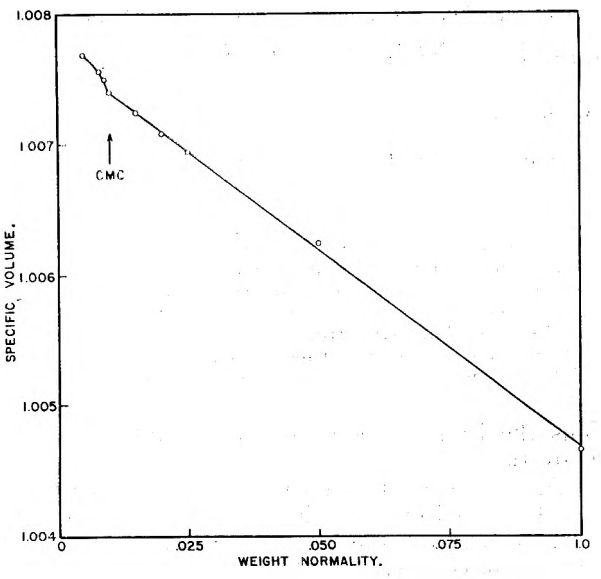

Fig. 1.—The variation of specific volume with concentration of aqueous solutions of sodium lauryl sulfonate at 40° (density data from ref. 7).

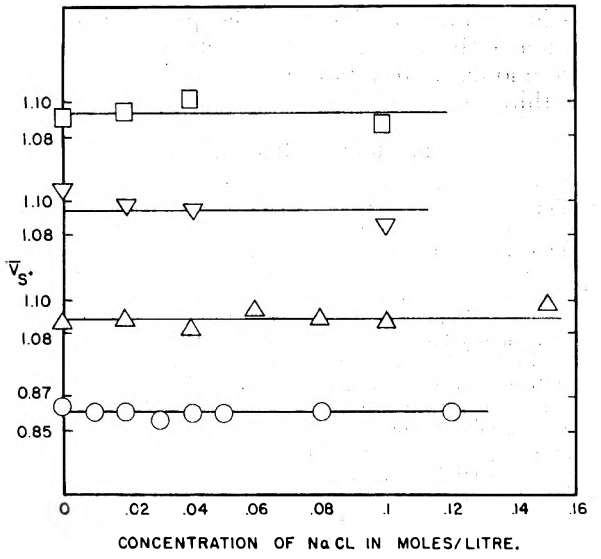

Fig. 2.—Variation of $\bar{V}_s$ with concentration of NaCl: ○, sodium lauryl sulfate, 23°; △, dodecylammonium chloride, 30°; ▽, dodecyltrimethylammonium chloride, 23°; □, tetradecyltrimethylammonium chloride, 23°.

change of only about 0.6 ml./mole,[13] the concentration effect on $\bar{V}_m'$ values of about 200 ml./mole can be neglected.

Assumption (b) is hard to evaluate theoretically. Approximately, however, we may note that the double layer potentials involved[6] (~100 mv.) correspond to maximum field intensities of about 1 million v./cm. Such a field at the surface of a monovalent ion in water, assuming the intervening dielectric constant to be unity, requires a radius of 38 Å. For a dielectric constant of 80, the distance is about 4 Å. Since intermediate values are more likely, the field intensity clearly corresponds to a fair distance from a monovalent ion, beyond one to several hydration layers, at which distance any residual electrostriction effects should be small.

Stronger support for assumption (b) can be obtained from the experimental density data.[14,15] In Fig. 2, the computed $\bar{V}_s$ values of four compounds in water and in various concentrations of sodium chloride are plotted against the salt concentration. The data can be represented by horizontal lines for all the compounds. The average deviations from the straight lines are 0.2% in the case of NaLS, 0.4% in the case of dodecylamine hydrochloride, 0.5% in the case of tetradecyltrimethylammonium chloride, and 0.6% in the case of dodecyltrimethylammonium chloride. Except for the last compound the deviations are random. We can conclude, therefore, that $\bar{V}_s$ changes very little with salt concentration over the range indicated. Since over this range of concentration the thickness of the double layer decreases by a factor of three to four, and the ζ-potential, in the typical case of sodium lauryl sulfate, decreases from about 100 to 66 mv.,[6] so that the field intensities double, it may be concluded also that the effect of the diffuse double layer on the volume of the system is negligible. This seems to be the first evidence of its kind and is of importance in the study of charged colloids in general.

To obtain the true anhydrous specific volume, V_s', and the density of the anhydrous micelles from $\bar{V}_m'$, allowance must be made for micelle–solvent interaction. This is confined to the micelle–water interface and is of three types: (1) the ion–water interaction, (2) the interaction between the hydrated ions, and (3) that between the exposed hydrocarbon surface and water.

The first factor causes electrostriction of the solvent, while the second factor influences the extent of it. Both are taken into account if the electrostriction is calculated for the "effective" concentration at the micelle surface. The electrostriction values at infinite dilution can be calculated on the basis of a recent study.[12,16] From geometrical considerations and the variation of $\bar{V}_m$ with counterions, the "effective" concentration for the lauryl sulfonates has been estimated to be 1–3 M.[17] We have used a mean value of 2 M and decreased the absolute values of the electrostrictions, calculated at infinite dilution, by 4 ml./mole, the average value pertaining to 1:1 electrolytes.[13]

The third factor is neglected. The partial molal volume of ACE's increase on micelle formation by about 5% for NaLS and much less for cationic compounds, as estimated from the density data.[14,15] A substantial part of this change is due to the decrease in electrostriction on micelle-formation. The reason for the rest is obscure, but even if it were all related to the change in the hydrocarbon area exposed to water, the residual effect must be small, since only a small fraction, about 10%, of this hydrocarbon area of the monomers remains exposed in the micelles.

To obtain the true volume from $\bar{V}_m'$ we add to $\bar{V}_m'$ the absolute value of the electrostriction for 1 mole of amphipathic ions and $1 - x$ mole of counterion, modified for the concentration effect. Division by the calculated mass now gives the true anhydrous specific volume V_s' and hence the density. For the monovalent counterions involved in our systems, the electrostriction corrections are 5 ml./mole or less. Uncertainties due to errors in these estimates in the final density figures are expected to be about 1%. The corrections are considerably larger for multivalent counterions.[12]

We have neglected the effect of temperature, which has only a small effect on the partial molal volumes of ordinary electrolytes.[18] Error due to this should be significant only in the case of sodium lauryl sulfonate.

Results

In Table I the data for several ACE's are shown. The average uncertainties are estimated to be about 0.5% for $\bar{V}_s$, 1% for $\bar{V}_s'$, and 1–2% for V_s' and the anhydrous micellar density.

The estimated densities are considerably higher than that of liquid dodecane (0.74 g./ml. at 25°.)[19]

(13) H. S. Harned and B. B. Owen, "The Physical Chemistry of Electrolytic Solutions," 3rd Edition, Reinhold Publ. Corp., New York, N. Y. 1958.

(14) L. M. Kushner, B. C. Duncan, and J. I. Hoffman, *J. Res. Natl. Bur. Std.*, **49**, 85 (1952).

(15) L. M. Kushner, W. D. Hubbard, and R. A. Parker, *ibid.*, **59**, 113 (1957).

(16) P. Mukerjee, *J. Phys. Chem.*, **65**, 744 (1961).

(17) P. Mukerjee, *ibid.*, **66**, 943 (1962).

(18) W. Geffken, *Z. physik. Chem.*, **A155**, 1 (1931).

(19) F. D. Rossini, *et al.*, "Selected Values of Physical and Thermodynamic Properties of Hydrocarbons and Related Compounds," American Petroleum Institute, Carnegie Press, 1953.

TABLE I

VOLUMES AND DENSITIES OF SOME ASSOCIATION COLLOIDS IN WATER AND NaCl SOLUTIONS

Substance	Medium	Temp., °C.	$\bar{V}_s$, ml./g.	$\bar{V}_s'$, ml./g.	V_s', ml./g.	Anhydrous micellar density, g./ml.	Source of density data, ref.
Sodium lauryl sulfate	Water and NaCl soln. up to 0.12 *M*	23	0.862	0.889	0.908	1.10_1	14
Dodecylamine hydrochloride	Water and NaCl soln. up to 0.15 *M*	30	1.088	1.111	1.132	0.882_0	15
Dodecyltrimethylammonium chloride	Water and NaCl soln. up to 0.1 *M*	23	1.095	1.114	1.120	$.893_3$	15
Tetradecyltrimethylammonium chloride	Water and NaCl soln. up to 0.1 *M*	23	1.094	1.111	1.116	$.896_6$	15
Sodium lauryl sulfonate	Water	40	0.901	0.931	0.950	1.052_0	7
		50	.906	.936	.956	1.046_0	7
		60	.916	.946	.966	1.035_0	7
		70	.925	.956	.975	1.026_0	7

This density has sometimes been assumed for the micelles[14] and has been derived from intrinsic viscosity data by neglecting all hydration.[15] This point will be examined in greater detail in a subsequent publication. The difference can be attributed mainly to the contribution of the effectively denser polar heads and counterions, which amounts to 30–60% of the total weight for all the compounds except dodecylammonium chloride, for which it is somewhat less. The rather pronounced difference between the anionic and the cationic electrolytes stems from the difference in densities between the sulfate or the sulfonate groups and the ammonium or substituted ammonium groups.

The decrease in the density of about 3% for sodium dodecyl sulfonate from 40 to 70° corresponds to about 7 ml. in molar volume and seems to be real since it is primarily in $\bar{V}_s$. The small effect of temperature on the partial volumes of ordinary electrolytes[18] suggests that only a small part of it is due to the increase in the volume of charged groups. However, the density of dodecane changes over this temperature range by about 3.0%.[19] Since about 62% of the weight of this surfactant is hydrocarbon, the contribution from the expansion of this part of the micelle with temperature should be about 2%, and this accounts for the major part of the observed change in density.

The final density values show that only a small error is made, 3–5%, on using the experimental $\bar{V}_s$ in our systems. Considerably larger errors are possible, however, in the case of dense or highly charged counterions. For a quaternary iodide, for example, $\bar{V}_s'$ may differ by 10% from $\bar{V}_s$. For monovalent counterions the electrostriction effects are small, and hence $\bar{V}_s'$ is a good approximation for V_s'. For multivalent counterions, however, V_s' may differ substantially from $\bar{V}_s'$.

Finally, we note that the general approach of this paper also is applicable to other systems of charged colloids, notably proteins.

Density of Giant Micelles.—In high concentrations of sodium chloride, the $\bar{V}_s$ of dodecyl ammonium chloride from the data of Kushner, *et al.*,[15] shows appreciable increases. Thus, compared to the average value of 1.088 at low salt concentrations, the values at 0.25 and 0.30 *M* salt concentrations are 1.103 and 1.134, respectively. Over this same range, the intrinsic viscosities, the molecular weights of the micelles, and the dissymmetry of the scattering of light all indicate that very large asymmetric micelles are present. Kushner, *et al.*,[15] have suggested that in these solutions the first stages of salting-out are evident, especially since the limits of solubility are approached and perhaps even exceeded. The curious decrease in the density suggests, however, that these giant micelles are not more solid-like but rather less so. The organization of the hydrocarbon chains is clearly different from that in ordinary micelles.

Acknowledgment.—The author is grateful to Professor Karol J. Mysels, without whose criticism, encouragement, and help this work would not have been possible.

NOTES

A STUDY OF ADSORPTION OF VARIOUS GASES AT 300°K.

BY J. TUUL

American Cyanamid Company, Stamford, Connecticut

Received February 5, 1962

While developing a method for a quick estimation of surface areas of catalyst materials by the use of an air pycnometer, the writer attempted to find some basic facts about the observed air adsorption. The method[1] referred to consisted of measuring the amount of air adsorbed on the sample at room temperature when the pressure of air surrounding the sample was increased from one to two atmospheres. Under specified conditions it was possible to correlate this adsorption with the surface area of the adsorbent. The investigations to be described here were carried out with the following three materials, all in the form of $^1/_{16}$ in. extrudates: (1) Al_2O_3, (2) 90% Al_2O_3 + 10% MoO_3, and (3) 82% Al_2O_3 + 15% MoO_3 + 3% CoO.

By carrying out measurements with nitrogen and oxygen separately, it had been found[1] that the amount of oxygen adsorbed was on the average close to 90% of the amount of nitrogen adsorbed under identical conditions. In order to illuminate further the problem of room temperature adsorption on inorganic oxides, similar measurements were carried out with carbon monoxide as pycnometer gas. CO adsorption was found to exceed that of air by about 50%. Otherwise, it was similar to the adsorption of air, being reversible and complete in less than 10 sec. Like the adsorption of air, the adsorption of CO could be increased by 100% or more by suitable heat treatments of hydrated samples. However, the ratio of CO adsorption to air adsorption on the same sample was always approximately 1.5.

When CO_2 was used as pycnometer gas, it was found to behave in a rather different manner. Its adsorption was about an order of magnitude larger than that of air, and much slower in reaching completion so that its progress could be conveniently followed. The process could best be approximated by a logarithmic function of time, indicating Elovich-type kinetics. When plotting the amount of CO_2 adsorbed *vs.* the logarithm of time, two portions of the curve could be approximated by a straight line. The first of these was in the range between 15 sec. and 3 min., and the second in the region above 5 min. About one half of the CO_2 taken up at 1 atm. pressure could be desorbed by 5-min. pumping with a mechanical pump, whereas the remainder, or at least most of it, could be desorbed by repeated evacuations alternated with exposures to atmospheric pressure of air.

Some samples were exposed to CO_2 without air having been evacuated from them. As can be seen from Fig. 1, the adsorption of CO_2 proceeded well on these samples and reached about the same proportions as on samples from which air had been evacuated prior to exposure to CO_2. The seemingly larger amount of adsorption on the unevacuated sample is not real but indicative of the limitations of the method. Thus, the equilibrium between gaseous CO_2 and the oxide surface, partly covered with adsorbed CO_2 molecules, is independent of a relatively small concentration of nitrogen or oxygen. It could be assumed that CO_2 and air are adsorbed on different surface sites. However, it also is possible that so many sites are available for the adsorption of CO_2 that a small fraction of sites covered by preadsorbed oxygen or nitrogen molecules would not make an observable difference with our method. Less CO_2 is adsorbed on hydrated than on dehydrated samples, but this effect is only about half as pronounced as in the case of the previously mentioned gases. As a consequence, the ratio of CO_2 to air adsorption is about 7 on dehydrated samples, but as high as 15 on hydrated samples.

An explanation was sought for the differences in adsorption of the various gases. It is generally accepted that the following kinds of forces are operative in physical adsorption: (1) dispersion forces, (2) repulsive forces, (3) electrostatic interactions with induced dipoles, and (4) electrostatic interactions with permanent electric moments. As far as the adsorption of nitrogen and oxygen is concerned, Drain[2] has suggested that the difference in their quadrupole moments might account for the difference in their heats of adsorption on ionic crystals. An inspection of Table I reveals that there is a positive correlation between the quadrupole moments and the relative adsorption of N_2, O_2, CO, and CO_2. It generally is assumed[3] that adsorption on dielectric surfaces is determined mainly by van der Waals and dipolar forces. When comparing the data for CO and CO_2 in Table I, it would seem that the quadrupole moment plays a more important role than the dipole moment. However, the overriding factor may be the polarizability. The principal polarizabilities of the molecules under study also are given in Table I. The relative adsorption coefficients for the four gases correlate with b_1 as well as b_2 and b_3, and also with the arithmetic mean of the polarizabilities.

In an attempt to determine which of the three polarizabilities, if any, is determining for the amount of adsorption, measurements were carried out with ammonia for which b_1 is smaller, but b_2 and b_3 are larger than for any of the previously used gases. Ammonia adsorption was found to be similar to that of CO_2, but much larger. When ammonia was included, the relative adsorption

(1) J. Tuul and W. B. Innes, *Anal. Chem.*, **34**, 818 (1962).

(2) L. E. Drain, *Trans. Faraday Soc.*, **49**, 650 (1953).

(3) A. C. Zettlemoyer, *Chem. Rev.*, **59**, 937 (1959).

TABLE I

RELATIVE ADSORPTION, DIPOLE MOMENTS, QUADRUPOLE MOMENTS, AND POLARIZABILITIES OF GASES STUDIED

Gas	Relative adsorption coefficient	Dipole moment, Debyes	Quadrupole moment ($Q \times 10^{16}$), cm.^{2}	Polarizabilities[a] $b_1 \times 10^{25}$, e.s.u.	b_2 and $b_3 \times 10^{25}$, e.s.u.
N_2	1.00	0	0.27	24.3	14.3
O_2	0.87	0	.09	24.3	11.9
CO	1.5	0.1	.34	26.0	16.2
CO_2	7–15	0	.65	41.0	19.3
C_2H_4	9–12	0	.48	56.1	35.9
NH_3	25–200	1.46	.28	24.2	21.9

[a] b_1, b_2, and b_3 are the principal semi-axes of the polarization ellipsoid.

coefficient could be correlated only with b_2 and b_3. However, the large dipole moment of the ammonia molecule might be responsible, at least in part, for the large amount of adsorption.

Finally, measurements with ethylene proved that no single property of the adsorbate molecule determines the extent of physical adsorption at room temperature, but rather a combination of the properties considered. The adsorption of ethylene was found to be approximately as large as CO_2 adsorption, but not as large as its polarizability would indicate. In addition, ethylene adsorption was fast, almost as fast as that of O_2, N_2, and CO. By the use of ethylene instead of air, the sensitivity of the previously described method of evaluating surface areas[1] could be increased considerably.

The extent of surface coverage occurring with the various gases in the pycnometer measurements has been estimated. Using the effective cross-sectional area of 16.2 Å.^{2} for nitrogen, and applying Henry's law, a total coverage of 3–4% was found for nitrogen at 2 atm. on freshly calcined samples (the exact figure depends on the type of material). Similarly, assuming an effective cross-sectional area of 14.1 Å.^{2} for the oxygen molecule, a coverage of 2–3% was calculated for oxygen under the same conditions. Using approximate cross-sectional areas for the other four molecules, calculated from the densities of these gases in the solid state, the following coverages were estimated at 2 atm. pressure: 5–7% for CO, 30–40% for CO_2, 40–50% for C_2H_4, and 50–60% for NH_3. These estimates may be too low, since the effective cross-sectional areas at room temperature may be larger than the ones assumed in these calculations. Nevertheless, the quoted figures give an indication of the large differences in the adsorption of the various gases under identical conditions of adsorbent, pressure, and temperature. Measurements with known mixtures of these gases would be of interest, as they might give an answer to the question of whether different gases are adsorbed on different surface sites.

The influence of preadsorbed water can be correlated with the affinity of the respective gases for water. The solubility of the gas in water may be taken as a manifestation of this affinity. The solubilities of N_2, O_2, and CO in water are very low. The adsorption of these gases on samples which contain about 10% water is less than 40% of the adsorption on the same samples immediately after calcination. The influence of preadsorbed water on the adsorption of ethylene and CO_2 is similar but smaller, since these two gases have considerably higher solubilities in water than the three above mentioned ones. The solubility of ammonia in water is about 100 times larger than that of N_2, O_2, or CO. This fact is reflected in the singular behavior of ammonia inasmuch as it is adsorbed to a larger extent on hydrated than on dehydrated samples. In Table I the adsorption of the other gases is related to the adsorption of nitrogen. A range of values of the relative adsorption coefficient has been assigned to CO_2, C_2H_4, and NH_3. The lowest value refers to freshly calcined samples, and the highest to samples hydrated by several months of atmospheric exposure.

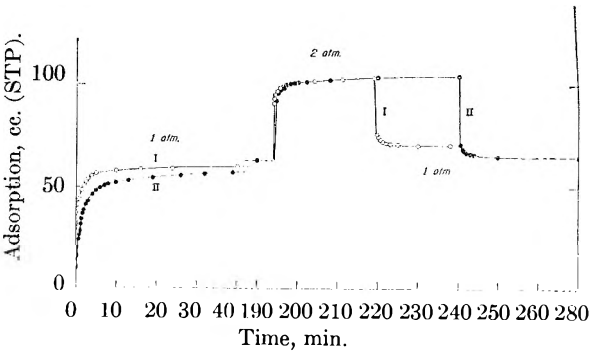

Fig. 1.—Adsorption of carbon dioxide on γ-alumina under various conditions: sample weight, 5.83 g.; surface area, 200 m.^{2}/g.; curve I, air not evacuated from sample; curve II, air evacuated from sample.

THE PREPARATION OF SOME RARE EARTH FORMATES AND THEIR CRYSTAL STRUCTURES

BY I. MAYER, M. STEINBERG, F. FEIGENBLATT, AND A. GLASNER[1]

Department of Inorganic and Analytical Chemistry, The Hebrew University, Jerusalem, Israel

Received March 10, 1962

In the course of the study of the thermal decomposition of lanthanon salts, a series of formates was prepared.[2] These were crystallized from formic acid solutions of the oxides or nitrates, washed with water, and then with ethanol or acetone.

The composition of the salts was determined[3] by the following procedures: (a) calcination of the formates to the corresponding sesquioxides (in the case of cerium, to the dioxide); (b) titration of the formate ion with potassium permanganate[2]; (c) determination of carbon and hydrogen by microanalysis; (d) absorption spectra in the infrared region (2–16 μ).

From the above analyses it was concluded that our preparations of cerium(III), praseodymium,

(1) On sabbatical leave at the Department of Chemistry, Princeton University, Princeton, N. J.

(2) F. Feigenblatt, M.Sc. Thesis, 1961.

(3) A. Glasner, M. Steinberg, F. Feigenblatt, and W. Bodenheimer, *Bull. Res. Council Israel*, **10A**, 8 (1961).

neodymium, and samarium formate all accord with the formula $La(HCOO)_3 \cdot 0.2H_2O$. The results are in good agreement with an earlier report.[4] The fractional water molecule could be removed only at 300° with simultaneous decomposition of the formate.

TABLE I

PARTIAL POWDER DIFFRACTION DATA FOR LANTHANON FORMATES

hkl Hex.	*hkl* Rhomb.	Ce-$(HCOO)_3$ *d*, Å.	Pr-$(HCOO)_3$ *d*, Å.	Nd-$(HCOO)_3$ *d*, Å.	Sm-$(HCOO)_3$ *d*, Å.
110	$10\bar{1}$	5.272	5.304	5.241	5.272
101	100	3.727	3.720	3.720	3.674
300, 021	$11\bar{2}$, $11\bar{1}$	3.066	3.055	3.055	3.035
220, 211	$20\bar{2}$, $20\bar{1}$	2.664	2.649	2.649	2.627
131	$21\bar{2}$	2.169	2.159	2.159	2.139
410, 401	$31\bar{2}$, $31\bar{1}$	2.012	2.018	2.000	1.987
012	110	1.991	1.983	1.979	1.963
321	$30\bar{2}$	1.882	1.871	1.868	1.853
202	200	1.860	1.860	1.857	1.836
330	$30\bar{3}$	1.776	1.769	1.766	1.753

X-Ray Results.—Powdered samples of the formates were examined by the X-ray diffraction method, using a General Electric diffractometer and filtered CuK radiation. Only samples that were proven to have a stoichiometric composition were taken; none of the lanthanum formate preparations came up to this requirement.

The powder patterns of the formates may be indexed on the basis of a hexagonal cell. Further examination of the hexagonal pattern showed that only lines of $h\text{-}l\text{-}k = 3n$ are present, indicating a rhombohedral lattice. Powder data are listed in Table I. The agreement between observed and calculated *d* values was ±0.015 Å. The 012, 202, 122, 312, and 232 lines (hexagonal indices) of cerium and praseodymium formates overlapped on the diffractometer pattern at the 410, 321, 330, 241, and 520 lines. They could be observed only by taking a powder picture with a high resolution focussing Guinier camera.

Unit cell dimensions of these compounds are recorded in Table II.

TABLE II

LATTICE CONSTANTS OF LANTHANON FORMATES

Formates of	Hexagonal cell *a*, Å.	Hexagonal cell *c*, Å.	Rhombohedral cell *a*, Å.	Rhombohedral cell α
Cerium(III)	10.67	4.08	6.31	115°36′
Praseodymium(III)	10.63	4.07	6.28	115°36′
Neodymium(III)	10.61	4.06	6.27	115°36′
Samarium(III)	10.53	4.02	6.22	115°36′
Gadolinium(III)[a]	10.44	3.98	6.17	115°30′

[a] See ref. 5.

Table II shows the regular decrease in unit cell dimensions in the order of diminishing crystal radii of the trivalent rare earth ions. This corresponds with the analytical results which indicated that the metal ions in these salts are all in the trivalent state.

Thus, there is ample evidence that the lanthanon formates here investigated are isomorphous with gadolinium formate.[5] Gadolinium formate has a trigonal unit cell and its space group is R3m. The positions in this space group are filled in the gadolinium formate as

		z	*x*
(a)	Gd atom in 000		
(b)	3 C atoms in *xxz*, *xzx*, *zxx*	0.43	0.85
(c)	3 O_1 atoms in *xxz*, *xzx*, *zxx*	0.19	0.81
	3 O_2 atoms in *xxz*, *xzx*, *zxx*	0.33	0.58

The oxygen atoms are placed in two non-equivalent sets of threefold positions, the O_1 atoms forming a ring about each metal atom, whereas the O_2 atoms form a somewhat closer ring around each threefold axis, equidistant between two metal atoms.

In order to prove the isomorphism between gadolinium formate and the formates investigated in this work, the calculated and the observed intensity values of neodymium formate were compared. Intensity measurements were made only for this compound, because the intensities of the reflections of the different compounds are similar. Intensity measurements were made with a diffractometer using filtered CuK radiation. Intensity data were recorded on a strip chart while scanning the reflections at $^1/_2°$ (2θ) per minute, the areas of the bands then were measured with a planimeter. The calculations were made by taking the same atomic parameters as determined for gadolinium formate. Absorption and temperature factors were omitted in these calculations.

In Table III observed and calculated intensities for the first six reflections of neodymium formate are listed. The agreement between the observed and calculated values leaves little doubt that these formates have the same structure as gadolinium formate. While in Pabst's work with gadolinium formate low intensity values were obtained for the $10\bar{1}$, 100, $11\bar{2}$, $11\bar{1}$ reflections, in our case this discrepancy was observed only for the 100 reflection.

TABLE III

OBSERVED AND CALCULATED INTENSITIES FOR NEODYMIUM FORMATE

hkl	I_{obs}	I_{calc}	
$10\bar{1}$	356	357	
100	30	90	
$11\bar{2}$	85	35	91
$11\bar{1}$		56	
$20\bar{2}$	197	87	217
$20\bar{1}$		130	
$21\bar{2}$	64	74	
$31\bar{2}$	100	62	103
$31\bar{1}$		41	

Acknowledgments.—The authors wish to thank Mr. Z. Kalman of the Department of Physics for help in carrying out the X-ray work, and Mrs. M. Goldstein of the Department of Organic Chemistry for analyzing the samples.

(4) B. Sahoo, S. Panda, and D. Patnaik, *J. Indian Chem. Soc.*, **37**, 594 (1960).

(5) A. Pabst, *J. Chem. Phys.*, **11**, 145 (1943).

RELAXATION TIMES AND "AVERAGED MUTUAL VISCOSITIES" OF SOME ALIPHATIC KETONES

By H. N. Srivastava,[1] K. C. Lal, and M. N. Sharma

Physics Department, Lucknow University, Lucknow, India

Received March 5, 1962

In an earlier communication,[2] the relaxation times of some aliphatic ketones in dilute solutions calculated from the equations proposed by Debye[3] and Wirtz and co-workers[4,5] were 10–15 times and twice the experimental values, respectively. On the basis of Debye's equation, the relaxation times of methyl ethyl ketone and methyl *n*-propyl ketone also were not proportional to the solvent viscosities, *i.e.*, benzene and decalin.[2]

Hill[6] has shown that relaxation time in dilute solution is related to the "mutual viscosity" between the solvent and the solute. More recently Vaughan, Purcell, and Smyth[7] have derived an expression for a quantity called "averaged mutual viscosity," $\bar{\eta}_{AB}$, defined by

$$\eta_m = f_A^2\eta_A + f_B^2\eta_B + 2f_Af_B\bar{\eta}_{AB} \qquad (1)$$

where η_m is the viscosity of the mixture, f_A and f_B the mole fractions of the solute and the solvent, and η_A and η_B the corresponding viscosities. It also has been shown that "mutual viscosity"[6] as well as "averaged mutual viscosity" have the same order of magnitude.

Equation 1 was rewritten as

$$y = x\bar{\eta}_{AB} + \eta_B \qquad (2)$$

where

$$x = \frac{2f_A}{f_B},\ y = \frac{\eta_m - f_A^2\eta_A}{f_B^2}$$

Table I

Relaxation Times and "Averaged Mutual Viscosities" of the Ketones

Temperature, 30°; viscosity of benzene = 0.593 cp., viscosity of decalin = 2.061 cp.

Ketone	Solvent	$\tau \times 10^{12}$ (sec.)[b]	$\bar{\eta}_{AB}$,[c] cp.	$\frac{\tau}{\eta_B} \times 10^{10}$	$\frac{\tau}{\bar{\eta}_{AB}} \times 10^{10}$
Methyl ethyl ketone	Benzene[a]	3.7	...	6.24	...
	Decalin	2.7	0.52	1.31	5.19
Methyl *n*-propyl ketone	Benzene	4.5	.54	7.59	8.34
	Decalin	4.4	.70	2.15	6.29
Methyl *n*-amyl ketone	Benzene	5.6	.64	9.44	8.75
Di-*n*-propyl ketone	Benzene	5.4	.63	9.11	8.57

[a] $\bar{\eta}_{AB}$ could not be measured for mixtures of benzene and methyl ethyl ketone because of the low viscosity. [b] Accuracy of relaxation time measurements was ±10%. [c] Accuracy of viscosity measurements was ±2%.

About five concentrations of different ketones were taken and from the slope of the straight line (2). $\bar{\eta}_{AB}$ was calculated by the least squares method.

Relaxation times were determined by a 3-cm. standing wave technique as described earlier.[8] The viscosities of different solutions were determined by Hoppler's precision viscometer.

The results recorded in Table I show that (a) the ratio of the relaxation time, τ, to the "averaged mutual viscosity" increases with the molecular size; (b) for the same ketone the ratio $\tau/\bar{\eta}_{AB}$ shows better agreement in decalin as well as benzene as compared to τ/η_B; and (c) on calculating the relaxation time by replacing η_B by $\bar{\eta}_{AB}$ in the Debye equation, the calculated values still are considerably higher than the experimental results.

Acknowledgment.—The authors are grateful to Dr. P. N. Sharma, D.Sc., Professor of Physics, for guidance.

(1) Meteorological Office, New Delhi, India.
(2) H. N. Srivastava, *J. Sci. Ind. Res.* (India), under publication.
(3) P. Debye, "Polar Molecules," Chemical Catalog Co., 1929.
(4) A. Spernol and K. Wirtz, *Z. Naturforsch.*, **8a**, 522 (1953).
(5) A. Gierrer and K. Wirtz, *ibid.*, **8a**, 532 (1953).
(6) N. E. Hill, *Proc. Phys. Soc.* (London), **67B**, 149 (1954).
(7) W. E. Vaughan, W. P. Purcell, and C. P. Smyth, *J. Am. Chem. Soc.*, **83**, 571 (1961).
(8) A. Vyas and H. N. Srivastava, *J. Sci. Ind. Res.* (India), **18B**, 399 (1959).

THE LUMINESCENCE OF CYCLOPENTANONE

By S. R. La Paglia and B. C. Roquitte[1]

Aeronautical Research Laboratory, Wright-Patterson Air Force Base, Dayton, Ohio

Received March 20, 1962

In several recent reports on the photochemistry of cyclopentanone[2-4] Srinivasan has suggested that the first excited singlet state (exciting wave length, 3130 Å.) of cyclopentanone has three distinct modes of unimolecular decomposition. Emission also may occur from the excited state(s); however, a previous attempt[3] to observe luminescence in liquid cyclopentanone failed, and only a weak afterglow was observed in solid solution at 77°K. It was deemed important to examine the luminescent properties of cyclopentanone as a solute in liquid and solid phases as a preliminary to any study of light emission by gaseous cyclopentanone. Only the gas phase luminescence behavior of cyclopentanone has a very direct bearing on the interpretation of the gas phase photolysis.

Eastman White Label cyclopentanone was analyzed by vapor phase chromatography and found to consist of only one component. However, before use, the cyclopentanone was freshly distilled and a middle fraction was taken. Absorption spectra of cyclopentanone solution were in complete agreement with literature spectra.[5,6] The fluorescence of cyclopentanone in hexane was observed spectrophotometrically with a double monochrometer device using a high pressure xenon light source, a photomultiplier detector, and a recording galvanometer. To record the phosphorescence spectrum, a dilute EPA solution of cyclopentanone was cooled to 77°K. in a quartz dewar. It was

(1) Visiting Research Associate at the Aeronautical Research Laboratory, 1961–1962.
(2) R. Srinivasan, *J. Am. Chem. Soc.*, **81**, 1546 (1959).
(3) R. Srinivasan, *ibid.*, **83**, 4344 (1961).
(4) R. Srinivasan, *ibid.*, **83**, 4348 (1961).
(5) D. J. Cram and H. Steinberg, *ibid.*, **76**, 2753 (1954).
(6) W. D. Kumler and A. C. Huitric, *ibid.*, **78**, 3374 (1956).

viewed by the spectrophotometer through a rotating can (~10,000 r.p.m.) type of shutter. For both fluorescence and phosphorescence the exciting light was of wave lengths 2900–3000 Å.

To measure the lifetime of phosphorescence, the cyclopentanone in a dilute glass at 77°K. was excited by a light flash of short duration. By means of a Corning 7–54 filter the exciting light was limited to the region 2400–4000 Å., while the emitted light that reached the photomultiplier was limited to wave lengths longer than 4600 Å. by a 4–65 filter. The flash triggered one sweep by a fast oscilloscope connected to the photomultiplier. Under identical conditions, the pure glassy solvent showed no emission, while a glass containing cyclopentanone (0.1 M) showed an easily measurable luminescent decay with a lifetime of 1.1×10^{-3} sec.

If the fluorescence spectrum is normalized to the absorption intensity and plotted on a wave number scale, the resultant spectra show an approximate "mirror image symmetry." The maximum of the fluorescence band lies at 4000–4100 Å. and is structureless. Dilute solutions (10^{-2}–10^{-3} M hexane, 25°) were used, to avoid self-quenching or re-absorption of fluorescence or the localization of the fluorescence near the incident face of the cuvette. Any of these reasons would account for the failure to observe fluorescence in the pure liquid.[3]

We found the phosphorescence, like the fluorescence of cyclopentanone, to be without structure; this probably is due in some measure to the low resolving power of the spectrophotometer. The phosphorescence maximum (4400–4500 Å.) and the lifetime of phosphorescence (1.1×10^{-3} sec.) of cyclopentanone are quite reasonable for an aliphatic ketone under these conditions. McClure[7] reported an average phosphorescence frequency of 23,000 cm.$^{-1}$ for the aliphatic ketones and lifetimes of 0.6×10^{-3} sec. (acetone), 1.26×10^{-3} sec. (diethyl ketone), and quite similar lifetimes for the triplet states of other aliphatic ketones under conditions equivalent to those described above. The observed phosphorescence and decay time therefore are ascribed to the triplet state of cyclopentanone.

(7) D. S. McClure, *J. Chem. Phys.*, **17**, 905 (1949).

THE DENSITY GRADIENT AND GRAVITATIONAL STABILITY DURING FREE DIFFUSION IN THREE-COMPONENT SYSTEMS

BY RICHARD P. WENDT[1]

Department of Chemistry and the Enzyme Institute, University of Wisconsin, Madison 6, Wisconsin

Received March 30, 1962

Several optical methods have been developed for studying the isothermal free diffusion process in liquids.[2] Each method requires the formation of an initially sharp boundary or interface between two solutions of different concentrations in a diffusion cell. At time $t = 0$ the diffusion process commences and the diffusing boundary between the two solutions is observed during the period of time before the concentrations at the top and bottom of the cell begin to change significantly. To prevent convective mixing in the diffusion cell, the two solutions are prepared so that d_B, the density of solution B below the interface, is greater than d_A, the density of solution A above the interface. The condition

$$d_B > d_A \qquad (1)$$

thus ensures gravitational stability at $t = 0$.

For a two-component system undergoing ideal diffusion, it can be readily proved[3] that condition 1 also ensures gravitational stability at all times $t > 0$ and at all positions, x, in the diffusing boundary ($x = 0$ at the interface and is positive if measured downward). That is, for binary systems condition 1 implies

$$(\partial d/\partial x)_t > 0 \qquad (2)$$

which is the necessary and sufficient condition for gravitational stability at all times $t > 0$ and at all positions x.

Procedures have been developed for studying free diffusion in three-component systems with the Gouy diffusiometer,[4-7] and for these experiments condition 1 for $t = 0$ also is required. However, for ternary systems it has not been shown that inequality 1 implies inequality 2 for all times $t > 0$ and for all positions in the diffusion cell. We will here derive the expression for the density gradient during the free diffusion process in a ternary system as a function of the variable y, where

$$y = x/(2\sqrt{t}) \qquad (3)$$

Conditions independent of y then will be found which are sufficient to ensure gravitational sta-

(1) Institute for Molecular Physics, University of Maryland, College Park, Maryland.

(2) Several methods are reviewed by L. J. Gosting in "Advances in Protein Chemistry," Vol. XI, Academic Press, Inc., New York, N. Y., 1956, pp. 462–485.

(3) Equation 71, ref. 2, for the concentration gradient during free diffusion in a binary system, reads

$$(\partial C/\partial x)_t = (\Delta C/2\sqrt{\pi Dt})e^{-x^2/(4Dt)}$$

where D is the diffusion coefficient, C is the solute concentration, and

$$\Delta C = C_B - C_A$$

Here C_B and C_A are the initial solute concentrations of the two solutions below and above, respectively, the initially sharp boundary in the diffusion cell. Because small values of ΔC are usually used in experimental work, D is assumed to be independent of C; it is also assumed that the solution density throughout the diffusion cell can be described by

$$d = d(\bar{C}) + H(C - \bar{C})$$

where $\bar{C}$ is the mean of C_A and C_B. Then

$$(\partial d/\partial x)_t = H(\partial C/\partial x)_t$$
$$\Delta d = (d)_B - (d)_A = H\Delta C$$

and

$$(\partial d/\partial x)_t = (\Delta d/2\sqrt{\pi Dt})e^{-x^2/(4Dt)}$$

Therefore, if

$$\Delta d > 0$$

at $t = 0$, then

$$(\partial d/\partial x)_t > 0$$

for all times $t > 0$ and for all positions x.

(4) R. L. Baldwin, P. J. Dunlop, and L. J. Gosting, *J. Am. Chem. Soc.*, **77**, 5235 (1955).

(5) H. Fujita and L. J. Gosting, *ibid.*, **78**, 1099 (1956).

(6) P. J. Dunlop, *J. Phys. Chem.*, **61**, 994 (1957).

(7) H. Fujita and L. J. Gosting, *ibid.*, **64**, 1256 (1960).

bility at all times $t \geq 0$ and at all positions x in the diffusing boundary. These conditions will be written in terms of the four volume-fixed diffusion coefficients[8] for the ternary system, $(D_{ij})_V$, where $i,j = 1,2$ denote the two solute components; the concentration differences, ΔC_i, where

$$\Delta C_i = (C_i)_B - (C_i)_A \quad (4)$$

and the density derivatives, H_i, which appear in the equation

$$d = d(\bar{C}_1, \bar{C}_2) + H_1(C_1 - \bar{C}_1) + H_2(C_2 - \bar{C}_2) \quad (5)$$

Equation 5 is valid if the concentrations (C_1, C_2) of the two solutions prepared for the experiment are sufficiently near their mean composition point $(\bar{C}_1, \bar{C}_2)$. Throughout this discussion the concentrations C_i have dimensions of moles/1000 cc.

The Density Gradient in a Three-Component System.—By using the boundary conditions for free diffusion, Fujita and Gosting[5] have integrated the continuity equations for convection-free diffusion of the solutes in a ternary system with constant diffusion coefficients to obtain

$$C_i = [(C_i)_A + (C_i)_B]/2 + K_i^+\Phi(\sqrt{\sigma_+}\, y) + K_i^-\Phi(\sqrt{\sigma_-}\, y) \quad (6)$$

where

$$\Phi(q) = (2/\sqrt{\pi})\int_0^q e^{-q^2}\, dq \quad (7)$$

$$\sigma_\pm = {}^1/_2\{S_{11} + S_{22} \pm [(S_{22} - S_{11})^2 + 4S_{12}S_{21}]^{1/2}\} \quad (8)$$

$$S_{ij} = [(D_{ij})_V]/[(D_{11})_V(D_{22})_V - (D_{12})_V(D_{21})_V] \quad (9)$$

$$K_i^\pm = \pm [(\sigma_\pm - S_{ii})\Delta C_i - S_{ij}\Delta C_j]/[2(\sigma_+ - \sigma_-)] \; (i \neq j) \quad (10)$$

Equation 3 defines the independent variable y. By using eq. 5 and assuming the density derivatives H_i to be independent of the concentrations C_i (and hence of x) we find

$$(\partial d/\partial x)_t = H_1(\partial C_1/\partial x)_t + H_2(\partial C_2/\partial x)_t \quad (11)$$

Equations 6 are differentiated with respect to x, and the resulting expressions for $(\partial C_i/\partial x)_t$ are inserted into (11) to obtain the expression for the density gradient in a ternary system during the free diffusion process

$$(\partial d/\partial x)_t = [1/\sqrt{\pi t}][\sqrt{\sigma_+}(H_1K_1^+ + H_2K_2^+)e^{-\sigma_+ y^2} + \sqrt{\sigma_-}(H_1K_1^- + H_2K_2^-)e^{-\sigma_- y^2}] \quad (12)$$

From this equation the density gradient could be calculated for any given values of $y = x/(2\sqrt{t})$ if the quantities $(D_{ij})_V$, H_i, and ΔC_i were known or could be estimated.

Conditions for Gravitational Stability.—For gravitational stability in a ternary system during the boundary sharpening process (or at $t = 0$) we find the condition

$$H_1\Delta C_1 + H_2\Delta C_2 > 0 \quad (13)$$

by using inequality 1 and eq. 4 and 5.

The condition for gravitational stability at any time $t > 0$ is found by inserting eq. 12 into 2 and multiplying both sides of the resulting inequality by $(\sqrt{\pi t/\sigma_+})e^{\sigma_+ y^2}$ to obtain

$$H_1K_1^+ + H_2K_2^+ + (\sqrt{\sigma_-/\sigma_+})(H_1K_1^- + H_2K_2^-)e^{(\sigma_+ - \sigma_-)y^2} > 0 \quad (14)$$

To find the conditions for gravitational stability that are independent of x and t (and hence y) we assume

$$\sigma_+ - \sigma_- > 0 \quad (15)$$

$$\sqrt{\sigma_+/\sigma_-} > 1 \quad (16)$$

These assumptions imply the very reasonable restrictions

$$[(D_{22})_V - (D_{11})_V]^2 > -4(D_{12})_V(D_{21})_V \quad (17)$$

$$(D_{11})_V(D_{22})_V > (D_{12})_V \quad (18)$$

on the diffusion coefficients. If (15) is satisfied, then for all values of y

$$e^{(\sigma_+ - \sigma_-)y^2} \geq 1 \quad (19)$$

From (14) and (19) it is apparent that, regardless of the value for $H_1K_1^+ + H_2K_2^+$, the condition[9]

$$H_1K_1^- + H_2K_2^- \geq 0 \quad (20)$$

must be satisfied if gravitational stability is to be maintained when $|y|$ is very large. Condition 20 is therefore necessary but not sufficient for inequality 2 to be satisfied for all values of y. However, if assumption 15 (which implies inequality 19) is valid, then condition 20 and a second condition

$$H_1K_1^+ + H_2K_2^+ + (\sqrt{\sigma_-/\sigma_+})(H_1K_1^- + H_2K_2^-) > 0 \quad (21)$$

together are seen to be sufficient to imply inequality 14 and hence gravitational stability, inequality 2, for *all* values of y, *i.e.*, for all values of $t > 0$ and all values of x.

The condition for gravitational stability at $t = 0$, inequality 13, also can be written

$$H_1K_1^+ + H_2K_2^+ + H_1K_1^- + H_2K_2^- > 0 \quad (22)$$

by using eq. 10. But we can show that condition 22 is implied by conditions 20 and 21 and is therefore a redundant condition for gravitational stability. From inequalities 16 and 20 it follows that

$$(\sqrt{\sigma_+/\sigma_-})(H_1K_1^- + H_2K_2^-) > H_1K_1^- + H_2K_2^- \quad (23)$$

which reads

$$-(\sqrt{\sigma_-/\sigma_+})(H_1K_1^- + H_2K_2^-) > -(H_1K_1^- + H_2K_2^-) \quad (24)$$

(8) Defined, for example, by eq. 20 of ref. 9.

(9) Throughout this derivation and the derivation of eq. 6 it is assumed that $\sigma_\pm \neq 0$; these inequalities are implied by condition 18.

after both sides of (23) are multiplied by $-\sqrt{\sigma_-/\sigma_+}$. From (21) we have

$$H_1K_1^+ + H_2K_2^+ > -(\sqrt{\sigma_-/\sigma_+})(H_1K_1^- + H_2K_2^-) \quad (25)$$

Inequalities 24 and 25 together imply

$$H_1K_1^+ + H_2K_2^+ > -(H_1K_1^- + H_2K_2^-) \quad (26)$$

which is identical with inequality 22. Thus, if inequality 16 is valid, then conditions 20 and 21 for gravitational stability at $t > 0$ also imply condition 22 for gravitational stability at $t = 0$. Therefore conditions 20 and 21 are sufficient to ensure gravitational stability for all times $t \geq 0$ during the free diffusion process and at all positions $\infty > x > -\infty$ in the diffusing boundary.

For the special case of a ternary system for which

$$(D_{12})_V = (D_{21})_V = 0 \quad (27)$$

where the faster diffusing solute is designated by the subscript 2, so that

$$(D_{22})_V > (D_{11})_V \quad (28)$$

then conditions 20 and 21, respectively, reduce to

$$H_2\Delta C_2 \geq 0 \quad (29)$$

and

$$H_1\Delta C_1/\sqrt{(D_{11})_V} + H_2\Delta C_2/\sqrt{(D_{22})_V} > 0 \quad (30)$$

Application.—From equations 20 and 21 the relative values of ΔC_1 and ΔC_2 which will give a gravitationally stable free diffusion experiment can be calculated, provided that values are available for H_1, H_2, and the four diffusion coefficients. If no estimates of values of the $(D_{ij})_V$ are available, two or more preliminary experiments which seem very likely to be gravitationally stable may be performed; the resulting preliminary data for the H_i and the $(D_{ij})_V$ then can be used to calculate whether other desired relative values of ΔC_1 and ΔC_2 may be safely used.

A simple illustration of the application of the criteria for gravitational stability is obtained by examining data for the system H_2O–glycine–KCl which was studied recently by Woolf, Miller, and Gosting.[10] For this system at $C_1 = 0.5$ and $C_2 = 0.5$ mole/l., where the subscripts 1 and 2 designate glycine and KCl, respectively, values obtained were $(D_{11})_V = 0.98_{42} \times 10^{-5}$ cm.^{2}/sec., $(D_{12})_V = -0.00_{57} \times 10^{-5}$ cm.^{2}/sec., $(D_{21})_V = -0.01_{34} \times 10^{-5}$ cm.^{2}/sec., $(D_{22})_V = 1.74_{45} \times 10^{-5}$ cm.^{2}/sec., $H_1 = 0.0301_4$ kg./mole, and $H_2 = 0.0447_9$ kg./mole. At this composition both cross-term diffusion coefficients are very small; if they are considered to be zero, conditions 29 and 30 then become

$$\Delta C_2 \geq 0 \quad (31)$$

and

$$\Delta C_1 + 1.1162\Delta C_2 > 0 \quad (32)$$

(10) L. A. Woolf, D. G. Miller, and L. J. Gosting, *J. Am. Chem. Soc.*, **84**, 317 (1962).

Also, inequality 22, the redundant condition for gravitational stability at $t = 0$, becomes

$$\Delta C_1 + 1.4861\Delta C_2 > 0 \quad (33)$$

It is apparent that (33) will be satisfied if (31) and (32) are satisfied. Furthermore, gravitational instability, or convection, will occur at some time t or some position x if condition 31 is not satisfied, because inequality 20 (and hence inequality 31) is a necessary condition for a positive density gradient (inequality 2). Thus, if we had been unaware of condition 31, we might have prepared solutions for a diffusion experiment so that $\Delta C_2 < 0$ and $\Delta C_1 > -1.4861\Delta C_2$, under the erroneous impression that condition 33 for gravitational stability at $t = 0$ also would ensure gravitational stability at all later times and at all positions.

The magnitude of the negative density gradient produced at some time during a diffusion experiment because condition 20 was not satisfied may be so small as to cause no observable disturbance of the diffusing boundary. Also, it should be emphasized that condition 21 was proved to be *sufficient* but not *necessary* for gravitational stability; therefore, if this condition is not satisfied, a negative density gradient will not necessarily be produced. But to be absolutely certain that no convective mixing will occur during a diffusion experiment, conditions 20 and 21 both should be satisfied for all studies of free diffusion in three-component systems.

Acknowledgments.—The author wishes to thank Professor L. J. Gosting for his helpful discussions of this research. This work was supported, in part, by research grants from the National Science Foundation (G-7401) and the National Institute of Arthritis and Metabolic Diseases (U.S.P.H.S.) (A-5177), and from the Research Committee of the University of Wisconsin Graduate School from funds supplied by the Wisconsin Alumni Research Foundation.

DECOMPOSITION OF *n*-PROPANE AND *n*-BUTANE ON CLEAN RHODIUM FILMS

BY RICHARD W. ROBERTS

General Electric Research Laboratory, Schenectady, N. Y.

Received March 31, 1962

The surface decomposition of saturated hydrocarbons has been investigated by a number of workers[1,2] on a variety of metal surfaces. In general, they concluded that carbon–carbon bond cleavage (cracking) did not occur at temperatures below about 140°. The vacuum conditions ($\sim 10^{-5}$ torr.) used in their experiments suggest that the metal surfaces were contaminated by adsorbed gases.

Recently, it has been demonstrated that adsorbed gases have a pronounced effect on hydrocarbon

(1) K. Morikawa, N. R. Trenner, and H. S. Taylor, *J. Am. Chem. Soc.*, **59**, 1103 (1937).

(2) R. C. Hansford in A. Farkas, Ed., "Physical Chemistry of the Hydrocarbons," Academic Press, New York, N. Y., 1953, Vol. II, p. 187.

cracking reactions.[3,4] For example, at 0° on a clean rhodium surface, *i.e.*, one prepared in a vacuum of 10^{-9} torr., ethane will decompose to yield gaseous methane and an adsorbed hydrocarbon residue. Observations of the interaction of *n*-propane and *n*-butane with clean films of rhodium are presented in this communication.

Experimental

The experimental procedure is similar to that published in detail elsewhere.[4] In brief, the rhodium film was deposited on the inside of a Pyrex glass sphere by pulse evaporating a 99.999% pure rhodium wire. The entire glass–metal system had previously been baked at 400° for 18 hr. The pressure in the system never rose above 2×10^{-9} torr. during the evaporation. Film thicknesses were measured at the completion of an experiment by X-ray emission spectroscopy and were about 50 Å. After the film was deposited, the reaction vessel was isolated from the pumping system by closing a metal valve. The *n*-propane and *n*-butane used were Phillips research grade and were admitted to the film by breaking a thin glass break-seal. After the desired reaction time, the gases were removed for mass spectrographic analysis. Blank experiments indicated that no reactions occurred on the freshly baked glass surfaces.

Results and Discussion

The results of experiments performed with *n*-propane and *n*-butane on clean rhodium films at 27 and 100° are given in Table I. The number of molecules of each species present in the gas phase, n_i, was determined mass spectrometrically and is listed. The numbers of carbon and hydrogen atoms remaining on the surface, $n_C(s)$ and $n_H(s)$, were calculated from the amount of gas introduced initially and the composition of the gas phase at the completion of the experiment.

TABLE I

SUMMARY OF EXPERIMENTS PERFORMED WITH *n*-PROPANE AND *n*-BUTANE ON CLEAN RHODIUM FILMS

Gas	C_3H_8	C_3H_8	C_4H_{10}	C_4H_{10}
Initial amt. of gas, molecules $\times 10^{-17}$	9.82	9.20	3.63	4.82
Rh temp., °C.	27	100	27	100
Rh av. thickness, Å.	56	48	42	32
Reaction time, min.	1200	14	3200	8
Products, molecules $\times 10^{-17}$				
n_{H_2}	0.93	..	2.83	..
n_{CH_4}	1.85	11.3	1.25	3.83
$n_{C_2H_6}$	0.21	0.23	0.11	..
$n_{C_3H_8}$	0.43	..	.11	..
$n_{C_4H_{10}}$	..	..	.87	..
$n_C(s)$	25.9	15.8	9.2	15.4
$n_H(s)$	64.6	26.9	15.4	32.9

It was observed that both *n*-propane and *n*-butane decomposed on clean rhodium surfaces at 27 and 100° to yield lower hydrocarbons and an adsorbed hydrocarbon residue. After 1200 min. on a rhodium film at 27°, *n*-propane decomposed to H_2, CH_4, and C_2H_6. Similarly, *n*-butane after 3200 min. at 27° decomposed to H_2, CH_4, C_2H_6, and C_3H_8. However, at a rhodium film temperature of 100°, the primary reaction product for both *n*-propane and *n*-butane was CH_4. The rate of decomposition at 100° was several hundred times greater than at 27° for both *n*-propane and *n*-butane.

Other experiments[4] indicate that there are about 3.5×10^{18} rhodium atoms present in the surface of the rhodium film. Thus, if all the carbon–carbon bonds were broken and all the hydrogen were bonded to the carbon, the rhodium film would be about 30 to 60% covered with the residue. Since the nature of the residue is unknown, these numbers are only a rough estimate.

Because the rhodium films were prepared in a vacuum of $\sim 2 \times 10^{-9}$ torr., they were not more than 5% contaminated at the time the hydrocarbon was admitted. Adsorbed gases greatly reduce the activity of these films. Neither ethane, *n*-propane, nor *n*-butane decomposed to lower hydrocarbons on a rhodium film which had adsorbed a monolayer of oxygen.

The reaction mechanism for these reactions is complex as there appears to be a number of consecutive processes occurring. However, at 100° the rate of all reactions is increased so that the end product is primarily methane.

Acknowledgment.—The author wishes to thank Miss Nancy Keary for assistance with the experiments.

(3) R. W. Roberts, *Nature*, **191**, 170 (1961).

(4) R. W. Roberts, *Trans. Faraday Soc.*, **58**, 1159 (1962).

EVIDENCE FOR THE FORMATION OF BIPHENYL BY *INTRA*MOLECULAR DIMERIZATION IN THE ELECTROÖXIDATION OF TETRAPHENYLBORATE ION

BY DAVID H. GESKE

Department of Chemistry, Cornell University, Ithaca, New York

Received April 2, 1962

The electroöxidation of tetraphenylborate ion at a platinum electrode in acetonitrile solution has previously been reported.[1] Evidence was presented showing that the primary electrode reaction was

$$B(C_6H_5)_4^- - 2e \longrightarrow B(C_6H_5)_2^+ + (C_6H_5)_2$$

It was not possible at that time to distinguish between the two possible mechanisms (Fig. 1) for formation of the biphenyl. Further work has now been done which suggests that the two phenyl radicals in the transition state of the oxidized tetraphenylborate undergo *intra*molecular dimerization (Fig. 1a).

Acetonitrile solution mixtures of tetramethylammonium perdeuteriotetraphenylborate, $(CH_3)_4N^+B(C_6D_5)_4^-$, and ordinary tetramethylammonium tetraphenylborate were electrolyzed. Mass spectral examination of the biphenyl produced showed that *only* $(C_6H_5)_2$ and $(C_6D_5)_2$ were formed, a result consistent with the reaction mechanism in Fig. 1a. The detection of mass 159, the unsymmetrical biphenyl which would be expected if the reaction in Fig. 1b were operative, was not obscured by the fragmentation pattern of perdeuteriobiphenyl; thus an upper limit of 1% of total biphenyl (the intrinsic instrumental limitation) can be set for the occurrence of $C_6H_5C_6D_5$. In two electrolyses in which the

(1) D. H. Geske, *J. Phys. Chem.*, **63**, 1062 (1959).

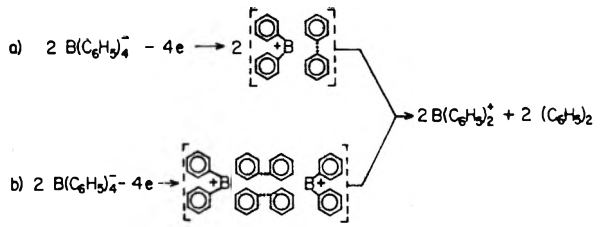

Fig. 1.—Alternative dimerization mechanisms in electrooxidation of tetraphenylborate ion.

initial mole ratios of $B(C_6D_5)_4^-/B(C_6H_5)_4^-$ were 0.91 and 0.30, the observed mole ratios of $(C_6D_5)_2/(C_6H_5)_2$ were 1.0 and 0.38, respectively.

It seems entirely reasonable to reject the suggestion that there are certain electrode sites on which the perdeuteriotetraphenylborate ion oxidation occurs and other sites on which ordinary tetraphenylborate ion oxidizes. On this basis the evidence points unequivocally to the reaction scheme in Fig. 1a as the correct one, *i.e.*, the dimerization is *intra*molecular.

Tetraphenylborate ion also is oxidized chemically in a two-electron process by ceric ammonium nitrate in acetonitrile. Analysis of the oxidized solutions shows that the dimerization mechanism is the same as for the electrooxidation.

Experimental

Reagents.—Tetramethylammonium perdeuteriotetraphenylborate, $(CH_3)_4^+B(C_6D_5)_4^-$, was synthesized by modification of the procedure of Nesmeyanov and Sazonova[2] for ordinary sodium tetraphenylborate. Bromobenzene-d_5 prepared from benzene-d_6 (99% isotopic purity, Volk Radiochemical Co., Chicago, Ill.) by the bromination procedure of Best and Wilson[3] was used to prepare the corresponding Grignard reagent. Sodium tetrafluoroborate was added to the Grignard reagent and the solution was refluxed for 90 min. and then poured into water and filtered. Addition of tetramethylammonium iodide to the aqueous filtrate precipitated tetramethylammonium perdeuteriotetraphenylborate. Deuterium analysis[4] of the tetramethylammonium perdeuteriotetraphenylborate gave 58.1 atom % excess deuterium compared with the calculated value of 62.5%.

The acetonitrile used as solvent in this work was purified as previously described.[1] The sodium perchlorate used as supporting electrolyte was purified by recrystallization from water followed by drying *in vacuo* at 130°.

Electrolyses and Analyses.—Acetonitrile solutions 0.2 *M* in sodium perchlorate as supporting electrolyte and approximately 5 m*M* in *total* tetramethylammonium tetraphenylborate were electrolyzed at a platinum electrode. The control potential was +1.0 volt *vs.* aqueous saturated calomel electrode. A modified Booman[5] potentiostat was employed. Solutions were degassed before and during the electrolyses. The total solution volume was 20 ml.

No attempt was made to obtain absolute biphenyl analyses but rather only the mole ratios of various isotopic species present. When a solution 2.53 m*M* in $(CH_3)_4N^+B(C_6D_5)_4^-$ and 2.78 m*M* in $(CH_3)_4N^+B(C_6H_5)_4^-$ was electrolyzed completely the mole ratio of $(C_6D_5)_2/(C_6H_5)_2$ in the electrolyzed solution as determined mass spectrometrically was found to be 1.0. The value of the ratio for electrolysis of a solution with an initial solution composition 1.26 m*M* in $(CH_3)_4^+B(C_6D_5)_4^-$ and 4.17 m*M* in $(CH_3)_4N^+B(C_6H_5)_4^-$ was 0.38.

In the previous study[1] sodium tetraphenylborate was electrolyzed in a solution containing lithium perchlorate as supporting electrolyte. It is quite likely that these salts as well as sodium perchlorate and tetramethylammonium tetraphenylborate are strong electrolytes. Thus there is little reason to suppose that the electrode process is altered by variation between the cationic species mentioned above.

The biphenyl analysis was completed in the following manner. A 5-ml. portion of the electrolyzed acetonitrile solution was equilibrated with 12 ml. of aqueous saturated mercuric chloride solution and then extracted with cyclohexane. The cyclohexane extract was dried over calcium chloride and transferred to a sample tube. The cyclohexane was evaporated on a steam bath leaving a small quantity of biphenyl which was subjected to mass spectrometric analysis. The molecular ions at mass 164 and 154 were used to establish the ratio of perdeuteriobiphenyl to biphenyl. The mass spectrum of an authentic sample of perdeuteriobiphenyl (Merck, Sharp and Dohme) was obtained for comparison.

Acknowledgment.—The author is indebted to Professor Richard Porter for performing the mass spectrometric analyses. The technical assistance of J. Taylor is acknowledged. Financial support was provided under grant AFOSR 61-18 from the Directorate of Chemical Sciences, Air Force Office of Scientific Research.

(2) A. N. Nesmeyanov and V. A. Sazonova, *Izv. Akad. Nauk SSSR, Otd. Khim. Nauk*, 187 (1955).

(3) A. P. Best and C. L. Wilson, *J. Chem. Soc.*, 239 (1946).

(4) Analyses were performed by Mr. J. D. Nemeth, Urbana, Illinois.

(5) G. L. Booman, *Anal. Chem.*, **29**, 213 (1957).

FARADAIC RECTIFICATION AND ELECTRODE PROCESSES. IV

BY HIDEO IMAI[1]

Coates Chemical Laboratory, Louisiana State University, Baton Rouge 3, Louisiana

Received April 9, 1962

Two methods have been applied in faradaic rectification measurements, namely direct measurement of rectification voltages[2,3] and compensation of the rectification voltage by a voltage step.[4] These methods allow the study of variations of the rectification voltage with frequency but have the disadvantage of requiring determination of the voltage applied to the faradaic impedance. This determination is not as easy as it might appear at high frequencies ($f > 1$ Mc.) because of stray capacity and the inductance of the cell circuit. A simple method is described here in which this difficulty is eliminated. The method rests on measurement of the frequency at which the rectification voltage is equal to zero. Measurement of the voltage applied to the faradaic impedance is not necessary and the attending experimental difficulties are avoided. Results are given for the reaction $Cr(CN)_6^{-3} + e = Cr(CN)_6^{-4}$ on mercury.

Experimental

Apparatus and techniques were previously described.[3,4b,4c] Special care was taken that the amplitude of the a.c. signal applied to the faradaic impedance did not exceed 5 mv. because theory did not apply very well for higher voltages (*cf.* ref. 2 for discussion). Zero rectification voltage could be observed 50 μsec. after application of the a.c. signal since transients had died out. $K_3Cr(CN)_6$ was obtained from the City Chemical Corp., New York, N.Y., and was used

(1) Postdoctoral research associate, 1960–1962, on leave from Minami College, Hiroshima University, Hiroshima, Japan.

(2) (a) P. Delahay, M. Senda, and C. H. Weis, *J. Am. Chem. Soc.*, **83**, 312 (1961); (b) for a review, *cf.* P. Delahay in "Advances in Electrochemistry and Electrochemical Engineering," Vol. I, P. Delahay, Editor, Interscience Division, John Wiley and Sons, New York, N. Y., 1961, pp. 279–300.

(3) H. Imai and P. Delahay, *J. Phys. Chem.*, **66**, 1108 (1962).

(4) (a) G. C. Barker, "Transactions of the Symposium on Electrode Processes, Philadelphia, 1959," E. Yeager, Editor, John Wiley and Sons, New York, N. Y., 1961, pp. 325–365; (b) M. Senda, H. Imai, and P. Delahay, *J. Phys. Chem.*, **65**, 1253 (1961); (c) H. Imai and P. Delahay, *ibid.*, **66**, 1683 (1962).

without further purification. Other reagents were of analytical grade. Solutions of $K_3Cr(CN)_6$ were prepared and kept in a darkroom because there appeared to be some photochemical decomposition.

Theory

We consider rectification for a simple charge transfer process without complication due to adsorption, coupled chemical reaction, etc. The rectification voltage $\Delta\bar{E}_\infty$ for a reaction $O + ne = R$ involving two soluble species is such that

$$\frac{RT}{nF}\frac{\Delta\bar{E}_\infty}{V_A^2} = \frac{2\alpha - 1}{4} - \frac{1}{2}\left(\alpha - \frac{C_O D_O^{1/2}}{C_O D_O^{1/2} + C_R D_R^{1/2}}\right)\frac{1 + \text{ctn}\,\theta}{1 + \text{ctn}^2\,\theta} \quad (1)$$

where V_A is the amplitude of the alternating voltage across the faradaic impedance, α the transfer coefficient, C's the concentrations, D's the diffusion coefficients, θ the phase angle between current and voltage, and n, F, R, T are as usual. The term $(2\alpha - 1)/4$ is positive or negative according to $\alpha \gtrless 0.5$. The second term is positive or negative depending on the value of ctn θ which depends on frequency. At sufficiently high frequencies ctn $\theta \gg 1$, and

$$\frac{1 + \text{ctn}\,\theta}{1 + \text{ctn}^2\,\theta} \approx \frac{1}{\text{ctn}\,\theta} = \frac{I_a^0}{2^{1/2}nF}\left(\frac{1}{C_O D_O^{1/2}} + \frac{1}{C_R D_R^{1/2}}\right)\frac{1}{\omega^{1/2}} \quad (2)$$

where I_a^0 is the apparent exchange current and $\omega = 2\pi f$, f being the frequency. Further

$$I_a^0 = nFk_a^0 C_O^{1-\alpha} C_R^{\alpha} \quad (3)$$

where k_a^0 is the apparent rate constant. The condition for $\Delta\bar{E}_\infty = 0$ is

$$\alpha - \frac{1}{2} = \left(\alpha - \frac{C_O D_O^{1/2}}{C_O D_O^{1/2} + C_R D_R^{1/2}}\right)\frac{k_a^0}{2^{1/2}\omega^{1/2}} C_O^{1-\alpha} C_R^{\alpha}\left(\frac{1}{C_O D_O^{1/2}} + \frac{1}{C_R D_R^{1/2}}\right) \quad (4)$$

The parameters α and k_a^0 can be determined from the value of ω for which $\Delta\bar{E}_\infty = 0$ provided C_O and C_R are known. We consider the case in which R is generated *in situ* by polarography. Thus

$$C_O = C_O^0[1 - (i/i_d)] \quad (5)$$

$$C_R = C_O^0(D_O/D_R)^{1/2}(i/i_d) \quad (6)$$

where C_O^0 is the bulk concentration of O, i the polarographic current, and i_d the diffusion current. By setting

$$C_R D_R^{1/2}/C_O D_O^{1/2} = p \quad (7)$$

with

$$p = (i/i_d)/[1 - (i/i_d)] \quad (8)$$

one deduces from eq. 4

$$k_a^0 = \frac{\left(\alpha - \frac{1}{2}\right)(4\pi f_p D_O)^{1/2}}{\left(\alpha - \frac{1}{1+p}\right)p^{\alpha-1}\left(\frac{D_O}{D_R}\right)^{\alpha/2}(1+p)} \quad (9)$$

where f_p is the frequency at which $\Delta\bar{E}_\infty = 0$ for the value of p given by eq. 8. Equation 9 can be applied at two potentials for which p has the values p_1 and p_2, and the resulting system of equations yields

$$\left(\frac{f_{p_1}}{f_{p_2}}\right)^{1/2} = \left(\frac{p_1}{p_2}\right)^{\alpha-1}\frac{\alpha(1+p_1) - 1}{\alpha(1+p_2) - 1} \quad (10)$$

or

$$\frac{1}{2}\log\frac{f_{p_1}}{f_{p_2}} + (1 - \alpha)\log\left(\frac{p_1}{p_2}\right) = \log\frac{\alpha(1+p_1) - 1}{\alpha(1+p_2) - 1} \quad (11)$$

The parameter α is determined from the intersection of the curves representing the left-hand and right-hand members of eq. 11, respectively, as functions of α. k_a^0 then is calculated from eq. 9.

The above procedure can be simplified when the frequency for which $\Delta\bar{E}_\infty = 0$ is measured at the half-wave potential and one can assume $D_O = D_R = D$. One then has

$$k_a^0 = (\pi f D)^{1/2} \quad (12)$$

The parameter α then is calculated from eq. 9.

Description and Discussion of Results

The above method was applied to $Cr(CN)_6^{-3} + e = Cr(CN)_6^{-4}$ on mercury under polarographic conditions. Results[5] for experimental conditions of Table I were as follows: $\alpha = 0.53$ for each combination II–III, III–IV, and II–IV; $k_a^0 = 1.58$, 1.14, and 1.00 cm. sec.$^{-1}$ for the data II, III, and IV, respectively. The value of k_a^0 based on eq. 12 was 1.06 cm. sec.$^{-1}$, and the corresponding α deduced from eq. 11 was 0.54. Results for α are excellent, whereas k_a^0 varies somewhat from one set of data to another. This variation in k_a^0 results, among other possible causes of departure from theory, from the approximation made by the use of eq. 2 (see below). It should be noted also that a decrease of k_a^0 as E becomes more negative is to be expected because of the double layer correction. (The potential across

TABLE I

EXPERIMENTAL CONDITIONS FOR 5 mM $K_3Cr(CN)_6$ IN 0.5 M KCN, 3 M KCl AT 25°

E, v. vs. s.c.e.	i/i_d	f, Mc. sec.$^{-1}$
−1.335[a]	0.500	0.050
−1.340	.552	.32
−1.345	.609	.95
−1.350	.646	1.60

[a] Half-wave potential.

(5) $D_O = 0.71 \times 10^{-5}$ cm.^{2} sec.$^{-1}$, as calculated from i_d. This compares quite well with the value 0.65×10^{-5} cm.^{2} sec.$^{-1}$ for 1 M KCN reported by D. N. Hume and I. M. Kolthoff, *J. Am. Chem. Soc.*, **65**, 1897 (1943).

the diffuse double layer from the plane of closest approach to solution increases as E becomes more negative.)

The above treatment is based on eq. 2, *i.e.*, on the assumption that $(1 + \text{ctn}\,\theta)/(1 + \text{ctn}^2\,\theta) \approx 1/\text{ctn}\,\theta$. The validity of this assumption was determined for the above case ($k = 1$ cm. sec.$^{-1}$) by computing ctn θ from the theory of the faradaic impedance.[6] Results were for $f = 0.05, 0.25, 0.5, 1, 2$ Mc. sec.$^{-1}$: $(1 + \text{ctn}\,\theta)/(1 + \text{ctn}^2\,\theta) = 0.54, 0.32, 0.24, 0.17, 0.13$; $1/\text{ctn}\,\theta = 0.45, 0.27, 0.21, 0.15, 0.11$. The assumption embodied in eq. 2 thus is fairly justified in this case, especially at the higher frequencies.

In conclusion, the above method has the merit of simplicity over other methods previously applied in faradaic rectification measurements. It allows indirect verification of the frequency dependence of the rectification voltage since measurements cover a fairly wide range of frequencies (*cf.* Table I). This method could be extended to electrode processes requiring a more involved frequency dependence than that of eq. 1 (charge transfer coupled with coupled chemical reaction, adsorption of reactants and/or products, etc.).

Acknowledgment.—This work was supported by the National Science Foundation. The author is indebted to Professor Paul Delahay for his interest and discussion of this investigation.

(6) *Cf.* ref. 2b, pp. 267–268.

RADIOLYSIS OF LIQUID 1,5-HEXADIENE

By H. B. van der Heijde and C. D. Wagner

Shell Development Company, Emeryville, California

Received April 9, 1962

There is now considerable evidence that the radiolysis of liquid and solid olefins frequently involves ionic reactions[1,2] and ion–molecule condensations.[3–6] It has been shown that the points at which condensation occurs in terminal olefins are at the carbons attached to the double bond. The importance of the double bond posed the interesting question of whether a non-conjugated diolefin would cyclize. For this reason the radiation chemistry of 1,5-hexadiene was studied.

Experimental

The 1,5-hexadiene was obtained from Farchan Chemical Co. After distillation it was found by gas–liquid chromatography (GLC) analysis to contain 0.08% 1-hexene and 0.03% of an unidentified hydrocarbon boiling slightly lower.

One irradiation was conducted with bremsstrahlung photons from the gold target of the 3 Mev. Van de Graaff accelerator.[7] To do this a 0.3-g. sample was sealed *in vacuo* in a 7 mm. o.d. glass tube, and placed in position in a thin metal tube under the target. Cold nitrogen gas maintained the temperature at −150° during the half-hour irradiation at an intensity of 1.3×10^8 rads/hr. The liquid phase was analyzed by GLC, using a 6 mm. o.d. × 6 m. "Ucon" column.

Most of the data obtained in this study were gathered from a radiolysis experiment in which hexadiene (90 g.) was irradiated at 25° in an aluminum circulating cell[8] with a 32 μa. 3 Mev. electron beam for 53 min. The dose was calculated to be 2.85×10^8 rads. Gas evolved was analyzed mass spectrometrically. Extensive gas chromatographic analyses were conducted on a distillate fraction, containing products $< C_5$ plus some of the unreacted feed, and on the residue, consisting of the remainder of the feed plus the heavier products. Fractional distillation of the residue provided a C_9–C_{12} fraction for detailed examination, and a yield value for heavier polymer.

The C_9 and C_{12} components were analyzed by gas chromatography, and some of the trapped fractions were examined by infrared and mass spectrometry. Then in order to obtain clear information on the carbon skeletons a sample was hydrogenated with platinic oxide catalyst in methanol–acetic acid. The hydrocarbon was isolated by dilution with water, separation, drying, and decanting. Completeness of hydrogenation was checked by infrared analysis. The hydrogenated products were analyzed by GLC, with identification by a combination of the mass spectral fragmentation patterns and GLC emergence times.

Results and Discussion

Yields of products from the irradiation at 25° are given in Table I. The yield of hydrogen, $G = 0.45$, is lower than that with 1-hexene, 0.8, as might be expected with this higher degree of unsaturation. The product pattern is similar to that from 1-hexene, except that products at C_3 (propylene) and C_9 are much more prominent. Like 1-hexene, the principal heavy products are formed by addition to one of the carbon atoms attached to a double bond with, again, a preference for joining at the end to produce a straight chain. The comparative rarity of C_2 branches again indicates a minor role for allyl-type radicals

$$CH_2{=}CH{-}CH_2{-}\dot{C}H{-}CH{=}CH_2$$

The gas–liquid chromatogram of products from the low-temperature irradiation was nearly identical with that of the irradiation at 25°. Thus, the products must arise from "hot" processes or from reactions involving no activation energy, an observation like that already made with 1-hexene.

Mass spectrometric examination of the C_9 products established that they consisted mostly of diolefins and triolefins, with mostly vinyl (terminal) but some vinylene (RCH = CHR) double bonds. The C_{12} products were di-, tri-, and some tetraolefins, always with vinyl unsaturation but frequently including vinylene double bonds.

The low yield of cyclic compounds ($G = 0.12$) may be attributed to the high collision efficiency of the ion–molecule reaction. The active positive center of the molecule readily polarizes a neighboring molecule and reacts with it, and only seldom finds its own opposite double bond in a position to react.

From these data the mechanism of formation of C_9 compounds is not clear. The similarity in structure between C_9 and C_{12} suggests condensation of the molecule ion with a molecule, followed in a fraction of the events by splitting at the relatively weak third bond to give C_9 and C_3.

(1) W. H. T. Davison, S. H. Pinner, and R. Worrall, *Chem. Ind.* (London), 1274 (1957).

(2) W. S. Anderson, *J. Phys. Chem.*, **63**, 765 (1959).

(3) P. C. Chang, N. C. Yang, and C. D. Wagner, *J. Am. Chem. Soc.*, **81**, 2060 (1959).

(4) C. D. Wagner, *Tetrahedron*, **14**, 164 (1961).

(5) C. D. Wagner, *J. Phys. Chem.*, **66**, 1158 (1962).

(6) E. Collinson, F. S. Dainton, and D. C. Walker, *Trans. Faraday Soc.*, **57**, 1732 (1961).

(7) C. D. Wagner and V. A. Campanile, *Nucleonics*, **17**, 99 (1959).

(8) C. D. Wagner, *J. Phys. Chem.*, **64**, 231 (1960).

TABLE I

PRODUCT YIELDS

Compound	G		G_{-M}[b]	
Hydrogen	0.45			
Ethylene		0.06		
Propylene		.09		
1-Butene		.06		
Unidentified C_5		.02		
$\Sigma C_2 - C_5$	0.23			
1-Hexene		0.17		0.17
Unidentified C_6 (3 cmpd.)		.22		.22
Cyclohexene		.02		.02
ΣC_6	0.41		0.41	
Product skeletal structures				
n-C_7		0.02		
n-C_8		.02		
$\Sigma C_7 - C_8$	0.04			
4-Methyloctane		.20		.30
n-Nonane		.21		.32
Butylcyclopentane		.01		.02
ΣC_9	0.42		0.63	
3-Methylnonane[a]		.01		
n-Decane		.01		
ΣC_{10}	0.02			
4,5-Diethyloctane[a]		.013		.026
4-Ethyl-5-methylnonane[a]		.045		.09
5,6-Dimethyldecane[a]		.015		.03
4-Ethyldecane[a] / 5-Methylundecane		.21		.42
n-Dodecane		.40		.80
Cyclane A[a]		.02		.04
Cyclane B[a]		.03		.06
Cyclane C[a]		.02		.04
Cyclane D[a]		.015		.03
ΣC_{12}	0.77		1.54	
Σ Heavy residue			4.80	

[a] Structure inferred from mass spectral fragmentation and emergence time. 4-Ethyldecane and 5-methylundecane were not resolved; the other C_{12} compounds were rather well defined from a 6 mm. × 13 m. column (Ucon) at 160°. [b] The sum for reaction, *ca.* 7.7, is undoubtedly too low. It is possibly due to evolved gas trapped within the cell, so that some of the energy of the electrons is dissipated in the cell wall beneath.

Conclusions

Radiolysis of liquid 1,5-hexadiene at −150 to 25° gives H_2 (G = 0.45), C_9 (G = 0.42), C_{12} (G = 0.78), and heavier polymers ($G_{(-M)}$ = 4.8). C_9 and C_{12} compounds are mainly diolefins and triolefins. Their carbon skeletons are those expected from the addition of the end of a straight C_3 or C_6 chain to either the end or second carbon of another straight chain. Cyclic products account for less than 10% of the products.

Independence of product distribution with temperature, the skeletal character of the dimer, and the small amount of cyclic products all agree with the concept that condensation occurs by the ion–molecule mechanism. The C_9 products apparently arise from the inherent weakness of the central carbon–carbon bond in 1,5-hexadiene.

NITRIC OXIDE DECOMPOSITION INDUCED BY EXCITED NITROGEN MOLECULES IN ACTIVE NITROGEN

BY A. N. WRIGHT AND C. A. WINKLER

The Physical Chemistry Laboratory, McGill University, Montreal, Quebec

Received April 9, 1962

In recent years, the N atom concentration in active nitrogen frequently has been estimated by determining, for optimal reaction conditions, either the extent of its reaction with hydrocarbons or hydrocarbon derivatives to produce HCN, or the extent to which it is capable of destroying NO. However, the ratio (NO destroyed)/(HCN produced) not only increases as the reaction pressure is increased,[1] but its value depends on the time of decay of the active nitrogen at a given pressure.[2] This seems to preclude an explanation[3] of the discrepancy based solely on an assumed pressure dependence of HCN production. It has been suggested,[2] therefore, that NO is destroyed, not only by N atoms present in the active nitrogen, but also by excitation to a state, such as the $^4\Sigma^-$ state, in collisions of the Second Kind with $N_2(A^3\Sigma_u^+)$, followed by decomposition to produce N atoms which might react further with NO. However, recent experiments[4] with isotopically labeled NO have given no evidence for the reaction of NO with N atoms derived from the decomposition of NO, even for reaction pressures[5] for which the ratio (NO destroyed)/(HCN produced) is considerably greater than unity.

An alternative decomposition of NO, induced by excited nitrogen molecules but without the formation of N atoms, may be suggested on the basis of the mechanism postulated recently by Strausz and Gunning[6] for the mercury photosensitized decomposition of NO. According to them, the long-lived, electronically excited[7] NO molecules, produced by energy transfer from Hg $6(^3P_1)$, appear to undergo the reactions

$$NO(^4\pi) + NO \xrightarrow{k_1} (NO)_2^* \xrightarrow{k_2} N_2 + \text{oxygen} \quad (1)$$

at a rate which is maximal at a pressure of 3.25 mm., which corresponds closely to the pressure in our experiments[2] with active nitrogen. In similar manner, spin-allowed collisions of the Second Kind between $N_2(A^3\Sigma_u^+)$ and $NO(X^2\pi)$, to yield $NO(^4\pi)$, might permit destruction of NO as in (1) above, and thereby account for a NO/HCN ratio greater than unity. Dissociation of the NO

(1) G. J. Verbeke and C. A. Winkler, *J. Phys. Chem.*, **64**, 319 (1960).

(2) A. N. Wright, R. L. Nelson, and C. A. Winkler, *Can. J. Chem.*, in press.

(3) W. G. Zinman, *J. Phys. Chem.*, **64**, 1343 (1960).

(4) J. T. Herron, *J. Res. Natl. Bur. Std.*, **A65**, 411 (1961).

(5) R. A. Back and J. Y. P. Mui, *J. Phys. Chem.*, **66**, 1362 (1962)

(6) O. P. Strausz and H. E. Gunning, *Can. J. Chem.*, **39**, 2549 (1961).

(7) R. J. Fallon, J. T. Vanderslice, and E. A. Mason, *J. Phys. Chem.*, **63**, 2082 (1959).

($^4\pi$) molecule, which requires a total energy of about 147 kcal. above the ground state, would be unlikely in view of the substantial potential energy well envisaged[8] for this bound electronic state.

The greater energy content of $N_2(A)$ molecules (142 kcal./mole for the zero vibrational level) would tend to reduce the cross section for energy transfer to NO below the large value (24.7 Å.^{2}) observed[9] for the resonance transfer[7] from excited mercury atoms. On the other hand, the greater energy content of the NO($^4\pi$) molecules so formed might be expected[10] to increase the apparent value of k_1 over the quite small value deduced by S and G from the low quantum yield of the over-all reaction in their system. The value of k_2 also should be increased over that for the photosensitized process, owing to the greater energy content of the $(NO)_2$ dimer.[11,12] Indeed, it is possible that, for the active nitrogen reaction, a simple bimolecular rearrangement process is involved.

Decomposition of NO induced by an electronically excited NO molecule of appreciable lifetime, as above, could maintain a factor of 2 between NO destroyed and the concentration of $N_2(A)$ molecules in active nitrogen, as used previously[2] to calculate the lifetime of the excited nitrogen molecule capable of causing NO destruction.

(8) J. T. Vanderslice, E. A. Mason, and W. G. Maisch, *J. Chem. Phys.*, **31**, 738 (1959).
(9) J. R. Bates, *J. Am. Chem. Soc.*, **54**, 569 (1932).
(10) J. L. Magee and W. H. Hamill, *J. Chem. Phys.*, **31**, 1380 (1959).
(11) G. B. Porter and B. T. Connelly, *ibid.*, **33**, 81 (1960).
(12) H. M. Frey and G. B. Kistiakowsky, *J. Am. Chem. Soc.*, **79**, 6373 (1957).

THE VISCOSITY OF LIQUIDS FROM THE HALF-TIME OF RISE IN A FINE VERTICAL CAPILLARY

BY LEONARD S. LEVITT

Chemistry Department, Seton Hall University, South Orange, New Jersey

Received April 16, 1962

The time of rise of a liquid of viscosity η, surface tension γ, and density ρ, in a vertical capillary of uniform radius r, is given by Washburn's formula[1,2]

$$t = \frac{-8\eta(h+d)}{r^2\rho g} - \frac{8}{r^2\rho g}\left[\eta\left(d + \frac{2\gamma}{r\rho g}\right) + \eta_a l\right] \times \ln\left(1 - \frac{d+h}{d+h_F}\right) \quad (1)$$

where g is the acceleration due to gravity, d is the depth of immersion of the capillary below the surface of the liquid, η_a is the viscosity of air, l is the total length of the capillary, h is the height the liquid has risen after time t, and h_F is the final height it can rise due to its surface tension. If the depth of immersion is made very small, $d \approx 0$, and if the viscosity of air is regarded as negligible, $\eta_a l \approx 0$; noting also[3] that $2\gamma/r\rho g = h_F$, the equation can be greatly simplified to

$$t = \frac{8\eta}{r^2\rho g}\left[h_F \ln\left(\frac{h_F}{h_F - h}\right) - h\right] \quad (2)$$

We can now define a half-time of rise,[4] $t_{1/2}$, as the time required for the liquid to rise to a distance $h_F/2$ in the capillary. The half-time of rise is seen to be simply

$$t_{1/2} = \frac{8\eta h_F}{r^2\rho g}\left(\ln 2 - \frac{1}{2}\right) = \frac{8\eta h_F}{r^2\rho g}(0.193) \quad (3)$$

Noting again that $h_F = 2\gamma/r\rho g$, eq. 3 also can be written

$$t_{1/2} = \frac{16\eta\gamma}{r^3\rho^2 g^2}(0.193) \quad (3a)$$

Thus the viscosity of the liquid is, from eq. 3, given by

$$\eta = 0.647 r^2 \rho g t_{1/2}/h_F \quad (4)$$

If the surface tension of the liquid already is known at the temperature of the experiment, then the radius of the capillary need not necessarily be calculated since $r = 2\gamma/\rho g h_F$, so that eq. 4 can also be written

$$\eta = \frac{2.59 t_{1/2}\gamma^2}{\rho g h_F^3} \quad (4a)$$

The experimental procedure is simply to determine h_F for a given capillary and liquid, and then mark off the distance $h_F/2$ directly on the capillary, and accurately determine the time, $t_{1/2}$, required for the liquid to rise to this mark. The smaller the radius of the capillary, the longer is the time of rise, and the greater the height to be measured. Therefore, the smaller the capillary bore, the more accurate will be the viscosity determined by this method. For practical results, a bore of $r \leq 0.005$ cm. should be used. Theoretically then, the total volume of liquid required for a viscosity determination by this method is very small indeed. For example, using water as the liquid at room temperature, $\rho \approx 1.0$ g./cm.^{3}, $\gamma = 72$ dynes/cm., $g = 980$ cm./sec.^{2}, and with $r = 0.0050$ cm., h_F is calculated to be about 30 cm. The quantity of water drawn up into the tube is therefore $\pi r^2 h_F = 2.4 \times 10^{-3}$ cm.^{3}, or about 1/20 of a drop. But in practice at least a few drops of the liquid should be used. The half-time of rise for the example under consideration is calculated from eq. 3 to be approximately 17 sec., which is seen to be a time of convenient duration for accurate measurement.

For two different liquids whose half-times of rise are measured in the same capillary, the relative viscosity of the liquids is

$$\frac{\eta_1}{\eta_2} = \frac{(\rho t_{1/2}/h_F)_1}{(\rho t_{1/2}/h_F)_2} = \frac{(\rho^2 t_{1/2}/\gamma)_1}{(\rho^2 t_{1/2}/\gamma)_2} \quad (5)$$

We have obtained preliminary results[5] with

(1) E. W. Washburn, *Phys. Rev.*, **17**, 273 (1921).
(2) J. R. Ligenza and R. B. Bernstein, *J. Am. Chem. Soc.*, **73**, 4636 (1951).
(3) We are assuming here that the liquid makes a contact angle of zero with the interior wall of the capillary during the course of the liquid's rise.
(4) More accurately, this should be called the "time of half-rise," but we defer to the established usage in the analogous case of chemical kinetics.
(5) The author wishes to thank Mr. Wm. Lane for obtaining the experimental data.

water, methanol, ethanol, benzene, acetone, and chloroform at room temperature, using marine barometer tubing supplied by the Corning Glass Co. The bore radius was determined by capillary rise of water to be 2.70×10^{-3} cm., and was checked by direct examination with a calibrated microscope, which gave $r = 2.71 \times 10^{-3}$ cm. With water at 27.4°, $\rho = 0.996$ g./cm.^{3}, h_F was 54.2 cm., and $t_{1/2}$ was found to be 98.7 and 98.9 sec. in two separate runs.[6] The viscosity calculated from eq. 4 is $\eta = (0.647)(2.70 \times 10^{-3})^2(0.996)(980)(98.8)/54.2 = 8.44 \times 10^{-3}$ poise = 0.844 cp. This value compares quite favorably with the value 0.846 cp. obtained by interpolation of recorded viscosity data[7] for water at various temperatures.

In conclusion it may be pointed out that the present work serves as a confirmation of the validity of Washburn's equation, as well as providing a new rapid method for simply and accurately determining the viscosity of a liquid, using samples considerably smaller than heretofore possible with other methods.

(6) If the same capillary tube is to be used again for a second liquid, it is, of course, necessary to clean the tube carefully with cleaning solution, followed by a few rinsings with distilled water and then acetone. Finally, the tube must be dried thoroughly. When the tube is not in use, it should be covered at both ends to prevent the smallest traces of dust from entering. If reproducible half-times cannot be obtained, the capillary is not clean, and in some cases the only remedy is to take a new section of capillary tubing.

(7) Handbook of Chemistry and Physics, 41st Ed., Chemical Rubber Publ. Co., Cleveland, Ohio, 1960, p. 2181.

CONDUCTANCE OF 2–2 ELECTROLYTES WITH MULTIPLE CHARGE SITES

BY JOHN E. LIND, JR.,[1] AND RAYMOND M. FUOSS

Contribution No. 1693 from the Sterling Chemistry Laboratory of Yale University, New Haven, Connecticut

Received April 18, 1962

The conductance theory of Fuoss and Onsager[2] has been applied extensively to 1–1 electrolytes, but there has been little examination of higher symmetrical charge types because the increased electrostatic fields reduce the range of applicability of the theory. Atkinson[3–5] and co-workers have investigated a number of metal salts of *m*-benzenedisulfonic acid (H_2BDS) and *p,p*-biphenyldisulfonic acid (H_2BPDS). However, no 2–2 salts have been investigated where the anions and cations are both large and of comparable size. For such salts the electrostatic interactions at contact are smaller and thus they better approximate the theoretical model. The purpose of this note is to present conductance data at 25° in water for two such salts: the N,N-dimethyltriethylenediammonium (DMD) salts of BDS and BPDS. DMD is the dimethyl quaternized ion of 1,4-diaza-bicyclo[2.2.2]octane with the structure $MeN^+(CH_2CH_2)_3N^+Me$.

(1) Du Pont Postdoctoral Research Fellow, 1960–1962.

(2) R. M. Fuoss and F. Accascina, "Electrolytic Conductance," Interscience Publishers, Inc., New York, N. Y., 1959.

(3) G. Atkinson, M. Yokoi, and C. J. Hallada, *J. Am. Chem. Soc.*, **83**, 1570 (1961).

(4) C. J. Hallada and G. Atkinson, *ibid.*, **83**, 3759 (1961).

(5) C. J. Hallada and G. Atkinson, *ibid.*, **83**, 4367 (1961).

Experimental

DMD–BDS was prepared from $DMDCl_2$, made by Houdry, and Eastman H_2BDS. After converting the $DMDCl_2$ to the sulfate by addition of silver sulfate, the $DMDSO_4$ was precipitated from the aqueous solution by evaporation and addition of ethanol, and was recrystallized from methanol containing a little water. These salts are very soluble in water but nearly insoluble in most other solvents. In order to remove sulfuric acid from H_2BDS, it was converted to the barium salt in aqueous solution by barium hydroxide, and the BaBDS (12.6 g./15 ml.) was recrystallized from water. The $DMDSO_4$ was titrated in aqueous solution to a nephelometric end-point with BaBDS. After filtering off the barium sulfate, the DMD–BDS was precipitated by addition of ethanol. The salt was recrystallized twice from methanol–water, washed with 7:1 methanol–water, and dried to constant weight at 30 μ and 138°. Water probably still was present in the salt, but a higher temperature was not risked. Wet tests for barium and silver were negative and the salt was neutral.

For the preparation of DMD–BPDS, the $DMDCl_2$ was recrystallized by dissolving 5 g. in 10 ml. of hot methanol, then adding an equal amount of ethanol, and evaporating to about one fourth the volume. The salt then was converted to the hydroxide by silver oxide. Eastman *p,p*-diphenyldisulfonic acid was converted to the potassium salt, which was recrystallized twice from water. The acid then was formed in aqueous solution by passing a solution of the potassium salt through a Duolite C-3 cation exchanger. The acid was titrated to a methyl orange end-point with $DMD(OH)_2$. After reducing the volume of solution, salt was precipitated by the addition of methanol. The salt was dried for two days at 78° and 30 μ.

The methods of measurement have been described previously[6]; the cell used in these measurements had a constant of 1.0109.

Results

The data for the conductance of DMD–BDS and DMD–BPDS are given in Table I.

TABLE I

CONDUCTANCE OF N,N-DIMETHYLTRIETHYLAMMONIUM SALTS IN WATER AT 25°

DMD–BDS			DMD–BPDS		
10^4c	Λ	$10^2\Delta\Lambda$	10^4c	Λ	$10^2\Delta\Lambda$
27.161	102.53	−2	20.747	101.14	−1
20.754	105.83	3	16.821	103.07	+2
15.529	109.22	1	12.472	105.62	0
10.996	112.94	−4	8.065	108.98	−2
5.657	119.09	1	4.143	113.22	+1
$c/m = 0.99707 - 0.32\ m$			$c/m = 0.99707 - 0.29\ m$		

They were analyzed by the Fuoss–Onsager equation

$$\Lambda = \Lambda_0 - S(c\gamma)^{1/2} + Ec\gamma \log c\gamma + Jc\gamma + J_2(c\gamma)^{3/2} - K_A c\gamma f^2\Lambda$$

The analysis was made on an IBM 709 computer with Kay's[7] program in Fortran which was modified by the addition of the $c^{3/2}$ term in the conductance equation. A second modification of the program was the addition of the condition that, if the association constant, K_A, becomes negative, the fraction of free ions is set equal to unity. This change was made because it appears that a small term in J was neglected which is by this analysis added as a small negative component to K_A. In Table I, $\Delta\Lambda$ is the difference between the observed conductance and the value computed from the

(6) J. E. Lind, Jr., and R. M. Fuoss, *J. Phys. Chem.*, **65**, 999 (1961).

(7) R. L. Kay, *J. Am. Chem. Soc.*, **82**, 2099 (1960). In order to adapt the program for 1–1 salts to data for 2–2 salts, one simply replaces the dielectric constant D by $D/4$ and the viscosity η by $\eta/2$.

Fuoss–Onsager equation. The dielectric constant and viscosity of water used in the computation were 78.54 and 0.008903 poise, respectively. The density of both salts is about 1.43. The maximum correction for solvent conductance was 1%.

The results of the analysis are given in Table II where Λ_0 = limiting conductance, a_J = ion size parameter from J-terms in the equation, K_A = association constant for the formation of ion pairs, and σ_Λ = standard deviation in Δ-units of the data points from the equation.

TABLE II

DERIVED CONSTANTS

Salt	Λ_0	a_J	K_A	σ_Λ
DMD–BDS	134.35 ± 0.15	4.30 ± 0.13	40 ± 5	0.04
DMD–BPDS	124.08 ± 0.09	4.41 ± .14	−5 ± 4	0.03

The association constant of the DMD–BDS is 40, compared to that of DMD–BPDS, which is essentially zero. This difference can be explained by the electrostatic interaction. The distances between the charges on the DMD and BDS ions are almost the same, so that when an ion pair forms, the charge sites of the two ions are very close to each other. Thus, greater association would be expected for the DMD–BDS than for DMD–BPDS, where the distance between the two charges on the anion is of the order of three times the charge separation in the cation.

The values of the limiting conductances are not precise because the salts are hygroscopic, but this uncertainty has little effect upon the other parameters of the equation. The limiting conductance of the DMD ion can be computed from Atkinson's values[3,5] for the BDS and BPDS ions; the two values are given in Table III. The difference of about 1% between them probably is due to a small amount of water still in our sample of DMD–BDS; this salt was unusually difficult to dehydrate. Also given in Table III are the (uncorrected) Stokes radii calculated for the DMD ion.

TABLE III

SINGLE ION CONDUCTANCES

Salt	λ_0^-	λ_0^+	10^8R^-	10^8R^+
DMD–BDS	59.94	74.4	3.07	2.47
DMD–BPDS	48.99	75.1	3.76	2.45

The center-to-center ion pair distances computed from the hydrodynamic radii of DMD–BDS and DMD–BPDS are 5.54 and 6.21 Å., respectively; these are higher than the values of a_J of 4.3 and 4.4, respectively. These hydrodynamic dimensions should be larger than the electrostatic because the charge sites are situated near the ends of the prolate ellipsoidal ions and thus the distance of closest approach of the charge sites might be expected to be less than the sum of the mean Stokes radii of the ions. Thus the Fuoss–Onsager eq. (1) can adequately represent data for 2–2 salts in aqueous solution up to concentrations of about 2.5×10^{-3} M to 0.02%. For the case of bolaform electrolytes, we note that the degree of association is sensitive to the ratios of the charge separations in the two ions, the association being greatly increased when this ratio is near unity.

THE HEAT OF FORMATION OF GASEOUS METHYL NITRITE[1]

BY JAMES D. RAY AND A. ARNOLD GERSHON

School of Chemistry, Georgia Institute of Technology, Atlanta 13, Georgia

Received July 11, 1961

Calculations which have been made recently by Gray and Pratt[2] indicate that the value for the heat of formation of methyl nitrite calculated from the equilibrium study of Leermakers and Ramsperger[3] is somewhat in error. Although Gray and Pratt[2] quote unpublished data of Baldrey, Lotzgesell, and Style as evidence for a revised value for the heat of formation of methyl nitrite, this value was obtained from solution calorimetry and depends ultimately on a small difference between two large numbers. Geiseler and Thierfelder[4] have determined the heat of combustion of methyl nitrite, but their value corresponds in precision to an uncertainty in entropy of ±3 e.u., which is not sufficiently accurate to determine the barrier to rotation of the methyl group. We felt that the direct determination of the heat of reaction between methyl alcohol and nitrosyl chloride to form methyl nitrite and hydrogen chloride, reaction 1, would be a much more sensitive method for measurement of the heat of formation of methyl

$$CH_3OH(g) + NOCl(g) = CH_3ONO(g) + HCl(g) \quad (1)$$

nitrite. In this reaction, the heats of formation of the other participants all have been determined with high accuracy; thus the precision of the Joule expansion reactant mixing gas calorimeter of Ogg and Ray[5] would be adequate to determine the barrier to rotation of the methyl group in methyl nitrite.

Experimental

Materials.—Methyl alcohol was purified by the method of Gillo.[6] Nitrosyl chloride was prepared as described previously[7] by the reaction of nitric oxide with chlorine. Methyl nitrite was prepared as described previously.[8] Dry hydrogen chloride gas was prepared by the reaction of C.P. sulfuric acid with reagent grade potassium chloride in a vacuum system.

Apparatus and Procedure.—The Joule expansion reactant mixing gas calorimeter employed has been described previously.[9] In the present case the calorimeter contained a 269.8-ml. gas reaction bottle. The energy equivalent of the calorimeter including 275 ml. of chlorobenzene liquid was found to be 161.0 cal./deg. by the heat of water vaporization method which has been described by Ray.[9] The value −10,520 cal./mole was used for the heat of vaporization of water at 25°. Reactions were carried out at 25°. The thermochemical calorie exactly equal to 4.184 absolute joules was used in calculations. The calorimeter was filled with gases from a vacuum system which was equipped with

(1) Presented in part at the American Chemical Society Meeting, St. Louis, Missouri, March 21–30, 1961.

(2) P. Gray and M. W. T. Pratt, *J. Chem. Soc.*, 3403 (1958).

(3) J. A. Leermakers and H. C. Ramsperger, *J. Am. Chem. Soc.*, **54**, 1832 (1932).

(4) G. Geiseler and W. Thierfelder, *Z. physik. Chem.* (Frankfurt), **29**, 248 (1961).

(5) R. A. Ogg, Jr., and J. D. Ray, *J. Phys. Chem.*, **61**, 1087 (1957).

(6) L. Gillo, *Ann. chim.*, [11] **12**, 281 (1939).

(7) J. D. Ray and R. A. Ogg, Jr., *J. Chem. Phys.*, **26**, 984 (1957).

(8) J. D. Ray and R. A. Ogg, Jr., *J. Phys. Chem.*, **63**, 1522 (1959).

(9) J. D. Ray, *Rev. Sci. Instr.*, **27**, 863 (1956).

glass Bourdon gages for measurement of the pressures of the corrosive gases.

The equilibrium constant for eq. 1 was found to be needed for interpretation of the calorimetric data. The old value for

$$K = \frac{(HCl)(CH_3ONO)}{(CH_3OH)(NOCl)}$$

given by Leermakers and Ramsperger[3] is 1.92 ± 0.6. The value of K determined by Cox and Ray[10] is 0.73 based on quantitative infrared spectroscopy and 0.69 based on the rate constants of the forward and reverse reactions. The value 0.73 is used in the present calculations.

Since the equilibrium constant for the reaction is nearly unity, it is necessary to employ a large excess of one reactant in order to obtain nearly complete reaction. Unfortunately, the reverse reaction of eq. 1 results in the formation of a liquid phase when a large excess of either reactant is used. The reaction of 100 mm. pressure of methyl alcohol in the 269.8-ml. calorimeter bottle at 25° with excess nitrosyl chloride was found to yield a liquid phase only at low NOCl pressures, and was used to evaluate the heat of the reaction.

In a typical run, the calorimeter bottle contained 100 mm. of MeOH. After measuring the initial temperature drift, NOCl was admitted to a final pressure of 244 mm. The observed temperature rise of the calorimeter was 0.0187°. From this was subtracted the temperature rise due to the Joule expansion of the nitrosyl chloride into the calorimeter bottle, 0.0079°, to give 0.0108° change in temperature due to the reaction. The heat of reaction per mole of methyl nitrite formed is given by

$$\Delta H = \frac{\text{(calorimeter energy equivalent)}}{\text{(moles of } CH_3ONO \text{ formed at equilib.)}} \text{(corr. temp. rise)}$$

$$\frac{(161.0)(0.0108)}{(0.000788)} = -2210 \text{ calories (exothermic)}$$

TABLE I

CALCULATED PRESSURES, $P_{calcd.} = n_{NOCl}RT/V$, AND OBSERVED PRESSURES OF WEIGHED AMOUNTS OF NOCl ADMITTED TO AN EVACUATED FLASK PLUS GAGE PLUS LEADS OF TOTAL VOLUME 310.8 ML.

NOCl, g.	T, °K.	P, mm. Calcd.	P, mm. Obsd.
0.489	298.0	446.5	444.5
0.6563	299.0	600.0	593.5
1.098	299.2	1008	984
1.566	299.8	1438	1388
1.720	299.0	1576	1511

Table II lists observed temperature rises associated with varying final pressures in the calorimeter bottle, and the respective pressures of CH_3ONO calculated to be present at equilibrium. A small correction was made by successive approximation to allow for the effect of the fugacity of NOCl on the equilibrium amount of methyl nitrite. This fugacity correction amounted to at most 30 small cal. in the heat of reaction per mole of methyl nitrite formed. Temperature rises due to the heat of expansion of the NOCl into the calorimeter bottle were allowed for. The heats of expansion include an almost negligible correction for the imperfection of the NOCl gas calculated from the data of Table I.

The Joule–Thompson heat of expansion, μC_p, was not present in the experiments. The calorimeter was filled by first opening the stopcock on the calorimeter bottle to the vacuum system manifold which contained a pressure of NOCl in excess of that of the methyl alcohol in the bottle. Then the stopcock to the NOCl storage flask was opened to fill the calorimeter slowly. Thus, the throttling took place at the NOCl storage flask outlet stopcock and the manifold and leads to the calorimeter bottle acted as a heat exchanger to eliminate the cooling effect of the Joule–Thompson expansion.

(10) J. R. Cox, Jr., and J. D. Ray, *J. Chem. Phys.*, **34**, 1072 (1961).

TABLE II

DATA FOR REACTION OF 100 MM. PRESSURE OF CH_3OH IN THE 269.8-ML. CALORIMETER BOTTLE WITH NOCl ADDED TO GIVE VARIOUS FINAL PRESSURES

The observed temperature rises, ΔT calorimeter, are corrected for the Joule expansion of the NOCl into the calorimeter bottle (3rd column) to give the temperature change associated with the reaction (4th column).

P_{final}, mm.	ΔT calorimeter uncorr.	ΔT Joule expansion	ΔT Reaction	P_{CH_3ONO}, mm. at equilib.	ΔH reaction 1, cal./mole CH_3ONO
244	0.0187	0.0079	0.0108	54.3	−2210
294	.0218	.0106	.0112	61.3	−2030
342	.0245	.0132	.0113	65.7	−1910
392	.0290	.0158	.0132	70.1	−2090
416	.0300	.0173	.0127	71.7	−1970
507	.0382	.0217	.0165	77.0	−2380
630	.0475	.0289	.0186	81.2	−2540
732	.0510	.0342	.0168	83.1	−2240
874	.0580	.0423	.0157	85.3	−2040
928	.0592	.0452	.0140	86.0	−1810
1027	.0692	.0507	.0185	87.1	−2360
1124	.0730	.0559	.0171	88.3	−2150
				Average	−2140 ± 200

Separate experiments showed that in the pressure range used in the above reactions, there was no detectable heat of reaction between HCl and NOCl, or between CH_3ONO and NOCl. Further experiments in which 100 mm. pressure of CH_3OH was admitted to a 310.8 ml. total volume system comprised of flask, gage, and leads, followed by admission of weighed amounts of NOCl, showed that no dimeric or trimeric compounds formed. The calculated pressures on mixing methyl alcohol and nitrosyl chloride agreed with those observed when allowance was made for the gas imperfection of NOCl given in Table I.

The value for the heat of reaction 1 at 25° found is −2,140 ± 200 cal. (standard deviation) when corrected to represent total reaction with the equilibrium constant 0.73 given by Cox and Ray.[10] The value calculated for the standard heat of formation of methyl nitrite gas at 25° is −15.64 ± 0.20 kcal./mole. The heat of formation of nitrosyl chloride was taken from Ray and Ogg.[11] The heats of formation of methyl alcohol and hydrogen chloride were taken from Rossini, *et al.*[12]

Discussion

The heat of formation $\Delta H^0_{298}CH_3ONO(g)$ calculated from the equilibrium study of Leermakers and Ramsperger[3] is −16.28 kcal./mole; the value of Baldrey, Lotzgesell, and Style[2] is −14.93 ± 0.26; that of Geiseler and Thierfelder[4] −16.8 ± 0.8; combination of the heat of combustion of methyl nitrate gas of Whittaker, Wheeler, and Pike,[13] −29.4 ± 0.8, with the value of Ray and Ogg[8] for the heat of reaction of nitrogen pentoxide gas with methyl nitrite gas gives −14.46 ± 0.9: that from the present study is −15.64 ± 0.20. The average of all five results is −15.62 ± 0.94. When the value of the present study, −15.64, is combined with the value of Cox and Ray[10] for equilibrium 1, the entropy of methyl nitrite gas is calculated to be 66.81 ± 0.67. The entropy calculated by Gray and Pratt[2] based on the geometry of the *cis–trans*

(11) J. D. Ray and R. A. Ogg, Jr., *ibid.*, **31**, 168 (1959).

(12) F. D. Rossini, D. D. Wagman, W. H. Evans, S. Levine, and I. Jaffe, "Selected Values of Chemical Thermodynamic Properties," Circular 500, U. S. Bur. Standards, 1952.

(13) H. H. Whittaker, W. H. Wheeler, and H. H. M. Pike, *J. Inst. Fuel*, **20**, 137 (1947).

isomers and their vibrational frequencies is 73.8, assuming free rotation. Gray and Reeves[14] have found a barrier 10,500 ± 2000 cal. ascribed to hindered rotation of the NO group. When an entropy deficit of 3.0 e.u. corresponding to this barrier is subtracted, there still remains an entropy deficit of 4 ± 0.7 e.u. between the calculated and experimental value. Gray and Pratt[2] calculated the maximum entropy due to free rotation of the methyl group to be 3.58 e.u. and that for the NO group to be 5.80. The entropy deficit 4 ± 0.7 e.u. found in the present work thus corresponds to an essentially fixed methyl group. Such a high barrier to rotation of the methyl group is reasonable since in methyl nitrate the distance of closest approach of a methyl group H to O is 1.8 Å., whereas the structural data given by Rogowski[15] indicate only 1.3 Å. for this distance in methyl nitrite. Further evidence for a large barrier to methyl group rotation in methyl nitrite is given by Tarte's[16] analysis of the C–D vibrational bands in CH_2DONO and Wagner's[17] interpretation of the intensity variation of the Raman –ONO lines which was ascribed to hydrogen bonding.

Acknowledgments.—This research was supported in part by a grant from the Research Corporation, and by a grant from the National Science Foundation.

(14) P. Gray and L. W. Reeves, *J. Chem. Phys.*, **32**, 1878 (1960).
(15) F. Rogowski, *Ber.*, **B75**, 244 (1942).
(16) P. Tarte, *Bull. soc. chim. Belges*, **62**, 401 (1953).
(17) J. Wagner, *J. phys. radium*, **15**, 526 (1954).

HAMMETT CORRELATIONS FOR THE SOLUBILITY OF GASEOUS HYDROGEN CHLORIDE IN CERTAIN AROMATIC SYSTEMS[1]

BY MORRIS RAPOPORT, C. KINNEY HANCOCK,[2] AND EDWARD A. MEYERS

Department of Chemistry, The A. and M. College of Texas, College Station, Texas

Received February 9, 1962

In the typical Hammett relation, a *functional group property*, such as an equilibrium or rate constant, is involved. In sharp contrast, there now are numerous quantitative relationships in the literature between a *molecular property*, such as the energy of electronic spectral excitations ($h\bar{\nu}$), and Hammett's σ-values. We have therefore looked for Hammett relations in the realm of solubility phenomena, which are also characterized by the lack of a localized "reaction" site and where gross molecular structure similarly plays an important role. We have found that the data collected by Brown and Brady[3] for the solubility of hydrogen chloride in solutions of some aromatic compounds follow a linear Hammett relation. Because of recent successful spectra–structure correlations[4] of 4-substituted, 2-nitrophenols, we have measured their solubility in heptane and in water, seeking a solubility–structure correlation. The solubility behavior of the 4-substituted, 2-nitrophenols, however, does not appear to correlate well with σ. These results are presented and discussed.

Experimental

The heptane (99 mole % minimum, Phillips Petroleum Co.) used for the solubility measurements was refluxed over sodium before distillation through a twelve-bulb Snyder column. The water was purified by passing distilled water through a mixed-bed ion exchange column (Amberlite MB-1, Rohm and Haas Co.). The preparation and purification of the 4-substituted, 2-nitrophenols have been discussed previously.[4] The stoppered test tubes which contained solvent and excess solute were shaken periodically while being kept at 25.00 ± 0.02° in a water bath.

The solubilities in water were determined in the following manner. Weighed amounts of solvent and excess solute, in stoppered test tubes, were allowed to approach equilibrium at 25° from both undersaturation and supersaturation.[5] The undissolved solute was carefully collected on a tared fritted-glass Gooch type crucible under vacuum and weighed after air-drying at room temperature. Four or more determinations were made for each compound. The average deviation from the mean of replicate values did not exceed 1.5%.

Solubilities in heptane were determined by a similar procedure. In addition, solubilities also were measured by removing saturated solution from the test tubes with filter-pipets[6] and collecting weighed amounts of saturated solution in tared aluminum foil dishes. The dishes containing residue were weighed after the heptane was evaporated at room temperature. Over-all results by these two methods for the heptane solubilities agreed within 2%.

Discussion

Data of Brown and Brady.—Brown and Brady measured the solubility of hydrogen chloride under low pressures at −78.15° in heptane, in toluene, and in these solvents containing, in addition, small amounts of dissolved aromatics.[3] Their data obey Henry's law closely, and the appropriate Henry's law constants, k_2, are given in Table I. In order to explain the variation in k_2 with these different solvents, they also calculated equilibrium constants for the dissociation of a complex. It was assumed that all the additional hydrogen chloride dissolved in the heptane–aromatic solutions (compared with the solubility of hydrogen chloride in heptane alone) was bound in a 1:1 Ar:HCl complex. In order to avoid, if possible, assumptions like these regarding the formation of complexes, the logarithms of the Henry's law constants themselves were subjected to linear regression analysis[7] to obtain the following good correlations for the data in Table I for the solubility of hydrogen chloride in: (1) solutions of 0.05 mole of aromatic per mole of heptane, (2) solutions of 0.10 mole of aromatic per mole of toluene, and (3) 0.52 M solutions of aromatic in heptane. The

$$\log k_2 = 3.53 + 0.206\sigma_p,\ r = 0.975,\ s = 0.020 \quad (1)$$

(1) Abstracted from a portion of the Ph.D. Dissertation of M. R., May, 1961.
(2) To whom inquiries should be addressed, at Department of Chemistry, The A. and M. College of Texas, College Station, Texas.
(3) H. C. Brown and J. D. Brady, *J. Am. Chem. Soc.*, **74**, 3570 (1952).
(4) M. Rapoport, C. K. Hancock, and E. A. Meyers, *ibid.*, **83**, 3489 (1961).
(5) R. D. Vold and M. J. Vold, "Physical Methods of Organic Chemistry," A. Weissberger, Editor, 2nd Ed., Interscience Publishers, Inc., New York, N. Y., 1949, Vol. I, Pt. I, p. 307.
(6) M. Rapoport and C. K. Hancock, *J. Chem. Educ.*, **39**, 98 (1962).
(7) G. W. Snedecor, "Statistical Methods," 5th Ed., The Iowa State College Press, Ames, Iowa, 1956, Chapters VI and VII.

TABLE I

SOLUBILITY AT −78.51° OF HYDROGEN CHLORIDE IN REPRESENTATIVE AROMATICS DISSOLVED IN HEPTANE OR TOLUENE

	Compound, A	Henry's law constant, k_2,[a] in mm. for the solubility of hydrogen chloride in 0.05 mole of A per mole of heptane	0.10 mole of A per mole of toluene	0.52 *M* soln. of A in heptane	σ[b]
1.	Iodobenzene			3750	0.276
2.	Bromobenzene			3660	.232
3.	Chlorobenzene	4000	318	3570	.227
4.	Fluorobenzene			3260	.062
5.	Toluene	3170	299	2790	− .170
6.	Ethylbenzene			2680	− .151
7.	Isopropylbenzene			2490	− .151
8.	*t*-Butylbenzene			2380	− .197
9.	*m*-Xylene	2980	278	2460	− .340[c]
10.	Mesitylene	2550	254	2210	− .510[d]
11.	Benzotrifluoride	4220	332		.551
12.	Benzene	3500	308		.000

[a] Data from ref. 3. [b] H. H. Jaffé, *Chem. Rev.*, **53**, 222 (1953). [c] 2(−0.170). [d] 3(−0.170).

$$\log k_2 = 2.48 + 0.103\sigma_p,\ r = 0.945,\ s = 0.013 \quad (2)$$

$$\log k_2 = 3.48 + 0.313\sigma_p,\ r = 0.964,\ s = 0.024 \quad (3)$$

correlation coefficient, r, and standard deviation from regression, s, are given above for each of the equations. The lines defined by eq. 1 and 3 are shown in Fig. 1. The deviations from the lower regression line of Fig. 1 for the points for isopropylbenzene and *t*-butylbenzene would seem to indicate that increased solubility accompanies an increase in the size of the aliphatic substituent. This seems reasonable in view of the solubility of hydrogen chloride in aliphatic solvents like heptane alone.

4-Substituted, 2-Nitrophenols.—Above, the ability of an aromatic molecule to act as a solvent was examined as a function of the σ_p-values of its substituents. It is more difficult to compare the solubilities of aromatic compounds in a common solvent, because it is necessary to use for all of them a reference state in which their vapor fugacities are the same.[8] One way of avoiding this difficulty is by comparing the solubilities of a related series of compounds in two different solvents. Then, if the solute has the same mole fraction activity coefficient in its saturated solution in the two different solvents, 1 and 2

$$\mu_2^* = \mu_1^* = RT \ln (X_1/X_2) \quad (4)$$

where X_1, X_2 = mole fraction of the solute in solvents 1 and 2, and μ_1^*, μ_2^* = chemical potentials of the solute in its standard state (extrapolated from infinite dilution to unit mole fraction[9]) in solvents 1 and 2.

Provided that the solubilities are sufficiently affected by changes in the σ_p-values of the substituents, and *yet not too strongly affected by the changes in size and shape of the molecule or the particular nature of the substituent*, it should be possible to obtain a correlation between the logarithm of the solubility ratio in the two solvents and the σ_p-values of the substituents present.

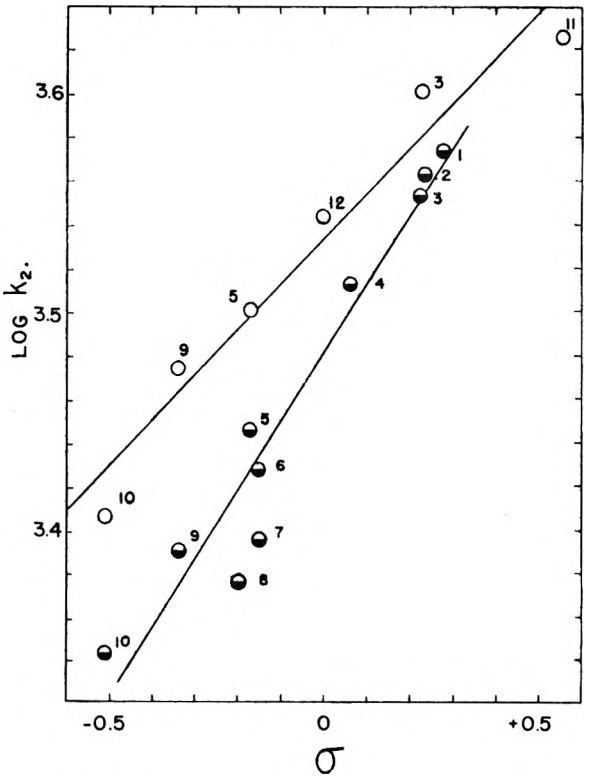

Fig. 1.—The relationship between log k_2 and σ for the data of Brown and Brady (ref. 3). Upper line refers to eq. 1, numbers to Table I. Lower line refers to eq. 3, numbers to Table I. The Henry's law constant, k_2, refers to the solution of gaseous HCl at low pressures in heptane–aromatic solutions at −78.51°.

The solubilities of a test series of five representative 4-substituted, 2-nitrophenols were measured in two solvents at 25°, one highly polar, water

TABLE II

SOLUBILITIES OF 4-SUBSTITUTED, 2-NITROPHENOLS IN HEPTANE AND IN WATER AT 25°

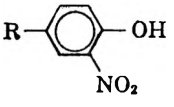

No.	R[a]	Solubility, g./100 g. soln. Heptane	Water	X_H/X_W[b]	σ[c]
1	OCH_3	1.72	0.0418	230.4	−0.268
2	H	10.3	.238[d]	247.3	.000
3	Cl	2.81	.0275	575.0	.227
4	$COCH_3$	0.117	.0451	14.43	.874
5	NO_2	0.151	.0482[e]	17.43	1.270

[a] Preparation and melting points are discussed in ref. 4. [b] X_H = mole fraction of solute in heptane. X_W = mole fraction of solute in water. [c] Footnote *b*, Table I. [d] Values of 0.24 (interpolated) and 0.25 are reported in A. Seidell, "Solubilities of Organic Compounds," D. Van Nostrand Co., Inc., Princeton, N. J., 3rd ed., 1941, pp. 361–362. [e] Values of 0.0465 and 0.041 (interpolated) are reported in ref. *d*, pp. 351–352.

(8) J. H. Hildebrand and R. L. Scott, "The Solubility of Non-Electrolytes," Reinhold Publ. Corp., New York, N. Y., 1948, p. 263.

(9) F. Daniels and R. A. Alberty, "Physical Chemistry," 2nd Ed., John Wiley and Sons, Inc., New York, N. Y., 1961, p. 157, Convention II.

(W), and one non-polar, heptane (H). The experimental data are recorded in Table II. Linear regression analysis of the data in Table II gives

$$\log (X_H/X_w) = 2.40 - 0.983\sigma_p,\ r = -0.853,\ s = 0.44 \quad (5)$$

Equation 5 is only statistically significant between the 5 and 10% levels and it is obvious that the agreement for this system is not as good as for solutions of hydrogen chloride in aromatics. This is understandable since, although the differences in solubility related to Hammett σ_p should be large for this solvent pair, the effects of size, shape, and nature of the substituent group might also be expected to be appreciable in such widely different solvents as water and heptane. Other solvent pairs such as *p*-dioxane and cyclohexane suggest themselves as possibilities for reducing the non-Hammett effects on solubility.

Acknowledgments.—This study was supported in part by a research grant from the Robert A. Welch Foundation. The statistical calculations were performed by the Data Processing Center, Texas Engineering Experiment Station, College Station, Texas.

MOLECULAR COMPLEXES OF TETRACYANOETHYLENE WITH TETRAHYDROFURAN, TETRAHYDROPYRAN, AND *p*-DIOXANE[1]

By Ruth Vars, Lucy A. Tripp, and Lucy W. Pickett

Carr Laboratory, Mount Holyoke College, South Hadley, Massachusetts

Received April 26, 1962

During the course of an investigation of molecular complexes of tetracyanoethylene (TCNE) and aromatic molecules, Merrifield and Phillips[2] noted evidence of complex formation with the solvent, diethyl ether. This fact suggested that such complexes might be used as a means of base strength comparison of the cyclic ethers whose absorption spectra have been under investigation in this Laboratory.[3] Preliminary studies showed that tetrahydrofuran, tetrahydropyran, and *p*-dioxane when mixed with a chloroform solution of TCNE all have absorption bands, absent in the unmixed reactants, which are suitable for the determination of association constants.

Experimental

Compounds.—The TCNE was a gift of the du Pont de Nemours Co. through the courtesy of Dr. D. D. Coffman.[4] This was used without further purification and kept in a dry atmosphere. Chloroform, Spectro Grade, from Eastman Kodak Co. was used.

Tetrahydrofuran, Certified Reagent, Fisher, and *p*-dioxane, Eastman Kodak, were distilled from barium oxide through a fractionating column in nitrogen atmosphere directly before use. Physical constants agreed with reported values, and peroxide tests before and after use were negative. Similar treatment of tetrahydropyran did not remove a slight persistent trace of benzene, nor did passage through chromatographic columns containing silica gel, alumina, and activated charcoal. The residual benzene was estimated at 5.3–5.9 $\times 10^{-4}$ *M*. This was sufficiently small so that there was no trace of the characteristic absorption band at 384 mμ identified as that of the complex of TCNE and benzene[2] and it is believed that the impurity did not interfere significantly with the results.

Measurement.—In the early measurements,[5] peroxide formation was found to occur before the completion of the measurements. A technique was developed whereby 1–5-ml. portions of the ether were added to 5-ml. aliquots of a standard TCNE–chloroform solution in a drybox with dry nitrogen atmosphere. The optical density of each solution was measured without delay with a calibrated Beckman DU spectrophotometer at a controlled temperature. Under these conditions no further difficulty with peroxides was experienced and results were reproducible when made by different persons.

Results

The absorption bands considered to be charge transfer bands of the TCNE complexes were broad structureless bands with maxima at the following wave lengths: tetrahydrofuran, 318 mμ; tetrahydropyran, 330 mμ; dioxane, 350 mμ. Measurements were made at these wave lengths since there was no interference from the other components in the solution. For example, dioxane, a mixture of dioxane and chloroform, and a chloroform solution of TCNE all were found to have negligible absorption at the wave length used. The molar extinction coefficient of the 1:1 complex and the association constant for its formation were calculated by the Benesi–Hildebrand method[6] from the intercept and slope of the straight line obtained when the ratio of the molar concentration of TCNE to the absorbance at the appropriate wave length was plotted against the reciprocal of the mole fraction of the ether. A characteristic set of data for dioxane and the corresponding plot are shown in Table I and Fig. 1.

Table I

Absorbance of TCNE–Dioxane Complex

Ml. dioxane added[a]	*A*, 25°	*A*, 35°	[TCNE]/*A* × 10^3, 25°	[TCNE]/*A* × 10^3, 35°	1/[B]
1	0.520	0.484	2.10	2.26	6.34
2	.645	.610	1.45	1.54	3.67
3	.675	.633	1.22	1.30	2.78
4	.659	.623	1.11	1.17	2.34
5	.633	.598	1.04	1.10	2.07

[a] In each case 5 ml. of a 1.31 $\times 10^{-3}$ *M* solution of TCNE in $CHCl_3$ was used, and solution was measured in 1.00-cm. cell.

Values of *K* also were calculated by the absolute method of Rose and Drago.[7] Comparable results were found when units were converted and there seemed to be no advantage in the use of this method for these complexes. Table II gives the results of individual runs and Table III summarizes the data and gives 95% confidence limits.

(1) This work was supported by a grant from The Petroleum Research Fund administered by the American Chemical Society. Grateful acknowledgment is hereby made to the donors of the fund.

(2) R. E. Merrifield and W. D. Phillips, *J. Am. Chem. Soc.*, **80**, 2778 (1958).

(3) L. W. Pickett, N. J. Hoeflich, and T. C. Liu, *ibid.*, **73**, 4865 (1951); G. Fleming, M. Anderson, A. Harrison, and L. Pickett, *J. Chem. Phys.*, **30**, 351 (1959).

(4) T. L. Cairns, *et al.*, *J. Am. Chem. Soc.*, **80**, 2775 (1958).

(5) R. A. Sturges, Honors Paper, Mount Holyoke College, 1959; R. A. Sturges, J. Maxwell, and L. W. Pickett, "4th Report on Research," Petroleum Research Fund, 1959, p. 38.

(6) H. A. Benesi and J. H. Hildebrand, *J. Am. Chem. Soc.*, **71**, 2703 (1949).

(7) N. J. Rose and R. S. Drago, *ibid.*, **81**, 6138 (1959).

TABLE II

VALUES OF ϵ AND K

Compound	Temp., °C.	ϵ	K
Tetrahydrofuran (THF)	25	3125	1.12
		3225	1.26
		3448	1.09
		3105	1.14
		3096	1.14
	35	3105	1.07
		3096	1.07
Tetrahydropyran (THP)	24.5	2632	1.30
		2778	1.36
		2816	1.37
p-Dioxane	20	1792	2.27
		1835	2.31
		1802	2.28
	25	1886	2.14
		1905	2.12
	35	1886	1.92
		1905	1.93

TABLE III

SUMMARY OF DATA[a]

Compound	λ, mμ	ϵ	K	ΔF^0, cal./mole	ΔH^0, kcal./mole	ΔS^0, e.u.
THF	318	3125 ± 57	1.15 ± 0.09	− 78	−1.14	−3.6
THP	330	2742 ± 242	1.34 ± .08	−173		
Dioxane	350	1859 ± 48	2.13 ± .13	−447	−1.83	−4.6

[a] 95% confidence limits given. Values at 25° except in case of THP (24.5°). Thermodynamic values refer to pure state as standard since activities are approximated effectively as mole fractions in the case of 1:1 complexes.

Discussion of Results

The absorption bands observed are believed to be charge transfer bands as explained by Mulliken[8] and others.[9] The results obtained are in reasonable accord with expectation. It will be seen that the value of the association constant increases with increasing wave length of the charge transfer band as was noted in a series of methylbenzenes by Merrifield and Phillips.[2] The value for ethyl ether, $K = 1.54$, with a band at 335 mμ reported by the latter authors, lies on the same smooth curve when the band maximum frequency is plotted against K for the four compounds.

Furthermore, it is reasonable that the complex in each case is less stable at higher temperatures and that ΔH^0 and ΔS^0 are of reasonable sign and magnitude. It also is in accord with reasonable expectation that the complexes of the five- and six-membered rings are similar in stability while that of the dioxane, with two equally probable points of attack, is approximately twice as great.

However, there are other points which were not anticipated. Studies of the complexes of these cyclic ethers with iodine[10] have given similar values for THF and THP with THF having the larger value for the dissociation constant. The values for ether and dioxane were smaller. The

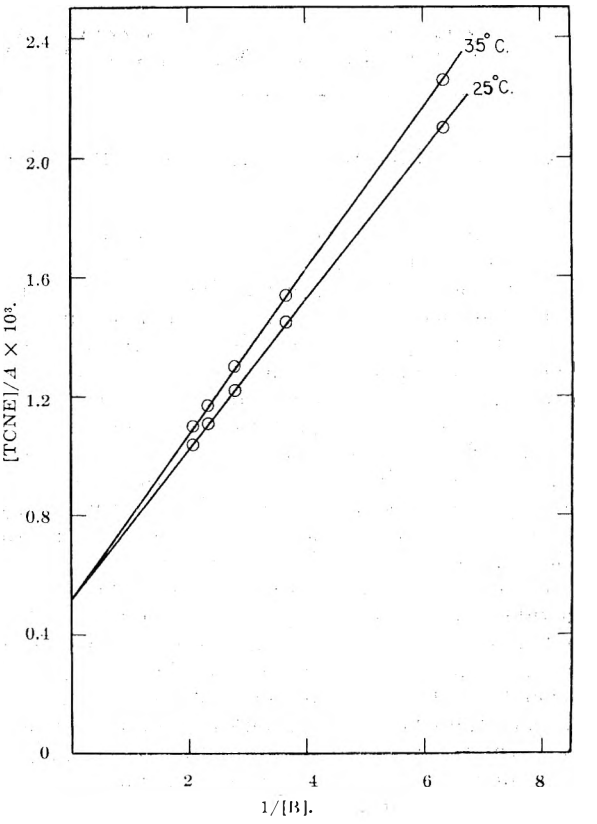

Figure 1.

different character of the acid and the steric factors involved may account for this difference. Tetracyanoethylene is a planar molecule and the other molecule may approach in a roughly perpendicular direction. The differences may be affected by association of the ethers[11] with the solvent chloroform where heat of mixing has been observed as a measure of hydrogen bonding. This suggests a competitive process whereby the compound most readily hydrogen bonded is least available for complex formation. It was not possible to find a solvent where some interaction with either donor or acceptor was not a possible factor.

Second, there would seem to be no obvious reason why a 2:1 as well as a 1:1 complex of TCNE–dioxane should not exist. Experiments devised to detect this gave no evidence of a second complex but the problem of dissolving sufficient TCNE in a solvent with which it does not complex meant that optimum conditions could not be achieved. In this connection it is of interest that Holliday[12] was able to prepare a 1:2 complex of dioxane with boron trifluoride but could make only a 1:1 complex with boron trichloride.

It is of interest that no evidence of complex formation with 1,3,5-trioxane was observed. No color developed as was observed in the case of dioxane and no absorption band was found in the region above 280 mμ. Possibly the acetal-like properties of this molecule overshadow its ether-like properties.

(8) R. S. Mulliken, *J. Am. Chem. Soc.*, **74**, 811 (1952); *J. Phys. Chem.*, **56**, 801 (1952).

(9) H. McConnell, J. S. Ham, and J. R. Platt, *J. Chem. Phys.*, **21**, 66 (1953).

(10) Sr. M. Brandon, M. Tamres, and S. Searles, *J. Am. Chem. Soc.*, **82**, 2129 (1960); M. Tamres and Sr. M. Brandon, *ibid.*, **82**, 2134 (1960).

(11) S. Searles and M. Tamres, *ibid.*, **73**, 3704 (1951).

(12) A. K. Holliday and J. Sowle, *J. Chem. Soc.*, 11 (1952); J. Grimley and A. K. Holliday, *ibid.*, 1215 (1954).

COMMUNICATION TO THE EDITOR

MASS SPECTRUM OF CARBON SUBOXIDE

Sir:

Recently, several articles have appeared in the literature dealing with carbon suboxide (C_3O_2). The presence of C_3O_2 in a reacting gas system has been identified by its infrared emission[1] and gas chromatography.[2] The published literature, however, does not appear to contain the mass spectrum of C_3O_2. Thus, we have undertaken the task of obtaining the cracking pattern of this compound.

The carbon suboxide was prepared by a modification of the method of Stock and Stoltzenburg.[3] From past experience, the impurities in the freshly prepared carbon suboxide were found to be acetic acid and carbon dioxide. The acetic acid was removed by fractional distillation. The carbon dioxide was removed by two techniques. The first involved the distillation of the C_3O_2 and CO_2 into an evaporator. Helium gas then was passed through the C_3O_2 at a temperature of *ca.* $-78°$ to displace the CO_2. The second technique used was to warm the C_3O_2 to *ca.* -40 to $-20°$, apply a vacuum for a period of 10–20 sec., and then refreeze the C_3O_2 in liquid nitrogen. This procedure was repeated several times. Both techniques showed the complete removal of CO_2 within the limits of detection of a Beckman GC-1 gas chromatograph using a silica gel column.

The spectrometer used was a General Electric analytical mass spectrometer. About 12 min. was required to sweep C_3O_2 from m/e = 12 to m/e = 70. The rate of leak of C_3O_2 expressed as % decrease of pressure in the 2-l. reservoir per min. was 2.6. The ion accelerating voltage was held constant at 1750 volts, and the magnetic field scanned from 45 ma. at m/e = 12 to 110 ma. at m/e = 70. The ionizing current and potential were operated at 50 μa. and 50 volts, respectively.

The operational procedure was as follows: low pressures of C_3O_2 in the 2-l. reservoir were obtained by expansion from a series of dosing volumes. Pressures were measured on a McLeod gage (tilting type). Samples were admitted to the leak 1 min. before beginning the sweep. The filament became carbonized as a result of the dissociation of C_3O_2. The filament therefore was conditioned with oxygen prior to each run until the m/e = 28 peak was approximately 7% of the m/e = 32 peak.

The results of two analyses are given in Table I. The 100% peak appears at m/e = 40. CO_2 was the only detectable impurity. The amount of CO_2 present was 0.17%.

TABLE I

MASS SPECTRUM OF C_3O_2

		Peak height		Relative intensity	
m/e	Ion	I	II	I	II
12	C^+	478.	254.	26.0	22.9
13		5.3	3.0	0.29	0.27
14	CO^{++}	1.8	0.8	0.10	0.07
16	O^+	14.0	7.8	0.76	0.70
24	C_2^+	244.	140.	13.3	12.6
25		6.0	3.0	0.33	0.27
26	C_2O^{++}	7.0	4.0	0.38	0.36
27		2.0	1.3	0.11	0.12
28	CO^+	498.	295.	27.0	26.1
29		5.5	3.0	0.30	0.27
30		1.0	0.4	0.05	0.04
34	$C_3O_2^{++}$	168.	98.1	9.1	8.9
34.5		5.2	3.0	0.28	0.27
35		0.6	0.5	0.03	0.04
36	C_3^+	22.8	13.5	1.2	1.2
40	C_2O^+	1839.	1110.	100.	100.
41		40.5	24.0	2.2	2.2
42		4.0	2.5	0.22	0.22
43		1.6	1.3	0.08	0.12
52	C_3O^+	44.2	25.9	2.4	2.3
53		1.5	1.0	0.08	0.09
68	$C_3O_2^+$	1734.	1044.	94.5	94.2
69		56.0	40.	3.0	3.6
70		7.5	4.5	0.41	0.40
Pressure (microns)		180.	110.		

The authors wish to acknowledge the assistance of Dr. F. J. Vastola of the Fuel Technology Department in preparing this note and the support of the above work by the Atomic Energy Commission, Contract No. AT(30-1)-1710.

FUEL TECHNOLOGY DEPARTMENT THOMAS J. HIRT
THE PENNSYLVANIA STATE UNIVERSITY
UNIVERSITY PARK, PENNSYLVANIA JAMES P. WIGHTMAN

RECEIVED AUGUST 10, 1962

(1) L. H. S. Roblee, Jr., J. T. Agnew, and K. Wark, Jr., *Combust. Flame*, **5**, 65 (1961).

(2) H. B. Palmer and T. J. Hirt, *J. Am. Chem. Soc.*, **84**, 113 (1962).

(3) A. Stock and H. Stoltzenburg, *Ber.*, **50**, 498 (1917).

NO. 27 EPR AT WORK SERIES

SECOND DERIVATIVE DISPLAY IN EPR

(ELECTRON PARAMAGNETIC RESONANCE)

The Varian V-4502 Spectrometer System permits display of both the first derivative and the second derivative of the resonance signal. The microwave bridge is designed for observation of either the absorption or the dispersion. This illustrates the versatility of Varian EPR Spectrometers.

EXAMPLE

DPPH in Benzene: First and second derivative of the absorption and dispersion.

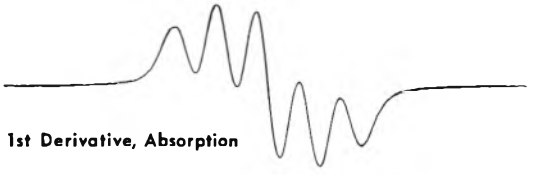

1st Derivative, Absorption

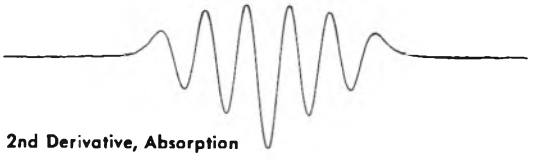

2nd Derivative, Absorption

1st Derivative, Dispersion

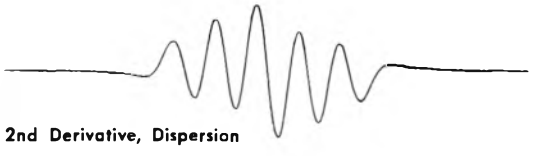

2nd Derivative, Dispersion

Recorder display of the second derivative of magnetic resonance absorption has been common in several laboratories for many years. Display of higher derivatives does not, of course, produce any new information. Nevertheless, the method has some definite advantages. For example, much of the information present in an EPR experiment lies in the *shape* of the resonance. The second derivative is very sensitive to the shape, and observation of it may permit ready detection of slight changes in curvature. Another application arises when two overlapping lines of different widths are encountered. The second derivative will suppress the broader line by the square of the ratio of line widths. A third application is to improve the resolution of overlapping hyperfine lines. In each of these illustrations, the visual display of the second derivative resulted in an easier interpretation of the resonance signals.

Detection of the second derivative is accomplished by using field modulations at two frequencies of about the same amplitude. The doubly modulated signal is subject to the following series of operations: Amplification at the high frequency → phase sensitive detection at the high frequency → amplification at the low frequency → phase sensitive detection at the low frequency → recorder display. The second derivative is obtained when the modulation amplitudes are small compared to the line width.

Resonances from the "classic" EPR material, DPPH dissolved in benzene, are illustrated in the figure. First and second derivatives of the absorption and dispersion result in the four curves. The display of the second derivative of the dispersion is less generally applicable, although there may be some uses in the study of inhomogeneously broadened systems such as donors in semiconductors and color centers in alkali halides.

We would be interested to hear from any readers who have further comments on second derivative presentation.

For literature which fully explains the 100 kc EPR Spectrometer and its application to basic and applied research in physics, chemistry, biology and medicine, write the Instrument Division.

VARIAN associates
PALO ALTO 52, CALIFORNIA